INSTITUTE FOR
Metal and Lightweight Structures
Prof. Dr.-Ing. habil. Natalie Stranghöner

UNIVERSITÄT DUISBURG ESSEN
Open-Minded

Universitätsstr. 15 | 45141 Essen | Phone: +49 (0)201 183-2757 | Fax: +49 (0)201 183-2710
E-Mail: iml@uni-due.de | www.uni-due.de/iml

# Preloading behaviour and preloading levels for stainless steel bolt assemblies including relaxation with detailed specifications for recommended preloading levels

## Deliverable report D5.4

## WP 5 – Task 5.3 / 5.4

***Prof. Dr.-Ing. habil. Natalie Stranghöner***
natalie.stranghoener@uni-due.de

***Christoph Abraham B.Sc.***
christoph.abraham@uni-due.de

***Nariman Afzali M.Sc.***
nariman.afzali@uni-due.de

***Dominik Jungbluth M.Sc.***
dominik.jungbluth@uni-due.de

Part of the RFCS Research Project

"SIROCO"
*Execution and reliability of slip-resistant connections for steel structures using CS and SS*

| | |
|---|---|
| RFCS Project No.: | RFSR-CT-2014-00024 |
| Project No. | 410410007-20003 |
| Report No.: | 2018-08 |

30.03.2018

## Table of contents Page

# 1 Introduction

## 1.1 General remarks

The construction industry demands more and more the application of preloaded stainless steel bolting assemblies, especially in offshore industry, oil rigs, pipelines and chemical industry, seawalls, security barriers, street furniture and other applications in highly corrosive environments.

The application of preloaded stainless steel bolting assemblies is currently not permitted in the execution standard for steel structures EN 1090-2 [1] – unless otherwise specified. If they have to be used, they have to be treated as special fasteners and procedure tests are mandatory. Because no product system neither product standard exist especially for stainless steel bolting assemblies for preloading, the lubrication must be adjusted in a procedure test in such a way that the demanded preload is adequately introduced with the chosen tightening procedure, overstressing has to be excluded, galling has to be avoided as much as possible, and losses of preloading caused by relaxation and creep effects (designated as viscoplastic deformation) have to be considered on the safe side. [2]

Preloaded stainless steel bolting assemblies mainly relax due to different parameters, like embedment/plastic deformation of the clamped component surfaces, the so called setting effect, and the viscoplastic deformation behaviour of stainless steel, which can be observed already at room temperature. The viscoplastic deformation behaviour in preloaded bolting assemblies is assumed to be divided into viscoplastic deformation under constant load condition for the plates (i.e. creep deformation) and viscoplastic deformation under constant strain condition for the bolts (i.e. stress relaxation). Therefore, it is important to estimate the amount of the preload losses from the combined creep and stress relaxation in the bolting assembly.

This deliverable report deals with Work Package (WP) 5, Task 5.3 and Task 5.4 from the RFCS Research Project SIROCO, "Execution and reliability of slip resistant connections for steel structures using CS and SS", funded by the Research Fund for Coal and Steel (RFCS) of the European Community (RFSR-CT-2014-00024). The main objective of WP 5 is to provide preloading levels and preloading methods for preloaded bolted stainless steel connections, taking into account the basic preloading behaviour of stainless steel bolting assemblies caused by nonlinear effects and considering the effects of material relaxation in the bolting assemblies themselves. For this reason, the tightening behaviour of stainless steel bolting assemblies and the relaxation of bolts and plates as isolated elements was studied as well as the relaxation behaviour of the whole bolting assemblies to clearly separate the base material behaviour from other effects resulting from the assemblies (such as friction of the threads, bearing surfaces and so on).

Investigating the basic preloading behaviour of stainless steel bolting assemblies implies in the first step to carry out tightening tests of stainless steel bolting assemblies to achieve information regarding the interaction behaviour between the applied torque and the achieved preload depending on the lubrication, the friction between the threads of the bolt and the nuts as well as the friction under the head of the bolt. For this reason, tightening tests according to EN ISO 16047 [3] resp. EN 14399-2 [4] have to be performed. These tests are necessary to be able to perform the relaxation tests on assembled plate-bolt-connections. It has to be known, on which level the boltin assemblies have to be preloaded in the relaxation tests.

## 1.2 Objectives

This deliverable report deals with the works undertaken in Task 5.3 "Preloading and Relaxation behaviour of SS bolt assemblies" and Task 5.4 "Preloading levels". Some parts and contents of this deliverable report were previously presented in the first and second annual report and are already published in the journal Steel Construction 10 (2017), Issue 4 [2].

## 1.3 Reference to Technical Annex

The Technical Annex of SIROCO defines Tasks 5.3 and 5.4 of WP 5, "Preloading of stainless steel bolts", as follows:

*Task 5.3 Basic preloading behaviour of stainless steel bolts assemblies and relaxation of preloaded stainless steel bolted connection assemblies (**UDE**, BFB, ARP, OSAB, OSOY)*

The basic preloading behaviour of bolt assemblies is highly depeding on various influencing parameters as there are for example

- the base material of the bolt, the nut and the washer (hardness, relaxation etc.),
- fitting of the paired threads of the bolt and the nut and
- lubrication of the nut.

Investigating the basic preloading behaviour of stainless steel bolt assemblies implies in the first step to carry out tightening tests of stainless steel bolt assemblies to achieve information regarding the interaction behaviour between the applied torque and the achieved preload depending on the lubrication, the friction between the threads of the bolt and the nuts as well as the fricttion under the head of the bolt. For this reason tightening tests according to EN ISO 16047 resp. EN 14399-2 have to be performed. These tests are necessary to be able to perform the relaxation tests on assembled plate-bolt-connections. It has to be known, on which level the bolts have to be preloaded in the relaxation tests.

It is assumed that only one lubrication method will be applied and tested during the programme. The lubriccation method will be defined in this task and will be kept constant for all other subsequent tasks in this WP and in WP 6. The most promising lubrication product for stainless steel applications is gleitmo 1952V, which is a product of Fuchs Lubritech GmbH. gleitmo 1952V is a dry film lubricant and is a typically lubrication for stainless steel bolts and nuts.

In a second step, the relaxation of the preload of bolts in bolted connection assemblies has to be investigated. For this reason, relxations test have to be performed of preloaded bolted connection assemblies considering stainless steel bolts and - for comparison reasons - in a first step carbon steel plates and in a second step stainless steel plates. The relaxation tests will be performed – comparable to task 3.3 - using two bolted steel plates (carbon and stainless steel) of the dimensions approx. 30 cm x 15 cm with eight preloaded bolts. Four of the eight bolts will be equiped with implanted strain gauges to measure the change of the preload in the bolts during the whole test time. The final test setup and the test time will be defined at the beginning of this task with respect to the results of task 5.2.

In these tests, firstly carbon steel plates (made of S235 or S355 with the same thickness as the stainless steel plates) will be used for the determination of the pure relaxation behaviour of the assembled stainless steel bolts in order to avoid any influenc of creep/relaxation effects from the assembled stainless steel plates themselves. The influence of creep/relaxation effects of carbon steel plates is negligible. Secondly, the same tests will be performed with stainless steel plates (steel grades as defined in task 5.1). With these tests the combined creep/relaxation effect of the whole assembly can be determined.

*Test specimens:*

| | |
|---|---|
| Steel grades of the clamped plates: | same 4 stainless steel grades as defined in task 5.1 + 1 carbon steel grade (S235 or S355) with same plate thickness. |
| Steel grades of the bolts: | same 3 stainless steel grades/4 strengths as defined in task 5.2 |
| Bolt dimensions: | same 2 bolt dimensions as defined in task 5.2 |

Number of test specimens:

*Tightening tests:*

2 bolt dimensions (M12 and M20), 4 grade strengths of stainless steel/strengths of the bolts, 1 type of lubrication (e.g. gleitmo 1952V, finally to be defined in the beginning of this task), 10 bolts per series

-> 2 x 4 x 1 x 10 = 80 tightening tests (i.e. 40 tightening tests per bolt dimension)

The tightening tests will be performed at UDE using the tightening torque testing machine at the institute. UDE possesses the largest tigthening torque testing machine at a research institute in Germany and is well experienced in performing thightening tests. BFB will produce and suplly the bolts for the tests. OSAB will supply the material to BFB for the production of the bolts

*Relaxation tests:*

2 bolt dimensions (M16 and M24), 4 grades of stainless steel/strengths for the bolts, 1 type of lubrication (e.g. gleitmo 1952V, finally to be defined in the beginning of this task), 5 steel grades for the assembled plate material (4 grades of stainless steel and 1 carbon steel), 3 test specimens for each configuration (2 assembled plates with 8 bolts, 4 bolts with implanted strain gauges -> 12 measurements of changes in the preolad per configuration)

-> 2 x 4 x 1 x 5 x 3 = 120 relaxation tests of bolted assemblies (-> 2 x 4 x 1 x 5 = 40 configurations)

The relaxation tests will be performed at UDE. UDE is well experienced in performing this kind of relaxation tests. BFB will produce and supply the bolts for the tests. OSAB will supply the material to BFB for the production of the bolts. OSAB and OSOY will supply the stainless steel plate material.

*Results and deliverables:*

- basic preloading behaviour of stainless steel bolts (torque-preload- and torque-rotation-behaviour as described in task 5.4)
- relaxation behaviour of preloaded bolted assemblies

*Relaxation tests:*

2 bolt dimensions (M16 and M24), 4 grades of stainless steel/strengths for the bolts, 1 type of lubrication (e.g. gleitmo 1952V, finally to be defined in the beginning of this task), 5 steel grades for the assembled plate material (4 grades of stainless steel and 1 carbon steel),

3 test specimens for each configuration (2 assembled plates with 8 bolts, 4 bolts with implanted strain gauges -> 12 measurements of changes in the preolad per configuration)

-> 2 x 4 x 1 x 5 x 3 = 120 relaxation tests of bolted assemblies (-> 2 x 4 x 1 x 5 = 40 configurations)

The relaxation tests will be performed at UDE. UDE is well experienced in performing this kind of relaxation tests. BFB will produce and supply the bolts for the tests. OSAB will supply the material to BFB for the production of the bolts. OSAB and OSOY will supply the stainless steel plate material.

Results and deliverables:

- basic preloading behaviour of stainless steel bolts (torque-preload- and torque rotation-behaviour as described in task 5.4)
- relaxation behaviour of preloaded bolted assemblies

*Task 5.4 Determination of recommended preloading levels (UDE, ARP, BFB)*

Recommended preloading levels can only be defined knowing the complex torque-preload- and torque- rotation-behaviour of each bolt diameter used in practice considering the relaxation effects. It is of great importance to show, that the functional characteristics of the bolt assemblies, described by the following parameters comparable to EN 14399-3 and -4 (valid for carbon steel bolts) are sufficient:

- maximum individual value of the bolt force during tightening test $F_{bi}$,
- angle by which the nut (or bolt) has to be turned starting from a defined preload $F_{p,C}$ (this value has to be defined in this task for stainless steel bolts),
- $F_{bi,max}$ is reached ($\Delta\Theta_1$),
- angle by which the nut (or bolt) has to be turned starting from the preload $F_{p,C}$ until $F_{bi}$ has dropped again to the $F_{p,C}$ and
- individual values of the k-factor ($k_i$), mean value of the k-factor (km) and coefficient of variation of the k- factor (VK).

The aforementioned parameters describe limiting criteria, which have to be redefined for stainless steel bolt assemblies during this task due to the fact that the limiting criteria given in EN 14399-3 and -4 are only valid for HR- or HV-bolt assemblies. For this reason, for each bolt diameter tightening tests have to be performed. In addition to those tests already performed in task 5.3, further tests have to be performed for bolt diameters which have not been tested in task 5.3 but should be covered in the EN 1993-1-4. It can be assumed that the relaxation effect might be transformed from the results already achieved in tasks 5.2 and 5.3, so that no further relaxation tests have to be carried out.

Furthermore, design specifications for preloaded connections made of stainless steel have to be defined.

*Test specimens:*

| | |
|---|---|
| Steel grades of the bolts: | same 3 stainless steel grades / 4 strengths as defined in task 5.2 |
| Bolt dimensions: | M16 and M24 -> M16 and M24 will already be tested in task 5.3 (The bolt dimensions covered in this research proposal are limited to M12, M16, M20 and M24) |

Number of test specimens:

*Tightening tests:*

2 bolt dimensions (M12 and M20), 4 stainless steel grades/strengths for the bolts, 1 type of lubrication (e.g. gleitmo 1952V, final decision to be made in the beginning of this task), 10 bolts per series

-> 2 x 4 x 1 x 10 = 80 tightening tests (i.e. 40 tightening tests per bolt dimension)

UDE will carry out the tightening tests. BFB will deliver the bolts. UDE, SCI and ARP will define the recommended preloading values with respect to practical needs. SCI will conclude the design specifications for preloaded bolted connections made of stainless steel.

Results and deliverables:

- recommended preloading levels for specified bolt diameter taking into account long term relaxation effects (Amndm. to EN 1090-2 and EN 1993-1-4),
- design specifications for preloaded bolted connections made of stainless steel (Amndm. to EN 1993-1-4)

# 2 State of the art

## 2.1 General

In this chapter, the state of the art of used bolting assemblies and bolted connections in the steel construction industry are introduced with special regard to preloaded bolting assemblies made of stainless steel. Firstly, a short overview of non-preloaded and preloaded carbon steel bolting assemblies is provided, based on the harmonized standards EN 15048-1 [5] (subchapter 2.2.1) and EN 14399-1 [6] (subchapter 2.2.2). Categories of bolted connections acc. to EN 1993-1-8 [7] are explained as well as the related target levels of preloading, see subchapter 2.2.3. The mechanical behaviour of bolting assemblies and bolted connections is essential, and for this reason the load-bearing behaviour of bolting assemblies under mono-axial tensile load is presented as well in subchapter 2.2.4.

An introduction about stainless steel bolting assemblies covered by EN ISO 3506-1 and -2 [8], [9] will be presented in subchapter 2.3. The information relates to the current revision of EN ISO 3506 which is due to be published in 2018, and the specification gives chemical compositions and mechanical properties for austenitic, martensitic, ferritic and also newly added duplex bolting assemblies. In addition, the main differences in mechanical behaviour of carbon steel and stainless steel are shortly summarized in subchapter 2.4.

The applicability of tightening methods is directly connected to the quality of calibrated bolting assemblies in their delivered condition. To achieve and guarantee a specified preloading level, appropriate tightening methods are required and underline the importance of adjusted, calibrated lubrication and k-classes. For this reason, the k-value, as a parameter for predominant friction conditions and quality of lubrication, is introduced according to EN 14399-2 as well as the related k-classes K0, K1, and K2 acc. to EN 14399-1 [6].

Looking at the preloading behaviour of stainless steel bolting assemblies, not only the tightening itself is of interest, but the whole procedure including all necessary tightening parameters and criteria: the level of suitable preloading, the associated lubrication, the tightening procedure (see subchapter 2.5) itself and the evaluation criteria, which do not exist so far for stainless steel bolting assemblies.

For this reason, the test procedure and suitability test for preloading according to EN 14399-2 is presented as well as the to be measured and/or to be determined parameters according to EN ISO 16047 (see subchapter 2.6 and 2.7). In absence of existing adequate criteria for preloaded stainless steel bolting assemblies, both standards form the basis for the evaluation of tightening tests of bolting assemblies made of stainless steel. The chosen criteria to evaluate the ductility of preloaded stainless steel bolting assemblies according to EN 14399-2 and EN 14399-3 [10] is summarized in subchapter 2.8.

Finally, the viscoplastic deformation behaviour of stainless steel bolting assemblies is introduced in subchapter 2.9.

## 2.2 Standards and categories of bolted connections

Bolting assemblies used in the steel construction industry are based on two European harmonized standards (CPR 305/2011), summarized in Figure 1:

- **Non-preloaded bolting assemblies** (categories A, D) refers to *EN 15048-1: 2007-07* and can be divided into standard bolts for metal construction (EN ISO

4014, 4016, 4017 and 4018) and german bolts for steel construction (DIN 7990 and DIN 7968).

- **Preloaded bolting assemblies** (categories B, C, E) according to *EN 14399-1:2015-04* include preloaded special bolts "H" like system HR acc. EN 14399-3 and HV acc. EN 14399-4 [11] (as examples of suitable bolting assemblies refered to the scope of EN 14399-1). Preloading of standard bolts acc. EN ISO 4014 [12] and EN ISO 4017 [13] is also possible.

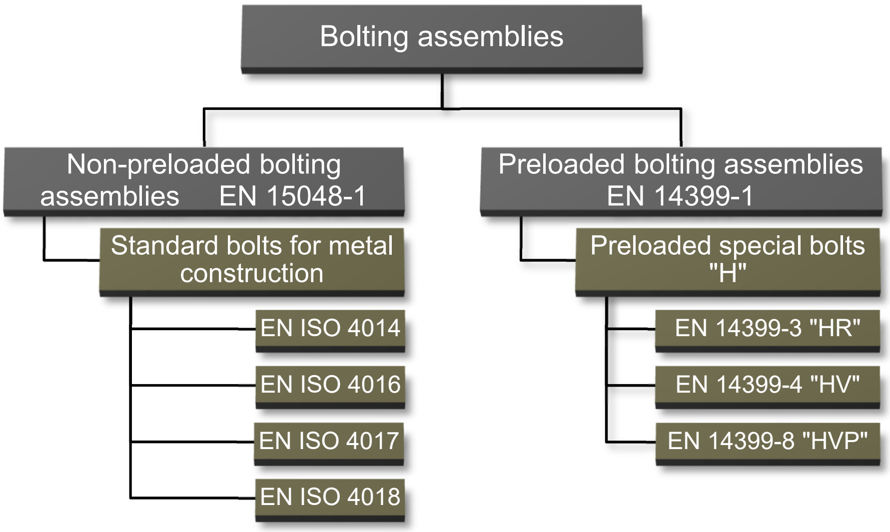


**Figure 1** Overview of bolting assemblies and harmonized standards used in the steel construction industry ([14][15])

### 2.2.1 Harmonized Standard EN 15048-1: Non-preloaded structural bolting assemblies

The European harmonized standard EN 15048-1:2007-07 [14] "Non-preloaded structural bolting assemblies – Part 1: General requirements" contains all technical requirements for bolting assemblies without referring to individual products in steel construction and is open-designed, meaning that various bolting assemblies must fulfil central claims like dimensions and tolerances in accordance to international or European standards, deliverable in bolting assemblies, CE certification of the manufacturer, and structural bolting (SB) marking [14].

Standard bolts for metal construction (EN ISO 4014, 4016, 4017 and 4018) are presented in a comparative overview in Table 1 together with German bolts according to DIN 7990 and DIN 7968 als fulfilling the criteriai of EN 15048-1. The advantages of these standard bolts for metal construction are that only a narrow stock range is necessary, and from a technical viewpoint, the selection is easy for the planning engineer and washers are not prescribed when normal round holes are used without special conditions. On the other hand, the shear load capacity of bolts with the thread in the clamped package is lower and deformations are a bit larger in shear/hole bearing connections. The normative references, main characteristics, and differences of nuts and washers for non-preloaded structural bolting assemblies are summarized in Table 2 and Table 3 [14].

**Table 1** Overview of non-preloaded structural bolting assemblies acc. EN 15048-1:2007-07 (based on [14])

| Designation | Product standard | Thread length | Shank diameters | Wrench width | Product class | Strength class |
|---|---|---|---|---|---|---|
| Standard bolts for metal construction | EN ISO 4014 | medium long: b ≈ (2.2 to 2.5) · d | normal: $d_{sh} = d$ | normal: s ≈ (1.5 to 1.6) · d | A/B[1)] | 5.6, 8.8, 10.9 |
| | EN ISO 4016 | | | | C | 4.6 |
| | EN ISO 4017 | long: b ≈ 1 | normal: $d_{sh} = d$ | normal: s ≈ (1.5 to 1.6) · d | A/B[1)] | 5.6, 8.8, 10.9 |
| | EN ISO 4018 | | | | C | 4.6 |
| German bolts for steel construction | DIN 7990 | particularly short: b ≈ (1.2 to 1.6) · d | normal: $d_{sh} = d$ | normal: s ≈ (1.5 to 1.6) · d | C | 4.6, 5.6 |
| | DIN 7968 | particularly short: b ≈ (1.2 to 1.5) · d | Pass-: $d_{sh} = d + 1$ | normal: s = (1.5 to 1.6) · d | C | 5.6 |

1) ≤ M24 / > M24

**Table 2** Overview of applicable nuts for non-preloaded structural bolting assemblies acc. EN 15048-1 (based on [14])

| Designation | Product standard | Height of the nut | Wrench width | Product class | Strength class |
|---|---|---|---|---|---|
| Standard bolts for metal construction | EN ISO 4032 | medium: m ≈ 0.9 · d | normal: s ≈ (1.5 to 1.6) · d | A/B[1)] | 6, 8, 10 |
| | EN ISO 4034 | medium: m ≈ 0..9 · d | normal: s ≈ (1.5 to 1.6) · d | C | 4, 5 |
| | EN ISO 4033 | medium: m ≈ 1.0 · d | normal: s ≈ (1.5 to 1.6) · d | A/B[1)] | 9, 12 |

1) ≤ M16 / > M16

**Table 3** Overview of applicable washers for non-preloaded structural bolting assemblies acc. EN 15048-1 [14] (based on [14])

| Designation | Product standard | Thickness[1)] | Outside diameter[1)] | Inside diameter[1)] | Chamfer | Product class | Hardness |
|---|---|---|---|---|---|---|---|
| Standard bolts for metal construction | EN ISO 7089 | thin: h = 2.5 to 5.0 mm | $d_a = e$ + (3 to 5) mm | $d_i = d$ +1 mm | no | A | 200/300 HV |
| | EN ISO 7090 | | | | outside | | 200/300 HV |
| | EN ISO 7091 | | | | no | C | 100 HV |
| German bolts for steel construction | DIN 7989-1 | thick: h = 8 mm | | $d_i = d$ + (2 to 3) mm | no | C | 100 HV |
| | DIN 7989-2 | | | | | A | |

1) Range: minimum value: M12 / maximum value: M36

Two types of bolting assemblies are possible [14]:

- *Standard bolting assemblies for metal construction* with EN ISO 4014 or 4017 bolts combined with ISO 4032 hexagon nuts and washers acc. to ISO 7089.
- *German bolting assemblies for steel construction* with DIN 7990 or DIN 7968 bolts, hexagon nuts acc. to EN ISO 4032, and washers acc. to DIN 7989 (only standardised in Germany).

### 2.2.2 Harmonized Standard EN 14399-1: High-strength structural bolting assemblies for preloading

The European harmonized standard EN 14399-1 "High-strength structural bolting assemblies for preloading – Part 1: General requirements" contains all technical requirements for bolting assemblies for preloading. The normative references, main characteristics, and differences of nuts and washers for preloaded structural bolting assemblies are summarized in Table 4, Table 5 and Table 6. Chapter 4.2.1 of EN 14399-1 describes two types of bolting assemblies for preloaded bolted connections:

- **Type HR** (including System HR acc. EN 14399-3 and System HRC acc. EN 14399-10) is structurally designed so that *ductility is predominantly achieved by plastic elongation of the bolt*. For this, the minimum height of the hexagon nut must be ≥ 0.9 *D* and the thread length of the bolt is acc. ISO 888:2012-04.
- **Type HV** is structurally designed so that ductility is *predominantly achieved by the plastic deformation of the paired threads*, realized by nut height ≈ 0.8 *D* and bolts with short thread length.

The special characteristics of HRC bolting assemblies with reference to EN 14399-10 and Direct Tension Indicators (DTI) according to EN 14399-9 are not explained here (see Deliverable report D3.3). Furthermore, preloading of standard bolting assemblies for metal construction in property class 8.8 according to EN ISO 4014 [21] and EN ISO 4017 [22] is also possible.

Compared to EN ISO 4014 and EN ISO 4017 bolting assemblies, high-strength structural bolting assemblies for preloading in System HR and HV are characterized by a larger wrench width, the height of the nut is equal to ISO 4017 (m ≈ 0.9 · d) and System HV bolt heads are larger than EN ISO 4014/4017 bolt heads.

**Table 4** Overview of preloaded high-strength structural bolts acc. EN 14399-1 [14]

| Designation | Product standard | Thread length | Shank diameter | Wrench width | Product class | Strength class |
|---|---|---|---|---|---|---|
| **Preloaded special bolts "H"** | EN 14399-4 "HV" | short: $b \approx (1.4 \text{ to } 1.9) \cdot d$ | normal: $d_{sch} = d$ | large: $s \approx (1.6 \text{ to } 1.7) \cdot d$ | B | 10.9 |
| | EN 14399-8 "HVP" | extremly short: $b \approx (1.2 \text{ to } 1.5) \cdot d$ | Pass-: $d_{sch} = d + 1$ | large: $s \approx (1.6 \text{ to } 1.7) \cdot d$ | B | 10.9 |
| | EN 14399-3 "HR " | medium: $b \approx (2.2 \text{ to } 3.3) \cdot d$ | normal: $d_{sch} = d$ | large: $s \approx (1.6 \text{ to } 1.7) \cdot d$ | B | 8.8, 10.9 |
| **Preloaded standard bolts for metal construction** | EN 14399-1 + EN ISO 4014 | medium: $b \approx (2.2 \text{ to } 2.5) \cdot d$ | normal: $d_{sch} = d$ | normal: $s \approx (1.5 \text{ to } 1.6) \cdot d$ | A/B[1)] | 8.8 |
| | EN 14399-1 + EN ISO 4017 | long: $b \approx 1$ | normal: $d_{sch} = d$ | normal: $s \approx (1.5 \text{ to } 1.6) \cdot d$ | A/B[1)] | 8.8 |

[1)] ≤ M24 / > M24

**Table 5** Overview of preloaded high-strength nuts acc. EN 14399-1 [14]

| Designation | Product standard | Height of the nut | Wrench width | Product class | Strength class |
|---|---|---|---|---|---|
| **Preloaded special bolts "H"** | EN 14399-4 "HV" | small: m ≈ 0.8 . d | large: s ≈ (1.6 to 1.7) · d | B | 10 |
| | EN 14399-3 "HR" | medium: m ≈ 0.9 . d | large: s ≈ (1.6 to 1.7) · d | B | 8, 10 |
| **Preloaded standard bolts for metal construction** | EN 14399-1 + EN ISO 4032 | medium: m ≈ 0.9 . d | normal: s ≈ (1.5 to 1.6) · d | A/B 1) | 8 |

1) ≤ M16 / > M16

**Table 6** Overview of preloaded high-strength washers acc. EN 14399-1 [14]

| Designation | Product standard | Thickness 1) | Outside diameter 1) | Inside diameter 1) | Chamfer | Product class | Hardness |
|---|---|---|---|---|---|---|---|
| **Preloaded special bolts "H"** | EN 14399-5 | medium: h = 3.0 to 6.0 mm | $d_a$ = e | $d_i$ = d +1 mm | no | A | 300 to 370 HV |
| | EN 14399-6 | | | | inside + outside | | |
| **Preloaded standard bolts for metal construction** | EN 14399-1 + DIN 34820 | thin: h = 2.5 to 5.0 mm | $d_a$ = e + (3 to 5) mm | $d_i$ = d +1 mm | | A | 300 HV |

1) Range: minimum value: M12 / maximum value: M36

## 2.2.3 Categories of bolted connections and preloading target levels

The primary distinction of bolted connections is between shear connections and tension connections, categorized based on the type of loading perpendicular or running parallel to the bolt axis. Based on the primary distinction, the Eurocode EN 1993-1-8 classifies bolted connections into categories A to E, presented in Table 7 and Figure 3.

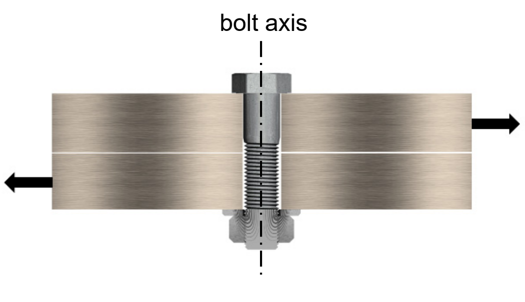


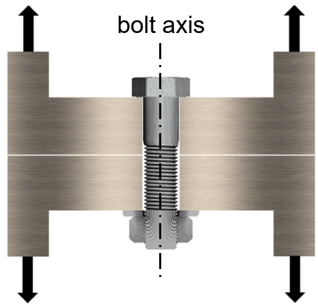


**Figure 2** Bolted shear connection (left) and tension connection (right)

**Table 7** Categories of bolted connections acc. EN 1993-1-8:2010-12

| Category | Design criterion | Annotations |
|---|---|---|
| **Shear connections** | | |
| A<br>bearing type | $F_{v,Ed} \leq F_{v,Rd}$<br>$F_{v,Ed} \leq F_{b,Rd}$ | No preloading required.<br>Bolt classes from 4.6 to 10.9 may be used. |
| B<br>slip resistant at serviceability | $F_{v,Ed,ser} \leq F_{s,Rd,ser}$<br>$F_{v,Ed} \leq F_{v,Rd}$<br>$F_{v,Ed} \leq F_{b,Rd}$ | Preloaded 8.8 or 10.9 bolts should be used. |
| C<br>slip resistant at ultimate | $F_{v,Ed} \leq F_{s,Rd}$<br>$F_{v,Ed} \leq F_{b,Rd}$<br>$\sum F_{v,Ed} \leq N_{net,Rd}$ | Preloaded 8.8 or 10.9 bolts should be used. |
| **Tension connections** | | |
| D<br>non-preloaded | $F_{t,Ed} \leq F_{t,Rd}$<br>$F_{t,Ed} \leq B_{p,Rd}$ | No preloading required.<br>Bolt classes from 4.6 to 10.9 may be used. |
| E<br>preloaded | $F_{t,Ed} \leq F_{t,Rd}$<br>$F_{t,Ed} \leq B_{p,Rd}$ | Preloaded 8.8 or 10.9 bolts should be used. |

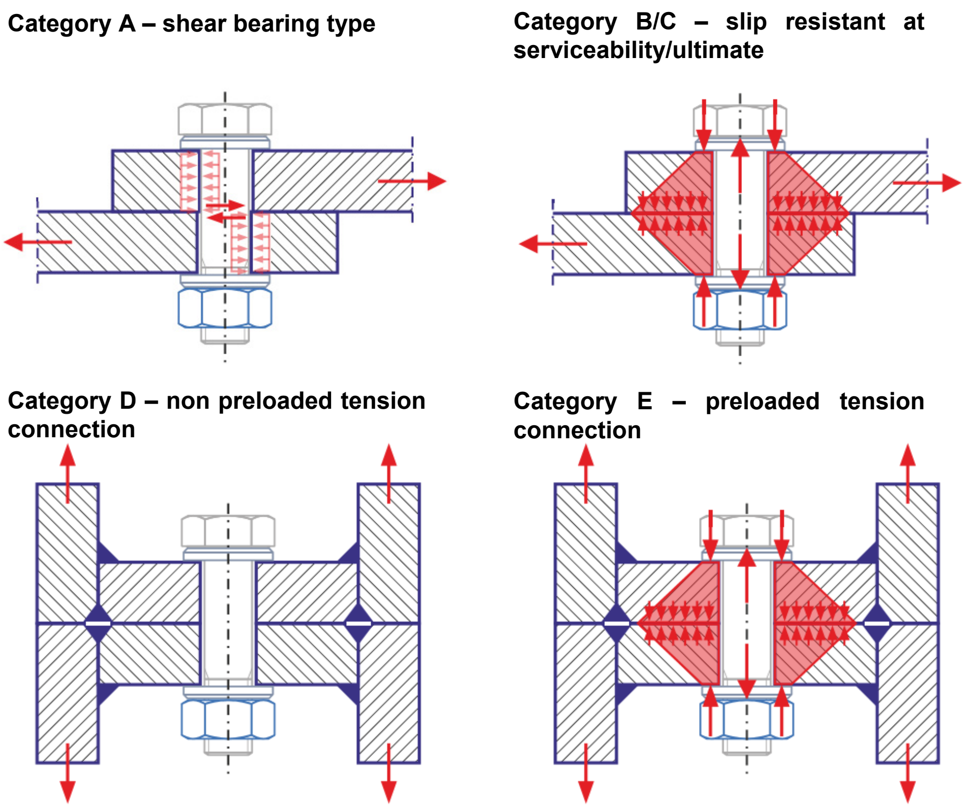


**Figure 3** Visualization of categories of bolted connections [© IML]

The preloading of high-strength, structural bolting assemblies can serve different purposes. The type of bolted connection must be considered, as well as the relevance of the security, which has of course the highest priority. From this perspective, further distinguishing between two target levels of preloading in steel construction is useful to take into account the required inspection of installation and testing accuracy:

- ***Target level I*** – *Guarantee structural safety:* slip-resistant connections in category B and C as well as preloaded tension connections in category E which are often used in fatigue loaded applications. In all cases, the preload must be sufficiently and safely guaranteed over the entire service life and periodical inspections are required.

  - *Specified preload in EN 1090-2:* $F_{p,C} = 0.7 \cdot f_{ub} \cdot A_s$,
    unless otherwise specified.
    with $F_{p,C}$ specified preloading level (see also EN 1090-2)
    $f_{ub}$ nominal tensile strength ($R_{m,nom}$) of the bolt
    $A_s$ nominal stress area of the bolt (see EN ISO 898-1 [16])

- ***Target level II*** – *Improvement of serviceability:* the shear-bearing connection in category A, as well as the non-preloaded tension connection in category D, can be executed as preloaded connections to improve the serviceability (e.g. slip minimisation, increasing the stiffness, minimisation of deformations).

  - *Posssible preload:* $F_p \leq F_{p,C}$, *e. g.* $F_{p,C}^* = 0.7 \cdot f_{yb} \cdot A_s$
    with $F_{p,C}^*$ reduced preloading level (see exemplary German Technical Annex, DIN EN 1993-1-8/NA [17])
    $f_{yb}$ nominal yield strength ($R_{m,nom}$) of the bolt
    $A_s$ nominal stress area of the bolt (see EN ISO 898-1)

The execution of preloaded bolted connections is summarized in Table 8 with a focus on the discussed target levels of preloading, normative references, tightening methods, and inspection requirements.

**Table 8** Execution of preloaded bolted connections acc. to EN 1090-2 and DIN EN 1993-1-8/NA [18]

| Target level preload | Category (according to design) | | Preload (according to execution) | Bolting assemblies: product standard | Bolting assemblies: strength class | k-cl. | Tightening methods[3] | Tightening parameters[4] | Control requirements |
|---|---|---|---|---|---|---|---|---|---|
| **I Quantitative improvement ultimate state** | B[1] C | relevant for design | $\mathbf{F_{p,C}}$ | EN 14399-1 | 10.9 8.8[5] | K2 K1 | CM | EN 1090-2 | EN 1090-2 |
| | E | | $\mathbf{F_{p,C}}$ | | | | | | |
| | | | $F_v < F_{p,C}$ | | specifications required[2] | | | | |
| | | | $F_{p,C}{}^*$ | Tab. NA.A.2[6] | 10.9 | K1 | MCM MTM CWM | Tab. NA.A.2[6] Tab. NA.A.3[6] | EN 1090-2 |
| | | | | Tab. NA.A.1[6] | 8.8 | | MTM CWM | Tab. NA.A.1[6] | |
| | | | $F_V < F_{p,C}{}^*$ | Tab. NA.A.2[6] | 10.9 | | MTM CWM | proportional to Tab. NA.A.2[6] | |
| | | | | Tab. NA.A.1[6] | 8.8 | | | proportional to Tab. NA.A.1[6] | |
| **II Qualitative improvement serviceability** | A D | not relevant for design | $\mathbf{F_{p,C}}$ | EN 14399-1 | 10.9 8.8[5] | K2 K1 | CM | EN 1090-2 | EN 1090-2 |
| | | | $F_v < F_{p,C}$ | | specifications required[2] | | | | |
| | | | $F_{p,C}{}^*$ | Tab. NA.A.2[6] | 10.9 | K1 | MCM MTM CWM | Tab. NA.A.2[6] Tab. NA.A.3[6] | EN 1090-2 – please note Quelle 1 |
| | | | | Tab. NA.A.1[6] | 8.8 | | MTM CWM | Tab. NA.A.1[6] | |
| | | | $F_V < F_{p,C}{}^*$ | Tab. NA.A.2[6] | 10.9 | | MTM CWM | proportional to Tab. NA.A.2[6] | |
| | | | | Tab. NA.A.1[6] | 8.8 | | | proportional to Tab. NA.A.1[6] | |

[1] In this case to guarantee serviceability. [2] Specifications regarding preload level. [3] Abbreviations of tightening methods: CM – combined method; TM – torque method; CWM – calibrated wrench method; MTM – modified torque method; MCM – modified combined method. [4] e.g. reference tightening torques. [5] The use of bolts in strength class 8.8 is not recommend. [6] Tables acc. Annex NA.A. of DIN EN 1993-1-8

## 2.2.4 Tensile loaded bolting assemblies and notch effects

The load-bearing behaviour of bolting assemblies under tensile load focuses on the question of converting a tightening torque to a useable and reliable preload. The total tightening torque $M_A$ is composed of the preload producing torque $M_{GSt}$ (which is, due to friction, only 10% of the total tightening torque), thread torque $M_{GR}$, and the nut respective to the bolt head bearing torque $M_{KR}$ (terminology from [19]). In the elastic range and with constant friction assumed, the relationship between tightening torque and the achieved preload is linear.

$$M_A = M_{GSt} + M_{GR} + M_{KR} = M_G + M_{KR} \qquad (2\text{-}1)$$

Derived from the equilibrium conditions for the inclined plane as a fundamental principle, the relationship between the preload and the torsional moment acting in the thread can be obtained. Considering the pitch diameter $d_2$, the pitch P, and flank angle $\alpha = 60°$ (ISO threads), the equation for thread torque can be simplified as:

$$M_G = F_V\,(0.159\,P + 0.577\,d_2\,\mu_G). \qquad (2\text{-}2)$$

The nut respective to the bolt head bearing torque for overcoming the friction is calculated by equation 2-3 with an adopted constant surface pressure and $D_{Km}$ as friction diameter:

$$M_{KR} = F_V\,\mu_K\,\frac{D_{Km}}{2} \;\wedge\; D_{Km} = \frac{(d_w + d_h)}{2}. \qquad (2\text{-}3)$$

The tightening torque can finally be determined by the following equation:

$$M_A = F_V\left(0.159\,P + 0.577\,d_2\,\mu_G + \frac{D_{Km}}{2}\mu_K\right). \qquad (2\text{-}4)$$

Figure 4 summarizes the occurring forces, torques, and frictions in a bolted connection when tightened (here, exemplary nut sided), the distribution in load-bearing paired threads, and the flow of forces.

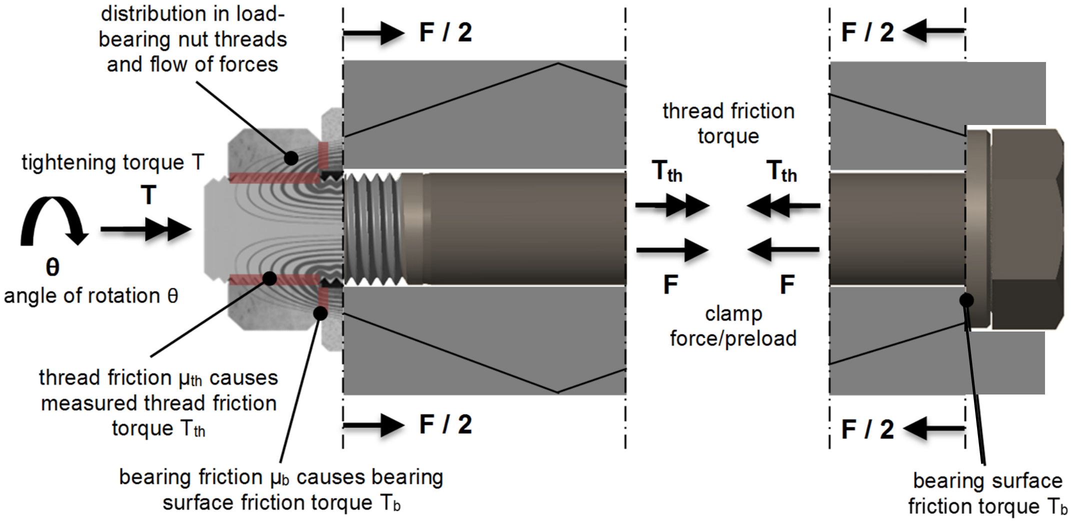


**Figure 4** Forces, torques and friction conditions in a bolted HV connection when tightened [19],[20]

The design of bolts in the context of load-bearing behaviour can be different depending on the required applications and target failure mode. For example, System HR bolts, according to EN 14399-3, are structurally designed such that ductility is predominantly achieved through plastic elongation of the bolt. For this, the minimum height of the hexagon nut must be ≥ 0.9 D so that fracture occurs in the free load loaded thread of the bolt. Related to security aspects, plastic deformations give notice of upcoming fracture. On the contrary, system HV bolts acc. EN 14399-4 achieve ductility through plastic deformation of the paired threads, realized by a nut height of ≈ 0.8 D and bolts with short thread lengths. The failure principle is the stripping of the hexagon nut.

Bolts are highly notched connecting elements and under tension load, local stresses can significantly increase. Figure 5 shows the ratio $\sigma_{max}/\sigma_{nom}$ (form factor $\alpha_K$) and displays places with high notch stresses at borders, like the bolt head-shank transition, in the free loaded thread of the bolt, and especially at the first load-bearing thread of the nut. It can be used to design failure modes of bolts, e.g. the different height of the System HR and System HV nuts to modify local stresses.

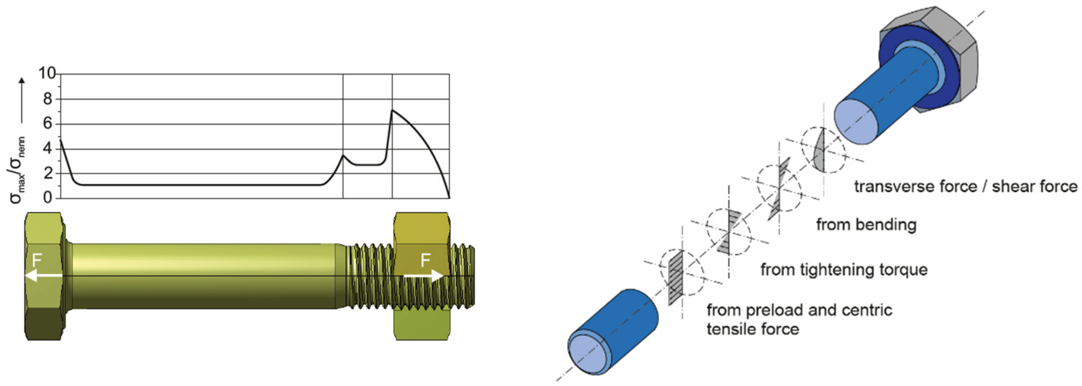


**Figure 5** Distribution and form factors $\alpha_K$ of notches in a bolt (left) and stresses in bolt shank (right) (© IML for left and right Figure)

Thomala and Kloos [19] emphasize that multiaxial stress states, which result from restricted transversal contractions (Poisson's ratio), are significantly influential on the load-bearing behaviour of bolts under rapid tensile loading depending on the material toughness. When the material toughness is sufficient, high stresses lead to better load-bearing behaviour due to notched strengthening, but also ductility and deformability decreases. On the other hand, notch softening as a strength-reducing effect occurs when material toughness drops below a limit value. The different (not multiaxial) stresses in the bolt shank are also shown in Figure 5. Furthermore, forces at load-bearing paired threads are unequally distributed. Numerical investigations at the IML indicate that local plastifying occurs at already at a specified preload of $F_{p,C}$* = 0.7 · $f_{yb}$ · $A_s$. [21].

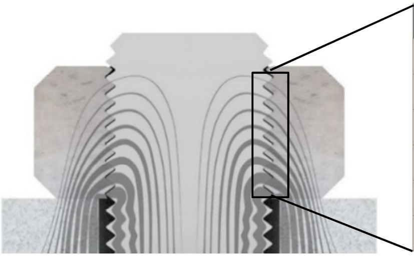

| Thread | % | % Sum |
|---|---|---|
| 1 | 34% | 34% |
| 2 | 23% | 55% |
| 3 | 16% | 71% |
| 4 | 11% | 82% |
| 5 | 9% | 91% |
| 6 | 7% | 98% |

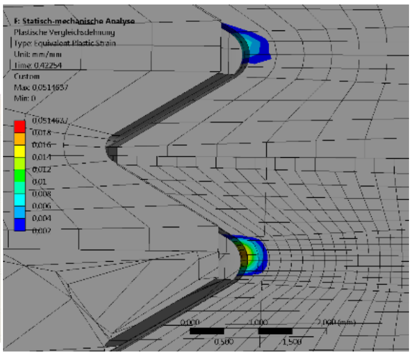

**Figure 6** Load distribution in the paired threads (left/middle) and plasticising at $F_{p,C}$* (right)

## 2.3 Bolting assemblies made of stainless steel covered by EN ISO 3506 (in revision)

Stainless steel bolts are covered by EN ISO 3506-1, *Corrosion-resistant stainless steel fasteners*. The information below relates to the revision of EN ISO 3506 which is due to be published in 2018. The specification gives chemical compositions and mechanical properties for austenitic, martensitic, ferritic and also duplex fasteners. Alternative materials not specifically covered in the specification are permitted if they meet the physical and mechanical property requirements and have equivalent corrosion resistance.

In EN ISO 3506-1/-2, bolt and nut materials are classified by a letter: "A" for austenitic, "F" for ferritic, "C" for martensitic and "D" for duplex. It is recommended that austenitic or duplex bolts are used in structural applications. The letter is followed by a number (1, 2, 3 4, 5, 6 or 8) which reflects the corrosion resistance; 1 representing the least durable and 8 the most durable one. Table 9 gives the chemical composition range for austenitic and duplex classes of bolts and Table 10 gives the common designations of stainless steels used for fasteners of each class.

**Table 9** Chemical compositions of bolts to EN ISO 3506

| Grade | | Chemical composition [a] weight, % | | | | | | | | | | Other elements and notes |
|---|---|---|---|---|---|---|---|---|---|---|---|---|
| | | C | Si | Mn | P | S | Cr | Mo | Ni | Cu | N | |
| Austenitic | **A1** | 0,12 | 1,0 | 6,5 | 0,020 | 0,15-0,35 | 16-19 | 0,7 | 5-10 | 1,75-2,25 | — | b, c, d |
| Austenitic | **A2** | 0,10 | 1,0 | 2,0 | 0,050 | 0,03 | 15-20 | — [e] | 8-19 | 4 | — | f, g |
| Austenitic | **A3** | 0,08 | 1,0 | 2,0 | 0,045 | 0,03 | 17-19 | — [e] | 9-12 | 1 | — | 5C ≤ Ti ≤ 0,8 and/or 10C ≤ Nb ≤ 1,0 |
| Austenitic | **A4** | 0,08 | 1,0 | 2,0 | 0,045 | 0,03 | 16-18,5 | 2,0-3,0 | 10-15 | 4 | — | g, h |
| Austenitic | **A5** | 0,08 | 1,0 | 2,0 | 0,045 | 0,03 | 16-18,5 | 2,0-3,0 | 10,5-14 | 1 | — | 5C ≤ Ti ≤ 0,8 and/or 10C ≤ Nb ≤ 1,0 h |
| Austenitic | **A8** | 0,03 | 1,0 | 2,0 | 0,040 | 0,03 | 19-22 | 6,0-7,0 | 17,5-26 | 1,5 | — | — |
| Duplex | **D2** | 0,04 | 1,0 | 6,0 | 0,040 | 0,030 | 19-24 | 0,10-1,0 | 1,5-5,5 | 3 | 0,05-0,20 | Cr+3,3Mo+16N ≤24 [j] |
| Duplex | **D4** | 0,04 | 1,0 | 6,0 | 0,040 | 0,030 | 21-25 | 0,10-2,0 | 1,0-5,5 | 3 | 0,05-0,30 | 24 < Cr+3,3Mo+16N [j] |
| Duplex | **D6** | 0,03 | 1,0 | 2,0 | 0,040 | 0,015 | 21-26 | 2,5-3,5 | 4,5-7,5 | — | 0,08-0,35 | — |
| Duplex | **D8** | 0,03 | 1,0 | 2,0 | 0,035 | 0,015 | 24-26 | 3,0-4,5 | 6,0-8,0 | 2,5 | 0,20-0,35 | W ≤ 1,0 |

a Values are maximum unless otherwise indicated.

b Selenium might be used to replace sulphur, however National regulations shall be taken into account in the countries or regions concerned.

c If the nickel content is below 8 %, the minimum manganese content shall be 5 %.

d There is no minimum limit to the copper content provided that the nickel content is greater than 8 %.

e Molybdenum may be present at the discretion of the manufacturer. However, if for some applications limiting of the molybdenum content is essential, this shall be stated at the time of ordering by the purchaser.

f If the chromium content is below 17 %, the minimum nickel content should be 12 %.

g For austenitic stainless steels having a maximum carbon content of 0,030 %, nitrogen may be present but shall not exceed 0,22 %.

h At the discretion of the manufacturer the carbon content may be higher where required in order to obtain the specified mechanical properties at larger diameters, but shall not exceed 0,12 % for austenitic steels.

j This formula is used for the purpose of classification of duplex steels in accordance with this standard; it is not intended to be used as a selection criterion for corrosion resistance.

**Table 10** Common designations of stainless steels used for fasteners

| Type | ISO 3506 class | Common designations of stainless steels used for fasteners | Comments |
|---|---|---|---|
| Austenitic | A1 | 1.4570, 1.4305 | Designed for machining [1)] |
| | A2 | 1.4301, 1.4307 | Basic austenitic |
| | A3 | 1.4541, 1.4550 | Stabilised basic austenitic |
| | A4 | 1.4401, 1.4404 | Molybdenum containing austenitic |
| | A5 | 1.4571 | Stabilised molybdenum austenitic |
| | A8 | 1.4529, 1.4547 | Super austenitic |
| Duplex | D2 | 1.4482, 1.4362 | Lean duplex |
| | D4 | 1.4162, 1.4062 | Lean duplex |
| | D6 | 1.4462 | Standard duplex |
| | D8 | 1.4410, 1.4501, 1.4507 | Super duplex |

[1)] The high sulphur content lowers resistance to corrosion compared to corresponding steels with normal sulphur content. Only specify with care.

Figure 7 shows the designation system and strength levels (property classes) available for austenitic and duplex fasteners. The different mechanical properties are usually achieved by work hardening and depend on the rate of cold working. Table 11 gives the mechanical properties of each property class. Austenitic bolts manufactured to property class 50 will be non-magnetic, but those in higher property classes may demonstrate some magnetic properties.

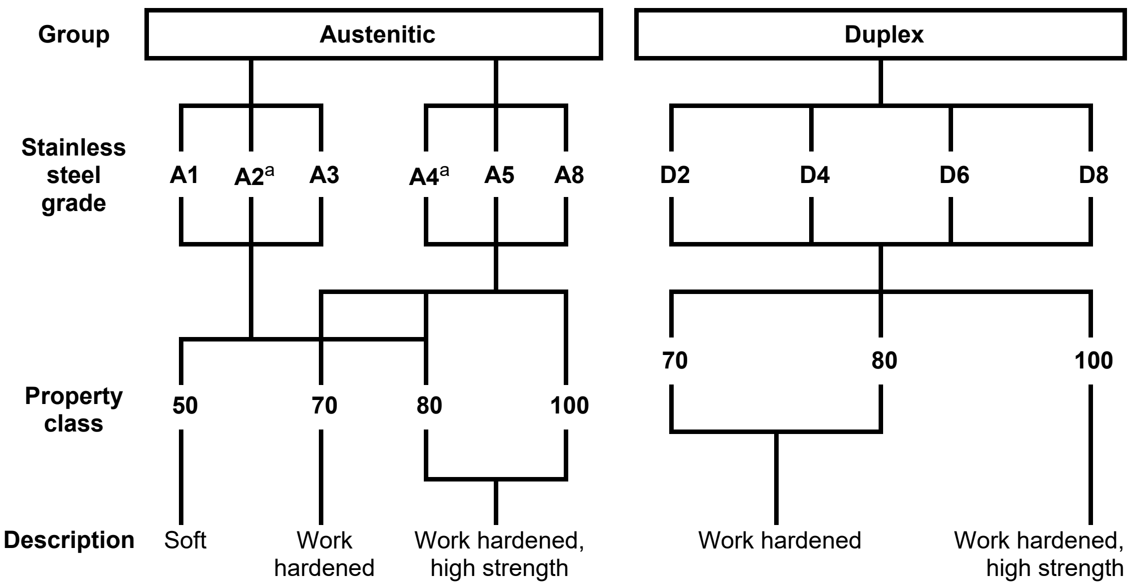


a Low carbon austenitic stainless steels with carbon content not exceeding 0,030 % may additionally be marked with an "L" after the grade. Example: **A4L–80**.

**Figure 7** Designation system for stainless steel grades and property classes for fasteners

The condition of the alloy in property class 50 bolts is soft. Property class 70 fasteners are made from cold drawn bar. Property class 80 fasteners are made from severely hard cold drawn bar. The cold working of the bar may have a slight effect on the corrosion resistance. Property class 50 bolts having machined threads are likely to be more prone to thread galling. The corrosion resistance of a stainless steel fastener should be at least equivalent to the material being joined, i.e. grade A2 bolts (or better) can be used to join grade 1.4301 material but grade A4 bolts (or better) should be used to join grade 1.4401 material. For calculating the resistance of a bolt under tension or shear or combined tension and shear, the basic strength $f_{ub}$ should be taken as the specified minimum tensile strength $R_m$ given in Table 11 for the appropriate property class.

Hydrogen embrittlement is not encountered in austenitic stainless steels, nor with duplex steels which are produced and used in accordance with standard quality control measures. On the few occasions where this phenomenon has occurred with duplex steels, it was associated either with poor production control or unusual service exposure conditions. The risk of hydrogen embrittlement should be assessed for high strength components such as bolts with strength greater than property class 80.

**Table 11** Minimum specified mechanical properties for bolts, screws and studs from austenitic and duplex steel grades

| **Stainless steel group** | **Stainless steel grade** | **Property class** | **Tensile strength, $R_m$** MPa | **Stress at 0,2 % non-proportional elongation, $R_{pf}$** MPa | **Elongation after fracture** mm |
|---|---|---|---|---|---|
| Austenitic | A1, A2, A3, A5 | 50 | 500 | 210 | 0,6 *d* |
| | | 70 | 700 | 450 | 0,4 *d* |
| | | 80 | 800 | 600 | 0,3 *d* |
| | A4 | 50 | 500 | 210 | 0,6 *d* |
| | | 70 | 700 | 450 | 0,4 *d* |
| | | 80 | 800 | 600 | 0,3 *d* |
| | | 100 | 1000 | 800 | 0,2 *d* |
| | A8 | 70 | 700 | 450 | 0,4 *d* |
| | | 80 | 800 | 600 | 0,3 *d* |
| | | 100 | 1000 | 800 | 0,2 *d* |
| Duplex | D2, D4 D6, D8 | 70 | 700 | 450 | 0,4 *d* |
| | | 80 | 800 | 600 | 0,3 *d* |
| | | 100 | 1000 | 800 | 0,2 *d* |

Austenitic bolts acc. to EN ISO 3506-1, property class 70 are the most widely available ones. Reference should be made to EN ISO 3506-1 for certain size and length restrictions. It is possible to have "specials" made to order and indeed, this sometimes produces an economical solution.

Bolts can be produced by a number of techniques, e.g. machining, cold rolling and forging. Rolled threads are stronger than machined threads because of the strain hardening which occurs during rolling. The compressive stresses at the surface of rolled threads improves the resistance to fatigue corrosion and, in some cases, stress corrosion cracking (SCC). Rolled threads also have greater resistance to thread galling. Thread rolling is the most common method of producing bolts and screws, especially for large volume production of common sizes. For larger bolts (say from M36 upwards), and especially for the stronger duplex bolts, threads are more likely to be cut.

## 2.4 Main differences in mechanical behaviour of carbon steel and stainless steel

The stress-strain curve of stainless steel is fundamentally different from that of structural carbon steel, presented as a comparative overview in Figure 8. While structural carbon steel shows a linear-elastic behaviour with a sharply defined yield strength, followed by plastic deformation before strain hardening, stainless steel exhibits a non-linear stress-strain curve without a well-marked elastic limit. In general, the curve progression is more rounded. Consequently, the non-linear behaviour of stainless steel is already valid for low levels of load, meaning plastic deformations occur at lower load levels compared to carbon steel. Because of the lack of a sharply-defined yield strength, the Eurocode standard EN 1993-1-4 [22] defines $R_{p,0.2}$ as the limit at 0.2% of the plastic strain. Additionally, stainless steels have a high energy absorption capacity paired with outstanding ductility. [23]

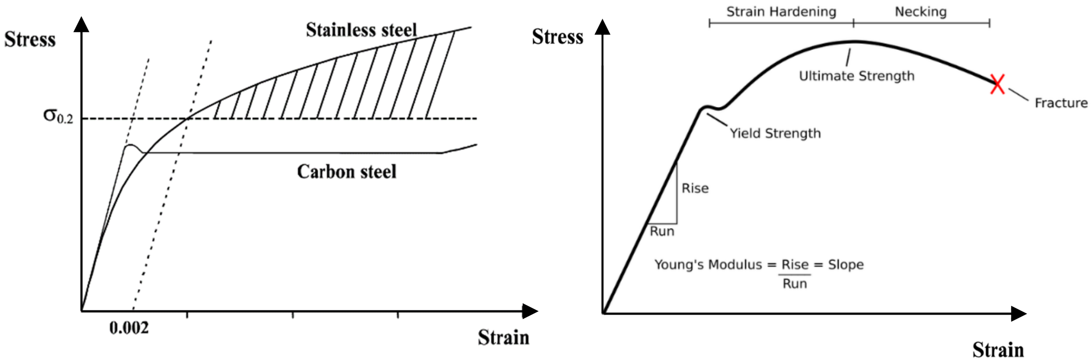


**Figure 8** Comparison of stress-strain curves for carbon steel and stainless steel (left) following [24]and characteristic values of stress-strain curves (right)

The ultimate strength of austenitic and ferritic-austenitic stainless steel is increased by strain hardening, realised, for example, through cold forming and additional rolling procedures. Martensitic and precipitation hardening stainless steel are hardenable by heat treatment. Ferritic and austenitic stainless steels, as well as duplex steels, are hardened by cold working. The increase in strength is linked to a decrease in ductility and toughness, schematically shown in Figure 9. Because of the relatively high basic ductility of stainless steel, the practical consequences for this are manageable in most cases.

It is important to note that strain hardened stainless steel tends to show asymmetric behaviour when tensile and compression loaded. Additionally, anisotropic behaviour can be observed, giving rise to different stress-strain characteristics depending on the rolling direction. Figure 9 visualizes asymmetric and anisotropic behaviour of stainless steel in longitudinal and transverse directions. As a result, using the conventional elastic-perfectly-plastic material model, known from structural carbon steel, does not consider the specific mechanical behaviour of stainless steel.

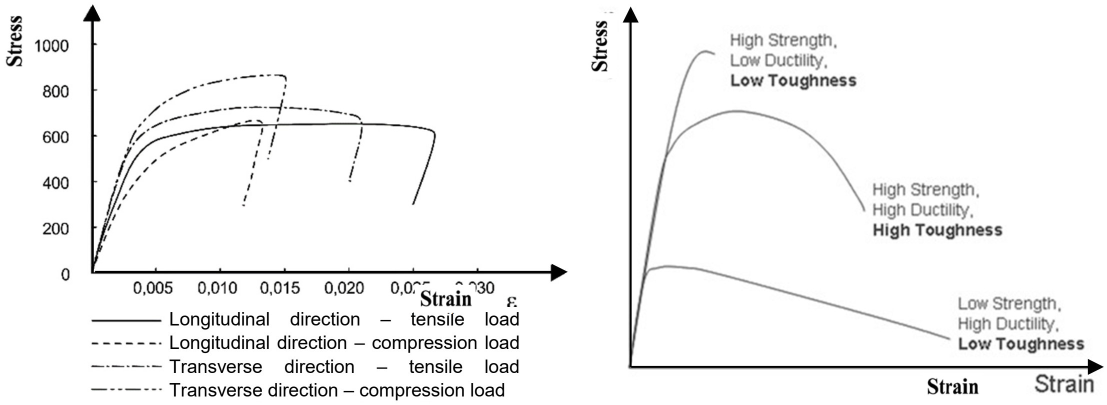


**Figure 9** Asymmetry and anisotropy of stainless steel (left) [23] and schematic overview of stress-strain behaviour depending on strength, ductility, and toughness (right) [© Ajax Bolt and Nut Co.]

## 2.5 Tightening methods and calibrated lubrication / k-classes

Tightening methods are required to achieve the specified preload in high-strength structural bolting assemblies with sufficient reliability. The accuracy of the achieved preload (respective to clamping load) depends on the following factors and demonstrates the importance of nearly constant conditions:

- friction conditions and lubrication,
- geometrical conditions of the bolted connection, like tolerances of the threads and the flexibility of the bolting assembly and clamped parts,
- tightening method.

Because there is still a degree of uncertainty regarding the preload achieved, the tightening factor $\alpha_A = F_{max}/F_{min}$ is used to describe the scatterings depending on the tightening method. Practically, the tightening factor $\alpha_A$ helps to avoid mechanical overload of the tightened bolting assemblies by increasing the designed and selected bolt area as a multiplication factor. A high tightening factor indicates a tightening method with low quality and high spreading[19].

Although a wide-range of tightening methods exist, like torsion free tightening for specific applications, EN 1090-2 [25] focuses on tightening methods which include the rotation of the nut or bolt head (in exceptional cases with reference to Annex H, or additional testing done acc. EN to 14399-2), the combined method and torque method. Other tightening methods (e.g. torsion- free axial preloading with hydraulic pressure) can be applied, too, but must be calibrated in accordance to recommendations from the manufacturer. If a bolt assembly is tightened up to the minimum preload $F_{p,C}$ and later untightened, it must be removed and the whole assembly must be discarded.

The applicability of tightening methods is connected to the quality of lubricated bolting assemblies in their delivered condition. For this reason, the k-value, as a measure for predominant friction conditions, is defined according to EN 14399-2, as well as k-classes K0, K1, and K2 defined acc. to EN 14399-1:

$$k_i = \frac{M_i}{F_{p,C} \cdot d} . \qquad (2\text{-}5)$$

For k-class K0, there are no special requirements for the k-value. The manufacturer only ensures that the delivered bolting assemblies are lubricated, while for k-class K1, the manufacturer must guarantee that the bolting assemblies are in a special range between 0.10–0.16, but additional statistical evaluations are not required. Finally, k-class K2 has the most demanding requirements, namely a special mean k-value $k_m$ and low coefficient of variation; a summary about classification of k-classes is presented in Table 12.

**Table 12** Classification of k-classes K0, K1, and K2 according to EN 14399-1:2015-04

| k-class | Information to be supplied | Criteria according EN 14399-3:2015 and -4 |
|---|---|---|
| K0 | No requirements for k-factor | — |
| K1 | Range of individual test value $k_i$ | $0.10 \leq k_i \leq 0.16$ |
| K2 | Mean test value $k_m$ | $0.10 \leq k_m \leq 0.23$ |
| | Coefficient of variation of k-factor $V_k$ | $V_k \leq 0.06$ |

The application of the *torque method* acc. to EN 1090-2 requires k-class K2. For the *combined method* acc. to EN 1090-2, k-class K1 or K2 are prescribed. The *combined method,* with reference to chapter 8.5.4 of EN 1090-2, consists of two steps:

- *First a torque-controlled tightening step* with a torque wrench in a suitable operating range to a tightening torque value of 0.75 $M_{r,i}$. This first tightening must be completed for all bolts in the connection before starting the second step. The torque reference values are calculated as:
  - $M_{r,2} = k_m \cdot d \cdot F_{p,C}$ with $k_m$ for k-class K2
  - $M_{r,1} = k_m \cdot d \cdot F_{p,C}$ with $k_m$ for k-class K1 $\wedge$ $k_m = 0.13$
- *Second an angle of rotation-controlled tightening step* where a specified part turn is applied to the turned part of the assembly. The position of the nut relative to the bolt should be marked after the first step. The additional rotation angles are dependent on the bolt diameter and total nominal thickness of parts to be connected, including all packs and washers.

A schematic overview of the first and second tightening steps is presented in Figure 10 by Schmidt and Stranghöner [14]. Starting with 75% of the reference tightening torque (depending on the k-class K1 or K2), and depending on the curve form in the bolt force-tightening torque-curve (left), a specific bolt force is reached for each bolting assembly. After additional rotation (e.g. 90° for 2d ≤ t < 6d), a new bolt force is achieved. Due to individual scattering, the achieved bolt forces may vary for each tightened bolting assembly.

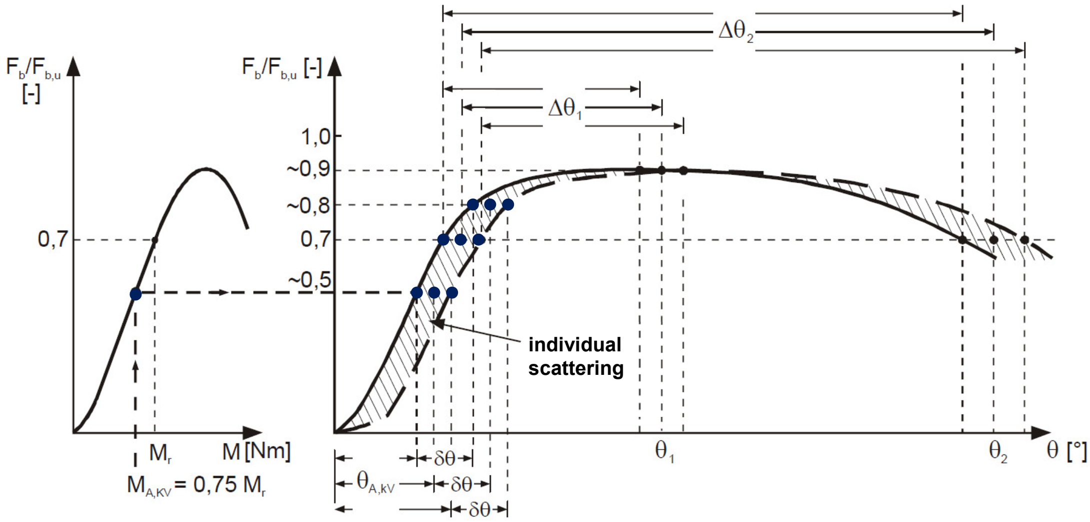


**Figure 10** Schematical overview of first and second tightening step of combined method acc. EN 1090-2:2011-10 [14] (© IML)

## 2.6 Test procedure and suitability for preloading acc. to EN 14399-2

According to EN 14399-2, "High-strength structural bolting assemblies for preloading – Part 2: Suitability for preloading", "the purpose of the tightening test is to check the behaviour of the bolting assembly to ensure that the required preload can be reliably obtained by the tightening methods specified in EN 1090-2 with sufficient margins against over tightening and against failure". Focusing on normative references, Table 13 summarizes some primary aspects of System HR and System HV bolting assemblies.

**Table 13** Systems of bolt/nut/washer assemblies according to EN 14399-1:2015-04

| | **Bolt/nut/washer assembly System HR** | | **Bolt/nut/washer assembly System HV** |
|---|---|---|---|
| **General require-ments** | EN 14399-1 | | |
| **Bolt/nut assembly** | EN 14399-3 | | EN 14399-4 |
| Marking | HR | | HV |
| Property classes | 8.8/8 | 10.9/10 | 10.9/10 |
| **Washer(s)** | EN 14399-5 or EN 14399-6 | | EN 14399-5 or EN 14399-6 |
| Marking | H | | H |
| **Suitability test for preloading** | EN 14399-2 | | EN 14399-2 |

To ensure that the required preload can be reliably obtained, the tightening procedure according to EN 14399-2 with test bolting assemblies is positioned such that:

- a washer of the assembly according to EN 14399-5 is placed under the hexagon nut, and plain chamfered washer according to EN 14399-6 may be placed under the bolt head;

- the clamp length $\Sigma t$, including shims and washer(s), is the minimum allowed in the relevant product standard;
- neither the bolt nor washer under the nut rotates during the test;
- the number of shims does not exceed four, with defined characteristics shown in Table 14 and presented in Figure 12 as examples;
- and the test apparatus is made of steel and the including stiffness of the test setup as high as practicable.

**Table 14** Characteristics of shims according to EN 14399-2

| Nominal bolt diameter | Hole diameter | Outside diameter | Thickness | Hardness for the outside shim | Parallelism |
|---|---|---|---|---|---|
| $d \leq$ M14 | $d + 1$ | Not less than the outside assembly washer diameter and sufficient to distribute load adequately to the device | $\geq 2$ | $\geq$ 45 HRC through hardened | $\leq 1$ % |
| M14 < $d \leq$ M24 | $d + 2$ | | | | |
| $d$ > M24 | $d + 3$ | | | | |

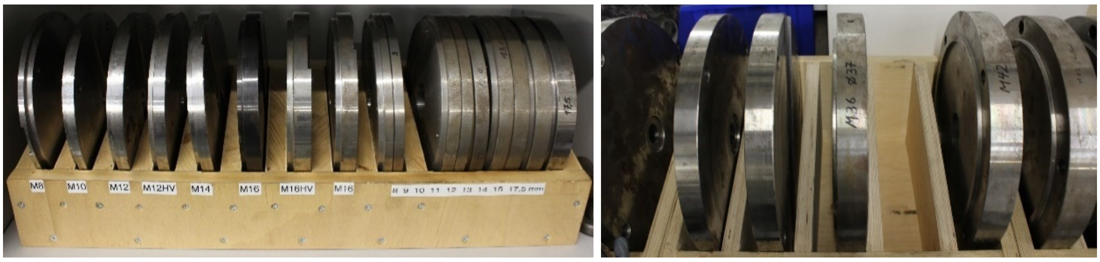

**Figure 11** Different shims with minor diameter (left) and major diameter (right) at IML laboratory of University of Duisburg-Essen

The tightening is completed through rotation of the nut in a continuous manner with the speed of rotation between 1 min$^{-1}$ and 10 min$^{-1}$ and an ambient temperature between 10–35° C.

The suitability for preloading of high-strength structural bolting assemblies and the tightening test procedure are typically regulated by EN 14399-2 and valid for System HR (EN 14399-3) and System HV (EN 14399-4). The main aspects of the test procedure and criteria of evaluation are summarized below. To ensure that the required preload can be reliably obtained, the tightening procedure must be performed as follows:

- The tightening procedure with test assemblies shall be positioned such that
  - a washer of the assembly is placed under the nut, and if possible placed under the bolt head;
  - the clamp length including shims and washer(s) is the minimum allowed in the relevant product standard.
- The tightening shall be carried out by rotation of the nut in a continuous manner with speed of rotation between 1 min$^{-1}$ and 10 min$^{-1}$.
- The test shall be stopped when one of the following conditions is first satisfied:
  - the angle of nut rotation exceeds ($\Theta_{pi} + \Delta\Theta_{2i,min}$);
  - the bolt force drops to $F_{p,C}$;
  - bolt failure by fracture occurs.

- For each of the bolting assemblies, determination of the *rotation/bolt force relationship* and *torque/bolt force relationship*, and additionally the *elongation/bolt force relationship* if required.

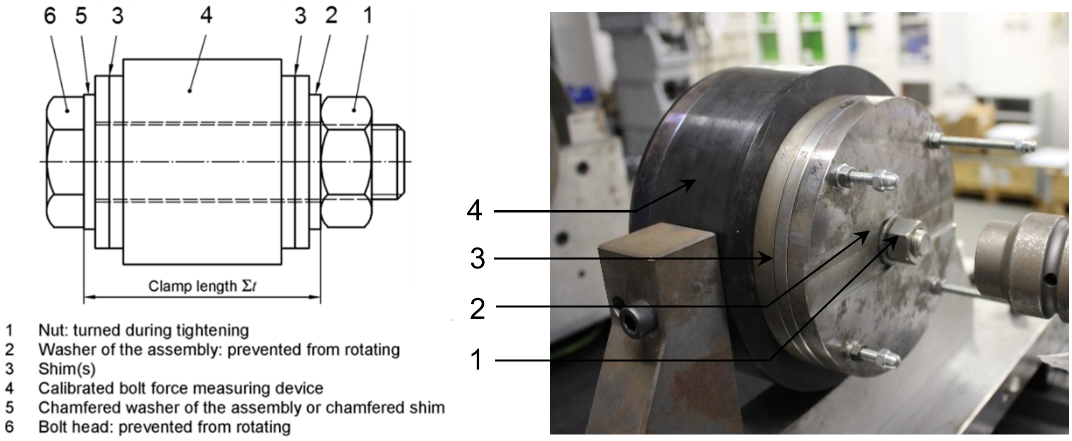


**Figure 12** Test setup for tightening tests at IML-UDE (exemplarily)

Figure 13 schematically visualizes a typical bolt force-angle of rotation curve and bolt force-tightening torque curve and defines relevant tightening and evaluation values like the maximum individual value of bolt force $F_{bi,max}$, the preloading level $F_{p,C}$, and the angle differences $\Delta\Theta_{1i}$ and $\Delta\Theta_{2i}$. Furthermore, the determination of the k-value is graphically displayed.

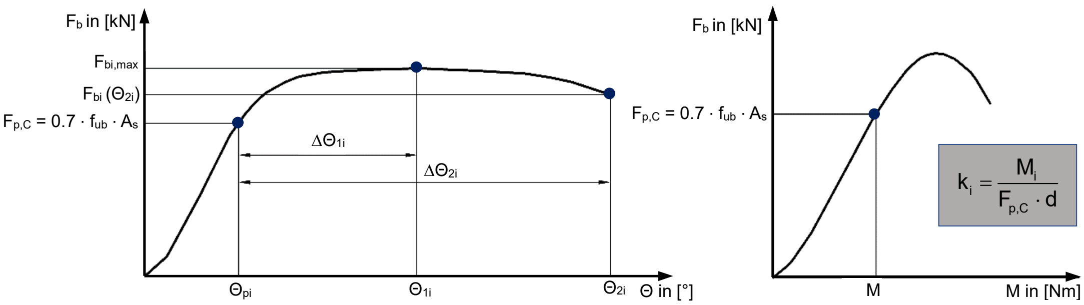


**Figure 13** Tightening curves and criteria of evaluation acc. EN 14399-2

The criteria of evaluation of high-strength structural bolting assemblies for preloading according to EN 14399-3 (System HR bolting assemblies made of carbon steel) are defined in subchapter 2.7 and 2.8.

## 2.7 Measured and determined parameters acc. to EN ISO 16047

Tightening of a bolted connection by a steadily applied tightening torque generates a clamp force/preload F in the bolted connection. By the influence of these two measured parameters, further tightening characteristics can be measured or determined, which characterize the tightening properties of the bolted connection. According to EN ISO 16047 the following tightening parameters are defined

- torque coefficient K (K-factor),
- coefficient of total friction $\mu_{tot}$,
- coefficient of friction between threads $\mu_{th}$,
- coefficient of friction between bearing surfaces $\mu_b$,

- yield clamp force $F_y$,
- yield tightening torque $T_y$,
- ultimate clamp force $F_u$, and
- ultimate tightening torque $T_u$.

For testing bolts/nuts under standard conditions, specified test components shall be used, either a test-bearing plate or a test washer of high (through-hardened, type HH) or low (type HL) hardness as well as suitable test nuts or test bolts. All traces of grease, oil or other contaminations shall be removed before testing.

The connecting element to be tested is either a nut or a bolt and is assembled with the corresponding test components, a test nut or test bolt to the entire bolted connection. The connecting element to be tested is supported by a test-bearing plate or a test washer. The specimen shall be assembled in the fixture (either the head of the test bolt or the test nut shall be fixed), and nut or bolt head, whichever is free to rotate, shall be driven by applying the tightening torque.

The tightening characteristics, which are not directly available as measured value, are determined by the following equations (2-6 to 2-10). The relationship between tightening characteristics and the parameters to be measured are shown in Table 15.

**Table 15** Parameters to be measured to obtain respective tightening characteristics

| **Tightening characteristics which may be determined** | | **Parameters to be measured** | | | |
|---|---|---|---|---|---|
| | | Clamp force F | Tightening torque T | Thread torque $T_{th}$ | Rotation angle $\Theta$ |
| Bearing surface friction torque | $T_b$ | – | • | • | – |
| K-factor | K | • | • | – | – |
| Coefficient of total friction | $\mu_{tot}$ | • | • | – | – |
| Coefficient of friction between threads | $\mu_{th}$ | • | – | • | – |
| Coefficient of friction between bearing surfaces | $\mu_b$ | • | • | • | – |

### Determination of bearing surface friction torque $T_b$

$$T_b = T - T_{th} \quad \text{[Nm]} \qquad (2\text{-}6)$$

with T: tightening torque,
defined as torque acting on a nut or a bolt during tightening,
$T_{th}$: thread torque,
defined as torque acting on paired threads on the bolt shank,
$T_b$: bearing surface friction torque,
defined as torque acting on the bearing surfaces on the clamped parts during tightening.

### Determination of torque coefficient K (K-factor)

$$K = \frac{T}{F \cdot d} \quad \text{[Nm]} \qquad (2\text{-}7)$$

with T: tightening torque,
F: clamp force/preload,
d: nominal thread diameter.

Unless otherwise specified, the determination of the K-factor is carried out under standard conditions and shall include the point with the clamp force at 75% of the proof load (0.75 $F_p$) of the test part, or the part to be tested, whichever is lower.

**Determination of coefficients of total friction $\mu_{tot}$**

$$\mu_{tot} = \frac{\frac{T}{F} - \frac{P}{2\pi}}{0{,}578 \cdot d_2 + 0{,}5 \cdot D_b} \qquad [-] \qquad (2\text{-}8)$$

with $D_b = \frac{D_o + d_h}{2}$ [mm]

T: tightening torque,
F: clamp force/preload,
P: pitch of the tread,
$d_2$: basic pitch diameter of the thread,
$D_b$: diameter of bearing surface under nut or bolt head for friction (theoretical or measured),
$D_o$: outer diameter of bearing surface, $d_{w,min}$ or $d_{k,min}$ (see product standards)
$d_h$: clearance hole diameter of washer or bearing part as nominal value

Unless otherwise specified, the determination of the total friction $\mu_{tot}$ is carried out under standard conditions and should include the point with the clamp force at 75% of the proof load (0.75 $F_p$) of the test part, or the part to be tested, whichever is lower.

**Determination of coefficient of friction between threads $\mu_{th}$**

$$\mu_{th} = \frac{\frac{T_{th}}{F} - \frac{P}{2\pi}}{0{,}578 \cdot d_2} \qquad [-] \qquad (2\text{-}9)$$

with $T_{th}$: thread torque,
F: clamp force/preload,
P: pitch of the tread,
$d_2$: basic pitch diameter of the thread,
T: tightening torque,
$T_b$: bearing surface friction torque.

Unless otherwise specified, the determination of the thread friction $\mu_{th}$ is carried out under standard conditions and should include the point with the clamp force at 75% of the proof load (0.75 $F_p$) of the test part, or the part to be tested, whichever is lower.

**Determination of coefficient of friction between bearing surfaces $\mu_b$**

$$\mu_b = \frac{T_b}{0{,}5 \cdot D_b \cdot F} \qquad [-] \qquad (2\text{-}10)$$

with $T_b$: bearing surface friction torque,
$D_b$: diameter of bearing surface under nut or bolt head for friction (theoretical or measured),
F: clamp force/preload,

T: tightening torque,
$T_{th}$: thread torque.

Unless otherwise specified, the determination of thread friction $\mu_{th}$ is carried out under standard conditions and should include the point with the clamp force at 75% of the proof load (0.75 $F_p$) of the test part, or the part to be tested, whichever is lower.

**Determination of further tightening characteristics**

The equations and methods for determining further tightening characteristics like the yield clamp force $F_y$, yield tightening torque $T_y$, ultimate clamp force $F_u$ and ultimate tightening torque $T_u$ according to EN ISO 16047 are not given in this summary.

In addition to EN ISO 16047, the statistical evaluation of the results of the tightening test is based on the following equations (2-11 to 2-14):

**Mean value**

$$\bar{x} = \frac{\sum_{i=1}^{n} x_i}{n} \qquad (2\text{-}11)$$

with $\bar{x}$: mean value,
$n$: number of tested specimens,
$x_i$: individual measured value.

**Standard deviation**

$$s = \sqrt{\frac{1}{n-1} \cdot \sum_{i=1}^{n} \left(x_i - \bar{x}\right)^2} \qquad (2\text{-}12)$$

with $s$: standard deviation,
$\bar{x}$: mean value,
$n$: number of tested specimens,
$x_i$: individual measured value.

**Range**

$$R = max - min \qquad (2\text{-}13)$$

with $s$: range,
$max$: highest measured value,
$min$: lowest measured value.

**Coefficient of variation**

$$\nu = \frac{s}{\bar{x}} \qquad (2\text{-}14)$$

with $\nu$: coefficient of variation,
$s$: standard deviation,
$\bar{x}$: mean value.

## 2.8 Evaluation of basic preloading behavior and ductility regarding EN 14399-2

The requirements regarding sufficient ductility of carbon steel HV and HR bolting assemblies are specified in EN 14399-4 and EN 14399-3. HR bolting assemblies are characterised by a longer thread and a higher nut than HV bolting assemblies. Herewith, HR bolts represent more likely bolting assemblies using EN ISO 4017 bolts and EN ISO 4032 [26] nuts. For this reason and in absence of existing adequate criteria for preloaded stainless steel bolting assemblies, the following criteria (2-15 to 2-18) acc. to EN 14399-2 and EN 14399-3, were chosen as a basis for qualification and evaluation of the ductility of preloaded stainless steel bolting assemblies. From these four criteria, only requirements (2-16) and (2-18) have to be fulfilled on $F_{p,C}$-level in the suitability test for preloading acc. to EN 14399-2/3.

- $F_{p,C} = 0.7 \cdot f_{ub} \cdot A_s$ (2-15)

  $F_{p,C}$ specified preloading level (see also EN 1090-2)
  $f_{ub}$ nominal tensile strength ($R_{m,nom}$) of the bolt
  $A_s$ nominal stress area of the bolt (see EN ISO 898-1)

- $F_{bi,max} \geq 0.9 \cdot f_{ub} \cdot A_s$ (2-16)

  $F_{bi,max}$ individual value of the maximum bolt force reached during the test
  $f_{ub}$ nominal tensile strength ($R_{m,nom}$) of the bolt
  $A_s$ nominal stress area of the bolt

- $\Delta\Theta_{1i} \geq \Delta\Theta_{1,min} = 90° / 120° / 150°$ (depending on the clamp length) (2-17)

  $\Delta\Theta_{1i}$ individual angle difference of the nut from the first time the preload $F_{p,C}$ is exceeded to the individual value of the maximum bolt force $F_{bi,max}$

- $\Delta\Theta_{2i} \geq \Delta\Theta_{2,min} = 210° / 240° / 270°$ (depending on the clamp length) (2-18)

  $\Delta\Theta_{2i}$ individual angle difference of the nut from the first time the preload $F_{p,C}$ is exceeded to the angle when bolt force drops below $F_{p,C}$ again

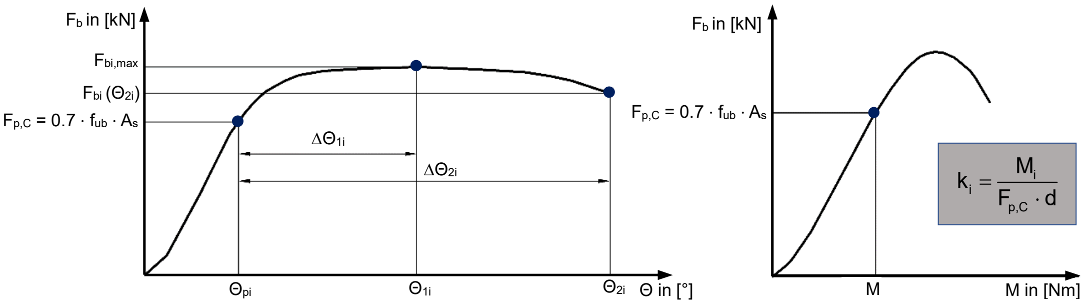


**Figure 14** Schematic bolt force-angle of rotation curve (left) and bolt force-tightening torque curve (right) according to EN 14399-2

## 2.9 Viscoplastic deformation behaviour of stainless steel bolting assemblies

### 2.9.1 General

Preloaded bolted connections made of stainless steel are not commonly used in stainless steel structures as their application is not allowed by the execution standard EN 1090-2 and the design standard EN 1993-1-4 for stainless steel structures unless otherwise specified, respectively unless their acceptability for a particular application has been demonstrated from test results. This restriction is mainly caused by three facts: firstly, it is feared that due to the viscoplastic deformation behaviour of stainless steel, severe preload losses have to be expected, secondly, neither stainless steel bolting assemblies for preloading nor tightening procedures exist on which could have been relied and thirdly, galling and seizure of stainless steel bolting assemblies lead to problems on site. These three questions, beside others, were treated in the frame of the European RFCS-research project "Execution and reliability of slip resistant connections for steel structures using CS and SS" SIROCO.

### 2.9.2 Creep and relaxation behaviour of stainless steel material

Relaxation of preloaded stainless steel bolted connections is mainly caused by setting effects due to embedment/plastic deformation of the surfaces of the clamped package and the viscoplastic deformation behaviour of the various stainless steel components themselves (clamped plates and bolts). The latter one can be divided into

- viscoplastic deformation under constant load in the plates (i.e. creep deformation) and
- viscoplastic deformation under constant strain in the bolts (i.e. stress relaxation).

The creep and stress relaxation behaviour of stainless steel plates and the stress relaxation behaviour of austenitic stainless steel bars has been investigated at Outokumpu Avesta R&D Center and Outokumpu Tornio R&D Center and has already been presented in detail in [27], [28] and [29]. To complete this comprehensive investigation, this task deals with determination of the amount of preload losses resulting from the combined creep and stress relaxation in a preloaded stainless steel bolted connection. The focus of this contribution is on the finally resulting preload losses of preloaded bolted connections of various stainless and carbon steel grades.

# 3 Experimental investigations – Tightening tests

## 3.1 Test equipment and test setup

Bolt force-tightening torque tests were carried out with the tightening torque testing machine (maximum torque: 15000 Nm and maximum bolt force: 1800 kN) at the Institute of Metal and Lightweight Structures of the University Duisburg-Essen, see also Figure 15. The torque and rotation are automatically generated by an electric gear motor. The tightening speed is set manually via an adjusting gear before starting the tightening test and was constant for all tests 5.0 rpm. The tightening torque testing machine is equipped with sensors for recording measurements from the company Schatz GmbH, Remscheid, Germany.

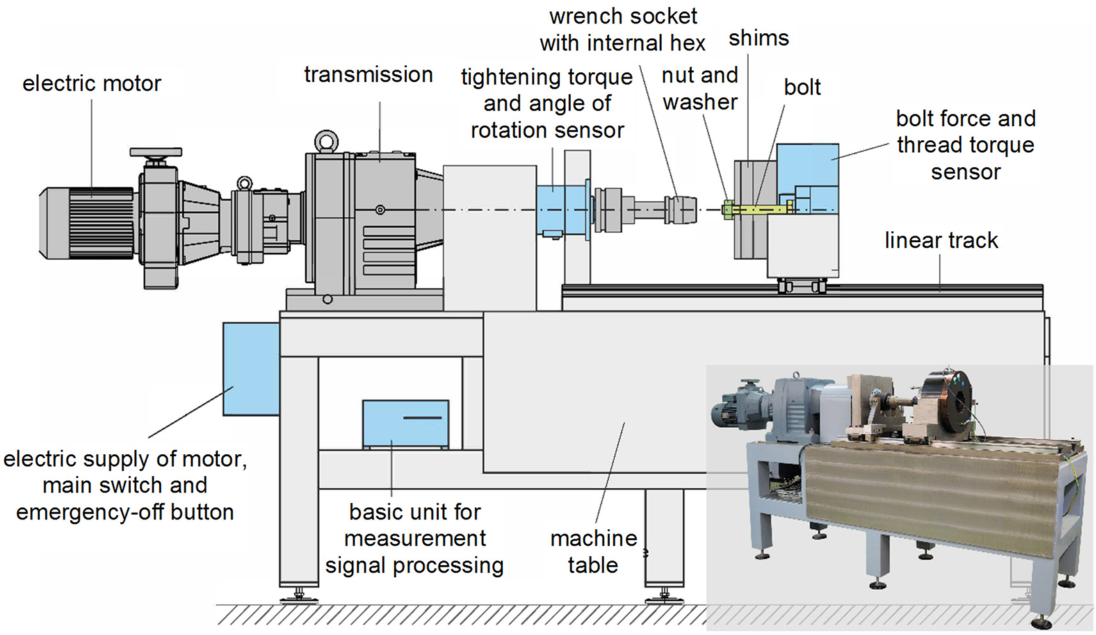


**Figure 15** Tightening torque testing machine of Institute for Metal and Lightweight Structures of University of Duisburg-Essen

## 3.2 Test programme

Investigating the basic preloading behaviour of stainless steel bolting assemblies implies in the first step to carry out tightening tests of stainless steel bolting assemblies to achieve information regarding the interaction behaviour between the applied torque and the achieved preload depending on the lubrication, the friction between the threads of the bolt and the nuts as well as the friction under the head of the bolt. For this reason, tightening tests according acc. to EN ISO 16047 resp. EN 14399-2 were performed with bolting assemblies M12, M16, M20 and M24 made of austenitic as well as duplex, super duplex and lean duplex steels with EN ISO 4014/4017 bolts, EN ISO 4032 nuts and EN ISO 7089 [30] washers in property classes 8.8/80 and 10.9/100. The tightening tests were carried out on the basis of EN 14399-2 and EN ISO 16047. In addition, various lubricants were tested to investigate the influence of lubrication regarding ductility and galling and to identify a suitable lubrication for preloaded bolting assemblies made of stainless steel, see Table 16.

Herein, the factory provided standard lubricant gleitmo® 1952V from Fuchs Lubritech GmbH was tested along with alternative lubricants as DOW Corning Molykote® P-74 Paste, DOW Corning Molykote® 1000 Paste, DOW Corning Molykote® 1000 Spray and DOW Corning Molykote® D-321 spray. All lubricants are suitable for stainless steels according to the information provided by the producer. Additionally, tightening tests were performed with M20 ISO 4017 bolts with the ceramic-based lubricant Interflon® HT1200 spray and paste for austenitic (property classes 8.8/80 and 10.9/100) and lean duplex (property class 10.9/100) bolting assemblies.

The tests were carried out in three steps. The factory provided standard lubrication was used in the first step, and the alternative lubricants from DOW Corning were used in the second step to identify suitable, alternative lubricants and to study the positive effects as extending the plastic plateau and avoiding galling. The austenitic bolts BUMAX 88 and 109 with property classes 8.8 and 10.9, and the lean duplex, duplex and super duplex bolts in property class 10.9 were provided by the Swedish bolt manufacturer BUMAX AB. Partially, they were specifically produced for these tests. The test matrix for all tightening tests is given in Table 17, and the main nominal mechanical properties are presented in Table 18.

In total, 37 series and 295 bolting assemblies were tested at UDE-IML which are significantly more than the test specimens prescribed in Task 5.3/5.4 technical annex (for each Task: 80 bolting assemblies = 2 bolt dimensions x 4 steel grades x 1 lubrication x 10 bolts per series). All tightening tests were carried out according to EN 14399-2 and EN ISO 16047. For reasons of comparability and in absence of regulations for stainless stseel bolting assemblies, the evaluation of the tested stainless steel bolting assemblies refers to EN 14399-3 for carbon steel bolts.

**Table 16** Types of alternative lubricants for bolting assemblies made of stainless steel

| | | | |
|---|---|---|---|
|  |  |  |  |
| **DOW Corning Molykote P-74 Paste** | **DOW Corning Molykote 1000 Spray / Paste** | **DOW Corning Molykote D-321R Spray** | **Interflon HT1200 Spray / Paste** |
| **Composition** | **Composition** | **Composition** | **Composition** |
| Solid lubricants | Solid lubricants | Solid lubricants | Mixture of mineral oil |
| Synthetic oil | Mineral oil | Solvents | Solids anorganic thickener |
| Thickener | Thickener | Binder | Additives |
| Adhesion promoter | Powdered metal | Air-curing dry film | MicPol® |
| **Friction coefficients** | **Friction coefficients** | **Friction coefficients** | **Friction coefficients** |
| $\mu_{th}$ 0.14 | $\mu_{th}$ 0.13 | $\mu_{th}$ 0.13 | μ = 0.12 (steel-steel) |
| $\mu_{b}$ 0.08 | $\mu_{b}$ 0.08 | $\mu_{b}$ 0.075 | μ = 0.08 (titanium-steel) |
| **Recommended applications** | **Recommended applications** | **Recommended applications** | **Recommended applications** |
| Wide range of applications/bolted joints | Bolted joints at elevated temperatures | Highly stressed sliding guides with low speeds | High temperature/ pressure applications |

**Table 17** Test matrix for the tightening tests of bolting assemblies made of austenitic, duplex, lean duplex and super duplex stainless steel

| Steel grade | Grade | Type of stainless steel | Lubrication | Bolt dimension | | | |
|---|---|---|---|---|---|---|---|
| | | | | M12 | M16 | M20 | M24 |
| **STEP 1: Tightening tests with standard lubrication** | | | | | | | |
| **Bumax 88** | bolts: EN 1.4432 nuts: EN 1.4436 | Austenitic | gleitmo 1952V[1)] | 4014[4)] | 4017[5)] | 4017 | 4017 |
| **Bumax 109** | | Austenitic | gleitmo 1952V | 4014 | 4017 | 4014 | - |
| **Bumax LDX** | EN 1.4162 | Lean Duplex | gleitmo 1952V | - | 4017 | 4017 | - |
| **Bumax DX** | EN 1.4462 | Duplex | gleitmo 1952V | - | 4017 | 4017 | - |
| **Bumax SDX** | EN 1.4410 | Super Duplex | gleitmo 1952V | 4017 | - | - | - |
| **STEP 2: Tightening tests with alternative lubrication** | | | | | | | |
| **Bumax 88** | bolts: EN 1.4432 nuts: EN 1.4436 | Austenitic | Molykote 1000 Spray[2)] | - | 4017 | 4017 | - |
| | | | Molykote 1000 Paste[2)] | - | - | 4017 | - |
| | | | Molykote P-74 Paste[2)] | - | - | 4017 | - |
| | | | Molykote D-321R Spray[2)] | - | - | 4017 | - |
| **Bumax 109** | | Austenitic | Molykote 1000 Spray | - | 4017 | 4014 | - |
| | | | Molykote P-74 Paste | - | - | 4014 | - |
| | | | Molykote D-321R Spray | - | 4017 | 4014 | - |
| **Bumax LDX** | EN 1.4162 | Lean Duplex | Molykote 1000 Spray | - | 4017 | 4017 | - |
| **Bumax DX** | EN 1.4462 | Duplex | Molykote 1000 Spray | - | 4017 | 4017 | - |
| **Bumax SDX** | EN 1.4410 | Super Duplex | Molykote 1000 Spray | 4017 | - | - | - |
| **STEP 3: Tightening tests with ceramic based lubrication** | | | | | | | |
| **Bumax 88** | bolts: EN 1.4432 nuts: EN 1.4436 | Austenitic | HT1200 Spray[3)] | - | - | 4017 | - |
| | | | HT1200 Paste[3)] | - | - | 4017 | - |
| **Bumax 109** | | Austenitic | HT1200 Spray | - | - | 4017 | - |
| | | | HT1200 Paste | - | - | 4017 | - |
| **Bumax LDX** | EN 1.4162 | Lean Duplex | HT1200 Spray | - | - | 4017 | - |
| | | | HT1200 Paste | - | - | 4017 | - |

[1)] gleitmo 1952V lubricant from Fuchs Lubritech GmbH
[2)] Molykote products from DOW Corning
[3)] HT1200 spray and paste from Interflon
[4)] 4014: EN ISO 4014 bolt, EN ISO 4032 nut and EN ISO 7089 washer
[5)] 4017: EN ISO 4017 bolt, EN ISO 4032 nut and EN ISO 7089 washer

**Table 18** Nominal mechanical properties of stainless steel bolting assemblies and bolt/washer/nut combinations [© BUMAX]

| Bolt Steel grade | Bolt type of stainless steel | Tensile strength $R_{m,min}$ | Yield strength $R_{p0.2,min}$ | Elong., min | Nut and washer steel grade | Nut and washer type of stainless steel | Nuts – Stress under proof load, min | Washers – Hardness, min |
|---|---|---|---|---|---|---|---|---|
| | | N/mm² | N/mm² | mm | | | N/mm² | HV |
| **Bumax 88** | Austenitic | 800 | 640 | 0.3 d | Bumax 88 | Austenitic | 800 | 200 |
| **Bumax 109** | Austenitic | 1000 | 900 | 0.2 d | Bumax 109 | Austenitic | 1000 | 300 |
| **Bumax LDX** | Lean Duplex | 1000 | 900 | 0.3 d | Bumax 109 | Austenitic | 1000 | 300 |
| **Bumax DX** | Duplex | 1000 | 900 | 0.3 d | Bumax 109 | Austenitic | 1000 | 300 |
| **Bumax SDX** | Super Duplex | 1000 | 900 | 0.3 d | Bumax 109 | Austenitic | 1000 | 300 |

The nomenclature of the specimens for the tightening tests is as follows:

**BU_Mxx_yyy-zz**

| | | | |
|---|---|---|---|
| **BU:** | BUMAX stainless steel bolt | **yyy:** | Property class 8.8/80 or 10.9/100 |
| **Mxx:** | bolt diameter | **zz:** | sequential number of bolt |

## 3.3 Tightening test results and evaluation – STEP 1: gleitmo® 1952V standard lubrication

In the following, every tested series – sorted by bolt dimension, strength class and steel grade – is described and evaluated in detail to give an overview about the performed tightening tests and basic preloading behaviour of bolting assemblies made of stainless steel (austenitic, lean duplex, duplex and super duplex) with Fuchs Lubritech GmbH gleitmo® 1952V standard lubrication (STEP 1).

### 3.3.1 Bolt dimension M12

For bolt dimension M12, tightening tests of stainless steel austenitic bolts M12x80 in property classes 8.8 and 10.9 were performed as well as super duplex bolting assemblies in strength class 10.9 with the same nominal length. Austenitic bolts were produced according to EN ISO 4014 whereas super duplex bolts were produced according to EN ISO 4017. The clamp length $\sum t$ was set to 64.0 mm (clamp length/bolt diameter ratio of 5.3) in reference to the corresponding tables of System HR – EN 14399-3 respectively System HV – EN 14399-4 standards. The bolting assemblies were tightened nut sided with a constant speed of rotation of 5.0 $min^{-1}$. The tightening tests of Bumax 88 – M12x80 and Bumax 109 – M12x80 were stopped when the angle of nut rotation exceeded $\Delta\Theta_{2i,min} \geq 240°$ or when the measured bolt force dropped to $F_{p,c} = 0.7 \cdot f_{ub} \cdot A_s$ (with $f_{ub}$: tensile strength of the bolt and $A_s$: tensile stress area of the bolt). In contrast, tightening tests of Bumax SDX – M12x80 in property class 10.9 were only stopped when the bolt force dropped to $F_{p,c}$ to allow a more detailed investigation of the basic preloading behaviour.

The criteria of evaluation acc. to EN 14399-3 for bolting assemblies in property class 8.8 (equal to Bumax 88) are defined as follows:

- $F_{p,C}^* = 0.7 \cdot f_{yb} \cdot A_s = 0.7 \cdot 640\ N/mm^2 \cdot 84.3\ mm^2 = 37.8\ kN$ (acc. to DIN EN 1993-1-8/NA)
- $F_{p,C} = 0.7 \cdot f_{ub} \cdot A_s = 0.7 \cdot 800\ N/mm^2 \cdot 84.3\ mm^2 = 47.2\ kN$
- $F_{bi,max} \geq 0.9 \cdot f_{ub} \cdot A_s = 0.9 \cdot 800\ N/mm^2 \cdot 84.3\ mm^2 = 60.7\ kN$
- $\Delta\Theta_{1i,min} \geq 120°$ with $\Sigma t = 64.0$ mm: $2d \leq \Sigma t < 6d$
- $\Delta\Theta_{2i,min} \geq 240°$ with $\Sigma t = 64.0$ mm: $2d \leq \Sigma t < 6d$

In addition, the criteria of evaluation for bolting assemblies in property class 10.9 (meaning Bumax 109 and Bumax SDX series) are defined as follows:

- $F_{p,C}^* = 0.7 \cdot f_{yb} \cdot A_s = 0.7 \cdot 900\ N/mm^2 \cdot 84.3\ mm^2 = 53.1\ kN$
- $F_{p,C} = 0.7 \cdot f_{ub} \cdot A_s = 0.7 \cdot 1000\ N/mm^2 \cdot 84.3\ mm^2 = 59.0\ kN$
- $F_{bi,max} \geq 0.9 \cdot f_{ub} \cdot A_s = 0.9 \cdot 1000\ N/mm^2 \cdot 84.3\ mm^2 = 75.9\ kN$
- $\Delta\Theta_{1i,min} \geq 120°$ with $\Sigma t = 64.0$ mm: $2d \leq \Sigma t < 6d$
- $\Delta\Theta_{2i,min} \geq 240°$ with $\Sigma t = 64.0$ mm: $2d \leq \Sigma t < 6d$

All tightening test were carried out in accordance with EN 14399-2 and EN ISO 16047 using the test setup shown in Table 19.

**Table 19** Test setup Bumax 88/109/SDX – M12x80 series.

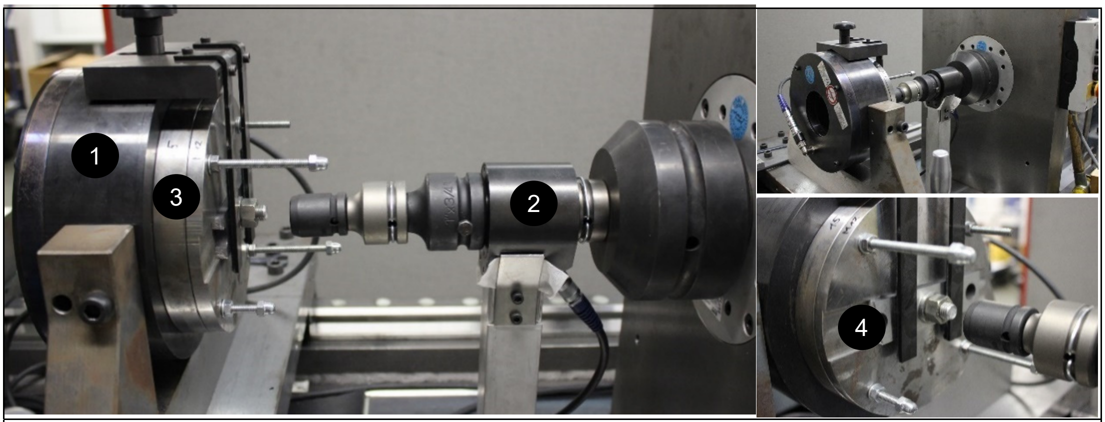


| | | |
|---|---|---|
| **1** | Sensor force – thread friction torque: SNo. 1016254 – 200 kN / 350 Nm | |
| **2** | Sensor total tightening torque – angle of rotation: SNo. 1016257 – 1,000 Nm | |
| **3** | Shims: DP 15mm + M12HV | Lubrication: gleitmo 1952V |
| **4** | Support bar: Yes | Adapter: Yes |
| | Speed of rotation: 2.0 $min^{-1}$ | Rotated component: Hexagon nut |
| | Number of bolting assemblies tested: 10 | Washers: placed under nut |
| | Clamp length $\sum t$ = 64.0 mm according to EN 14399-3:2015-03 | |
| | Clamp length/bolt diameter ratio: 5.3 | Stop criteria: dropped to $F_{p,C}$ or $\Delta\Theta_{2i,min}$ = 240° |

### *3.3.1.1 Bumax 88 – M12x80 – 8.8 – EN ISO 4014 – gleitmo 1952V*

The Bumax 88 – M12x80 austenitic stainless steel bolting assemblies, abbreviated below as BU_M12_88, are arranged of following components and descripted in detail including nominal mechanical properties based on Bumax datasheet from February 2014:

- *Bolts:* BUFAB Group Bumax 88 - M12x80 A4 according to EN ISO 4014; stainless steel EN 1.4432, 1.4436, 1.4435; manufact.: 2014-08-05; PRE = 27

  tensile strength $R_{m,min}$ (= $f_{ub}$): nominal 800 N/mm²
  yield strength $R_{p0.2,min}$ (= $f_{yb}$): nominal 640 N/mm²
  elongation, min: nominal 0.3d

- *Nuts:* BUFAB Group Bumax 88 - M12 M6M A4 according to EN ISO 4032; stainless steel EN 1.4432, 1.4436, 1.4435; PRE 27

  stress under proof load, min: nominal 800 N/mm²

- *Washers:* BUFAB Group Bumax RB A4-HV200 according to EN ISO 7089; stainless steel EN 1.4432, 1.4436, 1.4435; with dimensions d = 13.0 mm, D = 24.0 mm, t = 2.5 mm; PRE 27

  hardness, min: nominal 200 HV

The test results of Bumax 88 – M12x80 bolting assemblies are summarized in Table 20 and Table 21 including statistical evaluation. All tests were performed without any partial or total bolt fracture. Referring to the criteria of EN 14399-3, all bolting assemblies reached specified preloading levels $F_{p,C}$* and $F_{p,C}$, and 9 of 10 bolts achieved $F_{bi,max} \geq 0.9 \cdot f_{ub} \cdot A_s$. The k-values at specified preload level $F_{p,C}$ lie between k = 0.11 and k = 0.19 with a coefficient of variation in the amount of 18,61 % (compared to k = 0.11 – 0.16 and v = 12.69 % at $F_{p,C}$*). 3 of 10 tested bolts failed $\Delta\Theta_{1i,min}$ = 120° (with high coefficient of variation caused by specimens BU_M12_88-05 and -07) and 2 bolts also failed the criteria $\Delta\Theta_{2i,min}$ = 240°. In total, 8 of 10 bolting assemblies achieved k-class K1, k-class K2 was not accomplished. Furthermore, the reached maximum bolt force $F_{bi,max}$ and $\Delta\Theta_{2i}$ underlie high spreading. For further information and summarized criteria see Table 22. In addition, the tightening curves are shown in Figure 17 and Figure 18. The graphs show irregular bolt force-tightening torque curves because of galling in the nut bearing surface. The galling appears due to the high friction in the bearing surfaces and starts only when the bolts are tightened into the plastic range. In consequence, the washers began to rotate. After finishing the tightening tests, damages at the first load-bearing thread turn of the bolts, roughening of the paired threads and a minimal necking of the threaded shanks could be observed.

**Table 20** Test results of Bumax 88 – M12x80 series

| Legend | Specimen | $F_{p,C}$ | Max F | Max T | $\Theta_{pi}$ | $\Theta_{1i}$ | $\Theta_{2i}$ | $F_{bi}$ ($\Theta_{2i}$) | $\Delta\Theta_{1i}$ | $\Delta\Theta_{2i}$ | k ($F_{p,C}$) | $\mu_{tot}$ ($F_{p,C}$) | $\mu_{th}$ ($F_{p,C}$) | $\mu_b$ ($F_{p,C}$) | k ($F_{p,C*}$) | $M_i$ ($F_{p,C}$) | M ($F_{p,C}$*) | M ($F_{bi,max}$) |
|---|---|---|---|---|---|---|---|---|---|---|---|---|---|---|---|---|---|---|
| | | kN | kN | Nm | ° | ° | ° | kN | ° | ° | | | | | | Nm | Nm | Nm |
| max | | | --- | | | | | | --- | --- | 0,160 | | | | 0,16 | | | |
| min | | | 60,7 | | | | | | 120 | 240 | 0,100 | | | | 0,10 | | | |
| | BU_M12_88-01 | 47,2 | 61,5 | 191,5 | 158 | 268 | 298 | 60,2 | <112 | <142 | >0,188 | 0,145 | 0,187 | 0,109 | >0,16 | 106,5 | 73,7 | 180,8 |
| | BU_M12_88-03 | | 68,8 | 225,1 | 137 | 302 | 376 | 65,5 | 166 | 240 | 0,144 | 0,106 | 0,129 | 0,087 | 0,13 | 81,8 | 60,6 | 197,4 |
| | BU_M12_88-04 | | 68,4 | 252,0 | 154 | 315 | 393 | 59,3 | 163 | 240 | 0,150 | 0,111 | 0,157 | 0,072 | 0,14 | 84,7 | 62,2 | 216,3 |
| | BU_M12_88-05 | | <55,4 | 230,0 | 144 | 197 | 323 | 46,9 | <54 | <180 | >0,193 | 0,149 | 0,217 | 0,092 | >0,16 | 109,3 | 74,2 | 172,6 |
| | BU_M12_88-06 | | 74,9 | 190,2 | 147 | 354 | 387 | 74,1 | 208 | 240 | 0,113 | 0,079 | 0,103 | 0,059 | 0,11 | 64,2 | 51,4 | 174,5 |
| | BU_M12_88-07 | | 62,0 | 204,7 | 160 | 247 | 399 | 49,6 | <88 | 240 | 0,158 | 0,118 | 0,188 | 0,059 | 0,15 | 89,4 | 66,3 | 157,2 |
| | BU_M12_88-08 | | 72,0 | 201,3 | 136 | 359 | 376 | 71,7 | 224 | 240 | 0,119 | 0,084 | 0,110 | 0,062 | 0,12 | 67,4 | 53,6 | 192,4 |
| | BU_M12_88-09 | | 71,2 | 276,9 | 139 | 313 | 378 | 69,0 | 175 | 240 | 0,157 | 0,118 | 0,134 | 0,104 | 0,15 | 89,0 | 69,7 | 216,2 |
| | BU_M12_88-10 | | 68,8 | 259,3 | 159 | 304 | 398 | 64,1 | 146 | 240 | 0,153 | 0,114 | 0,156 | 0,079 | 0,14 | 86,9 | 63,2 | 210,4 |
| | BU_M12_88-11 | | 75,6 | 240,6 | 135 | 375 | 375 | 75,6 | 240 | 240 | 0,116 | 0,082 | 0,109 | 0,059 | 0,12 | 66,0 | 52,4 | 240,2 |

**Table 21** Statistical evaluation of Bumax 88 – M12x80

| BU_M12_88 (2014) | Max F | Max T | $\Theta_{pi}$ | $\Theta_{1i}$ | $\Theta_{2i}$ | $F_{bi}$ ($\Theta_{2i}$) | $\Delta\Theta_{1i}$ | $\Delta\Theta_{2i}$ | $\mu_{tot}$ ($F_{p,C}$) | $\mu_{th}$ ($F_{p,C}$) | $\mu_b$ ($F_{p,C}$) | $M_i$ ($F_{p,C}$) | k ($F_{p,C}$) | M ($F_{p,C}$*) | k ($F_{p,C*}$) | M ($F_{bi,max}$) |
|---|---|---|---|---|---|---|---|---|---|---|---|---|---|---|---|---|
| n = 10 | kN | Nm | ° | ° | ° | kN | ° | ° | | | | Nm | | Nm | | Nm |
| max | 75,6 | 276,9 | 160 | 375 | 399 | 75,6 | 240 | 240 | 0,149 | 0,217 | 0,109 | 109,3 | 0,19 | 74,2 | 0,16 | 240,2 |
| min | 55,4 | 190,2 | 135 | 197 | 298 | 46,9 | 54 | 142 | 0,079 | 0,103 | 0,059 | 64,2 | 0,113 | 51,4 | 0,11 | 157,2 |
| R | 20,2 | 86,7 | 25 | 178 | 101 | 28,7 | 186 | 98 | 0,070 | 0,114 | 0,050 | 45,1 | 0,080 | 22,8 | 0,05 | 83,0 |
| $\bar{x}$ | 67,9 | 227,2 | 147 | 303 | 370 | 63,6 | 158 | 224 | 0,111 | 0,149 | 0,078 | 84,5 | 0,149 | 62,7 | 0,14 | 195,8 |
| s | 6,4 | 30,1 | 10 | 55 | 33 | 9,8 | 60 | 34 | 0,024 | 0,039 | 0,019 | 15,6 | 0,028 | 8,4 | 0,02 | 25,3 |
| ν | 9,45 | 13,23 | 6,89 | 17,97 | 9,00 | 15,35 | 37,80 | 15,38 | 21,99 | 26,05 | 24,45 | 18,51 | 18,61 | 13,41 | 12,69 | 12,90 |

n: number; R: range; $\bar{x}$: mean value; s: standard deviation; ν: coefficient of variation in [%]

**Table 22** Evaluation of test results of Bumax 88 – M12x80 according to EN 14399-3

| n | $F_{p,C}^*$ | $F_{p,C}$ | $F_{bi,max}$ | $\Delta\Theta_{1i,min}$ | $\Delta\Theta_{2i,min}$ | k-values | k-class K1 | k-class K2 | | Fracture | Galling |
|---|---|---|---|---|---|---|---|---|---|---|---|
| [-] | 37.8 kN | 47.2 kN | ≥ 60.7 kN | ≥ 120° | ≥ 240° | [-] | $0.10 \leq k_i \leq 0.16$ | $0.10 \leq k_m \leq 0.23$ | $V_k \leq 0.06$ | | |
| 10 | 100% | 100% | 90% | 70% | 80% | 0.11 – 0.19 | 80% | 0.149 | 0.186 | 0% | 100% |

**Figure 16** BU_M12_88 test specimen after tightening

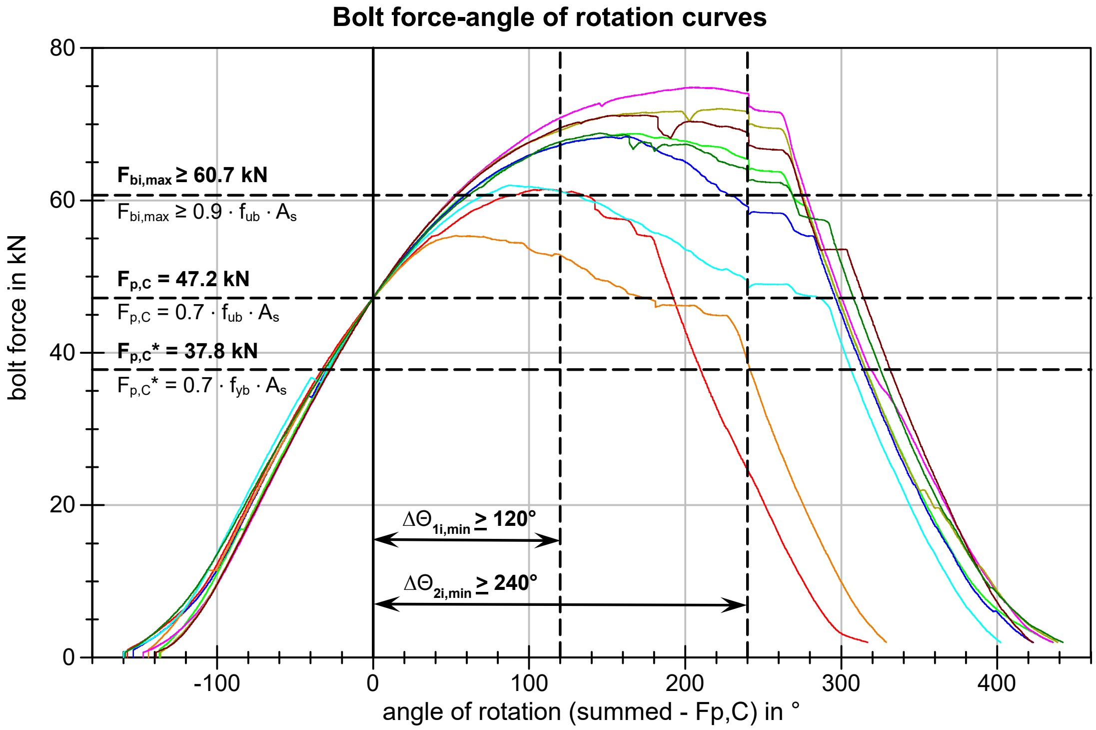


**Figure 17** BU_M12_88 Bolt force-angle of rotation curves

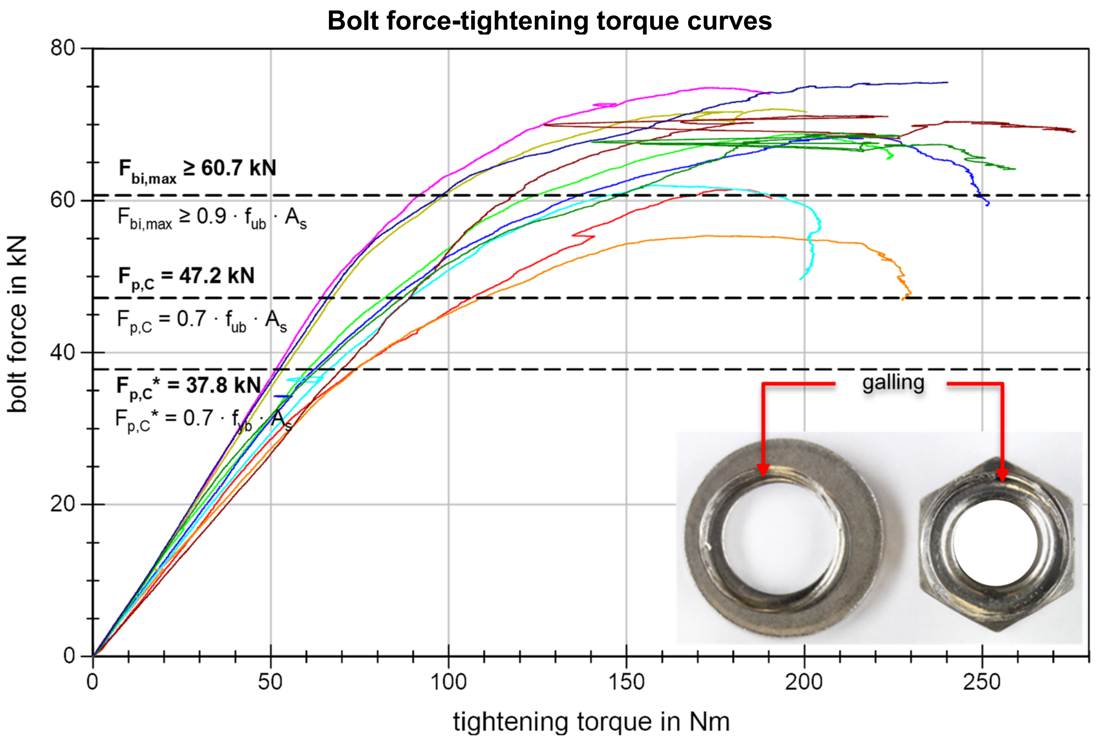


**Figure 18** BU_M12_88 Bolt force-tightening torque curves

#### *3.3.1.2 Bumax 109 – M12x80 – 10.9 – EN ISO 4014 – gleitmo 1952V*

The Bumax 109 – M12x80 austenitic stainless steel bolting assemblies, in short form BU_M12_109, are compiled and described in detail including nominal mechanical properties on the basis of Bumax datasheet:

- *Bolts:* BUFAB Group Bumax 109 - M12x80 A4 according to EN ISO 4014; stainless steel EN 1.4432, 1.4436, 1.4435; manufact.: 2013-11-20; PRE 27

  tensile strength $R_{m,min}$ (= $f_{ub}$): nominal 1000 N/mm²
  yield strength $R_{p0.2,min}$ (= $f_{yb}$): nominal 900 N/mm²
  elongation, min: nominal 0.2d

- *Nuts:* BUFAB Group Bumax 109 - M12 M6M A4 according to EN ISO 4032; stainless steel EN 1.4432, 1.4436, 1.4435; PRE 27

  stress under proof load, min: nominal 1000 N/mm²

- *Washers:* BUFAB Group Bumax RB A4-HV300 according to EN ISO 7089; stainless steel EN 1.4432, 1.4436, 1.4435; with dimensions d = 13.0 mm, D = 24.0 mm, t = 2.5 mm; PRE 27

  hardness, min: nominal 300 HV

Table 23, Table 24 and Table 25 summarize the test results and evaluation of Bumax 109 – M12x80 EN ISO 4014 bolting assemblies. The statistical evaluation is also presented as well as an overview about fulfilled and failed criteria according to EN 14399-3. The Bumax 109 – M12x80 bolts show a similar behaviour to the Bumax 88 – M12x80 bolts. Figure 20 and Figure 21 show the tightening graphs for the Bumax 109 - M12x80 – bolting assemblies. All tested specimens reached $F_{p,C}$* = 53.1 kN and $F_{p,C}$ = 59.0 kN. The bolt force plateau in the plastic range is less pronounced compared to the Bumax 88 – M12x80 bolts. In consequence, 4 of the 10 bolts failed $\Delta\Theta_{2i,min}$ = 240° according to EN 14399-3. The k-values at specified preload $F_{p,C}$ are between k = 0.12 and k = 0.24 (compared to k = 0.12 – 0.21 at $F_{p,C}$*), so that only 3 of the 10 tested bolts achieved k-class K1. k-class K2 is not achieved due to a coefficient of variation of v = 20.48 %. In addition, with attention to the demanded maximum bolt force, it is to noticeable that only 4 of 10 bolting assemblies reached $F_{bi,max} \geq 0.9 \cdot f_{ub} \cdot A_s$. Galling did occur when the bolts were tightened into the plastic range and lead to irregular bolt force-tightening torque curves shown in Figure 21. The statistical evaluation underlines high coefficients of variation for k-values at $F_{p,C}$* and $F_{p,C}$, $\Delta\Theta_{1i}$ and also high standard deviations and coefficients of variation for tightening torques $M_i$ at $F_{p,C}$*, $F_{p,C}$ and $F_{bi,max}$. Galling in the faying surface washer/nut, plastic deformations of the hexagon nut, damages at the first load-bearing thread turn of the bolts/nuts and roughening of paired threads are similar to what was observed for Bumax 88 – M12x80 tested bolting assemblies. Again, all tightening tests were performed without any partial or total bolt fracture.

**Table 23** Test results of Bumax 109 – M12x80

| Legend | Specimen | $F_{p,C}$ kN | Max F kN | Max T Nm | $\Theta_{pi}$ ° | $\Theta_{1i}$ ° | $\Theta_{2i}$ ° | $F_{bi}$ ($\Theta_{2i}$) kN | $\Delta\Theta_{1i}$ ° | $\Delta\Theta_{2i}$ ° | k ($F_{p,C}$) | $\mu_{tot}$ ($F_{p,C}$) | $\mu_{th}$ ($F_{p,C}$) | $\mu_b$ ($F_{p,C}$) | $F_{p,C}$* kN | k ($F_{p,C*}$) | $M_i$ ($F_{p,C}$) Nm | M ($F_{p,C}$*) Nm | M ($F_{bi,max}$) Nm |
|---|---|---|---|---|---|---|---|---|---|---|---|---|---|---|---|---|---|---|---|
| max | | | --- | | | | | | --- | --- | 0,160 | | | | | 0,16 | | | |
| min | | | 75,9 | | | | | | 120 | 240 | 0,100 | | | | | 0,10 | | | |
| | BU_M12_109-01 | 59 | <73,7 | 300,4 | 186 | 307 | 410 | 58,8 | 122 | <225 | >0,170 | 0,129 | 0,155 | 0,107 | 53,1 | >0,16 | 120,6 | 103,9 | 230,0 |
| | BU_M12_109-02 | | 78,5 | 340,7 | 181 | 317 | 420 | 63,9 | 137 | 240 | 0,159 | 0,119 | 0,089 | 0,145 | | 0,15 | 112,8 | 95,2 | 290,6 |
| | BU_M12_109-03 | | <72,6 | 300,8 | 184 | 315 | 423 | 61,7 | 133 | 240 | >0,185 | 0,142 | 0,157 | 0,128 | | >0,17 | 130,7 | 107,5 | 263,4 |
| | BU_M12_109-04 | | <70,5 | 333,8 | 177 | 283 | 388 | 58,8 | <107 | <212 | >0,185 | 0,142 | 0,118 | 0,161 | | 0,16 | 130,7 | 99,4 | 265,3 |
| | BU_M12_109-05 | | <72,7 | 298,1 | 179 | 272 | 391 | 58,8 | <94 | <213 | >0,202 | 0,157 | 0,140 | 0,171 | | >0,20 | 142,7 | 125,6 | 241,0 |
| | BU_M12_109-06 | | <69,0 | 297,1 | 197 | 288 | 397 | 58,8 | <91 | <200 | >0,223 | 0,175 | 0,128 | 0,215 | | >0,21 | 157,8 | 132,9 | 243,7 |
| | BU_M12_109-07 | | <73,5 | 339,0 | 183 | 315 | 423 | 63,8 | 132 | 240 | >0,211 | 0,165 | 0,093 | 0,227 | | >0,20 | 149,7 | 126,4 | 302,8 |
| | BU_M12_109-08 | | 78,3 | 350,6 | 182 | 313 | 422 | 72,8 | 132 | 240 | >0,241 | 0,191 | 0,108 | 0,261 | | >0,21 | 170,3 | 135,8 | 314,7 |
| | BU_M12_109-09 | | 78,7 | 203,4 | 164 | 290 | 404 | 68,9 | 125 | 240 | 0,127 | 0,091 | 0,122 | 0,065 | | 0,12 | 89,9 | 78,7 | 161,4 |
| | BU_M12_109-10 | | 81,1 | 238,8 | 174 | 324 | 415 | 74,7 | 150 | 240 | 0,131 | 0,095 | 0,097 | 0,092 | | 0,13 | 92,7 | 81,2 | 189,0 |

**Table 24** Statistical evaluation of Bumax 109 – M12x80

| BU_M12_109 (2013) n = 10 | Max F kN | Max T Nm | $\Theta_{pi}$ ° | $\Theta_{1i}$ ° | $\Theta_{2i}$ ° | $F_{bi}$ ($\Theta_{2i}$) kN | $\Delta\Theta_{1i}$ ° | $\Delta\Theta_{2i}$ ° | $\mu_{tot}$ ($F_{p,C}$) | $\mu_{th}$ ($F_{p,C}$) | $\mu_b$ ($F_{p,C}$) | $M_i$ ($F_{p,C}$) Nm | k ($F_{p,C}$) | M ($F_{p,C}$*) Nm | k ($F_{p,C*}$) | M ($F_{bi,max}$) Nm |
|---|---|---|---|---|---|---|---|---|---|---|---|---|---|---|---|---|
| max | 81,1 | 350,6 | 197 | 324 | 423 | 74,7 | 150 | 240 | 0,191 | 0,157 | 0,261 | 170,3 | 0,24 | 135,8 | 0,21 | 314,7 |
| min | 69,0 | 203,4 | 164 | 272 | 388 | 58,8 | 91 | 200 | 0,091 | 0,089 | 0,065 | 89,9 | 0,127 | 78,7 | 0,12 | 161,4 |
| R | 12,1 | 147,2 | 33 | 52 | 35 | 15,9 | 59 | 40 | 0,100 | 0,068 | 0,196 | 80,4 | 0,114 | 57,1 | 0,09 | 153,3 |
| $\bar{x}$ | 74,9 | 300,3 | 181 | 302 | 409 | 64,1 | 122 | 229 | 0,141 | 0,121 | 0,157 | 129,8 | 0,183 | 108,7 | 0,17 | 250,2 |
| s | 4,0 | 47,1 | 9 | 18 | 14 | 6,0 | 19 | 15 | 0,033 | 0,025 | 0,063 | 26,5 | 0,038 | 20,7 | 0,03 | 48,5 |
| ν | 5,36 | 15,69 | 4,71 | 5,82 | 3,31 | 9,44 | 15,68 | 6,71 | 23,39 | 20,34 | 39,93 | 20,43 | 20,48 | 19,08 | 19,19 | 19,37 |

n: number; R: range; $\bar{x}$: mean value; s: standard deviation; ν: coefficient of variation in [%]

**Table 25** Evaluation of test results of Bumax 109 – M12x80 according to EN 14399-3

| n | $F_{p,C}^*$ | $F_{p,C}$ | $F_{bi,max}$ | $\Delta\Theta_{1i,min}$ | $\Delta\Theta_{2i,min}$ | k-values | k-class K1 | k-class K2 | | Fracture | Galling |
|---|---|---|---|---|---|---|---|---|---|---|---|
| [-] | 53.1 kN | 59.0 kN | ≥ 75.9 kN | ≥ 120° | ≥ 240° | [-] | $0.10 \le k_i \le 0.16$ | $0.10 \le k_m \le 0.23$ | $V_k \le 0.06$ | | |
| 10 | 100% | 100% | 40% | 70% | 60% | 0.12 – 0.24 | 30% | 0.183 | 0.205 | 0% | 100% |

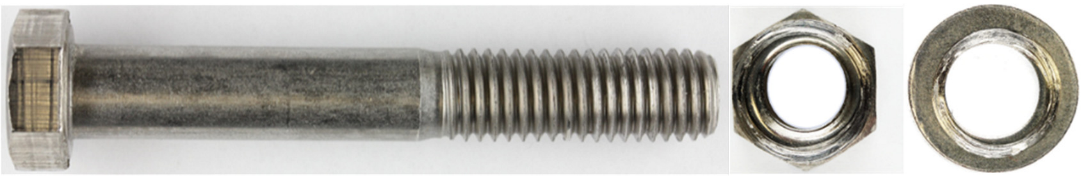

**Figure 19** BU_M12_109 test specimen after tightening

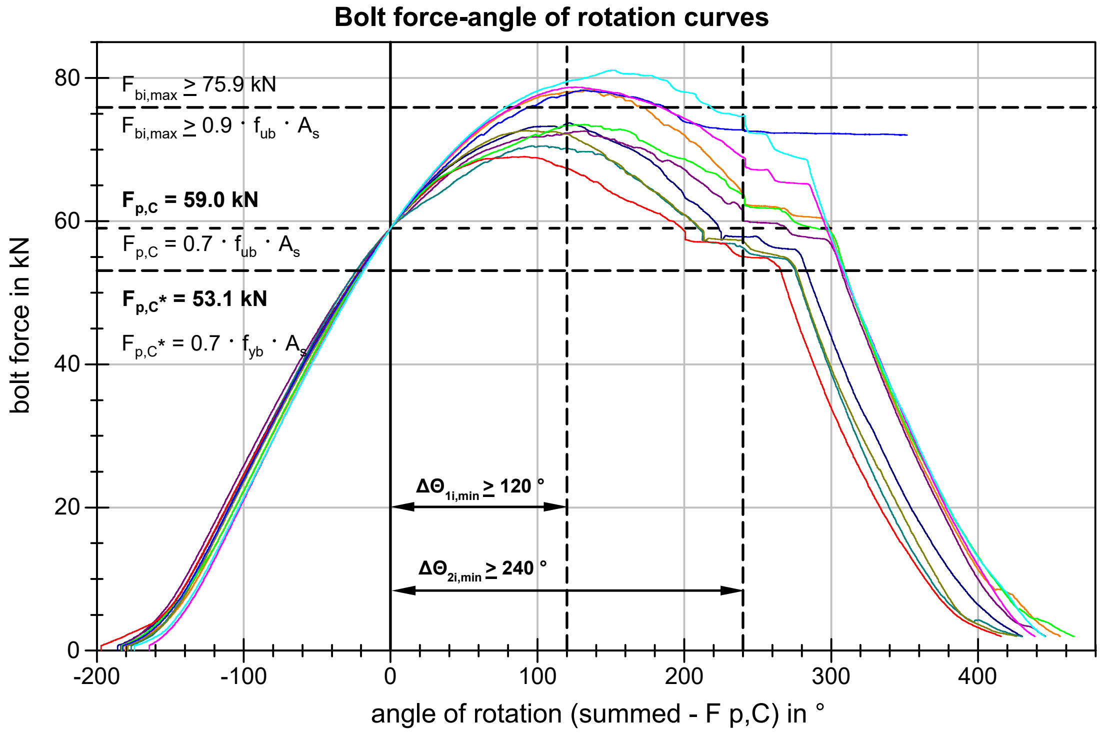


**Figure 20** BU_M12_109 Bolt force-angle of rotation curves

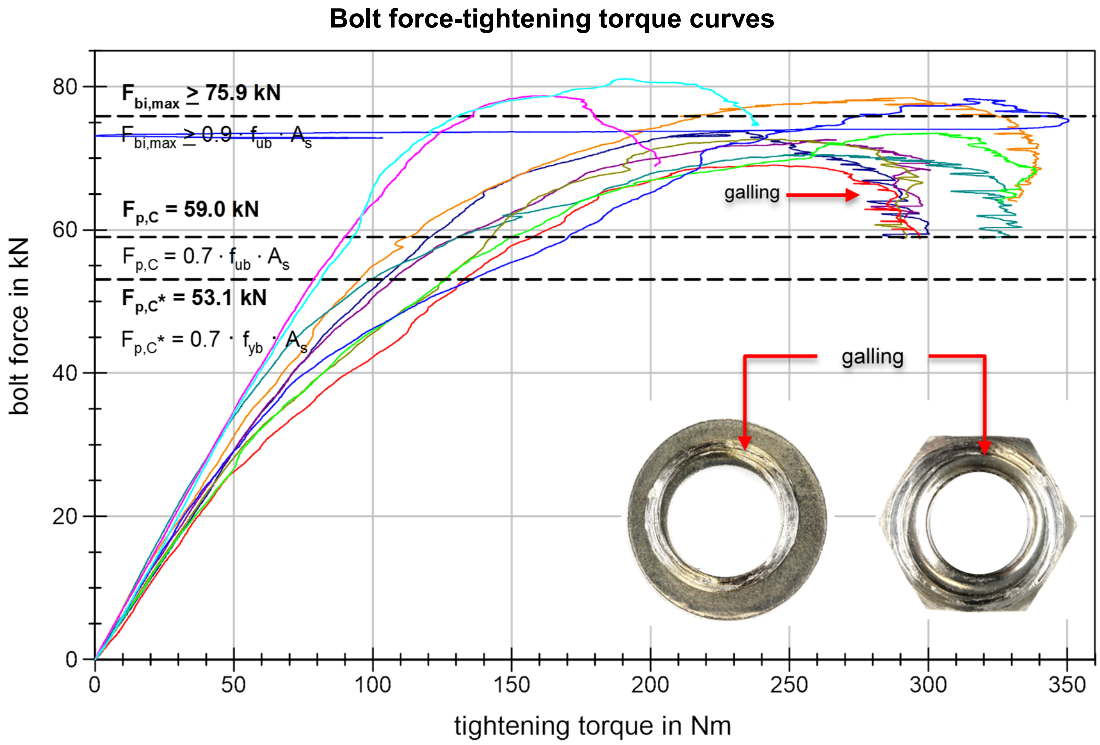


**Figure 21** BU_M12_109 Bolt force-tightening torque curves

#### *3.3.1.3 Bumax SDX – M12x80 – 10.9 – EN ISO 4017 – gleitmo 1952V*

The Bumax SDX – M12x80 super duplex stainless steel bolting assemblies in property class 10.9, abbreviated as BU_M12_SDX, are arranged as follows including mechanical properties based on Bumax datasheet:

- *Bolts:* BUFAB Group Bumax SDX - M12x80 according to EN ISO 4017; stainless steel EN 1.4410; manufact.: 2014-11-14; PRE 42

  tensile strength $R_{m,min}$ (= $f_{ub}$): nominal 1000 N/mm²
  yield strength $R_{p0.2,min}$ (= $f_{yb}$): nominal 900 N/mm²
  elongation, min: nominal 0.3d

- *Nuts:* BUFAB Group Bumax 109 - M12 M6M A4 according to EN ISO 4032; stainless steel EN 1.4432, 1.4436, 1.4435; manufact.: 2014-05-22; PRE 27

  stress under proof load, min: nominal 1000 N/mm²

- *Washers:* BUFAB Group Bumax RB A4-HV300 according to EN ISO 7089; stainless steel EN 1.4432, 1.4436, 1.4435; with dimensions d = 13.0 mm, D = 24.0 mm, t = 2.5 mm; manufact.: 2015-04-14; PRE 27

  hardness, min: nominal 300 HV

The test results of Bumax SDX – M12x80 super duplex bolting assemblies according to EN ISO 4017 and property class 10.9 are presented in Table 26, Table 27 and Table 28 including statistical data and evaluation. Referring to EN 14399-3, all bolting assemblies fulfilled the specified preload of $F_{p,C}$* and $F_{p,C}$, and additionally, 9 of 10 bolts achieved $F_{bi,max} \geq 0.9 \cdot f_{ub} \cdot A_s$ = 75.9 kN. The bolt force plateau in the plastic range is more pronounced compared to the austenitic Bumax 88 – M12x80 bolts. Furthermore, 6 of 10 tested bolts achieved k-class K1 with k-values at $F_{p,C}$ between 0.14 and 0.21 (compared to k = 0.14 – 0.20 at $F_{p,C}$*). Once more, k-class K2 is not achieved caused by a coefficient of variation of v = 13.82 %. Caused by high friction coefficients, specimen BU_M12_SDX-03 shows a noticeable low maximum force $F_{bi,max}$ = 70.8 kN and also low angles of rotation $\Delta\Theta_{1i}$ = 81° and $\Delta\Theta_{2i}$ = 209°. Neglecting this test, the k-values at $F_{p,C}$ lie between 0.10 and 0.18 with a significant lower coefficient of variation v = 9.22 %, and under those circumstances, all bolts achieved $F_{bi,max}$ as previously defined system HR criterion according to EN 14399-3. The tightening graphs of BU_M12_SDX 109 are presented in Figure 23. Figure 24 shows again irregular bolt force-tightening torque curves caused by galling in the nut bearing surface. Furthermore, the damages of the tested super duplex bolting assemblies are similar to those of the tested austenitic stainless steel bolts with damages mainly at the first and second load-bearing thread turns, roughening of paired threads and minimal necking of threaded shanks. Despite of galling in the faying surface washer/nut and plastic deformations of the paired threads it was possible to unscrew the hexagon nuts of all tested bolting assemblies manually by hand.

**Table 26** Test results of Bumax SDX – M12x80

| Legende | Probenbez. | $F_{p,C}$ kN | Max F kN | Max T Nm | $\Theta_{pi}$ ° | $\Theta_{1i}$ ° | $\Theta_{2i}$ ° | $F_{bi}$ ($\Theta_{2i}$) kN | $\Delta\Theta_{1i}$ ° | $\Delta\Theta_{2i}$ ° | k ($F_{p,C}$) | $\mu_{tot}$ ($F_{p,C}$) | $\mu_{th}$ ($F_{p,C}$) | $\mu_b$ ($F_{p,C}$) | $F_{p,C}$* kN | k ($F_{p,C*}$) | $M_i$ ($F_{p,C}$) Nm | M ($F_{p,C}$*) Nm | M ($F_{bi,max}$) Nm |
|---|---|---|---|---|---|---|---|---|---|---|---|---|---|---|---|---|---|---|---|
| max | | | --- | | | | | | --- | --- | 0,16 | | | | | 0,16 | | | |
| min | | | 75,9 | | | | | | 120 | 240 | 0,10 | | | | | 0,10 | | | |
| | BU_M12_SDX 109-01 | 59 | 78,0 | 281,0 | 183 | 320 | 454 | 59,0 | 137 | 271 | >0,16 | 0,123 | 0,157 | 0,094 | 53,1 | 0,16 | 115,6 | 101,4 | 227,1 |
| | BU_M12_SDX 109-02 | | 83,3 | 340,8 | 172 | 300 | 562 | 59,0 | 128 | 390 | >0,18 | 0,134 | 0,145 | 0,126 | | >0,17 | 124,9 | 109,4 | 237,7 |
| | BU_M12_SDX 109-03 | | <70,8 | 321,2 | 176 | 257 | 385 | 59,0 | <81 | <209 | >0,21 | 0,165 | 0,201 | 0,134 | | >0,20 | 149,6 | 129,4 | 261,1 |
| | BU_M12_SDX 109-04 | | 81,5 | 377,4 | 173 | 304 | 523 | 59,0 | 131 | 350 | 0,15 | 0,111 | 0,146 | 0,082 | | 0,14 | 106,0 | 89,9 | 222,6 |
| | BU_M12_SDX 109-05 | | 79,2 | 382,5 | 159 | 275 | 465 | 59,0 | <115 | 306 | 0,14 | 0,104 | 0,144 | 0,070 | | 0,14 | 100,6 | 87,7 | 230,9 |
| | BU_M12_SDX 109-06 | | 78,6 | 298,4 | 174 | 292 | 465 | 59,0 | <118 | 292 | >0,17 | 0,131 | 0,166 | 0,101 | | >0,16 | 121,9 | 104,5 | 214,6 |
| | BU_M12_SDX 109-07 | | 81,1 | 326,6 | 164 | 294 | 475 | 59,0 | 131 | 312 | 0,14 | 0,104 | 0,125 | 0,085 | | 0,14 | 100,0 | 88,2 | 227,6 |
| | BU_M12_SDX 109-08 | | 86,8 | 333,0 | 173 | 336 | 603 | 59,0 | 163 | 429 | 0,14 | 0,104 | 0,128 | 0,084 | | 0,14 | 100,6 | 88,8 | 209,2 |
| | BU_M12_SDX 109-09 | | 77,8 | 332,9 | 170 | 274 | 411 | 59,0 | <105 | 241 | 0,15 | 0,116 | 0,144 | 0,091 | | 0,15 | 109,7 | 93,1 | 216,6 |
| | BU_M12_SDX 109-10 | | 81,0 | 358,8 | 169 | 304 | 487 | 59,0 | 135 | 317 | 0,16 | 0,117 | 0,155 | 0,085 | | 0,15 | 111,1 | 95,0 | 241,7 |

**Table 27** Statistical evaluation of Bumax SDX – M12x80

| BU_M12_80_SDX 109 (2014) n = 10 | Max F kN | Max T Nm | $\Theta_{pi}$ ° | $\Theta_{1i}$ ° | $\Theta_{2i}$ ° | $F_{bi}$ ($\Theta_{2i}$) kN | $\Delta\Theta_{1i}$ ° | $\Delta\Theta_{2i}$ ° | $\mu_{tot}$ ($F_{p,C}$) | $\mu_{th}$ ($F_{p,C}$) | $\mu_b$ ($F_{p,C}$) | $M_i$ ($F_{p,C}$) Nm | k ($F_{p,C}$) | M ($F_{p,C}$*) Nm | k ($F_{p,C*}$) | M ($F_{bi,max}$) Nm |
|---|---|---|---|---|---|---|---|---|---|---|---|---|---|---|---|---|
| max | 86,8 | 382,5 | 183 | 336 | 603 | 59,0 | 163 | 429 | 0,165 | 0,201 | 0,134 | 149,6 | 0,21 | 129,4 | 0,20 | 261,1 |
| min | 70,8 | 281,0 | 159 | 257 | 385 | 59,0 | 81 | 209 | 0,104 | 0,125 | 0,070 | 100,0 | 0,14 | 87,7 | 0,14 | 209,2 |
| R | 16,0 | 101,5 | 24 | 79 | 218 | 0,0 | 82 | 220 | 0,061 | 0,076 | 0,064 | 49,6 | 0,07 | 41,7 | 0,06 | 51,9 |
| $\bar{x}$ | 79,8 | 335,3 | 171 | 296 | 483 | 59,0 | 124 | 312 | 0,121 | 0,151 | 0,095 | 114,0 | 0,16 | 98,7 | 0,16 | 228,9 |
| s | 4,2 | 31,9 | 7 | 23 | 65 | 0,0 | 22 | 66 | 0,019 | 0,021 | 0,020 | 15,3 | 0,02 | 13,1 | 0,02 | 15,2 |
| ν | 5,24 | 9,53 | 3,81 | 7,80 | 13,56 | 0,00 | 17,47 | 21,12 | 15,64 | 14,20 | 21,15 | 13,39 | 13,82 | 13,29 | 12,26 | 6,63 |

n: number; R: range; $\bar{x}$: mean value; s: standard deviation; ν: coefficient of variation in [%]

**Table 28** Evaluation of test results of Bumax SDX – M12x80 according to EN 14399-3

| n | $F_{p,C}^*$ | $F_{p,C}$ | $F_{bi,max}$ | $\Delta\Theta_{1i,min}$ | $\Delta\Theta_{2i,min}$ | k-values | k-class K1 | k-class K2 | | Fracture | Galling |
|---|---|---|---|---|---|---|---|---|---|---|---|
| [-] | 53.1 kN | 59.0 kN | ≥ 75.9 kN | ≥ 120° | ≥ 240° | [-] | $0.10 \leq k_i \leq 0.16$ | $0.10 \leq k_m \leq 0.23$ | $V_k \leq 0.06$ | | |
| 10 | 100% | 100% | 90% | 60% | 90% | 0.14 – 0.21 | 60% | 0.160 | 0.138 | 0% | 100% |

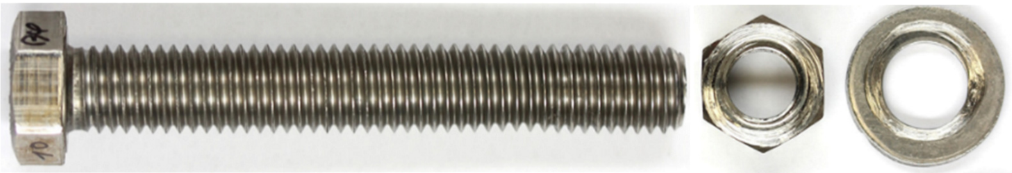


**Figure 22** BU_M12_SDX test specimen after tightening

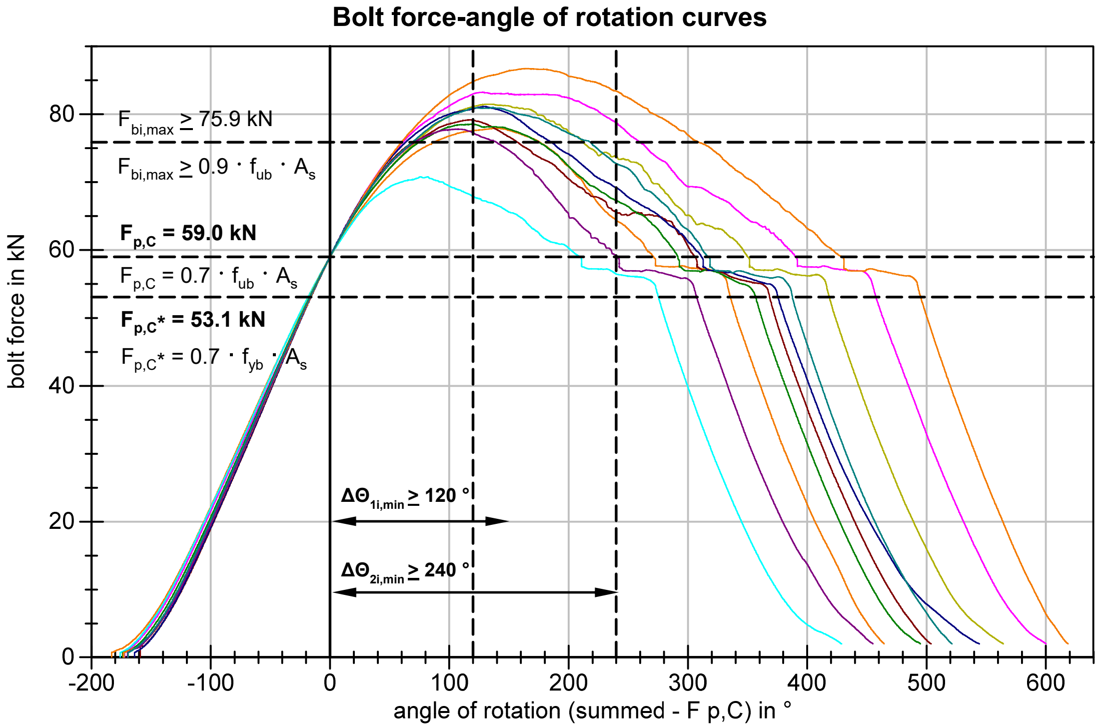


**Figure 23** BU_M12_SDX Bolt force-angle of rotation curves

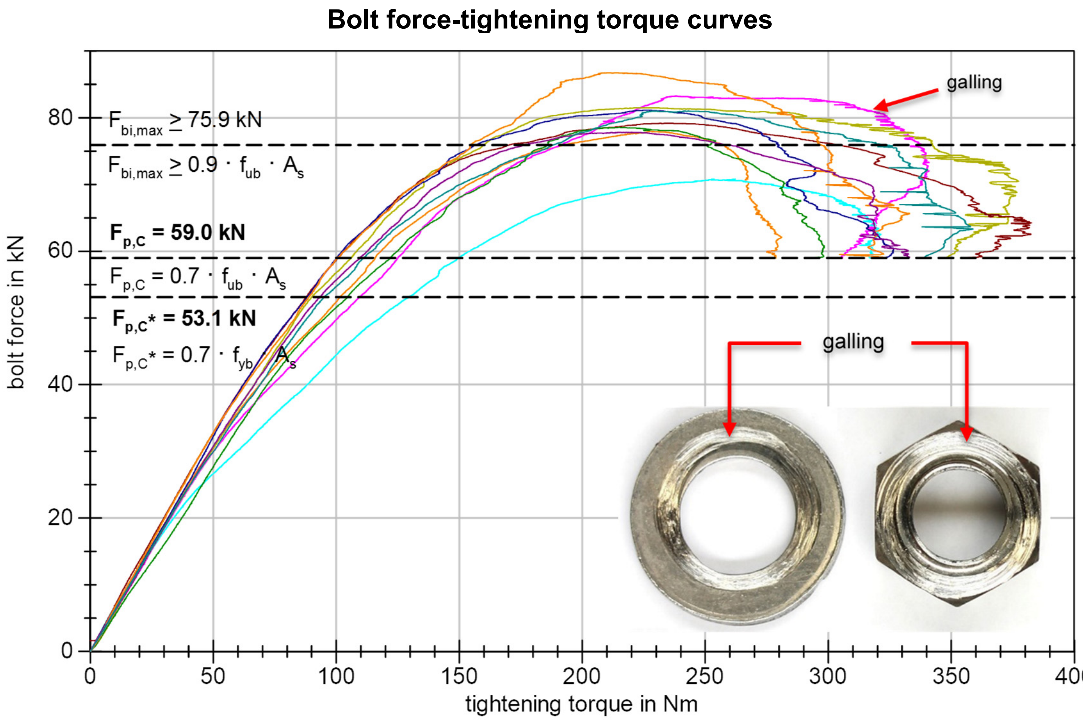


**Figure 24** BU_M12_SDX Bolt force-tightening torque curves

### 3.3.2 Bolt dimension M16

Tightening tests for bolt dimension M16 were carried out according to EN 14399-2 and EN ISO 16047. The test procedure contains a constant speed of rotation of 2.0 $min^{-1}$ for Bumax 88 bolting assemblies and speed of rotation of 5.0 $min^{-1}$ for Bumax 109, lean duplex and duplex steel grades. All series were tightened nut sided. The clamp length $\sum t$ for M16x80 bolts was set to 60.5 mm (clamp length/bolt diameter ratio of 3.8) in reference to the corresponding tables of System HR – EN 14399-3. In contrast, the clamp length $\sum t$ for property class 10.9 bolts (nominal length 100 mm) was set to 78.5 mm (clamp length/bolt diameter ratio of 4.9). In addition, the tests were stopped when the measured bolt force dropped to $F_{p,c} = 0.7 \cdot f_{ub} \cdot A_s$ (with $f_{ub}$: tensile strength of the bolt and $A_s$: tensile stress area of the bolt).

The criteria of evaluation for property class 8.8 according to EN 14399-3 are defined as follows:

- $F_{p,C}^* = 0.7 \cdot f_{yb} \cdot A_s = 0.7 \cdot 640\ N/mm^2 \cdot 157.0\ mm^2 = 70.3\ kN$ (see DIN EN 1993-1-8/NA:2010-10)
- $F_{p,C} = 0.7 \cdot f_{ub} \cdot A_s = 0.7 \cdot 800\ N/mm^2 \cdot 157.0\ mm^2 = 87.9\ kN$
- $F_{bi,max} \geq 0.9 \cdot f_{ub} \cdot A_s = 0.9 \cdot 800\ N/mm^2 \cdot 157.0\ mm^2 = 113.0\ kN$
- $\Delta\Theta_{1i,min} \geq 120°$ with $\Sigma t = 60.5$ mm: $2d \leq \Sigma t < 6d$
- $\Delta\Theta_{2i,min} \geq 240°$ with $\Sigma t = 60.5$ mm: $2d \leq \Sigma t < 6d$

In addition, the criteria of evaluation for bolting assemblies in property class 10.9 (meaning Bumax 109, Bumax lean duplex and Bumax duplex series) are defined as follows:

- $F_{p,C}^* = 0.7 \cdot f_{yb} \cdot A_s = 0.7 \cdot 800\ N/mm^2 \cdot 157.0\ mm^2 = 70.3\ kN$ (for Bumax 109 bolts)
- $F_{p,C}^* = 0.7 \cdot f_{yb} \cdot A_s = 0.7 \cdot 900\ N/mm^2 \cdot 157.0\ mm^2 = 87.9\ kN$ (for Bumax LDX and DX)
- $F_{p,C} = 0.7 \cdot f_{ub} \cdot A_s = 0.7 \cdot 1000\ N/mm^2 \cdot 157.0\ mm^2 = 109.9\ kN$
- $F_{bi,max} \geq 0.9 \cdot f_{ub} \cdot A_s = 0.9 \cdot 1000\ N/mm^2 \cdot 157.0\ mm^2 = 141.3\ kN$
- $\Delta\Theta_{1i,min} \geq 120°$ with $\Sigma t = 64.0$ mm: $2d \leq \Sigma t < 6d$
- $\Delta\Theta_{2i,min} \geq 240°$ with $\Sigma t = 64.0$ mm: $2d \leq \Sigma t < 6d$

All tightening test were carried out in accordance with EN 14399-2 and EN ISO 16047 using the test setup shown in Table 29 and Table 30.

**Table 29** Test setup Bumax 88 – M16x80 series

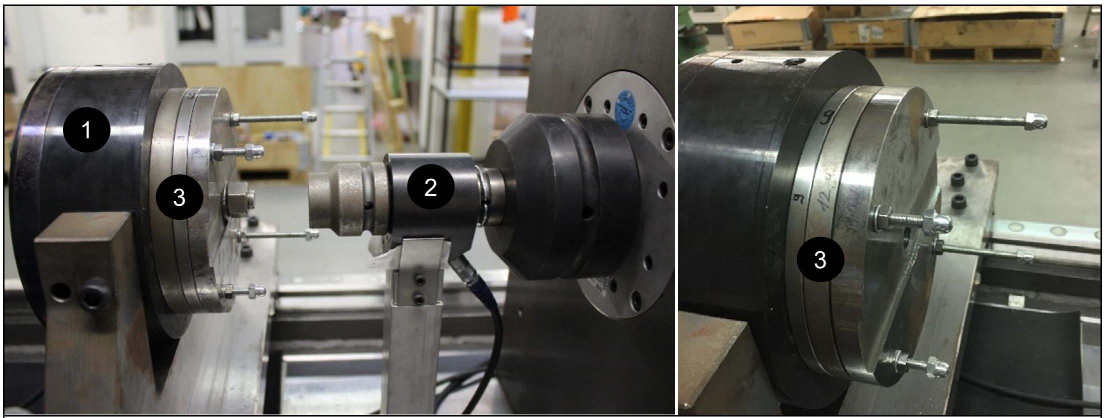


| | | |
|---|---|---|
| **1** | Sensor force – thread friction torque: SNo. 1016254 – 200 kN / 350 Nm | |
| **2** | Sensor total tightening torque – angle of rotation: SNo. 1016257 – 1,000 Nm | |
| **3** | Shims: DP 9mm + DP 12mm + M16HV | Lubrication: gleitmo 1952V |
| | Support bar: No | Adapter: Yes |
| | Speed of rotation: 2.0 $min^{-1}$ | Rotated component: Hexagon nut |
| | Number of bolting assemblies tested: 10 | Washers: placed under nut |
| | Clamp length $\sum t$ = 60.5 mm according to EN 14399-3:2015-03 | |
| | Clamp length/bolt diameter ratio: 3.8 | Stop criteria: bolt force dropped to $F_{p,C}$ |

**Table 30** Test setup Bumax 109/LDX/DX – M16x100 series (schematically)

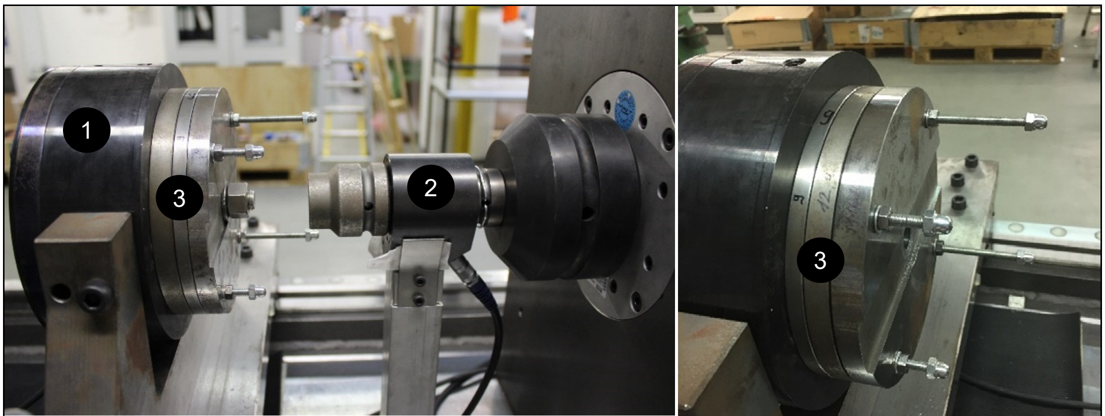


| | | |
|---|---|---|
| **1** | Sensor force – thread friction torque: SNo. 1016254 – 200 kN / 350 Nm | |
| **2** | Sensor total tightening torque – angle of rotation: SNo. 1016257 – 1,000 Nm | |
| **3** | Shims: DP 12mm + DP 22mm + M16HV | Lubrication: gleitmo 1952V |
| | Support bar: No | Adapter: Yes |
| | Speed of rotation: 5.0 $min^{-1}$ | Rotated component: Hexagon nut |
| | Number of bolting assemblies tested: 10 | Washers: placed under nut |
| | Clamp length $\sum t$ = 78.5 mm according to EN 14399-3:2015-03 | |
| | Clamp length/bolt diameter ratio: 4.9 | Stop criteria: bolt force dropped to $F_{p,C}$ |

#### *3.3.2.1 Bumax 88 – M16x80 – 8.8 – EN ISO 4017 – gleitmo 1952V*

The Bumax 88 – M16x80 austenitic stainless steel bolting assemblies in property class 8.8/80, in short form BU_M16_88, were arranged of following components including nominal mechanical properties based on Bumax datasheet:

- *Bolts:* BUFAB Group Bumax 88 - M16x80 A4 according to EN ISO 4017; stainless steel EN 1.4432, 1.4436, 1.4435; manufact.: 2015-09-05; PRE 27

| |
|---|
| tensile strength $R_{m,min}$ (= $f_{ub}$): nominal 800 N/mm² <br> yield strength $R_{p0.2,min}$ (= $f_{yb}$): nominal 640 N/mm² <br> elongation, min: nominal 0.3d |

- *Nuts:* BUFAB Group Bumax 88 - M16 M6M A4 according to EN ISO 4032; stainless steel EN 1.4432, 1.4436, 1.4435; manufact.: 2015-03-10; PRE 27

| |
|---|
| stress under proof load, min: nominal 800 N/mm² |

- *Washers:* BUFAB Group Bumax RB A4-HV200 according to EN ISO 7089; stainless steel EN 1.4432, 1.4436, 1.4435; with dimensions d = 17.0 mm, D = 30.0 mm, t = 3.0 mm; manufact.: 2014-04-16; PRE 27

| |
|---|
| hardness, min: nominal 200 HV |

Table 31, Table 32 and Table 33 summarize the test results and evaluation of tested stainless steel bolting assemblies. The statistical evaluation is shown as well with fulfilled and failed criteria according to EN 14399-3 (System HR). Figure 26 and Figure 27 present the tightening graphs. They show similar curves and pronounced bolt force plateaus in the plastic range compared to Bumax SDX – M12x80 super duplex bolting assemblies without any partial or total bolt fracture. All tested austenitic bolting assemblies reached $F_{p,C}$* = 70.3 kN, $F_{p,C}$ = 87.9 kN and also the maximum required bolt force $F_{bi,max} \geq 0.9 \cdot f_{ub} \cdot A_s$ = 113.0 kN. Furthermore, 9 of 10 tested bolts achieved k-class K1 with k-values in a narrow range between 0.13 and 0.17 and coefficient of variation v = 7.53 % (compared to k = 0.12 – 0.15 and v = 7.90 % at $F_{p,C}$*). On the contrary, k-class K2 was not accomplished. Indeed, the coefficient of variation $v_k$ is 7.53 % and quite close to the required criteria for classification of k-class K2. For further information and summarized criteria see Table 33.The graphs show irregular bolt force-tightening torque curves because of galling in the nut bearing surface when tightened into the plastic range including significant high ranges of values $M_i$ at $F_{bi,max}$ and at the end of the tests (bolt force dropped again to $F_{p,C}$) in the bolt force-tightening torque-curves. 6 of 10 tested bolts achieved $\Delta\Theta_{1i,min}$ = 120° and additionally, all bolts reached $\Delta\Theta_{2i,min}$ = 240°. Damages at the first and second load-bearing thread turn of the bolts and roughening of the paired threads could be observed; bolt failure by fracture did not occur. Galling in the faying surface washer/nut could be observed, too. Furthermore, in the context of functionality and re-use, it was possible to unscrew the hexagon nuts of all tested bolting assemblies manually but turning the nut on the whole threaded shank by hand was not possible.

**Table 31** Test results of Bumax 88 – M16x80

| | | $F_{p,C}$ | Max F | Max T | $\Theta_{pi}$ | $\Theta_{1i}$ | $\Theta_{2i}$ | $F_{bi}$ ($\Theta_{2i}$) | $\Delta\Theta_{1i}$ | $\Delta\Theta_{2i}$ | k ($F_{p,C}$) | $\mu_{tot}$ ($F_{p,C}$) | $\mu_{th}$ ($F_{p,C}$) | $\mu_b$ ($F_{p,C}$) | $F_{p,C}$* | k ($F_{p,C*}$) | $M_i$ ($F_{p,C}$) | M ($F_{p,C}$*) | M ($F_{bi,max}$) |
|---|---|---|---|---|---|---|---|---|---|---|---|---|---|---|---|---|---|---|---|
| | | kN | kN | Nm | ° | ° | ° | kN | ° | ° | | | | | kN | | Nm | Nm | Nm |
| max | | | --- | | | | | | --- | --- | 0,16 | | | | | 0,16 | | | |
| min | | | 113,0 | | | | | | 120 | 240 | 0,10 | | | | | 0,10 | | | |
| | BU_M16_88-01 | 88 | 125,0 | 502,8 | 183 | 332 | 537 | 88,0 | 149 | 355 | 0,14 | 0,104 | 0,163 | 0,053 | 70 | 0,14 | 196,0 | 159,6 | 366,7 |
| | BU_M16_88-02 | | 115,4 | 441,5 | 147 | 264 | 543 | 88,0 | <116 | 396 | >0,16 | 0,126 | 0,144 | 0,111 | | 0,14 | 232,2 | 162,3 | 378,6 |
| | BU_M16_88-03 | | 119,9 | 612,1 | 171 | 301 | 490 | 88,0 | 130 | 319 | 0,14 | 0,106 | 0,162 | 0,058 | | 0,14 | 199,6 | 158,9 | 378,1 |
| | BU_M16_88-04 | | 122,1 | 580,5 | 170 | 303 | 511 | 88,0 | 133 | 341 | 0,13 | 0,095 | 0,141 | 0,056 | | 0,12 | 181,8 | 135,3 | 318,4 |
| | BU_M16_88-05 | | 114,5 | 483,7 | 178 | 278 | 420 | 88,0 | <99 | 242 | 0,15 | 0,115 | 0,183 | 0,056 | | 0,15 | 213,2 | 165,4 | 415,9 |
| | BU_M16_88-06 | | 127,0 | 798,7 | 168 | 346 | 607 | 88,0 | 178 | 439 | 0,15 | 0,116 | 0,180 | 0,061 | | 0,15 | 215,0 | 171,9 | 473,1 |
| | BU_M16_88-07 | | 122,4 | 572,6 | 176 | 293 | 499 | 88,0 | <117 | 323 | 0,13 | 0,097 | 0,143 | 0,058 | | 0,12 | 185,4 | 139,8 | 346,4 |
| | BU_M16_88-08 | | 117,0 | 638,0 | 179 | 275 | 465 | 88,0 | <96 | 286 | 0,13 | 0,100 | 0,141 | 0,065 | | 0,13 | 190,0 | 144,4 | 417,0 |
| | BU_M16_88-09 | | 123,6 | 642,5 | 185 | 314 | 479 | 88,0 | 129 | 294 | 0,14 | 0,104 | 0,156 | 0,058 | | 0,14 | 195,4 | 156,5 | 419,5 |
| | BU_M16_88-10 | | 121,9 | 746,2 | 185 | 310 | 503 | 88,0 | 125 | 318 | 0,13 | 0,100 | 0,140 | 0,065 | | 0,13 | 189,0 | 150,9 | 564,7 |

**Table 32** Statistical evaluation of Bumax 88 – M16x80

| BU_M16_88 (2015) n = 10 | Max F kN | Max T Nm | $\Theta_{pi}$ ° | $\Theta_{1i}$ ° | $\Theta_{2i}$ ° | $F_{bi}$ ($\Theta_{2i}$) kN | $\Delta\Theta_{1i}$ ° | $\Delta\Theta_{2i}$ ° | $\mu_{tot}$ ($F_{p,C}$) | $\mu_{th}$ ($F_{p,C}$) | $\mu_b$ ($F_{p,C}$) | k ($F_{p,C}$) | $M_i$ ($F_{p,C}$) Nm | M ($F_{p,C}$*) Nm | M ($F_{bi,max}$) Nm |
|---|---|---|---|---|---|---|---|---|---|---|---|---|---|---|---|
| max | 127,0 | 798,7 | 185 | 346 | 607 | 88,0 | 178 | 439 | 0,126 | 0,183 | 0,111 | 0,16 | 232,2 | 171,9 | 564,7 |
| min | 114,5 | 441,5 | 147 | 264 | 420 | 88,0 | 96 | 242 | 0,095 | 0,140 | 0,053 | 0,13 | 181,8 | 135,3 | 318,4 |
| R | 12,5 | 357,2 | 38 | 82 | 187 | 0,0 | 82 | 197 | 0,031 | 0,043 | 0,058 | 0,03 | 50,4 | 36,6 | 246,3 |
| $\bar{x}$ | 120,9 | 601,9 | 174 | 302 | 505 | 88,0 | 127 | 331 | 0,106 | 0,155 | 0,064 | 0,14 | 199,8 | 154,5 | 407,8 |
| s | 4,1 | 112,3 | 11 | 26 | 50 | 0,0 | 24 | 56 | 0,010 | 0,016 | 0,017 | 0,01 | 15,8 | 11,7 | 70,2 |
| ν | 3,42 | 18,65 | 6,51 | 8,47 | 9,93 | 0,00 | 18,72 | 16,91 | 9,21 | 10,52 | 26,40 | 7,53 | 7,89 | 7,57 | 17,21 |

n: number; R: range; $\bar{x}$: mean value; s: standard deviation; ν: coefficient of variation in [%]

**Table 33** Evaluation of test results of Bumax 88 – M16x80 according to EN 14399-3

| n | $F_{p,C}$* | $F_{p,C}$ | $F_{bi,max}$ | $\Delta\Theta_{1i,min}$ | $\Delta\Theta_{2i,min}$ | k-values | k-class K1 | k-class K2 | | Fracture | Galling |
|---|---|---|---|---|---|---|---|---|---|---|---|
| [-] | 70.3 kN | 87.9 kN | ≥ 113.0 kN | ≥ 120° | ≥ 240° | [-] | $0.10 \le k_i \le 0.16$ | $0.10 \le k_m \le 0.23$ | $V_k \le 0.06$ | | |
| 10 | 100% | 100% | 100% | 60% | 100% | 0.13 – 0.17 | 90% | 0.136 | 0.075 | 0% | 100% |

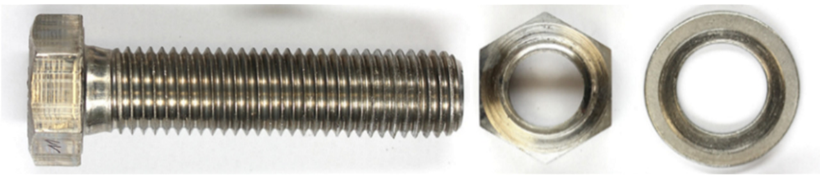

**Figure 25** BU_M16_88 test specimen after tightening

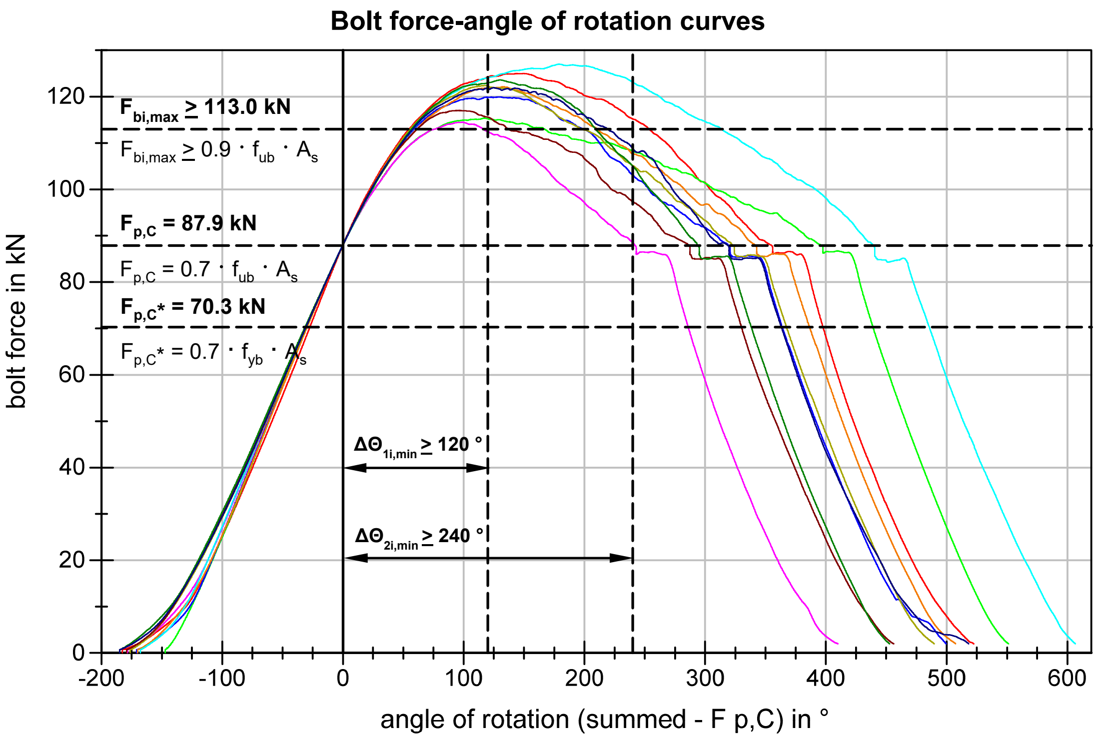


**Figure 26** BU_M16_88 Bolt force-angle of rotation curves

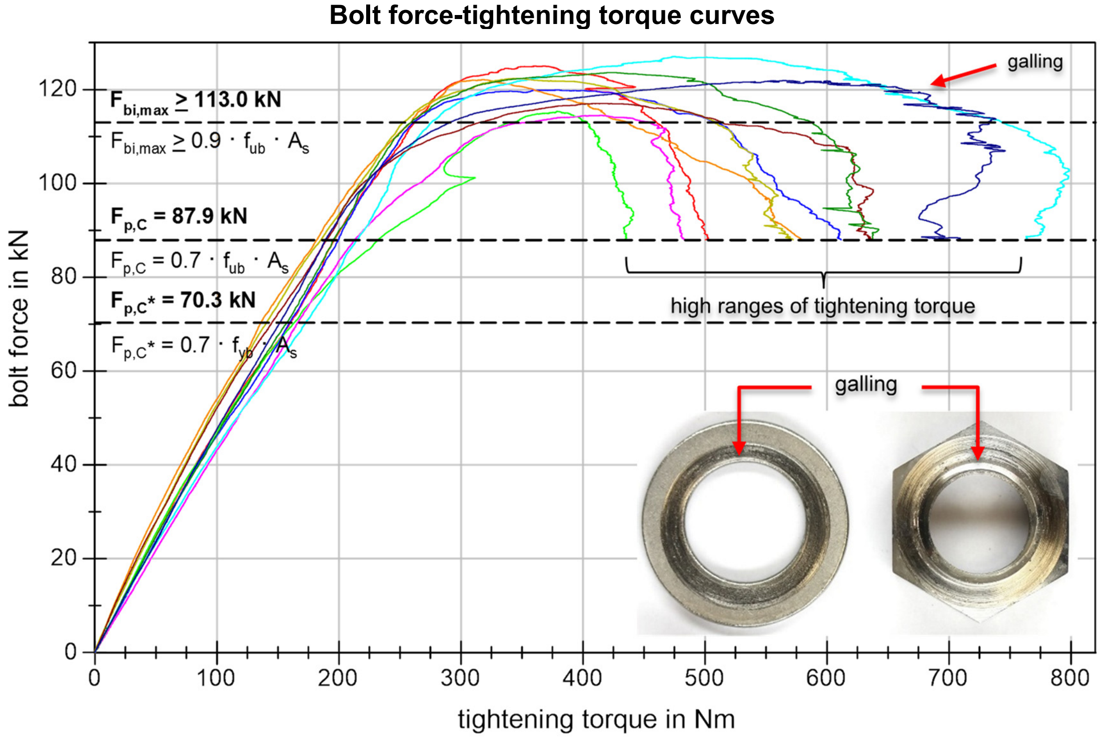


**Figure 27** BU_M16_88 Bolt force-tightening torque curves

### 3.3.2.2 *Bumax 109 – M16x100 – 10.9 – EN ISO 4017 – gleitmo 1952V*

The Bumax 109 – M16x100 austenitic stainless steel bolting assemblies in property class 10.9, in short form BU_M16_109, were arranged of following components including the nominal mechanical properties based on the Bumax datasheet:

- *Bolts:* BUFAB Group Bumax 109 - M16x100 A4 according to EN ISO 4017; stainless steel EN 1.4432, 1.4436, 1.4435; manufact.: 2016-04-28; PRE 27

  tensile strength $R_{m,min}$ (= $f_{ub}$): nominal 1000 N/mm²
  yield strength $R_{p0.2,min}$ (= $f_{yb}$): nominal 800 N/mm²
  elongation, min: nominal 0.3d

- *Nuts:* BUFAB Group Bumax 109 - M16 M6M A4 according to EN ISO 4032; stainless steel EN 1.4432, 1.4436, 1.4435; manufact.: 2015-02-26; PRE 27

  stress under proof load, min: nominal 1000 N/mm²

- *Washers:* BUFAB Group Bumax RB A4-HV300 according to EN ISO 7089; stainless steel EN 1.4432, 1.4436, 1.4435; with dimensions d = 17.0 mm, D = 30.0 mm, t = 3.0 mm; manufact.: 2015-12-14; PRE 27

  hardness, min: nominal 300 HV

The tightening test results of Bumax 109 – M16x100 bolting assemblies are summarized in Table 34, Table 35 and Table 36. The statistical evaluation is shown as well with fulfilled and failed criteria according to EN 14399-3 (System HR). In addition, the tightening curves are presented in Figure 29 andFigure 30. They show less pronounced bolt force plateaus in the plastic range compared to Bumax 88 – M16x80 bolting assemblies without any partial or total bolt fracture. All tested austenitic bolting assemblies reached $F_{p,C}$* = 87.9 kN and $F_{p,C}$ = 109.9 kN. On the contrary, only 3 of 10 bolts achieved $F_{bi,max} \geq 0.9 \cdot f_{ub} \cdot A_s$ = 141.3 kN. Due to the less pronounced plastic plateau, only 4 of the 10 bolts achieved $\Delta\Theta_{1i,min}$ = 120° and $\Delta\Theta_{2i,min}$ = 240° according to EN 14399-3. Furthermore, 6 of 10 tested bolts achieved k-class K1 with k-values in a wide range between 0.11 and 0.22 and a coefficient of variation of v = 23.07 % (compared to k = 0.10 – 0.20 and v = 21.57 % at $F_{p,C}$*). k-class K2 was not accomplished. For further information and summarized criteria see Table 36. Again, the graphs show irregular bolt force-tightening torque curves because of galling in the nut bearing surface when tightened into the plastic range including significant high ranges of values $M_i$ at $F_{p,C}$*, $F_{p,C}$, $F_{bi,max}$ and at end of test (bolt force dropped again to $F_{p,C}$) in the bolt force-tightening torque curves. The coefficients of friction $\mu_{tot}$, $\mu_{th}$ and $\mu_b$ show noticeable high scattering, especially the friction under nut bearing surface with a coefficient of variation of v = 61.38% at $F_{p,C}$. Damages at the first and second load-bearing thread turn of the bolts and roughening of paired threads could be observed. Galling especially in the faying surface washer/nut could be observed, too.

**Table 34** Test results of Bumax 109 – M16x100

| Legend | Specimens | $F_{p,C}$* kN | $F_{p,C}$ kN | Max F kN | Max T Nm | $\Theta_{pi}$ ° | $\Theta_{1i}$ ° | $\Theta_{2i}$ ° | $F_{bi}$ ($\Theta_{2i}$) kN | $\Delta\Theta_{1i}$ ° | $\Delta\Theta_{2i}$ ° | k ($F_{p,C*}$) | k ($F_{p,C}$) | $\mu_{tot}$ ($F_{p,C}$) | $\mu_{th}$ ($F_{p,C}$) | $\mu_b$ ($F_{p,C}$) | M ($F_{p,C}$*) Nm | $M_i$ ($F_{p,C}$) Nm | M ($F_{bi,max}$) Nm |
|---|---|---|---|---|---|---|---|---|---|---|---|---|---|---|---|---|---|---|---|
| max | | | | --- | | | | | | --- | --- | 0,16 | 0,16 | | | | | | |
| min | | | | 141,3 | | | | | | 120 | 240 | 0,10 | 0,10 | | | | | | |
| (red) | BU_M16_109-01 | 88 | 110 | <125,1 | 613,1 | 198 | 287 | 391 | 110,0 | <88 | <193 | 0,16 | >0,18 | 0,133 | 0,174 | 0,101 | 221,6 | 313,4 | 491,8 |
| (green) | BU_M16_109-02 | | | 145,3 | 787,7 | 187 | 348 | 550 | 110,0 | 161 | 363 | >0,20 | >0,22 | 0,169 | 0,133 | 0,197 | 286,2 | 386,9 | 664,9 |
| (blue) | BU_M16_109-03 | | | <132,7 | 716,0 | 187 | 292 | 403 | 110,0 | <105 | <216 | 0,13 | 0,13 | 0,094 | 0,138 | 0,058 | 177,1 | 230,6 | 472,5 |
| (orange) | BU_M16_109-04 | | | <137,0 | 649,4 | 184 | 307 | 444 | 110,0 | 123 | 260 | 0,13 | 0,13 | 0,093 | 0,149 | 0,048 | 182,9 | 229,3 | 403,0 |
| (magenta) | BU_M16_109-05 | | | <123,2 | 738,3 | 191 | 293 | 398 | 110,0 | <102 | <207 | >0,17 | >0,19 | 0,145 | 0,148 | 0,142 | 235,1 | 336,8 | 569,9 |
| (cyan) | BU_M16_109-06 | | | <123,2 | 608,7 | 197 | 278 | 372 | 110,0 | <81 | <175 | 0,14 | >0,17 | 0,123 | 0,213 | 0,050 | 203,2 | 292,0 | 418,0 |
| (yellow) | BU_M16_109-07 | | | <132,1 | 634,6 | 189 | 294 | 427 | 110,0 | <105 | <238 | 0,12 | 0,14 | 0,104 | 0,150 | 0,066 | 174,5 | 251,4 | 450,3 |
| (dark red) | BU_M16_109-08 | | | <136,3 | 575,4 | 184 | 302 | 401 | 110,0 | <118 | <216 | 0,13 | 0,14 | 0,097 | 0,155 | 0,051 | 178,7 | 237,9 | 443,6 |
| (dark green) | BU_M16_109-09 | | | 142,6 | 661,7 | 184 | 320 | 481 | 110,0 | 136 | 298 | 0,11 | 0,12 | 0,080 | 0,117 | 0,051 | 157,8 | 202,8 | 449,2 |
| (dark blue) | BU_M16_109-10 | | | 149,3 | 796,9 | 182 | 341 | 528 | 110,0 | 159 | 346 | 0,10 | 0,11 | 0,072 | 0,091 | 0,056 | 143,7 | 185,5 | 564,3 |

**Table 35** Statistical evaluation of Bumax 109 – M16x100

| BU_M16_109_100 - gleitmo 1952V n = 10 | Max F kN | Max T Nm | $\Theta_{pi}$ ° | $\Theta_{1i}$ ° | $\Theta_{2i}$ ° | $F_{bi}$ ($\Theta_{2i}$) kN | $\Delta\Theta_{1i}$ ° | $\Delta\Theta_{2i}$ ° | k ($F_{p,C*}$) | k ($F_{p,C}$) | $\mu_{tot}$ ($F_{p,C}$) | $\mu_{th}$ ($F_{p,C}$) | $\mu_b$ ($F_{p,C}$) | M ($F_{p,C}$*) Nm | $M_i$ ($F_{p,C}$) Nm | M ($F_{bi,max}$) Nm |
|---|---|---|---|---|---|---|---|---|---|---|---|---|---|---|---|---|
| max | 149,3 | 796,9 | 198 | 348 | 550 | 110,0 | 161 | 363 | 0,20 | 0,22 | 0,169 | 0,213 | 0,197 | 286,2 | 386,9 | 664,9 |
| min | 123,2 | 575,4 | 182 | 278 | 372 | 110,0 | 81 | 175 | 0,10 | 0,11 | 0,072 | 0,091 | 0,048 | 143,7 | 185,5 | 403,0 |
| R | 26,1 | 221,5 | 16 | 70 | 178 | 0,0 | 80 | 188 | 0,10 | 0,11 | 0,097 | 0,122 | 0,149 | 142,5 | 201,4 | 261,9 |
| $\bar{x}$ | 134,7 | 678,2 | 188 | 306 | 440 | 110,0 | 118 | 251 | 0,14 | 0,15 | 0,111 | 0,147 | 0,082 | 196,1 | 266,7 | 492,8 |
| s | 9,2 | 77,3 | 6 | 23 | 61 | 0,0 | 27 | 65 | 0,03 | 0,04 | 0,031 | 0,032 | 0,050 | 42,0 | 63,8 | 82,2 |
| ν | 6,84 | 11,40 | 2,94 | 7,59 | 13,86 | 0,00 | 23,23 | 25,71 | 21,57 | 23,07 | 27,67 | 22,10 | 61,38 | 21,41 | 23,92 | 16,69 |

with n: number; R: range; x: mean value; s: standard deviation; ν: coefficient of variation in [%]

**Table 36** Evaluation of test results of Bumax 109 – M16x100 according to EN 14399-3

| n | $F_{p,C}$* | $F_{p,C}$ | $F_{bi,max}$ | $\Delta\Theta_{1i,min}$ | $\Delta\Theta_{2i,min}$ | k-values | k-class K1 | k-class K2 | | Fracture | Galling |
|---|---|---|---|---|---|---|---|---|---|---|---|
| [-] | 87.9 kN | 109.9 kN | ≥ 141.3 kN | ≥ 120° | ≥ 240° | [-] | 0.10 ≤ $k_i$ ≤ 0.16 | 0.10 ≤ $k_m$ ≤ 0.23 | $V_k$ ≤ 0.06 | | |
| 10 | 100% | 100% | 30% | 40% | 40% | 0.11 – 0.22 | 60% | 0.151 | 0.231 | 0% | 100% |

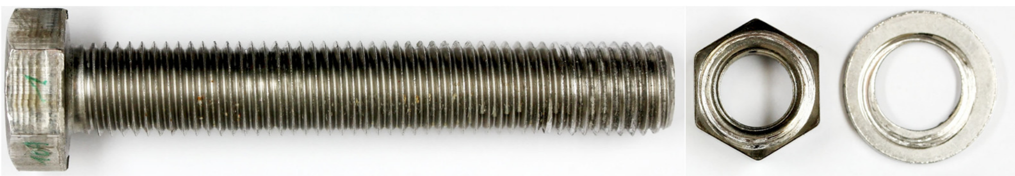

**Figure 28** BU_M16_109 test specimen after tightening

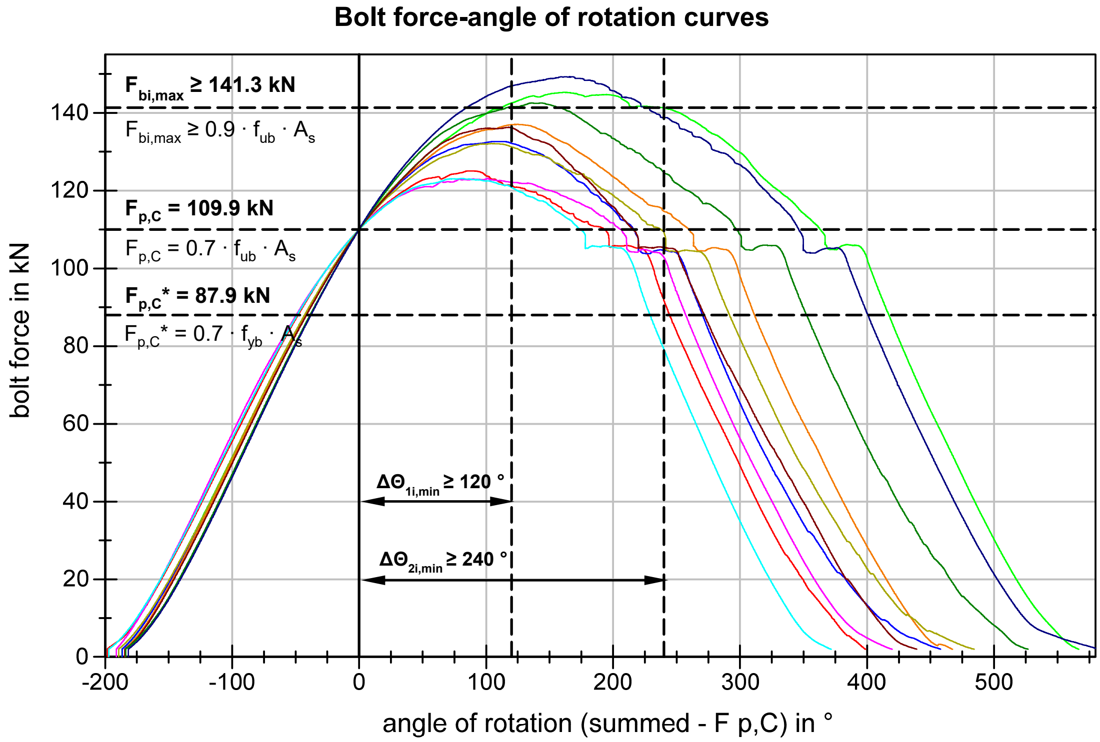


**Figure 29** BU_M16_109 Bolt force-angle of rotation curves

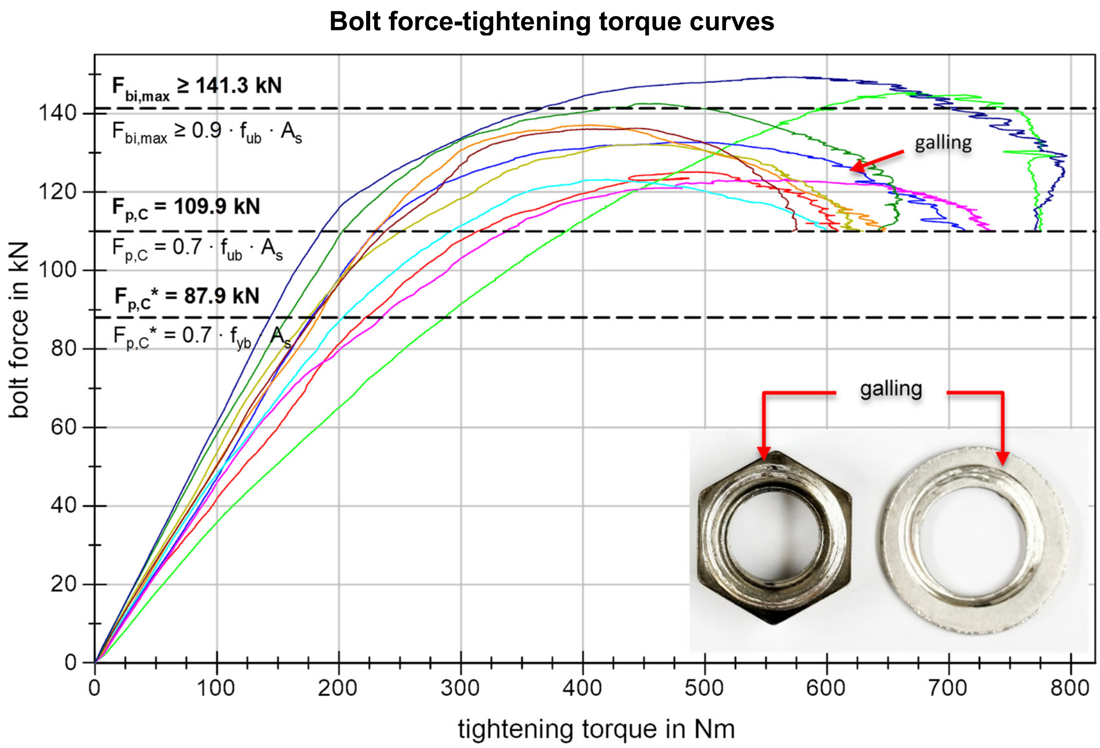


**Figure 30** BU_M16_109 Bolt force-tightening torque curves

#### *3.3.2.3 Bumax LDX – M16x100 – 10.9 – EN ISO 4017 – gleitmo 1952V*

The Bumax LDX – M16x100 lean duplex stainless steel bolting assemblies in property class 10.9, in short form BU_M16_LDX, were arranged of following components including nominal mechanical properties based on Bumax datasheet:

- *Bolts:* BUFAB Group Bumax LDX - M16x100 A4 according to EN ISO 4017; stainless steel EN 1.4162; manufact.: 2016-09-09; PRE 26

  tensile strength $R_{m,min}$ (= $f_{ub}$): nominal 1000 N/mm²
  yield strength $R_{p0.2,min}$ (= $f_{yb}$): nominal 900 N/mm²
  elongation, min: nominal 0.3d

- *Nuts:* BUFAB Group Bumax 109 - M16 M6M A4 according to EN ISO 4032; stainless steel EN 1.4432, 1.4436, 1.4435; manufact.: 2015-02-26; PRE 27

  stress under proof load, min: nominal 1000 N/mm²

- *Washers:* BUFAB Group Bumax RB A4-HV300 according to EN ISO 7089; stainless steel EN 1.4432, 1.4436, 1.4435; with dimensions d = 17.0 mm, D = 30.0 mm, t = 3.0 mm; manufact.: 2015-12-14; PRE 27

  hardness, min: nominal 300 HV

Table 37, Table 38 and Table 39 summarize the test results and evaluation of tested stainless steel bolting assemblies. The statistical evaluation is shown as well with fulfilled and failed criteria according to EN 14399-3 (System HR). Additionally, Figure 32 and Figure 33 present the tightening graphs. They show similar curves and pronounced bolt force plateaus in the plastic range compared to Bumax 109 – M16x100 austenitic bolting assemblies without any partial or total bolt fracture. All tested lean duplex bolting assemblies reached $F_{p,C}$* = 98.9 kN and $F_{p,C}$ = 109.9 kN, but on the contrary only 3 of 10 bolts achieved the maximum required bolt force $F_{bi,max} \geq 0.9 \cdot f_{ub} \cdot A_s$ = 141.3 kN. Furthermore, 10 of 10 tested bolts achieved k-class K1 with k-values in a narrow range between 0.11 and 0.15 and a coefficient of variation of v = 12.70 % (compared to k = 0.11 – 0.15 and v = 11.52 % at $F_{p,C}$*). However, k-class K2 was not accomplished due to a high coefficient of variation larger than 6 %. For further information and summarized criteria see Table 39. The graphs show irregular bolt force-tightening torque curves because of galling in the nut bearing surface when tightened into the plastic range especially after reaching $F_{bi,max}$, including significant high ranges of values $M_i$ at $F_{bi,max}$ and at the end of the tests (bolt force dropped again to $F_{p,C}$) in the bolt force-tightening torque curves. 4 of 10 tested bolts achieved $\Delta\Theta_{1i,min}$ = 120° and additionally, 8 of 10 bolts reached $\Delta\Theta_{2i,min}$ = 240°. Damages at the first and second load-bearing thread turn of the bolts and roughening of paired threads could be observed as well as galling in the faying surface washer/nut. Furthermore, in the context of functionality and re-use, it was possible to unscrew the hexagon nuts of all tested bolting assemblies manually but turning the nut on the whole threaded shank by hand was not possible.

**Table 37** Test results of Bumax LDX – M16x100

| Legend | Specimens | $F_{p,C*}$ kN | $F_{p,C}$ kN | Max F kN | Max T Nm | $\Theta_{pi}$ ° | $\Theta_{1i}$ ° | $\Theta_{2i}$ ° | $F_{bi}$ ($\Theta_{2i}$) kN | $\Delta\Theta_{1i}$ ° | $\Delta\Theta_{2i}$ ° | k ($F_{p,C*}$) | k ($F_{p,C}$) | $\mu_{tot}$ ($F_{p,C}$) | $\mu_{th}$ ($F_{p,C}$) | $\mu_b$ ($F_{p,C}$) | M ($F_{p,C*}$) Nm | $M_i$ ($F_{p,C}$) Nm | M ($F_{bi,max}$) Nm |
|---|---|---|---|---|---|---|---|---|---|---|---|---|---|---|---|---|---|---|---|
| max | | | | --- | | | | | | --- | --- | 0,16 | 0,16 | | | | | | |
| min | | | | 141,3 | | | | | | 120 | 240 | 0,10 | 0,10 | | | | | | |
| | BU_M16_LDX-01 | 98,9 | 110 | 141,9 | 638,1 | 173 | 313 | 434 | 109,9 | 141 | 261 | 0,11 | 0,12 | 0,083 | 0,117 | 0,054 | 176,5 | 203,3 | 448,0 |
| | BU_M16_LDX-02 | | | <138,4 | 692,0 | 174 | 289 | 454 | 110,0 | <116 | 280 | 0,11 | 0,11 | 0,083 | 0,117 | 0,053 | 180,3 | 202,3 | 411,0 |
| | BU_M16_LDX-03 | | | <137,6 | 538,9 | 174 | 293 | 439 | 110,0 | <118 | 265 | 0,11 | 0,11 | 0,081 | 0,115 | 0,052 | 179,5 | 198,6 | 367,1 |
| | BU_M16_LDX-04 | | | <129,3 | 714,6 | 176 | 247 | 420 | 110,0 | <72 | 244 | 0,13 | 0,14 | 0,104 | 0,109 | 0,101 | 203,0 | 245,9 | 447,6 |
| | BU_M16_LDX-05 | | | <138,2 | 702,9 | 172 | 286 | 461 | 110,0 | <114 | 289 | 0,11 | 0,11 | 0,082 | 0,111 | 0,057 | 180,8 | 200,6 | 414,8 |
| | BU_M16_LDX-06 | | | <139,3 | 632,4 | 174 | 301 | 418 | 110,0 | 126 | 243 | 0,12 | 0,12 | 0,085 | 0,121 | 0,054 | 182,7 | 206,0 | 371,5 |
| | BU_M16_LDX-07 | | | 141,5 | 642,8 | 176 | 311 | 474 | 110,0 | 135 | 299 | 0,11 | 0,11 | 0,078 | 0,112 | 0,048 | 172,4 | 191,8 | 349,9 |
| | BU_M16_LDX-08 | | | 144,2 | 750,9 | 178 | 322 | 493 | 110,0 | 144 | 315 | 0,11 | 0,11 | 0,080 | 0,109 | 0,054 | 174,6 | 196,2 | 396,0 |
| | BU_M16_LDX-09 | | | <126,3 | 787,0 | 183 | 276 | 401 | 109,9 | <93 | <218 | 0,15 | 0,15 | 0,118 | 0,160 | 0,081 | 232,0 | 272,6 | 524,8 |
| | BU_M16_LDX-10 | | | <131,8 | 740,3 | 181 | 275 | 374 | 110,0 | <94 | <192 | 0,13 | 0,14 | 0,103 | 0,141 | 0,070 | 210,6 | 243,4 | 454,5 |

**Table 38** Statistical evaluation of Bumax LDX – M16x100

| Bumax LDX - M16x100 ISO 4017 - Gleitmo 1952V n = 10 | Max F kN | Max T Nm | $\Theta_{pi}$ ° | $\Theta_{1i}$ ° | $\Theta_{2i}$ ° | $F_{bi}$ ($\Theta_{2i}$) kN | $\Delta\Theta_{1i}$ ° | $\Delta\Theta_{2i}$ ° | k ($F_{p,C*}$) | k ($F_{p,C}$) | $\mu_{tot}$ ($F_{p,C}$) | $\mu_{th}$ ($F_{p,C}$) | $\mu_b$ ($F_{p,C}$) | M ($F_{p,C*}$) Nm | $M_i$ ($F_{p,C}$) Nm | M ($F_{bi,max}$) Nm |
|---|---|---|---|---|---|---|---|---|---|---|---|---|---|---|---|---|
| max | 144,2 | 787,0 | 183 | 322 | 493 | 110,0 | 144 | 315 | 0,15 | 0,15 | 0,118 | 0,160 | 0,101 | 232,0 | 272,6 | 524,8 |
| min | 126,3 | 538,9 | 172 | 247 | 374 | 109,9 | 72 | 192 | 0,11 | 0,11 | 0,078 | 0,109 | 0,048 | 172,4 | 191,8 | 349,9 |
| R | 17,9 | 248,1 | 11 | 75 | 119 | 0,1 | 72 | 123 | 0,04 | 0,04 | 0,040 | 0,051 | 0,053 | 59,6 | 80,8 | 174,9 |
| $\bar{x}$ | 136,9 | 684,0 | 176 | 291 | 437 | 110,0 | 115 | 261 | 0,12 | 0,12 | 0,090 | 0,121 | 0,062 | 189,2 | 216,1 | 418,5 |
| s | 5,8 | 72,4 | 4 | 22 | 35 | 0,0 | 23 | 38 | 0,01 | 0,02 | 0,014 | 0,017 | 0,017 | 19,5 | 27,5 | 52,1 |
| ν | 4,26 | 10,58 | 2,03 | 7,59 | 8,11 | 0,04 | 20,08 | 14,44 | 11,52 | 12,70 | 15,14 | 13,63 | 26,91 | 10,31 | 12,74 | 12,45 |

with n: number; R: range; x: mean value; s: standard deviation; ν: coefficient of variation in [%]

**Table 39** Evaluation of test results of Bumax LDX – M16x100 according to EN 14399-3

| n | $F_{p,C}^*$ | $F_{p,C}$ | $F_{bi,max}$ | $\Delta\Theta_{1i,min}$ | $\Delta\Theta_{2i,min}$ | k-values | k-class K1 | k-class K2 | | Fracture | Galling |
|---|---|---|---|---|---|---|---|---|---|---|---|
| [-] | 98.9 kN | 109.9 kN | ≥ 141.3 kN | ≥ 120° | ≥ 240° | [-] | $0.10 \le k_i \le 0.16$ | $0.10 \le k_m \le 0.23$ | $V_k \le 0.06$ | | |
| 10 | 100% | 100% | 30% | 40% | 80% | 0.11 – 0.15 | 100% | 0.123 | 0.127 | 0% | 100% |

**Figure 31** BU_M16_LDX test specimen after tightening

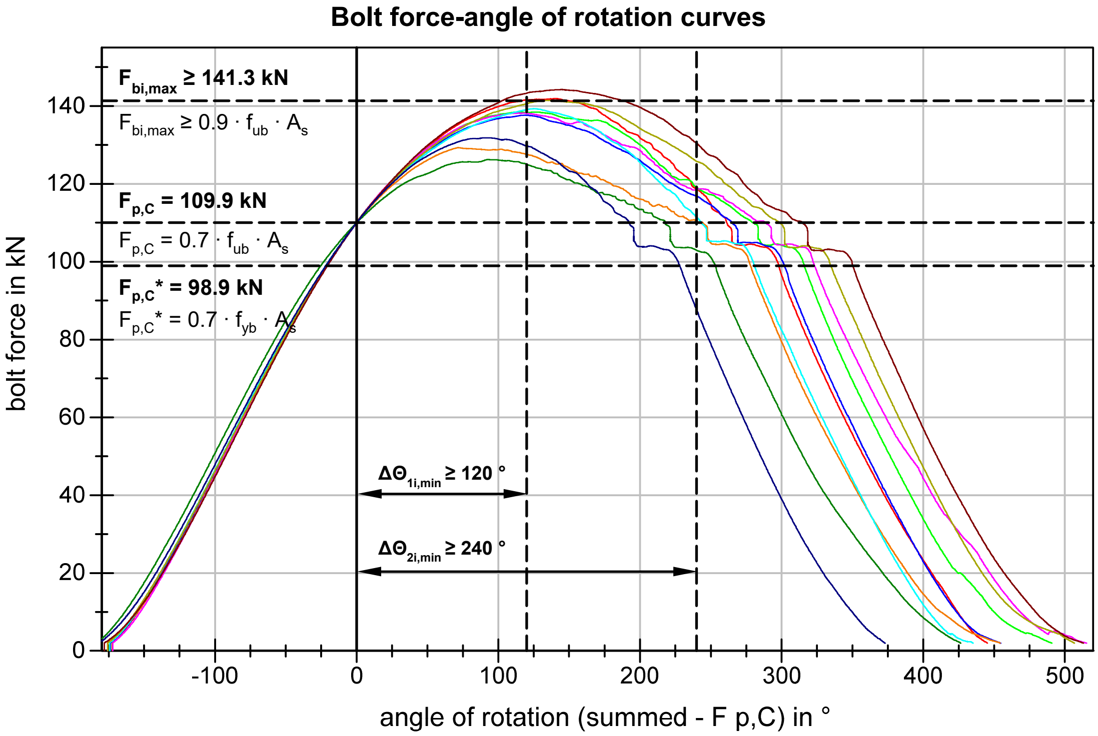


**Figure 32** BU_M16_LDX Bolt force-angle of rotation curves

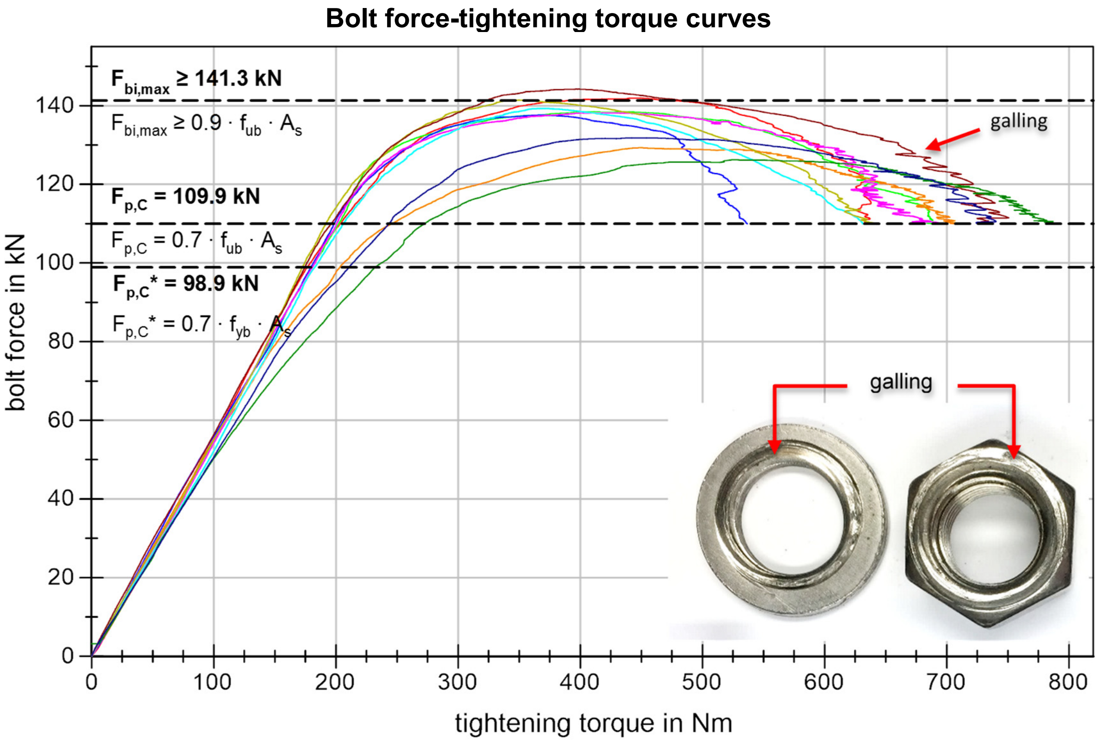


**Figure 33** BU_M16_LDX Bolt force-tightening torque curves

#### 3.3.2.4 Bumax DX – M16x100 – 10.9 – EN ISO 4017 – gleitmo 1952V

The Bumax DX – M16x100 duplex stainless steel bolting assemblies in property class 10.9, in short form BU_M16_DX, were arranged of following components including nominal mechanical properties based on Bumax datasheet:

- *Bolts:* BUFAB Group Bumax LDX - M16x100 A4 according to EN ISO 4017; stainless steel EN 1.4462; manufact.: 2016-06-20; PRE 36

  tensile strength $R_{m,min}$ (= $f_{ub}$): nominal 1000 N/mm²
  yield strength $R_{p0.2,min}$ (= $f_{yb}$): nominal 900 N/mm²
  elongation, min: nominal 0.3d

- *Nuts:* BUFAB Group Bumax 109 - M16 M6M A4 according to EN ISO 4032; stainless steel EN 1.4432, 1.4436, 1.4435; manufact.: 2015-02-26; PRE 27

  stress under proof load, min: nominal 1000 N/mm²

- *Washers:* BUFAB Group Bumax RB A4-HV300 according to EN ISO 7089; stainless steel EN 1.4432, 1.4436, 1.4435; with dimensions d = 17.0 mm, D = 30.0 mm, t = 3.0 mm; manufact.: 2015-12-14; PRE 27

  hardness, min: nominal 300 HV

The tightening test results of Bumax DX – M16x100 bolting assemblies are summarized in Table 40, Table 41 and Table 42. The statistical evaluation is shown as fulfilled and failed criteria according to EN 14399-3 (System HR). The tightening curves are presented in Figure 35 and Figure 36 and show, similar to the Bumax 109 – M16x100 and Bumax LDX – M16x100 series, less pronounced bolt force plateaus in the plastic range without any partial or total bolt fracture. All tested duplex bolting assemblies reached $F_{p,C}$* = 98.9 kN and $F_{p,C}$ = 109.9 kN. On the contrary, only 2 of 10 tested bolting assemblies achieved $F_{bi,max} \geq 0.9 \cdot f_{ub} \cdot A_s$ = 141.3 kN. Due to the less pronounced plastic plateaus, 2 of the 10 bolts achieved $\Delta\Theta_{1i,min}$ = 120°, 3 of 10 bolts fulfilled the $\Delta\Theta_{2i,min}$ = 240° criteria according to EN 14399-3. Furthermore, 7 of 10 tested bolts achieved k-class K1 with k-values in a wide range between 0.12 and 0.19 and a coefficient of variation of v = 16.92 % (compared to k = 0.12 – 0.17 and v = 13.58 % at $F_{p,C}$*). k-class K2 was not accomplished. For further information and summarized criteria see Table 42. The tightening graphs show irregular bolt force-tightening torque curves because of galling in the nut bearing surface when tightened into the plastic range especially after $F_{bi,max}$ including significant high ranges of values $M_i$ at end of the tests (bolt force dropped again to $F_{p,C}$). The coefficients of friction $\mu_{tot}$, $\mu_{th}$ and $\mu_b$ show noticeable high scattering, especially the friction under the nut bearing surface with a coefficient of variation of v = 35.62 % at $F_{p,C}$. Damages at the first and second load-bearing thread turn of the bolts and roughening of paired threads could be observed. Galling - especially in the faying surface washer/nut - could be observed, too.

**Table 40** Test results of Bumax DX – M16x100

| Legend | Specimens | $F_{p,C^*}$ kN | $F_{p,C}$ kN | Max F kN | Max T Nm | $\Theta_{pi}$ ° | $\Theta_{1i}$ ° | $\Theta_{2i}$ ° | $F_{bi}$ ($\Theta_{2i}$) kN | $\Delta\Theta_{1i}$ ° | $\Delta\Theta_{2i}$ ° | k ($F_{p,C^*}$) | k ($F_{p,C}$) | $\mu_{tot}$ ($F_{p,C}$) | $\mu_{th}$ ($F_{p,C}$) | $\mu_b$ ($F_{p,C}$) | M ($F_{p,C^*}$) Nm | $M_i$ ($F_{p,C}$) Nm | M ($F_{bi,max}$) Nm |
|---|---|---|---|---|---|---|---|---|---|---|---|---|---|---|---|---|---|---|---|
| max | | | | --- | | | | | | --- | --- | 0,16 | 0,16 | | | | | | |
| min | | | | 141,3 | | | | | | 120 | 240 | 0,10 | 0,10 | | | | | | |
| | BU_M16_DX-01 | 98,9 | 110 | <129,9 | 747,9 | 209 | 301 | 402 | 110,0 | <92 | <193 | >0,17 | >0,18 | 0,142 | 0,167 | 0,120 | 263,6 | 321,2 | 606,6 |
| | BU_M16_DX-02 | | | 145,4 | 608,5 | 187 | 316 | 463 | 110,0 | 129 | 277 | 0,12 | 0,12 | 0,089 | 0,127 | 0,055 | 188,7 | 213,9 | 385,5 |
| | BU_M16_DX-03 | | | <135,3 | 574,8 | 189 | 287 | 402 | 110,0 | <98 | <213 | 0,13 | 0,13 | 0,097 | 0,147 | 0,054 | 200,0 | 230,7 | 394,1 |
| | BU_M16_DX-04 | | | <131,3 | 821,1 | 193 | 274 | 496 | 110,0 | <81 | 303 | 0,13 | 0,14 | 0,105 | 0,139 | 0,076 | 208,1 | 247,3 | 450,4 |
| | BU_M16_DX-05 | | | <134,9 | 589,6 | 191 | 289 | 399 | 109,9 | <98 | <208 | 0,13 | 0,14 | 0,103 | 0,163 | 0,051 | 208,5 | 242,1 | 389,7 |
| | BU_M16_DX-07 | | | <133,7 | 829,1 | 189 | 292 | 393 | 110,0 | <103 | <204 | 0,14 | 0,16 | 0,123 | 0,150 | 0,100 | 227,3 | 284,1 | 585,8 |
| | BU_M16_DX-08 | | | <126,1 | 683,8 | 202 | 264 | 357 | 110,0 | <62 | <155 | 0,16 | >0,18 | 0,137 | 0,179 | 0,100 | 249,3 | 310,9 | 451,3 |
| | BU_M16_DX-10 | | | <123,1 | 693,4 | 192 | 254 | 333 | 110,0 | <62 | <141 | 0,16 | >0,19 | 0,152 | 0,170 | 0,137 | 257,2 | 342,1 | 560,1 |
| | BU_M16_DX-11 | | | 142,5 | 875,7 | 184 | 362 | 547 | 110,0 | 177 | 363 | 0,12 | 0,13 | 0,094 | 0,098 | 0,091 | 184,8 | 225,4 | 652,5 |
| | BU_M16_DX-12 | | | <135,4 | 648,5 | 192 | 290 | 399 | 110,0 | <98 | <206 | 0,12 | 0,13 | 0,093 | 0,132 | 0,060 | 186,0 | 223,6 | 475,9 |

**Table 41** Statistical evaluation of Bumax DX – M16x100

| Bumax DX - M16x100 ISO 4017 - Gleitmo 1952V n = 10 | Max F kN | Max T Nm | $\Theta_{pi}$ ° | $\Theta_{1i}$ ° | $\Theta_{2i}$ ° | $F_{bi}$ ($\Theta_{2i}$) kN | $\Delta\Theta_{1i}$ ° | $\Delta\Theta_{2i}$ ° | k ($F_{p,C^*}$) | k ($F_{p,C}$) | $\mu_{tot}$ ($F_{p,C}$) | $\mu_{th}$ ($F_{p,C}$) | $\mu_b$ ($F_{p,C}$) | M ($F_{p,C^*}$) Nm | $M_i$ ($F_{p,C}$) Nm | M ($F_{bi,max}$) Nm |
|---|---|---|---|---|---|---|---|---|---|---|---|---|---|---|---|---|
| max | 145,4 | 875,7 | 209 | 362 | 547 | 110,0 | 177 | 363 | 0,17 | 0,19 | 0,152 | 0,179 | 0,137 | 263,6 | 342,1 | 652,5 |
| min | 123,1 | 574,8 | 184 | 254 | 333 | 109,9 | 62 | 141 | 0,12 | 0,12 | 0,089 | 0,098 | 0,051 | 184,8 | 213,9 | 385,5 |
| R | 22,3 | 300,9 | 25 | 108 | 214 | 0,1 | 115 | 222 | 0,05 | 0,07 | 0,063 | 0,081 | 0,086 | 78,8 | 128,2 | 267,0 |
| $\bar{x}$ | 133,8 | 707,2 | 193 | 293 | 419 | 110,0 | 100 | 226 | 0,14 | 0,15 | 0,114 | 0,147 | 0,084 | 217,4 | 264,1 | 495,2 |
| s | 6,8 | 107,1 | 7 | 30 | 65 | 0,0 | 34 | 68 | 0,02 | 0,03 | 0,023 | 0,024 | 0,030 | 30,1 | 46,5 | 98,5 |
| ν | 5,06 | 15,14 | 3,83 | 10,27 | 15,41 | 0,03 | 33,51 | 30,20 | 13,58 | 16,92 | 20,33 | 16,50 | 35,62 | 13,87 | 17,61 | 19,89 |

with n: number; R: range; x: mean value; s: standard deviation; ν: coefficient of variation in [%]

**Table 42** Evaluation of test results of Bumax DX – M16x100 according to EN 14399-3

| n | $F_{p,C}^*$ | $F_{p,C}$ | $F_{bi,max}$ | $\Delta\Theta_{1i,min}$ | $\Delta\Theta_{2i,min}$ | k-values | k-class K1 | k-class K2 | | Fracture | Galling |
|---|---|---|---|---|---|---|---|---|---|---|---|
| [-] | 98.9 kN | 109.9 kN | ≥ 141.3 kN | ≥ 120° | ≥ 240° | [-] | $0.10 \leq k_i \leq 0.16$ | $0.10 \leq k_m \leq 0.23$ | $V_k \leq 0.06$ | | |
| 10 | 100% | 100% | 20% | 20% | 30% | 0.12 – 0.19 | 70% | 0.150 | 0.169 | 0% | 100% |

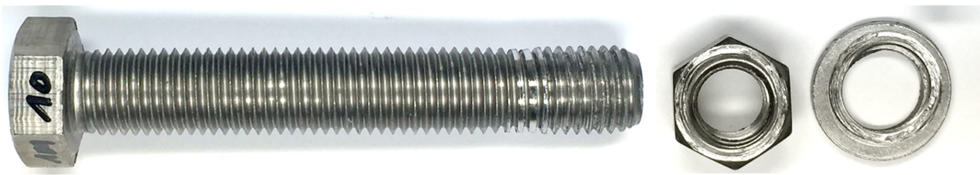


**Figure 34** BU_M16_DX test specimen after tightening

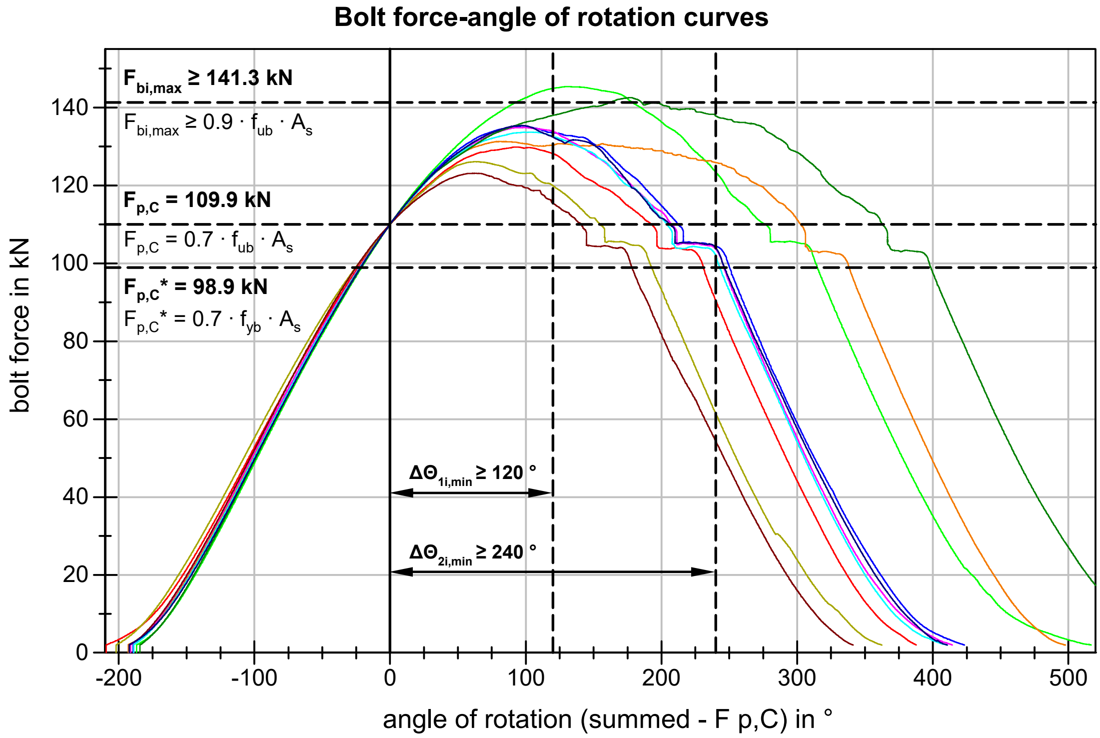


**Figure 35** BU_M16_DX Bolt force-angle of rotation curves

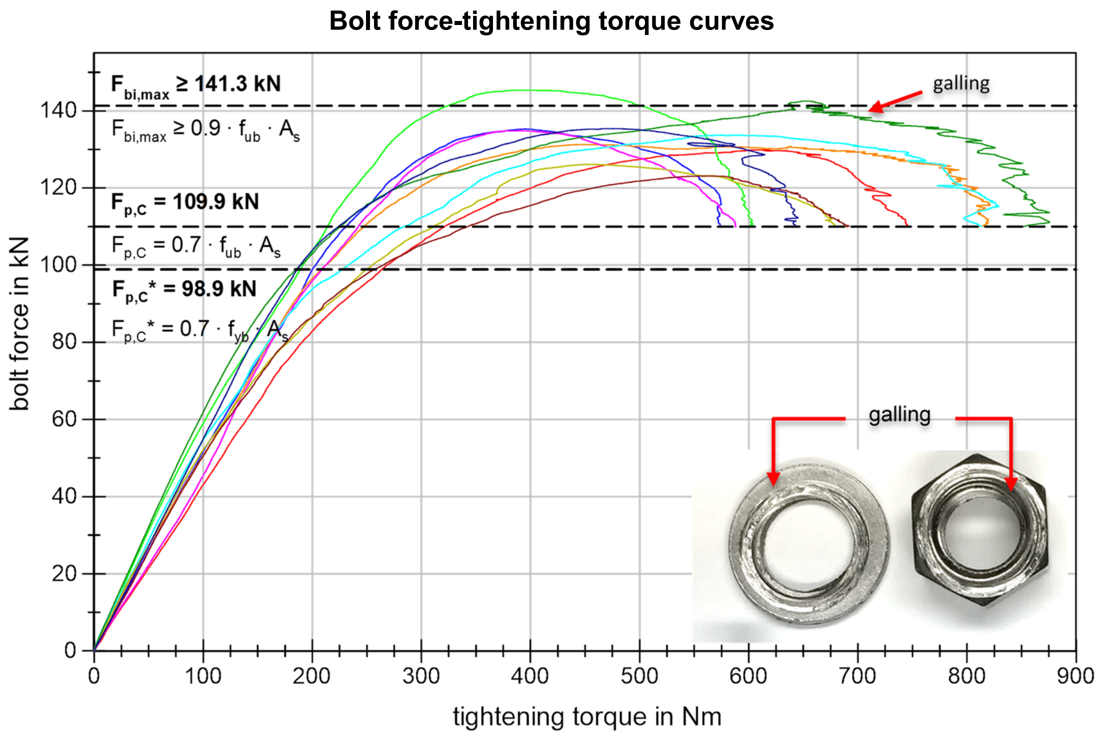


**Figure 36** BU_M16_DX Bolt force-tightening torque curves

### 3.3.3 Bolt dimension M20

The tests of Bumax 88 – M20x100 bolting assemblies according to EN ISO 4017 were performed with bolts manufactured in 2013 (first series) and in addition with bolts produced in the year 2015 (second series). Bumax 88 – M20x100 (2013) showed irregular results, so it has been decided to stop the tightening tests after five tested specimens and repeat testing with the bolts manufactured in 2015. Both series were tested with the same test setup to assure comparable testing conditions: The clamp length ∑t was set to 75.0 mm (clamp length/bolt diameter ratio of 3.8) in reference to EN 14399-3. As a complement to the Bumax 88 bolting assemblies, tightening tests of Bumax 109 austenitic stainless steel bolting assemblies according to EN ISO 4014 were performed to investigate basic preloading behaviour. The Bumax 109 – M20x140 bolts were tested with a clamping length of ∑t = 105.0 mm and a clamp length/bolt diameter ratio of 5.3. In addition, lean duplex and duplex bolts M20x100 (∑t = 72.0 mm and clamp length/bolt diameter ratio of 4.9) according to EN ISO 4017 were tested as well. The nut was turned to tighten the assembly with a constant speed of rotation of 2.0 $min^{-1}$ for Bumax 88 and 109 and 5.0 $min^{-1}$ for the lean duplex and duplex bolts. Overall, the tightening tests were stopped when the bolt force dropped to $F_{p,C}$ after exceeding $F_{p,C}$ once.

With normative reference to EN 14399-3, the relevant criteria for the evaluation of the Bumax 88 bolting assemblies were defined as follows:

- $F_{p,C}^* = 0.7 \cdot f_{yb} \cdot A_s = 0.7 \cdot 640$ N/mm² $\cdot$ 245.0 mm² = 109.7 kN (DIN EN 1993-1-8/NA:2010-10)
- $F_{p,C} = 0.7 \cdot f_{ub} \cdot A_s = 0.7 \cdot 800$ N/mm² $\cdot$ 245.0 mm² = 137.2 kN
- $F_{bi,max} \geq 0.9 \cdot f_{ub} \cdot A_s = 0.9 \cdot 800$ N/mm² $\cdot$ 245.0 mm² = 176.4 kN
- $\Delta\Theta_{1i,min} \geq 120°$ with $\Sigma t$ = 75.0 mm: $2d \leq \Sigma t < 6d$
- $\Delta\Theta_{2i,min} \geq 240°$ with $\Sigma t$ = 75.0 mm: $2d \leq \Sigma t < 6d$

Moreover, the criteria fro the evaluation of the bolting assemblies in property class 10.9 (meaning Bumax 109, Bumax lean duplex and Bumax duplex series) were defined as follows:

- $F_{p,C}^* = 0.7 \cdot f_{yb} \cdot A_s = 0.7 \cdot 800$ N/mm² $\cdot$ 245.0 mm² = 137.2 kN (for Bumax 109 bolts)
- $F_{p,C}^* = 0.7 \cdot f_{yb} \cdot A_s = 0.7 \cdot 900$ N/mm² $\cdot$ 245.0 mm² = 154.4 kN (for Bumax LDX and DX)
- $F_{p,C} = 0.7 \cdot f_{ub} \cdot A_s = 0.7 \cdot 1000$ N/mm² $\cdot$ 245.0 mm² = 171.5 kN
- $F_{bi,max} \geq 0.9 \cdot f_{ub} \cdot A_s = 0.9 \cdot 1000$ N/mm² $\cdot$ 245.0 mm² = 220.5 kN
- $\Delta\Theta_{1i,min} \geq 120°$ with $\Sigma t$ = 105.0 mm: $2d \leq \Sigma t < 6d$
- $\Delta\Theta_{2i,min} \geq 240°$ with $\Sigma t$ = 105.0 mm: $2d \leq \Sigma t < 6d$

All tightening tests were carried out in accordance to EN 14399-2 and EN ISO 16047 using the test setup shown in Table 43 and Table 44.

**Table 43** Test setup Bumax 88/LDX/DX – M20x100 series

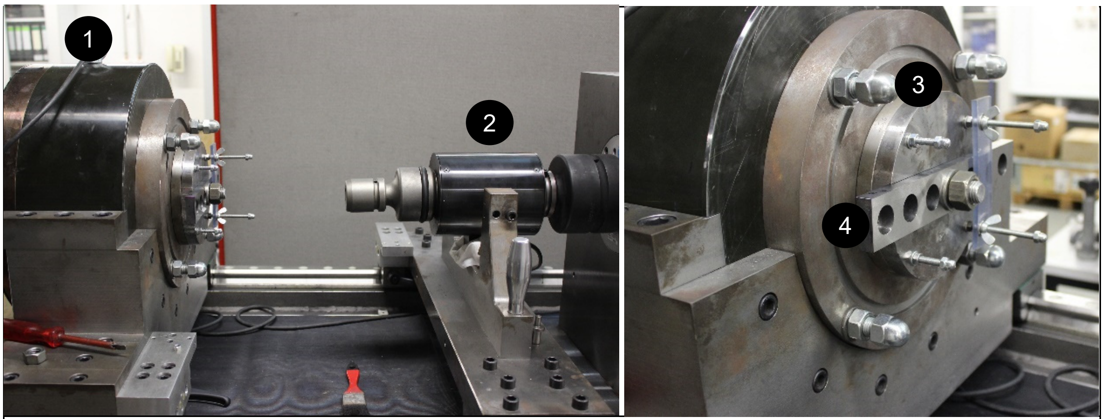


| | | |
|---|---|---|
| **1** | Sensor force – thread friction torque: SNo. 1016242 – 1,500 kN / 5,000 Nm | |
| **2** | Sensor total tightening torque – angle of rotation: SNo. 1024283 – 5,000 Nm | |
| **3** | Shims: DP 15mm + M20HV | Lubrication: gleitmo 1952V |
| **4** | Support bar: Yes | Adapter: Yes |
| | Speed of rotation: 2.0 $min^{-1}$ (88) and 5.0 $min^{-1}$ | Rotated component: Hexagon nut |
| | Number of bolting assemblies tested: 5/10 | Washers: placed under nut |
| | Clamp length ∑t = 75.0 mm according to EN 14399-3:2015-03 | |
| | Clamp length/bolt diameter ratio: 3.8 | Stop criteria: bolt force dropped to $F_{p,C}$ |

**Table 44** Test setup Bumax 109 – M20x140

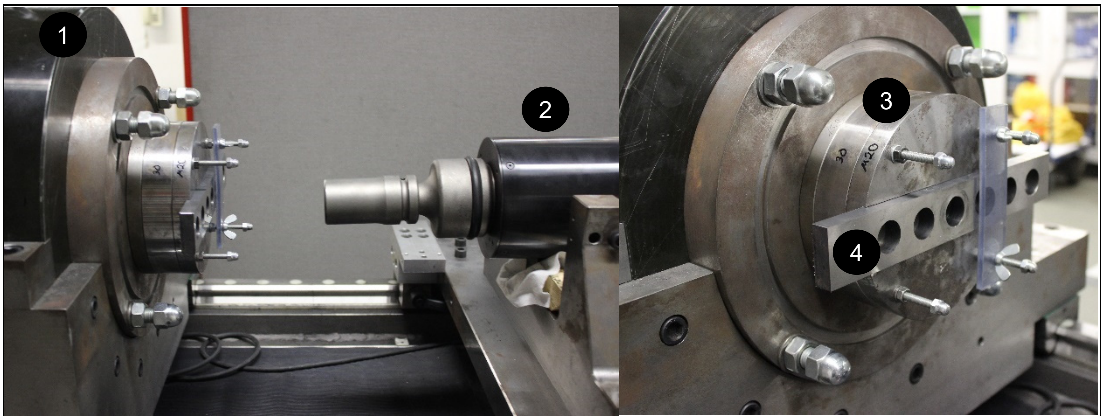


| | | |
|---|---|---|
| **1** | Sensor force – thread friction torque: SNo. 1016242 – 1,500 kN / 5,000 Nm | |
| **2** | Sensor total tightening torque – angle of rotation: SNo. 1024283 – 5,000 Nm | |
| **3** | Shims: DP 15mm + DP 30mm + M20HV | Lubrication: gleitmo 1952V |
| **4** | Support bar: Yes | Adapter: Yes |
| | Speed of rotation: 2.0 $min^{-1}$ | Rotated component: Hexagon nut |
| | Number of bolting assemblies tested: 10 | Washers: placed under nut |
| | Clamp length ∑t = 105.0 mm according to EN 14399-3:2015-03 | |
| | Clamp length/bolt diameter ratio: 5.3 | Stop criteria: bolt force dropped to $F_{p,C}$ |

#### *3.3.3.1 Bumax 88 – M20x100 (2013) – 8.8 – EN ISO 4017 – gleitmo 1952V*

Bumax 88 – M20x100 austenitic stainless steel bolting assemblies, property class 8.8 and bolts manufactured in 2013, abbreviated below as BU_M20_88 (2013), were arranged of following components including nominal mechanical properties based on Bumax datasheet:

- *Bolts:* BUFAB Group Bumax 88 – M20x100 A4 according to EN ISO 4017; stainless steel EN 1.4432, 1.4436, 1.4435; manufact.: 2013-12-12; PRE 27

  tensile strength $R_{m,min}$ (= $f_{ub}$): nominal 800 N/mm²
  yield strength $R_{p0.2,min}$ (= $f_{yb}$): nominal 640 N/mm²
  elongation, min: nominal 0.3d

- *Nuts:* BUFAB Group Bumax 88 – M20 M6M A4 according to EN ISO 4032; stainless steel EN 1.4432, 1.4436, 1.4435; manufact.: 2014-06-05; PRE 27

  stress under proof load, min: nominal 800 N/mm²

- *Washers:* BUFAB Group Bumax RB A4-HV200 according to EN ISO 7089; stainless steel EN 1.4432, 1.4436, 1.4435; with dimensions d = 21.0 mm, D = 37.0 mm, t = 3.0 mm; manufact.: 2014-03-19; PRE 27

  hardness, min: nominal 200 HV

The test results of Bumax 88 – M20x100 (2013 series) EN ISO 4017 bolting assemblies are summarized in Table 45, Table 46 and Table 47 showing the statistical evaluation as well as the summarized fulfilled and failed criteria according to EN 14399-3. In addition, Figure 38 and Figure 39 show the tightening graphs for these bolting assemblies. All tested bolting assemblies reached the specified preload of $F_{p,C}$* = 109.7 kN and $F_{p,C}$ = 137.2 kN. One of the specimens (BU_M20_88-03) reached $F_{bi,max}$ at 138 kN, near to $F_{p,C}$. A visual failure could not be noticed. The k-values at $F_{p,C}$ lie between 0.21 and 0.33 and result in a very high coefficient of variation of 21.71 % (compared to k = 0.20 – 0.28 and v = 16.02 % at $F_{p,C}$*) because of the one irregular test. Neglecting this test, the k-values at $F_{p,C}$ lie between 0.21 and 0.22 which equates to a very low coefficient of variation. Nevertheless, criteria for k-class K1 and k-class K2 failed. Also, all bolts failed the demanded maximum bolt force $F_{bi,max} \geq 0.9 \cdot f_{ub} \cdot A_s$ = 176.4 kN. Furthermore, they clearly not fullfilled the required angles of rotation $\Delta\Theta_{1i,min}$ and $\Delta\Theta_{2i,min}$. The graphs show also irregular bolt force-tightening torque curves because of galling in the nut bearing surface when the bolts are tightened into the plastic range. Similar to the previously described test series, damages at the first and second load-bearing thread turn of the bolts and roughening of the paired threads could be observed; bolt failure by partial or total fracture did not occur. In contrast to other tested series, galling in the faying surface washer/nut could be observed for only one tested specimen. Furthermore, the functionality and re-use of all tested bolting assemblies is limited.

**Table 45** Test results of Bumax 88 – M20x100 (2013)

| | | $F_{p,C}$ | Max F | Max T | $\Theta_{pi}$ | $\Theta_{1i}$ | $\Theta_{2i}$ | $F_{bi}$ ($\Theta_{2i}$) | $\Delta\Theta_{1i}$ | $\Delta\Theta_{2i}$ | k ($F_{p,C}$) | $\mu_{tot}$ ($F_{p,C}$) | $\mu_{th}$ ($F_{p,C}$) | $\mu_b$ ($F_{p,C}$) | $F_{p,C}$* | k ($F_{p,C*}$) | $M_i$ ($F_{p,C}$) | M ($F_{p,C}$*) | M ($F_{bi,max}$) |
|---|---|---|---|---|---|---|---|---|---|---|---|---|---|---|---|---|---|---|---|
| | | kN | kN | Nm | ° | ° | ° | kN | ° | ° | | | | | kN | | Nm | Nm | Nm |
| max | | | --- | | | | | | --- | --- | 0,16 | | | | | 0,16 | | | |
| min | | | 176,4 | | | | | | 120 | 240 | 0,10 | | | | | 0,10 | | | |
| | BU_M20_88-01 | 137,2 | <163,4 | 1021,4 | 205 | 279 | 381 | 137,2 | <74 | <176 | >0,21 | 0,166 | 0,234 | 0,106 | 109,7 | >0,20 | 572,0 | 439,5 | 873,4 |
| | BU_M20_88-02 | | <152,0 | 1054,3 | 222 | 267 | 345 | 137,1 | <45 | <123 | >0,22 | 0,174 | 0,254 | 0,104 | | >0,20 | 597,2 | 429,7 | 784,1 |
| | BU_M20_88-03 | | <137,9 | 985,1 | 245 | 248 | 263 | 137,2 | <3 | <18 | >0,33 | 0,271 | 0,351 | 0,201 | | >0,28 | 901,0 | 617,5 | 912,9 |
| | BU_M20_88-04 | | <161,7 | 985,3 | 208 | 281 | 421 | 137,2 | <74 | <214 | >0,21 | 0,171 | 0,215 | 0,133 | | >0,20 | 588,8 | 438,5 | 799,5 |
| | BU_M20_88-05 | | <151,6 | 902,6 | 210 | 259 | 363 | 137,2 | <49 | <152 | >0,22 | 0,178 | 0,290 | 0,079 | | >0,21 | 609,5 | 459,7 | 739,0 |

**Table 46** Statistical evaluation of Bumax 88 – M20x100 (2013)

| BU_M20_88 (2013) n = 5 | Max F kN | Max T Nm | $\Theta_{pi}$ ° | $\Theta_{1i}$ ° | $\Theta_{2i}$ ° | $F_{bi}$ ($\Theta_{2i}$) kN | $\Delta\Theta_{1i}$ ° | $\Delta\Theta_{2i}$ ° | $\mu_{tot}$ ($F_{p,C}$) | $\mu_{th}$ ($F_{p,C}$) | $\mu_b$ ($F_{p,C}$) | $M_i$ ($F_{p,C}$) Nm | k ($F_{p,C}$) | M ($F_{p,C}$*) Nm | k ($F_{p,C*}$) | M ($F_{bi,max}$) Nm |
|---|---|---|---|---|---|---|---|---|---|---|---|---|---|---|---|---|
| max | 163,4 | 1054,3 | 245 | 281 | 421 | 137,2 | 74 | 214 | 0,271 | 0,351 | 0,201 | 901,0 | 0,33 | 617,5 | 0,28 | 912,9 |
| min | 137,9 | 902,6 | 205 | 248 | 263 | 137,1 | 3 | 18 | 0,166 | 0,215 | 0,079 | 572,0 | 0,21 | 429,7 | 0,20 | 739,0 |
| R | 25,5 | 151,7 | 40 | 33 | 158 | 0,1 | 71 | 196 | 0,105 | 0,136 | 0,122 | 329,0 | 0,12 | 187,8 | 0,08 | 173,9 |
| $\bar{x}$ | 153,3 | 989,7 | 218 | 267 | 355 | 137,2 | 49 | 137 | 0,192 | 0,269 | 0,125 | 653,7 | 0,24 | 477,0 | 0,22 | 821,8 |
| s | 10,2 | 56,6 | 16 | 14 | 58 | 0,0 | 29 | 74 | 0,044 | 0,054 | 0,047 | 138,9 | 0,05 | 79,3 | 0,03 | 70,2 |
| ν | 6,64 | 5,72 | 7,53 | 5,18 | 16,48 | 0,03 | 59,34 | 54,33 | 23,11 | 19,97 | 37,55 | 21,25 | 21,71 | 16,63 | 16,02 | 8,55 |

with n: number; R: range; x: mean value; s: standard deviation; ν: coefficient of variation in [%]

**Table 47** Evaluation of test results of Bumax 88 – M20x100 (2013) according to EN 14399-3

| n | $F_{p,C}$* | $F_{p,C}$ | $F_{bi,max}$ | $\Delta\Theta_{1i,min}$ | $\Delta\Theta_{2i,min}$ | k-values | k-class K1 | k-class K2 | | Fracture | Galling |
|---|---|---|---|---|---|---|---|---|---|---|---|
| [-] | 109.7 kN | 137.2 kN | ≥ 176.4 kN | ≥ 120° | ≥ 240° | [-] | $0.10 \le k_i \le 0.16$ | $0.10 \le k_m \le 0.23$ | $V_k \le 0.06$ | | |
| 5 | 100% | 100% | 0% | 0% | 0% | 0.21 – 0.33 | 0% | 0.239 | 0.217 | 0% | 20% |

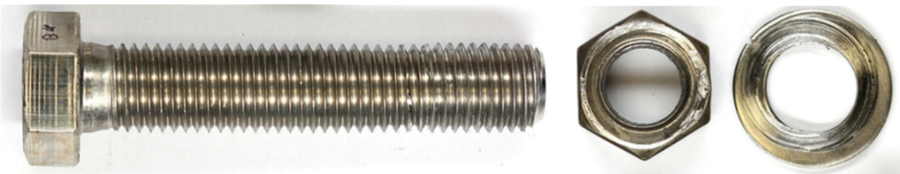

**Figure 37** BU_M20_88 (2013) test specimen after tightening

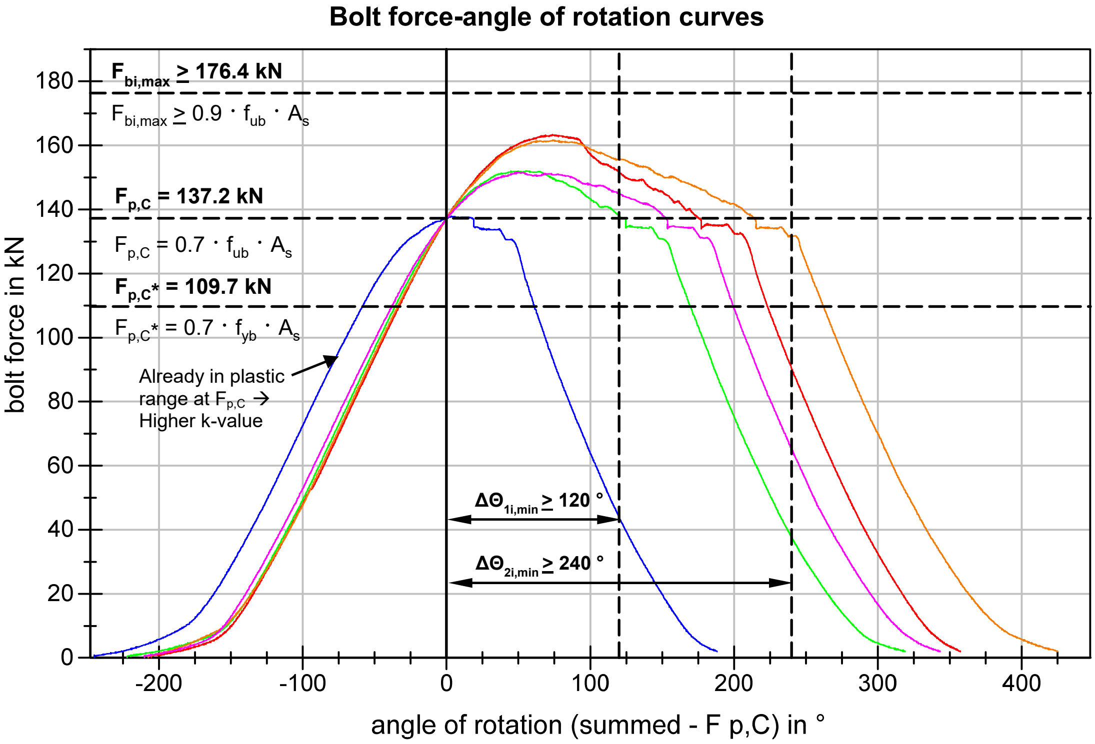


**Figure 38** BU_M20_88 (2013) Bolt force-angle of rotation curves

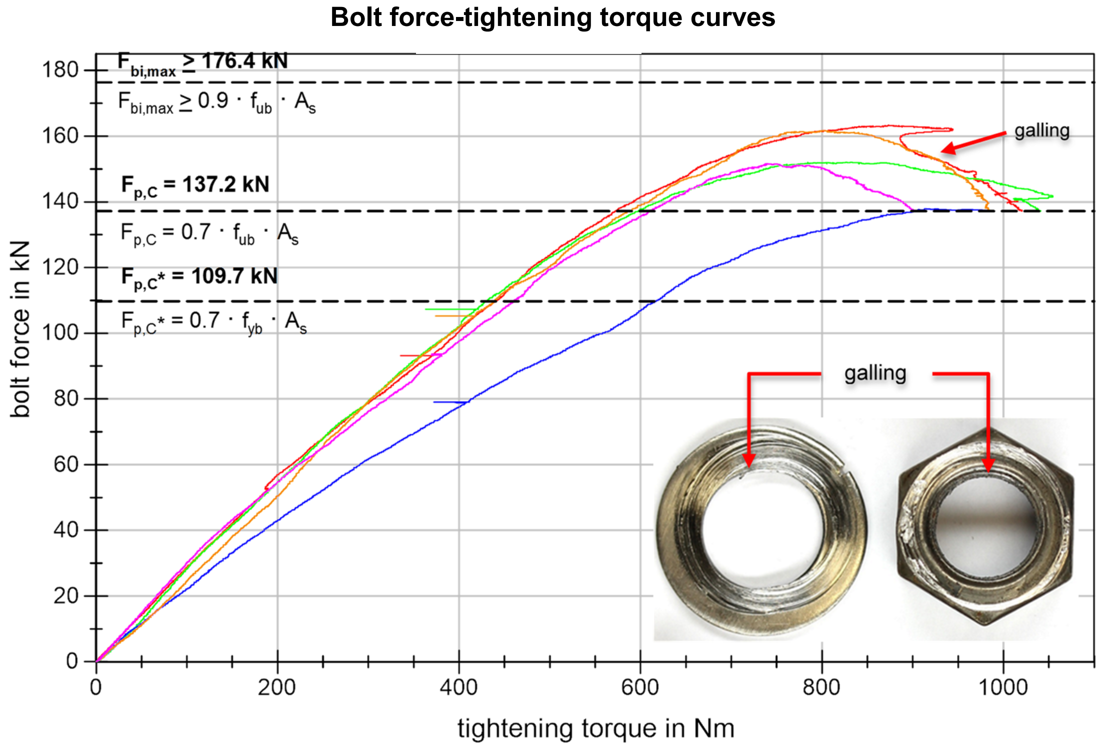


**Figure 39** BU_M20_88 (2013) Bolt force-tightening torque-curves

### *3.3.3.2 Bumax 88 – M20x100 (2015) – 8.8 – EN ISO 4017 – gleitmo 1952V*

In addition to the tightening tests described before and due to the irregular results, further Bumax 88 – M20x100 austenitic stainless steel bolting assemblies, property class 8.8 with bolts manufactured in 2015, abbreviated below as BU_M20_88 (2015), were tested and arranged of following components including the nominal mechanical properties based on Bumax datasheet:

- *Bolts:* BUFAB Group Bumax 88 – M20x100 A4 according to EN ISO 4017; stainless steel EN 1.4432, 1.4436, 1.4435; manufact.: 2015-06-05; PRE 27

  tensile strength $R_{m,min}$ (= $f_{ub}$): nominal 800 N/mm²
  yield strength $R_{p0.2,min}$ (= $f_{yb}$): nominal 640 N/mm²
  elongation, min: nominal 0.3d

- *Nuts:* BUFAB Group Bumax 88 – M20 M6M A4 according to EN ISO 4032; stainless steel EN 1.4432, 1.4436, 1.4435; manufact.: 2015-05-11; PRE 27

  stress under proof load, min: nominal 800 N/mm²

- *Washers:* BUFAB Group Bumax RB A4-HV200 according to EN ISO 7089; stainless steel EN 1.4432, 1.4436, 1.4435; with dimensions d = 21.0 mm, D = 37.0 mm, t = 3.0 mm; manufact.: 2014-03-19; PRE 27

  hardness, min: nominal 200 HV

As a continuation of the previously presented Bumax 88 – M20x100 series (bolts manufactured in 2013), the test results of the 2015 produced bolts according to EN ISO 4017, property class 8.8 with a nominal length of 100.0 mm are shown in Table 48, Table 49 and Table 50 including the evaluation of the tightening tests and the statistical data referred to EN 14399-3. Figure 41 and Figure 42 show the tightening graphs. In contrast to the 2013 series, the BU_M20_88 (2015) test series shows a different behaviour with a more pronounced bolt force plateau in the plastic range. All tested bolting assemblies reached $F_{p,C}$ = 137.2 kN and 9 of 10 bolting assemblies achieved $F_{bi,max} \geq 0.9 \cdot f_{ub} \cdot A_s$ = 176.4 kN. Furthermore, 8 of 10 tested bolts achieved k-class K1 with k-values between 0.12 and 0.17. On the contrary, k-class K2 was not accomplished because of a high coefficient of variation. It can be seen that 3 of 10 bolts reached $\Delta\Theta_{1i,min.}$, however 9 of 10 bolts achieved the criteria for $\Delta\Theta_{2i,min}$. For further information and summarized criteria see Table 50. Galling did occur when the bolts were tightened into the plastic range and leads to irregular bolt force-tightening torque curves as shown in Figure 42 including remarkable high ranges of tightening torque. The statistical evaluation underlines high coefficients of variation for friction and maximum torque. Damages at the first and second load-bearing thread turn of the bolts and nuts as well as minor and major roughening of paired threads occurred as well. Compared to the previously tested series, especially damages of the hexagon nut threads occured. Partial or total bolt fracture did not occur. Visible necking of the threaded shank and galling in the faying-surface washer/nut were detected, too.

**Table 48** Test results of Bumax 88 – M20x100 (2015)

| | | $F_{p,C}$ | Max F | Max T | $\Theta_{pi}$ | $\Theta_{1i}$ | $\Theta_{2i}$ | $F_{bi}$ ($\Theta_{2i}$) | $\Delta\Theta_{1i}$ | $\Delta\Theta_{2i}$ | k ($F_{p,C}$) | $\mu_{tot}$ ($F_{p,C}$) | $\mu_{th}$ ($F_{p,C}$) | $\mu_b$ ($F_{p,C}$) | $F_{p,C}$* | k ($F_{p,C*}$) | $M_i$ ($F_{p,C}$) | M ($F_{p,C}$*) | M ($F_{bi,max}$) |
|---|---|---|---|---|---|---|---|---|---|---|---|---|---|---|---|---|---|---|---|
| | | kN | kN | Nm | ° | ° | ° | kN | ° | ° | | | | | kN | | Nm | Nm | Nm |
| max | | | --- | | | | | | --- | --- | 0,16 | | | | | 0,16 | | | |
| min | | | 176,4 | | | | | | 120 | 240 | 0,10 | | | | | 0,10 | | | |
| | BU_M20_88-06 | 137,2 | 189,4 | 958,8 | 233 | 364 | 602 | 137,2 | 132 | 369 | 0,12 | 0,088 | 0,119 | 0,062 | 109,7 | 0,12 | 331,1 | 265,4 | 629,2 |
| | BU_M20_88-07 | | 188,1 | 1346,0 | 197 | 309 | 517 | 137,1 | <112 | 320 | 0,15 | 0,113 | 0,147 | 0,084 | | 0,14 | 409,2 | 299,0 | 768,7 |
| | BU_M20_88-08 | | 185,2 | 1005,1 | 214 | 328 | 542 | 137,2 | <114 | 328 | 0,14 | 0,103 | 0,139 | 0,071 | | 0,13 | 375,0 | 287,2 | 725,6 |
| | BU_M20_88-09 | | 179,7 | 1551,6 | 193 | 303 | 545 | 137,2 | <110 | 352 | >0,17 | 0,128 | 0,132 | 0,124 | | 0,15 | 453,9 | 339,7 | 1017,5 |
| | BU_M20_88-10 | | 177,4 | 1047,5 | 215 | 320 | 491 | 137,2 | <105 | 276 | 0,15 | 0,118 | 0,174 | 0,069 | | 0,15 | 423,9 | 323,6 | 704,8 |
| | BU_M20_88-11 | | 184,9 | 1260,9 | 190 | 302 | 523 | 137,2 | <112 | 333 | 0,16 | 0,122 | 0,172 | 0,079 | | 0,15 | 437,1 | 339,0 | 755,8 |
| | BU_M20_88-12 | | 178,0 | 969,5 | 203 | 308 | 463 | 137,2 | <105 | 260 | 0,15 | 0,115 | 0,178 | 0,059 | | 0,14 | 412,9 | 315,4 | 757,0 |
| | BU_M20_88-13 | | 191,7 | 872,2 | 204 | 326 | 608 | 137,2 | 121 | 403 | 0,13 | 0,093 | 0,131 | 0,060 | | 0,13 | 346,1 | 282,7 | 599,7 |
| | BU_M20_88-14 | | <171,4 | 1167,7 | 204 | 286 | 424 | 137,1 | <81 | <219 | >0,16 | 0,123 | 0,179 | 0,075 | | 0,15 | 440,3 | 323,9 | 705,1 |
| | BU_M20_88-15 | | 185,6 | 1084,1 | 217 | 340 | 507 | 137,1 | 122 | 289 | 0,12 | 0,090 | 0,117 | 0,066 | | 0,12 | 335,1 | 258,8 | 731,2 |

**Table 49** Statistical evaluation of Bumax 88 – M20x100 (2015)

| BU_M20_88 (2015) | Max F | Max T | $\Theta_{pi}$ | $\Theta_{1i}$ | $\Theta_{2i}$ | $F_{bi}$ ($\Theta_{2i}$) | $\Delta\Theta_{1i}$ | $\Delta\Theta_{2i}$ | $\mu_{tot}$ ($F_{p,C}$) | $\mu_{th}$ ($F_{p,C}$) | $\mu_b$ ($F_{p,C}$) | $M_i$ ($F_{p,C}$) | k ($F_{p,C}$) | M ($F_{p,C}$*) | k ($F_{p,C*}$) | M ($F_{bi,max}$) |
|---|---|---|---|---|---|---|---|---|---|---|---|---|---|---|---|---|
| n = 10 | kN | Nm | ° | ° | ° | kN | ° | ° | | | | Nm | | Nm | | Nm |
| max | 191,7 | 1551,6 | 233 | 364 | 608 | 137,2 | 132 | 403 | 0,128 | 0,179 | 0,124 | 453,9 | 0,17 | 339,7 | 0,15 | 1017,5 |
| min | 171,4 | 872,2 | 190 | 286 | 424 | 137,1 | 81 | 219 | 0,088 | 0,117 | 0,059 | 331,1 | 0,12 | 258,8 | 0,12 | 599,7 |
| R | 20,3 | 679,4 | 43 | 78 | 184 | 0,1 | 51 | 184 | 0,040 | 0,062 | 0,065 | 122,8 | 0,05 | 80,9 | 0,03 | 417,8 |
| $\bar{x}$ | 183,1 | 1126,3 | 207 | 319 | 522 | 137,2 | 111 | 315 | 0,109 | 0,149 | 0,075 | 396,5 | 0,15 | 303,5 | 0,14 | 739,5 |
| s | 6,3 | 207,9 | 13 | 22 | 57 | 0,0 | 14 | 55 | 0,015 | 0,025 | 0,019 | 46,1 | 0,02 | 29,3 | 0,01 | 112,1 |
| ν | 3,45 | 18,45 | 6,25 | 6,98 | 10,87 | 0,04 | 12,13 | 17,39 | 13,47 | 16,67 | 25,49 | 11,62 | 11,83 | 9,64 | 8,91 | 15,16 |

with n: number; R: range; x: mean value; s: standard deviation; ν: coefficient of variation in [%]

**Table 50** Evaluation of test results of Bumax 88 – M20x100 (2015) according to EN 14399-3

| n | $F_{p,C}$* | $F_{p,C}$ | $F_{bi,max}$ | $\Delta\Theta_{1i,min}$ | $\Delta\Theta_{2i,min}$ | k-values | k-class K1 | k-class K2 | | Fracture | Galling |
|---|---|---|---|---|---|---|---|---|---|---|---|
| [-] | 109.7 kN | 137.2 kN | ≥ 176.4 kN | ≥ 120° | ≥ 240° | [-] | 0.10 ≤ $k_i$ ≤ 0.16 | 0.10 ≤ $k_m$ ≤ 0.23 | $V_k$ ≤ 0.06 | | |
| 10 | 100% | 100% | 90% | 30% | 90% | 0.12 – 0.17 | 80% | 0.145 | 0.118 | 0% | 100% |

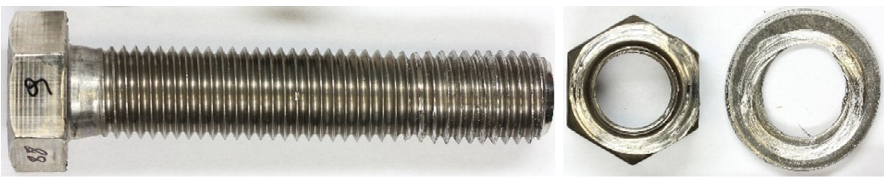

**Figure 40** BU_M20_88 (2015) test specimen after tightening

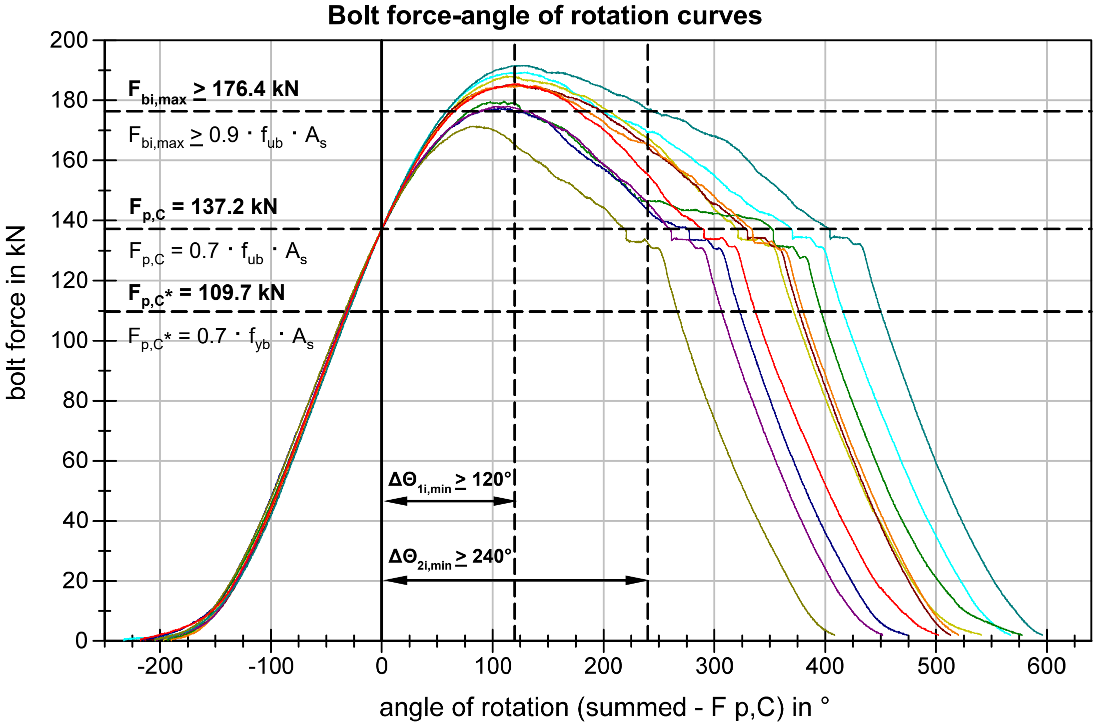


**Figure 41** BU_M20_88 (2015) Bolt force-angle of rotation curves

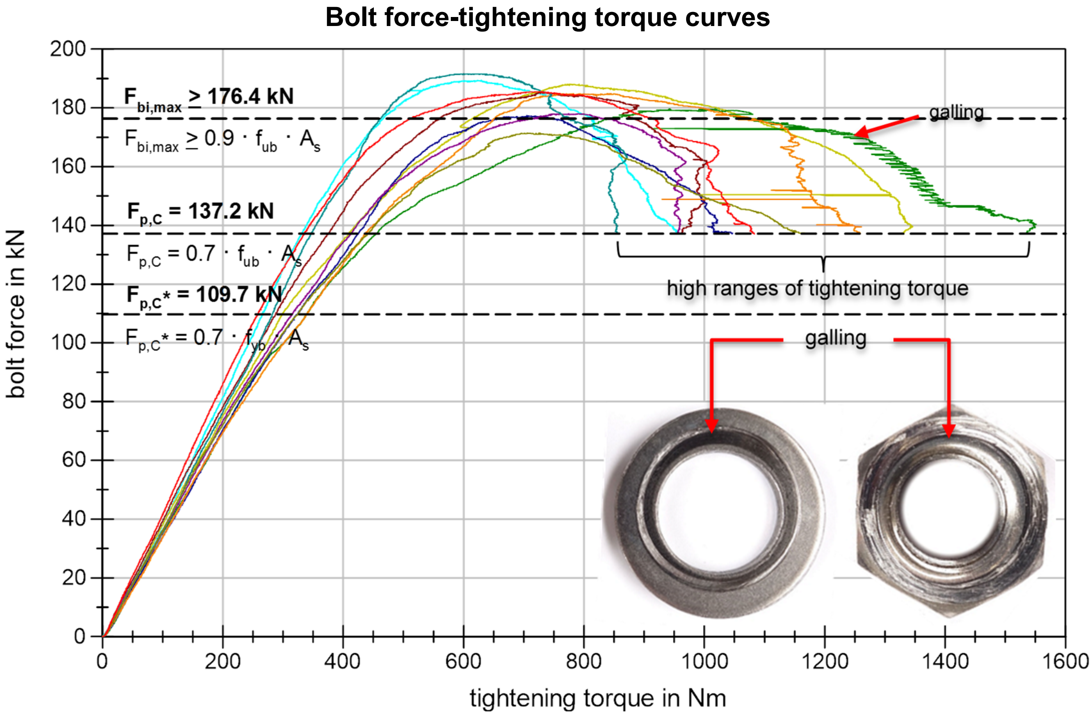


**Figure 42** BU_M20_88 (2015) Bolt force-tightening torque curves

### *3.3.3.3 Bumax 109 – M20x140 – 10.9 – EN ISO 4014 – gleitmo 1952V*

Bumax 109 – M20x140 austenitic stainless steel bolting assemblies in property class 10.9 according to EN ISO 4014, abbreviated below as BU_M20_109, were arranged of the following components including the nominal mechanical properties based on Bumax datasheet:

- *Bolts:* BUFAB Group Bumax 109 – M20x140 A4 according to EN ISO 4014; stainless steel EN 1.4432, 1.4436, 1.4435; manufact.: 2014-05-05; PRE 27

  tensile strength $R_{m,min}$ (= $f_{ub}$): nominal 1000 N/mm²
  yield strength $R_{p0.2,min}$ (= $f_{yb}$): nominal 800 N/mm²
  elongation, min: nominal 0.3d

- *Nuts:* BUFAB Group Bumax 109 – M20 M6M A4 according to EN ISO 4032; stainless steel EN 1.4432, 1.4436, 1.4435; manufact.: 2015-03-03; PRE 27

  stress under proof load, min: nominal 1000 N/mm²

- *Washers:* BUFAB Group Bumax RB A4-HV290 according to EN ISO 7089; stainless steel EN 1.4432, 1.4436, 1.4435; with dimensions d = 21.0 mm, D = 37.0 mm, t = 3.0 mm; manufact.: 2012-01-04; PRE 27

  hardness, min: nominal 200 HV

Table 51, Table 52 and Table 53 summarize the test results and evaluation of the Bumax 109 – M20x140 bolting assemblies. The statistical evaluation is also presented as well as an overview about the fulfilled and failed criteria according to EN 14399-3. The tightening graphs are shown in Figure 44 and Figure 45 and outline a shortened and barely visible pronounced bolt force plateaus in the plastic range. All tested bolting assemblies achieved $F_{p,C}$* = 137.2 kN, but only 4 of 10 tested bolting assemblies reached the specified preload $F_{p,C}$ = 171.5 kN. Furthermore, the tested stainless steel bolting assemblies failed in all additional criteria. The maximum bolt force $F_{bi,max} \geq 0.9 \cdot f_{ub} \cdot A_s$ = 220.5 kN as well as the prescribed angles of rotation were not achieved due to low ductile behaviour and high friction coefficients. With regard to the only partially reached preload level $F_{p,C}$, it must be considered that the statistical evaluation must be interpreted with caution: the coefficient of variation for the k-value lies between 0.25 and 0.26 and failed in criteria for k-class K1 as well as k-class K2; indeed only 4 of 10 tested bolts were considered in the statistical evaluation. Furthermore, the coefficients of friction are remarkably high at the specified preload level $F_{p,C}$: $\mu_b$ (0.218 – 0.225), $\mu_{th}$ (0.176 – 0.203) and $\mu_{tot}$ (0.199 – 0.203). The tightening graphs also show irregular bolt force-tightening torque curves like in the previous tested series because of galling in the nut bearing surface. Furthermore, the damages of the tested bolting assemblies show plastic deformations at the first load-bearing thread turn of the bolt and nut, roughening of the paired threads and minimal necking of the threaded shanks, comparable to the previously tested series. Total or partial bolt failure by fracture did not occur. Galling in the faying-surface washer/nut was detected in all tested bolting assemblies.

**Table 51** Test results of Bumax 109 – M20x140

| | | $F_{p,C}$ kN | Max F kN | Max T Nm | $\Theta_{pi}$ ° | $\Theta_{1i}$ ° | $\Theta_{2i}$ ° | $F_{bi}$ ($\Theta_{2i}$) kN | $\Delta\Theta_{1i}$ ° | $\Delta\Theta_{2i}$ ° | k ($F_{p,C}$) | $\mu_{tot}$ ($F_{p,C}$) | $\mu_{th}$ ($F_{p,C}$) | $\mu_b$ ($F_{p,C}$) | $F_{p,C}$* kN | k ($F_{p,C*}$) | $M_i$ ($F_{p,C}$) Nm | M ($F_{p,C}$*) Nm | M ($F_{bi,max}$) Nm |
|---|---|---|---|---|---|---|---|---|---|---|---|---|---|---|---|---|---|---|---|
| max | | | --- | | | | | | --- | --- | 0,16 | | | | | 0,16 | | | |
| min | | | 220,5 | | | | | | 120 | 240 | 0,10 | | | | | 0,10 | | | |
| | BU_M20_109-01 | 171,5 | <177,7 | 1223,4 | 260 | 295 | 334 | 171,5 | <34 | <74 | >0,25 | 0,203 | 0,184 | 0,219 | 137,2 | >0,19 | 860,5 | 531,3 | 1075,6 |
| | BU_M20_109-02 | | <160,1 | 1101,5 | - | 249 | - | - | - | - | - | - | - | - | | >0,24 | - | 654,6 | 923,7 |
| | BU_M20_109-03 | | <156,9 | 974,4 | - | 275 | 369 | 129,8 | - | <0 | - | - | - | - | | >0,27 | - | 746,6 | 949,8 |
| | BU_M20_109-04 | | <169,0 | 1147,9 | - | 276 | 387 | 128,3 | - | <0 | - | - | - | - | | >0,22 | - | 593,0 | 978,6 |
| | BU_M20_109-05 | | <166,1 | 1223,5 | - | 284 | 410 | 126,6 | - | <0 | - | - | - | - | | >0,27 | - | 727,8 | 1066,6 |
| | BU_M20_109-06 | | <179,2 | 1099,1 | 250 | 289 | 338 | 171,5 | <39 | <88 | >0,26 | 0,214 | 0,201 | 0,225 | | >0,22 | 904,3 | 607,1 | 1056,4 |
| | BU_M20_109-07 | | <177,5 | 1136,2 | 265 | 316 | 344 | 171,5 | <51 | <79 | >0,26 | 0,211 | 0,203 | 0,218 | | >0,21 | 893,2 | 585,9 | 1098,3 |
| | BU_M20_109-08 | | <175,6 | 1089,1 | 258 | 286 | 310 | 171,5 | <27 | <52 | >0,25 | 0,199 | 0,176 | 0,218 | | >0,20 | 844,6 | 539,1 | 1000,3 |
| | BU_M20_109-09 | | <168,7 | 1263,5 | - | 284 | 381 | 130,1 | - | <0 | - | - | - | - | | >0,23 | - | 631,3 | 1003,7 |
| | BU_M20_109-10 | | <169,8 | 981,8 | - | 275 | 399 | 122,7 | - | <0 | - | - | - | - | | >0,20 | - | 537,1 | 917,4 |

**Table 52** Statistical evaluation of Bumax 109 – M20x140

| BU_M20_109 (2014) n = 10 | Max F kN | Max T Nm | $\Theta_{pi}$ ° | $\Theta_{1i}$ ° | $\Theta_{2i}$ ° | $F_{bi}$ ($\Theta_{2i}$) kN | $\Delta\Theta_{1i}$ ° | $\Delta\Theta_{2i}$ ° | $\mu_{tot}$ ($F_{p,C}$) | $\mu_{th}$ ($F_{p,C}$) | $\mu_b$ ($F_{p,C}$) | $M_i$ ($F_{p,C}$) Nm | k ($F_{p,C}$) | M ($F_{p,C}$*) Nm | k ($F_{p,C*}$) | M ($F_{bi,max}$) Nm |
|---|---|---|---|---|---|---|---|---|---|---|---|---|---|---|---|---|
| max | 179,2 | 1263,5 | 265 | 316 | 410 | 171,5 | 51 | 88 | 0,214 | 0,203 | 0,225 | 904,3 | 0,26 | 746,6 | 0,27 | 1098,3 |
| min | 156,9 | 974,4 | 250 | 249 | 310 | 122,7 | 27 | 0 | 0,199 | 0,176 | 0,218 | 844,6 | 0,25 | 531,3 | 0,19 | 917,4 |
| R | 22,3 | 289,1 | 15 | 67 | 100 | 48,8 | 24 | 88 | 0,015 | 0,027 | 0,007 | 59,7 | 0,01 | 215,3 | 0,08 | 180,9 |
| $\bar{x}$ | 170,1 | 1124,0 | 258 | 283 | 364 | 147,1 | 38 | 33 | 0,207 | 0,191 | 0,220 | 875,7 | 0,26 | 615,4 | 0,23 | 1007,0 |
| s | 7,6 | 97,1 | 6 | 17 | 34 | 23,3 | 10 | 40 | 0,007 | 0,013 | 0,003 | 27,8 | 0,01 | 76,1 | 0,03 | 65,1 |
| ν | 4,47 | 8,64 | 2,42 | 6,02 | 9,26 | 15,84 | 26,79 | - | 3,36 | 6,88 | 1,53 | 3,18 | 2,26 | 12,36 | 12,44 | 6,46 |

with n: number; R: range; x: mean value; s: standard deviation; ν: coefficient of variation in [%]

**Table 53** Evaluation of test results of Bumax 109 – M20x140 according to EN 14399-3

| n | $F_{p,C}$* | $F_{p,C}$ | $F_{bi,max}$ | $\Delta\Theta_{1i,min}$ | $\Delta\Theta_{2i,min}$ | k-values | k-class K1 | k-class K2 | | Fracture | Galling |
|---|---|---|---|---|---|---|---|---|---|---|---|
| [-] | 137.2 kN | 171.5 kN | ≥ 220.5 kN | ≥ 120° | ≥ 240° | [-] | $0.10 \le k_i \le 0.16$ | $0.10 \le k_m \le 0.23$ | $V_k \le 0.06$ | | |
| 10 | 100% | 40% | 0% | 0% | 0% | 0.25 – 0.26 | 0% | 0.255 | 0.023 | 0% | 100% |

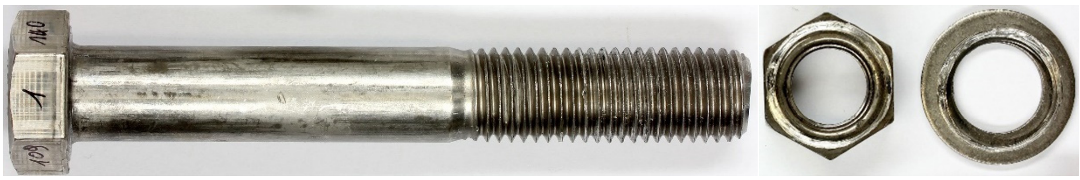

**Figure 43** BU_M20_109 test specimen after tightening

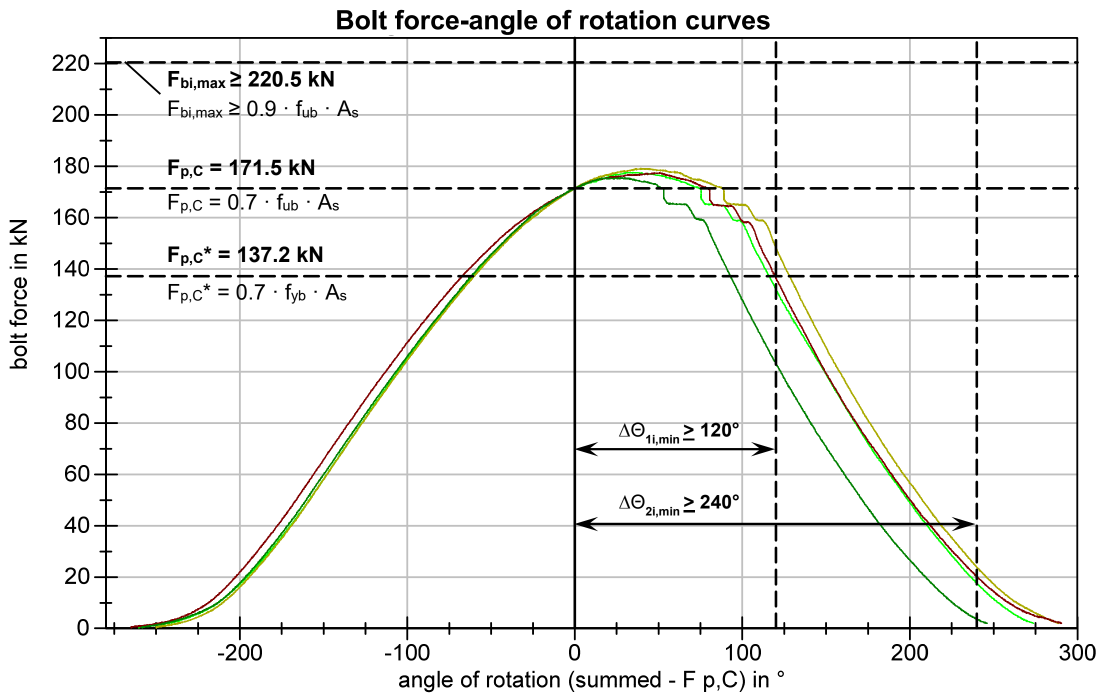


**Figure 44** BU_M20_109 bolt force-angle of rotation-curves (only specimens which achieved $F_{p,C}$)

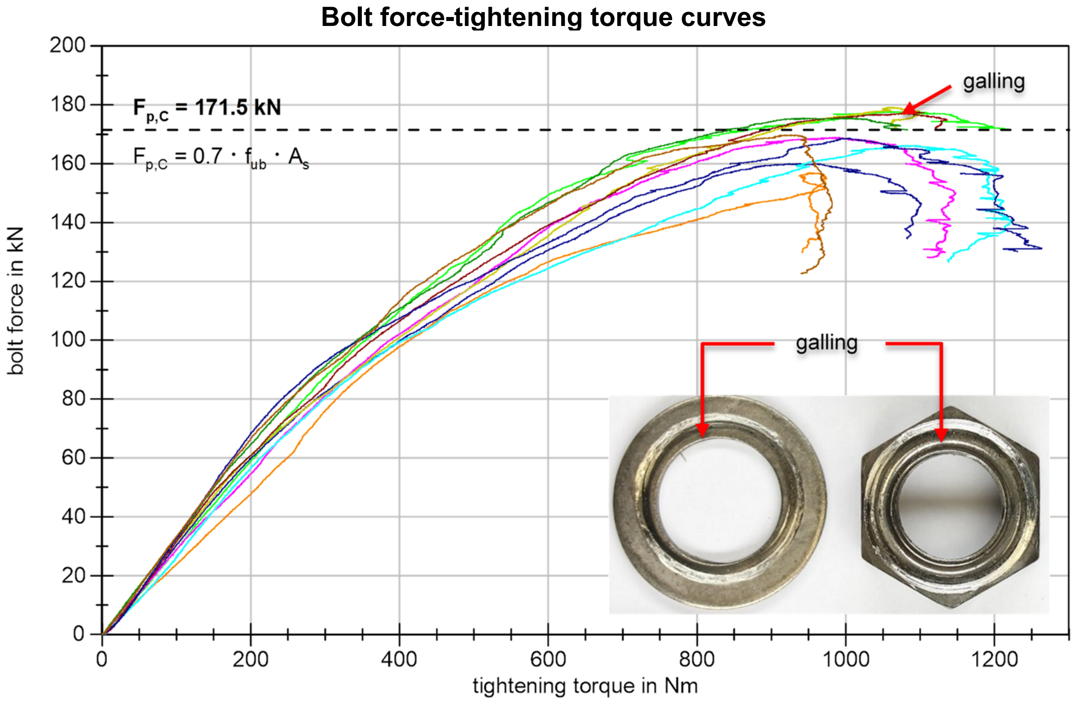


**Figure 45** BU_M20_109 bolt force-tightening torque-curves

### 3.3.3.4 *Bumax LDX – M20x100 – 10.9 – EN ISO 4017 – gleitmo 1952V*

The Bumax LDX – M20x100 ferrite-austenitic lean duplex stainless steel bolting assemblies in property class 10.9, in short form BU_M20_LDX, are arranged of the following components including nominal mechanical properties based on the Bumax datasheet:

- *Bolts:* BUFAB Group Bumax LDX – M20x100 A4 according to EN ISO 4017; stainless steel EN 1.4162; manufact.: 2016-09-09; PRE 26

  tensile strength $R_{m,min}$ (= $f_{ub}$): nominal 1000 N/mm²
  yield strength $R_{p0.2,min}$ (= $f_{yb}$): nominal 900 N/mm²
  elongation, min: nominal 0.3d

- *Nuts:* BUFAB Group Bumax 88 – M20 M6M A4 according to EN ISO 4032; stainless steel EN 1.4432, 1.4436, 1.4435; manufact.: 2016-04-08; PRE 27

  stress under proof load, min: nominal 800 N/mm²

- *Washers:* BUFAB Group Bumax RB A4-HV200 according to EN ISO 7089; stainless steel EN 1.4432, 1.4436, 1.4435; with dimensions d = 21.0 mm, D = 37.0 mm, t = 3.0 mm; manufact.: 2015-09-22; PRE 27

  hardness, min: nominal 200 HV

The tightening test results of Bumax LDX – M20x100 bolting assemblies are summarized in Table 54, Table 55 and Table 56. The statistical evaluation is shown as well with fulfilled and failed criteria according to EN 14399-3 (System HR). In addition, the tightening curves are presented in Figure 47 and Figure 48. They show less pronounced bolt force plateaus in the plastic range compared to Bumax LDX –

M16x100 and Bumax DX – M16x100 bolting assemblies without any partial or total bolt fracture. All tested lean duplex bolting assemblies reached $F_{p,C}$* = 154.4 kN and $F_{p,C}$ = 171.5 kN. On the contrary, the criteria of the maximum bolt force $F_{bi,max} \geq 0.9 \cdot f_{ub} \cdot A_s$ = 220.5 kN was not achieved in the whole tested series. Due to the less pronounced plastic plateau, criteria $\Delta\Theta_{1i,min}$ = 120° failed, too, and only 3 of 10 bolts achieved $\Delta\Theta_{2i,min}$ = 240° (with a coefficient of variation of 37.96 %) according to EN 14399-3. Furthermore, 10 of 10 tested bolts achieved k-class K1 with k-values between 0.10 and 0.15 and a coefficient of variation of v = 14.81 % (compared to k = 0.10 – 0.14 and v = 13.12 % at $F_{p,C}$*). k-class K2 was not accomplished. For further information and summarized criteria see Table 56. The graphs show irregular bolt force-tightening torque curves because of minor and major galling in the nut bearing surface when tightened into the plastic range. In addition, the coefficients of friction $\mu_{tot}$ (v = 17.80 %), $\mu_{th}$ (v = 20.45 %), and $\mu_b$ (v = 20.45 %) show a high scattering at $F_{p,C}$. Damages at the first and second load-bearing thread turn of the bolts and roughening of the paired threads could be observed. Galling especially in the faying surface washer/nut could be observed, too.

**Table 54** Test results of Bumax LDX – M20x100

| Legend | Specimens | $F_{p,C}$* kN | $F_{p,C}$ kN | Max F kN | Max T Nm | $\Theta_{pi}$ ° | $\Theta_{1i}$ ° | $\Theta_{2i}$ ° | $F_{bi}$ ($\Theta_{2i}$) kN | $\Delta\Theta_{1i}$ ° | $\Delta\Theta_{2i}$ ° | k ($F_{p,C*}$) | k ($F_{p,C}$) | $\mu_{tot}$ ($F_{p,C}$) | $\mu_{th}$ ($F_{p,C}$) | $\mu_b$ ($F_{p,C}$) | M ($F_{p,C}$*) Nm | $M_i$ ($F_{p,C}$) Nm | M ($F_{bi,max}$) Nm |
|---|---|---|---|---|---|---|---|---|---|---|---|---|---|---|---|---|---|---|---|
| max | | | | --- | | | | | | --- | --- | 0,16 | 0,16 | | | | | | |
| min | | | | 220,5 | | | | | | 120 | 240 | 0,10 | 0,10 | | | | | | |
| | BU_M20_LDX-01 | 154,4 | 171,5 | <214,7 | 956,0 | 273 | 397 | 605 | 171,4 | 124 | 333 | 0,10 | 0,10 | 0,085 | 0,087 | 0,084 | 365,7 | 415,4 | 679,6 |
| | BU_M20_LDX-02 | | | <187,6 | 936,2 | 267 | 321 | 380 | 171,4 | <53 | <112 | 0,13 | 0,14 | 0,127 | 0,168 | 0,090 | 496,7 | 576,3 | 766,2 |
| | BU_M20_LDX-03 | | | <198,2 | 954,0 | 263 | 350 | 451 | 171,4 | <86 | <188 | 0,11 | 0,11 | 0,100 | 0,120 | 0,082 | 396,6 | 471,5 | 711,6 |
| | BU_M20_LDX-04 | | | <199,1 | 828,9 | 276 | 361 | 512 | 171,3 | <84 | <235 | 0,12 | 0,13 | 0,114 | 0,165 | 0,070 | 454,7 | 528,9 | 717,2 |
| | BU_M20_LDX-05 | | | <200,0 | 936,5 | 255 | 348 | 437 | 171,4 | <93 | <182 | 0,10 | 0,11 | 0,095 | 0,119 | 0,075 | 383,5 | 454,2 | 715,0 |
| | BU_M20_LDX-06 | | | <205,7 | 897,9 | 256 | 362 | 516 | 171,3 | <107 | 260 | 0,10 | 0,11 | 0,093 | 0,115 | 0,074 | 379,3 | 445,4 | 746,2 |
| | BU_M20_LDX-07 | | | <189,5 | 998,0 | 252 | 305 | 362 | 171,4 | <53 | <110 | 0,13 | 0,14 | 0,125 | 0,139 | 0,113 | 480,8 | 571,2 | 797,2 |
| | BU_M20_LDX-08 | | | <184,0 | 989,2 | 271 | 311 | 376 | 171,4 | <40 | <105 | 0,14 | 0,15 | 0,141 | 0,167 | 0,118 | 509,2 | 632,4 | 804,3 |
| | BU_M20_LDX-09 | | | <201,9 | 926,2 | 251 | 333 | 447 | 171,4 | <81 | <195 | 0,10 | 0,10 | 0,085 | 0,109 | 0,065 | 360,8 | 415,9 | 696,4 |
| | BU_M20_LDX-10 | | | <206,6 | 1024,8 | 246 | 350 | 496 | 171,3 | <104 | 251 | 0,12 | 0,12 | 0,109 | 0,136 | 0,084 | 436,4 | 506,3 | 799,6 |

**Table 55** Statistical evaluation of Bumax LDX – M20x100

| BU_M20_LDX - Gleitmo 1952V n = 10 | Max F kN | Max T Nm | $\Theta_{pi}$ ° | $\Theta_{1i}$ ° | $\Theta_{2i}$ ° | $F_{bi}$ ($\Theta_{2i}$) kN | $\Delta\Theta_{1i}$ ° | $\Delta\Theta_{2i}$ ° | k ($F_{p,C*}$) | k ($F_{p,C}$) | $\mu_{tot}$ ($F_{p,C}$) | $\mu_{th}$ ($F_{p,C}$) | $\mu_b$ ($F_{p,C}$) | M ($F_{p,C}$*) Nm | $M_i$ ($F_{p,C}$) Nm | M ($F_{bi,max}$) Nm |
|---|---|---|---|---|---|---|---|---|---|---|---|---|---|---|---|---|
| max | 214,7 | 1024,8 | 276 | 397 | 605 | 171,4 | 124 | 333 | 0,14 | 0,15 | 0,141 | 0,168 | 0,118 | 509,2 | 632,4 | 804,3 |
| min | 184,0 | 828,9 | 246 | 305 | 362 | 171,3 | 40 | 105 | 0,10 | 0,10 | 0,085 | 0,087 | 0,065 | 360,8 | 415,4 | 679,6 |
| R | 30,7 | 195,9 | 30 | 92 | 243 | 0,1 | 84 | 228 | 0,04 | 0,05 | 0,056 | 0,081 | 0,053 | 148,4 | 217,0 | 124,7 |
| $\bar{x}$ | 198,7 | 944,8 | 261 | 344 | 458 | 171,4 | 83 | 197 | 0,12 | 0,12 | 0,107 | 0,133 | 0,086 | 426,4 | 501,8 | 743,3 |
| s | 9,4 | 55,3 | 10 | 27 | 76 | 0,0 | 27 | 75 | 0,02 | 0,02 | 0,019 | 0,028 | 0,017 | 56,4 | 74,1 | 46,0 |
| ν | 4,76 | 5,85 | 3,99 | 7,98 | 16,58 | 0,03 | 32,47 | 37,96 | 13,12 | 14,81 | 17,80 | 20,79 | 20,45 | 13,22 | 14,76 | 6,19 |

with n: number; R: range; x: mean value; s: standard deviation; ν: coefficient of variation in [%]

**Table 56** Evaluation of test results of Bumax LDX – M20x100 according to EN 14399-3

| n | $F_{p,C}^*$ | $F_{p,C}$ | $F_{bi,max}$ | $\Delta\Theta_{1i,min}$ | $\Delta\Theta_{2i,min}$ | k-values | k-class K1 | k-class K2 | | Fracture | Galling |
|---|---|---|---|---|---|---|---|---|---|---|---|
| [-] | 154.4kN | 171.5 kN | ≥ 220.5 kN | ≥ 120° | ≥ 240° | [-] | $0.10 \leq k_i \leq 0.16$ | $0.10 \leq k_m \leq 0.23$ | $V_k \leq 0.06$ | | |
| 10 | 100% | 100% | 0% | 0% | 30% | 0.10 – 0.15 | 100% | 0.120 | 0.148 | 0% | 100% |

**Figure 46** BU_M20_LDX test specimen after tightening

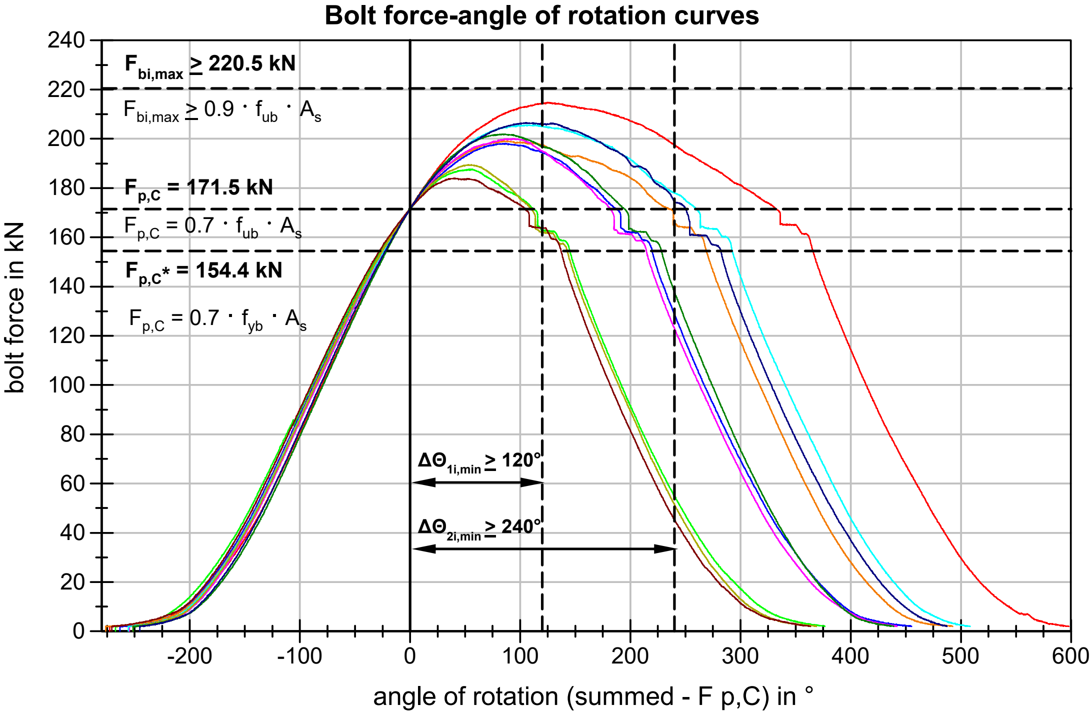


**Figure 47** BU_M20_LDX Bolt force-angle of rotation curves

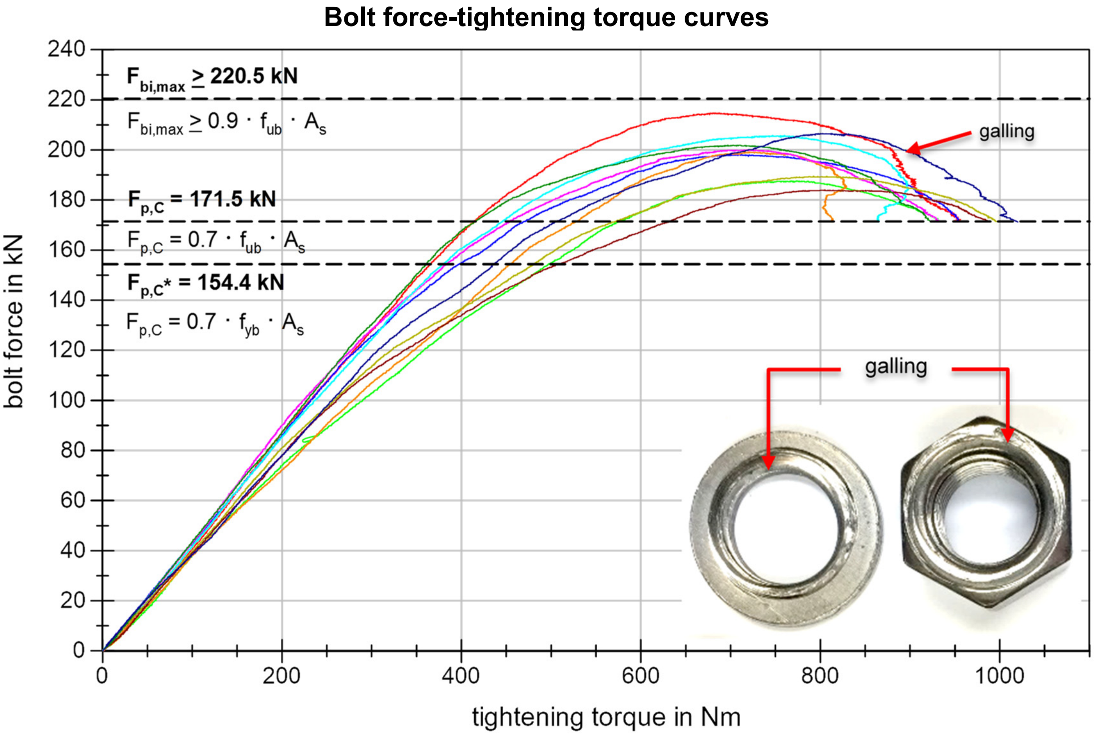


**Figure 48** BU_M20_LDX Bolt force-tightening torque curves

#### *3.3.3.5 Bumax DX – M20x100 – 10.9 – EN ISO 4017 – gleitmo 1952V*

The Bumax DX – M20x100 duplex stainless steel bolting assemblies in property class 10.9, in short form BU_M20_DX, are arranged of following components including nominal mechanical properties based on Bumax datasheet:

- *Bolts:* BUFAB Group Bumax LDX – M20x100 A4 according to EN ISO 4017; stainless steel EN 1.4462; manufact.: 2016-06-17; PRE 36

  tensile strength $R_{m,min}$ (= $f_{ub}$): nominal 1000 N/mm²
  yield strength $R_{p0.2,min}$ (= $f_{yb}$): nominal 900 N/mm²
  elongation, min: nominal 0.3d

- *Nuts:* BUFAB Group Bumax 88 – M20 M6M A4 according to EN ISO 4032; stainless steel EN 1.4432, 1.4436, 1.4435; manufact.: 2016-04-08; PRE 27

  stress under proof load, min: nominal 800 N/mm²

- *Washers:* BUFAB Group Bumax RB A4-HV200 according to EN ISO 7089; stainless steel EN 1.4432, 1.4436, 1.4435; with dimensions d = 21.0 mm, D = 37.0 mm, t = 3.0 mm; manufact.: 2015-09-22; PRE 27

  hardness, min: nominal 200 HV

The test results and evaluation of Bumax DX – M20x100 tested stainless steel bolting assemblies are summarized in Table 57, Table 58 and Table 59. The statistical evaluation is shown as well with fulfilled and failed criteria according to EN 14399-3 (System HR). Figure 50 and Figure 51 present the tightening graphs. They show nearly similar bolt force-angle of rotation-curves and also a less pronounced bolt force plateau in the plastic range comparable with Bumax LDX – M20x100 lean duplex bolting assemblies. All tested duplex bolting assemblies reached $F_{p,C}$* = 154.4 kN, $F_{p,C}$ = 171.5 kN, but on the contrary the maximum required bolt force $F_{bi,max} \geq 0.9 \cdot f_{ub} \cdot A_s$ = 220.5 kN is not achieved in the whole series. Furthermore, 10 of 10 tested bolts achieved k-class K1 with k-values between 0.10 and 0.15 and a coefficient of variation of v = 15.84 % (compared to k = 0.10 – 0.13 and v = 11.84 % at $F_{p,C}$*). k-class K2 was not accomplished. For further information and summarized criteria see Table 59. The graphs show irregular bolt force-tightening torque curves because of galling in the nut bearing surface when tightened into the plastic range including significant high ranges of values $M_i$ at the end of the tests (bolt force dropped again to $F_{p,C}$).The curve progressions are comparable with the results of the Bumax LDX – M20x100 series. Only 2 of 10 tested bolts achieved $\Delta\Theta_{1i,min}$ = 120° and 3 of 10 bolts reached $\Delta\Theta_{2i,min}$ = 240°. Damages at the first and second load-bearing thread turn of the bolts and roughening of the paired threads could be observed; bolt failure by fracture did not occur. Galling in the faying surface washer/nut could be observed, too. It was possible to unscrew the hexagon nuts of all tested bolting assemblies manually but turning on the nut on the whole threaded shank by hand was not possible.

**Table 57** Test results of Bumax DX – M20x100

| Legend | Specimens | $F_{p,C}$* kN | $F_{p,C}$ kN | Max F kN | Max T Nm | $\Theta_{pi}$ ° | $\Theta_{1i}$ ° | $\Theta_{2i}$ ° | $F_{bi}$ ($\Theta_{2i}$) kN | $\Delta\Theta_{1i}$ ° | $\Delta\Theta_{2i}$ ° | k ($F_{p,C^*}$) | k ($F_{p,C}$) | $\mu_{tot}$ ($F_{p,C}$) | $\mu_{th}$ ($F_{p,C}$) | $\mu_b$ ($F_{p,C}$) | M ($F_{p,C}$*) Nm | $M_i$ ($F_{p,C}$) Nm | M ($F_{bi,max}$) Nm |
|---|---|---|---|---|---|---|---|---|---|---|---|---|---|---|---|---|---|---|---|
| max | | | | --- | | | | | | --- | --- | 0,16 | 0,16 | | | | | | |
| min | | | | 220,5 | | | | | | 120 | 240 | 0,10 | 0,10 | | | | | | |
| | BU_M20_DX-01 | 154,4 | 171,5 | <204,7 | 1228,8 | 242 | 328 | 449 | 171,4 | <85 | <207 | 0,10 | 0,11 | 0,096 | 0,110 | 0,085 | 387,2 | 458,6 | 821,1 |
| | BU_M20_DX-02 | | | <193,6 | 1292,0 | 252 | 318 | 419 | 171,3 | <66 | <167 | 0,13 | 0,15 | 0,135 | 0,147 | 0,125 | 490,3 | 610,8 | 893,8 |
| | BU_M20_DX-03 | | | <197,2 | 1328,3 | 246 | 332 | 420 | 171,4 | <87 | <175 | 0,13 | 0,14 | 0,130 | 0,151 | 0,112 | 482,0 | 590,5 | 1004,8 |
| | BU_M20_DX-04 | | | <192,8 | 1157,5 | 243 | 303 | 388 | 171,4 | <60 | <145 | 0,10 | 0,11 | 0,100 | 0,122 | 0,081 | 381,5 | 473,0 | 784,8 |
| | BU_M20_DX-05 | | | <214,5 | 1802,3 | 242 | 372 | 582 | 171,3 | 130 | 340 | 0,10 | 0,10 | 0,085 | 0,086 | 0,085 | 374,5 | 415,9 | 1039,5 |
| | BU_M20_DX-06 | | | <197,7 | 1527,6 | 260 | 359 | 479 | 171,4 | <100 | <220 | 0,13 | 0,15 | 0,135 | 0,102 | 0,164 | 497,2 | 611,0 | 1136,1 |
| | BU_M20_DX-07 | | | <190,4 | 843,8 | 253 | 302 | 370 | 171,4 | <49 | <117 | 0,11 | 0,12 | 0,106 | 0,152 | 0,066 | 414,7 | 497,1 | 674,3 |
| | BU_M20_DX-08 | | | <216,2 | 908,5 | 237 | 369 | 653 | 171,4 | 132 | 416 | 0,10 | 0,10 | 0,082 | 0,111 | 0,057 | 366,9 | 403,1 | 636,7 |
| | BU_M20_DX-09 | | | <205,5 | 1007,3 | 242 | 348 | 461 | 171,4 | <106 | <219 | 0,12 | 0,13 | 0,114 | 0,135 | 0,095 | 461,8 | 526,6 | 782,4 |
| | BU_M20_DX-10 | | | <211,8 | 1258,3 | 229 | 347 | 583 | 171,4 | <118 | 354 | 0,11 | 0,11 | 0,101 | 0,105 | 0,098 | 412,8 | 477,2 | 814,3 |

**Table 58** Statistical evaluation of Bumax DX – M20x100

| BU_M20_DX - Gleitmo 1952V n = 10 | Max F kN | Max T Nm | $\Theta_{pi}$ ° | $\Theta_{1i}$ ° | $\Theta_{2i}$ ° | $F_{bi}$ ($\Theta_{2i}$) kN | $\Delta\Theta_{1i}$ ° | $\Delta\Theta_{2i}$ ° | k ($F_{p,C^*}$) | k ($F_{p,C}$) | $\mu_{tot}$ ($F_{p,C}$) | $\mu_{th}$ ($F_{p,C}$) | $\mu_b$ ($F_{p,C}$) | M ($F_{p,C}$*) Nm | $M_i$ ($F_{p,C}$) Nm | M ($F_{bi,max}$) Nm |
|---|---|---|---|---|---|---|---|---|---|---|---|---|---|---|---|---|
| max | 216,2 | 1802,3 | 260 | 372 | 653 | 171,4 | 132 | 416 | 0,13 | 0,15 | 0,135 | 0,152 | 0,164 | 497,2 | 611,0 | 1136,1 |
| min | 190,4 | 843,8 | 229 | 302 | 370 | 171,3 | 49 | 117 | 0,10 | 0,10 | 0,082 | 0,086 | 0,057 | 366,9 | 403,1 | 636,7 |
| R | 25,8 | 958,5 | 31 | 70 | 283 | 0,1 | 83 | 299 | 0,03 | 0,05 | 0,053 | 0,066 | 0,107 | 130,3 | 207,9 | 499,4 |
| $\bar{x}$ | 202,4 | 1235,4 | 245 | 338 | 480 | 171,4 | 93 | 236 | 0,11 | 0,12 | 0,108 | 0,122 | 0,097 | 426,9 | 506,4 | 858,8 |
| s | 9,4 | 286,3 | 9 | 25 | 94 | 0,0 | 29 | 100 | 0,01 | 0,02 | 0,020 | 0,023 | 0,031 | 51,1 | 76,4 | 159,9 |
| $\nu$ | 4,67 | 23,17 | 3,58 | 7,51 | 19,64 | 0,02 | 31,12 | 42,24 | 11,84 | 15,84 | 18,04 | 18,88 | 31,95 | 11,98 | 15,09 | 18,62 |

with n: number; R: range; x: mean value; s: standard deviation; $\nu$: coefficient of variation in [%]

**Table 59** Evaluation of test results of Bumax DX – M20x100 according to EN 14399-3

| n | $F_{p,C}^*$ | $F_{p,C}$ | $F_{bi,max}$ | $\Delta\Theta_{1i,min}$ | $\Delta\Theta_{2i,min}$ | k-values | k-class K1 | k-class K2 | | Fracture | Galling |
|---|---|---|---|---|---|---|---|---|---|---|---|
| [-] | 154.4kN | 171.5 kN | ≥ 220.5 kN | ≥ 120° | ≥ 240° | [-] | $0.10 \leq k_i \leq 0.16$ | $0.10 \leq k_m \leq 0.23$ | $V_k \leq 0.06$ | | |
| 10 | 100% | 100% | 0% | 20% | 30% | 0.10 – 0.15 | 100% | 0.121 | 0.158 | 0% | 100% |

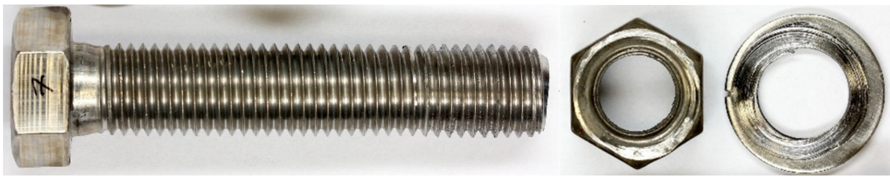

**Figure 49** BU_M20_DX test specimen after tightening

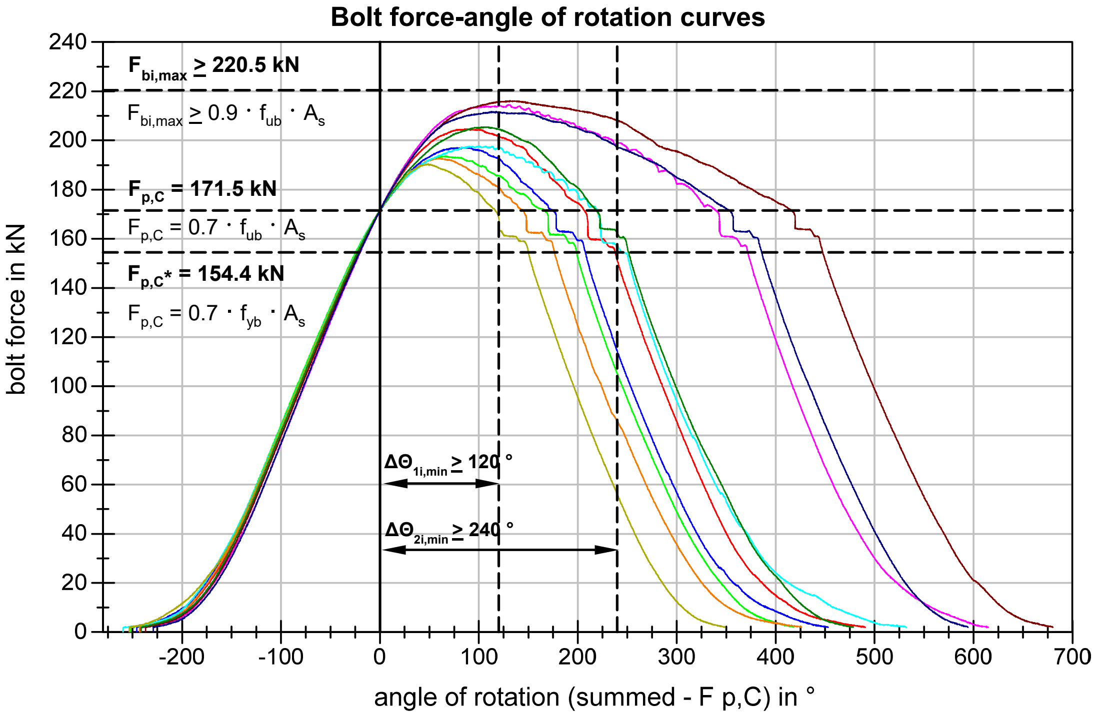


**Figure 50** BU_M20_DX Bolt force-angle of rotation curves

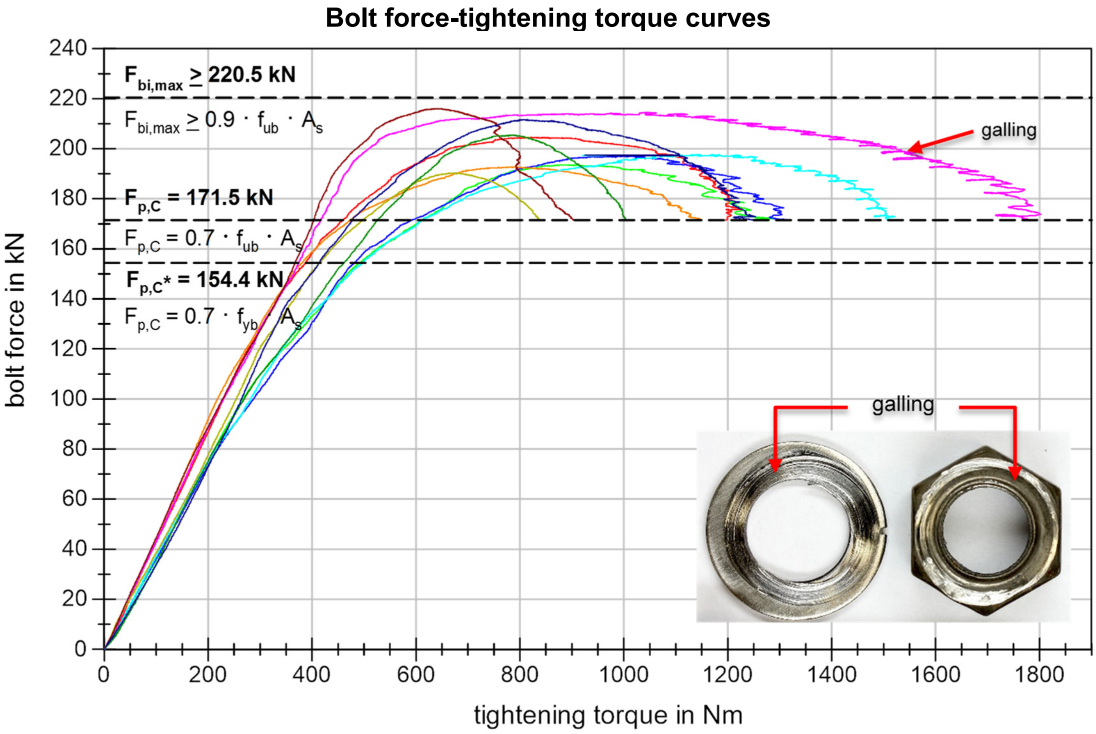


**Figure 51** BU_M20_DX Bolt force-tightening torque curves

### 3.3.4 Bolt dimension M24

In addition to the prescribed tightening tests in the technical annex of SIROCO, tightening tests for bolt dimension M24 in property class 8.8 were additionally carried out according to EN 14399-2 and EN ISO 16047. The test procedure was performed with a constant speed of rotation of 2.0 $min^{-1}$ and all bolting assemblies were tightened nut sided. The clamp length ∑t was set to 70.0 mm (clamp length/bolt diameter ratio of 2.9) in reference to the corresponding tables of System HR – EN 14399-3. The tightening tests were stopped when the measured bolt force dropped to $F_{p,c} = 0.7 \cdot f_{ub} \cdot A_s$ (with $f_{ub}$: tensile strength of the bolt and $A_s$: tensile stress area of the bolt).

The criteria of evaluation for property class 8.8 according to EN 14399-3 are defined as follows:

- $F_{p,C}^* = 0.7 \cdot f_{yb} \cdot A_s = 0.7 \cdot 640$ N/mm² $\cdot$ 353.0 mm² = 158.1 kN (DIN EN 1993-1-8/NA)
- $F_{p,C} = 0.7 \cdot f_{ub} \cdot A_s = 0.7 \cdot 800$ N/mm² $\cdot$ 353.0 mm² = 197.7 kN
- $F_{bi,max} \geq 0.9 \cdot f_{ub} \cdot A_s = 0.9 \cdot 800$ N/mm² $\cdot$ 353.0 mm² = 254.4 kN
- $\Delta\Theta_{1i,min} \geq 120°$ with $\Sigma t$ = 60.5 mm: $2d \leq \Sigma t < 6d$
- $\Delta\Theta_{2i,min} \geq 240°$ with $\Sigma t$ = 60.5 mm: $2d \leq \Sigma t < 6d$

All tightening test were carried out in accordance to EN 14399-2 and EN ISO 16047 using the test setup shown in Table 60.

**Table 60** Test setup Bumax 88 – M24x100

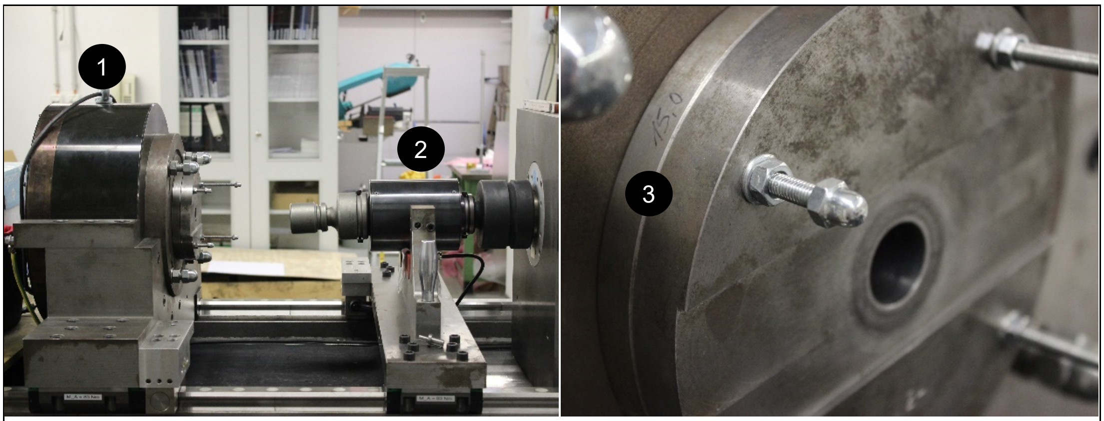


| | | |
|---|---|---|
| **1** | Sensor force – thread friction torque: SNo. 1016242 – 1,500 kN / 5,000 Nm | |
| **2** | Sensor total tightening torque – angle of rotation: SNo. 1024283 – 5,000 Nm | |
| **3** | Shims: DP 15mm + M24HV | Lubrication: gleitmo 1952V |
| | Support bar: No | Adapter: Yes |
| | Speed of rotation: 2.0 $min^{-1}$ | Rotated component: Hexagon nut |
| | Number of bolting assemblies tested: 10 | Washers: placed under nut |
| | Clamp length ∑t = 70.0 mm according to EN 14399-3:2015-03 | |
| | Clamp length/bolt diameter ratio: 2.9 | Stop criteria: bolt force dropped to $F_{p,C}$ |

#### *3.3.4.1 Bumax 88 – M24x100 – 8.8 – EN ISO 4017 – gleitmo 1952V*

The series Bumax 88 – M24x100 acc. EN ISO 4017 austenitic stainless steel bolting assemblies in property class 8.8 and abbreviated below as BU_M24_88 were arranged of the following components including the nominal mechanical properties based on Bumax datasheet:

- *Bolts:* BUFAB Group Bumax 88 – M24x100 A4 according to EN ISO 4017; stainless steel EN 1.4432, 1.4436, 1.4435; manufact.: 2015-06-05; PRE 27

  tensile strength $R_{m,min}$ (= $f_{ub}$): nominal 800 N/mm²
  yield strength $R_{p0.2,min}$ (= $f_{yb}$): nominal 640 N/mm²
  elongation, min: nominal 0.3d

- *Nuts:* BUFAB Group Bumax 88 – M24 M6M A4 according to EN ISO 4032; stainless steel EN 1.4432, 1.4436, 1.4435; manufact.: 2015-04-08; PRE 27

  stress under proof load, min: nominal 800 N/mm²

- *Washers:* BUFAB Group Bumax RB A4-HV200 according to EN ISO 7089; stainless steel EN 1.4432, 1.4436, 1.4435; with dimensions d = 25.0 mm, D = 44.0 mm, t = 4.0 mm; manufact.: 2013-11-25; PRE 27

  hardness, min: nominal 200 HV

Table 61, Table 62 and Table 63 summarize the test results including statistical evaluation and summarized criteria according to EN 14399-3. Due to technical problems, specimen BU_M24_88-08 was declared as invalid. With attention to the tightening curves shown in Figure 53 and Figure 54, all tested bolting assemblies reached $F_{p,C}$* = 158.1 kN and $F_{p,C}$ = 197.7 kN. Only 5 of 10 bolts reached the maximum bolt force $F_{bi,max} \geq 0.9 \cdot f_{ub} \cdot A_s$ = 254.2 kN. The bolt force-angle of rotation-curves show a narrow and shortened bolt force plateau in the plastic range. As a result, only 1 of 10 bolts achieved the angle of rotation $\Delta\Theta_{1i,min.}$ = 120° and 3 of 10 bolts reached $\Delta\Theta_{2i,min.}$ = 240°. The k-values lie between 0.10 and 0.22 with a high coefficient of variation of v = 23.45 %, accordingly 6 of 10 bolts accomplished the criteria for k-class K1 whereas the integration of the tested series referred to k-class K2 failed. The statistical evaluation shows very high coefficients of variation for $\Delta\Theta_{1i}$ (43.70 %) and $\Delta\Theta_{2i}$ (46.50 %). After all, the graphs show again irregular bolt force-tightening torque curves because of galling in the nut bearing surface when tightened into the plastic range. But it must be pointed out that, in contrast to the previously tested series, in the majority only minor galling occured.

The damage analysis in detail shows damages at the first load-bearing thread turn of the bolts and roughening of paired threads; bolt failure by fracture did not occur in all tested bolting assemblies made of stainless steel. Furthermore, it was possible to unscrew the hexagon nuts of all tested bolting assemblies manually.

**Table 61** Test results of Bumax 88 – M24x100

| Legende | Probenbez. | $F_{p,C}$ | Max F | Max T | $\Theta_{pi}$ | $\Theta_{1i}$ | $\Theta_{2i}$ | $F_{bi}$ ($\Theta_{2i}$) | $\Delta\Theta_{1i}$ | $\Delta\Theta_{2i}$ | k ($F_{p,C}$) | $\mu_{tot}$ ($F_{p,C}$) | $\mu_{th}$ ($F_{p,C}$) | $\mu_b$ ($F_{p,C}$) | $F_{p,C}$* | k ($F_{p,C*}$) | $M_i$ ($F_{p,C}$) | M ($F_{p,C}$*) | M ($F_{bi,max}$) |
|---|---|---|---|---|---|---|---|---|---|---|---|---|---|---|---|---|---|---|---|
| | | kN | kN | Nm | ° | ° | ° | kN | ° | ° | | | | | kN | | Nm | Nm | Nm |
| max | | | --- | | | | | | --- | --- | 0,16 | | | | | 0,16 | | | |
| min | | | 254,2 | | | | | | 120 | 240 | 0,10 | | | | | 0,10 | | | |
| | BU_M24_88-01 | 197,7 | <206,7 | 1303,8 | 169 | 191 | 232 | 197,7 | <21 | <63 | >0,22 | 0,172 | 0,226 | 0,125 | 158,1 | >0,20 | 1022,0 | 755,1 | 1161,3 |
| | BU_M24_88-02 | | <228,0 | 1301,4 | 163 | 214 | 292 | 197,7 | <51 | <130 | >0,17 | 0,134 | 0,182 | 0,091 | | >0,17 | 815,6 | 639,9 | 1087,0 |
| | BU_M24_88-03 | | 257,1 | 1475,3 | 154 | 236 | 379 | 197,6 | <82 | <225 | 0,15 | 0,111 | 0,092 | 0,128 | | 0,15 | 695,5 | 551,8 | 1025,5 |
| | BU_M24_88-04 | | <231,2 | 1349,2 | 157 | 206 | 295 | 197,6 | <49 | <139 | >0,17 | 0,133 | 0,148 | 0,120 | | >0,17 | 812,6 | 637,7 | 1093,3 |
| | BU_M24_88-05 | | <237,8 | 1343,4 | 162 | 224 | 327 | 197,5 | <63 | <166 | 0,16 | 0,122 | 0,126 | 0,118 | | 0,15 | 752,1 | 581,6 | 1066,3 |
| | BU_M24_88-06 | | 256,1 | 1569,5 | 154 | 232 | 354 | 197,6 | <78 | <200 | 0,14 | 0,106 | 0,093 | 0,117 | | 0,14 | 667,1 | 524,0 | 1032,8 |
| | BU_M24_88-07 | | 268,5 | 1258,7 | 155 | 263 | 481 | 197,7 | <109 | 326 | 0,11 | 0,076 | 0,074 | 0,079 | | 0,11 | 506,2 | 402,7 | 860,9 |
| | BU_M24_88-09 | | 273,9 | 1304,6 | 151 | 282 | 525 | 197,7 | 131 | 374 | 0,10 | 0,074 | 0,064 | 0,084 | | 0,10 | 495,7 | 387,4 | 897,7 |
| | BU_M24_88-10 | | 260,7 | 1453,6 | 156 | 247 | 416 | 197,6 | <91 | 261 | 0,12 | 0,090 | 0,082 | 0,097 | | 0,12 | 579,4 | 463,7 | 976,0 |
| | BU_M24_88-11 | | <235,3 | 1329,5 | 162 | 219 | 317 | 197,6 | <57 | <155 | >0,17 | 0,132 | 0,154 | 0,112 | | >0,17 | 804,4 | 646,0 | 1071,9 |

**Table 62** Statistical evaluation of Bumax 88 – M24x100

| BU_M24_88 (2015) n = 10 | Max F kN | Max T Nm | $\Theta_{pi}$ ° | $\Theta_{1i}$ ° | $\Theta_{2i}$ ° | $F_{bi}(\Theta_{2i})$ kN | $\Delta\Theta_{1i}$ ° | $\Delta\Theta_{2i}$ ° | $\mu_{tot}(F_{p,C})$ | $\mu_{th}(F_{p,C})$ | $\mu_b(F_{p,C})$ | $k(F_{p,C})$ | $M_i(F_{p,C})$ Nm | $M(F_{p,C}^*)$ Nm | $M(F_{bi,max})$ Nm |
|---|---|---|---|---|---|---|---|---|---|---|---|---|---|---|---|
| max | 273,9 | 1569,5 | 169 | 282 | 525 | 197,7 | 131 | 374 | 0,172 | 0,226 | 0,128 | 0,22 | 1022,0 | 755,1 | 1161,3 |
| min | 206,7 | 1258,7 | 151 | 191 | 232 | 197,5 | 21 | 63 | 0,074 | 0,064 | 0,079 | 0,10 | 495,7 | 387,4 | 860,9 |
| R | 67,2 | 310,8 | 18 | 91 | 293 | 0,2 | 110 | 311 | 0,098 | 0,162 | 0,049 | 0,12 | 526,3 | 367,7 | 300,4 |
| $\bar{x}$ | 245,5 | 1368,9 | 158 | 231 | 362 | 197,6 | 73 | 204 | 0,115 | 0,124 | 0,107 | 0,15 | 715,1 | 559,0 | 1027,3 |
| s | 21,1 | 98,0 | 5 | 27 | 90 | 0,1 | 32 | 95 | 0,030 | 0,053 | 0,018 | 0,04 | 161,9 | 117,1 | 92,2 |
| ν | 8,58 | 7,16 | 3,47 | 11,71 | 24,98 | 0,03 | 43,70 | 46,50 | 26,24 | 42,55 | 16,61 | 23,46 | 22,65 | 20,96 | 8,98 |

with n: number; R: range; x: mean value; s: standard deviation; ν: coefficient of variation in [%]

**Table 63** Evaluation of test results of Bumax 88 – M24x100 according to EN 14399-3

| n | $F_{p,C}^*$ | $F_{p,C}$ | $F_{bi,max}$ | $\Delta\Theta_{1i,min}$ | $\Delta\Theta_{2i,min}$ | k-values | k-class K1 | k-class K2 | | Fracture | Galling |
|---|---|---|---|---|---|---|---|---|---|---|---|
| [-] | 158.1 kN | 197.7 kN | ≥ 254.2 kN | ≥ 120° | ≥ 240° | [-] | $0.10 \le k_i \le 0.16$ | $0.10 \le k_m \le 0.23$ | $V_k \le 0.06$ | | |
| 10 | 100% | 100% | 50% | 10% | 30% | 0.10 – 0.22 | 60% | 0.151 | 0.235 | 0% | 30% |

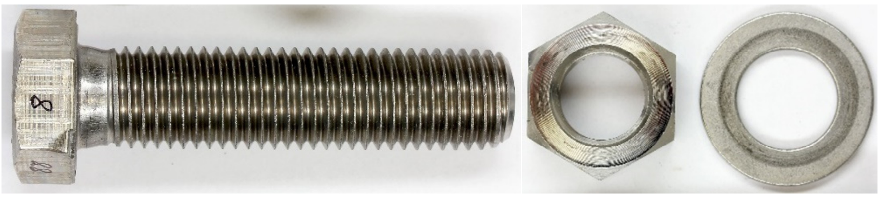

**Figure 52** BU_M24_88 test specimen after tightening

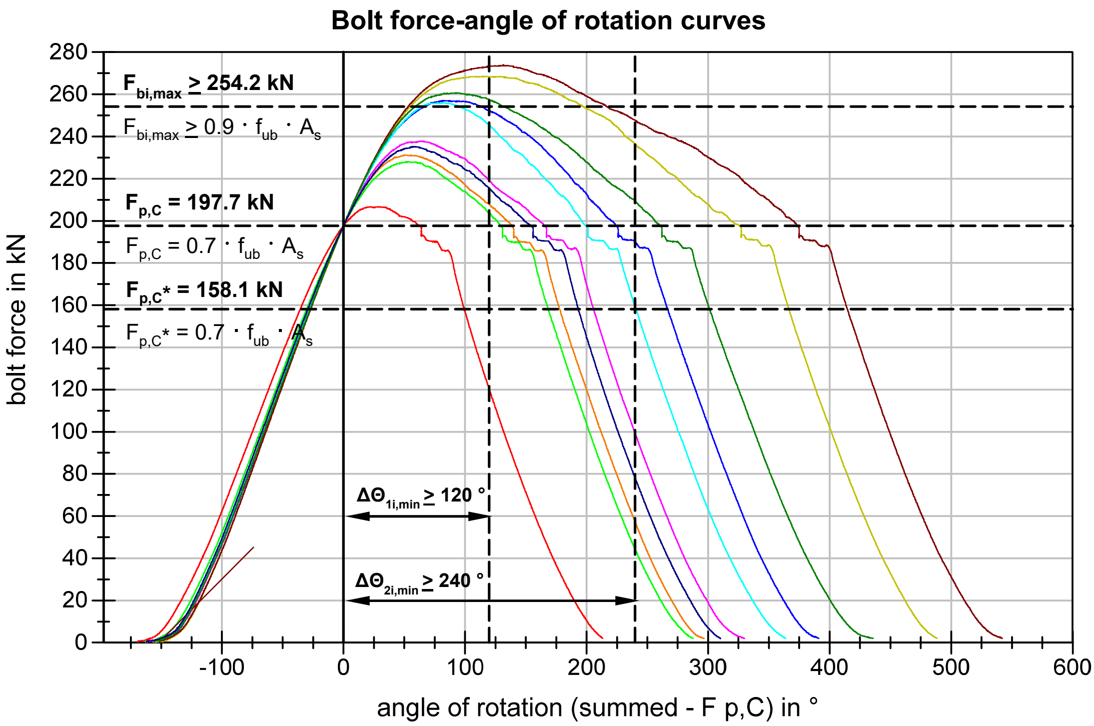


**Figure 53** BU_M20_88 (2015) Bolt force-angle of rotation curves

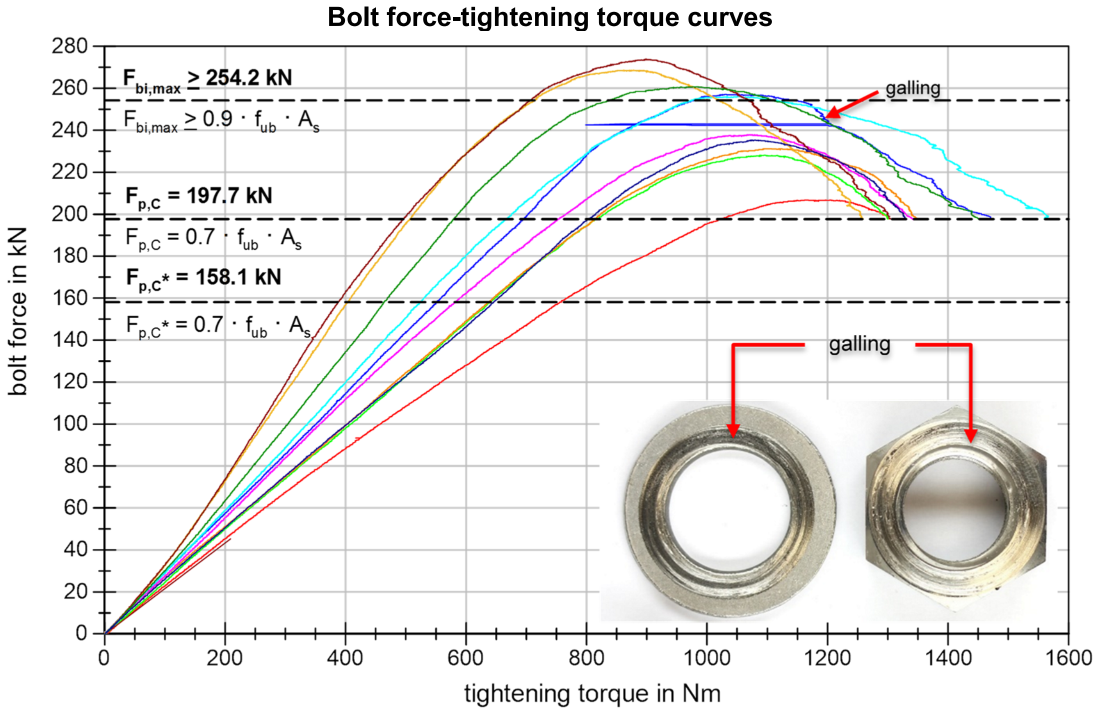


**Figure 54** BU_M20_88 (2015) Bolt force-tightening torque curves

## 3.4 Tightening test results and evaluation – STEP 2: alternative lubricants

### 3.4.1 Lubrication tests: Identification of suitable, alternative lubrication for stainless steel bolting assemblies

To identify suitable, alternative lubrication for stainless steel bolting assemblies, tightening tests were performed with Bumax 88 – M20x80 EN ISO 4017 bolting assemblies as well as Bumax 109 – M20x140 EN ISO 4014 bolting assemblies. For Bumax 88 – M20x80 austenitic series, the clamp length $\sum t$ was set to 60.5 mm (clamp length/bolt diameter ratio of 3.0) in reference to the corresponding tables of System HR – EN 14399-3. In addition, the Bumax 109 – M20x140 bolts were tested with a clamping length $\sum t$ = 105.0 mm and clamp length/ bolt diameter ratio of 5.3. The nut was turned to tighten the assembly with a constant speed of rotation of 5.0 min$^{-1}$. The tightening tests were stopped when the bolt force dropped to $F_{p,C}$ after reaching $F_{p,C}$ once to allow more detailed investigation of the basic preloading behaviour and the effects of alternative lubricants.

With normative reference to EN 14399-3, the relevant criteria for the evaluation of Bumax 88 bolting assemblies in property class 8.8 were defined as follows:

- $F_{p,C}^* = 0.7 \cdot f_{yb} \cdot A_s = 0.7 \cdot 640$ N/mm² $\cdot$ 245.0 mm² = 109.7 kN (DIN EN 1993-1-8/NA)
- $F_{p,C} = 0.7 \cdot f_{ub} \cdot A_s = 0.7 \cdot 800$ N/mm² $\cdot$ 245.0 mm² = 137.2 kN
- $F_{bi,max} \geq 0.9 \cdot f_{ub} \cdot A_s = 0.9 \cdot 800$ N/mm² $\cdot$ 245.0 mm² = 176.4 kN
- $\Delta\Theta_{1i,min} \geq 120°$ with $\Sigma t$ = 60.5 mm: $2d \leq \Sigma t < 6d$
- $\Delta\Theta_{2i,min} \geq 240°$ with $\Sigma t$ = 60.5 mm: $2d \leq \Sigma t < 6d$

In addition, the criteria for evaluation of the bolting assemblies in property class 10.9 (meaning Bumax 109) are defined as follows:

- $F_{p,C}^* = 0.7 \cdot f_{yb} \cdot A_s = 0.7 \cdot 800\ N/mm^2 \cdot 245.0\ mm^2 = 137.2\ kN$
- $F_{p,C} = 0.7 \cdot f_{ub} \cdot A_s = 0.7 \cdot 1000\ N/mm^2 \cdot 245.0\ mm^2 = 171.5\ kN$
- $F_{bi,max} \geq 0.9 \cdot f_{ub} \cdot A_s = 0.9 \cdot 1000\ N/mm^2 \cdot 245.0\ mm^2 = 220.5\ kN$
- $\Delta\Theta_{1i,min} \geq 120°$ with $\Sigma t = 105.0$ mm: $2d \leq \Sigma t < 6d$
- $\Delta\Theta_{2i,min} \geq 240°$ with $\Sigma t = 105.0$ mm: $2d \leq \Sigma t < 6d$

All tightening test were carried out in accordance to EN 14399-2 and EN ISO 16047 using the test setup shown in Table 64 and Table 65.

The following sections show exemplariliy the test results and evaluation of Bumax 88 – M20x80 series with alternative lubricants to provide an overview about the effects of alternative lubricants on ductility and galling. Finally, the results of all lubrication tests are discussed in subchapter 3.6.2.

**Table 64** Test setup Bumax 88 – M20x80 series

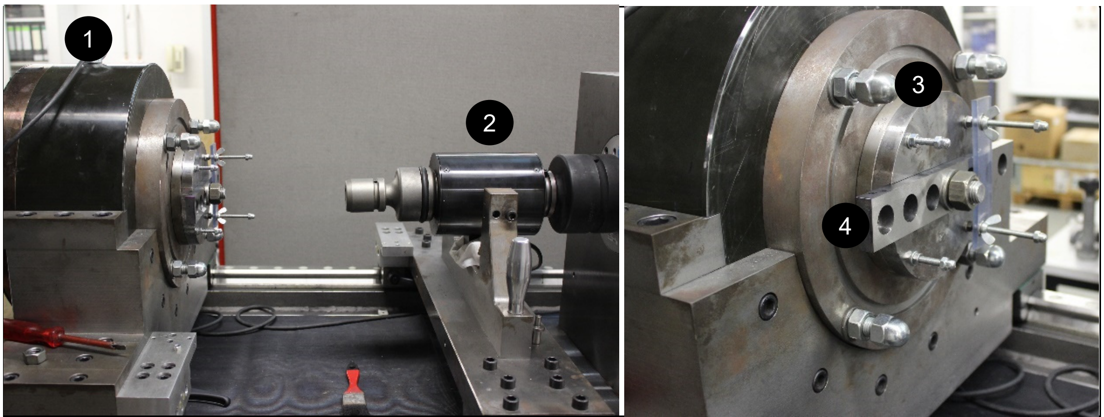


| | | |
|---|---|---|
| **1** | Sensor force – thread friction torque: SNo. 1016242 – 1,500 kN / 5,000 Nm | |
| **2** | Sensor total tightening torque – angle of rotation: SNo. 1024283 – 5,000 Nm | |
| **3** | Shims: DP 9mm + DP 12mm + M20 | Lubrication: Various |
| **4** | Support bar: Yes | Adapter: Yes |
| | Speed of rotation: 5.0 $min^{-1}$ | Rotated component: Hexagon nut |
| | Number of bolting assemblies tested: 5 | Washers: placed under nut |
| | Clamp length $\sum t$ = 60.5 mm according to EN 14399-3:2015-03 | |
| | Clamp length/bolt diameter ratio: 3.0 | Stop criteria: bolt force dropped to $F_{p,C}$ |

**Table 65** Test setup Bumax 109 – M20x140

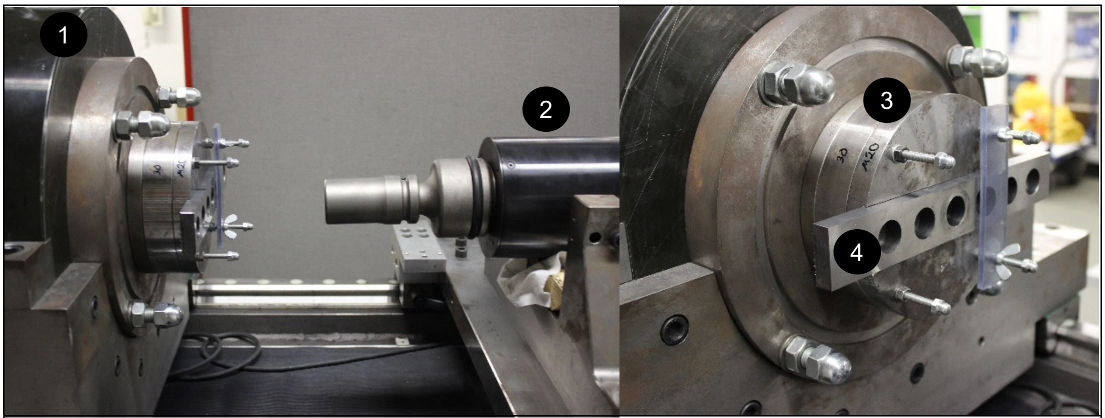


| | |
|---|---|
| **1** Sensor force – thread friction torque: SNo. 1016242 – 1,500 kN / 5,000 Nm | |
| **2** Sensor total tightening torque – angle of rotation: SNo. 1024283 – 5,000 Nm | |
| **3** Shims: DP 15mm + DP 30mm + M20HV | Lubrication: Various |
| **4** Support bar: Yes | Adapter: Yes |
| Speed of rotation: 5.0 $min^{-1}$ | Rotated component: Hexagon nut |
| Number of bolting assemblies tested: 5 | Washers: placed under nut |
| Clamp length ∑t = 105.0 mm according to EN 14399-3:2015-03 | |
| Clamp length/bolt diameter ratio: 5.3 | Stop criteria: bolt force dropped to $F_{p,C}$ |

### *3.4.1.1 Bumax 88 – M20x80 – 8.8 – EN ISO 4017 – gleitmo 1952V*

The Bumax 88 – M20x80 austenitic stainless steel bolting assemblies (used lubrication: Fuchs Lubritech gleitmo® 1952V standard lubrication) in property class 8.8, abbreviated below as BU_M20_88_80, were tested and arranged of following components including nominal mechanical properties based on Bumax datasheet:

- *Bolts:* BUFAB Group Bumax 88 – M20x80 A4 according to EN ISO 4017; stainless steel EN 1.4432, 1.4436, 1.4435; manufact.: 2015-06-05; PRE 27
  - tensile strength $R_{m,min}$ (= $f_{ub}$): nominal 800 N/mm²
  - yield strength $R_{p0.2,min}$ (= $f_{yb}$): nominal 640 N/mm²
  - elongation, min: nominal 0.3d
- *Nuts:* BUFAB Group Bumax 88 – M20 M6M A4 according to EN ISO 4032; stainless steel EN 1.4432, 1.4436, 1.4435; manufact.: 2015-05-11; PRE 27
  - stress under proof load, min: nominal 800 N/mm²
- *Washers:* BUFAB Group Bumax RB A4-HV200 according to EN ISO 7089; stainless steel EN 1.4432, 1.4436, 1.4435; with dimensions d = 21.0 mm, D = 37.0 mm, t = 3.0 mm; manufact.: 2014-03-19; PRE 27
  - hardness, min: nominal 200 HV

The tightening test results of Bumax 88 – M20x80 bolting assemblies (with gleitmo® 1952V standard lubrication) are summarized in Table 66, Table 67 and Table 68. The statistical evaluation is shown as well with fulfilled and failed criteria according to EN 14399-3 (System HR). In addition, the tightening curves are presented in Figure 56 and Figure 57. All tested bolting assemblies reached $F_{p,C}^*$ = 109.7 kN, $F_{p,C}$ = 137.2 kN, the criteria of maximum bolt force $F_{bi,max} \geq 0.9 \cdot f_{ub} \cdot A_s$ = 176.4 kN was achieved in the whole tested series. Due to the less pronounced plastic plateaus, only 2 of 5 bolts fulfilled criteria of $\Delta\Theta_{1i,min}$ = 120°. However, 5 of 5 bolts achieved $\Delta\Theta_{2i,min}$ = 240° (with coefficient of variation of 13.14 %) according to EN 14399-3. Furthermore, 5 of 5 tested bolts achieved k-class K1 with a narrow range of k-values between 0.12 and 0.13 and coefficient of variation v = 4.28 % (compared to k = 0.12 – 0.13 and v = 5.15 % at $F_{p,C}$*). For this reason, k-class K2 was accomplished. For further information and summarized criteria see Table 68. The graphs show irregular bolt force-tightening torque-curves because of minor galling in the nut bearing surface when tightened into the plastic range. Damages at the first and second load-bearing thread turn of the bolts and roughening of the paired threads could be observed. Minor galling especially in the faying surface washer/nut could be observed, too.

**Table 66** Test results of Bumax 88 – M20x80 – Gleitmo 1952V

| Legend | Specimens | $F_{p,C}$* | $F_{p,C}$ | Max F | Max T | $\Theta_{pi}$ | $\Theta_{1i}$ | $\Theta_{2i}$ | $F_{bi}$ ($\Theta_{2i}$) | $\Delta\Theta_{1i}$ | $\Delta\Theta_{2i}$ | k ($F_{p,C*}$) | k ($F_{p,C}$) | $\mu_{tot}$ ($F_{p,C}$) | $\mu_{th}$ ($F_{p,C}$) | $\mu_b$ ($F_{p,C}$) | M ($F_{p,C}$*) | $M_i$ ($F_{p,C}$) | M ($F_{bi,max}$) |
|---|---|---|---|---|---|---|---|---|---|---|---|---|---|---|---|---|---|---|---|
| | | kN | kN | kN | Nm | ° | ° | ° | kN | ° | ° | | | | | | Nm | Nm | Nm |
| max | | | | --- | | | | | | --- | --- | 0,16 | 0,16 | | | | | | |
| min | | | | 176,4 | | | | | | 120 | 240 | 0,10 | 0,10 | | | | | | |
| (red) | BU_M20_88_80-01 | 109,7 | 137,2 | 179,5 | 743,0 | 169 | 272 | 527 | 137,1 | <103 | 358 | 0,13 | 0,13 | 0,096 | 0,139 | 0,059 | 287,4 | 355,3 | 555,1 |
| (green) | BU_M20_88_80-02 | | | 180,2 | 770,3 | 161 | 254 | 455 | 137,0 | <93 | 295 | 0,12 | 0,12 | 0,086 | 0,112 | 0,064 | 262,3 | 324,7 | 550,2 |
| (blue) | BU_M20_88_80-03 | | | 184,6 | 832,3 | 170 | 281 | 475 | 137,1 | <110 | 305 | 0,13 | 0,13 | 0,097 | 0,144 | 0,055 | 291,1 | 356,7 | 567,3 |
| (orange) | BU_M20_88_80-04 | | | 184,3 | 846,5 | 149 | 270 | 548 | 137,1 | 120 | 399 | 0,12 | 0,12 | 0,088 | 0,119 | 0,060 | 265,2 | 328,5 | 606,4 |
| (magenta) | BU_M20_88_80-05 | | | 185,0 | 1122,9 | 152 | 259 | 464 | 137,1 | <107 | 311 | 0,12 | 0,12 | 0,092 | 0,114 | 0,072 | 264,3 | 340,9 | 710,3 |

**Table 67** Statistical evaluation of Bumax 88 – M20x80 – Gleitmo 1952V

| BU_M20_88_80 - Gleitmo 1952V | Max F | Max T | $\Theta_{pi}$ | $\Theta_{1i}$ | $\Theta_{2i}$ | $F_{bi}$ ($\Theta_{2i}$) | $\Delta\Theta_{1i}$ | $\Delta\Theta_{2i}$ | k ($F_{p,C*}$) | k ($F_{p,C}$) | $\mu_{tot}$ ($F_{p,C}$) | $\mu_{th}$ ($F_{p,C}$) | $\mu_b$ ($F_{p,C}$) | M ($F_{p,C}$*) | $M_i$ ($F_{p,C}$) | M ($F_{bi,max}$) |
|---|---|---|---|---|---|---|---|---|---|---|---|---|---|---|---|---|
| n = 5 | kN | Nm | ° | ° | ° | kN | ° | ° | | | | | | Nm | Nm | Nm |
| max | 185,0 | 1122,9 | 170 | 281 | 548 | 137,1 | 120 | 399 | 0,133 | 0,13 | 0,097 | 0,144 | 0,072 | 291,1 | 356,7 | 710,3 |
| min | 179,5 | 743,0 | 149 | 254 | 455 | 137,0 | 93 | 295 | 0,120 | 0,118 | 0,086 | 0,112 | 0,055 | 262,3 | 324,7 | 550,2 |
| R | 5,5 | 379,9 | 21 | 27 | 93 | 0,1 | 27 | 104 | 0,013 | 0,012 | 0,011 | 0,032 | 0,017 | 28,8 | 32,0 | 160,1 |
| $\bar{x}$ | 182,7 | 863,0 | 160 | 267 | 494 | 137,1 | 107 | 334 | 0,125 | 0,124 | 0,092 | 0,126 | 0,062 | 274,1 | 341,2 | 597,9 |
| s | 2,6 | 151,5 | 10 | 11 | 41 | 0,0 | 10 | 44 | 0,006 | 0,005 | 0,005 | 0,015 | 0,006 | 14,0 | 14,8 | 66,6 |
| ν | 1,45 | 17,55 | 5,98 | 4,03 | 8,34 | 0,03 | 9,25 | 13,14 | 5,15 | 4,28 | 5,25 | 11,82 | 10,39 | 5,10 | 4,33 | 11,14 |

n: number; R: range; $\bar{x}$: mean value; s: standard deviation; ν: coefficient of variation in [%]

**Table 68** Evaluation of test results of Bumax 88 – M20x80 – Gleitmo 1952V acc. EN 14399-3

| n | $F_{p,C}^*$ | $F_{p,C}$ | $F_{bi,max}$ | $\Delta\Theta_{1i,min}$ | $\Delta\Theta_{2i,min}$ | k-values | k-class K1 | k-class K2 | | Fracture | Galling |
|---|---|---|---|---|---|---|---|---|---|---|---|
| [-] | 109.7 kN | 137.2 kN | ≥ 176.4 kN | ≥ 120° | ≥ 240° | [-] | 0.10 ≤ $k_i$ ≤ 0.16 | 0.10 ≤ $k_m$ ≤ 0.23 | $V_k$ ≤ 0.06 | | |
| 5 | 100% | 100% | 100% | 20% | 100% | 0.12 – 0.13 | 100% | 0.124 | 0.043 | 0% | 60% |

**Figure 55** BU_M20_88 (Gleitmo 1952V) test specimen after tightening

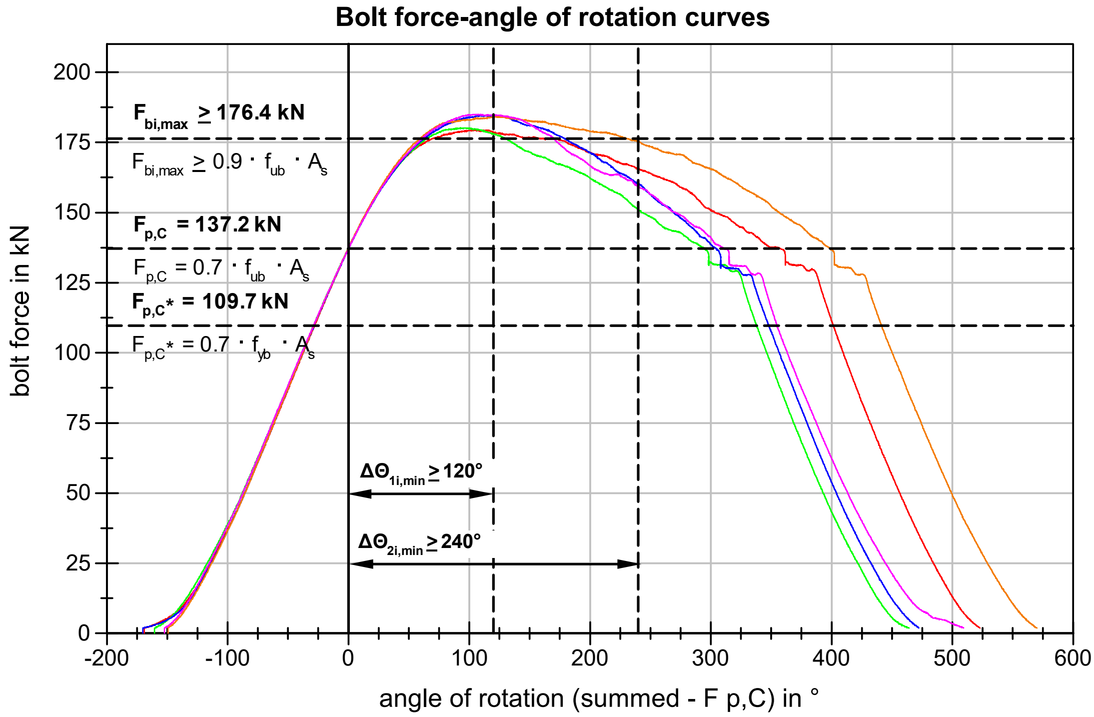


**Figure 56** BU_M20_88 (Gleitmo 1952V) Bolt force-angle of rotation curves

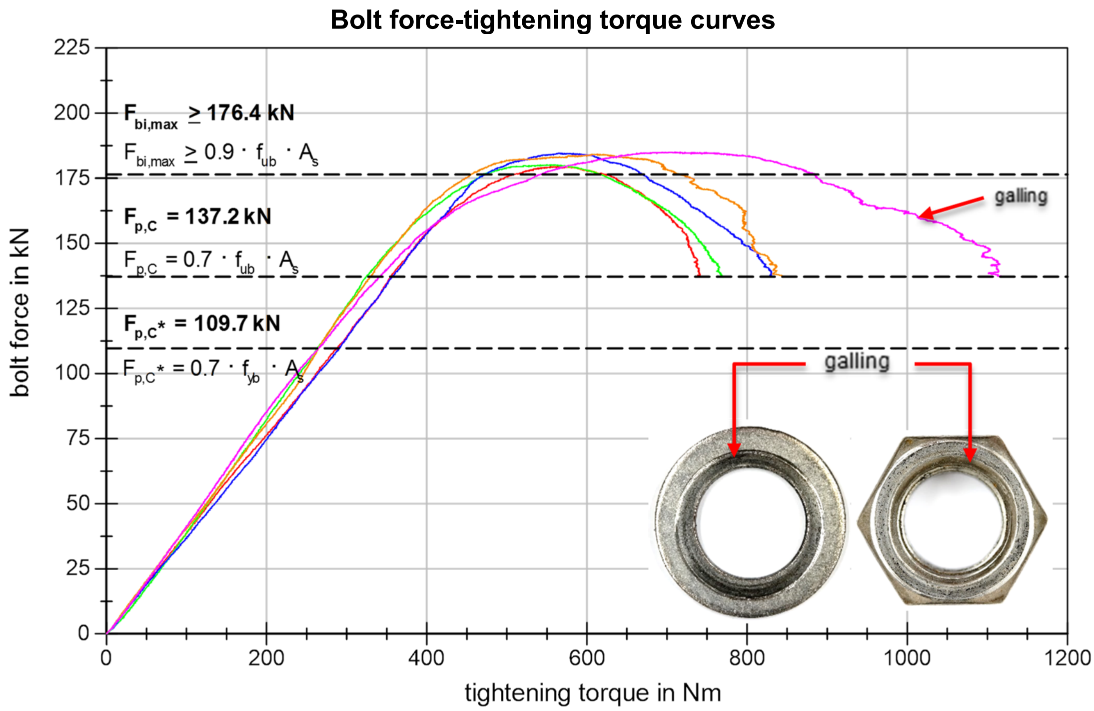


**Figure 57** BU_M20_88 (Gleitmo 1952V) Bolt force-tightening torque curves

### 3.4.1.2 Bumax 88 – M20x80 – 8.8 – EN ISO 4017 – Molykote 1000 spray

The Bumax 88 – M20x80 austenitic stainless steel bolting assemblies (used lubrication: Dow Corning Molykote® 1000 spray) in property class 8.8, abbreviated below as BU_M20_88_80, were tested and arranged of following components including nominal mechanical properties based on Bumax datasheet:

- *Bolts:* BUFAB Group Bumax 88 – M20x80 A4 according to EN ISO 4017; stainless steel EN 1.4432, 1.4436, 1.4435; manufact.: 2015-06-05; PRE 27

  tensile strength $R_{m,min}$ (= $f_{ub}$): nominal 800 N/mm²
  yield strength $R_{p0.2,min}$ (= $f_{yb}$): nominal 640 N/mm²
  elongation, min: nominal 0.3d

- *Nuts:* BUFAB Group Bumax 88 – M20 M6M A4 according to EN ISO 4032; stainless steel EN 1.4432, 1.4436, 1.4435; manufact.: 2015-05-11; PRE 27

  stress under proof load, min: nominal 800 N/mm²

- *Washers:* BUFAB Group Bumax RB A4-HV200 according to EN ISO 7089; stainless steel EN 1.4432, 1.4436, 1.4435; with dimensions d = 21.0 mm, D = 37.0 mm, t = 3.0 mm; manufact.: 2014-03-19; PRE 27

  hardness, min: nominal 200 HV

The test results and evaluation of Bumax 88 – M20x80 (Molykote 1000 spray) tested stainless steel bolting assemblies are summarized in Table 69, Table 70 and Table 71. The statistical evaluation is shown as well with fulfilled and failed criteria according to EN 14399-3 (System HR). Figure 59 and Figure 60 present the tightening graphs. Compared to the gleitmo 1952V series, they show significantly more pronounced bolt force plateaus in the plastic range. All tested austenitic bolting assemblies reached $F_{p,C}^*$ = 109.7 kN, $F_{p,C}$ = 137.2 kN as well as the maximum required bolt force $F_{bi,max} \geq 0.9 \cdot f_{ub} \cdot A_s$ = 176.4 kN. Furthermore, 5 of 5 tested bolts achieved k-class K1 with k-values between 0.12 and 0.14 and a coefficient of variation of v = 9.43 %. k-class K2 was not accomplished. For further information and summarized criteria see Table 71. The graphs show irregular bolt force-tightening torque-curves because of the strong galling in the nut bearing surface when tightened into the plastic range including significant high ranges of values $M_i$ at end of the tests (bolt force dropped again to $F_{p,C}$) in the bolt force-tightening torque-curves. 5 of 5 tested bolts achieved $\Delta\Theta_{1i,min}$ = 120° and $\Delta\Theta_{2i,min}$ = 240°. Damages at the first and second load-bearing thread turn of the bolts and roughening of paired threads could be observed; bolt failure by fracture did not occur. Strong galling in the faying surface washer/nut could be observed, too. It was possible to unscrew the hexagon nuts of all tested bolting assemblies manually but turning on the nut on thewhole threaded shank by hand was not possible.

**Table 69** Test results of Bumax 88 – M20x80 – Molykote 1000 spray

| Legend | Specimens | $F_{p,C}^*$ kN | $F_{p,C}$ kN | Max F kN | Max T Nm | $\Theta_{pi}$ ° | $\Theta_{1i}$ ° | $\Theta_{2i}$ ° | $F_{bi}$ ($\Theta_{2i}$) kN | $\Delta\Theta_{1i}$ ° | $\Delta\Theta_{2i}$ ° | k ($F_{p,C^*}$) | k ($F_{p,C}$) | $\mu_{tot}$ ($F_{p,C}$) | $\mu_{th}$ ($F_{p,C}$) | $\mu_b$ ($F_{p,C}$) | M ($F_{p,C}^*$) Nm | $M_i$ ($F_{p,C}$) Nm | M ($F_{bi,max}$) Nm |
|---|---|---|---|---|---|---|---|---|---|---|---|---|---|---|---|---|---|---|---|
| max | | | | --- | | | | | | --- | --- | 0,16 | 0,16 | | | | | | |
| min | | | | 176,4 | | | | | | 120 | 240 | 0,10 | 0,10 | | | | | | |
| | BU_M20_88_80-06 | 109,7 | 137,2 | 194,0 | 901,0 | 209 | 362 | 923 | 137,1 | 152 | 714 | 0,12 | 0,12 | 0,086 | 0,095 | 0,079 | 259,8 | 324,7 | 592,9 |
| | BU_M20_88_80-07 | | | 195,8 | 1268,4 | 186 | 335 | 880 | 137,1 | 149 | 694 | 0,12 | 0,12 | 0,087 | 0,084 | 0,090 | 260,6 | 326,6 | 649,2 |
| | BU_M20_88_80-08 | | | 185,8 | 1095,5 | 229 | 363 | 615 | 137,2 | 134 | 386 | 0,13 | 0,14 | 0,109 | 0,112 | 0,105 | 295,5 | 394,0 | 785,8 |
| | BU_M20_88_80-09 | | | 192,5 | 1343,3 | 186 | 337 | 820 | 136,9 | 151 | 634 | 0,14 | 0,14 | 0,107 | 0,110 | 0,103 | 312,3 | 387,5 | 833,4 |
| | BU_M20_88_80-10 | | | 193,7 | 1328,0 | 217 | 379 | 822 | 137,1 | 163 | 605 | 0,12 | 0,13 | 0,093 | 0,096 | 0,091 | 264,6 | 345,6 | 810,5 |

**Table 70** Statistical evaluation of Bumax 88 – M20x80 – Molykote 1000 spray

| BU_M20_88_80 - Molykote 1000 spray n = 5 | Max F kN | Max T Nm | $\Theta_{pi}$ ° | $\Theta_{1i}$ ° | $\Theta_{2i}$ ° | $F_{bi}$ ($\Theta_{2i}$) kN | $\Delta\Theta_{1i}$ ° | $\Delta\Theta_{2i}$ ° | k ($F_{p,C^*}$) | k ($F_{p,C}$) | $\mu_{tot}$ ($F_{p,C}$) | $\mu_{th}$ ($F_{p,C}$) | $\mu_b$ ($F_{p,C}$) | M ($F_{p,C}$*) Nm | $M_i$ ($F_{p,C}$) Nm | M ($F_{bi,max}$) Nm |
|---|---|---|---|---|---|---|---|---|---|---|---|---|---|---|---|---|
| max | 195,8 | 1343,3 | 229 | 379 | 923 | 137,2 | 163 | 714 | 0,142 | 0,14 | 0,109 | 0,112 | 0,105 | 312,3 | 394,0 | 833,4 |
| min | 185,8 | 901,0 | 186 | 335 | 615 | 136,9 | 134 | 386 | 0,118 | 0,118 | 0,086 | 0,084 | 0,079 | 259,8 | 324,7 | 592,9 |
| R | 10,0 | 442,3 | 43 | 44 | 308 | 0,3 | 29 | 328 | 0,024 | 0,026 | 0,023 | 0,028 | 0,026 | 52,5 | 69,3 | 240,5 |
| $\bar{x}$ | 192,4 | 1187,2 | 205 | 355 | 812 | 137,1 | 150 | 607 | 0,127 | 0,130 | 0,096 | 0,099 | 0,094 | 278,6 | 355,7 | 734,4 |
| s | 3,9 | 187,8 | 19 | 19 | 118 | 0,1 | 10 | 131 | 0,011 | 0,012 | 0,011 | 0,012 | 0,011 | 24,0 | 33,1 | 106,7 |
| ν | 2,00 | 15,82 | 9,29 | 5,29 | 14,56 | 0,08 | 6,93 | 21,59 | 8,54 | 9,43 | 11,35 | 11,68 | 11,35 | 8,60 | 9,31 | 14,53 |

n: number; R: range; $\bar{x}$: mean value; s: standard deviation; ν: coefficient of variation in [%]

**Table 71** Evaluation of test results of Bumax 88 – M20x80 Molykote 1000 spray acc. EN 14399-3

| n | $F_{p,C}^*$ | $F_{p,C}$ | $F_{bi,max}$ | $\Delta\Theta_{1i,min}$ | $\Delta\Theta_{2i,min}$ | k-values | k-class K1 | k-class K2 | | Fracture | Galling |
|---|---|---|---|---|---|---|---|---|---|---|---|
| [-] | 109.7 kN | 137.2 kN | ≥ 176.4 kN | ≥ 120° | ≥ 240° | [-] | $0.10 \le k_i \le 0.16$ | $0.10 \le k_m \le 0.23$ | $V_k \le 0.06$ | | |
| 5 | 100% | 100% | 100% | 100% | 100% | 0.12 – 0.14 | 100% | 0.130 | 0.094 | 0% | 100% |

**Figure 58** BU_M20_88 (Molykote 1000 spray) test specimen after tightening

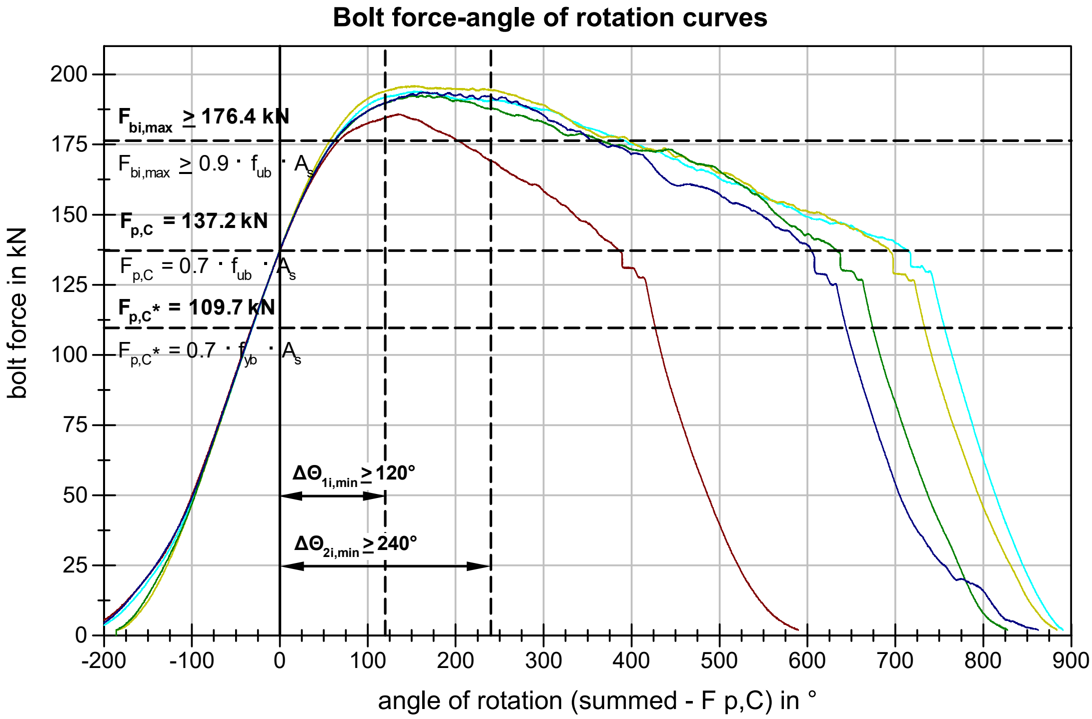


**Figure 59** BU_M20_88 (Molykote 1000 spray) Bolt force-angle of rotation curves

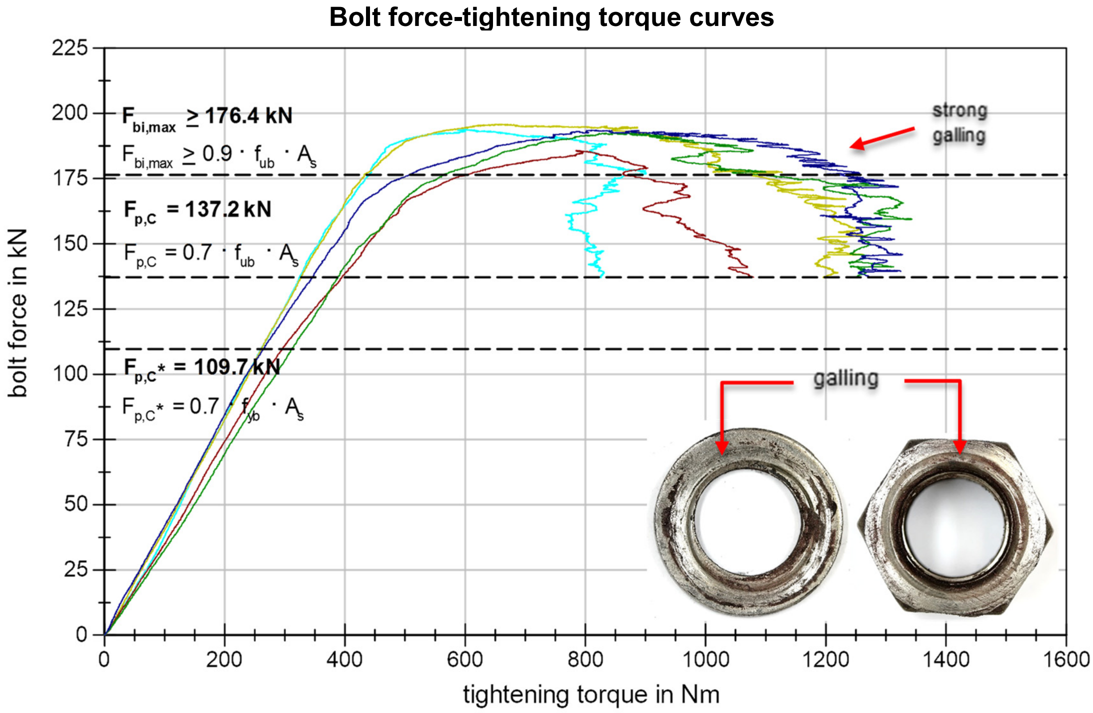


**Figure 60** BU_M20_88 (Molykote 1000 spray) Bolt force-tightening torque curves

### *3.4.1.3 Bumax 88 – M20x80 – 8.8 – EN ISO 4017 – Molykote 1000 paste*

The Bumax 88 – M20x80 austenitic stainless steel bolting assemblies (used lubrication: Dow Corning Molykote® 1000 paste) in property class 8.8, abbreviated below as BU_M20_88_80, were tested and arranged of following components including nominal mechanical properties based on Bumax datasheet:

- *Bolts:* BUFAB Group Bumax 88 – M20x80 A4 according to EN ISO 4017; stainless steel EN 1.4432, 1.4436, 1.4435; manufact.: 2015-06-05; PRE 27

  tensile strength $R_{m,min}$ (= $f_{ub}$): nominal 800 N/mm²
  yield strength $R_{p0.2,min}$ (= $f_{yb}$): nominal 640 N/mm²
  elongation, min: nominal 0.3d

- *Nuts:* BUFAB Group Bumax 88 – M20 M6M A4 according to EN ISO 4032; stainless steel EN 1.4432, 1.4436, 1.4435; manufact.: 2015-05-11; PRE 27

  stress under proof load, min: nominal 800 N/mm²

- *Washers:* BUFAB Group Bumax RB A4-HV200 according to EN ISO 7089; stainless steel EN 1.4432, 1.4436, 1.4435; with dimensions d = 21.0 mm, D = 37.0 mm, t = 3.0 mm; manufact.: 2014-03-19; PRE 27

  hardness, min: nominal 200 HV

Table 72, Table 73 and Table 74 summarize the test results and evaluation of tested stainless steel bolting assemblies. The statistical evaluation is shown as well as fulfilled and failed criteria according to EN 14399-3 (System HR). Figure 62 and Figure 63 present the tightening graphs. They show similar curves and pronounced bolt force plateaus in the plastic range compared to the Molykote 1000 spray series without any partial or total bolt fracture. All tested austenitic bolting assemblies reached specified preload $F_{p,C}$*, $F_{p,C}$ = 87.9 kN and also the maximum required bolt force $F_{bi,max} \geq 0.9 \cdot f_{ub} \cdot A_s$ = 176.4 kN. Furthermore, 5 of 5 tested bolts achieved k-class K1 with k-values in a narrow range between 0.13 and 0.15 and a coefficient of variation of v = 4.99 % (compared to k = 0.13 – 0.14 and v = 3.37 % at $F_{p,C}$*). k-class K2 was accomplished. The graphs show irregular bolt force-tightening torque-curves because of strong galling in the nut bearing surface when tightened into the plastic range including significant high ranges of values $M_i$ at $F_{bi,max}$ and at the end of the tests (bolt force dropped again to $F_{p,C}$) in the bolt force-tightening torque-curves. 4 of 5 tested bolts achieved $\Delta\Theta_{1i,min}$ = 120° and additionally, all bolts reached $\Delta\Theta_{2i,min}$ = 240°. Damages at the first and second load-bearing thread turn of the bolts and roughening of the paired threads could be observed; bolt failure by fracture did not occur. Galling in the faying surface washer/nut could be observed, too. Furthermore, in the context of functionality and re-use, it was possible to unscrew the hexagon nuts of all tested bolting assemblies manually but turning on the nut on the whole threaded shank by hand was not possible.

**Table 72** Test results of Bumax 88 – M20x80 – Molykote 1000 paste

| Legend | Specimens | $F_{p,C}$* kN | $F_{p,C}$ kN | Max F kN | Max T Nm | $\Theta_{pi}$ ° | $\Theta_{1i}$ ° | $\Theta_{2i}$ ° | $F_{bi}$ ($\Theta_{2i}$) kN | $\Delta\Theta_{1i}$ ° | $\Delta\Theta_{2i}$ ° | k ($F_{p,C*}$) | k ($F_{p,C}$) | $\mu_{tot}$ ($F_{p,C}$) | $\mu_{th}$ ($F_{p,C}$) | $\mu_b$ ($F_{p,C}$) | M ($F_{p,C}$*) Nm | $M_i$ ($F_{p,C}$) Nm | M ($F_{bi,max}$) Nm |
|---|---|---|---|---|---|---|---|---|---|---|---|---|---|---|---|---|---|---|---|
| max | | | | --- | | | | | | --- | --- | 0,16 | 0,16 | | | | | | |
| min | | | | 176,4 | | | | | | 120 | 240 | 0,10 | 0,10 | | | | | | |
| | BU_M20_88_80-11 | 109,7 | 137,2 | 184,9 | 1640,2 | 195 | 333 | 736 | 137,1 | 138 | 541 | 0,14 | 0,15 | 0,112 | 0,124 | 0,101 | 311,6 | 403,7 | 940,0 |
| | BU_M20_88_80-12 | | | 189,0 | 1214,3 | 179 | 324 | 710 | 137,1 | 146 | 531 | 0,14 | 0,14 | 0,104 | 0,115 | 0,094 | 308,4 | 378,9 | 854,4 |
| | BU_M20_88_80-13 | | | 188,7 | 1388,7 | 214 | 371 | 776 | 137,1 | 157 | 562 | 0,13 | 0,13 | 0,098 | 0,118 | 0,081 | 295,7 | 360,8 | 812,4 |
| | BU_M20_88_80-14 | | | 192,5 | 1255,3 | 183 | 325 | 695 | 137,1 | 143 | 512 | 0,14 | 0,13 | 0,099 | 0,106 | 0,094 | 297,2 | 364,8 | 822,7 |
| | BU_M20_88_80-15 | | | 181,7 | 1119,8 | 216 | 324 | 610 | 137,1 | <108 | 394 | 0,13 | 0,13 | 0,098 | 0,118 | 0,079 | 287,4 | 359,6 | 740,7 |

**Table 73** Statistical evaluation of Bumax 88 – M20x80 – Molykote 1000 paste

| BU_M20_88_80 - Molykote 1000 paste n = 5 | Max F kN | Max T Nm | $\Theta_{pi}$ ° | $\Theta_{1i}$ ° | $\Theta_{2i}$ ° | $F_{bi}$ ($\Theta_{2i}$) kN | $\Delta\Theta_{1i}$ ° | $\Delta\Theta_{2i}$ ° | k ($F_{p,C*}$) | k ($F_{p,C}$) | $\mu_{tot}$ ($F_{p,C}$) | $\mu_{th}$ ($F_{p,C}$) | $\mu_b$ ($F_{p,C}$) | M ($F_{p,C}$*) Nm | $M_i$ ($F_{p,C}$) Nm | M ($F_{bi,max}$) Nm |
|---|---|---|---|---|---|---|---|---|---|---|---|---|---|---|---|---|
| max | 192,5 | 1640,2 | 216 | 371 | 776 | 137,1 | 157 | 562 | 0,142 | 0,15 | 0,112 | 0,124 | 0,101 | 311,6 | 403,7 | 940,0 |
| min | 181,7 | 1119,8 | 179 | 324 | 610 | 137,1 | 108 | 394 | 0,131 | 0,131 | 0,098 | 0,106 | 0,079 | 287,4 | 359,6 | 740,7 |
| R | 10,8 | 520,4 | 37 | 47 | 166 | 0,0 | 49 | 168 | 0,011 | 0,016 | 0,014 | 0,018 | 0,022 | 24,2 | 44,1 | 199,3 |
| $\bar{x}$ | 187,4 | 1323,7 | 197 | 335 | 705 | 137,1 | 138 | 508 | 0,137 | 0,136 | 0,102 | 0,116 | 0,090 | 300,1 | 373,6 | 834,0 |
| s | 4,2 | 201,6 | 17 | 20 | 62 | 0,0 | 18 | 66 | 0,005 | 0,007 | 0,006 | 0,007 | 0,009 | 9,9 | 18,5 | 72,4 |
| ν | 2,22 | 15,23 | 8,68 | 6,04 | 8,72 | 0,00 | 13,27 | 13,04 | 3,37 | 4,99 | 5,89 | 5,66 | 10,49 | 3,29 | 4,96 | 8,68 |

n: number; R: range; $\bar{x}$: mean value; s: standard deviation; ν: coefficient of variation in [%]

**Table 74** Evaluation of test results of Bumax 88 – M20x80 – Molykote 1000 paste acc. EN 14399-3

| n | $F_{p,C}$* | $F_{p,C}$ | $F_{bi,max}$ | $\Delta\Theta_{1i,min}$ | $\Delta\Theta_{2i,min}$ | k-values | k-class K1 | k-class K2 | | Fracture | Galling |
|---|---|---|---|---|---|---|---|---|---|---|---|
| [-] | 109.7 kN | 137.2 kN | ≥ 176.4 kN | ≥ 120° | ≥ 240° | [-] | $0.10 \leq k_i \leq 0.16$ | $0.10 \leq k_m \leq 0.23$ | $V_k \leq 0.06$ | | |
| 5 | 100% | 100% | 100% | 80% | 100% | 0.13 – 0.15 | 100% | 0.136 | 0.050 | 0% | 100% |

**Figure 61** BU_M20_88 (Molykote 1000 paste) test specimen after tightening

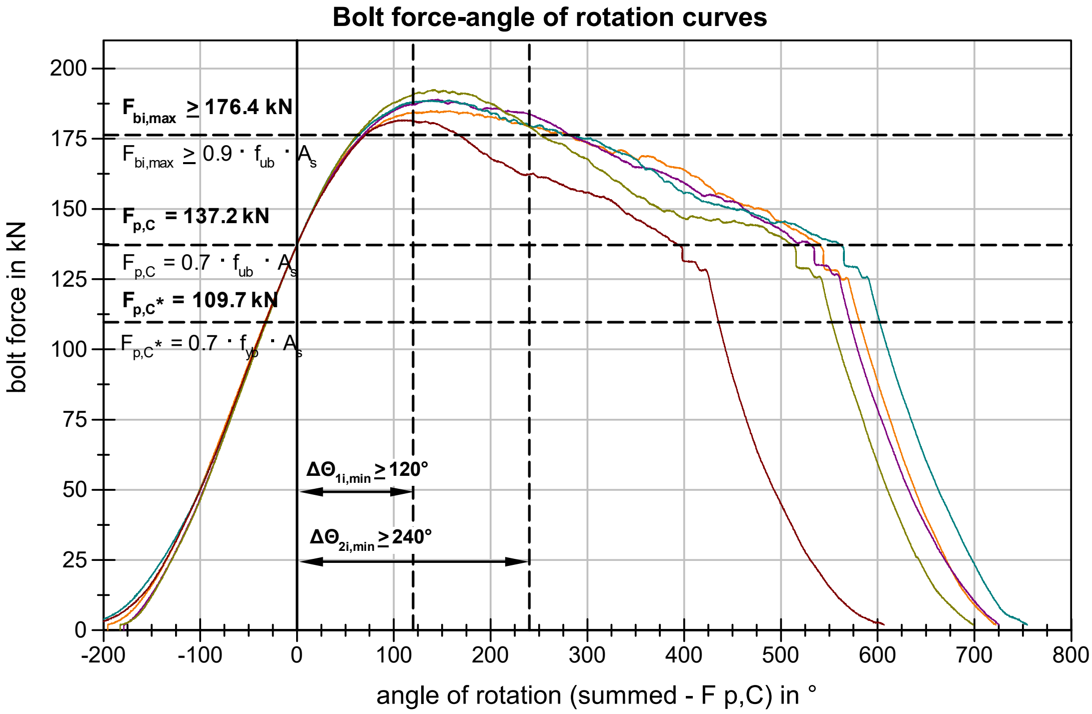


**Figure 62** BU_M20_88 (Molykote 1000 paste) Bolt force-angle of rotation curves

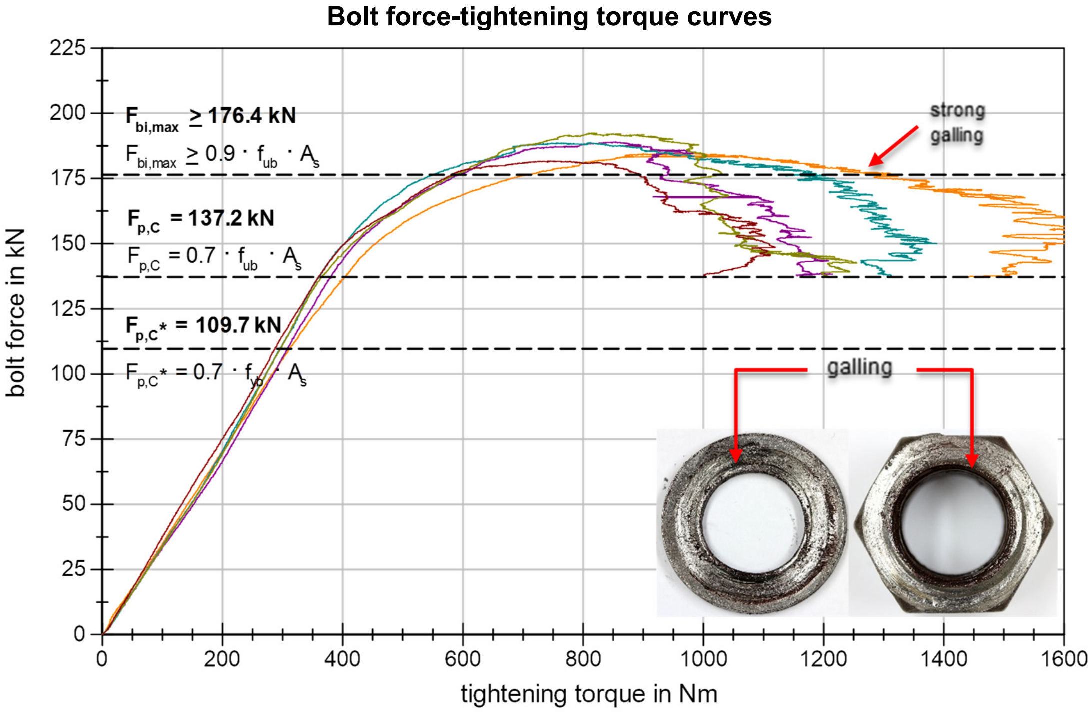


**Figure 63** BU_M20_88 (Molykote 1000 paste) Bolt force-tightening torque curves

#### *3.4.1.4 Bumax 88 – M20x80 – 8.8 – EN ISO 4017 – Molykote P-74 paste*

The Bumax 88 – M20x80 austenitic stainless steel bolting assemblies (used lubrication: Dow Corning Molykote® P-74 paste) in strength class 8.8, abbreviated below as BU_M20_88_80, were tested and arranged of following components including nominal mechanical properties based on Bumax datasheet:

- *Bolts:* BUFAB Group Bumax 88 – M20x80 A4 according to EN ISO 4017; stainless steel EN 1.4432, 1.4436, 1.4435; manufact.: 2015-06-05; PRE 27

  tensile strength $R_{m,min}$ (= $f_{ub}$): nominal 800 N/mm²
  yield strength $R_{p0.2,min}$ (= $f_{yb}$): nominal 640 N/mm²
  elongation, min: nominal 0.3d

- *Nuts:* BUFAB Group Bumax 88 – M20 M6M A4 according to EN ISO 4032; stainless steel EN 1.4432, 1.4436, 1.4435; manufact.: 2015-05-11; PRE 27

  stress under proof load, min: nominal 800 N/mm²

- *Washers:* BUFAB Group Bumax RB A4-HV200 according to EN ISO 7089; stainless steel EN 1.4432, 1.4436, 1.4435; with dimensions d = 21.0 mm, D = 37.0 mm, t = 3.0 mm; manufact.: 2014-03-19; PRE 27

  hardness, min: nominal 200 HV

The tightening test results of Bumax 88 – M20x80 (Molykote P-74 paste) bolting assemblies are summarized in Table 75, Table 76 and Table 77. The statistical evaluation is shown as well with fulfilled and failed criteria according to EN 14399-3 (System HR). In addition, the tightening curves are presented in Figure 65 and Figure 66. All tested austenitic bolting assemblies reached $F_{p,C}$* = 109.7 kN and $F_{p,C}$ = 137.2 kN as well as the criteria of maximum bolt force $F_{bi,max} \geq 0.9 \cdot f_{ub} \cdot A_s$ = 176.4kN. 4 of 5 bolts achieved angle of nut rotation $\Delta\Theta_{1i,min}$ = 120°, in addition 5 of 5 bolts achieved $\Delta\Theta_{2i,min}$ = 240° (with coefficient of variation of 21.92 %) according to EN 14399-3. Furthermore, 3 of 5 tested bolts achieved k-class K1 with k-values between 0.14 and 0.17 and coefficient of variation v = 8.34 % (compared to k = 0.13 – 0.15 and v = 5.83 % at $F_{p,C}$*). k-class K2 was not accomplished. For further information and summarized criteria see Table 77. Again, the graphs show irregular bolt force-tightening torque-curves because of minor and major galling in the nut bearing surface when tightened into the plastic range. In addition, the coefficients of friction $\mu_{tot}$ (v = 9.65 %), $\mu_{th}$ (v = 12.57 %), and $\mu_b$ (v = 23.79 %) show high scatterings at $F_{p,C}$. Damages at the first and second load-bearing thread turn of the bolts and roughening of the paired threads could be observed. Strong galling especially in the faying surface washer/nut could be observed, too.

**Table 75** Test results of Bumax 88 – M20x80 – Molykote P-74 paste

| Legend | Specimens | $F_{p,C}$* kN | $F_{p,C}$ kN | Max F kN | Max T Nm | $\Theta_{pi}$ ° | $\Theta_{1i}$ ° | $\Theta_{2i}$ ° | $F_{bi}$ ($\Theta_{2i}$) kN | $\Delta\Theta_{1i}$ ° | $\Delta\Theta_{2i}$ ° | k ($F_{p,C^*}$) | k ($F_{p,C}$) | $\mu_{tot}$ ($F_{p,C}$) | $\mu_{th}$ ($F_{p,C}$) | $\mu_b$ ($F_{p,C}$) | M ($F_{p,C}$*) Nm | $M_i$ ($F_{p,C}$) Nm | M ($F_{bi,max}$) Nm |
|---|---|---|---|---|---|---|---|---|---|---|---|---|---|---|---|---|---|---|---|
| max | | | | --- | | | | | | --- | --- | 0,16 | 0,16 | | | | | | |
| min | | | | 176,4 | | | | | | 120 | 240 | 0,10 | 0,10 | | | | | | |
| (green) | BU_M20_88_80-16 | 109,7 | 137,2 | 177,8 | 1147,9 | 213 | 338 | 620 | 137,0 | 126 | 407 | 0,15 | 0,16 | 0,119 | 0,141 | 0,100 | 320,1 | 427,6 | 866,6 |
| (blue) | BU_M20_88_80-17 | | | 179,4 | 1101,8 | 210 | 329 | 534 | 137,2 | <118 | 324 | 0,15 | >0,16 | 0,127 | 0,131 | 0,122 | 326,0 | 450,1 | 817,1 |
| (orange) | BU_M20_88_80-18 | | | 187,4 | 1173,5 | 212 | 351 | 766 | 137,0 | 138 | 553 | 0,13 | 0,13 | 0,101 | 0,120 | 0,084 | 288,4 | 369,1 | 802,2 |
| (magenta) | BU_M20_88_80-19 | | | 185,3 | 1219,1 | 241 | 373 | 589 | 137,1 | 132 | 348 | 0,15 | >0,17 | 0,131 | 0,101 | 0,158 | 332,3 | 465,0 | 863,7 |
| (cyan) | BU_M20_88_80-20 | | | 186,8 | 1329,7 | 227 | 364 | 684 | 137,1 | 136 | 456 | 0,14 | 0,15 | 0,119 | 0,115 | 0,121 | 303,7 | 425,1 | 965,4 |

**Table 76** Statistical evaluation of Bumax 88 – M20x80 – Molykote P-74 paste

| BU_M20_88_80 - Molykote P-74 paste n = 5 | Max F kN | Max T Nm | $\Theta_{pi}$ ° | $\Theta_{1i}$ ° | $\Theta_{2i}$ ° | $F_{bi}$ ($\Theta_{2i}$) kN | $\Delta\Theta_{1i}$ ° | $\Delta\Theta_{2i}$ ° | k ($F_{p,C^*}$) | k ($F_{p,C}$) | $\mu_{tot}$ ($F_{p,C}$) | $\mu_{th}$ ($F_{p,C}$) | $\mu_b$ ($F_{p,C}$) | M ($F_{p,C^*}$) Nm | $M_i$ ($F_{p,C}$) Nm | M ($F_{bi,max}$) Nm |
|---|---|---|---|---|---|---|---|---|---|---|---|---|---|---|---|---|
| max | 187,4 | 1329,7 | 241 | 373 | 766 | 137,2 | 138 | 553 | 0,151 | 0,17 | 0,131 | 0,141 | 0,158 | 332,3 | 465,0 | 965,4 |
| min | 177,8 | 1101,8 | 210 | 329 | 534 | 137,0 | 118 | 324 | 0,131 | 0,135 | 0,101 | 0,101 | 0,084 | 288,4 | 369,1 | 802,2 |
| R | 9,6 | 227,9 | 31 | 44 | 232 | 0,2 | 20 | 229 | 0,020 | 0,034 | 0,030 | 0,040 | 0,074 | 43,9 | 95,9 | 163,2 |
| $\bar{x}$ | 183,3 | 1194,4 | 221 | 351 | 639 | 137,1 | 130 | 418 | 0,143 | 0,156 | 0,119 | 0,122 | 0,117 | 314,1 | 427,4 | 863,0 |
| s | 4,4 | 86,7 | 13 | 18 | 89 | 0,1 | 8 | 92 | 0,008 | 0,013 | 0,012 | 0,015 | 0,028 | 17,9 | 36,5 | 63,8 |
| ν | 2,42 | 7,26 | 6,00 | 5,15 | 14,01 | 0,06 | 6,25 | 21,92 | 5,83 | 8,34 | 9,65 | 12,57 | 23,79 | 5,69 | 8,54 | 7,40 |

n: number; R: range; $\bar{x}$: mean value; s: standard deviation; ν: coefficient of variation in [%]

**Table 77** Evaluation of test results of Bumax 88 – M20x80 – Molykote P-74 paste acc. EN 14399-3

| n | $F_{p,C}^*$ | $F_{p,C}$ | $F_{bi,max}$ | $\Delta\Theta_{1i,min}$ | $\Delta\Theta_{2i,min}$ | k-values | k-class K1 | k-class K2 | | Fracture | Galling |
|---|---|---|---|---|---|---|---|---|---|---|---|
| [-] | 109.7 kN | 137.2 kN | ≥ 176.4 kN | ≥ 120° | ≥ 240° | [-] | $0.10 \le k_i \le 0.16$ | $0.10 \le k_m \le 0.23$ | $V_k \le 0.06$ | | |
| 5 | 100% | 100% | 100% | 80% | 100% | 0.14 – 0.17 | 60% | 0.156 | 0.083 | 0% | 80% |

**Figure 64** BU_M20_DX test specimen after tightening

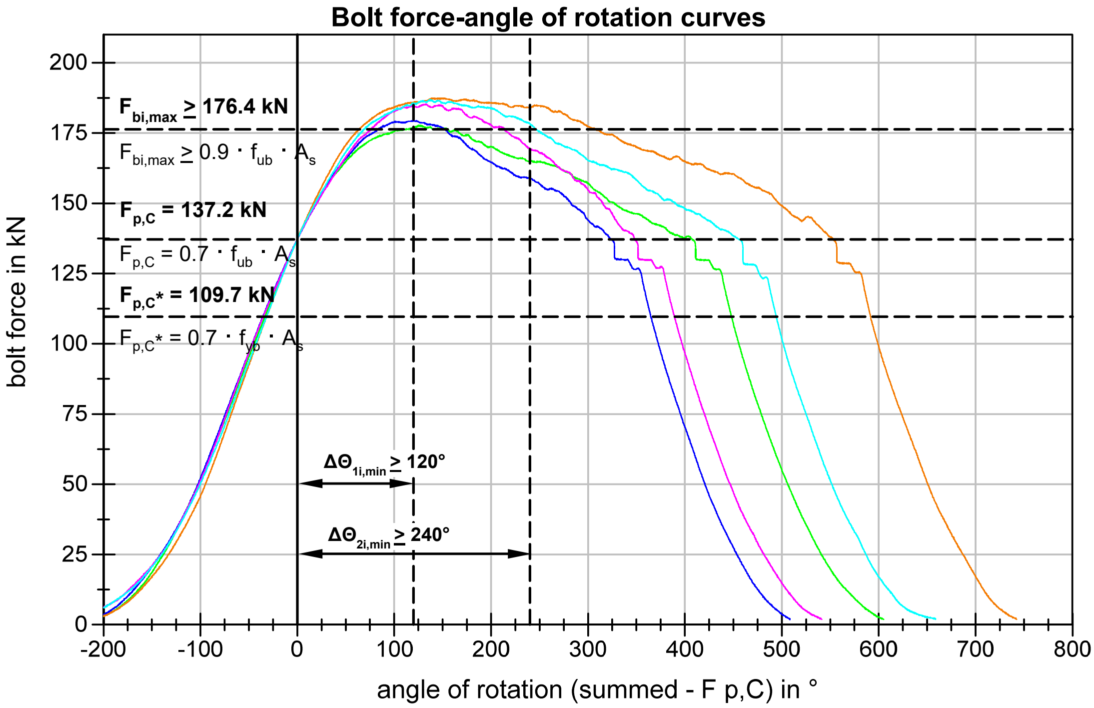


**Figure 65** BU_M20_88 (Molykote P-74 paste) Bolt force-angle of rotation curves

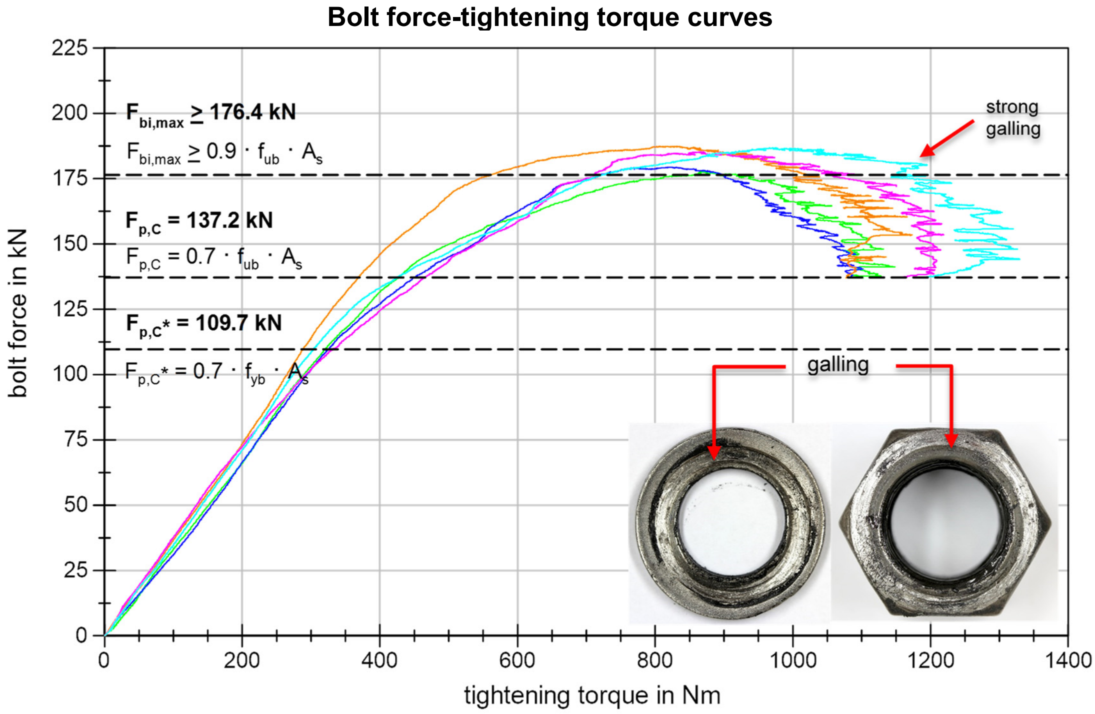


**Figure 66** BU_M20_88 (Molykote P-74 paste) Bolt force-tightening torque curves

### *3.4.1.5 Bumax 88 – M20x80 – 8.8 – EN ISO 4017 – Molykote D-321R spray*

The Bumax 88 – M20x80 austenitic stainless steel bolting assemblies (used lubrication: Dow Corning Molykote® D-321R spray) in property class 8.8/80, abbreviated below as BU_M20_88_80, were tested and arranged of following components including nominal mechanical properties based on Bumax datasheet:

- *Bolts:* BUFAB Group Bumax 88 – M20x80 A4 according to ISO 4017; stainless steel EN 1.4432, 1.4436, 1.4435; manufact.: 2015-06-05; PRE 27

  tensile strength $R_{m,min}$ (= $f_{ub}$): nominal 800 N/mm²
  yield strength $R_{p0.2,min}$ (= $f_{yb}$): nominal 640 N/mm²
  elongation, min: nominal 0.3d

- *Nuts:* BUFAB Group Bumax 88 – M20 M6M A4 according to ISO 4032; stainless steel EN 1.4432, 1.4436, 1.4435; manufact.: 2015-05-11; PRE 27

  stress under proof load, min: nominal 800 N/mm²

- *Washers:* BUFAB Group Bumax RB A4-HV200 according to ISO 7089; stainless steel EN 1.4432, 1.4436, 1.4435; with dimensions d = 21.0 mm, D = 37.0 mm, t = 3.0 mm; manufact.: 2014-03-19; PRE 27

  hardness, min: nominal 200 HV

The test results and evaluation tested stainless steel bolting assemblies are summarized in Table 78, Table 79 and Table 80. The statistical evaluation is shown as well with fulfilled and failed criteria according to EN 14399-3 (System HR). Figure 68 and Figure 69 present the tightening graphs. All tested bolting assemblies reached $F_{p,C}$*, $F_{p,C}$ and maximum required bolt force $F_{bi,max} \geq 0.9 \cdot f_{ub} \cdot A_s = 176.4$ kN.

Furthermore, 5 of 5 tested bolts achieved k-class K1 with low k-values between 0.10 and 0.11 and coefficient of variation v = 4.71 % (compared to k = 0.10 – 0.12 and v = 5.42 % at $F_{p,C}$*). For this reason, k-class K2 was accomplished. For further information and summarized criteria see Table 80. The graphs show irregular bolt force-tightening torque-curves because of galling in the nut bearing surface when tightened into the plastic range, especially at the end of the tests (bolt force dropped again to $F_{p,C}$). Due to the improved ductility, all tested bolts achieved $\Delta\Theta_{1i,min}$ = 120° and $\Delta\Theta_{2i,min}$ = 240°. Damages at the first and second load-bearing thread turn of the bolts and roughening of the paired threads could be observed; bolt failure by fracture did not occur. Galling in the faying surface washer/nut could be observed, too. It was possible to unscrew the hexagon nuts of all tested bolting assemblies manually but turning on the nut on the whole threaded shank by hand was not possible.

**Table 78** Test results of Bumax 88 – M20x80 – Molykote D-321R spray

| Legend | Specimens | $F_{p,C}$* kN | $F_{p,C}$ kN | Max F kN | Max T Nm | $\Theta_{pi}$ ° | $\Theta_{1i}$ ° | $\Theta_{2i}$ ° | $F_{bi}$ ($\Theta_{2i}$) kN | $\Delta\Theta_{1i}$ ° | $\Delta\Theta_{2i}$ ° | k ($F_{p,C^*}$) | k ($F_{p,C}$) | $\mu_{tot}$ ($F_{p,C}$) | $\mu_{th}$ ($F_{p,C}$) | $\mu_b$ ($F_{p,C}$) | M ($F_{p,C}$*) Nm | $M_i$ ($F_{p,C}$) Nm | M ($F_{bi,max}$) Nm |
|---|---|---|---|---|---|---|---|---|---|---|---|---|---|---|---|---|---|---|---|
| max | | | | --- | | | | | | --- | --- | 0,16 | 0,16 | | | | | | |
| min | | | | 176,4 | | | | | | 120 | 240 | 0,10 | 0,10 | | | | | | |
| (yellow) | BU_M20_88_80-21 | 109,7 | 137,2 | 197,3 | 1187,6 | 190 | 332 | 714 | 137,1 | 142 | 525 | 0,10 | 0,10 | 0,074 | 0,081 | 0,067 | 225,5 | 284,6 | 487,8 |
| (dark red) | BU_M20_88_80-22 | | | 198,8 | 1317,7 | 176 | 343 | 854 | 137,0 | 167 | 678 | 0,12 | 0,11 | 0,082 | 0,086 | 0,078 | 252,6 | 310,9 | 502,7 |
| (green) | BU_M20_88_80-23 | | | 198,0 | 1512,4 | 185 | 342 | 698 | 137,1 | 157 | 513 | 0,10 | 0,10 | 0,071 | 0,060 | 0,081 | 224,2 | 277,0 | 489,0 |
| (blue) | BU_M20_88_80-24 | | | 201,7 | 1525,3 | 208 | 367 | 865 | 137,1 | 159 | 657 | 0,10 | 0,10 | 0,071 | 0,070 | 0,072 | 221,5 | 277,5 | 471,8 |
| (orange) | BU_M20_88_80-25 | | | 194,1 | 1449,5 | 175 | 338 | 704 | 137,0 | 163 | 529 | 0,11 | 0,11 | 0,075 | 0,072 | 0,078 | 234,2 | 289,9 | 817,3 |

**Table 79** Statistical evaluation of Bumax 88 – M20x80 – Molykote D-321R spray

| BU_M20_88_80 - Molykote D-321R n = 5 | Max F kN | Max T Nm | $\Theta_{pi}$ ° | $\Theta_{1i}$ ° | $\Theta_{2i}$ ° | $F_{bi}$ ($\Theta_{2i}$) kN | $\Delta\Theta_{1i}$ ° | $\Delta\Theta_{2i}$ ° | k ($F_{p,C^*}$) | k ($F_{p,C}$) | $\mu_{tot}$ ($F_{p,C}$) | $\mu_{th}$ ($F_{p,C}$) | $\mu_b$ ($F_{p,C}$) | M ($F_{p,C}$*) Nm | $M_i$ ($F_{p,C}$) Nm | M ($F_{bi,max}$) Nm |
|---|---|---|---|---|---|---|---|---|---|---|---|---|---|---|---|---|
| max | 201,7 | 1525,3 | 208 | 367 | 865 | 137,1 | 167 | 678 | 0,115 | 0,11 | 0,082 | 0,086 | 0,081 | 252,6 | 310,9 | 817,3 |
| min | 194,1 | 1187,6 | 175 | 332 | 698 | 137,0 | 142 | 513 | 0,101 | 0,101 | 0,071 | 0,060 | 0,067 | 221,5 | 277,0 | 471,8 |
| R | 7,6 | 337,7 | 33 | 35 | 167 | 0,1 | 25 | 165 | 0,014 | 0,012 | 0,011 | 0,026 | 0,014 | 31,1 | 33,9 | 345,5 |
| $\bar{x}$ | 198,0 | 1398,5 | 187 | 344 | 767 | 137,1 | 158 | 580 | 0,106 | 0,105 | 0,075 | 0,074 | 0,075 | 231,6 | 288,0 | 553,7 |
| s | 2,7 | 143,8 | 13 | 13 | 85 | 0,1 | 10 | 80 | 0,006 | 0,005 | 0,005 | 0,010 | 0,006 | 12,7 | 13,9 | 147,8 |
| ν | 1,38 | 10,28 | 7,18 | 3,88 | 11,05 | 0,04 | 6,05 | 13,80 | 5,42 | 4,71 | 6,04 | 13,70 | 7,49 | 5,47 | 4,82 | 26,68 |

n: number; R: range; $\bar{x}$: mean value; s: standard deviation; ν: coefficient of variation in [%]

**Table 80** Evaluation of test results of Bumax 88 – M20x80 – Molykote D-321R spray acc. EN 14399-3

| n | $F_{p,C}$* | $F_{p,C}$ | $F_{bi,max}$ | $\Delta\Theta_{1i,min}$ | $\Delta\Theta_{2i,min}$ | k-values | k-class K1 | k-class K2 | | Fracture | Galling |
|---|---|---|---|---|---|---|---|---|---|---|---|
| [-] | 109.7 kN | 137.2 kN | ≥ 176.4 kN | ≥ 120° | ≥ 240° | [-] | $0.10 \leq k_i \leq 0.16$ | $0.10 \leq k_m \leq 0.23$ | $V_k \leq 0.06$ | | |
| 5 | 100% | 100% | 100% | 100% | 100% | 0.10 – 0.11 | 100% | 0.105 | 0.047 | 0% | 80% |

**Figure 67** BU_M20_88 (Molykote D-321R spray) test specimen after tightening

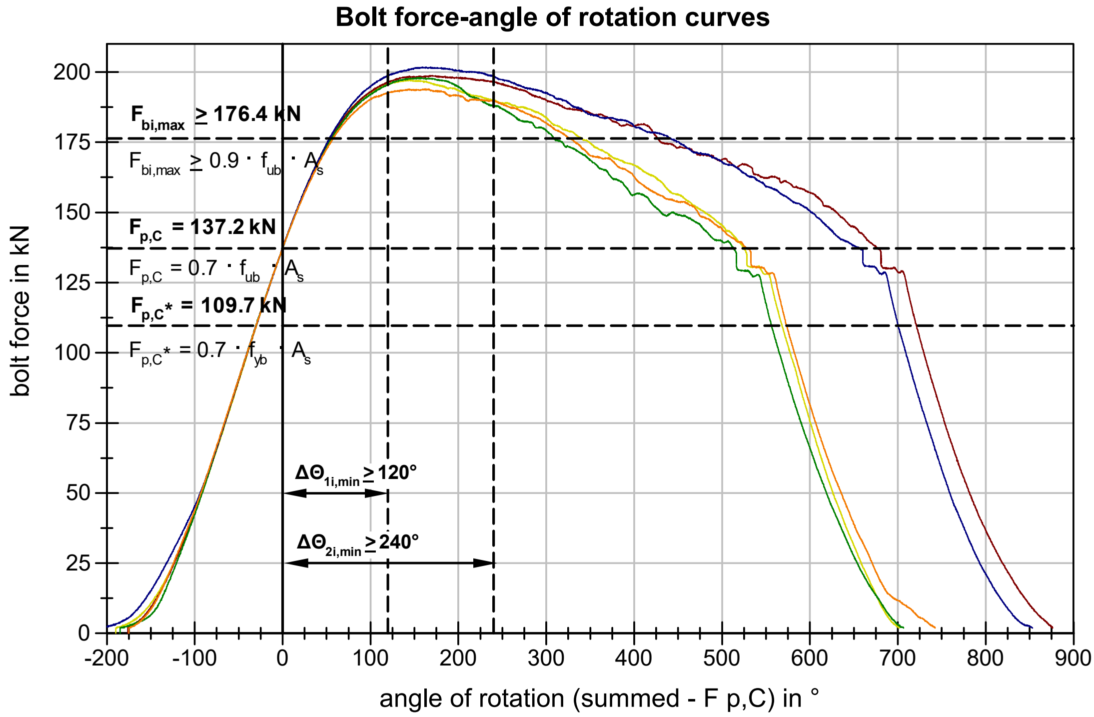


**Figure 68** BU_M20_88 (Molykote D-321R spray) Bolt force-angle of rotation curves

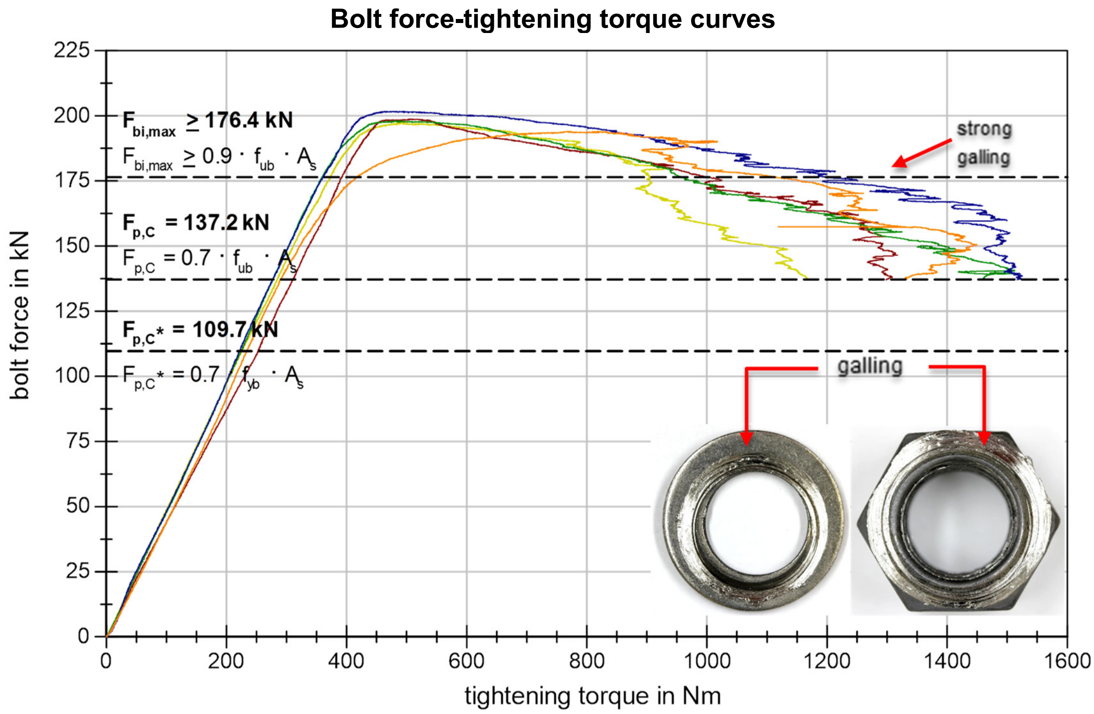


**Figure 69** BU_M20_88 (Molykote D-321R spray) bolt force-tightening torque curves

## 3.4.2 Additional tightening tests: Bolt dimension M12

For bolt dimension M12, additional tightening tests of stainless steel super duplex bolts M12x80 in property class 10.9 were performed. The tested super duplex bolts were produced according to EN ISO 4017. The clamp length $\Sigma t$ was set to 64.0 mm (clamp length/bolt diameter ratio of 5.3) in reference to the corresponding tables of System HR – EN 14399-3 respectively System HV – EN 14399-4. The bolting assemblies were tightened nut sided with constant speed of rotation of 5.0 $min^{-1}$ and stopped when the bolt force dropped to $F_{p,c}$ again to allow a more detailed investigation of the basic preloading behaviour.

The criteria of evaluation regarding to EN 14399-3 for bolting assemblies in property class 10.9 (equal to Bumax SDX series) are defined as follows:

- $F_{p,C}^* = 0.7 \cdot f_{yb} \cdot A_s = 0.7 \cdot 900$ N/mm² · 84.3 mm² = 53.1 kN
- $F_{p,C} = 0.7 \cdot f_{ub} \cdot A_s = 0.7 \cdot 1000$ N/mm² · 84.3 mm² = 59.0 kN
- $F_{bi,max} \geq 0.9 \cdot f_{ub} \cdot A_s = 0.9 \cdot 1000$ N/mm² · 84.3 mm² = 75.9 kN
- $\Delta\Theta_{1i,min} \geq 120°$ with $\Sigma t$ = 64.0 mm: $2d \leq \Sigma t < 6d$
- $\Delta\Theta_{2i,min} \geq 240°$ with $\Sigma t$ = 64.0 mm: $2d \leq \Sigma t < 6d$

#### *3.4.2.1 Bumax SDX – M12x80 – Molykote 1000 spray*

The Bumax SDX – M12x80 super duplex stainless steel bolting assemblies (used lubrication: Dow Corning Molykote® 1000 spray) in property class 10.9, abbreviated as BU_M12_SDX, were arranged as follows including mechanical properties based on Bumax datasheet:

- *Bolts:* BUFAB Group Bumax SDX - M12x80 according to EN ISO 4017; stainless steel EN 1.4410; manufact.: 2014-11-14; PRE 42

  tensile strength $R_{m,min}$ (= $f_{ub}$): nominal 1000 N/mm²
  yield strength $R_{p0.2,min}$ (= $f_{yb}$): nominal 900 N/mm²
  elongation, min: nominal 0.3d

- *Nuts:* BUFAB Group Bumax 109 - M12 M6M A4 according to EN ISO 4032; stainless steel EN 1.4432, 1.4436, 1.4435; manufact.: 2014-05-22; PRE 27

  stress under proof load, min: nominal 1000 N/mm²

- *Washers:* BUFAB Group Bumax RB A4-HV300 according to EN ISO 7089; stainless steel EN 1.4432, 1.4436, 1.4435; with dimensions d = 13.0 mm, D = 24.0 mm, t = 2.5 mm; manufact.: 2015-04-14; PRE 27

  hardness, min: nominal 300 HV

The test results of Bumax SDX – M12x80 super duplex bolting assemblies (used lubrication: Dow Corning Molykote 1000 spray) according to EN ISO 4017 and property class 10.9 are presented in Table 81, Table 82 and Table 83 including statistical data and evaluation. Referring to EN 14399-3, all bolting assemblies fulfilled the specified preload of $F_{p,C}^*$ and $F_{p,C}$, and additionally, 10 of 10 bolts achieved $F_{bi,max} \geq 0.9 \cdot f_{ub} \cdot A_s$ = 75.9 kN. The bolt force plateaus in the plastic range are significantly more pronounced compared to the Bumax SDX – M12x80 gleitmo 1952V series. Furthermore, 10 of 10 tested bolts achieved k-class K1 with k-values at $F_{p,C}$ between 0.12 and 0.16 (equal to k = 0.12 – 0.16 at $F_{p,C}^*$). Once more, k-class K2 is not achieved caused by a coefficient of variation of v = 9.72 %. Additionally, all bolts achieved $F_{bi,max} \geq 0.9 \cdot f_{ub} \cdot A_s$ = 75.9 kN according to EN 14399-3. The tightening graphs of BU_M12_SDX 109 (Molykote 1000 spray) are presented in Figure 71 and

Figure 72 and show again irregular bolt force-torque-curves caused by strong galling in the nut bearing surface. Furthermore, the damages of the tested super duplex bolting assemblies are similar to the austenitic stainless steel bolts with damages mainly at the first and second load-bearing thread turns, roughening of the paired threads and minimal necking of the threaded shanks. Strong galling occurred in all tested bolting assemblies, fracture occurred in 7 of 10 bolts only after the end of the test when turning off the nut. Furthermore, it was possible to unscrew the hexagon nuts of all tested bolting assemblies manually by hand.

**Table 81** Test results of Bumax SDX – M12x80 – Molykote 1000 spray

| Legend | Specimens | $F_{p,C}$* kN | $F_{p,C}$ kN | Max F kN | Max T Nm | $\Theta_{pi}$ ° | $\Theta_{1i}$ ° | $\Theta_{2i}$ ° | $F_{bi}$ ($\Theta_{2i}$) kN | $\Delta\Theta_{1i}$ ° | $\Delta\Theta_{2i}$ ° | k ($F_{p,C^*}$) | k ($F_{p,C}$) | $\mu_{tot}$ ($F_{p,C}$) | $\mu_{th}$ ($F_{p,C}$) | $\mu_b$ ($F_{p,C}$) | M ($F_{p,C}$*) Nm | $M_i$ ($F_{p,C}$) Nm | M ($F_{bi,max}$) Nm |
|---|---|---|---|---|---|---|---|---|---|---|---|---|---|---|---|---|---|---|---|
| max | | | | --- | | | | | | --- | --- | 0,16 | 0,16 | | | | | | |
| min | | | | 75,9 | | | | | | 120 | 240 | 0,10 | 0,10 | | | | | | |
| | BU_M12_SDX-11 | 53,1 | 59 | 95,5 | 370,5 | 150 | 365 | 752 | 59,0 | 216 | 603 | 0,13 | 0,13 | 0,092 | 0,087 | 0,097 | 81,4 | 91,0 | 257,4 |
| | BU_M12_SDX-12 | | | 88,9 | 310,5 | 158 | 350 | 719 | 58,9 | 191 | 560 | 0,12 | 0,12 | 0,086 | 0,080 | 0,090 | 77,1 | 85,5 | 222,9 |
| | BU_M12_SDX-13 | | | 90,2 | 312,4 | 152 | 400 | 838 | 59,0 | 248 | 687 | 0,12 | 0,12 | 0,085 | 0,085 | 0,084 | 75,6 | 84,8 | 255,6 |
| | BU_M12_SDX-14 | | | 92,5 | 259,5 | 156 | 400 | 872 | 59,0 | 244 | 716 | 0,16 | 0,16 | 0,120 | 0,138 | 0,105 | 99,1 | 113,3 | 234,7 |
| | BU_M12_SDX-15 | | | 94,1 | 308,2 | 158 | 411 | 872 | 59,0 | 253 | 714 | 0,14 | 0,14 | 0,105 | 0,100 | 0,110 | 86,6 | 101,4 | 270,9 |
| | BU_M12_SDX-16 | | | 92,7 | 356,8 | 149 | 398 | 984 | 58,9 | 249 | 836 | 0,15 | 0,15 | 0,115 | 0,112 | 0,118 | 95,0 | 109,4 | 269,8 |
| | BU_M12_SDX-17 | | | 84,9 | 286,6 | 153 | 332 | 781 | 59,0 | 179 | 628 | 0,14 | 0,15 | 0,109 | 0,109 | 0,108 | 88,9 | 104,0 | 226,6 |
| | BU_M12_SDX-18 | | | 89,0 | 329,7 | 157 | 317 | 640 | 58,9 | 160 | 483 | 0,14 | 0,14 | 0,104 | 0,090 | 0,117 | 86,7 | 100,7 | 255,7 |
| | BU_M12_SDX-19 | | | 91,4 | 333,8 | 155 | 359 | 730 | 59,0 | 204 | 575 | 0,13 | 0,13 | 0,095 | 0,094 | 0,096 | 82,5 | 93,1 | 258,5 |
| | BU_M12_SDX-20 | | | 87,1 | 368,7 | 153 | 358 | 939 | 59,0 | 205 | 787 | 0,14 | 0,14 | 0,104 | 0,116 | 0,093 | 87,7 | 100,0 | 271,6 |

**Table 82** Statistical evaluation of Bumax SDX – M12x80 – Molykote 1000 spray

| Bumax SDX - M12x80 ISO 4017 - Molykote 1000 spray n = 10 | Max F kN | Max T Nm | $\Theta_{pi}$ ° | $\Theta_{1i}$ ° | $\Theta_{2i}$ ° | $F_{bi}$ ($\Theta_{2i}$) kN | $\Delta\Theta_{1i}$ ° | $\Delta\Theta_{2i}$ ° | k ($F_{p,C^*}$) | k ($F_{p,C}$) | $\mu_{tot}$ ($F_{p,C}$) | $\mu_{th}$ ($F_{p,C}$) | $\mu_b$ ($F_{p,C}$) | M ($F_{p,C}$*) Nm | $M_i$ ($F_{p,C}$) Nm | M ($F_{bi,max}$) Nm |
|---|---|---|---|---|---|---|---|---|---|---|---|---|---|---|---|---|
| max | 95,5 | 370,5 | 158 | 411 | 984 | 59,0 | 253 | 836 | 0,156 | 0,16 | 0,120 | 0,138 | 0,118 | 99,1 | 113,3 | 271,6 |
| min | 84,9 | 259,5 | 149 | 317 | 640 | 58,9 | 160 | 483 | 0,119 | 0,120 | 0,085 | 0,080 | 0,084 | 75,6 | 84,8 | 222,9 |
| R | 10,6 | 111,0 | 9 | 94 | 344 | 0,1 | 93 | 353 | 0,037 | 0,040 | 0,035 | 0,058 | 0,034 | 23,5 | 28,5 | 48,7 |
| $\bar{x}$ | 90,6 | 323,7 | 154 | 369 | 813 | 59,0 | 215 | 659 | 0,135 | 0,139 | 0,102 | 0,101 | 0,102 | 86,1 | 98,3 | 252,4 |
| s | 3,3 | 35,7 | 3 | 32 | 107 | 0,0 | 33 | 109 | 0,012 | 0,013 | 0,012 | 0,018 | 0,012 | 7,3 | 9,6 | 18,1 |
| ν | 3,59 | 11,04 | 2,08 | 8,66 | 13,17 | 0,08 | 15,24 | 16,53 | 8,53 | 9,72 | 11,61 | 17,58 | 11,34 | 8,53 | 9,74 | 7,17 |

n: number; R: range; $\bar{x}$: mean value; s: standard deviation; ν: coefficient of variation in [%]

**Table 83** Evaluation of test results of Bumax SDX – M12x80 – Molykote 1000 spray acc. EN 14399-3

| n | $F_{p,C}$* | $F_{p,C}$ | $F_{bi,max}$ | $\Delta\Theta_{1i,min}$ | $\Delta\Theta_{2i,min}$ | k-values | k-class K1 | k-class K2 | | Fracture | Galling |
|---|---|---|---|---|---|---|---|---|---|---|---|
| [-] | 53.1 kN | 59.0 kN | ≥ 75.9 kN | ≥ 120° | ≥ 240° | [-] | $0.10 \le k_i \le 0.16$ | $0.10 \le k_m \le 0.23$ | $V_k \le 0.06$ | | |
| 10 | 100% | 100% | 100% | 100% | 100% | 0.12 – 0.16 | 100% | 0.139 | 0.097 | 70% | 100% |

**Figure 70** BU_M12_SDX test specimen after tightening

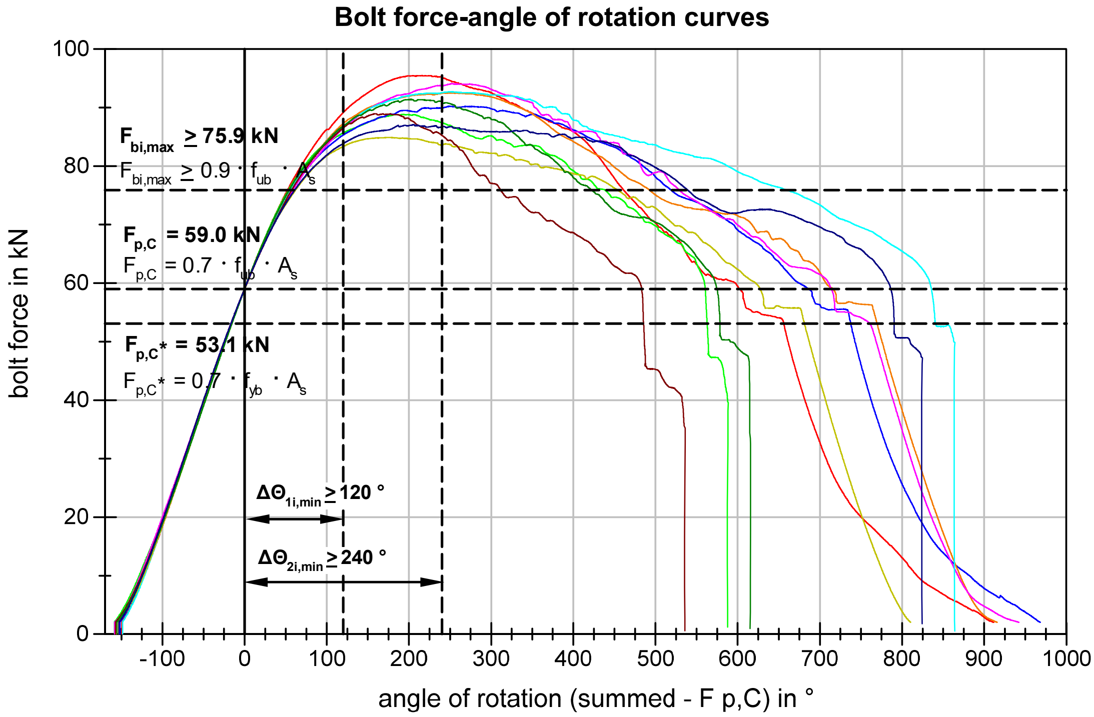


**Figure 71** BU_M12_SDX Bolt force-angle of rotation curves

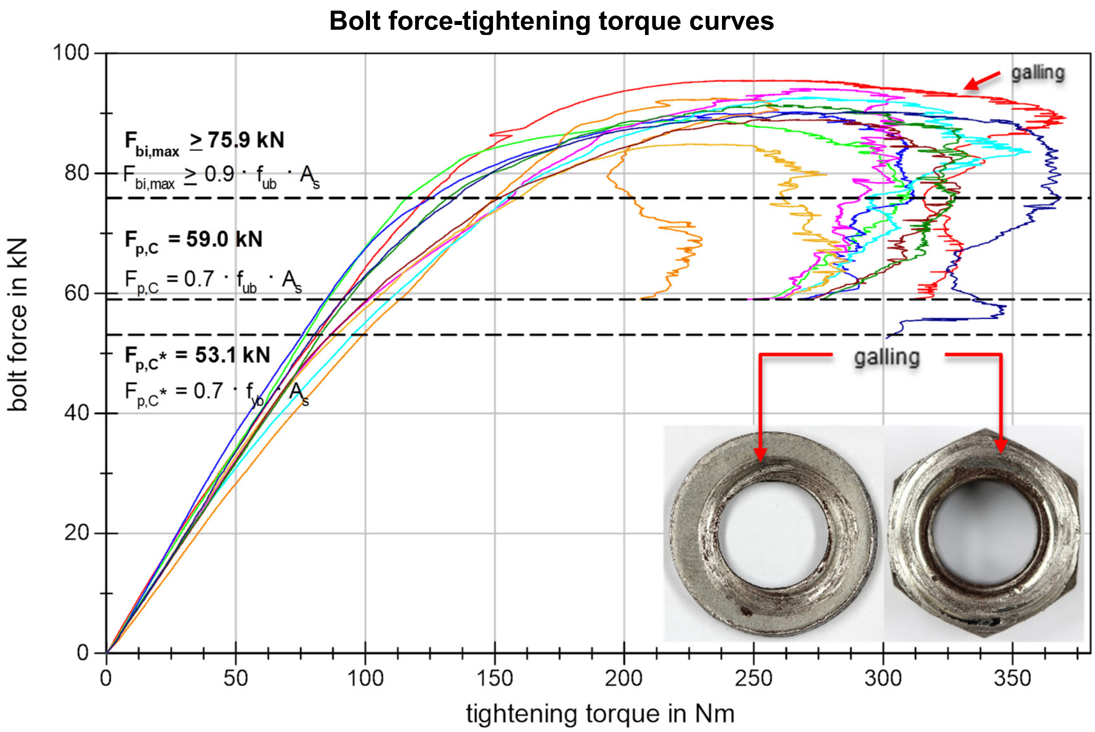


**Figure 72** BU_M12_SDX Bolt force-tightening torque curves

## 3.4.3 Additional tightening tests: Bolt dimension M20

Tightening tests for bolt dimension M20 were performed according to EN 14399-2 and EN ISO 16047. The test procedure contains a constant speed of rotation of 5.0 $min^{-1}$

for Bumax 109, lean duplex and duplex steel grades. All series were tightened nut sided, the clamping length ∑t was set to 72.0 mm (clamp length/bolt diameter ratio of 3.6) in reference to the corresponding tables of System HR – EN 14399-3. The tightening tests were stopped when the measured bolt force dropped to $F_{p,c} = 0.7 \cdot f_{ub} \cdot A_s$ (with $f_{ub}$: tensile strength of the bolt and $A_s$: tensile stress area of the bolt).

The criteria of evaluation for bolting assemblies in property class 10.9 (meaning Bumax 109, Bumax lean duplex and Bumax duplex series) are defined as follows:

- $F_{p,C}^* = 0.7 \cdot f_{yb} \cdot A_s = 0.7 \cdot 800$ N/mm² $\cdot$ 245.0 mm² = 137.2 kN (for Bumax 109 bolts)
- $F_{p,C}^* = 0.7 \cdot f_{yb} \cdot A_s = 0.7 \cdot 900$ N/mm² $\cdot$ 245.0 mm² = 154.4 kN (for Bumax LDX and DX)
- $F_{p,C} = 0.7 \cdot f_{ub} \cdot A_s = 0.7 \cdot 1000$ N/mm² $\cdot$ 245.0 mm² = 171.5 kN
- $F_{bi,max} \geq 0.9 \cdot f_{ub} \cdot A_s = 0.9 \cdot 1000$ N/mm² $\cdot$ 245.0 mm² = 220.5 kN
- $\Delta\Theta_{1i,min} \geq 120°$ with $\Sigma t$ = 105.0 mm: $2d \leq \Sigma t < 6d$
- $\Delta\Theta_{2i,min} \geq 240°$ with $\Sigma t$ = 105.0 mm: $2d \leq \Sigma t < 6d$

### *3.4.3.1 Bumax 109 – M20x100 – 10.9 – EN ISO 4017 – Molykote 1000 spray*

The Bumax 109 – M20x100 austenitic stainless steel bolting assemblies in property class 10.9 according to EN ISO 4017 (used lubrication: Dow Corning Molykote® 1000 spray), abbreviated below as BU_M20_109, were arranged of the following components including nominal mechanical properties based on Bumax datasheet:

- *Bolts:* BUFAB Group Bumax 109 – M20x100 A4 according to EN ISO 4017; stainless steel EN 1.4432, 1.4436, 1.4435; manufact.: 2016-04-28; PRE 27

  tensile strength $R_{m,min}$ (= $f_{ub}$): nominal 1000 N/mm²
  yield strength $R_{p0.2,min}$ (= $f_{yb}$): nominal 800 N/mm²
  elongation, min: nominal 0.3d

- *Nuts:* BUFAB Group Bumax 88 – M20 M6M A4 according to EN ISO 4032; stainless steel EN 1.4432, 1.4436, 1.4435; manufact.: 2016-04-08; PRE 27

  stress under proof load, min: nominal 800 N/mm²

- *Washers:* BUFAB Group Bumax RB A4-HV200 according to EN ISO 7089; stainless steel EN 1.4432, 1.4436, 1.4435; with dimensions d = 21.0 mm, D = 37.0 mm, t = 3.0 mm; manufact.: 2015-09-22; PRE 27

  hardness, min: nominal 200 HV

Table 84, Table 85 and Table 86 summarize the test results and evaluation of Bumax 109 – M20x100 bolting assemblies (used lubrication: Molykote 1000 spray). The statistical evaluation is presented as well with an overview about the fulfilled and failed criteria according to EN 14399-3. The tightening graphs are shown in Figure 74 and Figure 75 and outline slightly improved bolt force plateaus in the plastic range. All tested bolting assemblies achieved $F_{p,C}^*$ = 137.2 kN and 10 of 10 tested bolting assemblies reached the specified preload $F_{p,C}$ = 171.5 kN. The maximum bolt force $F_{bi,max} \geq 0.9 \cdot f_{ub} \cdot A_s$ = 220.5 kN was not achieved caused by low ductile behaviour and high friction coefficients. 6 of the 10 bolts achieved $\Delta\Theta_{1i,min}$ = 120° and additionally, 7 of 10 bolts fulfilled the $\Delta\Theta_{2i,min}$ = 240° criteria according to EN 14399-3. Especially the coefficient of variation of $\mu_b$ is remarkably high (v = 24.30 % at $F_{p,C}$). The tightening graphs also show irregular bolt force-torque-curves like in the previous tested series because of galling in the nut bearing surface. Furthermore, the damages of the tested bolting assemblies show plastic deformations at the first load-bearing thread turn of the bolt and nut, roughening of the paired threads and minimal necking of the threaded shanks, comparable to previously tested series. Total or partial bolt failure by fracture did not occur. Strong galling in the faying-surface washer/nut was detected in all tested bolting assemblies.

**Table 84** Test results of Bumax 109 – M20x100 – Molykote 1000 spray

| Legend | Specimens | $F_{p,C^*}$ kN | $F_{p,C}$ kN | Max F kN | Max T Nm | $\Theta_{pi}$ ° | $\Theta_{1i}$ ° | $\Theta_{2i}$ ° | $F_{bi}(\Theta_{2i})$ kN | $\Delta\Theta_{1i}$ ° | $\Delta\Theta_{2i}$ ° | k ($F_{p,C^*}$) | k ($F_{p,C}$) | $\mu_{tot}$ ($F_{p,C}$) | $\mu_{th}$ ($F_{p,C}$) | $\mu_b$ ($F_{p,C}$) | M ($F_{p,C^*}$) Nm | $M_i$ ($F_{p,C}$) Nm | M ($F_{bi,max}$) Nm |
|---|---|---|---|---|---|---|---|---|---|---|---|---|---|---|---|---|---|---|---|
| max | | | | --- | | | | | | --- | --- | 0,16 | 0,16 | | | | | | |
| min | | | | 220,5 | | | | | | 120 | 240 | 0,10 | 0,10 | | | | | | |
| | BU_M20_109-31 | 137,2 | 171,5 | <213,7 | 1429,7 | 239 | 377 | 616 | 171,4 | 137 | 376 | 0,10 | 0,10 | 0,091 | 0,086 | 0,095 | 324,9 | 436,7 | 903,0 |
| | BU_M20_109-32 | | | <213,3 | 1513,8 | 248 | 400 | 841 | 171,3 | 152 | 593 | 0,10 | 0,10 | 0,090 | 0,101 | 0,081 | 340,8 | 434,1 | 879,6 |
| | BU_M20_109-33 | | | <191,5 | 1434,5 | 260 | 361 | 486 | 171,4 | <102 | <226 | 0,13 | 0,15 | 0,141 | 0,118 | 0,162 | 431,5 | 634,2 | 1044,5 |
| | BU_M20_109-34 | | | <211,5 | 1444,5 | 253 | 394 | 705 | 171,4 | 140 | 452 | 0,12 | 0,14 | 0,130 | 0,093 | 0,162 | 409,6 | 589,3 | 1016,9 |
| | BU_M20_109-36 | | | <195,5 | 1070,1 | 251 | 352 | 450 | 171,3 | <101 | <199 | 0,13 | 0,14 | 0,132 | 0,106 | 0,154 | 440,3 | 596,4 | 892,5 |
| | BU_M20_109-37 | | | <203,0 | 1370,1 | 262 | 416 | 580 | 171,4 | 154 | 319 | 0,13 | 0,15 | 0,139 | 0,110 | 0,165 | 443,5 | 626,6 | 1084,7 |
| | BU_M20_109-38 | | | <212,1 | 1771,2 | 243 | 428 | 754 | 171,2 | 185 | 511 | 0,12 | 0,13 | 0,123 | 0,114 | 0,130 | 414,0 | 561,3 | 1116,9 |
| | BU_M20_109-39 | | | <198,0 | 1219,1 | 263 | 363 | 520 | 171,4 | <99 | 257 | 0,12 | 0,12 | 0,111 | 0,120 | 0,102 | 386,4 | 513,7 | 845,9 |
| | BU_M20_109-40 | | | <192,2 | 1260,6 | 248 | 319 | 452 | 171,4 | <70 | <203 | 0,12 | 0,13 | 0,115 | 0,126 | 0,106 | 393,9 | 532,4 | 831,1 |
| | BU_M20_109-41 | | | <207,7 | 1405,5 | 256 | 380 | 622 | 171,3 | 124 | 366 | 0,12 | 0,14 | 0,124 | 0,115 | 0,132 | 410,3 | 567,0 | 853,7 |

**Table 85** Statistical evaluation of Bumax 109 – M20x100 – Molykote 1000 spray

| BU_M20_109 - Molykote 1000 Spray n = 10 | Max F kN | Max T Nm | $\Theta_{pi}$ ° | $\Theta_{1i}$ ° | $\Theta_{2i}$ ° | $F_{bi}(\Theta_{2i})$ kN | $\Delta\Theta_{1i}$ ° | $\Delta\Theta_{2i}$ ° | k ($F_{p,C^*}$) | k ($F_{p,C}$) | $\mu_{tot}$ ($F_{p,C}$) | $\mu_{th}$ ($F_{p,C}$) | $\mu_b$ ($F_{p,C}$) | M ($F_{p,C^*}$) Nm | $M_i$ ($F_{p,C}$) Nm | M ($F_{bi,max}$) Nm |
|---|---|---|---|---|---|---|---|---|---|---|---|---|---|---|---|---|
| max | 213,7 | 1771,2 | 263 | 428 | 841 | 171,4 | 185 | 593 | 0,133 | 0,15 | 0,141 | 0,126 | 0,165 | 443,5 | 634,2 | 1116,9 |
| min | 191,5 | 1070,1 | 239 | 319 | 450 | 171,2 | 70 | 199 | 0,097 | 0,104 | 0,090 | 0,086 | 0,081 | 324,9 | 434,1 | 831,1 |
| R | 22,2 | 701,1 | 24 | 109 | 391 | 0,2 | 115 | 394 | 0,036 | 0,048 | 0,051 | 0,040 | 0,084 | 118,6 | 200,1 | 285,8 |
| $\bar{x}$ | 203,9 | 1391,9 | 252 | 379 | 603 | 171,4 | 126 | 350 | 0,120 | 0,132 | 0,120 | 0,109 | 0,129 | 399,5 | 549,2 | 946,9 |
| s | 8,9 | 187,4 | 8 | 32 | 132 | 0,1 | 34 | 136 | 0,012 | 0,017 | 0,018 | 0,013 | 0,031 | 39,8 | 70,7 | 107,5 |
| ν | 4,39 | 13,46 | 3,19 | 8,50 | 21,97 | 0,04 | 26,80 | 38,75 | 10,04 | 12,83 | 15,05 | 11,50 | 24,30 | 9,97 | 12,87 | 11,35 |

n: number; R: range; $\bar{x}$: mean value; s: standard deviation; ν: coefficient of variation in [%]

**Table 86** Evaluation of test results of Bumax 109 – M20x140 – Molykote 1000 spray acc. EN 14399-3

| n | $F_{p,C}^*$ | $F_{p,C}$ | $F_{bi,max}$ | $\Delta\Theta_{1i,min}$ | $\Delta\Theta_{2i,min}$ | k-values | k-class K1 | k-class K2 | | Fracture | Galling |
|---|---|---|---|---|---|---|---|---|---|---|---|
| [-] | 137.2 kN | 171.5 kN | ≥ 220.5 kN | ≥ 120° | ≥ 240° | [-] | $0.10 \le k_i \le 0.16$ | $0.10 \le k_m \le 0.23$ | $V_k \le 0.06$ | | |
| 10 | 100% | 100% | 0% | 60% | 70% | 0.10 – 0.15 | 100% | 0.132 | 0.128 | 0% | 100% |

**Figure 73** BU_M20_109 test specimen after tightening

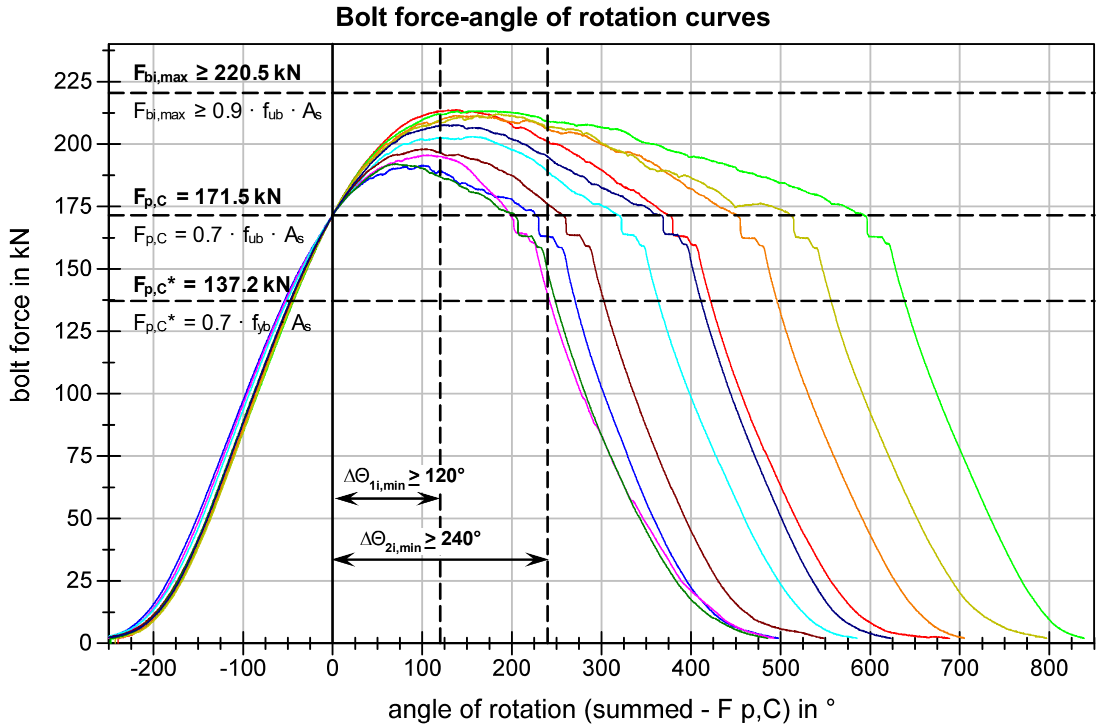


**Figure 74** BU_M20_109 Bolt force-angle of rotation curves

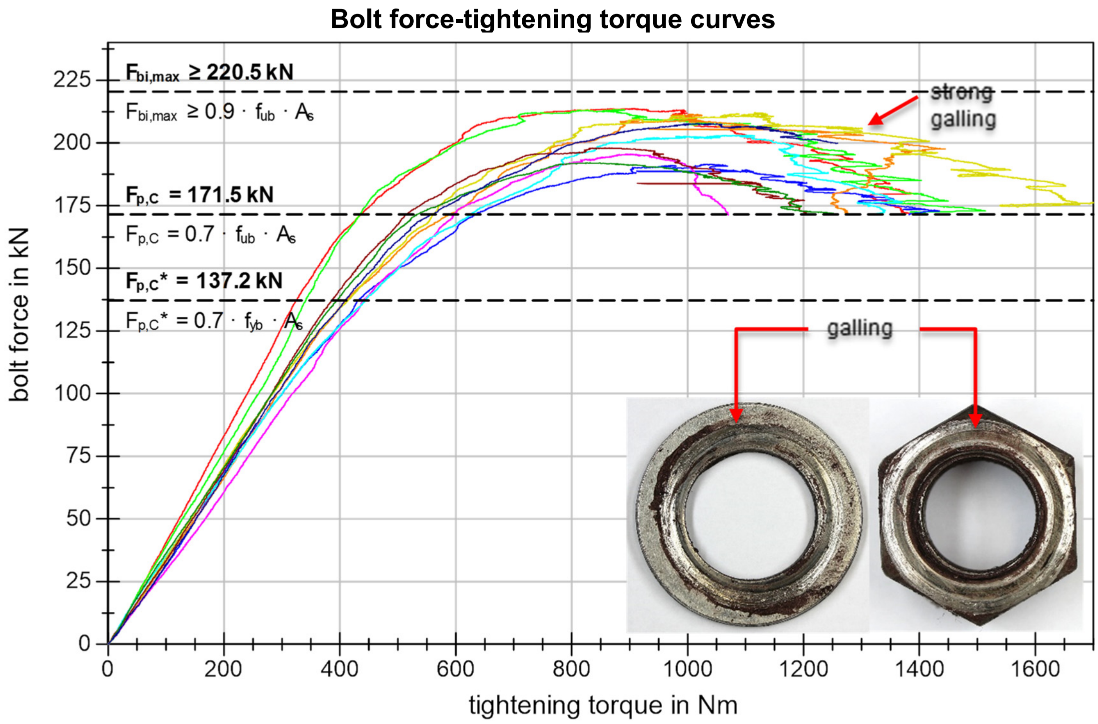


**Figure 75** BU_M20_109 Bolt force-tightening torque curves

### *3.4.3.2 Bumax LDX – M20x100 – 10.9 – EN ISO 4017 – Molykote 1000 spray*

The Bumax LDX – M20x100 lean duplex stainless steel bolting assemblies in property class 10.9 (used lubrication: Dow Corning Molykote® 1000 spray), in short form

BU_M20_LDX, were arranged of the following components including nominal mechanical properties based on Bumax datasheet:

- *Bolts:* BUFAB Group Bumax LDX – M20x100 A4 according to EN ISO 4017; stainless steel EN 1.4162; manufact.: 2016-09-09; PRE 26

  tensile strength $R_{m,min}$ (= $f_{ub}$): nominal 1000 N/mm²
  yield strength $R_{p0.2,min}$ (= $f_{yb}$): nominal 900 N/mm²
  elongation, min: nominal 0.3d

- *Nuts:* BUFAB Group Bumax 88 – M20 M6M A4 according to EN ISO 4032; stainless steel EN 1.4432, 1.4436, 1.4435; manufact.: 2016-04-08; PRE 27

  stress under proof load, min: nominal 800 N/mm²

- *Washers:* BUFAB Group Bumax RB A4-HV200 according to EN ISO 7089; stainless steel EN 1.4432, 1.4436, 1.4435; with dimensions d = 21.0 mm, D = 37.0 mm, t = 3.0 mm; manufact.: 2015-09-22; PRE 27

  hardness, min: nominal 200 HV

The tightening test results of the Bumax LDX – M20x100 bolting assemblies are summarized in Table 87, Table 88 and Table 89. The statistical evaluation is shown as well with fulfilled and failed criteria according to EN 14399-3 (System HR). In addition, the tightening curves are presented in Figure 77 and Figure 78. All tested lean duplex bolting assemblies reached $F_{p,C}$* = 154.4 kN and $F_{p,C}$ = 171.5 kN. On the contrary, the criteria of the maximum bolt force $F_{bi,max} \geq 0.9 \cdot f_{ub} \cdot A_s$ = 220.5 kN was not achieved in the whole tested series. Due to the less pronounced plastic plateaus, only 3 of 10 tested bolting assemblies achieved criteria $\Delta\Theta_{1i,min}$ = 120°, and 7 of 10 bolts achieved $\Delta\Theta_{2i,min}$ = 240° (with a high coefficient of variation of 32.70 %) according to EN 14399-3. Furthermore, 10 of 10 tested bolts achieved k-class K1 with k-values between 0.10 and 0.13 and a coefficient of variation of v = 8.23 % (compared to k = 0.10 – 0.12 and v = 6.88 % at $F_{p,C}$*). k-class K2 was not accomplished. For further information and summarized criteria see Table 89. The graphs show irregular bolt force-tightening torque curves because of minor and major galling in the nut bearing surfaces when tightened into the plastic range. Damages at the first and second load-bearing thread turn of the bolts and roughening of paired threads could be observed. Strongly pronounced galling especially in the faying surface washer/nut could be observed, too.

**Table 87** Test results of Bumax LDX – M20x100 – Molykote 1000 spray

| Legend | Specimens | $F_{p,C}$* kN | $F_{p,C}$ kN | Max F kN | Max T Nm | $\Theta_{pi}$ ° | $\Theta_{1i}$ ° | $\Theta_{2i}$ ° | $F_{bi}$ ($\Theta_{2i}$) kN | $\Delta\Theta_{1i}$ ° | $\Delta\Theta_{2i}$ ° | k ($F_{p,C^*}$) | k ($F_{p,C}$) | $\mu_{tot}$ ($F_{p,C}$) | $\mu_{th}$ ($F_{p,C}$) | $\mu_b$ ($F_{p,C}$) | M ($F_{p,C}$*) Nm | $M_i$ ($F_{p,C}$) Nm | M ($F_{bi,max}$) Nm |
|---|---|---|---|---|---|---|---|---|---|---|---|---|---|---|---|---|---|---|---|
| max | | | | --- | | | | | | --- | --- | 0,16 | 0,16 | | | | | | |
| min | | | | 220,5 | | | | | | 120 | 240 | 0,10 | 0,10 | | | | | | |
| | BU_M20_LDX-11 | 154,4 | 171,5 | <219,5 | 1512,9 | 247 | 387 | 725 | 171,4 | 140 | 478 | 0,10 | 0,10 | 0,086 | 0,085 | 0,088 | 373,7 | 418,8 | 730,1 |
| | BU_M20_LDX-12 | | | <202,4 | 1164,6 | 278 | 373 | 504 | 171,4 | <95 | <226 | 0,11 | 0,12 | 0,108 | 0,096 | 0,118 | 423,0 | 504,0 | 837,0 |
| | BU_M20_LDX-13 | | | <210,7 | 1514,9 | 245 | 360 | 659 | 171,4 | <116 | 414 | 0,12 | 0,13 | 0,117 | 0,107 | 0,125 | 462,3 | 539,4 | 907,9 |
| | BU_M20_LDX-14 | | | <199,0 | 1088,7 | 249 | 335 | 433 | 171,2 | <86 | <184 | 0,12 | 0,13 | 0,114 | 0,126 | 0,104 | 434,0 | 528,8 | 766,2 |
| | BU_M20_LDX-15 | | | <218,3 | 1254,1 | 242 | 439 | 661 | 171,4 | 197 | 418 | 0,11 | 0,11 | 0,100 | 0,089 | 0,109 | 413,5 | 470,8 | 866,7 |
| | BU_M20_LDX-16 | | | <206,9 | 1400,2 | 258 | 372 | 609 | 171,5 | <114 | 351 | 0,10 | 0,11 | 0,095 | 0,101 | 0,090 | 381,0 | 453,6 | 863,8 |
| | BU_M20_LDX-17 | | | <215,5 | 1305,1 | 253 | 411 | 673 | 171,4 | 158 | 420 | 0,11 | 0,11 | 0,102 | 0,106 | 0,098 | 423,5 | 479,4 | 971,1 |
| | BU_M20_LDX-18 | | | <198,0 | 1182,1 | 261 | 360 | 455 | 171,4 | <99 | <194 | 0,12 | 0,13 | 0,120 | 0,125 | 0,116 | 456,4 | 551,2 | 887,2 |
| | BU_M20_LDX-19 | | | <207,4 | 1235,8 | 242 | 342 | 504 | 171,4 | <101 | 262 | 0,12 | 0,12 | 0,104 | 0,117 | 0,092 | 436,2 | 486,8 | 843,3 |
| | BU_M20_LDX-20 | | | <206,3 | 1341,4 | 244 | 367 | 541 | 171,3 | 123 | 297 | 0,12 | 0,12 | 0,108 | 0,129 | 0,090 | 441,0 | 503,5 | 900,9 |

**Table 88** Statistical evaluation of Bumax LDX – M20x100 – Molykote 1000 spray

| BU_M20_LDX - Molykote 1000 Spray n = 10 | Max F kN | Max T Nm | $\Theta_{pi}$ ° | $\Theta_{1i}$ ° | $\Theta_{2i}$ ° | $F_{bi}$ ($\Theta_{2i}$) kN | $\Delta\Theta_{1i}$ ° | $\Delta\Theta_{2i}$ ° | k ($F_{p,C^*}$) | k ($F_{p,C}$) | $\mu_{tot}$ ($F_{p,C}$) | $\mu_{th}$ ($F_{p,C}$) | $\mu_b$ ($F_{p,C}$) | M ($F_{p,C^*}$) Nm | $M_i$ ($F_{p,C}$) Nm | M ($F_{bi,max}$) Nm |
|---|---|---|---|---|---|---|---|---|---|---|---|---|---|---|---|---|
| max | 219,5 | 1514,9 | 278 | 439 | 725 | 171,5 | 197 | 478 | 0,123 | 0,13 | 0,120 | 0,129 | 0,125 | 462,3 | 551,2 | 971,1 |
| min | 198,0 | 1088,7 | 242 | 335 | 433 | 171,2 | 86 | 184 | 0,099 | 0,100 | 0,086 | 0,085 | 0,088 | 373,7 | 418,8 | 730,1 |
| R | 21,5 | 426,2 | 36 | 104 | 292 | 0,3 | 111 | 294 | 0,024 | 0,032 | 0,034 | 0,044 | 0,037 | 88,6 | 132,4 | 241,0 |
| $\bar{x}$ | 208,4 | 1300,0 | 252 | 375 | 576 | 171,4 | 123 | 324 | 0,113 | 0,118 | 0,105 | 0,108 | 0,103 | 424,5 | 493,6 | 857,4 |
| s | 7,6 | 143,9 | 11 | 31 | 102 | 0,1 | 34 | 106 | 0,008 | 0,010 | 0,010 | 0,016 | 0,013 | 29,0 | 40,6 | 69,5 |
| $\nu$ | 3,64 | 11,07 | 4,47 | 8,32 | 17,68 | 0,05 | 27,57 | 32,70 | 6,88 | 8,23 | 9,81 | 14,54 | 13,04 | 6,82 | 8,22 | 8,11 |

n: number; R: range; $\bar{x}$: mean value; s: standard deviation; $\nu$: coefficient of variation in [%]

**Table 89** Evaluation of test results of Bumax LDX – M20x100 – Molykote 1000 spray acc. EN 14399-3

| n | $F_{p,C}^*$ | $F_{p,C}$ | $F_{bi,max}$ | $\Delta\Theta_{1i,min}$ | $\Delta\Theta_{2i,min}$ | k-values | k-class K1 | k-class K2 | | Fracture | Galling |
|---|---|---|---|---|---|---|---|---|---|---|---|
| [-] | 154.4kN | 171.5 kN | ≥ 220.5 kN | ≥ 120° | ≥ 240° | [-] | $0.10 \le k_i \le 0.16$ | $0.10 \le k_m \le 0.23$ | $V_k \le 0.06$ | | |
| 10 | 100% | 100% | 0% | 40% | 70% | 0.10 – 0.13 | 100% | 0.118 | 0.082 | 0% | 100% |

**Figure 76** BU_M20_LDX test specimen after tightening

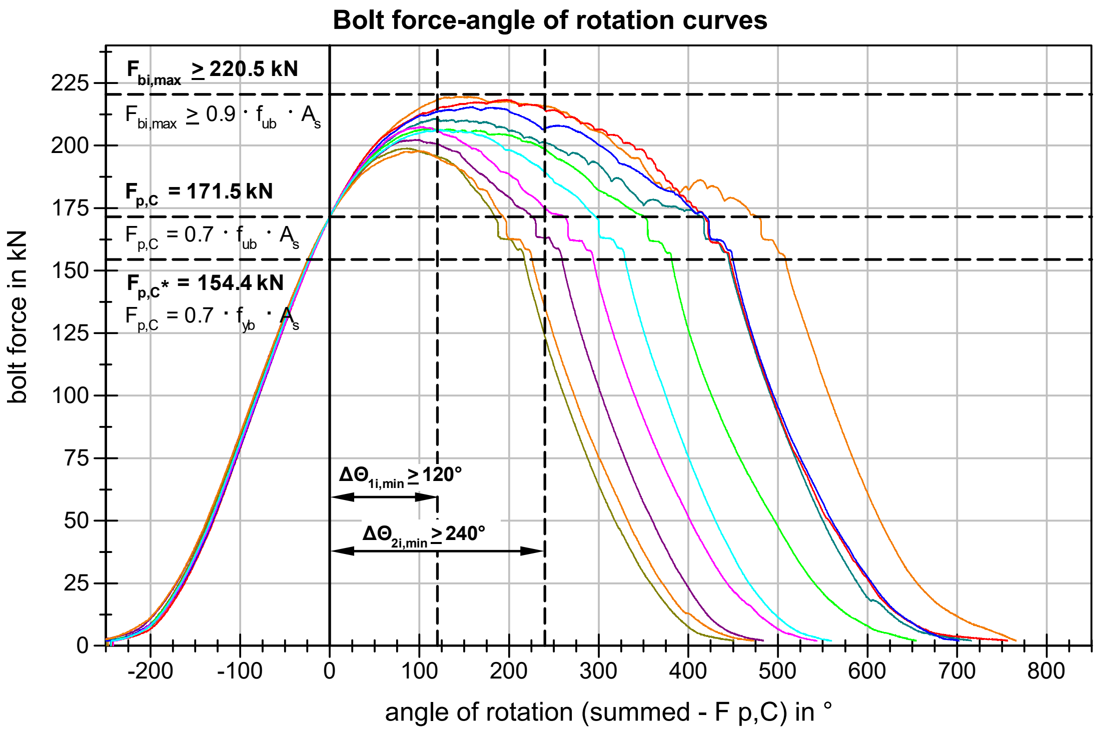


**Figure 77** BU_M20_LDX Bolt force-angle of rotation curves

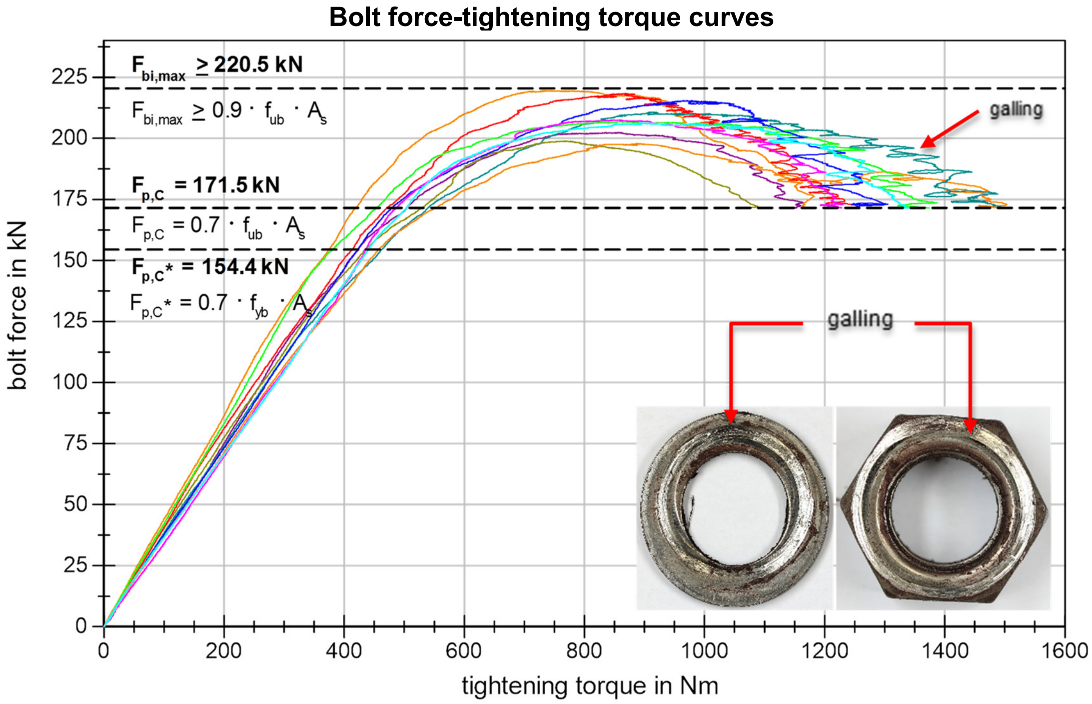


**Figure 78** BU_M20_LDX Bolt force-tightening torque curves

### *3.4.3.3 Bumax DX – M20x100 – 10.9 – EN ISO 4017 – Molykote 1000 spray*

The Bumax DX – M20x100 duplex stainless steel bolting assemblies in property class 10.9 (used lubrication: Dow Corning Molykote® 1000 spray), in short form BU_M20_DX, were arranged of the following components including nominal mechanical properties based on Bumax datasheet:

- *Bolts:* BUFAB Group Bumax LDX – M20x100 A4 according to EN ISO 4017; stainless steel EN 1.4462; manufact.: 2016-06-17; PRE 36

  tensile strength $R_{m,min}$ (= $f_{ub}$): nominal 1000 N/mm²
  yield strength $R_{p0.2,min}$ (= $f_{yb}$): nominal 900 N/mm²
  elongation, min: nominal 0.3d

- *Nuts:* BUFAB Group Bumax 88 – M20 M6M A4 according to EN ISO 4032; stainless steel EN 1.4432, 1.4436, 1.4435; manufact.: 2016-04-08; PRE 27

  stress under proof load, min: nominal 800 N/mm²

- *Washers:* BUFAB Group Bumax RB A4-HV200 according to EN ISO 7089; stainless steel EN 1.4432, 1.4436, 1.4435; with dimensions d = 21.0 mm, D = 37.0 mm, t = 3.0 mm; manufact.: 2015-09-22; PRE 27

  hardness, min: nominal 200 HV

The test results and evaluation of Bumax DX – M20x100 (Molykote 1000 spray) tested stainless steel bolting assemblies are summarized in Table 90, Table 91 and Table 92. The statistical evaluation is shown as well with fulfilled and failed criteria according to EN 14399-3 (System HR). Figure 80 and Figure 81 present the tightening graphs. Similar to the Bumax LDX – M20x100 (Molykote 1000 spray) test series, all bolts reached $F_{p,C}$* = 154.4 kN and $F_{p,C}$ = 171.5 kN. On the contrary, 3 of 10 tested duplex bolting assemblies achieved the maximum required bolt force $F_{bi,max} \geq 0.9 \cdot f_{ub} \cdot A_s$ = 220.5 kN. Furthermore, 9 of 10 tested bolts achieved k-class K1 with k-values between 0.09 and 0.15 and a coefficient of variation of v = 12.76 % (compared to k = 0.09 – 0.14 and v = 12.36 % at $F_{p,C}$*). k-class K2 was not accomplished. For further information and summarized criteria see Table 92. The graphs show irregular bolt force-tightening torque curves because of galling in the nut bearing surface when tightened into the plastic range including significant high ranges of values $M_i$ at end of the tests (bolt force dropped again to $F_{p,C}$) in the bolt force-tightening torque curves. 7 of 10 tested bolts achieved $\Delta\Theta_{1i,min}$ = 120° and 7 of 10 bolts reached $\Delta\Theta_{2i,min}$ = 240°. Damages at the first and second load-bearing thread turn of the bolts and roughening of the paired threads could be observed; bolt failure by fracture did not occur. Strong pronounced galling in the faying surface washer/nut could be observed, too. It was possible to unscrew the hexagon nuts of all tested bolting assemblies manually but turning on the nut on the whole threaded shank by hand was not possible.

**Table 90** Test results of Bumax DX – M20x100 – Molykote 1000 spray

| Legend | Specimens | $F_{p,C}$* | $F_{p,C}$ | Max F | Max T | $\Theta_{pi}$ | $\Theta_{1i}$ | $\Theta_{2i}$ | $F_{bi}$ ($\Theta_{2i}$) | $\Delta\Theta_{1i}$ | $\Delta\Theta_{2i}$ | k ($F_{p,C}$*) | k ($F_{p,C}$) | $\mu_{tot}$ ($F_{p,C}$) | $\mu_{th}$ ($F_{p,C}$) | $\mu_b$ ($F_{p,C}$) | M ($F_{p,C}$*) | $M_i$ ($F_{p,C}$) | M ($F_{bi,max}$) |
|---|---|---|---|---|---|---|---|---|---|---|---|---|---|---|---|---|---|---|---|
| | | kN | kN | kN | Nm | ° | ° | ° | kN | ° | ° | | | | | | Nm | Nm | Nm |
| max | | | | --- | | | | | | --- | --- | 0,16 | 0,16 | | | | | | |
| min | | | | 220,5 | | | | | | 120 | 240 | 0,10 | 0,10 | | | | | | |
| | BU_M20_DX-11 | 154,4 | 171,5 | 225,2 | 1121,9 | 249 | 404 | 812 | 171,4 | 156 | 563 | <0,09 | <0,09 | 0,079 | 0,084 | 0,075 | 346,9 | 391,3 | 729,7 |
| | BU_M20_DX-12 | | | <199,2 | 1024,6 | 240 | 320 | 399 | 171,4 | <80 | <159 | 0,12 | 0,12 | 0,107 | 0,139 | 0,079 | 437,9 | 500,1 | 822,1 |
| | BU_M20_DX-13 | | | 221,7 | 1176,3 | 235 | 393 | 753 | 171,4 | 158 | 518 | 0,11 | 0,11 | 0,100 | 0,092 | 0,107 | 408,4 | 472,4 | 842,9 |
| | BU_M20_DX-14 | | | <202,7 | 1215,6 | 245 | 333 | 449 | 171,4 | <88 | <204 | 0,13 | 0,14 | 0,124 | 0,132 | 0,118 | 502,3 | 568,2 | 881,4 |
| | BU_M20_DX-15 | | | 220,5 | 1853,8 | 237 | 451 | 791 | 171,4 | 214 | 554 | 0,11 | 0,11 | 0,102 | 0,094 | 0,109 | 431,3 | 480,0 | 1018,5 |
| | BU_M20_DX-16 | | | <206,1 | 1579,6 | 257 | 401 | 559 | 171,4 | 144 | 301 | 0,12 | 0,12 | 0,109 | 0,070 | 0,142 | 439,4 | 506,2 | 1014,6 |
| | BU_M20_DX-17 | | | <211,8 | 1290,0 | 238 | 361 | 529 | 171,3 | 122 | 290 | 0,12 | 0,12 | 0,111 | 0,102 | 0,119 | 441,4 | 516,7 | 980,2 |
| | BU_M20_DX-18 | | | <207,0 | 1402,0 | 247 | 354 | 482 | 171,4 | <107 | <236 | 0,14 | 0,15 | 0,135 | 0,129 | 0,140 | 530,8 | 609,3 | 1039,2 |
| | BU_M20_DX-19 | | | <209,5 | 1559,8 | 236 | 363 | 545 | 171,4 | 127 | 309 | 0,11 | 0,12 | 0,109 | 0,096 | 0,121 | 428,6 | 508,6 | 969,7 |
| | BU_M20_DX-20 | | | <213,6 | 1443,0 | 239 | 368 | 619 | 171,3 | 129 | 380 | 0,14 | 0,15 | 0,135 | 0,100 | 0,165 | 518,9 | 610,0 | 1057,0 |

**Table 91** Statistical evaluation of Bumax DX – M20x100 – Molykote 1000 spray

| BU_M20_DX - Molykote 1000 Spray | Max F | Max T | $\Theta_{pi}$ | $\Theta_{1i}$ | $\Theta_{2i}$ | $F_{bi}$ ($\Theta_{2i}$) | $\Delta\Theta_{1i}$ | $\Delta\Theta_{2i}$ | k ($F_{p,C}$*) | k ($F_{p,C}$) | $\mu_{tot}$ ($F_{p,C}$) | $\mu_{th}$ ($F_{p,C}$) | $\mu_b$ ($F_{p,C}$) | M ($F_{p,C}$*) | $M_i$ ($F_{p,C}$) | M ($F_{bi,max}$) |
|---|---|---|---|---|---|---|---|---|---|---|---|---|---|---|---|---|
| n = 10 | kN | Nm | ° | ° | ° | kN | ° | ° | | | | | | Nm | Nm | Nm |
| max | 225,2 | 1853,8 | 257 | 451 | 812 | 171,4 | 214 | 563 | 0,141 | 0,15 | 0,135 | 0,139 | 0,165 | 530,8 | 610,0 | 1057,0 |
| min | 199,2 | 1024,6 | 235 | 320 | 399 | 171,3 | 80 | 159 | 0,092 | 0,094 | 0,079 | 0,070 | 0,075 | 346,9 | 391,3 | 729,7 |
| R | 26,0 | 829,2 | 22 | 131 | 413 | 0,1 | 134 | 404 | 0,049 | 0,052 | 0,056 | 0,069 | 0,090 | 183,9 | 218,7 | 327,3 |
| $\bar{x}$ | 211,7 | 1366,7 | 242 | 375 | 594 | 171,4 | 133 | 351 | 0,119 | 0,124 | 0,111 | 0,104 | 0,118 | 448,6 | 516,3 | 935,5 |
| s | 8,6 | 251,4 | 7 | 38 | 146 | 0,0 | 39 | 147 | 0,015 | 0,016 | 0,017 | 0,022 | 0,028 | 55,3 | 66,2 | 109,8 |
| ν | 4,04 | 18,40 | 2,91 | 10,23 | 24,58 | 0,02 | 29,25 | 41,84 | 12,36 | 12,76 | 15,21 | 21,58 | 23,48 | 12,32 | 12,82 | 11,74 |

n: number; R: range; $\bar{x}$: mean value; s: standard deviation; ν: coefficient of variation in [%]

**Table 92** Evaluation of test results of Bumax DX – M20x100 – Molykote 1000 spray acc. EN 14399-3

| n | $F_{p,C}^*$ | $F_{p,C}$ | $F_{bi,max}$ | $\Delta\Theta_{1i,min}$ | $\Delta\Theta_{2i,min}$ | k-values | k-class K1 | k-class K2 | | Fracture | Galling |
|---|---|---|---|---|---|---|---|---|---|---|---|
| [-] | 154.4kN | 171.5 kN | ≥ 220.5 kN | ≥ 120° | ≥ 240° | [-] | $0.10 \leq k_i \leq 0.16$ | $0.10 \leq k_m \leq 0.23$ | $V_k \leq 0.06$ | | |
| 10 | 100% | 100% | 30% | 70% | 70% | 0.09 – 0.15 | 90% | 0.124 | 0.128 | 0% | 100% |

**Figure 79** BU_M20_DX test specimen after tightening

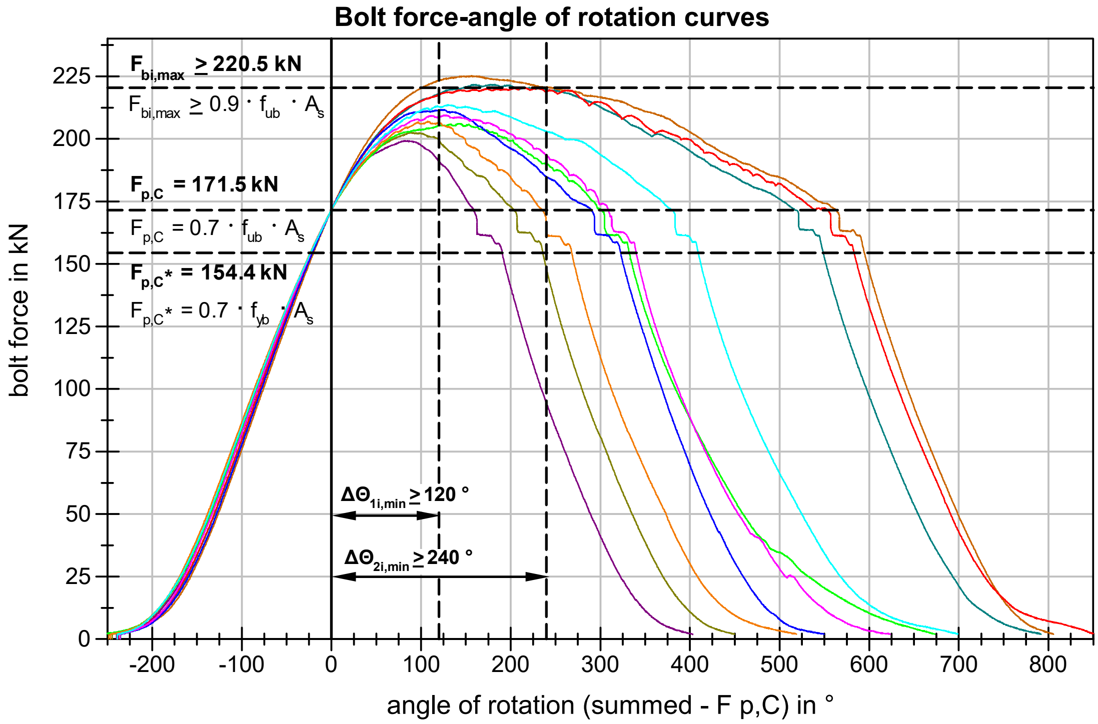


**Figure 80** BU_M20_DX Bolt force-angle of rotation curves

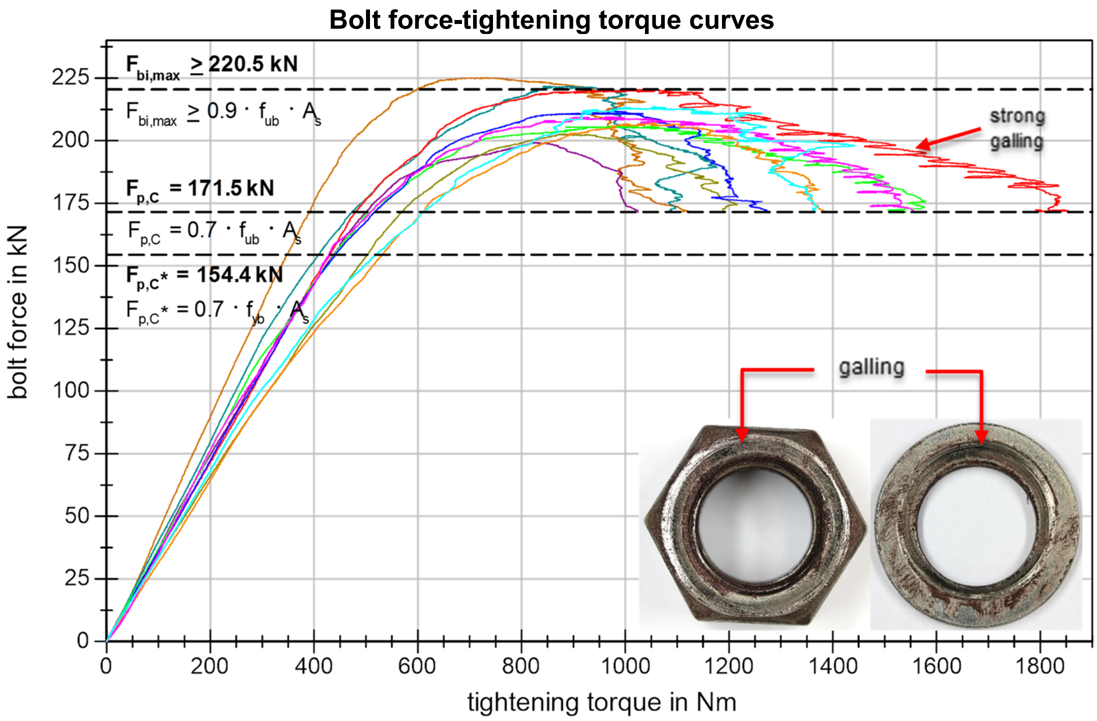


**Figure 81** BU_M20_DX Bolt force-tightening torque curves

### 3.4.4 Additional tightening tests: Bolt dimension M16

Tightening tests for bolt dimension M16 were carried out as well according to EN 14399-2 and EN ISO 16047. The test procedure contains a constant speed of rotation of 5.0 $min^{-1}$ for Bumax 88, Bumax 109, lean duplex and duplex steel grades. All series were tightened nut sided, the clamping length $\sum t$ was set to 78.5 mm (clamp length/bolt diameter ratio of 4.9) in reference to the corresponding tables of System HR – EN 14399-3. In contrast, the clamp length $\sum t$ for property class 10.9 bolts (nominal length 100 mm) was set to 78.5 mm (clamp length/bolt diameter ratio of 4.9). In addition, the test were stopped when the measured bolt force dropped to $F_{p,c} = 0.7 \cdot f_{ub} \cdot A_s$ (with $f_{ub}$: tensile strength of the bolt and $A_s$: tensile stress area of the bolt).

The criteria of evaluation for property class 8.8 (Bumax 88 series) according to EN 14399-3 are defined as follows:

- $F_{p,C}* = 0.7 \cdot f_{yb} \cdot A_s = 0.7 \cdot 640$ N/mm² $\cdot$ 157.0 mm² = 70.3 kN (DIN EN 1993-1-8/NA)
- $F_{p,C} = 0.7 \cdot f_{ub} \cdot A_s = 0.7 \cdot 800$ N/mm² $\cdot$ 157.0 mm² = 87.9 kN
- $F_{bi,max} \geq 0.9 \cdot f_{ub} \cdot A_s = 0.9 \cdot 800$ N/mm² $\cdot$ 157.0 mm² = 113.0 kN
- $\Delta\Theta_{1i,min} \geq 120°$ with $\sum t = 60.5$ mm: $2d \leq \sum t < 6d$
- $\Delta\Theta_{2i,min} \geq 240°$ with $\sum t = 60.5$ mm: $2d \leq \sum t < 6d$

In addition, the criteria of evaluation for bolting assemblies in property class 10.9/100 (meaning Bumax 109, Bumax lean duplex and Bumax duplex series) are defined as follows:

- $F_{p,C}* = 0.7 \cdot f_{yb} \cdot A_s = 0.7 \cdot 800$ N/mm² $\cdot$ 157.0 mm² = 70.3 kN (for Bumax 109 bolts)
- $F_{p,C}* = 0.7 \cdot f_{yb} \cdot A_s = 0.7 \cdot 900$ N/mm² $\cdot$ 157.0 mm² = 87.9 kN (for Bumax LDX and DX)
- $F_{p,C} = 0.7 \cdot f_{ub} \cdot A_s = 0.7 \cdot 1000$ N/mm² $\cdot$ 157.0 mm² = 109.9 kN
- $F_{bi,max} \geq 0.9 \cdot f_{ub} \cdot A_s = 0.9 \cdot 1000$ N/mm² $\cdot$ 157.0 mm² = 141.3 kN
- $\Delta\Theta_{1i,min} \geq 120°$ with $\sum t = 64.0$ mm: $2d \leq \sum t < 6d$
- $\Delta\Theta_{2i,min} \geq 240°$ with $\sum t = 64.0$ mm: $2d \leq \sum t < 6d$

#### *3.4.4.1 Bumax 88 – M16x100 – 8.8 – EN ISO 4017 – Molykote 1000 spray*

The Bumax 88 – M16x100 austenitic stainless steel bolting assemblies in property class 8.8 (used lubrication: Dow Corning Molykote® 1000 spray), in short form BU_M16_88, were arranged of the following components including nominal mechanical properties based on Bumax datasheet:

- *Bolts:* BUFAB Group Bumax 88 - M16x100 A4 according to EN ISO 4017; stainless steel EN 1.4432, 1.4436, 1.4435; manufact.: 2016-04-28; PRE 27

| |
|---|
| tensile strength $R_{m,min}$ (= $f_{ub}$): nominal 800 N/mm² |
| yield strength $R_{p0.2,min}$ (= $f_{yb}$): nominal 640 N/mm² |
| elongation, min: nominal 0.3d |

- *Nuts:* BUFAB Group Bumax 88 - M16 M6M A4 according to EN ISO 4032; stainless steel EN 1.4432, 1.4436, 1.4435; manufact.: 2015-04-22; PRE 27 stress under proof load, min: nominal 800 N/mm²

- *Washers:* BUFAB Group Bumax RB A4-HV200 according to EN ISO 7089; stainless steel EN 1.4432, 1.4436, 1.4435; with dimensions d = 17.0 mm, D = 30.0 mm, t = 3.0 mm; manufact.: 2014-04-16; PRE 27

hardness, min: nominal 200 HV

Table 93, Table 94 and Table 95 summarize the test results and evaluation of the tested stainless steel bolting assemblies. The statistical evaluation is shown as well with fulfilled and failed criteria according to EN 14399-3 (System HR). Figure 83 and Figure 84 present the tightening graphs. All tested austenitic bolting assemblies reached $F_{p,C}$* = 70.3 kN, $F_{p,C}$ = 87.9 kN, 9 of 10 bolts the maximum required bolt force $F_{bi,max} \geq 0.9 \cdot f_{ub} \cdot A_s$ = 113.0 kN. Furthermore, 10 of 10 tested bolts achieved k-class K1 with k-values between 0.10 and 0.16 and coefficient of variation v = 14.95 % (compared to k = 0.10 – 0.15 and v = 12.66 % at $F_{p,C}$*). On the contrary, k-class K2 was not accomplished. For further information and summarized criteria see Table 95. The graphs show irregular bolt force-tightening torque curves because of strong galling in the nut bearing surface when tightened into the plastic range including significant high ranges of values $M_i$ at $F_{bi,max}$ and at end of the tests (bolt force dropped again to $F_{p,C}$) in the bolt force-tightening torque curves. 9 of 10 tested bolts achieved $\Delta\Theta_{1i,min}$ = 120° and $\Delta\Theta_{2i,min}$ = 240°. Damages at the first and second load-bearing thread turn of the bolts and roughening of the paired threads could be observed; bolt failure by fracture occurred in 5 of 10 tested bolts when the bolt force dropped again to $F_{p,C}$. Galling in the faying surface washer/nut could be observed ,too. Furthermore, in the context of functionality and re-use, it was possible to unscrew the hexagon nuts of all tested bolting assemblies manually, but turning on the nut on the whole threaded shank by hand was not possible.

**Table 93** Test results of Bumax 88 – M16x100 – Molykote 1000 spray

| Legend | Specimens | $F_{p,C}$* kN | $F_{p,C}$ kN | Max F kN | Max T Nm | $\Theta_{pi}$ ° | $\Theta_{1i}$ ° | $\Theta_{2i}$ ° | $F_{bi}$ ($\Theta_{2i}$) kN | $\Delta\Theta_{1i}$ ° | $\Delta\Theta_{2i}$ ° | k ($F_{p,C*}$) | k ($F_{p,C}$) | $\mu_{tot}$ ($F_{p,C}$) | $\mu_{th}$ ($F_{p,C}$) | $\mu_b$ ($F_{p,C}$) | M ($F_{p,C}$*) Nm | $M_i$ ($F_{p,C}$) Nm | M ($F_{bi,max}$) Nm |
|---|---|---|---|---|---|---|---|---|---|---|---|---|---|---|---|---|---|---|---|
| max | | | | --- | | | | | | --- | --- | 0,16 | 0,16 | | | | | | |
| min | | | | 113,0 | | | | | | 120 | 240 | 0,10 | 0,10 | | | | | | |
| | BU_M16_88-11 | 70,3 | 88 | 140,7 | 696,0 | 144 | 387 | 852 | 87,9 | 242 | 708 | 0,10 | 0,10 | 0,072 | 0,068 | 0,076 | 116,7 | 144,4 | 414,7 |
| | BU_M16_88-12 | | | 113,9 | 649,5 | 171 | 292 | 470 | 88,0 | 121 | 298 | 0,14 | 0,15 | 0,110 | 0,136 | 0,087 | 156,2 | 205,6 | 421,5 |
| | BU_M16_88-13 | | | 127,4 | 632,3 | 163 | 347 | 655 | 88,0 | 184 | 492 | 0,14 | 0,15 | 0,116 | 0,136 | 0,098 | 160,7 | 214,8 | 437,2 |
| | BU_M16_88-14 | | | 134,0 | 634,6 | 158 | 329 | 691 | 88,0 | 171 | 533 | 0,13 | 0,13 | 0,094 | 0,098 | 0,090 | 141,6 | 180,2 | 408,5 |
| | BU_M16_88-15 | | | 138,9 | 675,8 | 150 | 367 | 909 | 87,8 | 217 | 759 | 0,11 | 0,11 | 0,079 | 0,083 | 0,076 | 124,4 | 156,0 | 353,2 |
| | BU_M16_88-16 | | | 135,1 | 811,2 | 158 | 351 | 712 | 87,9 | 193 | 553 | 0,11 | 0,11 | 0,082 | 0,083 | 0,082 | 120,6 | 161,2 | 393,0 |
| | BU_M16_88-17 | | | 139,1 | 616,2 | 157 | 405 | 837 | 87,9 | 248 | 680 | 0,12 | 0,12 | 0,083 | 0,105 | 0,064 | 135,0 | 162,3 | 468,9 |
| | BU_M16_88-18 | | | 114,9 | 563,0 | 161 | 286 | 490 | 88,0 | 125 | 329 | 0,13 | 0,14 | 0,107 | 0,135 | 0,083 | 150,7 | 200,9 | 427,2 |
| | BU_M16_88-19 | | | 134,8 | 574,2 | 151 | 373 | 783 | 87,8 | 222 | 631 | 0,12 | 0,12 | 0,087 | 0,105 | 0,072 | 135,9 | 169,0 | 465,3 |
| | BU_M16_88-20 | | | <110,2 | 483,2 | 163 | 250 | 403 | 88,0 | <87 | <240 | 0,15 | 0,16 | 0,119 | 0,179 | 0,068 | 170,1 | 220,8 | 342,0 |

**Table 94** Statistical evaluation of Bumax 88 – M16x100 – Molykote 1000 spray

| BU_M16_88_100 - Molykote 1000 Spray n = 10 | Max F kN | Max T Nm | $\Theta_{pi}$ ° | $\Theta_{1i}$ ° | $\Theta_{2i}$ ° | $F_{bi}$ ($\Theta_{2i}$) kN | $\Delta\Theta_{1i}$ ° | $\Delta\Theta_{2i}$ ° | k ($F_{p,C*}$) | k ($F_{p,C}$) | $\mu_{tot}$ ($F_{p,C}$) | $\mu_{th}$ ($F_{p,C}$) | $\mu_b$ ($F_{p,C}$) | M ($F_{p,C}$*) Nm | $M_i$ ($F_{p,C}$) Nm | M ($F_{bi,max}$) Nm |
|---|---|---|---|---|---|---|---|---|---|---|---|---|---|---|---|---|
| max | 140,7 | 811,2 | 171 | 405 | 909 | 88,0 | 248 | 759 | 0,151 | 0,16 | 0,119 | 0,179 | 0,098 | 170,1 | 220,8 | 468,9 |
| min | 110,2 | 483,2 | 144 | 250 | 403 | 87,8 | 87 | 240 | 0,104 | 0,103 | 0,072 | 0,068 | 0,064 | 116,7 | 144,4 | 342,0 |
| R | 30,5 | 328,0 | 27 | 155 | 506 | 0,2 | 161 | 519 | 0,047 | 0,054 | 0,047 | 0,111 | 0,034 | 53,4 | 76,4 | 126,9 |
| $\bar{x}$ | 128,9 | 633,6 | 158 | 339 | 680 | 87,9 | 181 | 522 | 0,126 | 0,129 | 0,095 | 0,113 | 0,080 | 141,2 | 181,5 | 413,2 |
| s | 11,6 | 87,5 | 8 | 49 | 175 | 0,1 | 55 | 182 | 0,016 | 0,019 | 0,017 | 0,033 | 0,010 | 18,0 | 27,0 | 41,8 |
| ν | 9,02 | 13,81 | 4,90 | 14,55 | 25,74 | 0,09 | 30,27 | 34,75 | 12,66 | 14,95 | 17,73 | 29,66 | 13,11 | 12,72 | 14,89 | 10,13 |

n: number; R: range; $\bar{x}$: mean value; s: standard deviation; ν: coefficient of variation in [%]

**Table 95** Evaluation of test results of Bumax 88 – M16x100 – Molykote 1000 spray acc. EN 14399-3

| n | $F_{p,C}^*$ | $F_{p,C}$ | $F_{bi,max}$ | $\Delta\Theta_{1i,min}$ | $\Delta\Theta_{2i,min}$ | k-values | k-class K1 | k-class K2 | | Fracture | Galling |
|---|---|---|---|---|---|---|---|---|---|---|---|
| [-] | 70.3 kN | 87.9 kN | $\geq$ 113.0 kN | $\geq$ 120° | $\geq$ 240° | [-] | $0.10 \leq k_i \leq 0.16$ | $0.10 \leq k_m \leq 0.23$ | $V_k \leq 0.06$ | | |
| 10 | 100% | 100% | 90% | 90% | 90% | 0.10 – 0.16 | 100% | 0.129 | 0.150 | 50% | 70% |


**Figure 82** BU_M16_88 test specimen after tightening

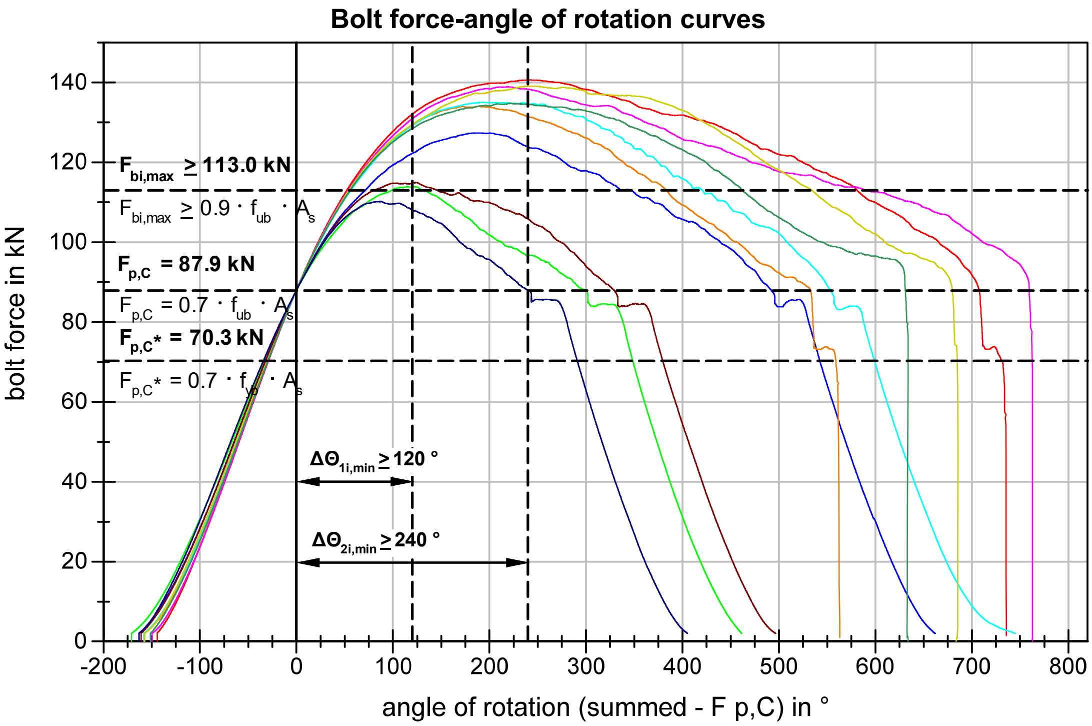


**Figure 83** BU_M20_88 Bolt force-angle of rotation curves

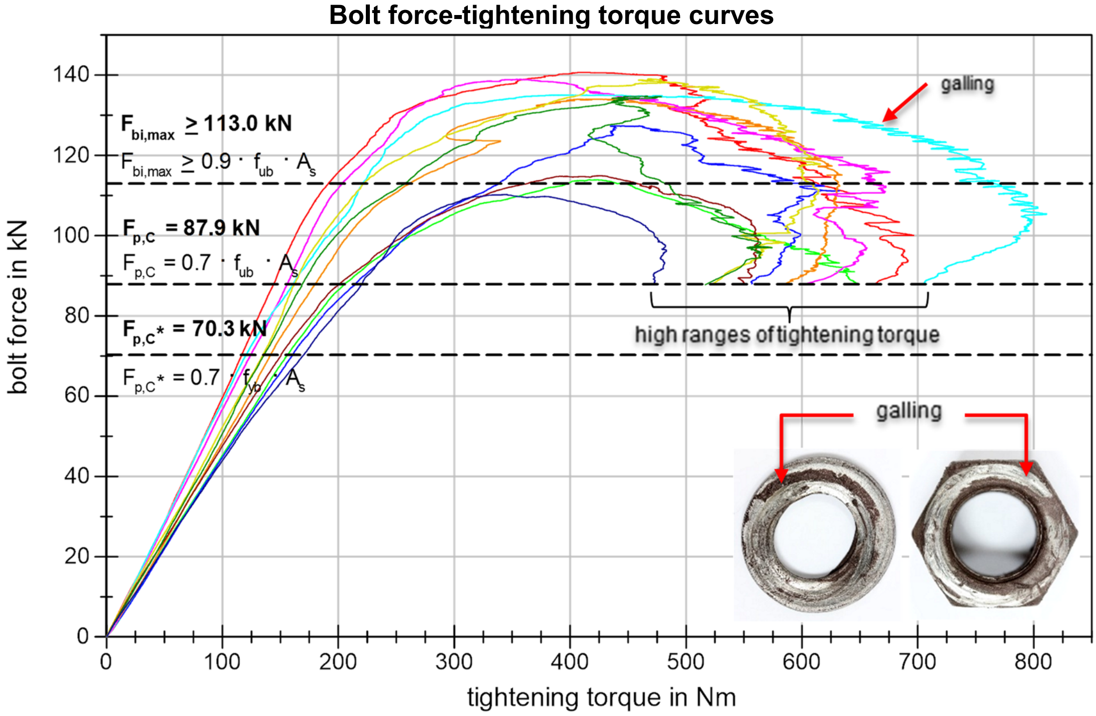


**Figure 84** BU_M20_88 Bolt force-tightening torque curves

### 3.4.4.2 Bumax 109 – M16x100 – 10.9 – EN ISO 4017 – Molykote 1000 spray

The Bumax 109 – M16x100 austenitic stainless steel bolting assemblies in property class 10.9/100 (used lubrication: Dow Corning Molykote® 1000 spray), in short form BU_M16_109, were arranged of the following components including nominal mechanical properties based on Bumax datasheet:

- *Bolts:* BUFAB Group Bumax 109 - M16x100 A4 according to EN ISO 4017; stainless steel EN 1.4432, 1.4436, 1.4435; manufact.: 2016-04-28; PRE 27

  tensile strength $R_{m,min}$ (= $f_{ub}$): nominal 1000 N/mm²
  yield strength $R_{p0.2,min}$ (= $f_{yb}$): nominal 800 N/mm²
  elongation, min: nominal 0.3d

- *Nuts:* BUFAB Group Bumax 109 - M16 M6M A4 according to EN ISO 4032; stainless steel EN 1.4432, 1.4436, 1.4435; manufact.: 2015-02-26; PRE 27

  stress under proof load, min: nominal 1000 N/mm²

- *Washers:* BUFAB Group Bumax RB A4-HV300 according to EN ISO 7089; stainless steel EN 1.4432, 1.4436, 1.4435; with dimensions d = 17.0 mm, D = 30.0 mm, t = 3.0 mm; manufact.: 2015-12-14; PRE 27

  hardness, min: nominal 300 HV

The tightening test results of Bumax 109 – M16x100 bolting assemblies (used lubrication: Molykote 1000 spray) are summarized in Table 86, Table 87 and Table 88. The statistical evaluation is shown as well with fulfilled and failed criteria according to EN 14399-3 (System HR). In addition, the tightening curves are presented in Figure

86 and Figure 87. All tested austenitic bolting assemblies reached $F_{p,C}^{*}$ = 87.9 kN and $F_{p,C}$ = 109.9 kN as well as $F_{bi,max} \geq 0.9 \cdot f_{ub} \cdot A_s$ = 141.3 kN. Due to the more pronounced plastic plateaus, consequently 10 of the 10 bolts achieved $\Delta\Theta_{1i,min}$ = 120° and $\Delta\Theta_{2i,min}$ = 240° according to EN 14399-3. Furthermore, 10 of 10 tested bolts achieved k-class K1 with k-values in a narrow range between 0.11 and 0.14 and coefficient of variation of v = 8.03 % (compared to k = 0.11– 0.15 and v = 8.48 % at $F_{p,C}^{*}$). k-class K2 was not accomplished. For further information and summarized criteria see Table 88. Again, the graphs show irregular bolt force-tightening torque curves because of galling in the nut bearing surface when tightened into the plastic range including significant high ranges of values $M_i$ at $F_{bi,max}$ and at the end of the tests (bolt force dropped again to $F_{p,C}$) in the bolt force-tightening torque curves. Damages at the first and second load-bearing thread turn of the bolts and roughening of the paired threads could be observed without partial or total bolt fracture. Strong pronounced galling especially in the faying surface washer/nut could be observed, too.

**Table 96** Test results of Bumax 109 – M16x100 – Molykote 1000 spray

| Legend | Specimens | $F_{p,C}$* | $F_{p,C}$ | Max F | Max T | $\Theta_{pi}$ | $\Theta_{1i}$ | $\Theta_{2i}$ | $F_{bi}$ ($\Theta_{2i}$) | $\Delta\Theta_{1i}$ | $\Delta\Theta_{2i}$ | k ($F_{p,C*}$) | k ($F_{p,C}$) | $\mu_{tot}$ ($F_{p,C}$) | $\mu_{th}$ ($F_{p,C}$) | $\mu_b$ ($F_{p,C}$) | M ($F_{p,C}$*) | $M_i$ ($F_{p,C}$) | M ($F_{bi,max}$) |
|---|---|---|---|---|---|---|---|---|---|---|---|---|---|---|---|---|---|---|---|
| | | kN | kN | kN | Nm | ° | ° | ° | kN | ° | ° | | | | | | Nm | Nm | Nm |
| max | | | | --- | | | | | | --- | --- | 0,16 | 0,16 | | | | | | |
| min | | | | 141,3 | | | | | | 120 | 240 | 0,10 | 0,10 | | | | | | |
| | BU_M16_109-06 | 88 | 110 | 150,5 | 738,6 | 181 | 358 | 593 | 110,0 | 177 | 412 | 0,14 | 0,14 | 0,098 | 0,099 | 0,097 | 191,8 | 238,8 | 479,4 |
| | BU_M16_109-07 | | | 156,8 | 891,2 | 184 | 394 | 684 | 110,0 | 210 | 500 | 0,14 | 0,14 | 0,098 | 0,101 | 0,096 | 194,3 | 239,7 | 544,7 |
| | BU_M16_109-08 | | | 148,6 | 762,5 | 187 | 336 | 507 | 110,0 | 149 | 320 | 0,13 | 0,13 | 0,093 | 0,117 | 0,074 | 181,4 | 229,6 | 457,3 |
| | BU_M16_109-09 | | | 150,1 | 769,7 | 179 | 353 | 582 | 110,0 | 174 | 403 | 0,14 | 0,14 | 0,103 | 0,104 | 0,103 | 197,4 | 250,3 | 447,4 |
| | BU_M16_109-10 | | | 151,7 | 806,8 | 181 | 362 | 636 | 110,0 | 181 | 455 | 0,15 | 0,14 | 0,105 | 0,123 | 0,091 | 206,8 | 254,1 | 522,0 |
| | BU_M16_109-11 | | | 155,8 | 692,2 | 180 | 370 | 693 | 110,0 | 190 | 513 | 0,13 | 0,13 | 0,093 | 0,102 | 0,086 | 182,8 | 228,4 | 481,0 |
| | BU_M16_109-12 | | | 158,1 | 799,5 | 180 | 380 | 632 | 110,0 | 200 | 452 | 0,12 | 0,12 | 0,087 | 0,104 | 0,074 | 169,9 | 217,1 | 557,6 |
| | BU_M16_109-13 | | | 149,1 | 696,1 | 177 | 335 | 605 | 110,0 | 157 | 428 | 0,12 | 0,13 | 0,090 | 0,104 | 0,079 | 174,8 | 222,5 | 421,7 |
| | BU_M16_109-14 | | | 154,8 | 743,4 | 182 | 362 | 698 | 109,9 | 180 | 515 | 0,11 | 0,11 | 0,076 | 0,089 | 0,066 | 154,3 | 193,9 | 420,6 |
| | BU_M16_109-15 | | | 151,2 | 839,1 | 180 | 346 | 652 | 110,0 | 166 | 472 | 0,12 | 0,12 | 0,084 | 0,099 | 0,072 | 170,1 | 210,9 | 534,7 |

**Table 97** Statistical evaluation of Bumax 109 – M16x100 – Molykote 1000 spray

| BU_M16_109_100 - Molykote 1000 spray n = 10 | Max F | Max T | $\Theta_{pi}$ | $\Theta_{1i}$ | $\Theta_{2i}$ | $F_{bi}$ ($\Theta_{2i}$) | $\Delta\Theta_{1i}$ | $\Delta\Theta_{2i}$ | k ($F_{p,C*}$) | k ($F_{p,C}$) | $\mu_{tot}$ ($F_{p,C}$) | $\mu_{th}$ ($F_{p,C}$) | $\mu_b$ ($F_{p,C}$) | M ($F_{p,C}$*) | $M_i$ ($F_{p,C}$) | M ($F_{bi,max}$) |
|---|---|---|---|---|---|---|---|---|---|---|---|---|---|---|---|---|
| | kN | Nm | ° | ° | ° | kN | ° | ° | | | | | | Nm | Nm | Nm |
| max | 158,1 | 891,2 | 187 | 394 | 698 | 110,0 | 210 | 515 | 0,147 | 0,14 | 0,105 | 0,123 | 0,103 | 206,8 | 254,1 | 557,6 |
| min | 148,6 | 692,2 | 177 | 335 | 507 | 109,9 | 149 | 320 | 0,110 | 0,110 | 0,076 | 0,089 | 0,066 | 154,3 | 193,9 | 420,6 |
| R | 9,5 | 199,0 | 10 | 59 | 191 | 0,1 | 61 | 195 | 0,037 | 0,034 | 0,029 | 0,034 | 0,037 | 52,5 | 60,2 | 137,0 |
| $\bar{x}$ | 152,7 | 773,9 | 181 | 360 | 628 | 110,0 | 178 | 447 | 0,130 | 0,130 | 0,093 | 0,104 | 0,084 | 182,4 | 228,5 | 486,6 |
| s | 3,4 | 62,2 | 3 | 19 | 59 | 0,0 | 19 | 60 | 0,011 | 0,010 | 0,009 | 0,010 | 0,013 | 15,7 | 18,4 | 50,6 |
| ν | 2,23 | 8,03 | 1,53 | 5,17 | 9,41 | 0,03 | 10,41 | 13,37 | 8,48 | 8,03 | 9,57 | 9,15 | 14,99 | 8,59 | 8,04 | 10,39 |

with n: number; R: range; x: mean value; s: standard deviation; ν: coefficient of variation in [%]

**Table 98** Evaluation of test results of Bumax 109 – M16x100 – Molykote 1000 spray acc. EN 14399-3

| n | $F_{p,C}^{*}$ | $F_{p,C}$ | $F_{bi,max}$ | $\Delta\Theta_{1i,min}$ | $\Delta\Theta_{2i,min}$ | k-values | k-class K1 | k-class K2 | | Fracture | Galling |
|---|---|---|---|---|---|---|---|---|---|---|---|
| [-] | 87.9 kN | 109.9 kN | ≥ 141.3 kN | ≥ 120° | ≥ 240° | [-] | 0.10 ≤ $k_i$ ≤ 0.16 | 0.10 ≤ $k_m$ ≤ 0.23 | $V_k$ ≤ 0.06 | | |
| 10 | 100% | 100% | 100% | 100% | 100% | 0.11 – 0.14 | 100% | 0.130 | 0.080 | 0% | 100% |

**Figure 85** BU_M16_109 test specimen after tightening

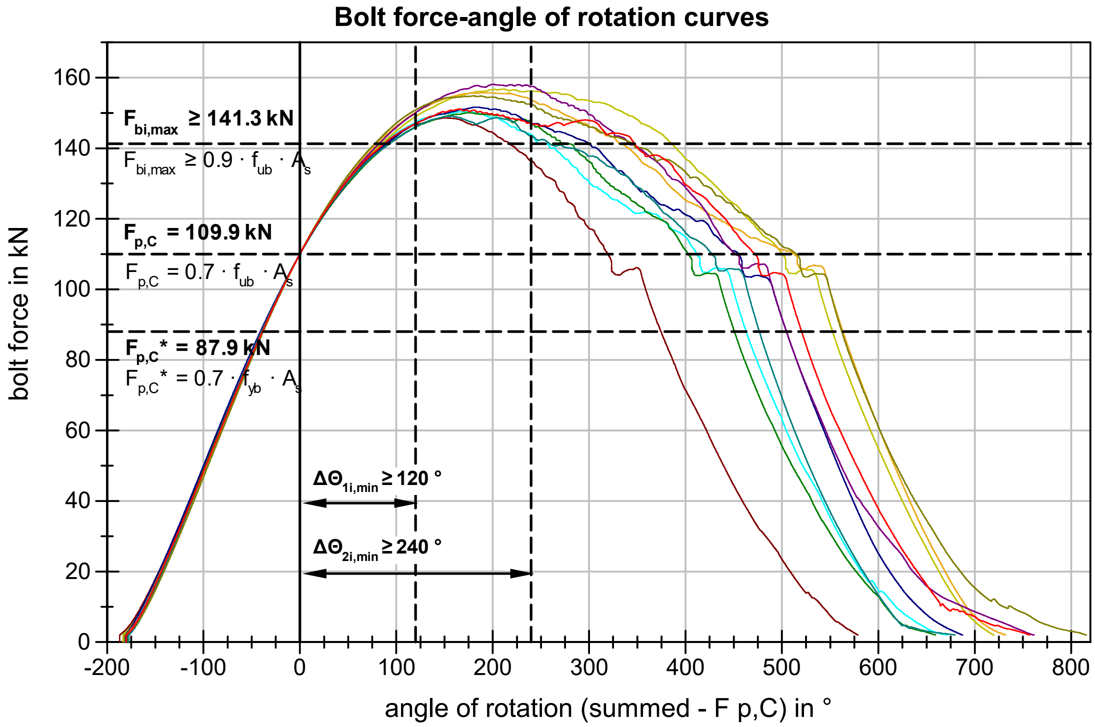


**Figure 86** BU_M16_109 Bolt force-angle of rotation curves

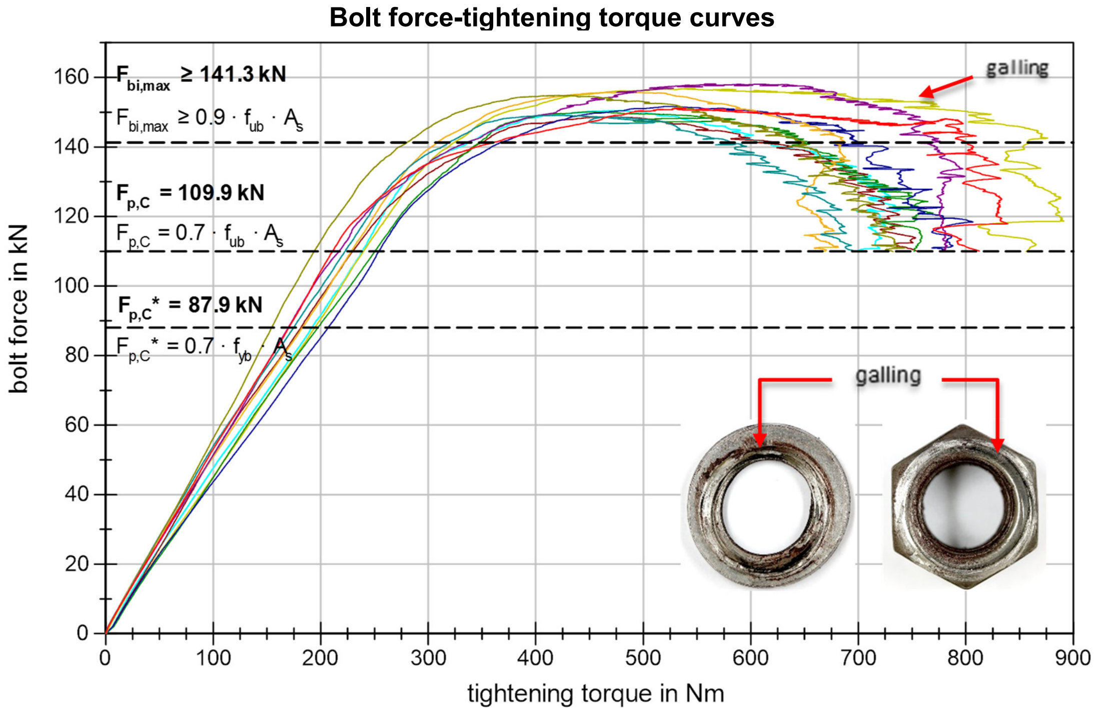


**Figure 87** BU_M16_109 Bolt force-tightening torque curves

#### *3.4.4.3 Bumax 109 – M16x100 – 10.9 – EN ISO 4017 – Molykote D-321R spray*

The Bumax 109 – M16x100 austenitic stainless steel bolting assemblies in property class 10.9 (used lubrication: Dow Corning Molykote® D-321R spray), in short form BU_M16_109, were arranged of the following components including nominal mechanical properties based on Bumax datasheet:

- *Bolts:* BUFAB Group Bumax 109 - M16x100 A4 according to EN ISO 4017; stainless steel EN 1.4432, 1.4436, 1.4435; manufact.: 2016-04-28; PRE 27

  tensile strength $R_{m,min}$ (= $f_{ub}$): nominal 1000 N/mm²
  yield strength $R_{p0.2,min}$ (= $f_{yb}$): nominal 800 N/mm²
  elongation, min: nominal 0.3d

- *Nuts:* BUFAB Group Bumax 109 - M16 M6M A4 according to EN ISO 4032; stainless steel EN 1.4432, 1.4436, 1.4435; manufact.: 2015-02-26; PRE 27

  stress under proof load, min: nominal 1000 N/mm²

- *Washers:* BUFAB Group Bumax RB A4-HV300 according to EN ISO 7089; stainless steel EN 1.4432, 1.4436, 1.4435; with dimensions d = 17.0 mm, D = 30.0 mm, t = 3.0 mm; manufact.: 2015-12-14; PRE 27

  hardness, min: nominal 300 HV

Table 99, Table 100 and Table 101 summarize the test results and evaluation of tested stainless steel bolting assemblies (used lubrication: Molykote D-321R). The statistical evaluation is shown as well with fulfilled and failed criteria according to EN 14399-3 (System HR). Figure 89 and Figure 90 present the tightening graphs. All tested austenitic bolting assemblies reached the specified preload levels $F_{p,C}$* = 87.9, $F_{p,C}$ = 109.9 kN and the maximum bolt force $F_{bi,max} \geq 0.9 \cdot f_{ub} \cdot A_s$ = 141.3 kN. Furthermore, 10 of 10 tested bolts achieved k-class K1 with k-values in a narrow range between 0.10 and 0.12 and a low coefficient of variation of v = 5.29 % (compared to k = 0.10 – 0.12 and v = 4.57 % at $F_{p,C}$*). Consequently, k-class K2 was accomplished. For further information and summarized criteria see Table 101. The graphs show irregular bolt force-tightening torque curves because of galling in the nut bearing surface when tightened into the plastic range including significant high ranges of values $M_i$ at $F_{bi,max}$ and at the end of the tests (bolt force dropped again to $F_{p,C}$) in the bolt force-tightening torque curves. 10 of 10 tested bolts achieved $\Delta\Theta_{1i,min}$ = 120° and additionally, all bolts reached $\Delta\Theta_{2i,min}$ = 240°. Damages at the first and second load-bearing thread turn of the bolts and roughening of the paired threads could be observed; bolt failure by fracture occurred once only. Strong galling in the faying surface washer/nut could be observed, too. Furthermore, in the context of functionality and re-use, it was possible to unscrew the hexagon nuts of all tested bolting assemblies manually but turning on the nut on whole threaded shank by hand was not possible.

**Table 99** Test results of Bumax 109 – M16x100 – Molykote D-321R spray

| Legend | Specimens | $F_{p,C}$* kN | $F_{p,C}$ kN | Max F kN | Max T Nm | $\Theta_{pi}$ ° | $\Theta_{1i}$ ° | $\Theta_{2i}$ ° | $F_{bi}$ ($\Theta_{2i}$) kN | $\Delta\Theta_{1i}$ ° | $\Delta\Theta_{2i}$ ° | k ($F_{p,C^*}$) | k ($F_{p,C}$) | $\mu_{tot}$ ($F_{p,C}$) | $\mu_{th}$ ($F_{p,C}$) | $\mu_b$ ($F_{p,C}$) | M ($F_{p,C}$*) Nm | $M_i$ ($F_{p,C}$) Nm | M ($F_{bi,max}$) Nm |
|---|---|---|---|---|---|---|---|---|---|---|---|---|---|---|---|---|---|---|---|
| max | | | | --- | | | | | | --- | --- | 0,16 | 0,16 | | | | | | |
| min | | | | 141,3 | | | | | | 120 | 240 | 0,10 | 0,10 | | | | | | |
| (yellow) | BU_M16_109-16 | 88 | 110 | 156,4 | 803,5 | 175 | 370 | 770 | 110,0 | 194 | 595 | 0,11 | 0,11 | 0,073 | 0,082 | 0,066 | 148,9 | 188,1 | 329,7 |
| (dark red) | BU_M16_109-17 | | | 143,7 | 605,7 | 181 | 307 | 492 | 110,0 | 126 | 311 | 0,11 | 0,11 | 0,077 | 0,090 | 0,067 | 157,5 | 196,6 | 351,0 |
| (green) | BU_M16_109-18 | | | 154,7 | 709,5 | 181 | 398 | 678 | 110,0 | 216 | 496 | 0,12 | 0,12 | 0,082 | 0,100 | 0,068 | 162,5 | 206,6 | 398,6 |
| (dark blue) | BU_M16_109-19 | | | 154,3 | 643,9 | 177 | 379 | 627 | 110,0 | 203 | 450 | 0,12 | 0,12 | 0,082 | 0,101 | 0,067 | 164,8 | 206,4 | 394,9 |
| (orange) | BU_M16_109-20 | | | 164,5 | 623,2 | 174 | 412 | 904 | 110,0 | 238 | 730 | 0,11 | 0,11 | 0,075 | 0,080 | 0,071 | 154,0 | 191,7 | 449,3 |
| (purple) | BU_M16_109-21 | | | 142,0 | 582,6 | 186 | 323 | 515 | 110,0 | 137 | 329 | 0,12 | 0,12 | 0,087 | 0,113 | 0,066 | 167,4 | 215,9 | 386,6 |
| (teal) | BU_M16_109-22 | | | 146,3 | 660,4 | 183 | 337 | 513 | 110,0 | 153 | 330 | 0,11 | 0,11 | 0,076 | 0,090 | 0,065 | 155,8 | 193,9 | 422,8 |
| (olive) | BU_M16_109-23 | | | 151,9 | 623,6 | 178 | 428 | 785 | 110,0 | 249 | 607 | 0,10 | 0,11 | 0,074 | 0,084 | 0,065 | 147,8 | 188,7 | 507,7 |
| (red) | BU_M16_109-24 | | | 158,4 | 648,5 | 184 | 398 | 592 | 110,0 | 213 | 408 | 0,10 | 0,10 | 0,070 | 0,081 | 0,062 | 145,9 | 182,0 | 355,1 |
| (light green) | BU_M16_109-25 | | | 157,0 | 649,1 | 184 | 384 | 719 | 110,0 | 200 | 535 | 0,11 | 0,11 | 0,078 | 0,097 | 0,063 | 157,8 | 197,7 | 335,7 |

**Table 100** Statistical evaluation of Bumax 109 – M16x100 – Molykote D-321R spray

| BU_M16_109_100 - Molykote D-321R n = 10 | Max F kN | Max T Nm | $\Theta_{pi}$ ° | $\Theta_{1i}$ ° | $\Theta_{2i}$ ° | $F_{bi}$ ($\Theta_{2i}$) kN | $\Delta\Theta_{1i}$ ° | $\Delta\Theta_{2i}$ ° | k ($F_{p,C^*}$) | k ($F_{p,C}$) | $\mu_{tot}$ ($F_{p,C}$) | $\mu_{th}$ ($F_{p,C}$) | $\mu_b$ ($F_{p,C}$) | M ($F_{p,C}$*) Nm | $M_i$ ($F_{p,C}$) Nm | M ($F_{bi,max}$) Nm |
|---|---|---|---|---|---|---|---|---|---|---|---|---|---|---|---|---|
| max | 164,5 | 803,5 | 186 | 428 | 904 | 110,0 | 249 | 730 | 0,119 | 0,12 | 0,087 | 0,113 | 0,071 | 167,4 | 215,9 | 507,7 |
| min | 142,0 | 582,6 | 174 | 307 | 492 | 110,0 | 126 | 311 | 0,104 | 0,103 | 0,070 | 0,080 | 0,062 | 145,9 | 182,0 | 329,7 |
| R | 22,5 | 220,9 | 12 | 121 | 412 | 0,0 | 123 | 419 | 0,015 | 0,020 | 0,017 | 0,033 | 0,009 | 21,5 | 33,9 | 178,0 |
| $\bar{x}$ | 152,9 | 655,0 | 180 | 374 | 660 | 110,0 | 193 | 479 | 0,111 | 0,112 | 0,077 | 0,092 | 0,066 | 156,2 | 196,8 | 393,1 |
| s | 7,0 | 62,3 | 4 | 40 | 136 | 0,0 | 41 | 139 | 0,005 | 0,006 | 0,005 | 0,011 | 0,003 | 7,3 | 10,3 | 55,6 |
| ν | 4,61 | 9,51 | 2,28 | 10,60 | 20,69 | 0,00 | 21,49 | 29,11 | 4,57 | 5,29 | 6,51 | 11,75 | 3,85 | 4,67 | 5,22 | 14,13 |

with n: number; R: range; x: mean value; s: standard deviation; ν: coefficient of variation in [%]

**Table 101** Evaluation of test results of Bumax 109 – M16x100 – Molykote D-321R spray

| n | $F_{p,C}^*$ | $F_{p,C}$ | $F_{bi,max}$ | $\Delta\Theta_{1i,min}$ | $\Delta\Theta_{2i,min}$ | k-values | k-class K1 | k-class K2 | | Fracture | Galling |
|---|---|---|---|---|---|---|---|---|---|---|---|
| [-] | 87.9 kN | 109.9 kN | ≥ 141.3 kN | ≥ 120° | ≥ 240° | [-] | $0.10 \le k_i \le 0.16$ | $0.10 \le k_m \le 0.23$ | $V_k \le 0.06$ | | |
| 10 | 100% | 100% | 100% | 100% | 100% | 0.10 – 0.12 | 100% | 0.112 | 0.053 | 10% | 100% |

**Figure 88** BU_M16_109 test specimen after tightening

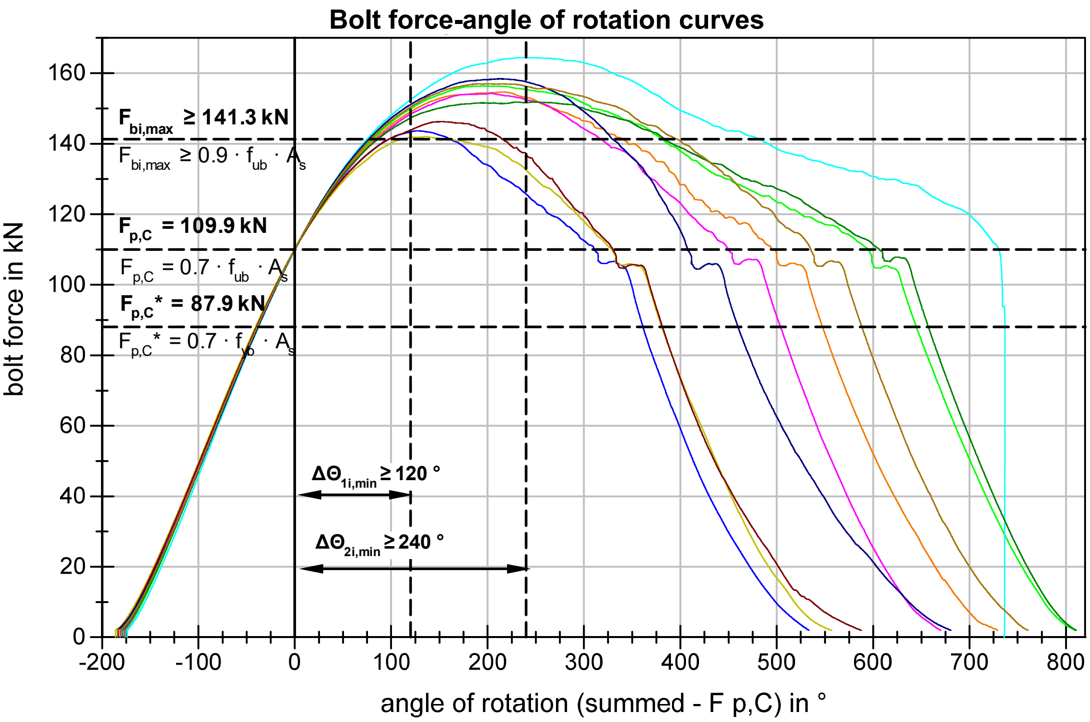


**Figure 89** BU_M16_109 Bolt force-angle of rotation curves

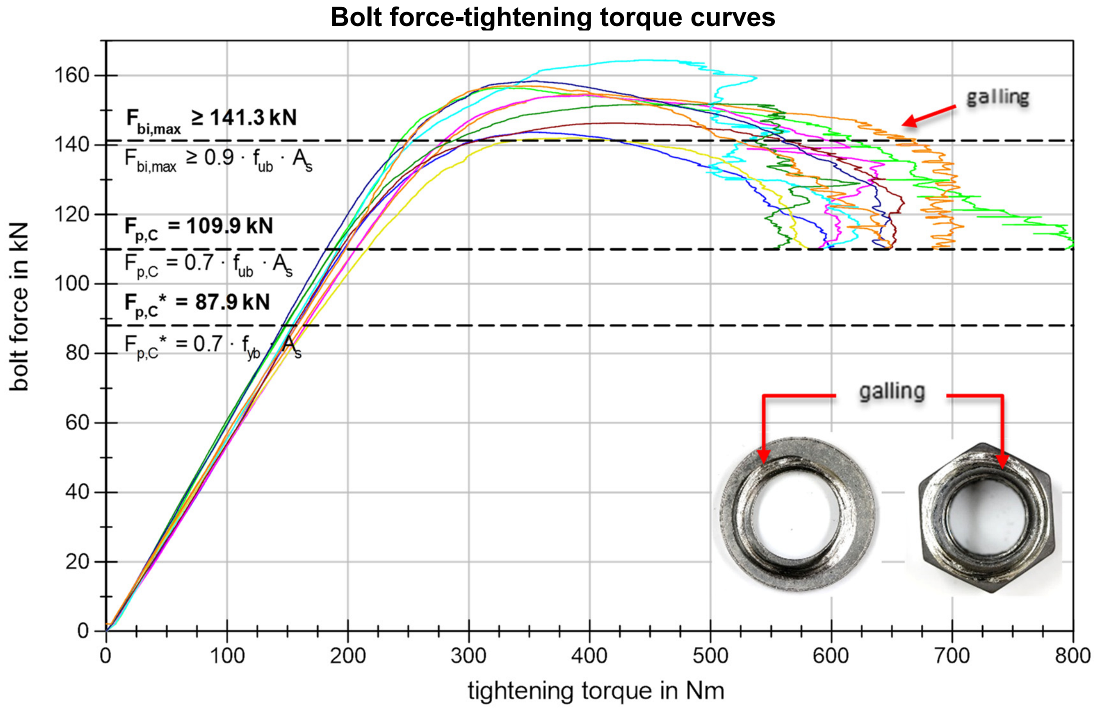


**Figure 90** BU_M16_109 Bolt force-tightening torque curves

### *3.4.4.4 Bumax LDX – M16x100 – 10.9 – EN ISO 4017 – Molykote 1000 spray*

The Bumax LDX – M16x100 lean duplex stainless steel bolting assemblies in property class 10.9/100 (used lubrication: Dow Corning Molykote® 1000 spray), in short form BU_M16_LDX, were arranged of the following components including nominal mechanical properties based on Bumax datasheet:

- *Bolts:* BUFAB Group Bumax LDX - M16x100 A4 according to EN ISO 4017; stainless steel EN 1.4162; manufact.: 2016-09-09; PRE 26

  tensile strength $R_{m,min}$ (= $f_{ub}$): nominal 1000 N/mm²
  yield strength $R_{p0.2,min}$ (= $f_{yb}$): nominal 900 N/mm²
  elongation, min: nominal 0.3d

- *Nuts:* BUFAB Group Bumax 109 - M16 M6M A4 according to EN ISO 4032; stainless steel EN 1.4432, 1.4436, 1.4435; manufact.: 2015-02-26; PRE 27

  stress under proof load, min: nominal 1000 N/mm²

- *Washers:* BUFAB Group Bumax RB A4-HV300 according to EN ISO 7089; stainless steel EN 1.4432, 1.4436, 1.4435; with dimensions d = 17.0 mm, D = 30.0 mm, t = 3.0 mm; manufact.: 2015-12-14; PRE 27

  hardness, min: nominal 300 HV

Table 102, Table 103 and Table 104 summarize the test results and evaluation of the Bumax LDX – M16x100 tested stainless steel bolting assemblies (used lubrication: Molykote 1000 spray). The statistical evaluation is shown as well with fulfilled and failed criteria according to EN 14399-3:2015-03 (System HR). Figure 92 and Figure 93 present the tightening graphs. All tested austenitic bolting assemblies reached the specified preload levels $F_{p,C}$* = 98.9, $F_{p,C}$ = 109.9 kN, and 9 of 10 bolts achieved the maximum bolt force $F_{bi,max} \geq 0.9 \cdot f_{ub} \cdot A_s$ = 141.3 kN. Furthermore, 10 of 10 tested bolts achieved k-class K1 with k-values in a narrow range between 0.12 and 0.15 and coefficient of variation v = 7.53 % (compared to k = 0.12 – 0.15 and v = 7.82 % at $F_{p,C}$*). Consequently, k-class K2 was accomplished. For further information and summarized criteria see Table 104. The graphs show irregular bolt force-tightening torque curves because of strong galling in the nut bearing surface when tightened into the plastic range including significant high ranges of values $M_i$ at $F_{bi,max}$ and at the end of the tests (bolt force dropped again to $F_{p,C}$) in the bolt force-tightening torque curves. 10 of 10 tested bolts achieved $\Delta\Theta_{1i,min}$ = 120° and additionally, all bolts reached $\Delta\Theta_{2i,min}$ = 240°. Damages at the first and second load-bearing thread turn of the bolts and roughening of the paired threads could be observed without partial or total bolt fracture. Strong galling in the faying surface washer/nut could be observed, too. Furthermore, in the context of functionality and re-use, it was possible to unscrew the hexagon nuts of all tested bolting assemblies manually, but turning on the nut on the whole threaded shank by hand was not possible.

**Table 102** Test results of Bumax LDX – M16x100 – Molykote 1000 spray

| Legend | Specimens | $F_{p,C}$* kN | $F_{p,C}$ kN | Max F kN | Max T Nm | $\Theta_{pi}$ ° | $\Theta_{1i}$ ° | $\Theta_{2i}$ ° | $F_{bi}(\Theta_{2i})$ kN | $\Delta\Theta_{1i}$ ° | $\Delta\Theta_{2i}$ ° | k ($F_{p,C^*}$) | k ($F_{p,C}$) | $\mu_{tot}$ ($F_{p,C}$) | $\mu_{th}$ ($F_{p,C}$) | $\mu_b$ ($F_{p,C}$) | M ($F_{p,C}$*) Nm | $M_i$ ($F_{p,C}$) Nm | M ($F_{bi,max}$) Nm |
|---|---|---|---|---|---|---|---|---|---|---|---|---|---|---|---|---|---|---|---|
| max | | | | --- | | | | | | --- | --- | 0,16 | 0,16 | | | | | | |
| min | | | | 141,3 | | | | | | 120 | 240 | 0,10 | 0,10 | | | | | | |
| | BU_M16_LDX-11 | 98,9 | 110 | 153,2 | 869,2 | 180 | 423 | 892 | 110,0 | 242 | 712 | 0,12 | 0,12 | 0,088 | 0,101 | 0,077 | 188,6 | 213,1 | 623,6 |
| | BU_M16_LDX-12 | | | 150,6 | 666,3 | 182 | 352 | 616 | 110,0 | 170 | 434 | 0,12 | 0,12 | 0,092 | 0,109 | 0,077 | 194,9 | 220,0 | 384,7 |
| | BU_M16_LDX-13 | | | 150,7 | 645,6 | 172 | 384 | 681 | 110,0 | 212 | 509 | 0,12 | 0,12 | 0,089 | 0,105 | 0,076 | 195,7 | 215,6 | 442,5 |
| | BU_M16_LDX-14 | | | 154,5 | 746,0 | 168 | 468 | 834 | 110,0 | 300 | 666 | 0,13 | 0,13 | 0,093 | 0,085 | 0,101 | 200,8 | 223,8 | 532,3 |
| | BU_M16_LDX-15 | | | 147,2 | 758,5 | 175 | 414 | 791 | 110,0 | 239 | 616 | 0,14 | 0,14 | 0,109 | 0,085 | 0,130 | 225,2 | 255,2 | 640,2 |
| | BU_M16_LDX-16 | | | <139,4 | 781,9 | 178 | 387 | 637 | 110,0 | 210 | 460 | 0,12 | 0,13 | 0,093 | 0,089 | 0,096 | 192,8 | 223,2 | 614,8 |
| | BU_M16_LDX-17 | | | 150,3 | 764,7 | 175 | 387 | 630 | 110,0 | 212 | 455 | 0,14 | 0,15 | 0,110 | 0,111 | 0,108 | 226,8 | 256,8 | 524,3 |
| | BU_M16_LDX-18 | | | 150,2 | 794,9 | 175 | 389 | 709 | 110,0 | 213 | 533 | 0,13 | 0,14 | 0,101 | 0,097 | 0,104 | 208,7 | 238,0 | 558,4 |
| | BU_M16_LDX-19 | | | 155,7 | 893,1 | 165 | 386 | 813 | 110,0 | 221 | 648 | 0,13 | 0,14 | 0,102 | 0,097 | 0,106 | 212,7 | 240,6 | 578,0 |
| | BU_M16_LDX-20 | | | 149,0 | 685,9 | 174 | 385 | 716 | 110,0 | 211 | 542 | 0,15 | 0,15 | 0,110 | 0,111 | 0,109 | 235,6 | 256,9 | 526,1 |

**Table 103** Statistical evaluation of Bumax LDX – M16x100 – Molykote 1000 spray

| Bumax LDX - M16x100 ISO 4017 - Molykote 1000 spray n = 10 | Max F kN | Max T Nm | $\Theta_{pi}$ ° | $\Theta_{1i}$ ° | $\Theta_{2i}$ ° | $F_{bi}(\Theta_{2i})$ kN | $\Delta\Theta_{1i}$ ° | $\Delta\Theta_{2i}$ ° | k ($F_{p,C^*}$) | k ($F_{p,C}$) | $\mu_{tot}$ ($F_{p,C}$) | $\mu_{th}$ ($F_{p,C}$) | $\mu_b$ ($F_{p,C}$) | M ($F_{p,C}$*) Nm | $M_i$ ($F_{p,C}$) Nm | M ($F_{bi,max}$) Nm |
|---|---|---|---|---|---|---|---|---|---|---|---|---|---|---|---|---|
| max | 155,7 | 893,1 | 182 | 468 | 892 | 110,0 | 300 | 712 | 0,149 | 0,15 | 0,110 | 0,111 | 0,130 | 235,6 | 256,9 | 640,2 |
| min | 139,4 | 645,6 | 165 | 352 | 616 | 110,0 | 170 | 434 | 0,119 | 0,121 | 0,088 | 0,085 | 0,076 | 188,6 | 213,1 | 384,7 |
| R | 16,3 | 247,5 | 17 | 116 | 276 | 0,0 | 130 | 278 | 0,030 | 0,025 | 0,022 | 0,026 | 0,054 | 47,0 | 43,8 | 255,5 |
| $\bar{x}$ | 150,1 | 760,6 | 174 | 398 | 732 | 110,0 | 223 | 558 | 0,132 | 0,133 | 0,099 | 0,099 | 0,098 | 208,2 | 234,3 | 542,5 |
| s | 4,5 | 80,9 | 5 | 31 | 96 | 0,0 | 33 | 98 | 0,010 | 0,010 | 0,009 | 0,010 | 0,017 | 16,4 | 17,5 | 80,6 |
| $\nu$ | 3,02 | 10,64 | 2,95 | 7,83 | 13,07 | 0,00 | 14,96 | 17,50 | 7,82 | 7,53 | 8,91 | 10,26 | 17,68 | 7,87 | 7,45 | 14,86 |

with n: number; R: range; x: mean value; s: standard deviation; $\nu$: coefficient of variation in [%]

**Table 104** Evaluation of test results of Bumax LDX – M16x100 – Molykote 1000 spray acc. EN 14399-3

| n | $F_{p,C}^*$ | $F_{p,C}$ | $F_{bi,max}$ | $\Delta\Theta_{1i,min}$ | $\Delta\Theta_{2i,min}$ | k-values | k-class K1 | k-class K2 | | Fracture | Galling |
|---|---|---|---|---|---|---|---|---|---|---|---|
| [-] | 98.9 kN | 109.9 kN | ≥ 141.3 kN | ≥ 120° | ≥ 240° | [-] | $0.10 \leq k_i \leq 0.16$ | $0.10 \leq k_m \leq 0.23$ | $V_k \leq 0.06$ | | |
| 10 | 100% | 100% | 90% | 100% | 100% | 0.12 – 0.15 | 100% | 0.133 | 0.075 | 0% | 100% |

**Figure 91** BU_M16_LDX test specimen after tightening

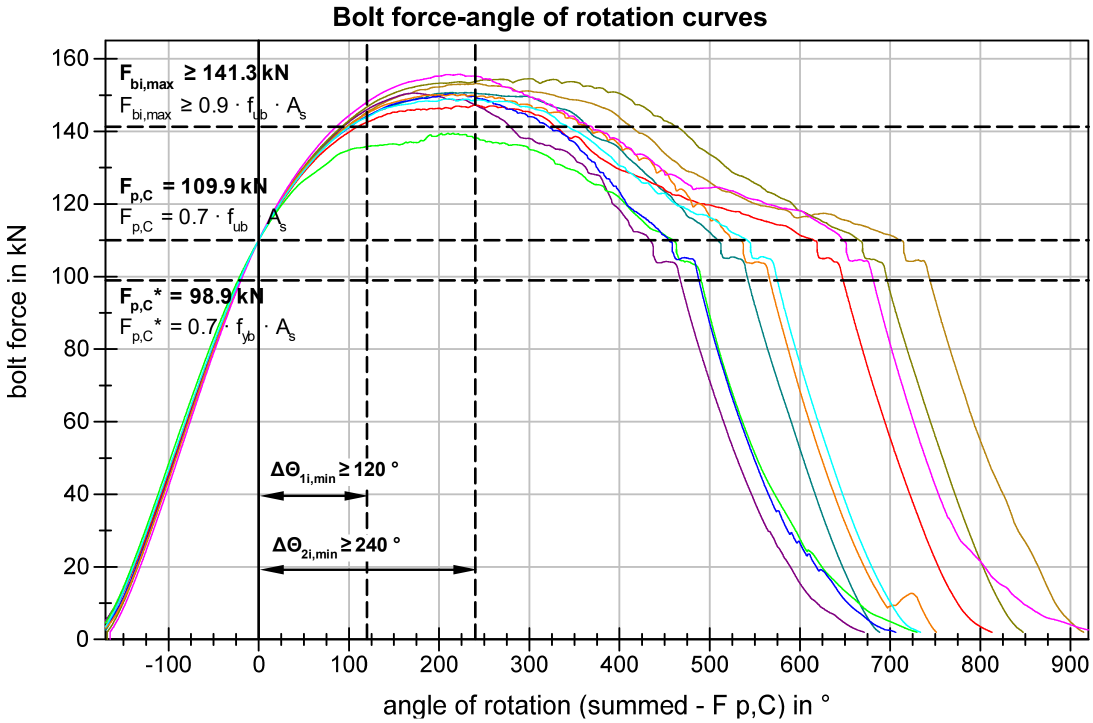


**Figure 92** BU_M16_LDX Bolt force-angle of rotation curves

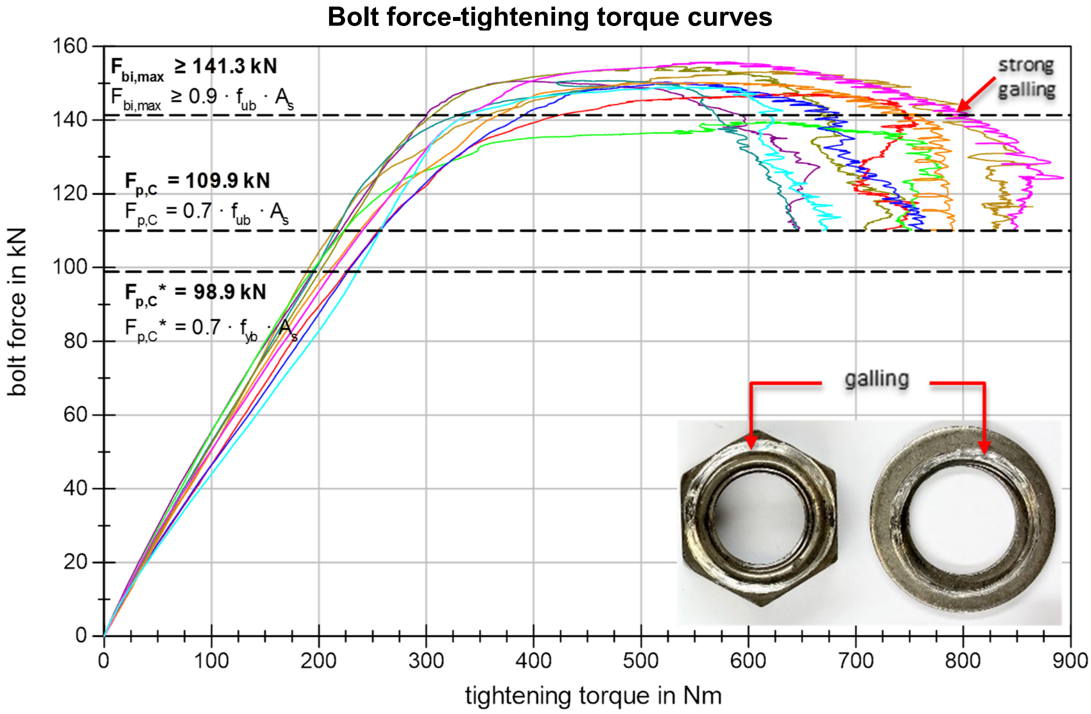


**Figure 93** BU_M16_LDX Bolt force-tightening torque curves

### *3.4.4.5 Bumax DX – M16x100 – 10.9 – EN ISO 4017 – Molykote 1000 spray*

The Bumax DX – M16x100 duplex stainless steel bolting assemblies in property class 10.9 (used lubrication: Dow Corning Molykote® 1000 spray), in short form BU_M16_DX, were arranged of the following components including nominal mechanical properties based on Bumax datasheet:

- *Bolts:* BUFAB Group Bumax LDX - M16x100 A4 according to EN ISO 4017; stainless steel EN 1.4462; manufact.: 2016-06-20; PRE 36

  tensile strength $R_{m,min}$ (= $f_{ub}$): nominal 1000 N/mm²
  yield strength $R_{p0.2,min}$ (= $f_{yb}$): nominal 900 N/mm²
  elongation, min: nominal 0.3d

- *Nuts:* BUFAB Group Bumax 109 - M16 M6M A4 according to EN ISO 4032; stainless steel EN 1.4432, 1.4436, 1.4435; manufact.: 2015-02-26; PRE 27

  stress under proof load, min: nominal 1000 N/mm²

- *Washers:* BUFAB Group Bumax RB A4-HV300 according to EN ISO 7089; stainless steel EN 1.4432, 1.4436, 1.4435; with dimensions d = 17.0 mm, D = 30.0 mm, t = 3.0 mm; manufact.: 2015-12-14; PRE 27

  hardness, min: nominal 300 HV

The tightening test results of Bumax DX – M16x100 bolting assemblies are summarized in Table 105, Table 106 and Table 107. The statistical evaluation is shown as well with fulfilled and failed criteria according to EN 14399-3 (System HR). The tightening curves are presented in Figure 95 and Figure 96 and show improved pronounced bolt force plateaus in the plastic range without any partial or total bolt fracture. All tested duplex bolting assemblies reached $F_{p,C}^{*} = 98.9$ kN and $F_{p,C} = 109.9$ kN as well as $F_{bi,max} \geq 0.9 \cdot f_{ub} \cdot A_s = 141.3$ kN. Due to the more pronounced plastic plateaus, 10 of the 10 bolts achieved $\Delta\Theta_{1i,min} = 120°$ and $\Delta\Theta_{2i,min} = 240°$ criteria according to EN 14399-3. Furthermore, 10 of 10 tested bolts achieved k-class K1 with k-values in a wide range between 0.14 and 0.17 and coefficient of variation v = 5.73 % (compared to k = 0.14 – 0.16 and v = 6.16 % at $F_{p,C}^{*}$). k-class K2 was accomplished. For further information and summarized criteria see Table 107. Again, the tightening graphs show irregular bolt force-tightening torque-curves because of galling in the nut bearing surface when tightened into the plastic range especially after $F_{bi,max}$ including significant high ranges of values $M_i$ at $F_{bi,max}$ and at the end of the tests (bolt force dropped again to $F_{p,C}$) in the bolt force-tightening torque curves. Damages at the first and second load-bearing thread turn of the bolts and roughening of the paired threads could be observed without partial or total bolt fracture. Strong galling especially in the faying surface washer/nut could be observed, too.

**Table 105** Test results of Bumax DX – M16x100 – Molykote 1000 spray

| Legend | Specimens | $F_{p,C}$* | $F_{p,C}$ | Max F | Max T | $\Theta_{pi}$ | $\Theta_{1i}$ | $\Theta_{2i}$ | $F_{bi}$ ($\Theta_{2i}$) | $\Delta\Theta_{1i}$ | $\Delta\Theta_{2i}$ | k ($F_{p,C*}$) | k ($F_{p,C}$) | $\mu_{tot}$ ($F_{p,C}$) | $\mu_{th}$ ($F_{p,C}$) | $\mu_b$ ($F_{p,C}$) | M ($F_{p,C}$*) | $M_i$ ($F_{p,C}$) | M ($F_{bi,max}$) |
|---|---|---|---|---|---|---|---|---|---|---|---|---|---|---|---|---|---|---|---|
| | | kN | kN | kN | Nm | ° | ° | ° | kN | ° | ° | | | | | | Nm | Nm | Nm |
| max | | | | --- | | | | | | --- | --- | 0,16 | 0,16 | | | | | | |
| min | | | | 141,3 | | | | | | 120 | 240 | 0,10 | 0,10 | | | | | | |
| | BU_M16_DX-12 | 98,9 | 110 | 148,0 | 862,4 | 193 | 359 | 636 | 110,0 | 166 | 443 | 0,14 | 0,14 | 0,109 | 0,111 | 0,106 | 223,3 | 254,2 | 497,8 |
| | BU_M16_DX-13 | | | 151,6 | 741,0 | 193 | 396 | 692 | 110,0 | 203 | 499 | 0,15 | 0,15 | 0,116 | 0,129 | 0,105 | 237,3 | 269,2 | 552,9 |
| | BU_M16_DX-14 | | | 158,6 | 925,8 | 182 | 430 | 867 | 110,0 | 247 | 685 | 0,14 | 0,15 | 0,113 | 0,103 | 0,121 | 226,2 | 262,9 | 621,6 |
| | BU_M16_DX-15 | | | 150,7 | 850,6 | 183 | 377 | 705 | 110,0 | 194 | 522 | 0,16 | >0,16 | 0,126 | 0,102 | 0,147 | 247,5 | 289,8 | 636,8 |
| | BU_M16_DX-16 | | | 147,9 | 830,9 | 186 | 339 | 698 | 110,0 | 153 | 512 | 0,15 | 0,15 | 0,114 | 0,113 | 0,115 | 229,7 | 264,9 | 555,6 |
| | BU_M16_DX-17 | | | 155,2 | 921,5 | 184 | 415 | 786 | 110,0 | 231 | 601 | 0,14 | 0,14 | 0,104 | 0,094 | 0,113 | 217,1 | 246,0 | 749,2 |
| | BU_M16_DX-18 | | | 150,5 | 979,4 | 187 | 385 | 828 | 110,0 | 198 | 641 | 0,15 | 0,15 | 0,112 | 0,109 | 0,114 | 237,2 | 261,5 | 569,9 |
| | BU_M16_DX-19 | | | 144,7 | 808,8 | 187 | 360 | 639 | 110,0 | 172 | 451 | 0,16 | 0,16 | 0,121 | 0,135 | 0,109 | 251,1 | 279,9 | 560,5 |
| | BU_M16_DX-20 | | | 142,0 | 886,2 | 193 | 337 | 568 | 110,0 | 144 | 375 | >0,16 | >0,16 | 0,126 | 0,147 | 0,109 | 260,2 | 290,2 | 588,1 |
| | BU_M16_DX-21 | | | 154,1 | 888,8 | 189 | 389 | 680 | 110,0 | 200 | 491 | 0,14 | 0,14 | 0,108 | 0,116 | 0,101 | 218,4 | 253,3 | 658,5 |

**Table 106** Statistical evaluation of Bumax DX – M16x100 – Molykote 1000 spray

| Bumax DX - M16x100 ISO 4017 - Molykote 1000 spray n = 10 | Max F kN | Max T Nm | $\Theta_{pi}$ ° | $\Theta_{1i}$ ° | $\Theta_{2i}$ ° | $F_{bi}$ ($\Theta_{2i}$) kN | $\Delta\Theta_{1i}$ ° | $\Delta\Theta_{2i}$ ° | k ($F_{p,C^*}$) | k ($F_{p,C}$) | $\mu_{tot}$ ($F_{p,C}$) | $\mu_{th}$ ($F_{p,C}$) | $\mu_b$ ($F_{p,C}$) | M ($F_{p,C^*}$) Nm | $M_i$ ($F_{p,C}$) Nm | M ($F_{bi,max}$) Nm |
|---|---|---|---|---|---|---|---|---|---|---|---|---|---|---|---|---|
| max | 158,6 | 979,4 | 193 | 430 | 867 | 110,0 | 247 | 685 | 0,164 | 0,17 | 0,126 | 0,147 | 0,147 | 260,2 | 290,2 | 749,2 |
| min | 142,0 | 741,0 | 182 | 337 | 568 | 110,0 | 144 | 375 | 0,137 | 0,140 | 0,104 | 0,094 | 0,101 | 217,1 | 246,0 | 497,8 |
| R | 16,6 | 238,4 | 11 | 93 | 299 | 0,0 | 103 | 310 | 0,027 | 0,025 | 0,022 | 0,053 | 0,046 | 43,1 | 44,2 | 251,4 |
| $\bar{x}$ | 150,3 | 869,5 | 188 | 379 | 710 | 110,0 | 191 | 522 | 0,148 | 0,152 | 0,115 | 0,116 | 0,114 | 234,8 | 267,2 | 599,1 |
| s | 4,9 | 67,2 | 4 | 31 | 92 | 0,0 | 33 | 95 | 0,009 | 0,009 | 0,007 | 0,016 | 0,013 | 14,5 | 15,2 | 70,5 |
| $\nu$ | 3,29 | 7,73 | 2,23 | 8,09 | 12,98 | 0,00 | 17,17 | 18,22 | 6,16 | 5,73 | 6,48 | 14,16 | 11,34 | 6,19 | 5,68 | 11,77 |

with n: number; R: range; x: mean value; s: standard deviation; $\nu$: coefficient of variation in [%]

**Table 107** Evaluation of test results of Bumax DX – M16x100 – Molykote 1000 spray acc. EN 14399-3

| n | $F_{p,C}^*$ | $F_{p,C}$ | $F_{bi,max}$ | $\Delta\Theta_{1i,min}$ | $\Delta\Theta_{2i,min}$ | k-values | k-class K1 | k-class K2 | | Fracture | Galling |
|---|---|---|---|---|---|---|---|---|---|---|---|
| [-] | 98.9 kN | 109.9 kN | ≥ 141.3 kN | ≥ 120° | ≥ 240° | [-] | $0.10 \le k_i \le 0.16$ | $0.10 \le k_m \le 0.23$ | $V_k \le 0.06$ | | |
| 10 | 100% | 100% | 100% | 100% | 100% | 0.14 – 0.17 | 80% | 0.152 | 0.057 | 0% | 100% |

**Figure 94** BU_M16_DX test specimen after tightening

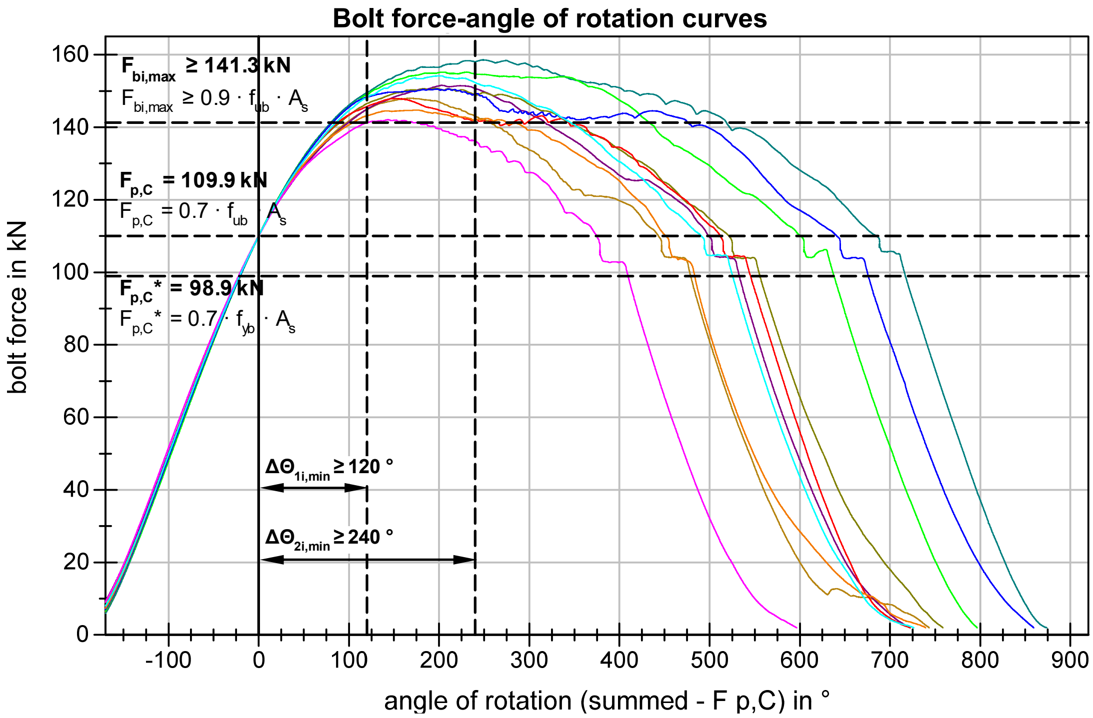


**Figure 95** BU_M16_DX Bolt force-angle of rotation curves

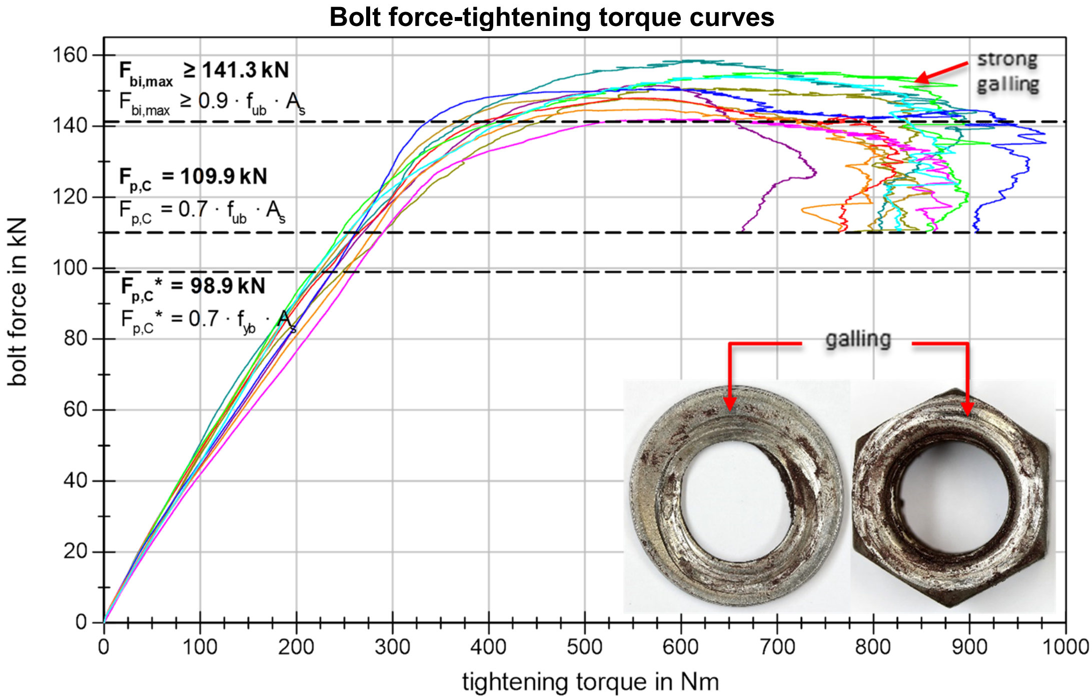


**Figure 96** BU_M16_DX Bolt force-tightening torque curves

## 3.5 Tightening test results and evaluation – STEP 3:

Additionally, tightening tests for bolt dimension M20 for austenitic and lean duplex/duplex were performed in STEP 3 with Interflon® HT1200 spray and paste according to EN 14399-2 and EN ISO 16047. The objective was to test additional lubricants and to investigate the effects on ductility and galling during tightening and to compare them with those of DOW Corning from STEP 2.

The test procedure contains a constant speed of rotation of 5.0 $min^{-1}$ for all tested steel grades. All series were tightened nut sided, the clamping length $\sum t$ was set to 72.0 mm (clamp length/bolt diameter ratio of 3.6) in reference to the corresponding tables of System HR – EN 14399-3. The tightening tests were stopped when the measured bolt force dropped to $F_{p,c} = 0.7 \cdot f_{ub} \cdot A_s$ (with $f_{ub}$: tensile strength of the bolt and $A_s$: tensile stress area of the bolt).

The criteria of evaluation for property class 8.8 (Bumax 88 series) according to EN 14399-3 are defined as follows:

- $F_{p,C}^* = 0.7 \cdot f_{yb} \cdot A_s = 0.7 \cdot 640$ N/mm² $\cdot$ 157.0 mm² = 70.3 kN (DIN EN 1993-1-8/NA)
- $F_{p,C} = 0.7 \cdot f_{ub} \cdot A_s = 0.7 \cdot 800$ N/mm² $\cdot$ 157.0 mm² = 87.9 kN
- $F_{bi,max} \geq 0.9 \cdot f_{ub} \cdot A_s = 0.9 \cdot 800$ N/mm² $\cdot$ 157.0 mm² = 113.0 kN
- $\Delta\Theta_{1i,min} \geq 120°$ with $\Sigma t = 60.5$ mm: $2d \leq \Sigma t < 6d$
- $\Delta\Theta_{2i,min} \geq 240°$ with $\Sigma t = 60.5$ mm: $2d \leq \Sigma t < 6d$

The criteria of evaluation for bolting assemblies in property class 10.9 (meaning Bumax 109, Bumax lean duplex and Bumax duplex series) are defined as follows:

- $F_{p,C}{}^* = 0.7 \cdot f_{yb} \cdot A_s = 0.7 \cdot 800$ N/mm² $\cdot$ 245.0 mm² = 137.2 kN (for Bumax 109 bolts)
- $F_{p,C}{}^* = 0.7 \cdot f_{yb} \cdot A_s = 0.7 \cdot 900$ N/mm² $\cdot$ 245.0 mm² = 154.4 kN (for Bumax LDX and DX)
- $F_{p,C} = 0.7 \cdot f_{ub} \cdot A_s = 0.7 \cdot 1000$ N/mm² $\cdot$ 245.0 mm² = 171.5 kN
- $F_{bi,max} \geq 0.9 \cdot f_{ub} \cdot A_s = 0.9 \cdot 1000$ N/mm² $\cdot$ 245.0 mm² = 220.5 kN
- $\Delta\Theta_{1i,min} \geq 120°$ with $\Sigma t$ = 105.0 mm: $2d \leq \Sigma t < 6d$
- $\Delta\Theta_{2i,min} \geq 240°$ with $\Sigma t$ = 105.0 mm: $2d \leq \Sigma t < 6d$

The following sections show exemplariliy the test results and evaluation of Bumax LDX – M20x100 series in property class 10.9 with Interflon HT1200 spray and paste and provide an overview about the effects of these alternative lubricants on ductility and galling. Finally, the results of all lubrication tests will be discussed in subchapter 3.6.3.

### 3.5.1 Bumax LDX – M20x100 – 10.9 – EN ISO 4017 – Interflon HT1200 spray

The Bumax LDX – M20x100 lean duplex stainless steel bolting assemblies in property class 10.9 with Interflon® HT1200 spray lubricants, in short form BU_M20_LDX, were arranged of the following components including nominal mechanical properties based on Bumax datasheet:

- *Bolts:* BUFAB Group Bumax LDX – M20x100 A4 according to EN ISO 4017; stainless steel EN 1.4162; manufact.: 2016-09-09; PRE 26

  tensile strength $R_{m,min}$ (= $f_{ub}$): nominal 1000 N/mm²
  yield strength $R_{p0.2,min}$ (= $f_{yb}$): nominal 900 N/mm²
  elongation, min: nominal 0.3d

- *Nuts:* BUFAB Group Bumax 88 – M20 M6M A4 according to EN ISO 4032; stainless steel EN 1.4432, 1.4436, 1.4435; manufact.: 2016-04-08; PRE 27

  stress under proof load, min: nominal 800 N/mm²

- *Washers:* BUFAB Group Bumax RB A4-HV200 according to EN ISO 7089; stainless steel EN 1.4432, 1.4436, 1.4435; with dimensions d = 21.0 mm, D = 37.0 mm, t = 3.0 mm; manufact.: 2015-09-22; PRE 27

  hardness, min: nominal 200 HV

The tightening curves of Bumax LDX – M20x100 bolting assemblies with Interflon® HT1200 spray are presented in Table 108. In general, the tightening curves are comparable to the already tested bolting assemblies using DOW Corning Molykote 1000 spray and are shown in Figure 98 and Figure 99. All tested lean duplex bolting assemblies reached $F_{p,C}{}^*$ = 154.4 kN and $F_{p,C}$ = 171.5 kN. On the contrary, the criteria of the maximum bolt force $F_{bi,max} \geq 0.9 \cdot f_{ub} \cdot A_s$ = 220.5 kN was not achieved in the whole tested series. Due to the less pronounced plastic plateaus, criteria $\Delta\Theta_{1i,min}$ = 120° and $\Delta\Theta_{2i,min}$ = 240° were only partially achieved (1 of 5 bolt). Furthermore, 4 of 5 tested bolts achieved k-class K1 with k-values between 0.14 and 0.19 and coefficient of variation v = 12.60 %. k-class K2 was not accomplished. For further information and summarized criteria see Table 108. Damages at the first and second load-bearing thread turn of the bolts and roughening of the paired threads could be observed. Minor galling especially in the faying surface washer/nut could be observed when tightened into the plastic range.

**Table 108** Evaluation of test results of Bumax LDX – M20x100 according to EN 14399-3 – Interflon HT1200 spray

| n | $F_{p,C}^*$ | $F_{p,C}$ | $F_{bi,max}$ | $\Delta\Theta_{1i,min}$ | $\Delta\Theta_{2i,min}$ | k-values | k-class K1 | k-class K2 | | Fracture | Galling |
|---|---|---|---|---|---|---|---|---|---|---|---|
| [-] | 154.4 kN | 171.5 kN | $\geq$ 220.5 kN | $\geq$ 120° | $\geq$ 240° | [-] | $0.10 \leq k_i \leq 0.16$ | $0.10 \leq k_m \leq 0.23$ | $V_k \leq 0.06$ | | |
| 5 | 100% | 100% | 0% | 20% | 20% | 0.14 – 0.19 | 80% | 0.162 | 0.126 | 0% | 60% |

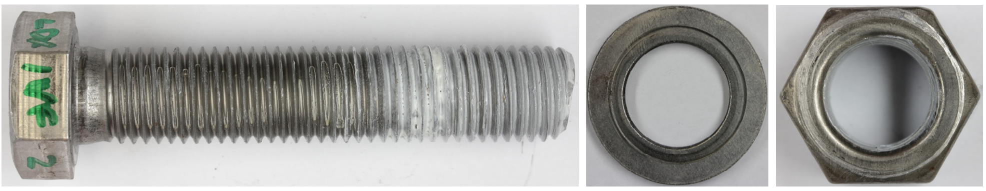

**Figure 97** BU_M20_LDX test specimen after tightening – Interflon HT1200 spray

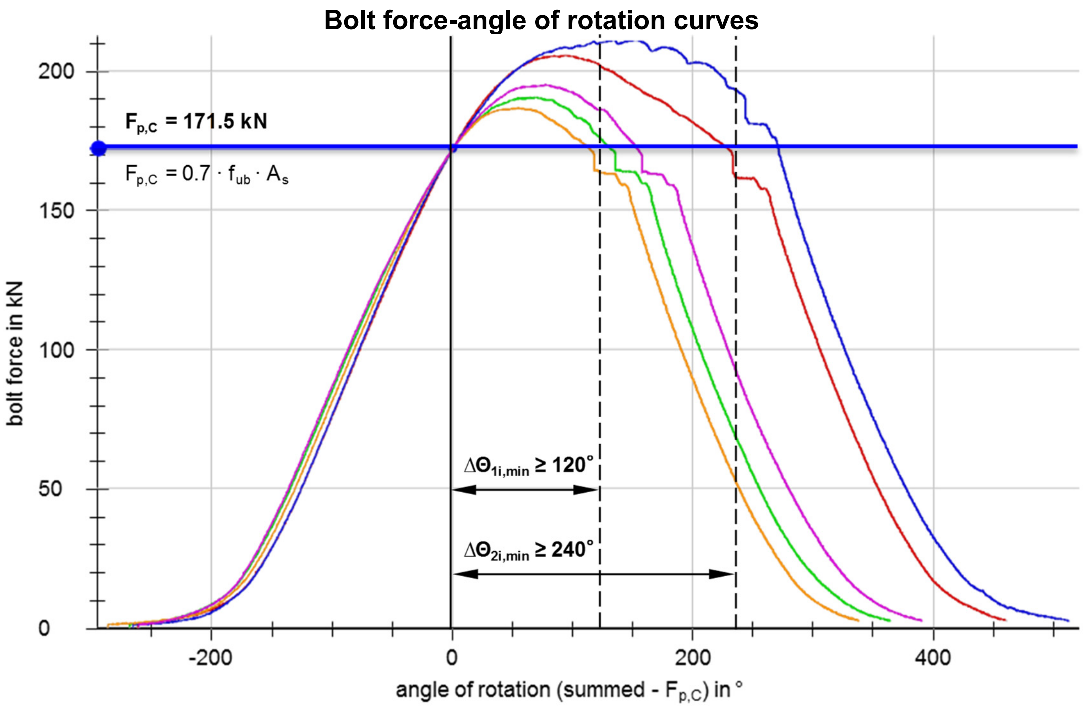


**Figure 98** BU_M20_LDX Bolt force-angle of rotation curves – Interflon HT1200 spray

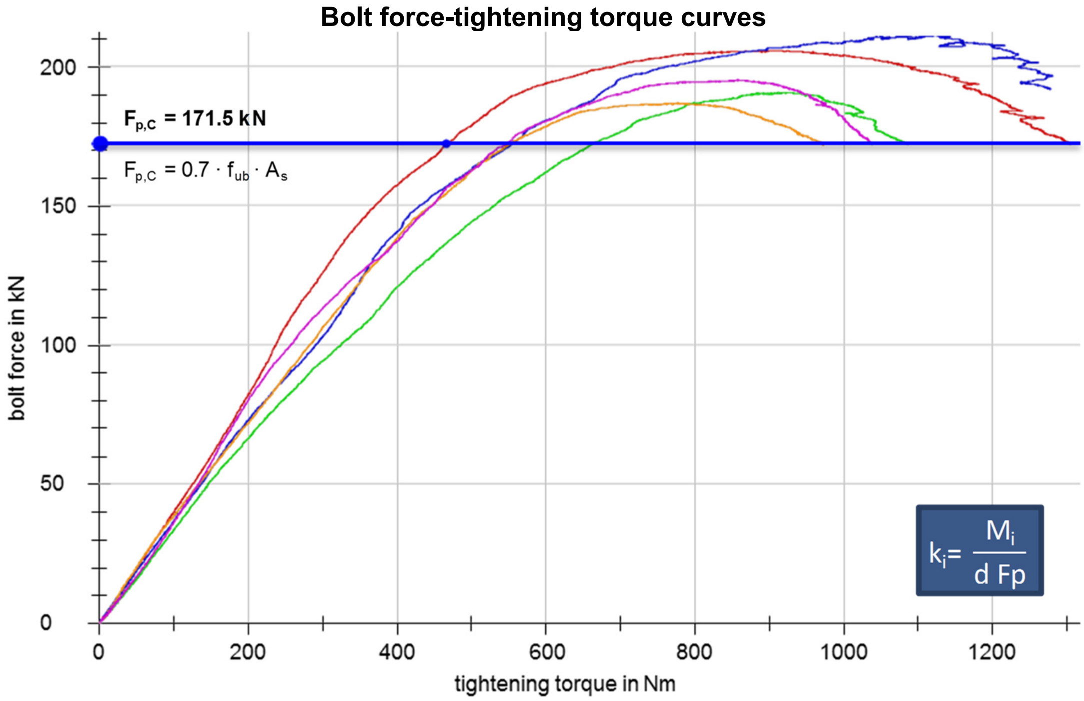


**Figure 99** BU_M20_LDX Bolt force-tightening torque curves – Interflon HT1200 spray

### 3.5.2 Bumax LDX – M20x100 – 10.9 – EN ISO 4017 – Interflon HT1200 paste

The Bumax LDX – M20x100 lean duplex stainless steel bolting assemblies in property class 10.9 and Interflon® HT1200 paste lubricants, in short form BU_M20_LDX, were arranged of the following components including nominal mechanical properties based on Bumax datasheet:

- *Bolts:* BUFAB Group Bumax LDX – M20x100 A4 according to EN ISO 4017; stainless steel EN 1.4162; manufact.: 2016-09-09; PRE 26

  tensile strength $R_{m,min}$ (= $f_{ub}$): nominal 1000 N/mm²
  yield strength $R_{p0.2,min}$ (= $f_{yb}$): nominal 900 N/mm²
  elongation, min: nominal 0.3d

- *Nuts:* BUFAB Group Bumax 88 – M20 M6M A4 according to EN ISO 4032; stainless steel EN 1.4432, 1.4436, 1.4435; manufact.: 2016-04-08; PRE 27

  stress under proof load, min: nominal 800 N/mm²

- *Washers:* BUFAB Group Bumax RB A4-HV200 according to EN ISO 7089; stainless steel EN 1.4432, 1.4436, 1.4435; with dimensions d = 21.0 mm, D = 37.0 mm, t = 3.0 mm; manufact.: 2015-09-22; PRE 27

  hardness, min: nominal 200 HV

The tightening curves of Bumax LDX – M20x100 bolting assemblies with Interflon® HT1200 paste are presented in Table 109. Again, the tightening curves (see Figure 101 and Figure 102) are comparable to the already tested bolting assemblies using DOW Corning Molykote 1000 spray. All tested lean duplex bolting assemblies reached $F_{p,C}^*$ = 154.4 kN and $F_{p,C}$ = 171.5 kN. On the contrary, only one bolting assembly achieved the criteria of maximum bolt force $F_{bi,max} \geq 0.9 \cdot f_{ub} \cdot A_s = 220.5$ kN. Due to the less pronounced plastic plateaus, criteria $\Delta\Theta_{1i,min} = 120°$ and $\Delta\Theta_{2i,min} = 240°$ were only partially achieved (2 of 5 bolt). Furthermore, 5 of 5 tested bolts achieved k-class K1 with k-values between 0.14 and 0.16 and a coefficient of variation of v = 4.70 %. k-class K2 was accomplished. For further information and summarized criteria see Table 109. Damages at the first and second load-bearing thread turn of the bolts and roughening of the paired threads could be observed. Minor galling especially in the faying surface washer/nut could be observed when tightened into the plastic range.

**Table 109** Evaluation of test results of Bumax LDX – M20x100 according to EN 14399-3 – Interflon HT1200 paste

| n | $F_{p,C}^*$ | $F_{p,C}$ | $F_{bi,max}$ | $\Delta\Theta_{1i,min}$ | $\Delta\Theta_{2i,min}$ | k-values | k-class K1 | k-class K2 | | Fracture | Galling |
|---|---|---|---|---|---|---|---|---|---|---|---|
| [-] | 154.4 kN | 171.5 kN | ≥ 220.5 kN | ≥ 120° | ≥ 240° | [-] | $0.10 \leq k_i \leq 0.16$ | $0.10 \leq k_m \leq 0.23$ | $V_k \leq 0.06$ | | |
| 5 | 100% | 100% | 20% | 40% | 40% | 0.14 – 0.16 | 100% | 0.149 | 0.047 | 0% | 40% |

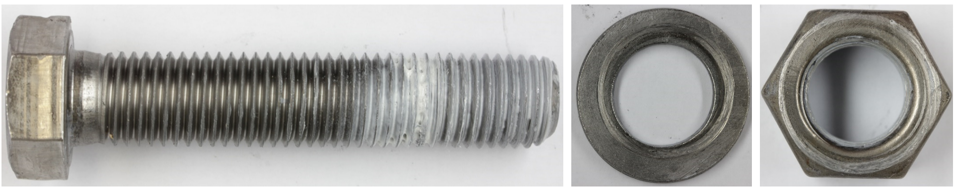

**Figure 100** BU_M20_LDX test specimen after tightening – Interflon HT1200 paste

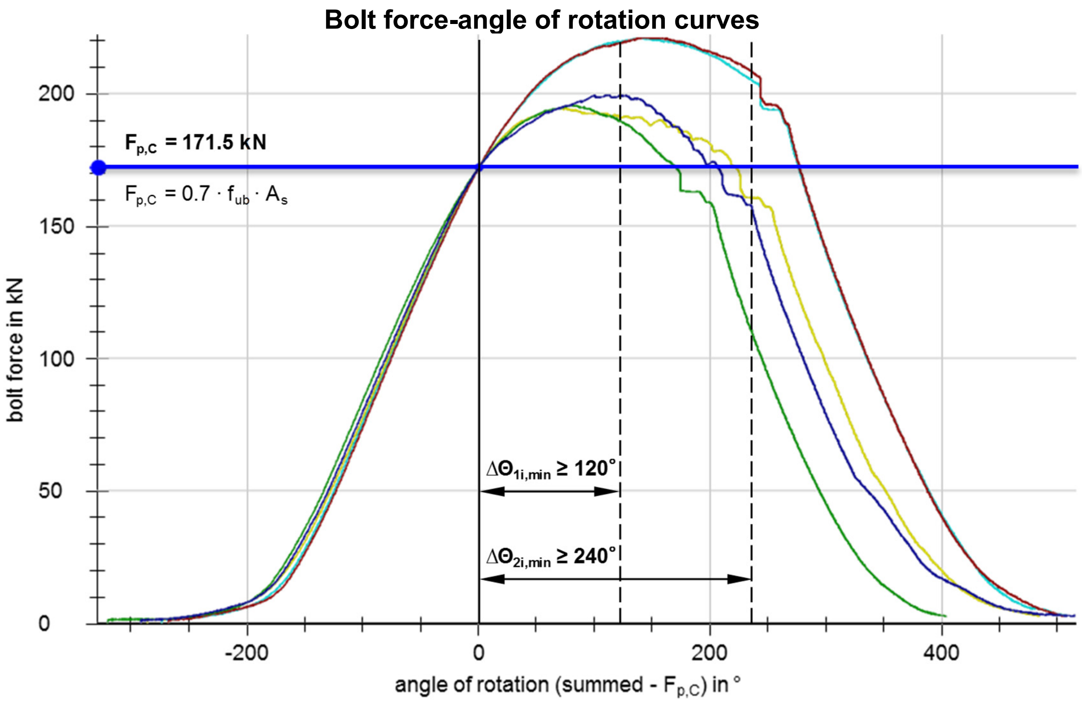


**Figure 101** BU_M20_LDX Bolt force-angle of rotation curves – Interflon HT1200 paste

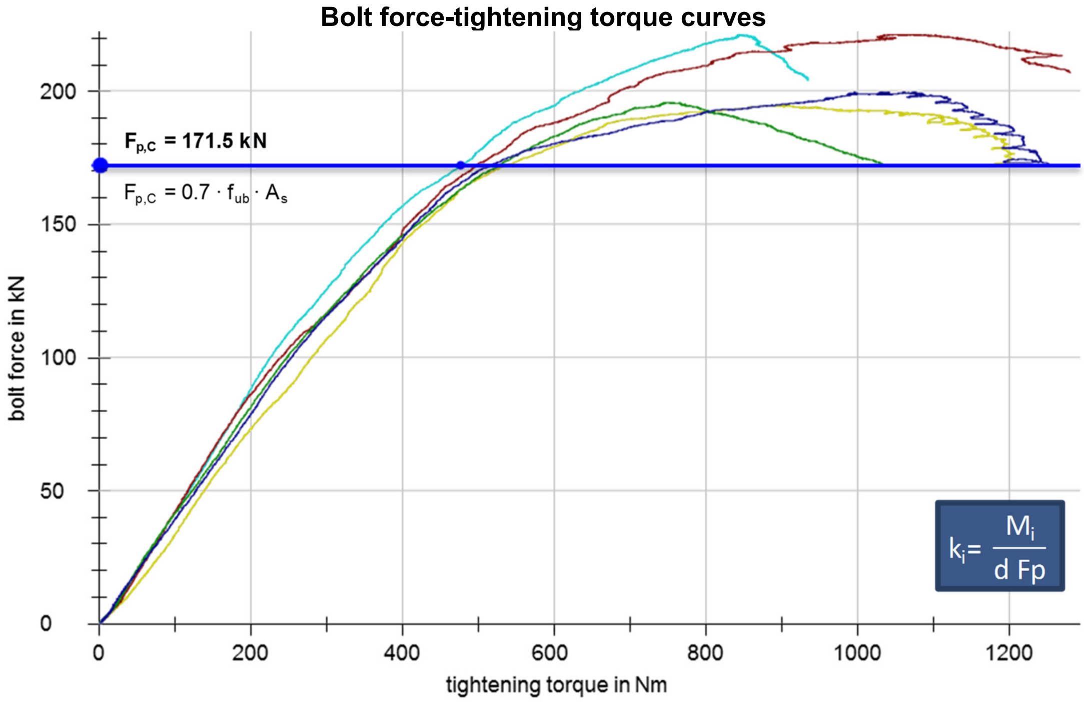


**Figure 102** BU_M20_LDX Bolt force-tightening torque curves – Interflon HT1200 paste

## 3.6 Results and Discussion

In the context of WP 5 – Preloading of SS bolts, Task 5.3/5.4, tightening tests of austenitic, lean duplex, duplex and super duplex stainless steel bolting assemblies were performed at the Institute for Metal and Lightweight Structures, University of Duisburg-Essen (UDE-IML). The objective was to investigate the basic preloading behaviour of stainless steel bolting assemblies and to achieve information regarding the complex interaction behaviour between the applied torque and the achieved preload. Bumax stainless steel bolts (acc. EN ISO 4014 and EN ISO 4017), hexagon nuts (acc. EN ISO 4032) and washers (acc. EN ISO 7089) were used. All bolting assemblies were tightened according to EN 14399-2 (valid for carbon steel bolts). Due to the fact that no evaluation criteria exist so far for preloaded stainless steel bolting assemblies (as they exist for carbon bolting assemblies with EN 14399), the evaluation of the tightening tests was referred to EN 14399-3 and follows for reasons of comparability the requirements and criteria of the HR system.

In addition, various lubricants were tested to investigate the influence of lubrication regarding ductility and galling and to identify a suitable lubrication for preloaded stainless steel bolting assemblies.

The tests were carried out in three steps:

1. The factory provided standard lubrication gleitmo 1952V from Fuchs Lubritech GmbH was used in the first step. Tightening tests of austenitic, lean duplex, duplex and super duplex stainless steel bolting assemblies in bolt dimension M12, M16, M20 and M24 were performed.
2. The alternative lubricants from DOW Corning (Molykote 1000 spray/paste, D-321R spray and P-74 paste) were used in the second step to identify suitable, alternative lubricants and to study the positive effects as extending the plastic plateau and avoiding galling. Tightening tests of austenitic, lean duplex, duplex and super duplex stainless steel bolting assemblies in bolt dimensions

M12, M16 and M20 were performed, covering EN ISO 4014 and EN ISO 4017 bolts and property classes 8.8 and 10.9.

3. Additionally, tightening tests were performed with M20 EN ISO 4017 bolts with the ceramic-based lubricant Interflon HT1200 spray and paste for austenitic (property classes 8.8 and 10.9) and lean duplex (property class 10.9) bolting assemblies.

The austenitic bolts BUMAX 88 and 109 with property classes 8.8 and 10.9, and the lean duplex, duplex and super duplex bolts in property class 10.9 were provided by the Swedish bolt manufacturer BUMAX AB. Partially, they were specifically produced for these tests.

### 3.6.1 Evaluation of tightening tests – Step 1: gleitmo 1952V

Table 110 shows the summary of the evaluation of the tested series after finishing the tightening tests with gleitmo® 1952V standard lubrication from Fuchs Lubritech GmbH. In conclusion, it can be figured out that fracture of bolts did not occur and, with the exception of Bumax 109 – M20x140, all tested stainless steel bolting assemblies reached the preload level $F_{p,C}^* = 0.7 \cdot f_{yb} \cdot A_s$ and $F_{p,C} = 0.7 \cdot f_{ub} \cdot A_s$. In contrast, caused by the fact that the bolt force plateaus in the plastic range were less pronounced compared to those of EN 14399-carbon steel bolting assemblies, the criteria of the maximum bolt force $F_{bi,max} \geq 0.9 \cdot f_{ub} \cdot A_s$ was only partially achieved. It can be shown that in total only Bumax 88 – M16x80 series reached $F_{bi,max} \geq 0.9 \cdot f_{ub} \cdot A_s$. Indeed, for the series Bumax 88 – M12x80, Bumax SDX – M12x80 and Bumax 88 – M20x100 (bolts manufactured in 2015) only one bolt failed in each series. On the contrary, Bumax 88 – M20x100 (2013), Bumax 109 – M20x140, Bumax LDX – M20x100 and Bumax DX – M20x100 test series failed completely. Furthermore, also referred to the less pronounced bolt force plateaus in plastic range, the required angles of nut rotation $\Delta\Theta_{1i,min}$ and $\Delta\Theta_{2i,min}$ are unequally distributed, which can be seen in Table 110. The analysis of k-values tends to show two groups:

- *a narrow range of k-values* like Bumax 88 – M16x80 (0.13 to 0.17), Bumax 109 – M20x140 (0.25 to 0.26) and Bumax LDX – M16x100 (0.11 to 0.15),
- *a wide range of k-values* like Bumax 88 – M12x80 (0.11 to 0.19), Bumax 88 – M24x100 (0.10 to 0.22) and other tested series.

Consequently, the classification in k-class K1 is also unequally distributed in all tested series and confirming a general high dispersion of all tested values, markedly friction. In addition, all tested stainless steel bolting assemblies did not achieve the criteria for classification to k-class K2, mainly caused by a higher coefficient of variation $v_k$ than 0.06 referring to EN 14399-1. It is noticeable that Bumax 88 – M20x100 (bolts manufactured in 2013) failed as well as Bumax 109 – M20x140 – in most criteria, caused by very high coefficients of friction as a possible evidence for insufficient or ineffective lubrication. In addition, lean duplex and duplex steel grades for bolt dimension M16 and M20 did not achieve $F_{bi,max} \geq 0.9 \cdot f_{ub} \cdot A_s$, and the required angles of nut rotation $\Delta\Theta_{1i,min}$ and $\Delta\Theta_{2i,min}$ were only partially fulfilled. In total, the tested bolting assemblies showed up light to heavy galling in the nut bearing surfaces, when tightened into the plastic range. The damage analysis underlines that all tested bolt assemblies have similar damages at the first (and in some cases second) load-bearing thread turn of the bolt, roughening of paired threads and minimal necking of threaded shanks without bolt or nut fracture. With the exception of Bumax 88 – M20x100 (2013 series) and Bumax 88 – M24x100 series, all tested bolting assemblies showed damages caused by galling, especially in the faying surface between the washer and nut as shown exemplary in Figure 103. There are a variety of possible reasons for such an occurrence. Considering the use of bolting assemblies made of stainless steel as high-strength bolting assembly for preloading, the tightening behaviour had to be investigated by using alternative lubrications to increase the ductility and to avoid galling.

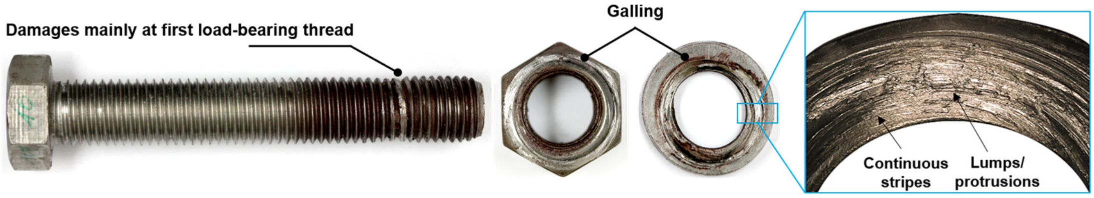


**Figure 103** Galling of the nut bearing surface when tightened into plastic range: bolt (left), nut and washer (middle), and detailed view of washer (right)

**Table 110** Summary of the evaluation of stainless steel tightening tests according to EN 14399-3 (valid for clamp lengths: 2d ≤ ∑t ≤ 6d)

| Tested series | n | $F_{p,C}^{*}$ | $F_{p,C}$ | $F_{bi,max}$ | $\Delta\Theta_{1i,min}$ | $\Delta\Theta_{2i,min}$ | k-values | k-class K1 | k-class K2 | | Fracture | Galling |
|---|---|---|---|---|---|---|---|---|---|---|---|---|
| | [-] | | | | ≥ 120° | ≥ 240° | [-] | $0.10 \le k_i \le 0.16$ | $0.10 \le k_m \le 0.23$ | $V_k \le 0.06$ | | |
| **M12** | | | | | | | | | | | | |
| Bumax 88 - M12x80 | 10 | 100% | 100% | 90% | 70% | 80% | 0.11 – 0.19 | 80% | 0.149 | 0.186 | 0% | 100% |
| Bumax 109 - M12x80 | 10 | 100% | 100% | 40% | 70% | 60% | 0.12 – 0.24 | 30% | 0.183 | 0.205 | 0% | 100% |
| Bumax SDX - M12x80 | 10 | 100% | 100% | 90% | 60% | 90% | 0.14 – 0.21 | 60% | 0.138 | 0.138 | 0% | 100% |
| **M16** | | | | | | | | | | | | |
| Bumax 88 - M16x80 | 10 | 100% | 100% | 100% | 60% | 100% | 0.13 – 0.17 | 90% | 0.136 | 0.075 | 0% | 100% |
| Bumax 109 - M16x100 | 10 | 100% | 100% | 30% | 40% | 40% | 0.11 – 0.22 | 60% | 0.151 | 0.231 | 0% | 100% |
| Bumax LDX - M16x100 | 10 | 100% | 100% | 30% | 40% | 80% | 0.11 – 0.15 | 100% | 0.123 | 0.127 | 0% | 100% |
| Bumax DX - M16x100 | 10 | 100% | 100% | 20% | 20% | 30% | 0.12 – 0.19 | 70% | 0.150 | 0.169 | 0% | 100% |
| **M20** | | | | | | | | | | | | |
| Bumax 88 - M20x100 (2013) | 5 | 100% | 100% | 0% | 0% | 0% | 0.21 – 0.33 | 0% | 0.239 | 0.217 | 0% | 20% |
| Bumax 88 - M20x100 (2015) | 10 | 100% | 100% | 90% | 30% | 90% | 0.12 – 0.17 | 80% | 0.145 | 0.118 | 0% | 100% |
| Bumax 109 - M20x140 | 10 | 100% | 40% | 0% | 0% | 0% | 0.25 – 0.26 | 0% | 0.255 | 0.023 | 0% | 100% |
| Bumax LDX - M20x100 | 10 | 100% | 100% | 0% | 0% | 30% | 0.10 – 0.15 | 100% | 0.120 | 0.148 | 0% | 100% |
| Bumax DX - M20x100 | 10 | 100% | 100% | 0% | 20% | 30% | 0.10 – 0.15 | 100% | 0.121 | 0.158 | 0% | 100% |
| **M24** | | | | | | | | | | | | |
| Bumax 88 - M24x100 | 10 | 100% | 100% | 50% | 10% | 30% | 0.10 – 0.22 | 60% | 0.151 | 0.235 | 0% | 30% |

Because galling occurs frequently, especially when stainless steel surfaces are in contact with or sliding against each other, the control of lubrication is required. A detailed view of friction as a dynamic link between the applied torque and the achieved preload is essential for understanding the basic preloading behaviour of bolting assemblies. Although gleitmo® 1952V is used as a special lubrication for stainless steel applications and has promising constant friction coefficients with low spreading, the test results delivered high ranges in $\mu_{tot}$, $\mu_{th}$, and $\mu_b$, the friction coefficients vary significantly in all tested austenitic and austenitic-ferritic series. Hence, a constant level of friction was not achieved in the tightening tests of the stainless steel bolting assemblies. To identify preloading levels for stainless steel bolting assemblies (Task 5.4), it is required to perform additional tightening tests to clarify the use of alternative, suitable lubrications. The scattering and unequally distribution of friction coefficients at different preload levels is exemplary presented in Figure 104, showing $\mu_{tot}$, $\mu_{th}$ and $\mu_b$ of Bumax 88 – M12x80 series. The summary of the friction coefficients of the tested stainless steel series is presented in Table 111.

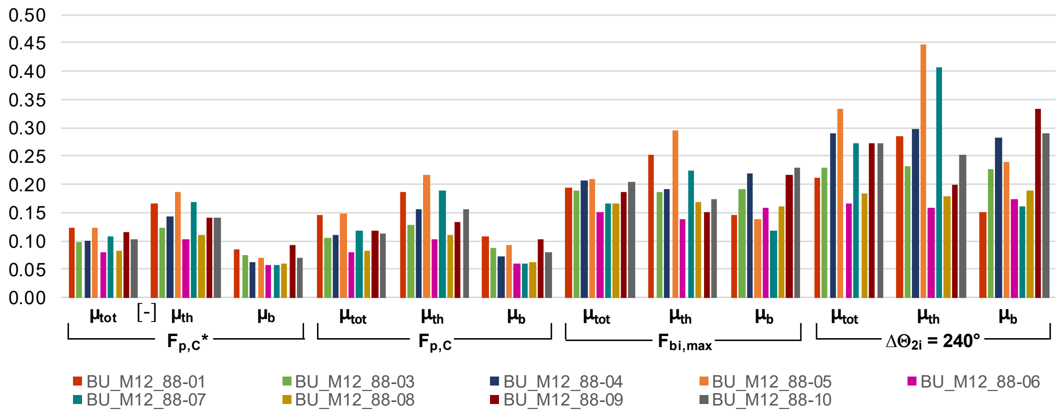


**Figure 104** BU_M12_88 distribution of friction at selected bolt force levels

**Table 111** Summary of the friction coefficients of tested stainless steel series with gleitmo 1952V standard lubrication

| Series | $\mu_{tot}$ | | | $\mu_{th}$ | | | $\mu_b$ | | |
|---|---|---|---|---|---|---|---|---|---|
| | Min - Max | Range | $V_K$ [%] | Min - Max | Range | $V_K$ [%] | Min - Max | Range | $V_K$ [%] |
| **M12** | | | | | | | | | |
| **Bumax 88 - M12x80** | 0.079 - 0.149 | 0.070 | **20.65** | 0.103 - 0.217 | 0.114 | **25.01** | 0.059 - 0.109 | 0.050 | 23.62 |
| **Bumax 109 - M12x80** | 0.119 - 0.191 | 0.068 | **21.20** | 0.089 - 0.157 | 0.068 | **21.20** | 0.107 - 0.261 | 0.154 | **29.93** |
| **Bumax SDX - M12x80** | 0.104 - 0.165 | 0.061 | **15.64** | 0.125 - 0.201 | 0.076 | **14.20** | 0.070 - 0.134 | 0.064 | **21.15** |
| **M16** | | | | | | | | | |
| **Bumax 88 - M16x80** | 0.095 - 0.126 | 0.031 | **9.21** | 0.140 - 0.183 | 0.043 | **10.52** | 0.053 - 0.111 | 0.058 | **26.40** |
| **Bumax 109 - M16x100** | 0.072 - 0.169 | 0.097 | **27.67** | 0.091 - 0.213 | 0.122 | **22.10** | 0.048 - 0.197 | 0.149 | **61.38** |
| **Bumax LDX - M16x100** | 0.078 - 0.118 | 0.040 | **15.14** | 0.109 - 0.160 | 0.051 | **13.63** | 0.048 - 0.101 | 0.053 | **26.91** |
| **Bumax DX - M16x100** | 0.089 - 0.152 | 0.063 | **20.33** | 0.098 - 0.179 | 0.081 | **16.50** | 0.051 - 0.137 | 0.086 | **35.62** |
| **M20** | | | | | | | | | |
| **Bumax 88 - M20x100 (2013)** | 0.166 - 0.271 | 0.105 | **23.11** | 0.215 - 0.351 | 0.136 | **19.97** | 0.079 - 0.201 | 0.122 | **37.55** |
| **Bumax 88 - M20x100 (2015)** | 0.088 - 0.128 | 0.040 | **13.47** | 0.117 - 0.179 | 0.062 | **16.67** | 0.059 - 0.124 | 0.065 | **25.49** |
| **Bumax 109 - M20x140** | 0.199 - 0.214 | 0.015 | **3.36** | 0.176 - 0.203 | 0.027 | **6.88** | 0.218 - 0.225 | 0.007 | **1.53** |
| **Bumax LDX - M20x100** | 0.085 - 0.141 | 0.056 | **17.80** | 0.087 - 0.168 | 0.081 | **20.79** | 0.065 - 0.118 | 0.053 | **20.45** |
| **Bumax DX - M20x100** | 0.082 - 0.135 | 0.053 | **18.04** | 0.086 - 0.152 | 0.066 | **18.88** | 0.057 - 0.164 | 0.066 | **31.95** |
| **M24** | | | | | | | | | |
| **Bumax 88 - M24x100** | 0.074 - 0.172 | 0.098 | **26.24** | 0.064 - 0.226 | 0.162 | **42.55** | 0.079 - 0.128 | 0.049 | **16.61** |

The mechanical behaviour of EN ISO 4014/4017 stainless steel bolting assemblies using gleitmo® 1952V standard lubrication compared to system HR and system HV carbon steel bolting assemblies is shown exemplary in Figure 105, Figure 106 (system HR), and Figure 107, Figure 108 (system HV). The tightening curves visualize a comparison between Bumax 88 – M24x100 stainless steel bolting assemblies (black curves) and M24x100 HR 8.8 bolting assemblies (yellow curves), as well as M24x100 HV 10.9 bolting assemblies (yellow curves). Note that these are simply examples to present main differences because the shape of tightening curves is multifactorial influenced (e. g. by lubrication used) and may differ. From the beginning of the tightening test to the defined preload level $F_{p,C}$* and $F_{p,C}$, stainless steel and carbon steel bolting assemblies show a nearly similar and approximately linear behaviour in the bolt force-angle of rotation curves, differentiated only by the slope of the line. Additionally, in this region, the scattering of curves in all tested series is negligible. The bolt force plateau in the plastic range of SS bolting assemblies are less pronounced compared to CS bolts, leading to lower angles of rotation $\Delta\Theta_{1i}$ and $\Delta\Theta_{2i}$. Furthermore, the tightening curves of the tested SS bolting assemblies show a greater distribution in both axes, meaning scattering of the maximum individual bolt force $F_{bi,max}$ and scattering of the angles of rotation when the bolt force again drops to

$F_{p,C}$ again. The bolt force-tightening torque curves of HR and HV bolting assemblies tend to display a relatively narrow range of tightening torque. On the other hand, SS bolting assemblies display a wide range of torque. In total, these circumstances create difficulties in defining predictable, calculable, and securely tightening torques for bolting assemblies made of stainless steel.

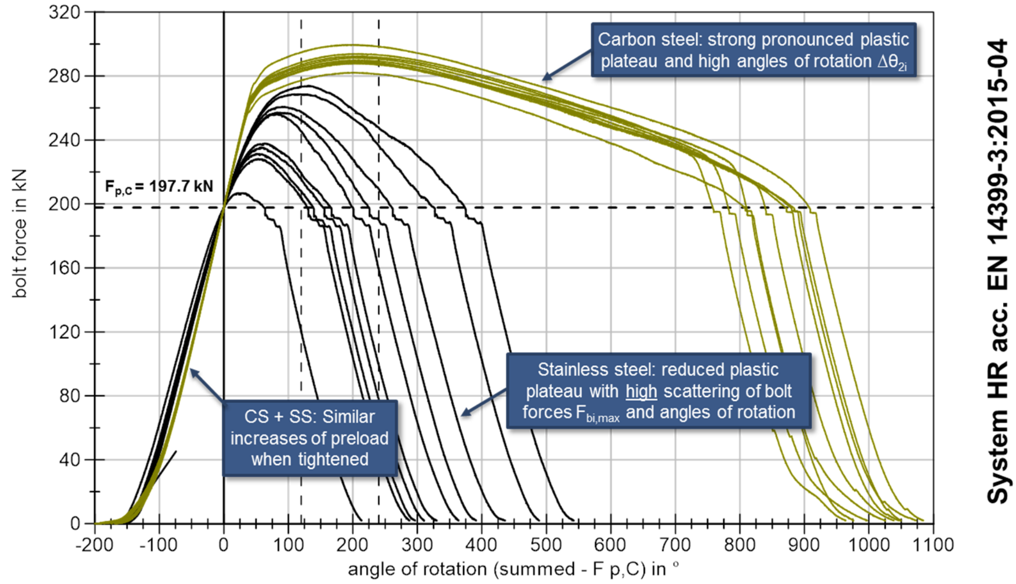


**Figure 105** Comparison of bolt force-angle of rotation-curves between Bumax 88 – M24x100 - gleitmo 1952V (black) and M24x100 HR 8.8 (yellow)

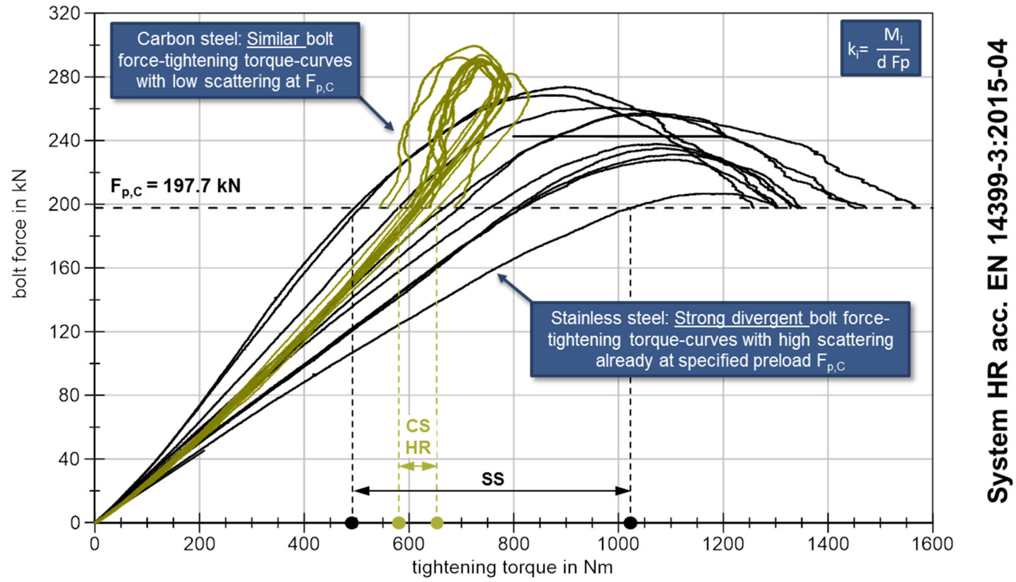


**Figure 106** Comparison of bolt force-tightening torque-curves between Bumax 88 – M24x100 - gleitmo 1952V (black) and M24x100 HR 8.8 (yellow)

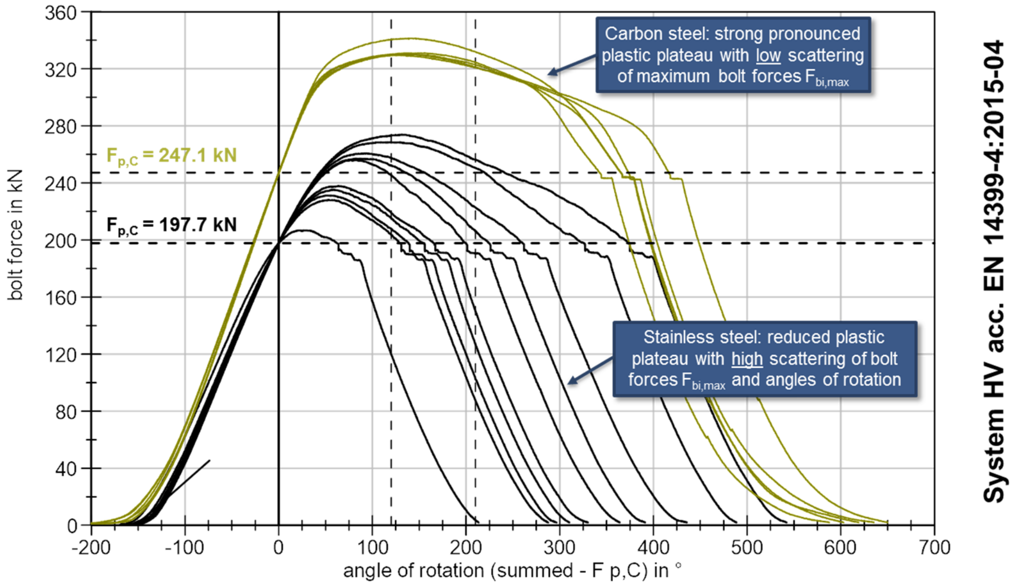


**Figure 107** Comparison of bolt force-angle of rotation-curves between Bumax 88 – M24x100 - gleitmo 1952V (black) and M24x100 HV 10.9 (yellow)

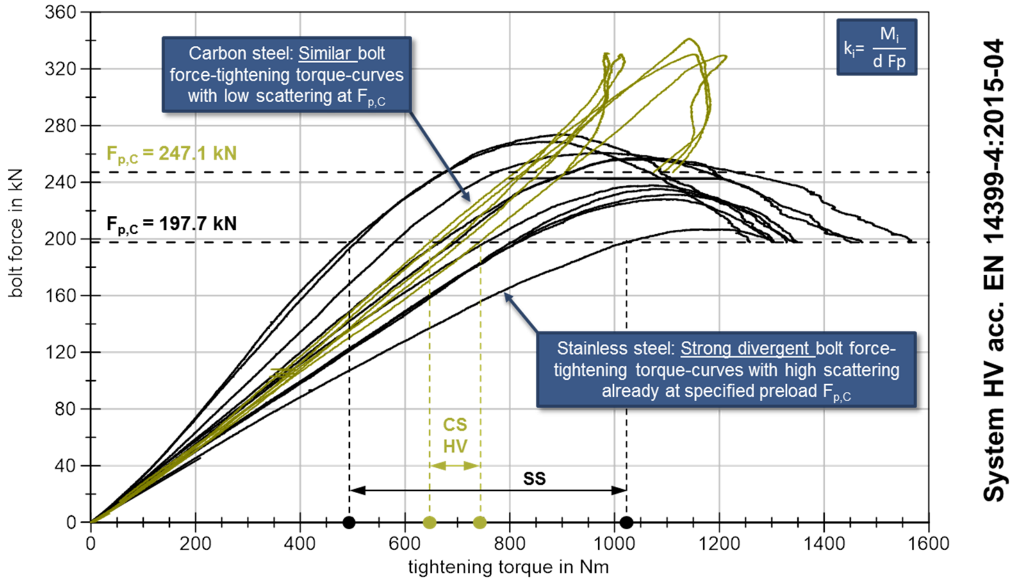


**Figure 108** Comparison of bolt force-tightening torque-curves between Bumax 88 – M24x100 - gleitmo 1952V (black) and M24x100 HV 10.9 (yellow)

Further tightening tests with alternative lubrications were performed in step 2 and step 3 to investigate their influence on the friction and to optimize the tightening procedure of stainless steel bolting assemblies with low deviations and constant, calculable friction coefficients.

### 3.6.2 Evaluation of tightening tests – Step 2: alternative lubricants

In the context of WP 5 – Preloading levels Task 5.4, tightening tests with various lubrications were performed to identify suitable, alternative lubrications for stainless steel bolting assemblies.

The summary of the evaluation of lubrication tests with various alternative lubricants is shown in Table 112. These lubrication tests identified Molykote® 1000 spray as an alternative lubrication for gleitmo® 1952V standard lubrication, and Molykote® D-321R spray as a promising alternative under difficult friction conditions. As a next step, additional tightening tests of austenitic, lean duplex, duplex and super duplex stainless steel bolting assemblies were performed at the Institute for Metal and Lightweight Structures, University of Duisburg-Essen (UDE-IML). Regarding the determination of the recommended preloading levels, the objective was again to investigate the basic preloading behaviour of stainless steel bolting assemblies and gather information regarding the complex interactions between the applied torque and the achieved preload. For this purpose, Bumax stainless steel bolts (acc. to EN ISO 4014 and EN ISO 4017), hexagon nuts (acc. to EN ISO 4032) and washers (acc. to EN ISO 7089) were used. The bolting assemblies were tightened according to EN 14399-2 (valid for carbon steel bolting assemblies). The evaluation of the tightening tests referred to EN 14399-3 and follows for reasons of comparability the requirements and criteria of the HR system.

Table 113 shows a summary of the additional tested series (using alternative lubrication Molykote® 1000 spray and D-321R spray) after finishing the tightening tests for Task 5.4. In conclusion, bolt fractures occurred in three tested series, but only at the end of the test procedure when turning off the nut: Bumax SDX – M12x80 series (lubrication: Molykote® 1000 spray), Bumax 88 – M16x100 series (lubrication: Molykote® 1000 spray) and Bumax 109 – M16x100 (lubrication: Molykote® D-321R spray). All tested stainless steel bolting assemblies achieved the preload level $F_{p,C}^* = 0.7 \cdot f_{yb} \cdot A_s$ and $F_{p,C} = 0.7 \cdot f_{ub} \cdot A_s$. Regarding the criteria of the individual maximum bolt force $F_{bi,max} \geq 0.9 \cdot f_{ub} \cdot A_s$ and sufficient ductility, in particular the required angles of nut rotation $\Delta\Theta_{1i,min}$ and $\Delta\Theta_{2i,min}$, the test results tend to generate two groups:

- For bolt dimension M16 – austenitic and austenitic-ferritic stainless steel bolting assemblies, the application of alternative lubrication significantly improves the preloading behaviour and expands the plastic plateau and angles of nut rotation $\Delta\Theta_{1i,min}$ and $\Delta\Theta_{2i,min}$. Furthermore, the tested series show a narrow range of k-values including coefficients of variation less than 8% (with the exception of Bumax 88 – M16x100 Molykote® 1000 series). Consequently, each series achieved criteria for k-class K1 (with exception of Bumax DX – M16x100 series, 8 of 10 bolts achieved k-class K1). Additionally, Bumax 109 – M16x100 (used lubrication: Dow Corning Molykote® D-321R spray) and Bumax DX – M16x100 (used lubrication: Dow Corning Molykote® 1000 spray) also accomplished k-class K2.
- For bolt dimension M20 – austenitic and austenitic-ferritic stainless steel bolting assemblies, the positive effects of alternative lubrication are relatively small compared to those of M16. The effects on ductility are only weakly defined, especially the criteria of the individual maximum bolt force $F_{bi,max} = 0.9 \cdot f_{ub} \cdot A_s$ is not achieved in Bumax 109 – M20x100 and Bumax LDX – M20x100 series, and only partially achieved (3 of 10 bolts) in Bumax DX – M20x100 series. The k-values show a range between 0.09 – 0.15, but the coefficient of variation is larger than 8%.

The damage analysis emphasizes that all tested bolting assemblies have similar damages at the first (and in some cases second) load-bearing thread turn of the bolt, roughening of the paired threads, and minimal necking of threaded shanks. All tested bolting assemblies showed damages caused by strong pronounced galling, especially in the faying surface between the washer and nut, see Figure 109. In addition, deformations of the washer occurred when turning off the nut in each tested series, as well as heat generation due to the cold-welded stainless steel nut and washer as well as the paired threads.

**Table 112** Task 5.4 – Summary of the evaluation of lubrication tests

| Tested series | n | $F_{p,C}^{*}$ | $F_{p,C}$ | $F_{bi,max}$ | $\Delta\Theta_{1i,min}$ | $\Delta\Theta_{2i,min}$ | k-values | k-class K1 | k-class K2 | | Fracture | Galling |
|---|---|---|---|---|---|---|---|---|---|---|---|---|
| | [-] | | | | ≥ 120° | ≥ 240° | [-] | $0.10 \leq k_i \leq 0.16$ | $0.10 \leq k_m \leq 0.23$ | $V_k \leq 0.06$ | | |
| **Bumax 88 - M20x80 EN ISO 4017 bolting assemblies** | | | | | | | | | | | | |
| Gleitmo 1952V | 5 | 100% | 100% | 100% | 20% | 100% | 0.12 – 0.13 | 100% | 0.124 | 0.043 | 0% | 60% |
| Molykote 1000 spray | 5 | 100% | 100% | 100% | 100% | 100% | 0.12 – 0.14 | 100% | 0.130 | 0.094 | 0% | 100% |
| Molykote 1000 paste | 5 | 100% | 100% | 100% | 80% | 100% | 0.13 – 0.15 | 100% | 0.136 | 0.050 | 0% | 100% |
| Molykote P-74 paste | 5 | 100% | 100% | 100% | 80% | 100% | 0.14 – 0.17 | 60% | 0.156 | 0.083 | 0% | 80% |
| Molykote D-321R spray | 5 | 100% | 100% | 100% | 100% | 100% | 0.10 – 0.11 | 100% | 0.105 | 0.047 | 0% | 80% |
| **Bumax 109 - M20x140 EN ISO 4014 bolting assemblies** | | | | | | | | | | | | |
| Gleitmo 1952V | 10 | 100% | 40% | 0% | 0% | 0% | 0.25 – 0.26 | 0% | 0.255 | 0.032 | 0% | 100% |
| Molykote 1000 paste | 5 | 100% | 100% | 0% | 0% | 80% | 0.16 – 0.20 | 40% | 0.178 | 0.105 | 0% | 100% |
| Molykote P-74 paste | 5 | 100% | 100% | 0% | 0% | 20% | 0.15 – 0.25 | 20% | 0.187 | 0.188 | 0% | 80% |
| Molykote D-321R spray | 5 | 100% | 100% | 20% | 60% | 60% | 0.11 – 0.13 | 100% | 0.115 | 0.071 | 0% | 100% |

**Table 113** Task 5.4 – Summary of the evaluation of additional stainless steel tightening tests according to EN 14399-3 (used lubrication: Molykote 1000 and Molykote D-321R spray)

| Tested series | n | $F_{p,C}^{*}$ | $F_{p,C}$ | $F_{bi,max}$ | $\Delta\Theta_{1i,min}$ | $\Delta\Theta_{2i,min}$ | k-values | k-class K1 | k-class K2 | | Fracture | Galling |
|---|---|---|---|---|---|---|---|---|---|---|---|---|
| | [-] | | | | ≥ 120° | ≥ 240° | [-] | $0.10 \leq k_i \leq 0.16$ | $0.10 \leq k_m \leq 0.23$ | $V_k \leq 0.06$ | | |
| **M12x80** | | | | | | | | | | | | |
| SDX - Molykote 1000 spray | 10 | 100% | 100% | 100% | 100% | 100% | 0.12 – 0.16 | 100% | 0.139 | 0.097 | 70% | 100% |
| **M16x100** | | | | | | | | | | | | |
| 88 - Molykote 1000 spray | 10 | 100% | 100% | 90% | 90% | 90% | 0.10 – 0.16 | 100% | 0.129 | 0.150 | 50% | 70% |
| 109 - Molykote 1000 spray | 10 | 100% | 100% | 100% | 100% | 100% | 0.11 – 0.14 | 100% | 0.130 | 0.080 | 0% | 100% |
| 109 - Molykote D-321R spray | 10 | 100% | 100% | 100% | 100% | 100% | 0.10 – 0.12 | 100% | 0.112 | 0.053 | 10% | 100% |
| LDX - Molykote 1000 spray | 10 | 100% | 100% | 90% | 100% | 100% | 0.12 – 0.15 | 100% | 0.133 | 0.075 | 0% | 100% |
| DX - Molykote 1000 spray | 10 | 100% | 100% | 100% | 100% | 100% | 0.14 – 0.17 | 80% | 0.152 | 0.057 | 0% | 100% |
| **M20x100** | | | | | | | | | | | | |
| 109 - Molykote 1000 spray | 10 | 100% | 100% | 0% | 60% | 70% | 0.10 – 0.15 | 100% | 0.132 | 0.128 | 0% | 100% |
| LDX - Molykote 1000 spray | 10 | 100% | 100% | 0% | 40% | 70% | 0.10 – 0.13 | 100% | 0.118 | 0.082 | 0% | 100% |
| DX - Molykote 1000 spray | 10 | 100% | 100% | 30% | 70% | 70% | 0.09 – 0.15 | 90% | 0.124 | 0.128 | 0% | 100% |


**Figure 109** Galling of the nut bearing surface when tightened into plastic range: nut (left), washer (middle) and detailed view of washer (right)

Although gleitmo® 1952V from Fuchs Lubritech GmbH is used as a special lubrication for stainless steel applications and has promising constant friction coefficients with low spreading, the test results of Task 5.3 delivered high ranges in $\mu_{tot}$, $\mu_{th}$, and $\mu_b$, significantly vary in all tested austenitic and austenitic-ferritic series. Hence, while using gleitmo® 1952V a constant level of friction was not achieved in tightening tests of stainless steel bolting assemblies. For Task 5.4, summaries of the friction coefficients of lubrication tests and additional tightening tests are presented in Table 114 and Table 115. Here, focus is given to additional tightening tests. The test results for bolt dimension M16 show reduced coefficients of variation $\mu_{th}$ and $\mu_b$ compared to gleitmo® 1952V series (with the exception of the thread friction of Bumax 88 – M16x100 Molykote® 1000 spray series), though for bolt dimension M20, a generalised statement is not possible due to inhomogeneous test results.

**Table 114** Task 5.4 – Summary of the friction coefficients of tested stainless steel series for lubrication tests

| Series | $\mu_{tot}$ ($F_{p,C}$) | | | $\mu_{th}$ ($F_{p,C}$) | | | $\mu_{b}$ ($F_{p,C}$) | | |
|---|---|---|---|---|---|---|---|---|---|
| | min | max | Vk | min | max | Vk | min | max | Vk |
| Lubrication tests: Bumax 88 - M20x80 ISO 4017 | | | | | | | | | |
| Gleitmo 1952V | 0.086 | 0.097 | **0.053** | 0.112 | 0.144 | **0.118** | 0.055 | 0.072 | **0.104** |
| Molykote 1000 spray | 0.086 | 0.109 | **0.114** | 0.084 | 0.112 | **0.117** | 0.079 | 0.105 | **0.114** |
| Molykote 1000 paste | 0.098 | 0.112 | **0.059** | 0.106 | 0.124 | **0.057** | 0.079 | 0.101 | **0.105** |
| Molykote P-74 paste | 0.101 | 0.131 | **0.097** | 0.101 | 0.141 | **0.126** | 0.084 | 0.158 | **0.238** |
| Molykote D-321R spray | 0.071 | 0.082 | **0.060** | 0.060 | 0.086 | **0.137** | 0.060 | 0.081 | **0.075** |
| Lubrication tests: Bumax 109 - M20x140 ISO 4014 | | | | | | | | | |
| Gleitmo 1952V | 0.199 | 0.214 | **0.034** | 0.176 | 0.203 | **0.069** | 0.218 | 0.225 | **0.015** |
| Molykote 1000 paste | 0.122 | 0.159 | **0.117** | 0.126 | 0.191 | **0.163** | 0.114 | 0.152 | **0.116** |
| Molykote P-74 paste | 0.117 | 0.198 | **0.208** | 0.129 | 0.212 | **0.184** | 0.106 | 0.187 | **0.251** |
| Molykote D-321R spray | 0.078 | 0.094 | **0.085** | 0.078 | 0.112 | **0.159** | 0.073 | 0.080 | **0.034** |

**Table 115** Task 5.4 – Summary of the friction coefficients of additional tested stainless steel series

| Series | $\mu_{tot}$ ($F_{p,C}$) | | | $\mu_{th}$ ($F_{p,C}$) | | | $\mu_{b}$ ($F_{p,C}$) | | |
|---|---|---|---|---|---|---|---|---|---|
| | min | max | Vk | min | max | Vk | min | max | Vk |
| Additional tightening tests: M12x80 | | | | | | | | | |
| SDX - Molykote 1000 spray | 0.085 | 0.120 | **0.116** | 0.080 | 0.138 | **0.176** | 0.084 | 0.118 | **0.113** |
| Additional tightening tests: M16x100 | | | | | | | | | |
| 88 - Molykote 1000 spray | 0.072 | 0.119 | **0.177** | 0.068 | 0.179 | **0.297** | 0.064 | 0.098 | **0.131** |
| 109 - Molykote 1000 spray | 0.076 | 0.105 | **0.096** | 0.089 | 0.123 | **0.092** | 0.066 | 0.103 | **0.150** |
| 109 - Molykote D-321R spray | 0.070 | 0.087 | **0.065** | 0.080 | 0.113 | **0.118** | 0.062 | 0.071 | **0.039** |
| LDX - Molykote 1000 spray | 0.088 | 0.110 | **0.089** | 0.085 | 0.111 | **0.103** | 0.076 | 0.130 | **0.177** |
| DX - Molykote 1000 spray | 0.104 | 0.126 | **0.065** | 0.094 | 0.147 | **0.142** | 0.101 | 0.147 | **0.113** |
| Additional tightening tests: M20x100 | | | | | | | | | |
| 109 - Molykote 1000 spray | 0.090 | 0.141 | **0.151** | 0.086 | 0.126 | **0.115** | 0.081 | 0.165 | **0.243** |
| LDX - Molykote 1000 spray | 0.086 | 0.120 | **0.098** | 0.085 | 0.129 | **0.145** | 0.088 | 0.125 | **0.130** |
| DX - Molykote 1000 spray | 0.079 | 0.135 | **0.152** | 0.070 | 0.139 | **0.216** | 0.075 | 0.165 | **0.235** |

When tightened into the plastic range, galling in form of "spikes" is also visible in tightening curves and helps in identifying the starting-point of galling, especially in the bolt force-tightening torque curves. Figure 110 shows an example: galling begins after the maximum individual bolt force $F_{bi,max}$ is reached. Moreover, Figure 111 demonstrates strong pronounced galling starting at $F_{bi,max}$. Future investigations will attempt to determine in detail when galling starts and aspects that influence the galling behaviour of stainless steel bolting assemblies. So far, it can be noted that galling always starts after the specified preload level $F_{p,C} = 0.7 \cdot f_{ub} \cdot A_s$ when tightened into the plastic range.

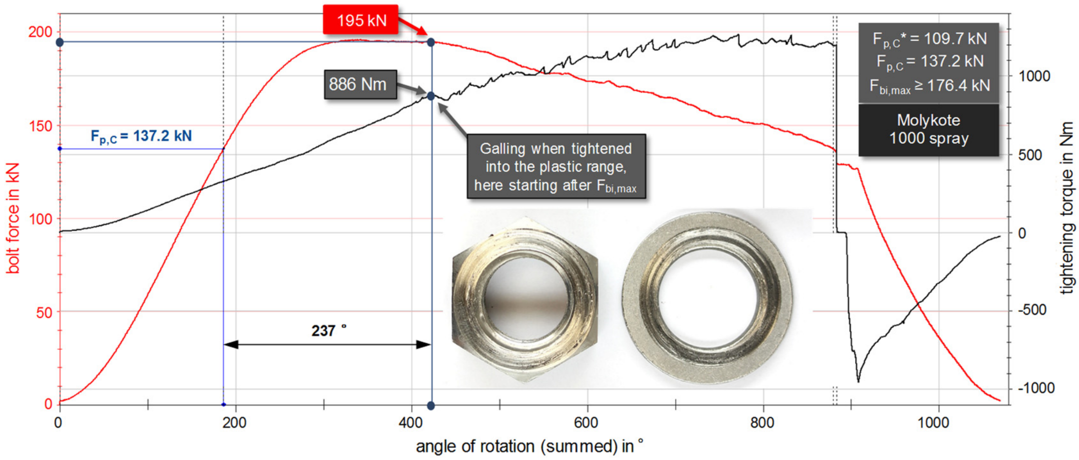


**Figure 110** BU_M20_88-07 – Example of minor galling in the tightening curves starting at maximum load

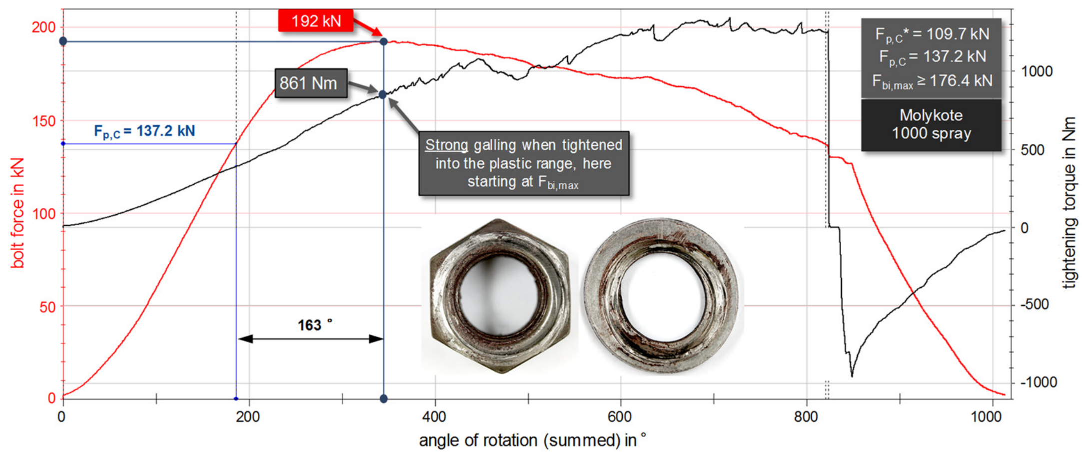


**Figure 111** BU_M20_88-09 – Example of major galling in the tightening curves starting at maximum load

In addition, a comparison between gleitmo® 1952V standard lubrication and Molykote® 1000 spray for Bumax LDX – M16x100 ISO 4017 lean duplex stainless steel bolting assemblies is presented in Figure 112. When using gleitmo® 1952V, the tightening curves show a typically less pronounced plastic plateau and low angles of rotation $\Delta\Theta_{1i,min}$ and $\Delta\Theta_{2i,min}$. $F_{p,C}$* and $F_{p,C}$ are achieved, but the criteria of individual maximum bolt force $F_{bi,max} \geq 0.9 \cdot f_{ub} \cdot A_s$ failed for the most part. However, the application of Molykote 1000 spray extends significantly the plastic range as well as the maximum bolt force. “Spikes” in the bolt force-tightening torque curves indicate strong galling after $F_{bi,max}$, especially when using Molykote 1000 spray.

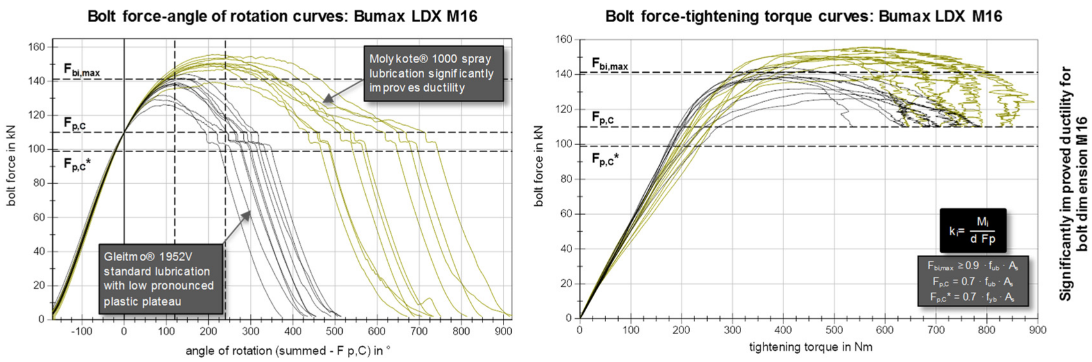


**Figure 112** Comparison of BU_M16_LDX tightening curves between gleitmo 1952V standard lubrication (black curves) and Molykote 1000 spray (yellow curves)

A comparison between gleitmo® 1952V standard lubrication and Molykote® 1000 spray for Bumax DX – M20x100 ISO 4017 duplex stainless steel bolting assemblies is presented in Figure 113. Compared to bolt dimension M16, the positive effects of alternative lubrication on the ductility and the plastic plateau, more specifically the maximum individual bolt force and angles of rotation $\Delta\Theta_{1i,min}$ and $\Delta\Theta_{2i,min}$, are significantly lower. Again, the tightening curves of tested bolts using gleitmo® 1952V show less pronounced plastic plateaus and low angles of rotation $\Delta\Theta_{1i,min}$ and $\Delta\Theta_{2i,min}$. Compared to Bumax LDX – M16x100 gleitmo® 1952V series, the bolt force-angle of rotation curves spread more. $F_{p,C}$* and $F_{p,C}$ are achieved, but the criteria of the individual maximum bolt force $F_{bi,max} \geq 0.9 \cdot f_{ub} \cdot A_s$ failed. The application of Molykote® 1000 spray slightly improved the plastic range as well as the maximum bolt force. The bolt force-tightening torque curves show strong pronounced galling with the use of Molykote® 1000 spray, starting at $F_{bi,max}$ when tightened into the plastic range.

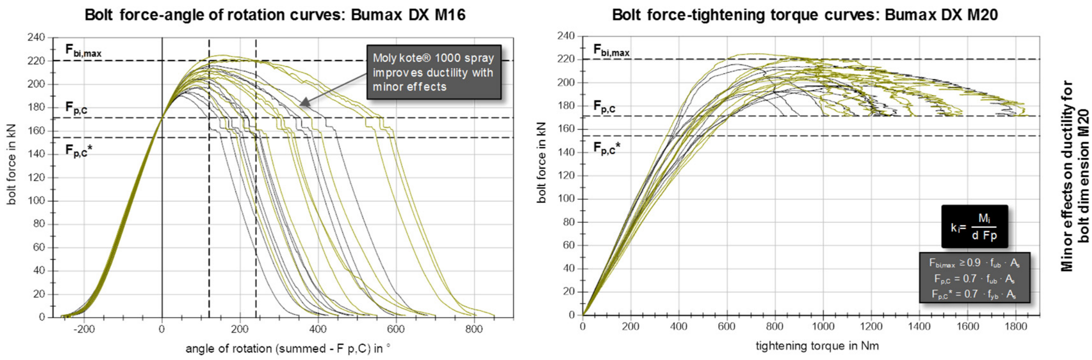


**Figure 113** Comparison of BU_M20_DX tightening curves between gleitmo® 1952V standard lubrication (black curves) and Molykote® 1000 spray (yellow curves)

### 3.6.3 Evaluation of tightening tests – Step 3: ceramic-based lubricants

The summary of the evaluation of tightening tests with ceramic-based lubricants Interflon® HT1200 spray and paste are shown in Table 116. Again, all tested bolting assemblies made of stainless steel achieved specified preload levels $F_{p,C}$* and $F_{p,C}$ without galling, comparable to DOW Corning Molykote® 1000 spray and Molykote® D-321R spray. In general, the tightening test results are comparable to the tested series with DOW Corning Molykote® 1000 spray. The criteria of $\Delta\Theta_{1i,min}$ and $\Delta\Theta_{2i,min}$ are again unequally distributed, k-class K1 was achieved in all tested series with the exception of Bumax LDX – M20x100 HT1200 spray (8 of 10 bolting assemblies achieved k-class K1).

Overall, the use of the ceramic based lubrication Interflon® HT1200 spray and paste has nearly similar results to DOW Corning Molykote 1000 spray regarding tightening behaviour and ductility. Further investigations were not performed due to the fact that the tested ceramic-based lubricants react with differing sensitivity to drying times and do not create a homogeneous abrasion-resistant layer in all cases which leads to scattering of friction coefficients $\mu_{tot}$, $\mu_{th}$ and $\mu_b$ and all related tightening parameters. Figure 114 shows exemplary Bumax – M20x100 bolting assemblies after tightening with Interflon® HT1200 spray and Interflon® HT1200 paste.

**Table 116** Task 5.4 – Summary of the evaluation of tightening tests with Interflon® HT1200 spray and paste

| Tested series | n | $F_{p,C}$* | $F_{p,C}$ | $F_{bi,max}$ | $\Delta\Theta_{1i,min}$ | $\Delta\Theta_{2i,min}$ | k-values | k-class K1 | k-class K2 | | Fracture | Galling |
|---|---|---|---|---|---|---|---|---|---|---|---|---|
| | [-] | | | | ≥ 120° | ≥ 240° | [-] | 0.10 ≤ $k_i$ ≤ 0.16 | 0.10 ≤ $k_m$ ≤ 0.23 | $V_k$ ≤ 0.06 | | |
| Bumax 88 - M20x100 EN ISO 4017 bolting assemblies | | | | | | | | | | | | |
| 88 - HT1200 spray | 5 | 100% | 100% | 100% | 60% | 100% | 0.12 – 0.14 | 100% | 0.127 | 0.065 | 0% | 40% |
| 88 - HT1200 paste | 5 | 100% | 100% | 100% | 60% | 100% | 0.13 – 0.16 | 100% | 0.139 | 0.084 | 0% | 40% |
| Bumax 109 - M20x100 EN ISO 4017 bolting assemblies | | | | | | | | | | | | |
| 109 - HT1200 spray | 5 | 100% | 100% | 0% | 20% | 100% | 0.12 – 0.16 | 100% | 0.133 | 0.148 | 0% | 40% |
| 109 - HT1200 paste | 5 | 100% | 100% | 0% | 40% | 100% | 0.14 – 0.16 | 100% | 0.147 | 0.070 | 0% | 60% |
| Bumax LDX - M20x100 EN ISO 4017 bolting assemblies | | | | | | | | | | | | |
| LDX - HT1200 spray | 5 | 100% | 100% | 0% | 20% | 20% | 0.14 – 0.19 | 80% | 0.162 | 0.126 | 0% | 60% |
| LDX - HT1200 paste | 5 | 100% | 100% | 20% | 40% | 40% | 0.14 – 0.16 | 100% | 0.149 | 0.047 | 0% | 40% |


**Figure 114** Bumax – M20x100 bolting assemblies after tightening with Interflon HT1200 spray (above) and Interflon HT1200 paste (below)

Again, galling as a form of cold-welding only occurred when tightened into the plastic range, but starting after the maximum individual bolt force $F_{bi,max}$ is reached. It must be emphasized that no galling occurs when the paired threads are suitably lubricated (e.g. DOW Corning Molykote 1000, DOW Corning Molykote D-321R or Interflon HT1200 spray and paste) and tightened only into the elastic range. This is an important finding. Figure 115, Figure 116 and Figure 117 show a comparison between Fuchs Lubritech gleitmo® 1952V standard lubrication, Molykote® 1000 spray and Interflon® HT1200 paste at preloading levels $F_{p,C}$*, $F_{p,C}$ and $F_{bi,max}$ focussing on galling of the washer and nut.

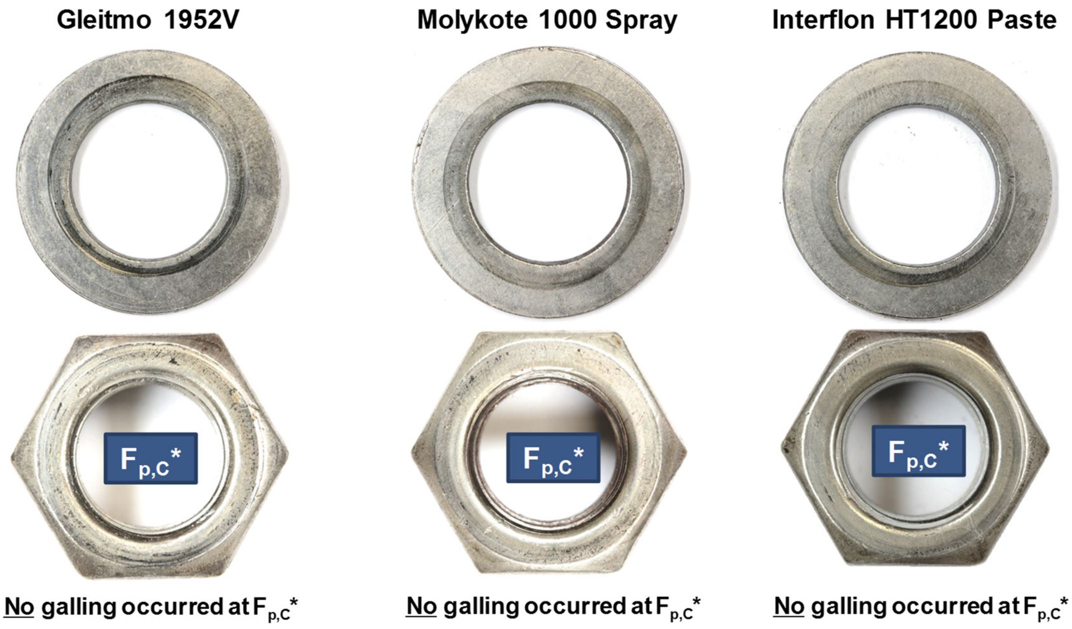


**Figure 115** Inspection of galling of austenitic M20 HV200 washers and M20 Bumax 88 austenitic nuts in property class 8.8 after tightening at specified preload level $F_{p,C}^* = 0.7\ f_{yb}\ A_s$

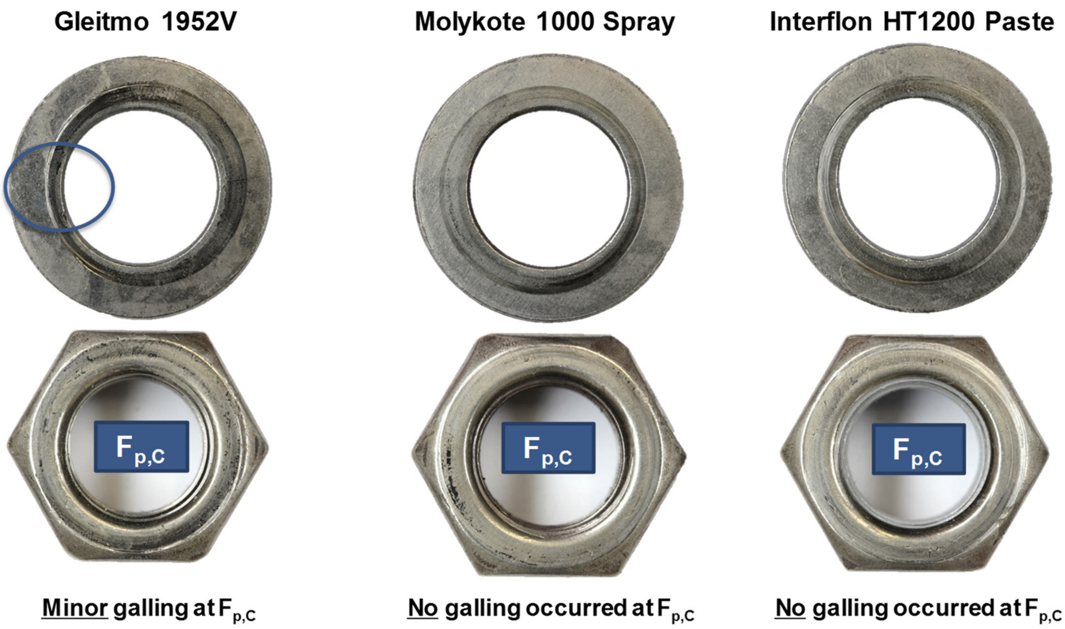


**Figure 116** Inspection of galling of austenitic M20 HV200 washers and M20 Bumax 88 austenitic nuts in property class 8.8 after tightening at specified preload level $F_{p,C} = 0.7\ f_{ub}\ A_s$

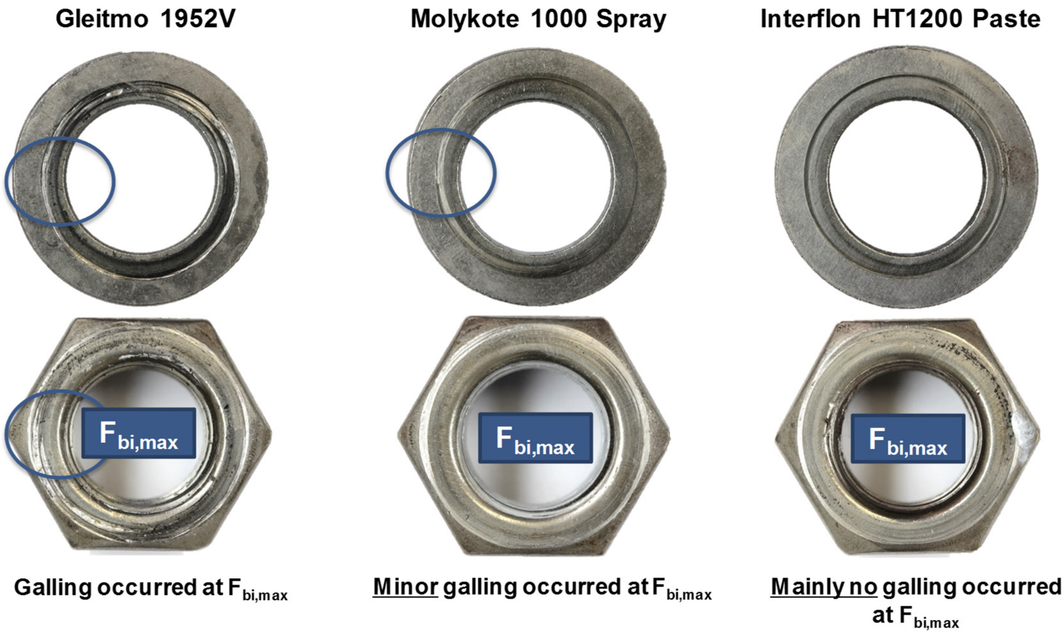


**Figure 117** Inspection of galling of austenitic M20 HV200 washers and M20 Bumax 88 austenitic nuts in property class 8.8 after tightening at specified preload level $F_{bi,max} \geq 0.9\ f_{ub}\ A_s$

## 3.7 Preloading levels and design specifications

In principle, the preloading of austenitic and lean duplex, duplex and super duplex stainless steel bolting assemblies, property classes 8.8 and 10.9 is possible by choosing a suitable material pairing and lubrication. The higher surface pressures of the EN ISO 4014/4017 systems, resulting from smaller geometrical dimensions than the HR/HV systems, are uncritically up to the preload level $F_{p,C}$ when structural steel is used with yield strength larger than or equal to 355 N/mm$^2$ [2].

The presented investigations and findings can only provide an initial insight into the tightening behaviour of stainless steel bolting assemblies. Further investigations are necessary in order to finally determine the tightening procedure including all requirements. It seems, as if a preload level of $F_{p,C}$* and also $F_{p,C}$ can be reliably achieved with a suitable lubricant using the torque method. Based on the presented investigations, the most promising lubricants for stainless steel bolting assemblies are DOW Corning Molykote® 1000 spray and Molykote® D-321R spray. Also, long term relaxation effects must be investigated and systematically considered.

Regarding the preloading levels and design specifications, it is important to note that the tightening procedure and the required preload level are well-matched. For this reason, the suitability test for preloading according to EN 14399-2 must be carried out to check if the bolting assemblies made of stainless steel are in principle suitable for preloading. Subsequently, the boundary conditions regarding the required preload level and tightening procedure as well as the tightening parameters have to be defined in each specific case, so that the test of suitability for preloading for the determination of all functional characteristics and parameters of stainless steel bolting assemblies can be successfully carried out. In addition, the inspection requirements have to be defined depending on the required target level of preloading and the individual and specific boundary conditions.

The process to verify the suitability of the stainless bolting assemblies for preloading and the determination of tightening method and tightening parameters to achieve the required target preload is illustrated in the flow chart shown in Figure 118.

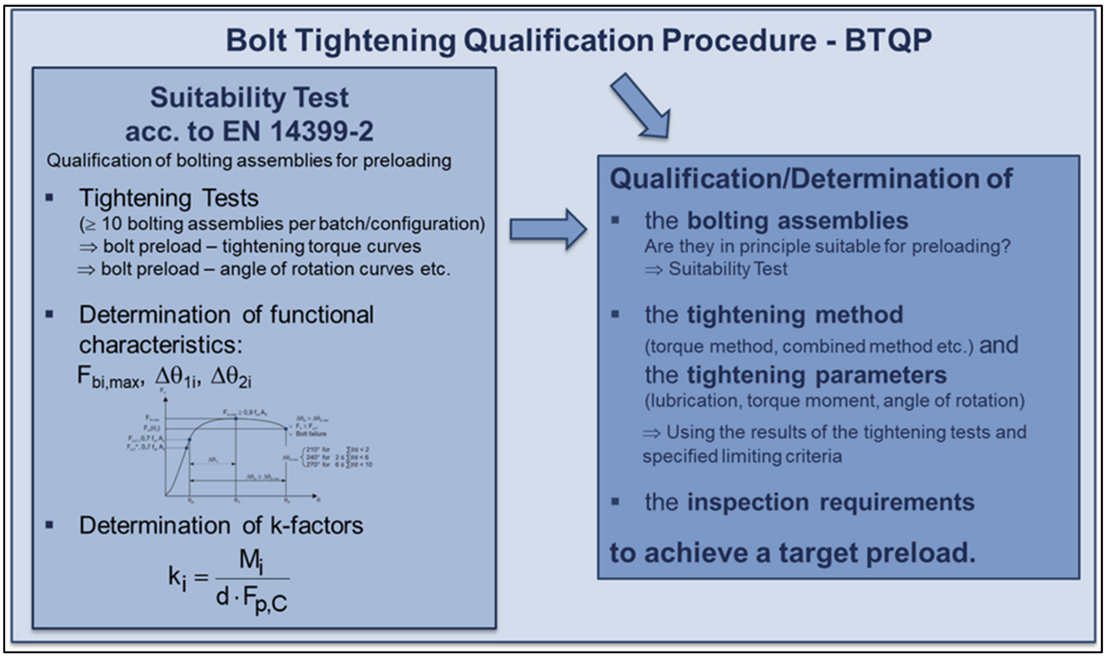


**Figure 118** Flowchart for suitability test and tightening method qualification of stainless steel bolts for preloading

Nonetheless, the complete load-bearing behaviour of a bolted connection should be considered, and for property class 10.9, the unique qualities and benefits of HR and HV bolting assemblies still destine them for use in preloaded applications, which lead to the idea to create a new type of stainless steel bolting assemblies approaching the geometrical dimensions of carbon steel HV/HR bolting assemblies taking into account the specifics of stainless steel bolting assemblies.

One important finding is that the problem of galling on the bolt head and nut bearing surfaces as well as on the paired threads can be for sure avoided by secure tightening with limitations in the elastic range using a suitable lubricant. With proper lubrication, galling only occurs when the stainless steel bolting assemblies are tightened into the plastic range close to the maximum bolt force $F_{bi,max}$, which must be avoided in all cases.

# 4 Experimental investigations – Relaxation tests

## 4.1 General

Preloading of bolted connections is necessary either for ultimate limit reasons when the preload is used in the design process to achieve a specific design resistance (category B, C and E connections according to EN 1993-1-8) or for serviceability reasons "only" to limit slip and deformation in the connections themselves (category A and D connections according to EN 1993-1-8). Whereas in the latter case, the specific amount of preloading does not have to be met absolutely, in the first case it has to be proven that the preload level is at least met and will remain over the whole service life of the structural detail with the value applied in the design process.

Whereas preloading of bolted connections is commonly used for carbon steel connections, it is seldom applied for stainless steel connections. The execution standard for steel structures EN 1090-2 does not allow preloaded stainless steel bolting assemblies, unless otherwise specified. Furthermore, the design standard for stainless structures in the frame to the Eurocode 3-family, EN 1993-1-4, requires that the acceptability in a particular application has to be demonstrated from test results. This restriction is mainly caused by three facts: firstly, it is feared that due to the viscoplastic deformation behaviour of stainless steel, severe preload losses might be expected, secondly, neither stainless steel bolting assemblies for preloading nor tightening procedures exist on which could have been relied and thirdly, galling and seizure of stainless steel bolting assemblies lead to problems on site. The results regarding the preloading procedure of stainless steel bolting assemblies and galling have already been presented in this deliverable, see also [31], [32] and [2]. The present chapter gives an initial insight into the viscoplastic deformation behaviour of stainless steel bolting assemblies which were achieved in SIROCO which shows that preloaded bolted stainless steel connections can be treated similar to those made of carbon steel.

## 4.2 Relaxation behaviour of bolted connections

The preload level in a bolted connection is not a constant level and it can be defined as a function of time. In general, a reduction in the preload level is referred as bolt relaxation. Many researches have been carried out in order to investigate the relaxation behaviour of bolted connections theoretically and experimentally, see also [33], [34], [35], [36] and [37].

Preloaded stainless steel bolting assemblies mainly relax due to different parameters, like embedment/plastic deformation of the clamped component surfaces, so called setting effect and the viscoplastic deformation behaviour of the stainless steels. The viscoplastic deformation behaviour in preloaded bolting assemblies are assumed to be divided into viscoplastic deformation under constant load condition for the plates (i.e. creep deformation) and viscoplastic deformation under constant strain condition for the bolts (i.e. stress relaxation). These two-related phenomena have to be considered not only in the preloading procedure to achieve a precise preload level for the bolting assemblies but also for the already mentioned serviceability and ultimate limit reasons. Therefore, it is important to estimate the amount of the preload losses from the combined creep and stress relaxation in the bolted assembly. Herewith, the clarification of the influence of the mentioned parameters on the relaxation behaviour of stainless steel bolted connections is an important issue.

## 4.3 Experimental investigations

### 4.3.1 General

Preloaded stainless steel (SS) bolting assemblies relax due to the setting effect of the clamped components surfaces and creep and relaxation of stainless steel material as a result of the applied pretension. As a result of additional relaxing and creeping of the stainless steel bolts and the clamped parts compared to carbon steel, there might be preload losses in the bolts which must be taken into account when defining suitable tightening parameters. Otherwise, it would not be possible to achieve a precise preloading level of bolting assemblies made of stainless steel for connections which are preloaded for load-bearing safety reasons.

### 4.3.2 Different methods for measuring the preload in stainless steel bolts

An important question to be answered is the amount of preload losses to be expected from relaxation and creep of the preloaded bolt and creep of the associated clamped parts.

The first step to investigate the relaxation behaviour of the SS bolting assemblies is to find the most reliable method to measure the preload inside the bolt. For this reason, additional creep tests on stainless steel bolts were carried out to investigate the influence of the creeping of the bolt material on the measured preload level. For this purpose, three different types of strain gauge were selected (BTM-6C, BTM-1C and BTMC-3). For each test specimen the bolts were instrumented with a strain gauge embedded in a 2 mm hole along the bolt shank, see Figure 119.

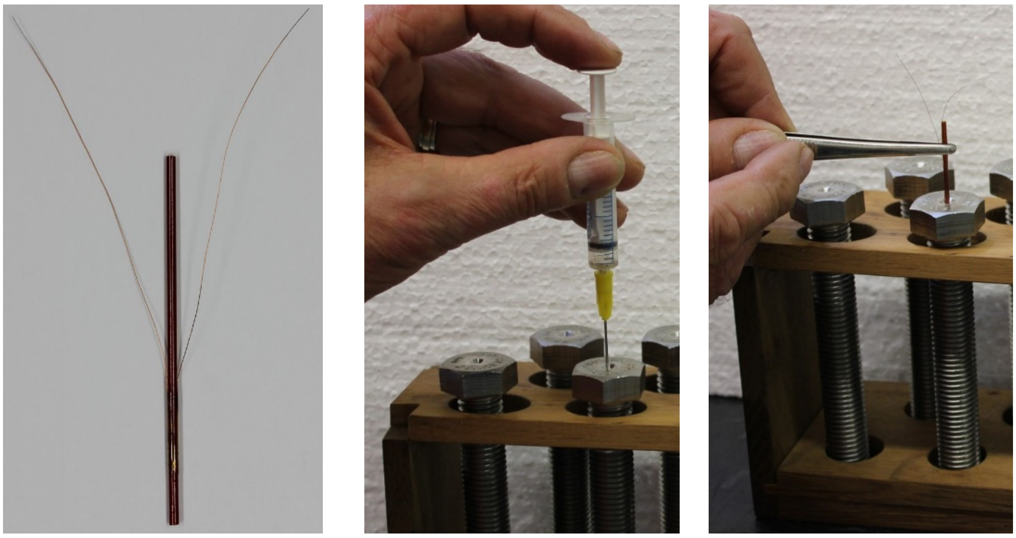

**Figure 119** Exemplary production phases of instrumented stainless steel bolts

Each instrumented bolt was calibrated under stepwise tensile loading and the calibration factors were evaluated. Those bolts, which showed a linear load-strain-behaviour, were selected for application within the creep tests, see Figure 120.

The creep tests were performed in a universal testing machine (with a maximum load capacity of ±200 kN), applying a constant tensile load to the bolts. The preload in the bolts was measured constantly and compared to the constant tensile load (the load level that actually existed in the bolts). All bolts were loaded to the $F_{p,C}$ level in the universal testing machine.

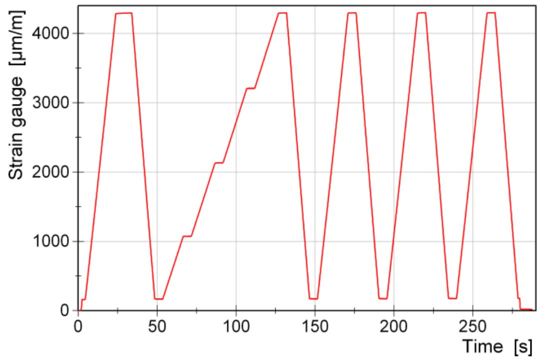


a) measured strain

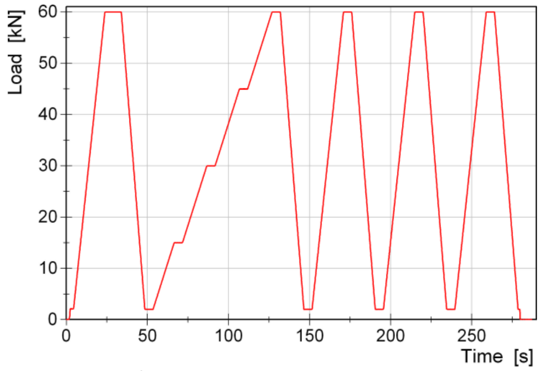


b) stepwise tensile loading

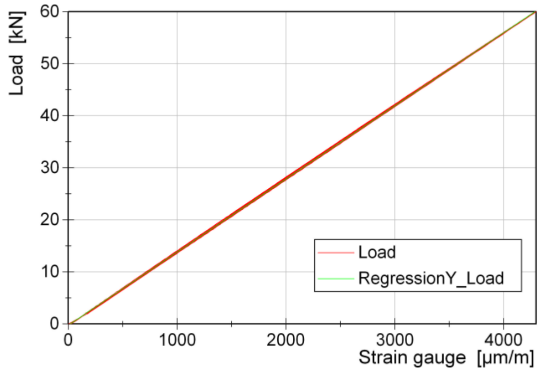


c) load-strain-behaviour

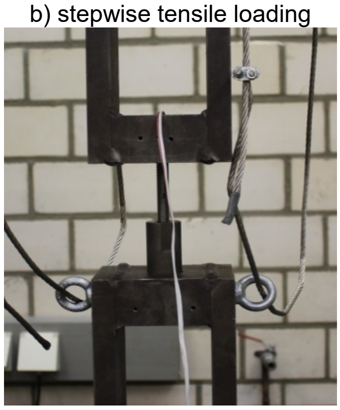

d) calibration test setup

**Figure 120** Calibration of instrumented M12 super duplex bolt

In total ten tests were performed: one test on a carbon steel bolt and nine tests on stainless steel bolts, see Table 117. For each type of stainless steel bolts, one creep test was repeated to proof the reusability of the stainless steel bolts.

**Table 117** Creep test program

| Series ID | Material | Grade | Dimension | Standard | Level of load | Duration [days] | $\Delta_{max}$ 1) [%] | ER 2) [%] |
|---|---|---|---|---|---|---|---|---|
| | | | | Strain gauge type: BTM-6C | | | | |
| CS | Carbon | HV 10.9 | M20 x 110 | EN 14399-4 | $F_{p,C}$=172 kN | 14 | ≈ 0 | ≈ 0 |
| A-1 | Austenitic (1.4436) | Bumax 109 | M20 x 100 | ISO 4017 | $F_{p,C}$=172 kN | 5 | ≈ 1.4 | ≈ 50 |
| A-1R | Austenitic (1.4436) | Bumax 109 | M20 x 100 | ISO 4017 | $F_{p,C}$=172 kN | 14 | ≈ 0.6 | ≈ 60 |
| A-2 | Austenitic (1.4436) | Bumax 109 | M20 x 100 | ISO 4017 | $F_{p,C}$=172 kN | 8 | ≈ 4 | - |
| SDX-1 | Super duplex (1.441) | Bumax 109 | M12 x 80 | ISO 4017 | $F_{p,C}$=59 kN | 14 | ≈ 4 | ≈ 20 |
| | | | | Strain gauge type: BTM-1C | | | | |
| SDX-2 | Super duplex (1.441) | Bumax 109 | M12 x 80 | ISO 4017 | $F_{p,C}$=59 kN | 14 | ≈ 6 | ≈ 5 |
| SDX-2R | Super duplex (1.441) | Bumax 109 | M12 x 80 | ISO 4017 | $F_{p,C}$=59 kN | 29 | ≈ 1 | ≈ 15 |
| | | | | Strain gauge type: BTMC-3 | | | | |
| A-3 | Austenitic (1.4436) | Bumax 88 | M20 x 80 | ISO 4017 | $F_{p,C}$=140 kN | 4 | ≈ 1.6 | ≈ 50 |
| A-4 | Austenitic (1.4436) | Bumax 109 | M16 x 100 | ISO 4017 | $F_{p,C}$=110 kN | 8 | ≈ 4 | - |
| A-5 | Austenitic (1.4436) | Bumax 88 | M16 x 80 | ISO 4017 | $F_{p,C}$=88 kN | 11 | ≈ 6.5 | ≈ 7 |

1) maximum difference between measured preload and constant tensile load
2) elastic recovery of the bolt when the specimen is unloaded

Table 117 shows that both repeated tests (A-1R and SDX-2R) show more accurate results in comparison to the first creep test. This phenomenon can be explained by the plastic creep in the stainless bolts during the first creep test. For this reason, a very small amount of creep was occurred in the second creep test, see an example in Figure 121.

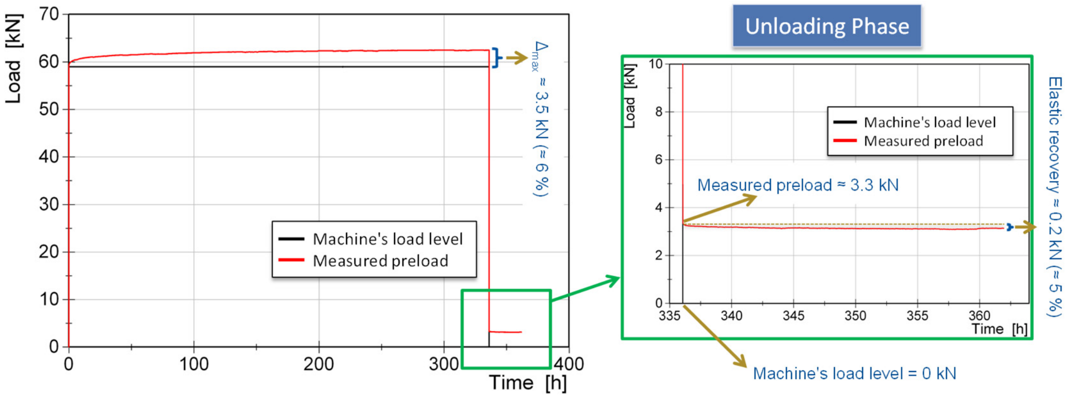


(a) creep test for first time (SDX-2)

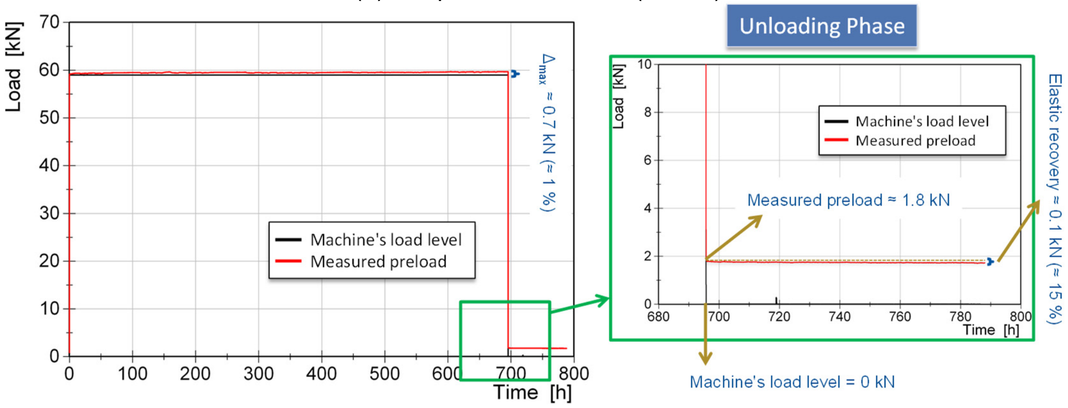


(b) repeated creep test (SDX-2R)

**Figure 121** Creep test M12 super duplex bolt

Table 117 shows that the accuracy of the instrumented bolts with implanted strain gauges for measuring the preload inside the bolts is acceptable but it has also to be pointed out that already during the preloading process of the stainless steel, creep occurs. These changes in the strain were measured by strain gauges and caused different values in comparison to the real preload level, see Figure 121. This phenomenon cannot be observed in carbon steel bolts since they do not creep. For this reason, it was decided to prepare some small load cells to measure the preload level. The advantage of using load cells is that creep has no influence on the measured preload level. For this purpose, different load cells were prepared by UDE, see Figure 122. All load cells were calibrated under stepwise tensile loading in a similar way as carried out for instrumented bolts with strain gauges. The combination of the instrumented bolt and load cell was also tested in the tightening testing machine in order to confirm the accuracy of both methods, see Figure 123.

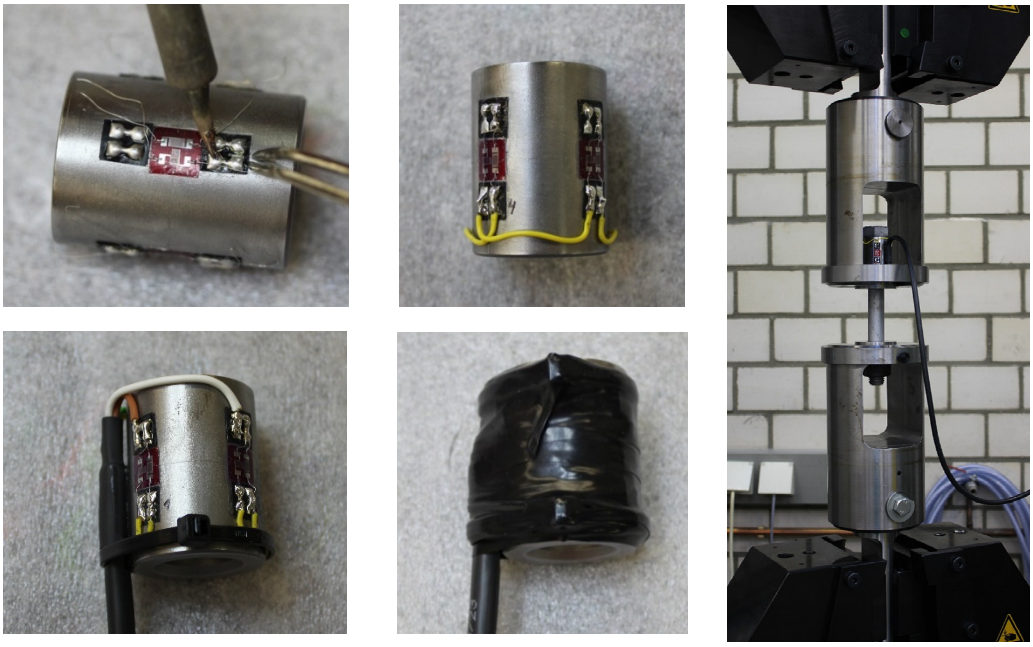

(a) some production phases of load cells (LC) at the University of Duisburg-Essen

(b) calibration phases

**Figure 122** Production calibration phases of load cells and test setup of relaxation test

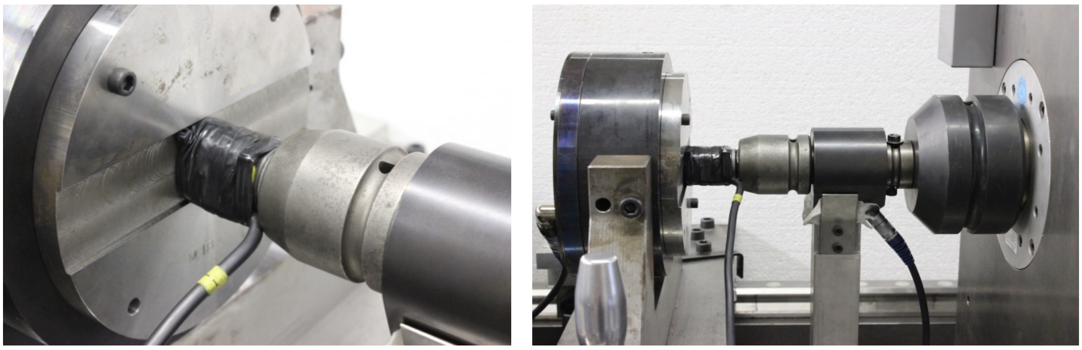

**Figure 123** Testing of the bolts with SG and LC in the tightening testing machine of the Institute for Metal and Lightweight Structures of University of Duisburg-Essen

#### *4.3.2.1 Preliminary relaxation tests*

The additional relaxation tests were carried out in two different groups. In the first group, the preload was measured by instrumented bolts with a clamping length range of $\sum t / d = 2$ in order to take account of the fact that shorter clamping lengths lead to greater preload losses, see Table 118. In the second group, the preload measured with two different methods (instrumented bolts (SG) + load cell (LC)). Using LCs leads to a relatively larger clamping length in comparison to the first group.

In the first phase all tests were carried out using 75 mm × 75 mm plates with thicknesses of 8 mm (ferritic ss), 16 mm (ferritic ss) and 20 mm (carbon steel), see Figure 124.

**Table 118** Relaxation test program – First group (Instrumented bolts)

| Specimen ID | Σt[1)]/d [-] | Preload level | Bolt material | Material and geometry of the clamped plates | Surface roughness (Rz) [µm] | Loss of preload determined with strain gages: measured after 68 d [%] | Loss of preload determined with strain gages: after 50 years (extrapolated) [%] |
|---|---|---|---|---|---|---|---|
| M20 – HV-bolts | | | | | | | |
| CS_M20_06 | 2.4 | $F_{p,C}$ [2)] | HV-bolt Class[4)] 10.9 | Carbon steel, 2 × 75 mm × 75 mm × 20 mm | 57.2[5)] | 5.4 | 8.1 |
| CS_M20_14 | | | | | | 8.9 | 11.0 |
| CS_M20_15 | | 0.9 $F_{p,C}$*[3)] | | | | 5.6 | 7.4 |
| CS_M20_25 | | | | | | 3.7 | 5.0 |
| CS_M20_30 | | | | | | 5.9 | 7.4 |
| M20 – ISO 4017-Bolts made of Austenitic stainless steel | | | | | | | |
| SS-A_M20_2 | 1.9 | $F_{p,C}$ | Austenitic 1.4436 Class[4)] 10.9 | Ferritic 1.4003, 2 × 75 mm × 75 mm × 16 mm | 57.4[5)] | 3.4 | 5.0 (7.0)[7)] |
| SS-A_M20_3 | | | | | | 3,3 | 4.7 (7.7)[7)] |
| SS-A_M20_4 | | | | | | 2,0 | 3.0 (5.0)[7)] |
| M12 – ISO 4017- Bolts made of Super Duplex stainless steel | | | | | | | |
| SS-SD_M12_2 | 1.75 | 0.9 $F_{p,C}$* | Super Duplex 1.4410 Class[4)] 10.9 | Ferritic 1.4003, 2 × 75 mm × 75 mm × 8 mm | 24.4[6)] | 2.9 | 4.4 (6.4)[7)] |
| SS-SD_M12_3 | | | | | | 3.7 | 5.5 (7.5)[7)] |
| SS-SD_M12_4 | | $F_{p,C}$ | | | | 4.3 | 5.6 (7.6)[7)] |
| SS-SD_M12_6 | | | | | | 6.9 | 9.4 (11.4)[7)] |

[1)] Clamping length | [2)] $F_{p,C} = 0.7\ f_{ub} \times A_s$ | [3)] $F_{p,C}* = 0.7 \times f_{yb} \times A_s$ | [4)] Property class | [5)] Blasted (glass particle – 300 µm) | [6)] 1D surface | [7)] Increase of loss of preload by 2% after 50 years for the eliminating the preload increase measured by strain gauge due to creep

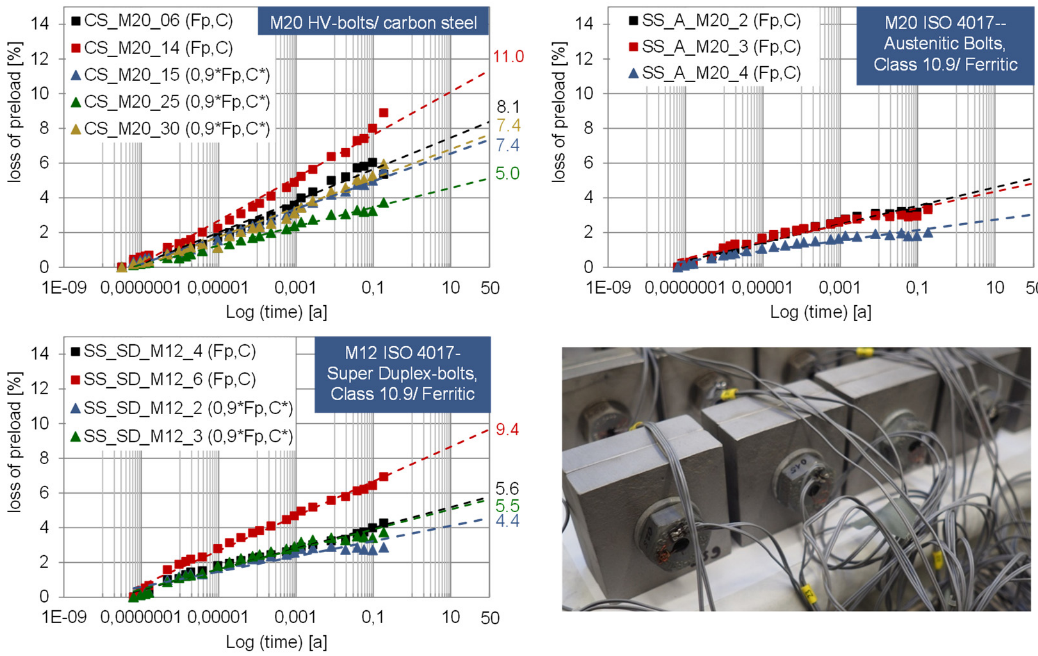


**Figure 124** Preload losses after 50 years in preload losses-log (time) diagrams exemplary for M20 HV-bolts in a clamping package made of carbon steel as well as austenitic M20-ISO 4017 bolts and super duplex M20 ISO 4017 bolts, each in clamping packages made of ferritic stainless steel; presentation of the test samples

Two different preload levels $F_{p,C}$ and 0.9 $F_{p,C}$* were selected. For each test specimen the bolts M20 were instrumented with a strain gauge to measure the preload continuously by measuring the strain at a specific point in the shank. Herewith, it was possible to achieve the exact level of preload while the fastener is tightened.

Figure 124 shows the test specimens as well as the preload losses after 50 years in preload loss-log (time) diagrams exemplary for M20 HV-bolts in a clamping package made of carbon steel as well as austenitic M20-ISO 4017 bolts and super duplex M20 ISO 4017 bolts, each in clamping packages made of ferritic stainless steel.

In the second phase all tests were performed using 75 mm × 75 mm plates with thicknesses of 8 mm and 16 mm (ferritic ss), see Figure 125. Two different bolt property classes 8.8 and 10.9 were selected. All bolts were preloaded to $F_{p,C}$ preload level, see Table 119. For each test specimen, the preload level was measured with two different methods to investigate the difference between these two measurements (strain gauge and load cell).

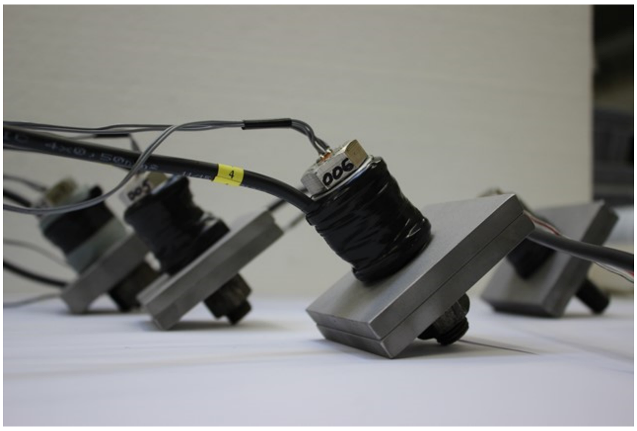

**Figure 125** Relaxation test samples (combination of strain gauge and load cell)

**Table 119** Relaxation test program – Second group (Instrumented bolts + Load cells)

| Specimen ID | Σt[1]/d [-] | L [2] | Bolt class[3] | Number of plates | Geometry of the clamped plates [4] [mm] | Surface roughness (Rz) [µm] | Loss of preload: measured after 15 d (SG[5]/LC[6]) [%] | Loss of preload: after 50 years (extrapolated) (SG[5]/LC[6]) [%] |
|---|---|---|---|---|---|---|---|---|
| ISO 4017-Bolts made of Austenitic stainless steel | | | | | | | | |
| SS-A_M20-S+L | 3.0 | 40 | 8.8 | 1 | 75 × 75 × 16 | 57.4[7] | 4.5 / 3.5 | 5.4 / 4.8 |
| SS-A_M16-S+L_1 | 4.6 | 55 | 10.9 | 2 | 75 × 75 × 8 | 44.2[7] | 4.5 / 3.3 | 4.8 / 5.2 |
| SS-A_M16-S+L_2 | 3.7 | 40 | 10.9 | | | | 5.6 / 3.9 | 6.2 / 5.8 |
| SS-A_M16-S+L_3 | | | 8.8 | | | | 2.3 / 3.5 | 3.4 / 5.2 |
| SS-A_M16-S+L_4 | | | 8.8 | | | | 2.2 / 2.6 | 3.2 / 4.0 |
| SS-A_M16-S+L_5 | | | 8.8 | | | | - / 3.1 | - / 4.3 |

[1] Clamping length | [2] Length of the load cell | [3] Property class | [4] Material: Ferritic 1.4003 |
[5] measured by strain gauge | [6] measured by load cell | [7] Blasted (glass particle - 300 µm)

- Preload in all the tests were selected as $F_{p,C} = 0.7\ f_{ub} \times A_s$
- All bolts were instrumented with BTMC-3 strain gauges

The relaxation experiments show that the loss of preload due to relaxation and creep between HV bolts and stainless steel bolts are comparable. The results show that a higher preload level causes higher losses of preload. The test results in this investigation have shown that the highest loss of preload was observed for HV-bolts by about 11 % for $F_{p,C}$ and 7.4 % for the preload level 0.9 $F_{p,C}$*. For the austenitic stainless steel bolts, the maximum preload losses were approx. 7.7 % for $F_{p,C}$ and for super duplex bolts approx. 11.4 % for $F_{p,C}$ and approx. 7.5 % for 0.9 $F_{p,C}$*.

It can be seen from Table 119 that the results of instrumented bolts and the load cell are comparable, see Figure 126. Even though, the load cells provide more reliable test results in the long term relaxation tests. In the second group of tests, the strain gauges show a deep increase in measuring the loss of preload. It seems that it can be neglected due to measuring errors. Further investigations have to be carried out to investigate this phenomenon.

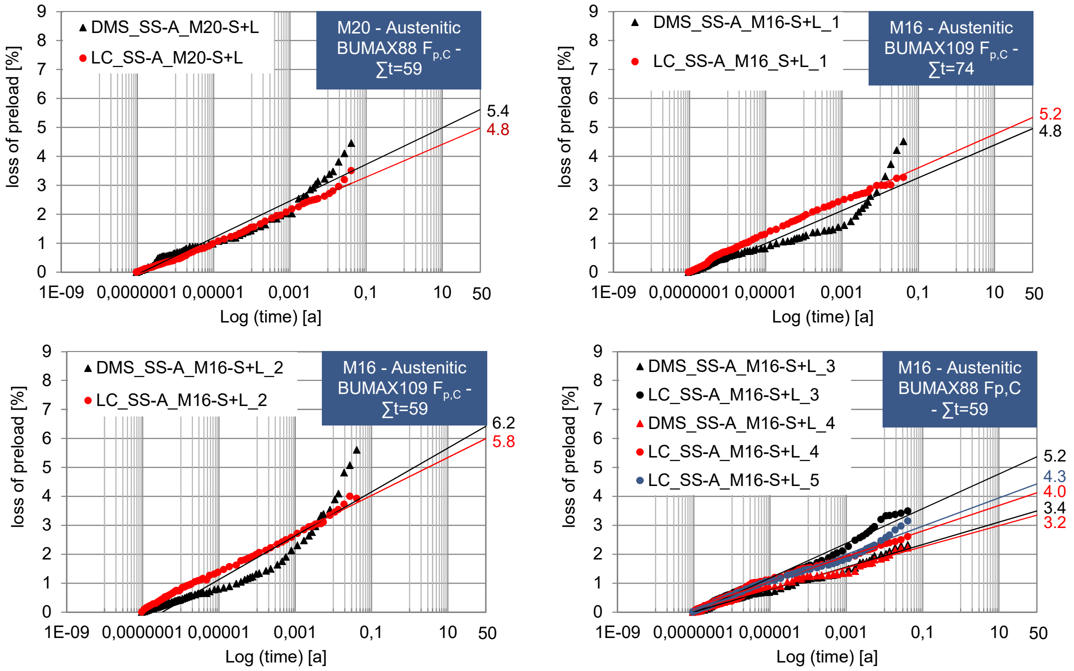


**Figure 126** Preload losses after 50 years in preload losses-log (time) diagrams for M20 and M16 Austenitic-bolts

The first efforts show that the high concern about the loss of preload due to relaxation and creep seems to be unreasonable and stainless steel connections can be treated similar to those made of carbon steel.

### 4.3.3 Relaxation tests according to the Technical annex

To complete the investigations into the creep and relaxation behaviour of stainless steel bolted connections, various sets of bolted plates were tested in order to achieve results for the whole clamped and preloaded connection detail.

Within SIROCO, austenitic (1.4404), ferritic (1.4003), duplex (1.4462), and lean duplex (1.4162) stainless steel plates and austenitic (1.4432), duplex (1.4462) and lean duplex (1.4162) stainless steel bolting assemblies according to EN ISO 4017 were used for experimental testing of the loss of preload of stainless steel bolted connections. All stainless steel plates were used in the "as delivered" 1D surface condition without any further surface treatment, see Figure 127 (a) and (b).

Additionally, further test series were conducted with S355 carbon steel plates (in the "as received" surface condition, see Figure 127 (c) and (d)) in combination with stainless steel bolts (M16 and M20 austenitic bolts (Bumax 88)) and carbon steel bolts (M16 and M20 HV 10.9 bolts) according to EN 14399-4 and stainless steel plate.

These additional tests were carried out in order to be able to separate the creep effect from the stainless steel plates and bolts.

(a) Eight-bolts duplex specimens in 1D surface condition

(b) One-bolt austenitic specimens in 1D surface condition

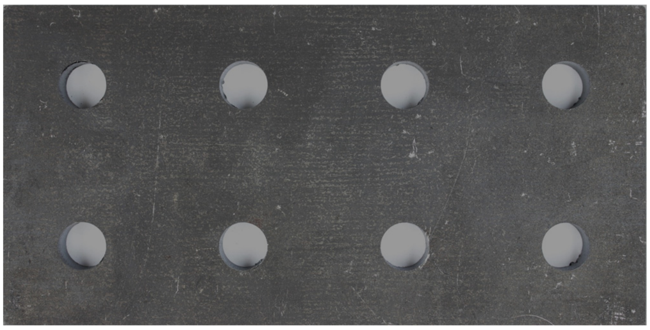

(c) Eight-bolts carbon steel specimens in 1D surface condition

(d) One-bolt carbon steel specimens in 1D surface condition

**Figure 127** Exemplary photos for stainless steel and carbon steel test specimens

Furthermore, some test series were conducted with carbon steel HV bolts and S355 carbon steel plates in order to be able to compare the preload losses in stainless steel and carbon steel bolting assemblies. The carbon steel plates were only shot blasted to clean the surfaces from rust. The test matrix of all investigated combinations is given in Table 120.

**Table 120** Different test combinations

| Bolt material type | Pc[2)] [-] | Plate material type | Surface condition |
|---|---|---|---|
| Austenitic EN 1.4436 | 8.8/10.9 | Austenitic EN 1.4404 | 1D |
| | | Ferritic EN 1.4003 | |
| | | Duplex EN 1.4462 | |
| | | Lean Duplex EN 1.4162 | |
| | | S355 | as received |
| Duplex EN 1.4462 | 10.9 | Austenitic EN 1.4404 | 1D |
| | | Ferritic EN 1.4003 | |
| | | Duplex EN 1.4462 | |
| | | Lean Duplex EN 1.4162 | |
| | | S355 | as received |
| Lean Duplex EN 1.4162 | 10.9 | Austenitic EN 1.4404 | 1D |
| | | Ferritic EN 1.4003 | |
| | | Duplex EN 1.4462 | |
| | | Lean Duplex EN 1.4162 | |
| | | S355 | as received |
| Carbon steel HV | 10.9 | Austenitic EN 1.4404 | 1D |
| | | Duplex EN 1.4462 | |
| | | S355* | as received |
| * the results from Task 3.3 | | | |

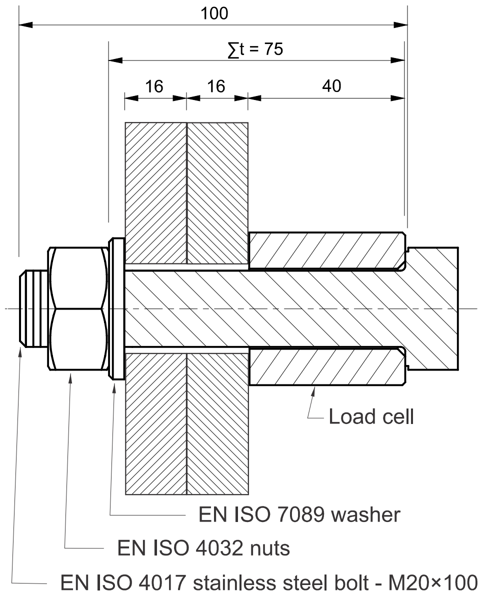


(a) M20 test specimen

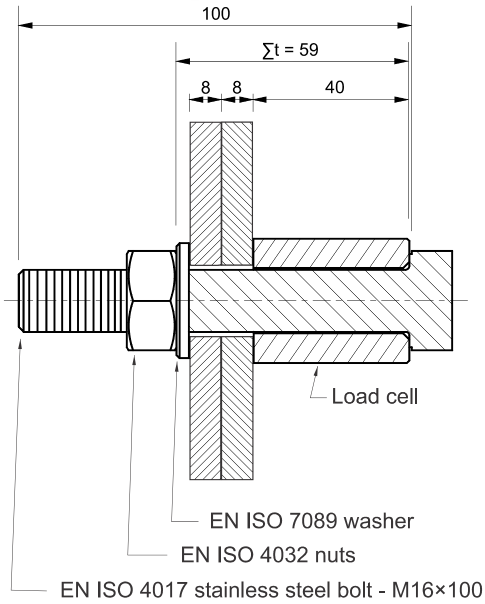


(b) M16 test specimen

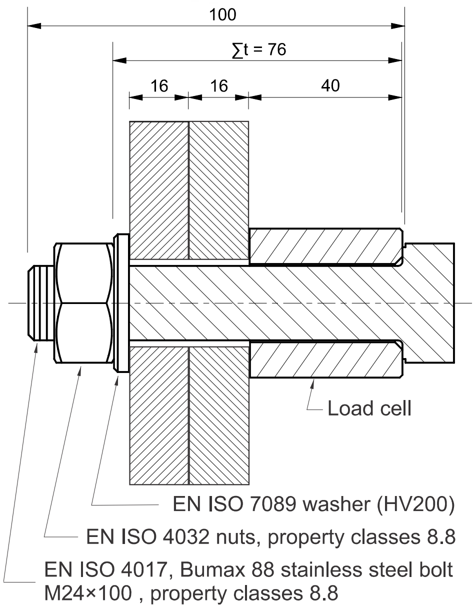


(c) M24 test specimen

**Figure 128** Clamping length of the stainless steel bolting assemblies for the relaxation test tests

The investigations were carried out at the Institute for Metal and Lightweight Structures of the University of Duisburg-Essen. The bolts used were austenitic stainless steel bolts M16 and M20 of grade Bumax 88 and 109 which relate to property classes 8.8 and 10.9 according to EN ISO 898-1 comparable to those of carbon steel bolts, as well as duplex (M16 and M20) and lean duplex (M16) stainless steel bolts with property class 10.9 bolts. All bolts used were full threaded bolts acc. to EN ISO 4017. All stainless steel bolts were supplied by BUAMX AB, which produces stainless steel bolting assemblies of these property classes deviating from EN ISO 3506-1 and EN ISO 3506-2 [9].

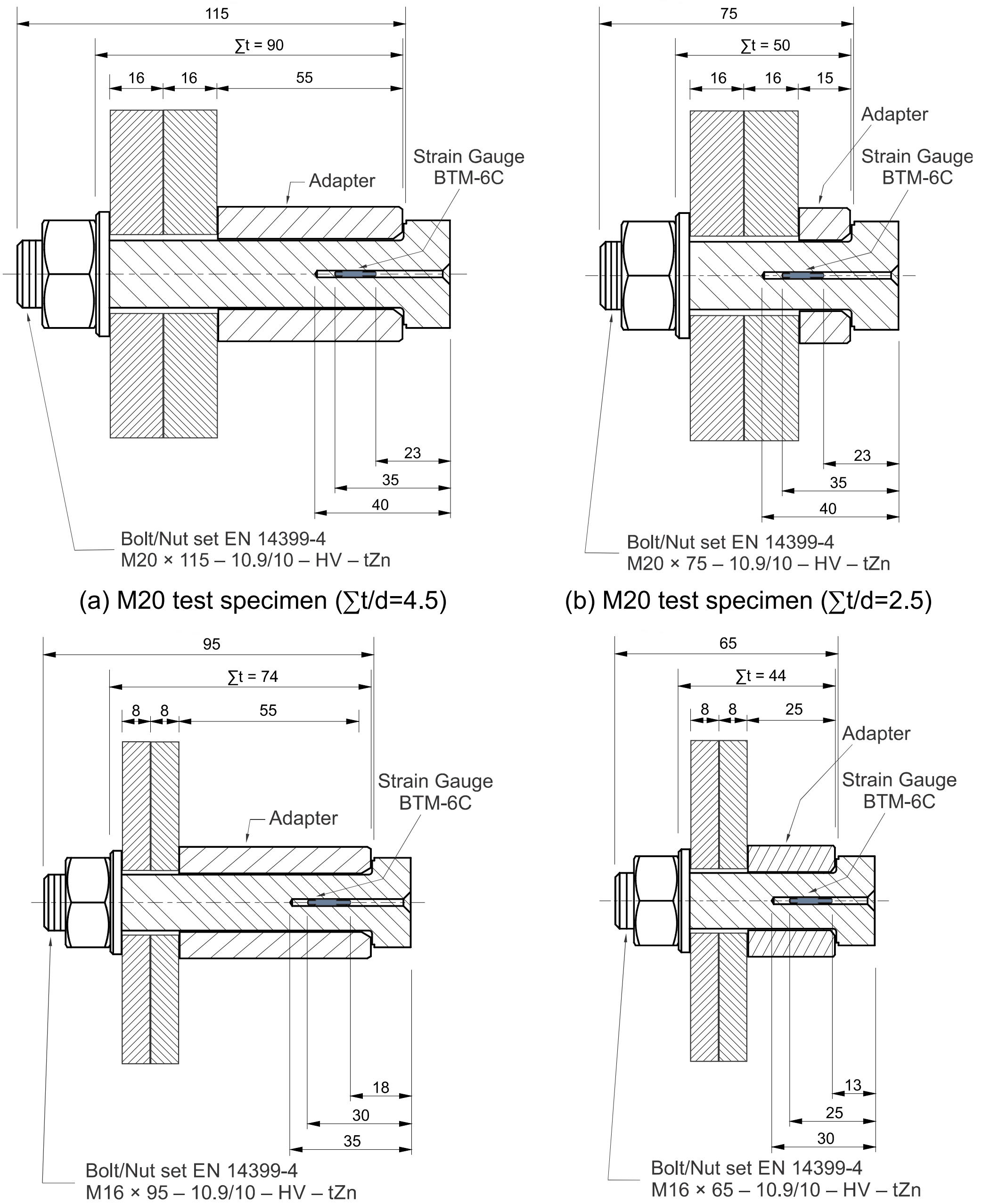


(a) M20 test specimen (∑t/d=4.5) (b) M20 test specimen (∑t/d=2.5)

(c) M20 test specimen (∑t/d=4.6) (d) M20 test specimen (∑t/d=2.8)

**Figure 129** Clamping length of the carbon steel HV-bolting assemblies for the relaxation test tests in two different clamping lengths for each bolt dimension

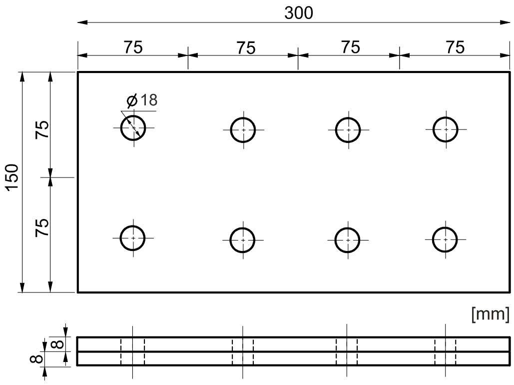


(a) Test specimen with eight M16 bolts

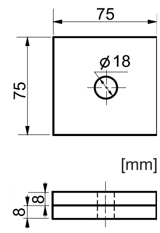


(b) Test specimen with one M16 bolt

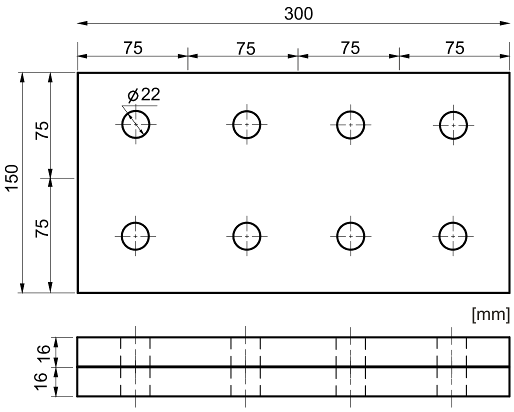


(c) Test specimen with eight M20 bolts

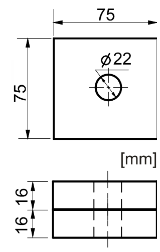


(d) Test specimen with one M20 bolt

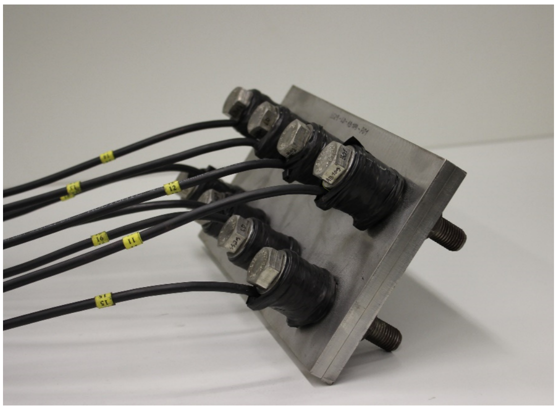

(e) Eight-bolt-specimen (150 mm × 150 mm plates)

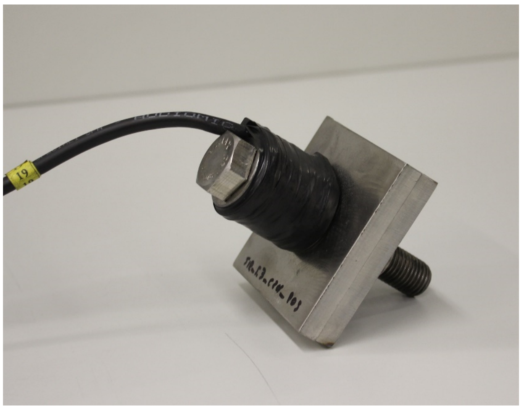

(f) One-bolt-specimen (75 mm × 75 mm plates)

**Figure 130** Test specimen geometry for the relaxation tests of the bolted connections (test specimens for M16 and M20 bolts)

One of the most accurate method to measure preloads in bolts is to use instrumented bolts with implanted strain gauges, see Figure 119. Using load cells is also very accurate, but has the rather big disadvantage of an artificial increased clamping length, which is of importance when the change of the preload in the bolt shall be measured: as already mentioned before, with increasing clamping length the loss of preload decreases. For this reason, in carbon steel bolts, implanted strain gauges should be used in order to avoid additional adjustments to cover the influence of a high clamping length. Unfortunately, using instrumented bolts is not possible for stainless steel bolts as viscoplastic deformation already occurs during the preloading process of the stainless steel bolt and the rate of this change decreases when time elapses. This means that this change of the strain would be measured by the strain gauges as well which would lead to deviating\unreal values of the measured preload in comparison to the real preload level in the bolt, see further explanations in chapter 2.3.2. As it is mentioned there, using the load cell will be the more accurate method compared to instrumented bolts for measuring the preload level in stainless steel bolting assemblies. For this reason, special small load cells for stainless steel bolts were developed, produced and calibrated at the Institute for Metal and Lightweight Structures of the University of Duisburg-Essen, see Figure 122 and Figure 131. In order to compare the influence of different types of stainless steel and bolt sizes, the same preload level of $F_{p,C}$ = 0.7 $f_{ub}$ $A_s$ was considered for all tests. Herewith, the preload level for M16 Bumax 109 and Bumax 88 yielded to about 110 kN and 88 kN respectively. Both M20 Bumax 88 and HV-bolts were preloaded to 137 and 172 kN respectively.

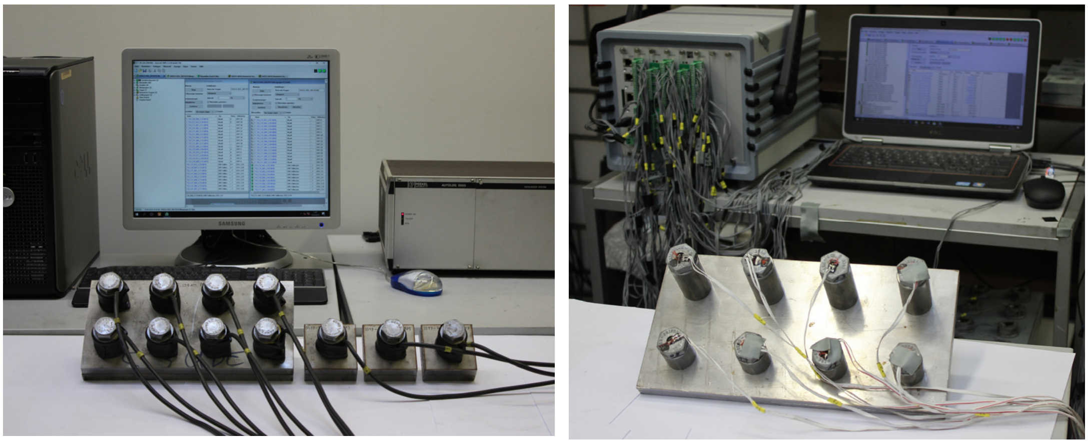

(a) performing relaxation test wit load cells

(b) performing relaxation test wit instrumented bolts

**Figure 131** Test setup

Of great importance is the definition of the starting point for the evaluation of the preload measurement as in the first seconds after tightening of the bolts, a considerable drop in the measured preload level can be observed. The main amount of this instance drop can be explained by turning back of the nut and elastic recovery of the bolt threads when the wrench is removed. This phenomenon it is not entirely related to the relaxation behaviour of the bolting assemblies and it has to be extracted and must not be considered in the calculation of the loss of preload. For this reason, the first three seconds of the measurements should not be taken into account. By removing the first three seconds and by considering the linear behaviour of the loss of preload in a logarithmic scale, it is possible to derive the exact starting point of the relaxation test. Figure 132 and Figure 133 show exemplary the preload losses-log (time) diagrams for the austenitic stainless steel SS16 test series with M20 lean Duplex bolts with property class 10.9. Table 121 presents the results of all test series extrapolated to 50 years. Further preload losses-log (time) diagrams other tests series are given in Annex A.

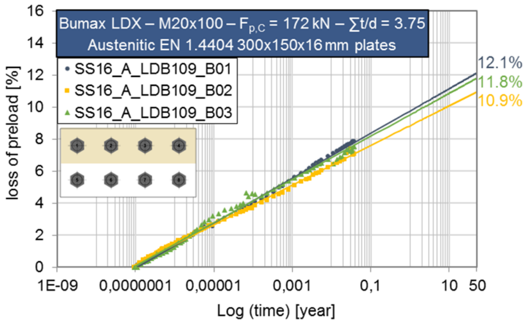


(a) preload losses-log (time) diagrams for eight-bolts specimens - first row

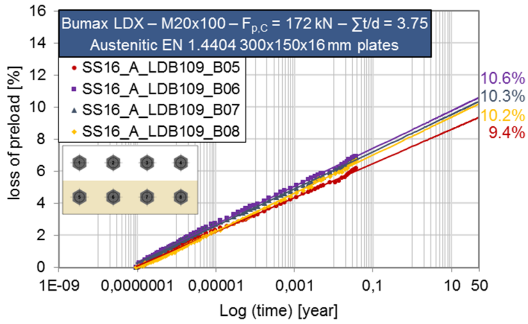


(b) preload losses-log (time) diagrams for eight-bolts specimens - second row

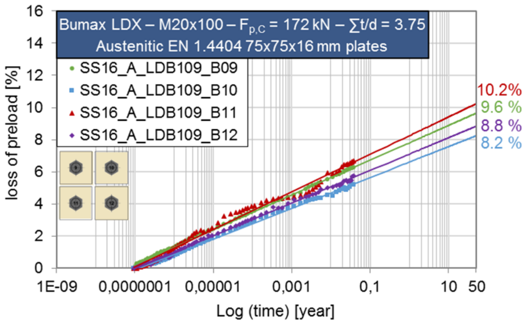


(c) preload losses-log (time) diagrams for one-bolt specimens

| Loss of preload min / mean / max [%] | |
|---|---|
| measured after 14 days | after 50 years (extrapolated) |
| 5.2 / 6.6 / 7.9 | 8.2 / 10.2 / 12.1 |

(d) loss preload measured/extrapolated after 14 days/ 50 years

**Figure 132** Preload losses for SS16

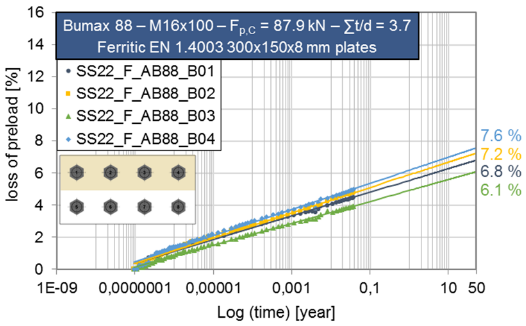


(a) preload losses-log (time) diagrams for eight-bolts specimens - first row

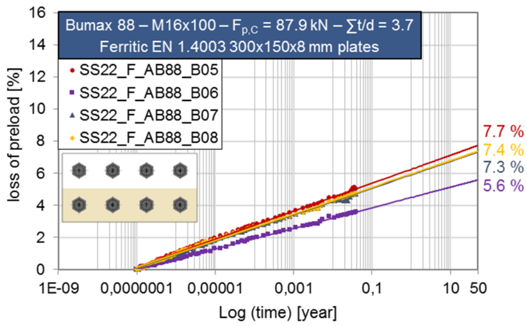


(b) preload losses-log (time) diagrams for eight-bolts specimens - second row

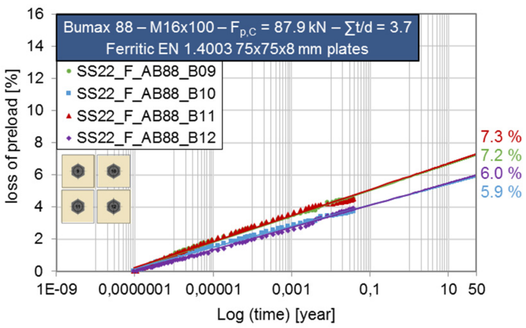


(c) preload losses-log (time) diagrams for one-bolt specimens

| Loss of preload min / mean / max [%] | |
|---|---|
| measured after 14 days | after 50 years (extrapolated) |
| 3.6 / 4.4 / 5.0 | 5.6 / 6.8 / 7.7 |

(d) loss preload measured/extrapolated after 14 days/ 50 years

**Figure 133** Preload losses for SS22

**Table 121** Loss of preload for the relaxation tests of M20 stainless steel bolting assemblies

| Ser. ID | Type of specimen | | No. of tests | Σt/d [1] [-] | Clamped package: Bolt | Clamped package: Plate | $F_{p,C}$ [2] [kN] | Loss of preload: measured after days - min / mean / max [%] | Loss of preload: after 50 years (extrapolated) min / mean / max [%] |
|---|---|---|---|---|---|---|---|---|---|
| Bumax 88 Austenitic bolts (M20x100) | | | | | | | | | |
| SS01 | 8 bolt | First row | 4 | 3.75 | Bumax 88 | Austenitic | 137 | 14 – 3.7 / 4.6 / 6.0 | 6.0 / 6.8 / 7.2 |
| | | Sec. row | 4 | 3.75 | | | 137 | 14 – 4.3 / 4.6 / 4.8 | 7.0 / 7.1 / 7.2 |
| | 1 bolt | - | 4 | 3.75 | | | 137 | 14 – 4.2 / 4.5 / 5.2 | 6.7 / 7.2 / 8.3 |
| SS02 | 8 bolt | First row | 4 | 3.75 | | Ferritic | 137 | 14 – 4.0 / 4.4 / 4.7 | 6.4 / 6.7 / 7.1 |
| | | Sec. row | 4 | 3.75 | | | 137 | 14 – 3.4 / 3.7 / 4.1 | 5.4 / 5.9 / 6.4 |
| | 1 bolt | - | 4 | 3.75 | | | 137 | 14 – 3.5 / 4.1 / 4.6 | 5.5 / 6.4 / 7.3 |
| SS03 | 8 bolt | First row | 4 | 3.75 | | Duplex | 137 | 14 – 3.4 / 4.0 / 4.4 | 5.4 / 6.2 / 7.0 |
| | | Sec. row | 4 | 3.75 | | | 137 | 14 – 4.0 / 4.1 / 4.4 | 6.2 / 6.5 / 7.2 |
| | 1 bolt | - | 4 | 3.75 | | | 137 | 14 – 3.6 / 4.1 / 4.6 | 5.5 / 6.3 / 7.0 |
| SS04 | 8 bolt | First row | 3 | 3.75 | | Lean Duplex | 137 | 14 – 4.0 / 4.8 / 6.0 | 6.0 / 7.3 / 9.0 |
| | | Sec. row | 4 | 3.75 | | | 137 | 14 – 4.4 / 4.6 / 5.0 | 6.8 / 7.0 / 7.5 |
| | 1 bolt | - | 4 | 3.75 | | | 137 | 14 – 4.0 / 4.4 / 4.5 | 6.4 / 6.8 / 7.0 |
| CS05 | 8 bolt | First row | 4 | 3.75 | | S355 | 137 | 20 – 2.9 / 3.7 / 4.7 | 4.6 / 5.8 / 7.1 |
| | | Sec. row | 2 | 3.75 | | | 137 | 20 – 3.0 / 3.0 / 3.0 | 4.6 / 4.7 / 4.7 |
| Bumax 109 Austenitic bolts (M20x100) | | | | | | | | | |
| SS06 | 8 bolt | First row | 3 | 3.75 | Bumax 109 | Austenitic | 172 | 14 –5.0 / 5.3 / 5.6 | 7.8 / 8.2 / 8.6 |
| | | Sec. row | 3 | 3.75 | | | 172 | 14 –5.6 / 5.8 / 5.9 | 8.6 / 8.8 / 8.9 |
| SS07 | 1 bolt | - | 3 | 3.75 | | Ferritic | 172 | 25 –4.4 / 4.6 / 4.8 | 6.4 / 6.7 / 7.0 |
| SS09 | 8 bolt | First row | 2 | 3.75 | | Lean Duplex | 172 | 20 –4.4 / 4.6 / 4.8 | 6.9 / 7.0 / 7.1 |
| | | Sec. row | 4 | 3.75 | | | 172 | 20 – 4.2 / 4.8 / 5.3 | 6.8 / 7.5 / 8.2 |
| CS10 | 8 bolt | First row | 3 | 3.75 | | S355 | 172 | 20 – 3.9 / 4.0 / 4.0 | 5.8 / 5.9 / 6.0 |
| | | Sec. row | 3 | 3.75 | | | 172 | 20 – 4.3 / 4.5 / 4.7 | 6.5 / 6.7 / 7.0 |
| Bumax DX Duplex bolts (M20x100) | | | | | | | | | |
| SS11 | 8 bolt | First row | 4 | 3.75 | Bumax DX | Austenitic | 172 | 14 – 3.5 / 4.3 / 5.2 | 5.5 / 6.6 / 7.9 |
| | | Sec. row | 3 | 3.75 | | | 172 | 14 – 4.1 / 4.2 / 4.5 | 6.4 / 6.5 / 6.8 |
| SS12 | 8 bolt | First row | 4 | 3.75 | | Ferritic | 172 | 20 – 3.9 / 4.7 / 5.2 | 5.7 / 7.2 / 8.0 |
| | | Sec. row | 4 | 3.75 | | | 172 | 20 – 4.7 / 5.2 / 5.7 | 7.2 / 7.8 / 8.6 |
| SS13 | 1 bolt | - | 3 | 3.75 | | Duplex | 172 | 20 – 4.9 / 5.1 / 5.2 | 7.5 / 7.8 / 8.0 |
| SS14 | 1 bolt | - | 3 | 3.75 | | Lean Duplex | 172 | 10 – 4.3 / 4.7 / 5.0 | 7.3 / 7.9 / 8.4 |
| CS15 | 1 bolt | - | 3 | 3.75 | | S355 | 172 | 20 – 4.7 / 4.8 / 4.9 | 7.2 / 7.4 / 7.6 |
| Bumax LDX Lean Duplex bolts (M20x100) | | | | | | | | | |
| SS16 | 8 bolt | First row | 3 | 3.75 | Bumax LDX | Austenitic | 172 | 14 – 7.1 / 7.5 / 7.9 | 10.9 / 11.6 / 12.1 |
| | | Sec. row | 4 | 3.75 | | | 172 | 14 – 6.2 / 6.7 / 6.9 | 9.4 / 10.1 /10.6 |
| | 1 bolt | - | 4 | 3.75 | | | 172 | 14 – 5.2 / 6.0 / 6.7 | 8.2 / 9.2 / 10.2 |
| SS17 | 8 bolt | First row | 3 | 3.75 | | Ferritic | 172 | 14 – 5.1 / 5.2 / 5.3 | 7.9 / 8.0 / 8.2 |
| | | Sec. row | 3 | 3.75 | | | 172 | 14 – 5.3 / 5.4 / 5.6 | 8.0 / 8.2 / 8.6 |
| | 1 bolt | - | 3 | 3.75 | | | 172 | 14 – 4.1 / 4.6 / 5.1 | 6.8 / 7.3 / 8.0 |
| SS18 | 1 bolt | - | 4 | 3.75 | | Duplex | 172 | 14 – 5.2 / 5.6 / 5.9 | 8.3 / 8.9 / 9.5 |
| SS19 | 1 bolt | - | 3 | 3.75 | | Lean Duplex | 172 | 14 – 5.0 / 5.4 / 5.4 | 7.9 / 8.2 / 8.4 |

[1] clamping length ratio (Σt = clamping length and d = bolt dimension) | [2] preload level

**Table 122** Loss of preload for the relaxation tests of M16 stainless steel bolting assemblies

| Ser. ID | Type of specimen | | No. of tests | Σt/d[1] [-] | Clamped package: Bolt | Clamped package: Plate | $F_{p,C}$[2] [kN] | Loss of preload: measured after days - min / mean / max [%] | Loss of preload: after 50 years (extrapolated) min / mean / max [%] |
|---|---|---|---|---|---|---|---|---|---|
| Bumax 88 Austenitic bolts (M16x100) | | | | | | | | | |
| SS21 | 8 bolt | First row | 4 | 3.7 | Bumax 88 | Austenitic | 88 | 14 – 4.7 / 5.0 / 5.5 | 7.3 / 7.7 / 8.5 |
| | | Sec. row | 4 | 3.7 | | | 88 | 14 – 4.5 / 4.8 / 5.1 | 6.8 / 7.3 / 7.7 |
| | 1 bolt | - | 4 | 3.7 | | | 88 | 14 – 3.9 / 4.5 / 5.0 | 6.1 / 6.8 / 7.8 |
| SS22 | 8 bolt | First row | 4 | 3.7 | | Ferritic | 88 | 14 – 3.9 / 4.5 / 5.0 | 6.1 / 6.9 / 7.6 |
| | | Sec. row | 4 | 3.7 | | | 88 | 14 – 3.6 / 4.5 / 5.0 | 5.6 / 7.0 / 7.7 |
| | 1 bolt | - | 4 | 3.7 | | | 88 | 14 – 3.7 / 4.2 / 4.5 | 5.9 / 6.6 / 7.3 |
| SS23 | 8 bolt | First row | 4 | 3.7 | | Duplex | 88 | 14 – 4.5 / 5.2 / 5.8 | 6.7 / 7.8 / 8.7 |
| | | Sec. row | 4 | 3.7 | | | 88 | 14 – 4.6 / 4.8 / 4.9 | 7.1 / 7.3 / 7.6 |
| | 1 bolt | - | 4 | 3.7 | | | 88 | 14 – 3.9 / 4.8 / 5.8 | 6.1 / 7.3 / 8.9 |
| SS24 | 8 bolt | First row | 4 | 3.7 | | Lean Duplex | 88 | 30 – 4.2 / 5.2 / 6.0 | 6.2 / 7.5 / 8.6 |
| | | Sec. row | 4 | 3.7 | | | 88 | 30 – 4.7 / 5.1 / 5.8 | 6.7 / 7.4 / 8.4 |
| | 1 bolt | - | 4 | 3.7 | | | 88 | 14 – 4.7 / 5.1 / 5.5 | 7.3 / 7.8 / 8.5 |
| CS25 | 8 bolt | First row | 1 | 3.7 | | S355 | 88 | 30 – 4.8 | 7.0 |
| | | Sec. row | 4 | 3.7 | | | 88 | 30 – 4.1 / 4.5 / 4.7 | 5.8 / 6.4 / 6.7 |
| | 1 bolt | - | 3 | 3.7 | | | 88 | 30 – 4.3 / 4.6 / 5.0 | 6.2 / 6.6 / 7.2 |
| Bumax 109 Austenitic bolts (M16x100) | | | | | | | | | |
| SS26 | 8 bolt | First row | 4 | 3.7 | Bumax 109 | Austenitic | 110 | 14 – 5.6 / 5.7 / 5.9 | 8.6 / 8.9 / 9.2 |
| | | Sec. row | 4 | 3.7 | | | 110 | 14 – 5.8 / 6.0 / 6.3 | 9.0 / 9.3 / 9.6 |
| | 1 bolt | - | 3 | 3.7 | | | 110 | 25 – 5.1 / 5.2 / 5.3 | 7.3 / 7.6 / 7.8 |
| SS27 | 8 bolt | First row | 3 | 3.7 | | Ferritic | 110 | 40 – 6.2 / 6.3 / 6.4 | 9.0 / 9.1 / 9.3 |
| | | Sec. row | 4 | 3.7 | | | 110 | 40 – 6.1 / 6.3 / 6.6 | 8.9 / 9.0 / 9.2 |
| | 1 bolt | - | 3 | 3.7 | | | 110 | 40 – 5.4 / 5.8 / 6.3 | 7.7 / 8.3 / 9.2 |
| SS28 | 8 bolt | First row | 4 | 3.7 | | Duplex | 110 | 55 – 4.6 / 5.0 / 5.4 | 6.4 / 7.1 / 7.7 |
| | | Sec. row | 4 | 3.7 | | | 110 | 55 – 4.9 / 5.4 / 6.1 | 7.0 / 7.6 / 8.5 |
| | 1 bolt | - | 4 | 3.7 | | | 110 | 55 – 5.0 / 5.3 / 5.7 | 7.1 / 7.7 / 8.2 |
| SS29 | 8 bolt | First row | 4 | 3.7 | | Lean Duplex | 110 | 14 – 5.6 / 5.7 / 5.9 | 8.6 / 9.0 / 9.4 |
| | | Sec. row | 4 | 3.7 | | | 110 | 14 – 5.8 / 6.0 / 6.3 | 9.1 / 9.3 / 9.6 |
| | 1 bolt | - | 4 | 3.7 | | | 110 | 14 – 4.8 / 5.2 / 5.7 | 7.4 / 8.0 / 8.9 |
| CS30 | 8 bolt | First row | 4 | 3.7 | | S355 | 110 | 20 – 3.8 / 4.4 / 4.7 | 6.0 / 6.8 / 7.2 |
| | | Sec. row | 4 | 3.7 | | | 110 | 20 – 4.6 / 4.7 / 4.8 | 7.1 / 7.3 / 7.5 |
| Bumax DX Duplex bolts (M16x100) | | | | | | | | | |
| SS31 | 8 bolt | First row | 4 | 3.7 | Bumax DX | Austenitic | 110 | 20 – 6.2 / 6.6 / 6.8 | 9.5 / 9.9 / 10.3 |
| | | Sec. row | 4 | 3.7 | | | 110 | 20 – 6.9 / 7.2 / 7.4 | 9.4 / 10.4 / 10.9 |
| | 1 bolt | - | 3 | 3.7 | | | 110 | 12 – 5.5 / 5.8 / 6.1 | 8.9 / 9.4 / 9.8 |
| SS32 | 1 bolt | - | 4 | 3.7 | | Ferritic | 110 | 14 – 5.4 / 5.8 / 6.6 | 8.3 / 9.0 / 10.3 |
| SS33 | 1 bolt | - | 3 | 3.7 | | Duplex | 110 | 14 – 5.2 / 5.8 / 6.4 | 8.2 / 9.0 / 9.9 |
| SS34 | 1 bolt | - | 4 | 3.7 | | Lean Duplex | 110 | 9 – 4.3 / 4.7 / 5.0 | 6.9 / 7.6 / 8.1 |
| CS35 | 1 bolt | - | 4 | 3.7 | | S355 | 110 | 14 – 4.7 / 5.0 / 5.5 | 7.2 / 7.7 / 8.2 |
| Bumax LDX Lean Duplex bolts (M16x100) | | | | | | | | | |
| SS36 | 8 bolt | First row | 2 | 3.7 | Bumax LDX | Austenitic | 110 | 20 –5.2 / 6.1 / 7.0 | 7.9 / 9.3 / 10.7 |
| | | Sec. row | 4 | 3.7 | | | 110 | 20 – 4.4 / 4.6 / 5.0 | 6.9 / 7.2 / 7.6 |
| | 1 bolt | - | 3 | 3.7 | | | 110 | 14 – 6.1 / 6.3 / 6.4 | 9.3 / 9.7 / 10.0 |
| SS37 | 8 bolt | First row | 4 | 3.7 | | Ferritic | 110 | 55 – 5.0 / 5.3 / 5.6 | 7.1 / 7.5 / 8.0 |
| | | Sec. row | 4 | 3.7 | | | 110 | 55 – 5.0 / 5.3 / 5.5 | 7.1 / 7.5 / 7.9 |
| | 1 bolt | - | 3 | 3.7 | | | 110 | 55 – 4.9 / 5.3 / 5.6 | 7.0 / 7.4 / 7.8 |
| SS38 | 1 bolt | - | 4 | 3.7 | | Duplex | 110 | 14 – 4.9 / 5.5 / 6.3 | 7.4 / 8.2 / 9.2 |
| SS39 | 8 bolt | First row | 4 | 3.7 | | Lean Duplex | 110 | 20 – 4.1 / 4.4 / 4.6 | 6.3 / 6.7 / 7.0 |
| | | Sec. row | 4 | 3.7 | | | 110 | 20 – 5.7 / 6.1 / 6.4 | 8.8 / 9.3 / 9.9 |
| | 1 bolt | - | 3 | 3.7 | | | 110 | 20 – 5.3 / 5.7 / 6.0 | 7.9 / 8.5 / 9.1 |
| CS40 | 1 bolt | - | 3 | 3.7 | | S355 | 110 | 55 – 5.0 / 5.6 / 6.1 | 7.0 / 7.9 / 8.6 |

[1] clamping length ratio (Σt = clamping length and d = bolt dimension) | [2] preload level

**Table 123** Loss of preload for the relaxation tests of M24 stainless steel bolting assemblies

| Ser. ID | Type of specimen | | No. of tests | Σt/d[1] [-] | Clamped package: Bolt | Clamped package: Plate | $F_{p,C}$[2] [kN] | Loss of preload: measured after days - min / mean / max [%] | Loss of preload: after 50 years (extrapolated) min / mean / max [%] |
|---|---|---|---|---|---|---|---|---|---|
| Bumax 88 Austenitic bolts (M24x100) | | | | | | | | | |
| SS41 | 8 bolt | First row | 3 | 3.2 | Bumax 88 | Austenitic | 198 | 14 – 5.3 / 5.7 / 6.2 | 8.2 / 8.5 / 8.9 |
| SS41 | 8 bolt | Sec. row | 4 | 3.2 | Bumax 88 | Austenitic | 198 | 14 – 5.1 / 5.6 / 6.0 | 8.0 / 8.7 / 9.2 |
| SS43 | 8 bolt | First row | 4 | 3.2 | Bumax 88 (re-used) | Austenitic (re-used) | 198 | 25 – 2.6 / 2.8 / 3.6 | 3.9 / 4.3 / 5.4 |
| SS43 | 8 bolt | Sec. row | 4 | 3.2 | Bumax 88 (re-used) | Austenitic (re-used) | 198 | 25 – 2.7 / 2.8 / 3.0 | 4.1 / 4.2 / 4.5 |

[1] clamping length ratio (Σt = clamping length and d = bolt dimension) | [2] preload level

**Table 124** Loss of preload for the relaxation tests of M20 and M16 HV bolting assemblies

| Ser. ID | Type of specimen | | No. of tests | Σt/d[1] [-] | Clamped package: Bolt | Clamped package: Plate | $F_{p,C}$[2] [kN] | Loss of preload: measured after days - min / mean / max [%] | Loss of preload: after 50 years (extrapolated) min / mean / max [%] |
|---|---|---|---|---|---|---|---|---|---|
| HV bolts M20 | | | | | | | | | |
| SS45 | 8 bolt | First row | 4 | 2.5 | HV M20x75/ M20x115 | Duplex | 172 | 14 – 3.0 / 4.3 / 5.2 | 4.7 / 6.7 / 8.0 |
| SS45 | 8 bolt | Sec. row | 4 | 4.5 | HV M20x75/ M20x115 | Duplex | 172 | 14 – 2.9 / 3.5 / 4.4 | 4.6 / 5.5 / 6.8 |
| DTI05[3] | 8 bolt | First row | 4 | 2.4 | HV M20 × 75 | S355 | 172 | 14 – 4.0 / 5.1 / 6.5 | 6.0 / 7.7 / 9.7 |
| DTI05[3] | 8 bolt | Sec. row | - | 2.4 | HV M20 × 75 | S355 | 172 | - | - |
| DTI05[3] | 1 bolt | - | 4 | 2.4 | HV M20 × 75 | S355 | 172 | 35 – 9.4 / 10.1 / 10.8 | 5.5 / 6.2 / 7.1 |
| DTI06[3] | 8 bolt | First row | 4 | 4.4 | HV M20 × 115 | S355 | 172 | 14 – 3.6 / 4.0 / 5.0 | 5.3 / 6.1 / 7.6 |
| DTI06[3] | 8 bolt | Sec. row | 4 | 4.4 | HV M20 × 115 | S355 | 172 | 14 – 2.9 / 4.3 / 5.4 | 4.4 / 6.4 / 8.0 |
| DTI06[3] | 1 bolt | - | 3 | 4.4 | HV M20 × 115 | S355 | 172 | 40 – 4.7 / 5.0 / 5.5 | 6.6 / 7.1 / 7.7 |
| HV bolts M16 | | | | | | | | | |
| SS46 | 8 bolt | First row | 2 | 2.75 | HV M16x65/ M16x95 | Austenitic | 110 | 20 – 1.8 / 2.4 / 3.3 | 2.8 / 3.6 / 4.8 |
| SS46 | 8 bolt | Sec. row | 4 | 4.6 | HV M16x65/ M16x95 | Austenitic | 110 | 20 – 1.3 / 1.6 / 2.0 | 2.0 / 2.4 / 3.0 |
| SS47 | 8 bolt | First row | 4 | 2.75 | HV M16x65/ M16x95 | Duplex | 110 | 14 – 2.6 / 2.8 / 3.0 | 4.0 / 4.4 / 4.6 |
| SS47 | 8 bolt | Sec. row | 4 | 4.6 | HV M16x65/ M16x95 | Duplex | 110 | 14 – 2.0 / 2.3 / 2.6 | 3.0 / 3.5 / 3.9 |
| DTI11[3] | 8 bolt | First row | 4 | 2.5 | HV M16 × 65 | S355 | 110 | 14 – 3.6 / 4.4 / 5.5 | 5.7 / 6.7 / 8.2 |
| DTI11[3] | 8 bolt | Sec. row | 4 | 2.5 | HV M16 × 65 | S355 | 110 | 14 – 4.1 / 5.2 / 7.9 | 6.4 / 7.9 / 11.9 |
| DTI11[3] | 1 bolt | - | 3 | 2.5 | HV M16 × 65 | S355 | 110 | 40 – 6.2 / 6.5 / 6.7 | 9.0 / 9.4 / 9.8 |
| DTI12[3] | 8 bolt | First row | 4 | 4.5 | HV M16 × 95 | S355 | 110 | 12 – 5.2 / 5.4 / 5.7 | 8.2 / 8.4 / 8.8 |
| DTI12[3] | 8 bolt | Sec. row | 4 | 4.5 | HV M16 × 95 | S355 | 110 | 12 – 3.9 / 4.1 / 4.3 | 6.5 / 6.7 / 7.0 |
| DTI12[3] | 1 bolt | - | 2 | 4.5 | HV M16 × 95 | S355 | 110 | 40 – 5.0 / 5.0 / 5.1 | 7.0 / 7.0 / 7.1 |

[1] clamping length ratio (Σt = clamping length and d = bolt dimension) | [2] preload level | [3] test results from Task 3.3

#### *4.3.3.1 Results and discussions*

After tightening of the bolts, the loss of preload starts immediately and continues gradually over time. Figure 132 shows that the rate of loss of preload decreases as time elapses. The highest rate can be observed at the beginning of testing.

The results show that the highest loss of preload was observed for austenitic lean-duplex M20 and M16 duplex bolted assemblies in combination with austenitic plates by about 10 %, see Figure 135. It can also be seen that the amount of loss of preload between M16, M20 and M24 stainless steel bolting assemblies are comparable for different types of stainless steel with the same clamping length ratio and preload level.

The asymptotic stress relaxation of the cold drawn bar was found to be 8.6 % for initial stress comparable to the preload for Bumax 88 and 10.1 % for the initial stress comparable to the preload for Bumax 109 whereby the 0.2 proof stress $R_{p0.2}$ of the cold drawn bar was 823 MPa. $R_{p0.2}$ of the actual bolts was 869 MPa for the Bumax 88 (M16)-bolts, 973 MPa for the Bumax 88 (M20)-bolts and 1060 MPa for the Bumax 109 (M16)-bolts. Herewith, it can be assumed that the asymptotic stress relaxation for the actual bolt material lies under the curve of the Hart's model as shown in Figure 136 which is in agreement with the extrapolated loss of preload in Table 124.

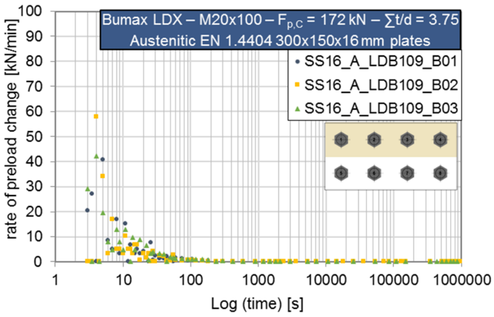


(a) log (rate of loss of preload) – time diagrams for eight-bolts specimens - first row

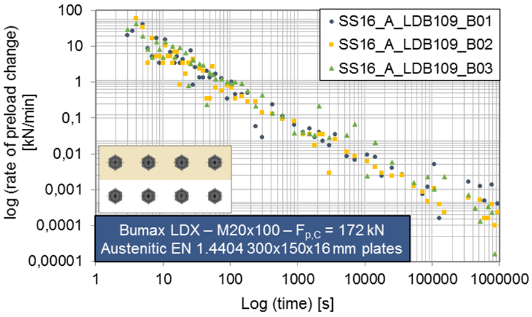


(b) log (rate of loss of preload) – log (time) diagrams for eight-bolts specimens - first row

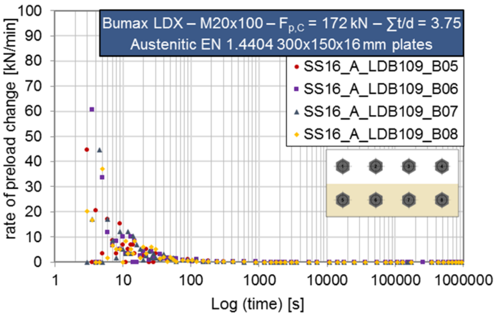


(c) log (rate of loss of preload) – time diagrams for eight-bolts specimens - second row

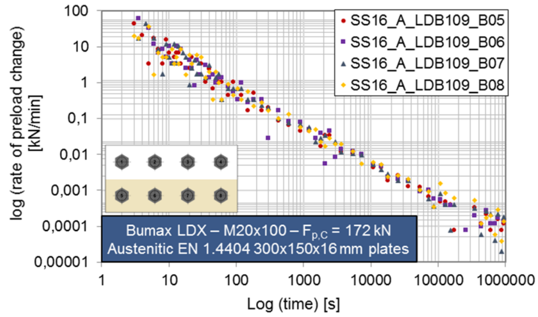


(d) log (rate of loss of preload) – log (time) diagrams for eight-bolts specimens - second row

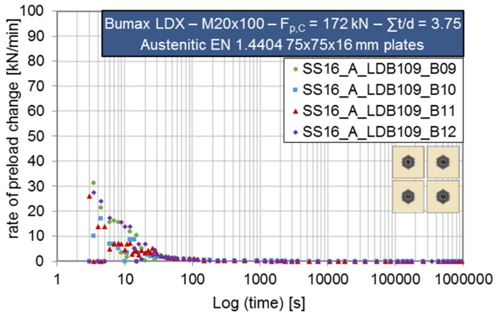


(e) log (rate of loss of preload) – time diagrams for one-bolt specimens

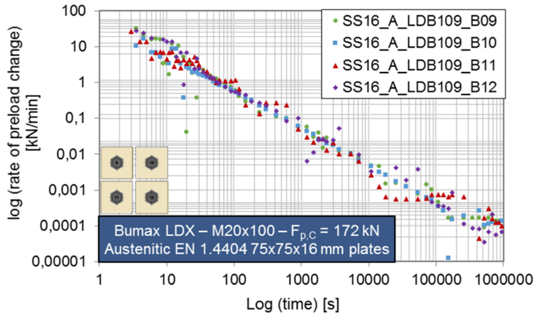


(f) log (rate of loss of preload) – log (time) diagrams for one-bolt specimens

**Figure 134** Exemplary rate of loss of preload for SS16 test series (M20 bolting assemblies, preload level: $F_{p,C}$ 172 kN, $\sum t/d = 3.75$)

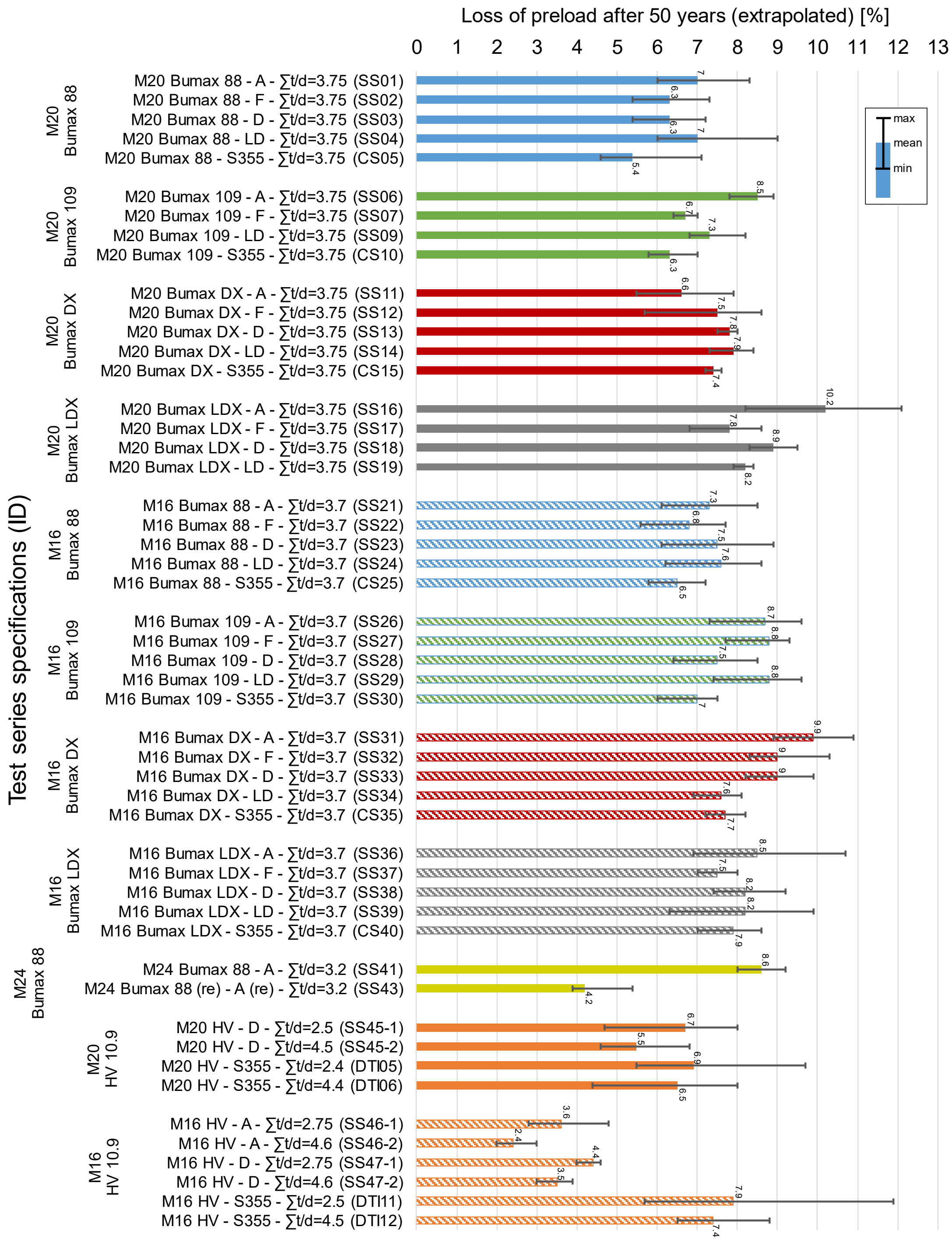


A: Austenitic EN 1.4404 | F: Ferritic EN 1.4003 | D: Duplex EN 1.4462 | LD: Lean Duplex EN 1.4162

**Figure 135** Comparing the loss of preload after 50 years (extrapolated) for different test series

In order to investigate the influence of the creep in the plate material on the loss of preload of stainless steel bolted connections, two series of tests were conducted with carbon steel plates (S355) in the as received condition with M20 austenitic, duplex and M16 austenitic, duplex and lean duplex bolting assemblies. As the amount of creep in the carbon steel material is negligible, the loss of preload is mainly caused by the initial setting effects and creep and stress relaxation of the stainless steel bolting assemblies. From Figure 135 it can be seen that there is a tendency towards a slightly lower loss of preload after 50 years. The results of the combination of stainless steel bolting assemblies with carbon steel and stainless steel clamped plates are - with some exceptions but in general - comparable.

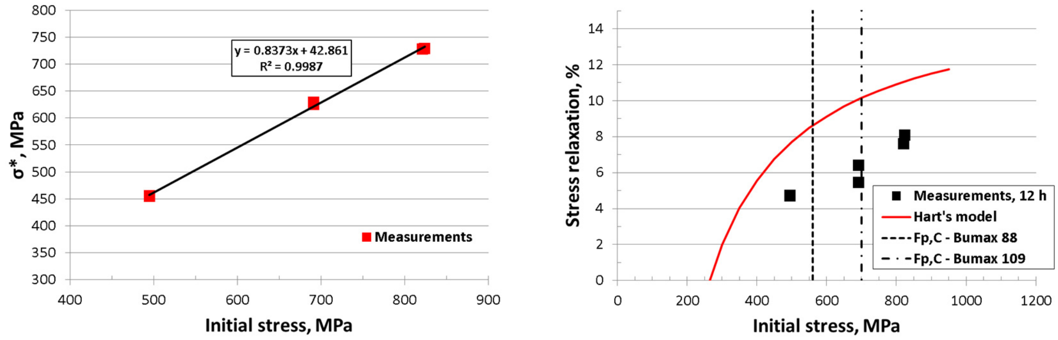


(a) σ* as a function of the initial stress for 1.4436 cold drawn bar

(b) Asymptotic stress relaxation of 1.4436 cold drawn bar

**Figure 136** Stress relaxation results fitted to the Hart's model for 1.4436 cold drawn bar material, see[1]/[29] and [29]

As it was seen in the creep tests on stainless steel bolts, a very small creep will happen if the stainless steel bolts are preloaded for the second time, see Figure 121. This phenomenon can also be confirmed in the relaxation test. For M24 Bumax 88 bolted assemblies the relaxation test was repeated with the same bolt and clamp components and the results show about 50 % lower preload losses extrapolated after 50 years. This phenomenon can be explained by remaining viscopelastic deformation in the stainless bolts during the first relaxation test. For this reason, in the second test a very small amount of viscopelastic deformation appeared in the components.

As it can also be seen in Table 124, the smaller clamping length leads to a higher loss of preload in the preloaded bolted assemblies. This phenomenon can be confirmed for both bolt dimensions (M20 and M16).

Herewith, the conclusion can be drawn that the loss of preload in the preloaded connections investigated in this work was mainly attributed to the embedment/plastic deformation of the clamped component surfaces while the creep in the plates was negligible. Table 121, Table 122, Table 123 and Table 124 also show that the estimated preload losses over 50 years for different grades of stainless steel bolting assemblies (austenitic, duplex and lean-duplex) are similar (between 6% to 10 %). It is clear that the creep and stress relaxation in the bolt material is detectable but the influence of these parameters on the amount of preload losses are insignificant.

The present relaxation experiments are compared with the results of carbon steel bolted connections from Task 3.3 with approximately the same clamping length ratio and without any DTIs (series names: DTI05, DTI06, DTI11 and DTI12). The results show that the loss of preload in preloaded carbon steel bolted connections and preloaded stainless steel bolted connections are comparable, see Table 1 and Figure 135, as the preload loss for the carbon steel bolted connections yield to approximately the same value of between 7% to 8 % which is comparable to the values achieved over all stainless steel test samples.

# 5 Conclusions

The application of preloaded stainless steel bolting assemblies is currently not permitted in the execution standard for steel structures EN 1090-2 – unless otherwise specified. If they have to be used, they have to be treated as special fasteners and procedure tests are mandatory. Because no product system neither product standard exist especially for stainless steel bolting assemblies for preloading, the lubrication must be adjusted in a procedure test in such a way that the demanded preload is adequately introduced with the chosen tightening procedure, overstressing is excluded, galling is avoided as much as possible, and losses of preloading caused by relaxation and creep effects (designated as viscoplastic deformation) are considered to be on the safe side.

Preloaded stainless steel bolting assemblies mainly relax due to different parameters, like embedment/plastic deformation of the clamped component surfaces, so called setting effect and the viscoplastic deformation behaviour of the stainless steels, which have already been observed at room temperature. The viscoplastic deformation behaviour in preloaded bolting assemblies are assumed to be divided into viscoplastic deformation under constant load condition for the plates (i.e. creep deformation) and viscoplastic deformation under constant strain condition for the bolts (i.e. stress relaxation). Therefore, it is important to estimate the amount of the preload losses from the combined creep and stress relaxation in the bolted assembly.

Due to the fact that the viscoplastic deformation behaviour was unknown for preloaded stainless steel bolting assemblies, it was feared, that it might cause higher amount of preload losses in this kind of preloaded bolted connections than in carbon steel bolted connections. For this reason, a comprehensive investigation has been conducted to investigate not only the creep behaviour of different stainless steel plates and stress relaxation behaviour of austenitic stainless steel bars but also the relaxation behaviour of different combinations of preloaded bolted connections made of stainless steel.

Investigating the basic preloading behaviour of stainless steel bolting assemblies implies in the first step to carry out tightening tests of stainless steel bolting assemblies to achieve information regarding the interaction behaviour between the applied torque and the achieved preload depending on the lubrication, the friction between the threads of the bolt and the nuts as well as the friction under the head of the bolt. For this reason, tightening tests according to EN ISO 16047 resp. EN 14399-2 have to be performed.

Finally, it can be summarized that preloading of austenitic and lean duplex, duplex and super duplex stainless steel bolting assemblies in property classes 8.8 and 10.9 to specified preload levels $F_{p,C}$* and $F_{p,C}$ is in principle possible by choosing a suitable material pairing and lubrication. It seems, as if a preload level of $F_{p,C}$* can be reliably achieved with a suitable lubricant using the torque method. Although the torque method is not the best tightening method in form of reliability, it is the most applied tightening procedure in the daily practice of erection steel structures. Taking this for the practitioners very important circumstance into account, in future work, the parameters for secure tightening of stainless steel bolting assemblies using bolts acc. to EN ISO 4014/4017 shall be determined for all bolt dimensions.

The presented investigations and findings can only provide an initial insight into the tightening behaviour of stainless steel bolting assemblies. Based on the presented investigations, the most promising lubricants for stainless steel bolting assemblies are DOW Corning Molykote® 1000 spray and DOW Corning Molykote® D-321R-spray.

As a result of these investigations, it can be summarized that the loss of preload is mainly due to the embedment/plastic deformation of the clamped component surfaces and stress relaxation of the bolts. The influence of creep and stress relaxation in the plate material on the loss of preload seems to be negligible. The overall loss of preload extrapolated to 50 years in bolted connections is in agreement with the asymptotic stress relaxation by the Hart's model found from stress relaxation testing of cold drawn bar.

The loss of preload in preloaded stainless steel bolted connections with different grades of bolts and plates is similar to preloaded carbon steel bolted connections. This shows that the high concern about the loss of preload due to relaxation and creep seems to be unreasonable.

Essen, 30.03.2018

Univ.-Prof. Dr.-Ing. habil. Natalie Stranghöner

Christoph Abraham B.Sc.

Nariman Afzali M.Sc.

Dominik Jungbluth M.Sc.

# 6 References

[1] EN 1090-2:2008+A1:2011, Execution of steel structures and aluminium structures - Part 2: Technical requirements for steel structures.

[2] Stranghöner, N.; Jungbluth, D.; Abraham, Chr.; Söderman, A.: Tightening behaviour of preloaded stainless steel bolting assemblies, Steel Construction 10 (2017), No. 4, pp. 319-332.

[3] EN ISO 16047:2013-01, Fasteners — Torque/clamp force testing (ISO 16047:2005 + Amd 1:2012).

[4] EN 14399-2:2015, High-strength structural bolting assemblies for preloading — Part 2: Suitability for preloading.

[5] EN 15048-1:2007, Non-preloaded structural bolting assemblies - Part 1: General requirements

[6] EN 14399-1:2015, High-strength structural bolting assemblies for preloading - Part 1: General requirements

[7] EN 1993-1-8:2010-12, Eurocode 3: Design of steel structures — Part 1-8: Design of joints (EN 1993-1-8:2005 + AC:2009).

[8] EN ISO 3506-1, Mechanical properties of corrosion-resistant stainless steel fasteners – Part 1: Bolts, screws and studs (ISO 3506-1:2009).

[9] EN ISO 3506-2, Mechanical properties of corrosion-resistant stainless steel fasteners – Part 2: Nuts (ISO 3506-2:2009).

[10] EN 14399-3:2015, High-strength structural bolting assemblies for preloading – Part 3: System HR – Hexagon bolt and nut assemblies.

[11] EN 14399-4:2015, High-strength structural bolting assemblies for preloading – Part 4: System HV – Hexagon bolt and nut assemblies.

[12] EN ISO 4014:2011, Hexagon head bolts — Product grades A and B (ISO 4014:2011).

[13] EN ISO 4017:2014, Fasteners – Hexagon head screws — Product grades A and B (ISO 4017:2014).

[14] Schmidt, H.; Stranghöner, N. Ausführung geschraubter Verbindungen nach DIN EN 1090-2. In (Kuhlmann, U. Ed.): Stahlbau-Kalender 2011. Eurocode 3 - Grundnorm, Verbindungen. Ernst & Sohn GmbH & Co. KG, Berlin, 2011; pp. 283–340.

[15] Kindmann, R.; Vette, J. Merkblatt 322. Geschraubte Verbindungen im Stahlbau, 2012.

[16] EN ISO 898-1:2013, Mechanical properties of fasteners made of carbon steel and alloy steel – Part 1: Bolts, screws and studs with specified property classes – Coarse thread and fie pitch thread (ISO 898-1:2013).

[17] DIN EN 1993-1-8/NA:2010-12, National Annex – Nationally determined parameters – Eurocode 3: Design of steel structures – Part 1-8: Design of joints.

[18] bauforumstahl e.V. Arbeitshilfe 5.3. Ausführung von Stahlbauten - Geschraubte Verbindungen - Planmäßiges Vorspannen, 2013.

[19] Thomala, W.; Kloos, K.-H. Schraubenverbindungen. Grundlagen, Berechnung, Eigenschaften, Handhabung. Springer-Verlag, Berlin, Heidelberg, 2007.

[20] Abraham, Chr., Tightening behaviour of stainless steel bolting assemblies with regard to suitability as high strength structural bolting assemblies for preloading, Bachelor-Thesis, Institute for Metal and Lightweight Structures, University of Duisburg-Essen, 2016.

[21] Stranghöner, N.; Lorenz, C. Numerische Simulation des Anzieh-verhaltens von

Schraubenverbindungen unter Berücksichtigung des plastischen Materialverhaltens: 20. DASt-Forschungskolloquium; pp. 101–106.

[22] EN 1993-1-4:2015, Eurocode 3: Design of steel structures – Part 1-4: General rules – Supplementary rules for stainless steels; EN 1993-1-4:2006 + A1:2015.

[23] Euro Inox and The Steel Construction Institute Bemessungshilfen zu nichtrostenden Stählen im Bauwesen. Euro Inox, Brussels, 2006.

[24] Salih, E. L.; Gardner, L.; Nethercot, D. A. Numerical investigation of net section failure in stainless steel bolted connections. In Journal of Constructional Steel Research, 2010, 66; pp. 1455–1466.

[25] EN 1090-1, Execution of steel structures and aluminium structures - Part 1: Requirements for conformity assessment of structural components; German version EN 1090-1:2009+A1:2011

[26] EN ISO 4032:2013-04, Hexagon regular nuts (style 1) — Product grades A and B (ISO 4032:2012).

[27] Afzali, N., Pilhagen, J., Manninen, T., Schedin, E., Stranghöner, N.: Creep and Relaxation Behaviour of Stainless Steel Bolted Assemblies, Fifth International Experts Seminar, Stainless Steel in Structures, Organised by The Steel Construction Institute (SCI), London, UK, 18-19 September 2017.

[28] Manninen, T., Pilhagen, J.: Deliverable 5.2 - Creep and stress relaxation behavior of stainless steel plates at room temperature, SIROCO, March 2018.

[29] Pilhagen, J.: Deliverable 5.3 - Mechanical properties and stress relaxation of stainless bolts, SIROCO, June 2017.

[30] EN ISO 7089:2000-11, Plain washers — Normal series, Product grade A (ISO 7089:2000).

[31] Stranghöner, N.; Jungbluth, D.; Afzali, N.; Lorenz, C.: Einblick in das Vorspannverhalten von geschraubten Verbindungen aus nichtrostendem Stahl, Stahlbau 86 (2017), Heft 4, S. 302-314.

[32] Stranghöner, N.; Jungbluth, D.; Afzali, N.: Preloading of stainless steel bolting assemblies, Proceedings of Eurosteel 2017 Conference, Copenhagen, Denmark, ce/papers 1 (2017), Issue 2-3, p. 342–351.

[33] Heistermann, C. (2011). Behaviour of Pretensioned Bolts in Friction Connections. Licentiate Thesis, Luleå University of Technology, Lulea.

[34] Katzung, W./Pfeiffer, H./Schneider, A.: Zum Vorspannkraftabfall in planmäßig vorgespannten Schraubenverbindungen mit beschichteten Kontaktflächen. Stahlbau 65 (1996), 307–311.

[35] Reuther, D., Baker, I., Yetka, A., Cleary, D. B., & Riddell, W. (2014). Relaxation of ASTM A325 Bolted Assemblies. Journal of Structural Engineering, 140(9), 01014060-1 - 04014060-7.

[36] Yang, J., & DeWolf, J. T. (1999). Mathematical Model for Relaxation in High Strength Bolted Connections. Journal of Structural Engineering, 125(8), 803-809.

[37] Yang, J., & DeWolf, J. T. (2000). Relaxation in High-Strength Bolted Connections Using Galvanized Steel. Journal of Bridge Engineering, 5(2), 99-106.

# 7 Annex A: Loss of preload

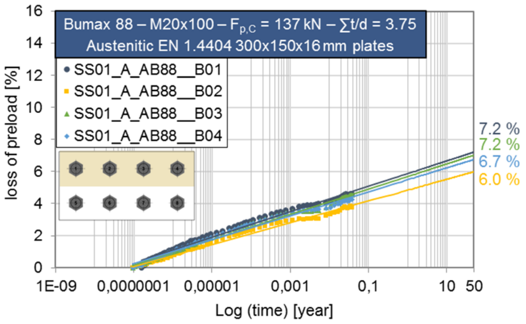


(a) preload losses-log (time) diagrams for eight-bolts specimens - first row

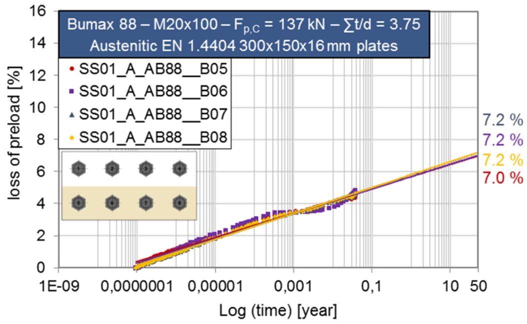


(b) preload losses-log (time) diagrams for eight-bolts specimens - second row

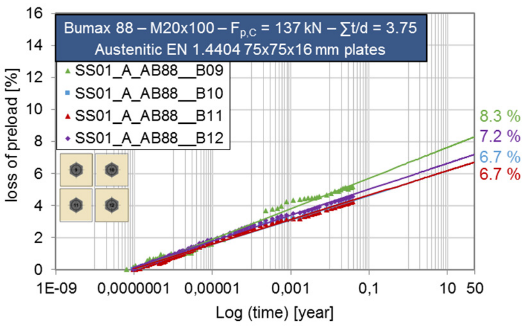


(c) preload losses-log (time) diagrams for one-bolt specimens

| Loss of preload min / mean / max [%] | |
|---|---|
| measured after 14 days | after 50 years (extrapolated) |
| 3.7 / 4.6 / 6.0 | 6.0 / 7.0 / 8.3 |

(d) loss preload measured/extrapolated after 14 days/ 50 years

**Figure 137** Preload losses for SS01

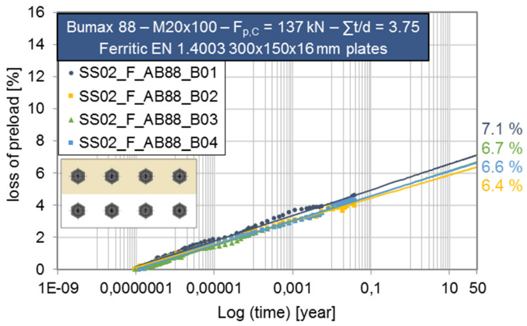


(a) preload losses-log (time) diagrams for eight-bolts specimens - first row

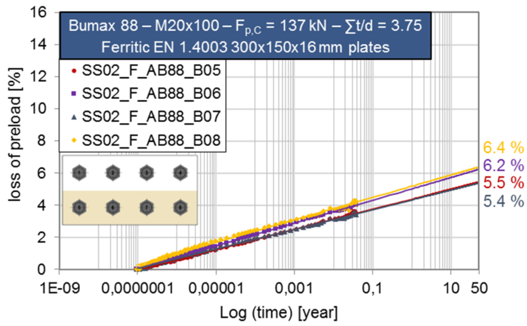


(b) preload losses-log (time) diagrams for eight-bolts specimens - second row

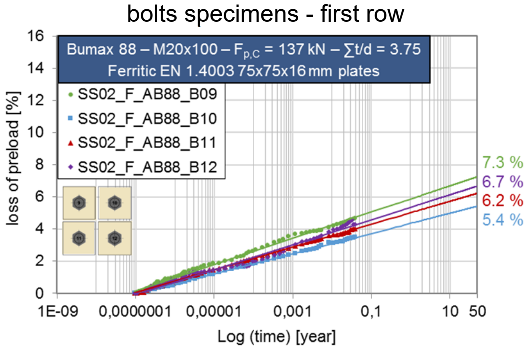


(c) preload losses-log (time) diagrams for one-bolt specimens

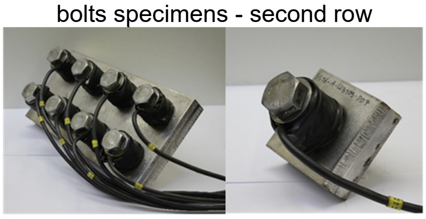

| Loss of preload min / mean / max [%] | |
|---|---|
| measured after 14 days | after 50 years (extrapolated) |
| 3.4 / 4.1 / 4.7 | 5.4 / 6.3 / 7.3 |

(d) loss preload measured/extrapolated after 14 days/ 50 years

**Figure 138** Preload losses for SS02

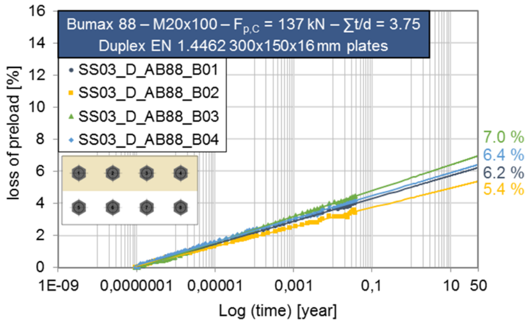


(a) preload losses-log (time) diagrams for eight-bolts specimens - first row

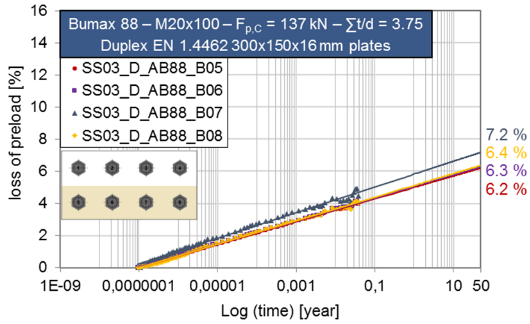


(b) preload losses-log (time) diagrams for eight-bolts specimens - second row

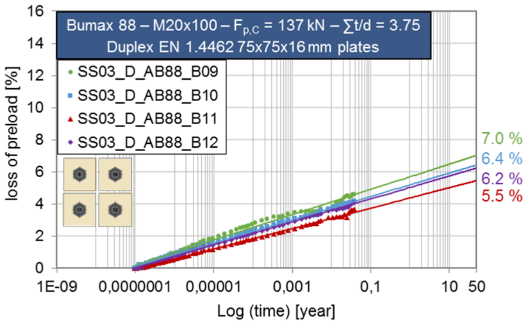


(c) preload losses-log (time) diagrams for one-bolt specimens

| Loss of preload min / mean / max [%] | |
|---|---|
| measured after 14 days | after 50 years (extrapolated) |
| 3.4 / 4.1 / 4.6 | 5.4 / 6.3 / 7.2 |

(d) loss preload measured/extrapolated after 14 days/ 50 years

**Figure 139** Preload losses for SS03

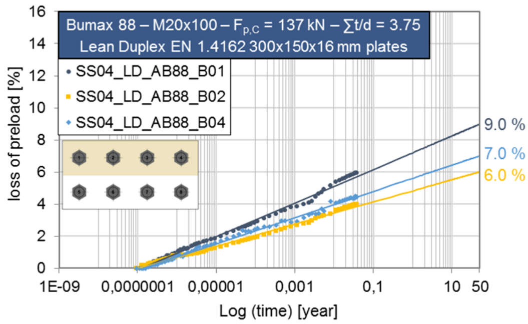


(a) preload losses-log (time) diagrams for eight-bolts specimens - first row

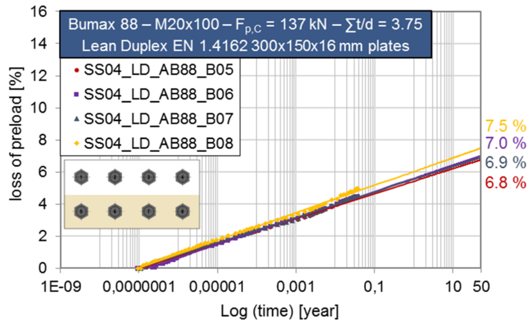


(b) preload losses-log (time) diagrams for eight-bolts specimens - second row

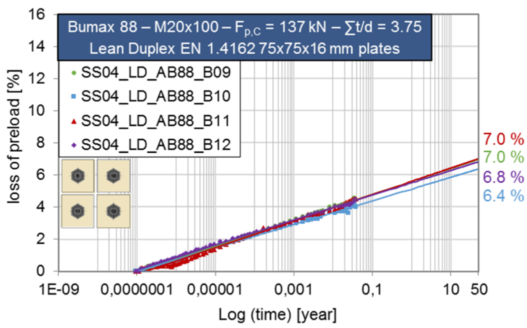


(c) preload losses-log (time) diagrams for one-bolt specimens

| Loss of preload min / mean / max [%] | |
|---|---|
| measured after 14 days | after 50 years (extrapolated) |
| 4.0 / 4.6 / 6.0 | 6.0 / 7.0 / 9.0 |

(d) loss preload measured/extrapolated after 14 days/ 50 years

**Figure 140** Preload losses for SS04

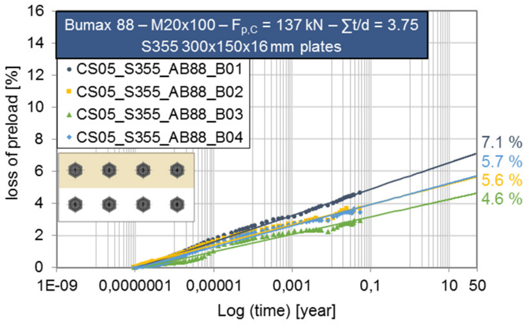


(a) preload losses-log (time) diagrams for eight-bolts specimens - first row

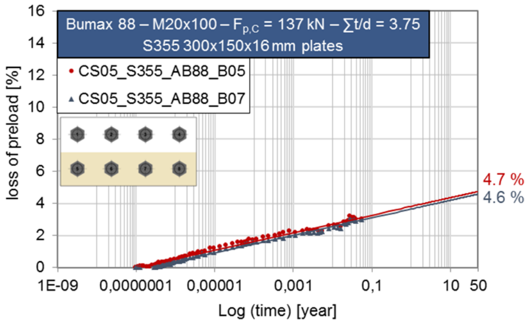


(b) preload losses-log (time) diagrams for eight-bolts specimens - second row

| Loss of preload min / mean / max [%] | |
|---|---|
| measured after 20 days | after 50 years (extrapolated) |
| 2.9 / 3.4 / 4.7 | 4.6 / 5.4 / 7.1 |

(c) loss preload measured/extrapolated after 20 days/ 50 years

**Figure 141** Preload losses for CS05

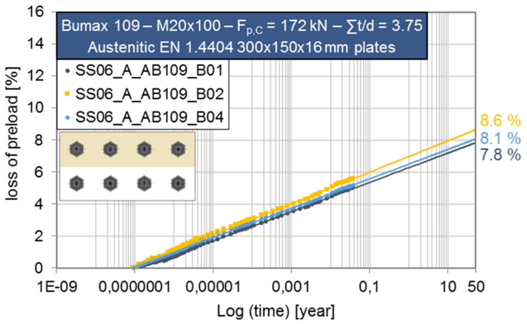


(a) preload losses-log (time) diagrams for eight-bolts specimens - first row

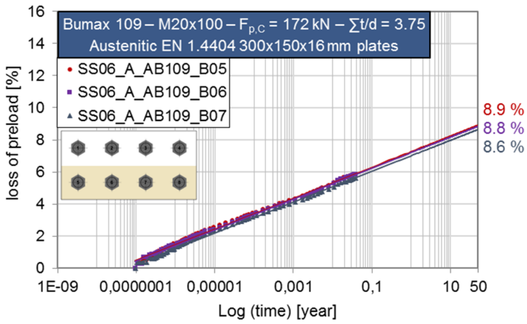


(b) preload losses-log (time) diagrams for eight-bolts specimens - second row

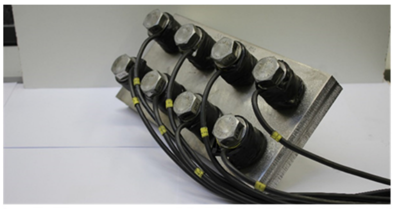

| Loss of preload min / mean / max [%] | |
|---|---|
| measured after 14 days | after 50 years (extrapolated) |
| 5.0 / 5.5 / 5.9 | 7.8 / 8.5 / 8.9 |

(c) loss preload measured/extrapolated after 14 days/ 50 years

**Figure 142** Preload losses for SS06

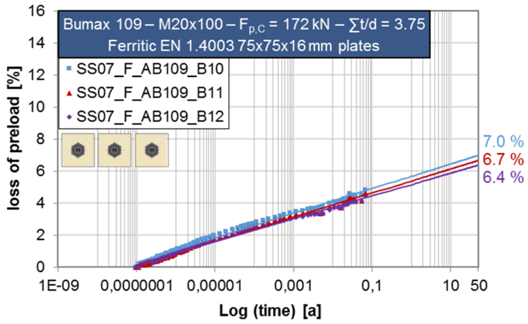


(a) preload losses-log (time) diagrams for one-bolt specimens

| Loss of preload min / mean / max [%] | |
|---|---|
| measured after 25 days | after 50 years (extrapolated) |
| 4.4 / 4.6 / 4.8 | 6.4 / 6.7 / 7.0 |

(b) loss preload measured/extrapolated after 20 days/ 50 years

**Figure 143** Preload losses for SS07

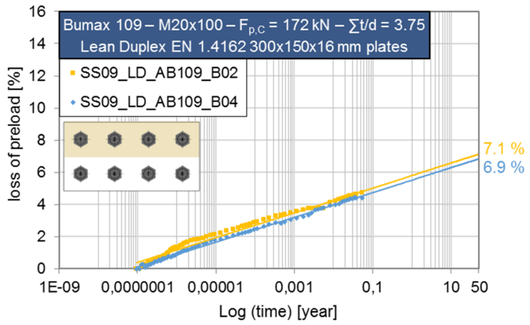


(a) preload losses-log (time) diagrams for eight-bolts specimens - first row

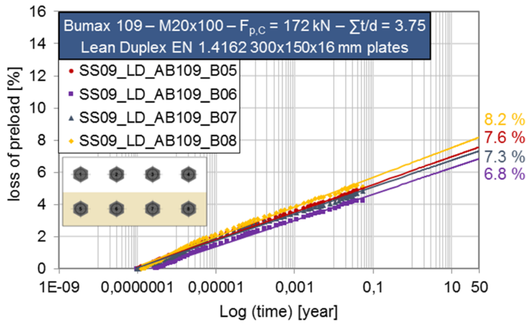


(b) preload losses-log (time) diagrams for eight-bolts specimens - second row

| Loss of preload min / mean / max [%] | |
|---|---|
| measured after 20 days | after 50 years (extrapolated) |
| 4.2 / 4.7 / 5.3 | 6.8 / 7.3 / 8.2 |

(c) loss preload measured/extrapolated after 20 days/ 50 years

**Figure 144** Preload losses for SS09

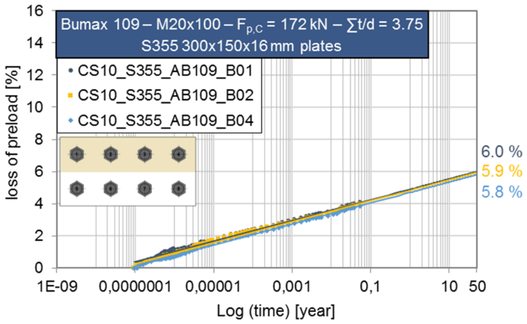


(a) preload losses-log (time) diagrams for eight-bolts specimens - first row

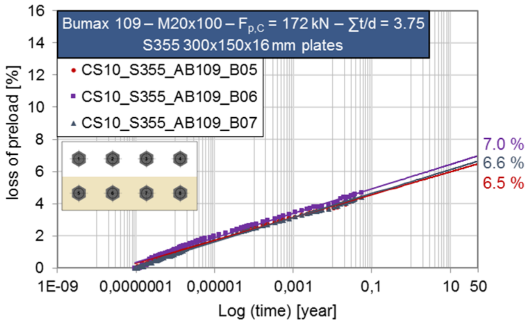


(b) preload losses-log (time) diagrams for eight-bolts specimens - second row

| Loss of preload min /  / max [%] | |
|---|---|
| measured after 14 days | after 50 years (extrapolated) |
| 3.9 / 4.2 / 4.7 | 5.8 / 6.3 / 7.0 |

(c) loss preload measured/extrapolated after 14 days/ 50 years

**Figure 145** Preload losses for CS10

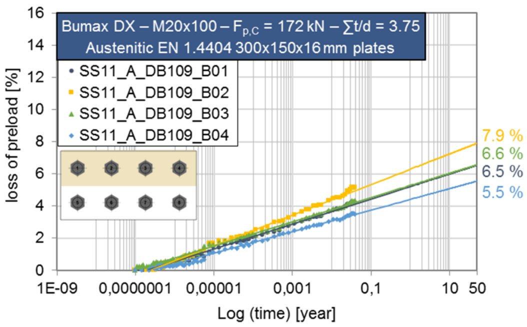


(a) preload losses-log (time) diagrams for eight-bolts specimens - first row

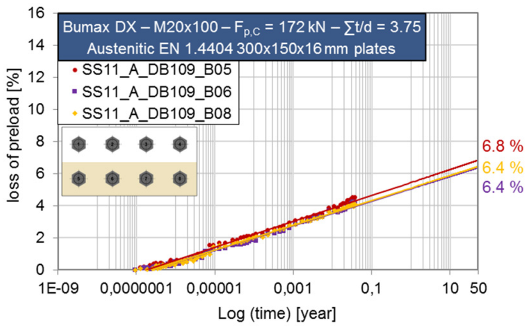


(b) preload losses-log (time) diagrams for eight-bolts specimens - second row

| Loss of preload min / mean / max [%] | |
|---|---|
| measured after 14 days | after 50 years (extrapolated) |
| 3.5 / 4.3 / 5.2 | 5.5 / 6.6 / 7.9 |

(c) loss preload measured/extrapolated after 14 days/ 50 years

**Figure 146** Preload losses for SS11

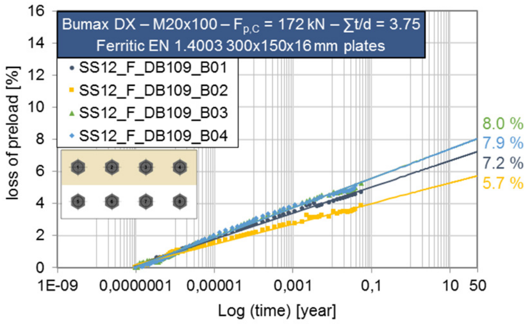


(a) preload losses-log (time) diagrams for eight-bolts specimens - first row

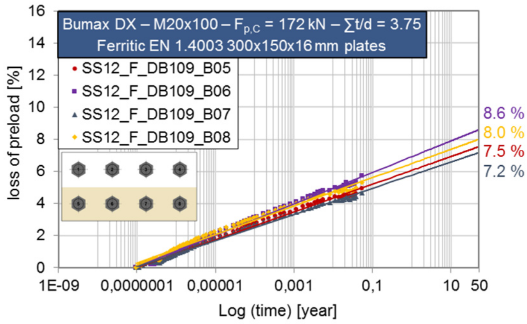


(b) preload losses-log (time) diagrams for eight-bolts specimens - second row

| Loss of preload min / mean / max [%] | |
|---|---|
| measured after 20 days | after 50 years (extrapolated) |
| 3.9 / 5.0 / 5.7 | 5.7 / 7.5 / 8.6 |

(c) loss preload measured/extrapolated after 20 days/ 50 years

**Figure 147** Preload losses for SS12

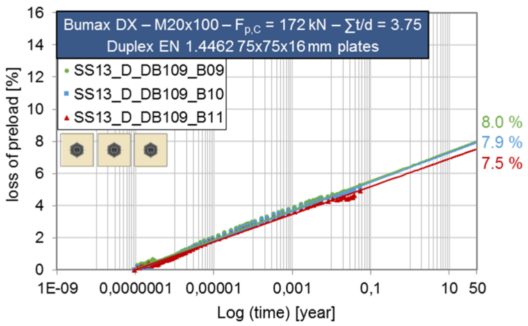


(a) preload losses-log (time) diagrams for one-bolt specimens

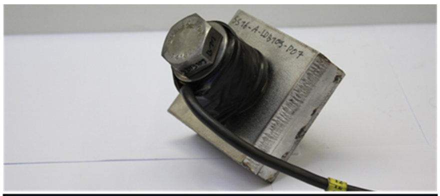

| Loss of preload min / mean / max [%] | |
|---|---|
| measured after 20 days | after 50 years (extrapolated) |
| 4.9 / 5.1 / 5.2 | 7.5 / 7.8 / 8.0 |

(b) loss preload measured/extrapolated after 20 days/ 50 years

**Figure 148** Preload losses for SS13

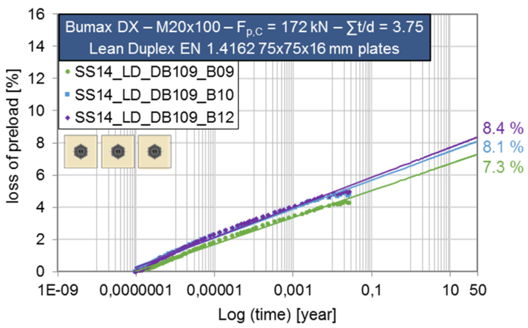


(a) preload losses-log (time) diagrams for one-bolt specimens

| Loss of preload min / mean / max [%] | |
|---|---|
| measured after 10 days | after 50 years (extrapolated) |
| 4.3 / 4.7 / 5.0 | 7.3 / 7.9 / 8.4 |

(b) loss preload measured/extrapolated after 10 days/ 50 years

**Figure 149** Preload losses for SS14

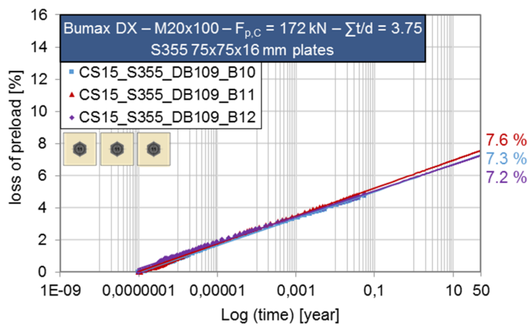


(a) preload losses-log (time) diagrams for one-bolt specimens

| Loss of preload min / mean / max [%] | |
|---|---|
| measured after 20 days | after 50 years (extrapolated) |
| 4.7 / 4.8 / 4.9 | 7.2 / 7.4 / 7.6 |

(b) loss preload measured/extrapolated after 20 days/ 50 years

**Figure 150** Preload losses for CS15

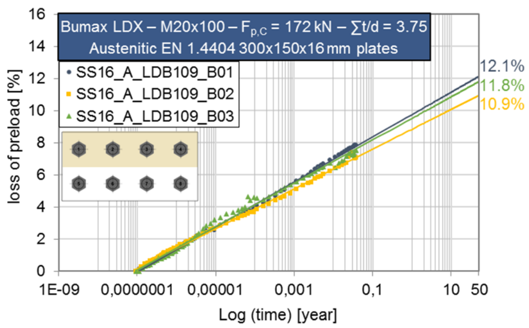


(a) preload losses-log (time) diagrams for eight-bolts specimens - first row

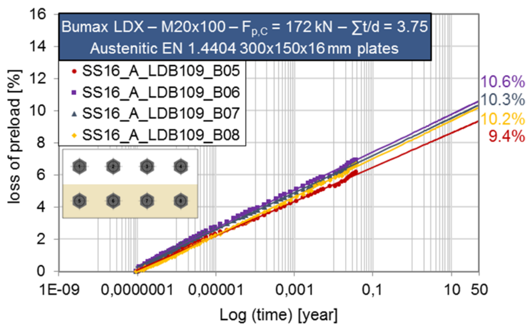


(b) preload losses-log (time) diagrams for eight-bolts specimens - second row

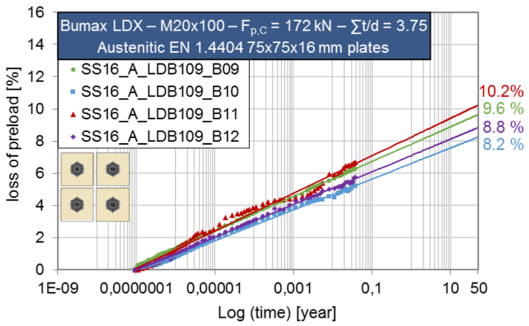


(c) preload losses-log (time) diagrams for one-bolt specimens

| Loss of preload min / mean / max [%] | |
|---|---|
| measured after 14 days | after 50 years (extrapolated) |
| 5.2 / 6.6 / 7.9 | 8.2 / 10.2 / 12.1 |

(d) loss preload measured/extrapolated after 14 days/ 50 years

**Figure 151** Preload losses for SS16

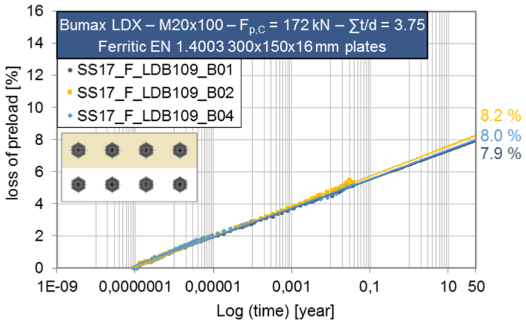


(a) preload losses-log (time) diagrams for eight-bolts specimens - first row

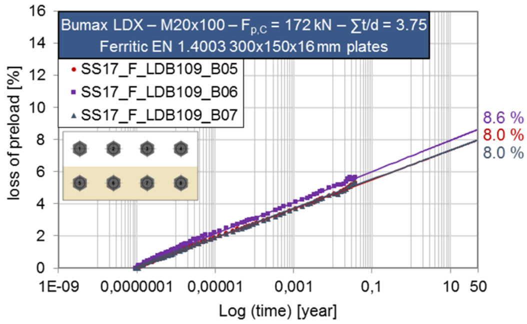


(b) preload losses-log (time) diagrams for eight-bolts specimens - second row

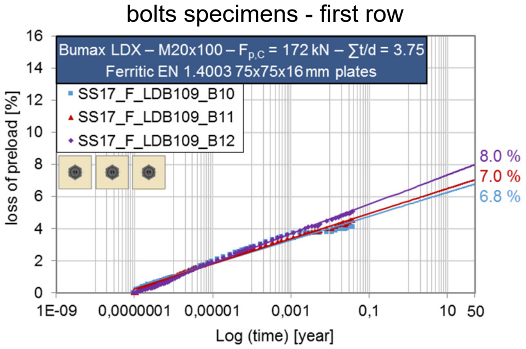


(c) preload losses-log (time) diagrams for one-bolt specimens

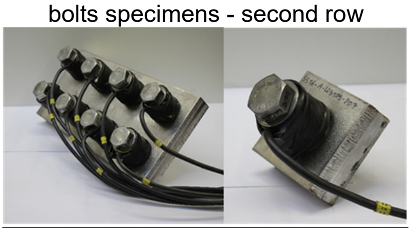

| Loss of preload min / mean / max [%] | |
|---|---|
| measured after 14 days | after 50 years (extrapolated) |
| 4.1 / 5.1 / 5.6 | 6.8 / 7.8 / 8.6 |

(d) loss preload measured/extrapolated after 14 days/ 50 years

**Figure 152** Preload losses for SS17

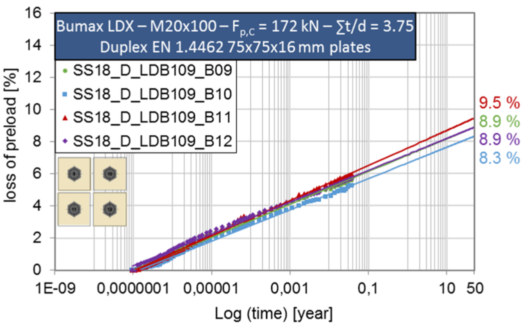


(a) preload losses-log (time) diagrams for one-bolt specimens

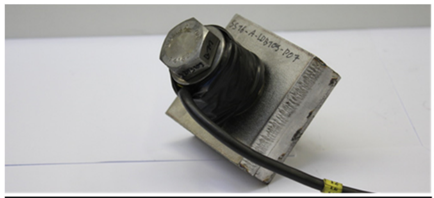

| Loss of preload min / mean / max [%] | |
|---|---|
| measured after 14 days | after 50 years (extrapolated) |
| 5.2 / 5.6 / 5.9 | 8.3 / 8.9 / 9.5 |

(b) loss preload measured/extrapolated after 14 days/ 50 years

**Figure 153** Preload losses for SS18

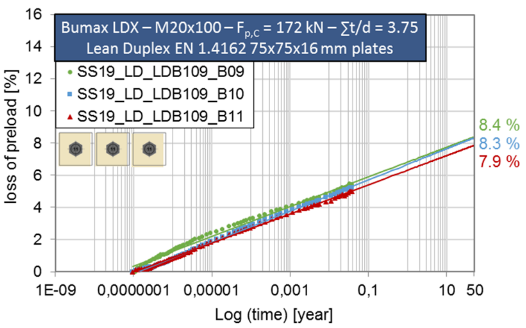


(a) preload losses-log (time) diagrams for one-bolt specimens

| Loss of preload min / mean / max [%] | |
|---|---|
| measured after 14 days | after 50 years (extrapolated) |
| 5.0 / 5.2 / 5.4 | 7.9 / 8.2 / 8.4 |

(b) loss preload measured/extrapolated after 14 days/ 50 years

**Figure 154** Preload losses for SS19

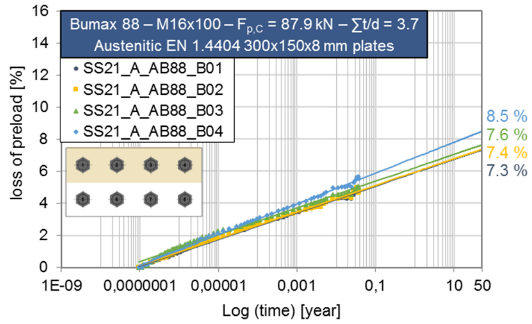


(a) preload losses-log (time) diagrams for eight-bolts specimens - first row

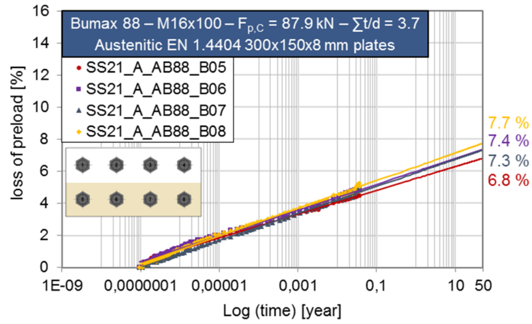


(b) preload losses-log (time) diagrams for eight-bolts specimens - second row

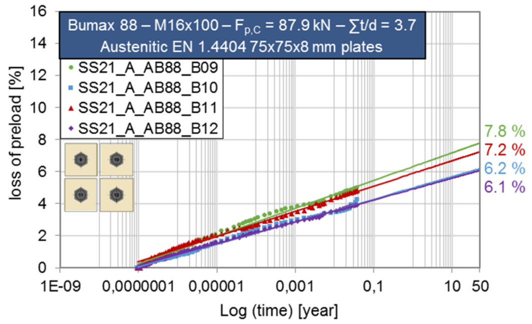


(c) preload losses-log (time) diagrams for one-bolt specimens

| Loss of preload min / mean / max [%] | |
|---|---|
| measured after 14 days | after 50 years (extrapolated) |
| 3.9 / 4.8 / 5.5 | 6.1 / 7.3 / 8.5 |

(d) loss preload measured/extrapolated after 14 days/ 50 years

**Figure 155** Preload losses for SS21

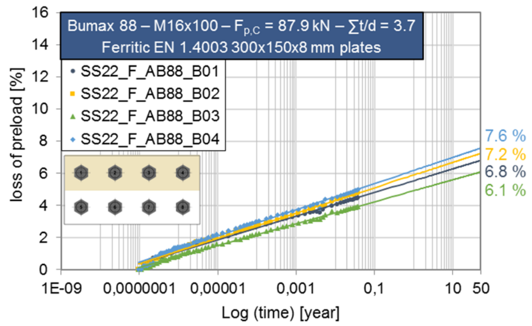


(a) preload losses-log (time) diagrams for eight-bolts specimens - first row

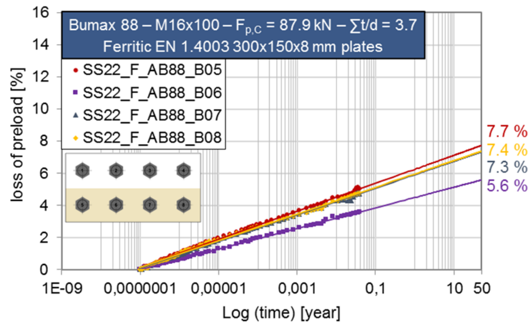


(b) preload losses-log (time) diagrams for eight-bolts specimens - second row

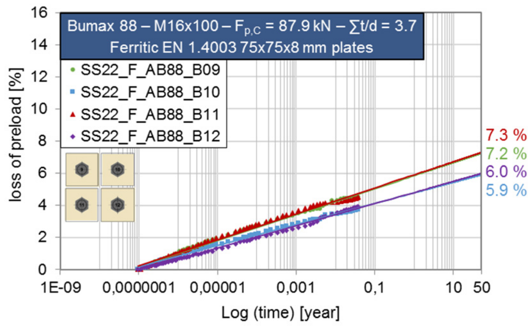


(c) preload losses-log (time) diagrams for one-bolt specimens

| Loss of preload min / mean / max [%] | |
|---|---|
| measured after 14 days | after 50 years (extrapolated) |
| 3.6 / 4.4 / 5.0 | 5.6 / 6.8 / 7.7 |

(d) loss preload measured/extrapolated after 14 days/ 50 years

**Figure 156** Preload losses for SS22

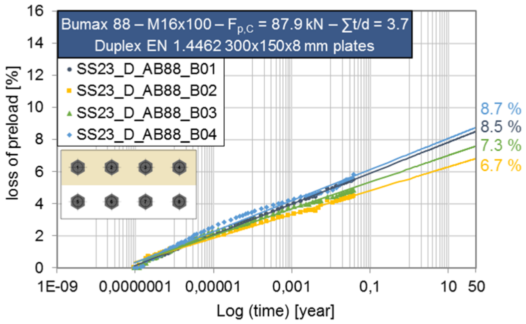


(a) preload losses-log (time) diagrams for eight-bolts specimens - first row

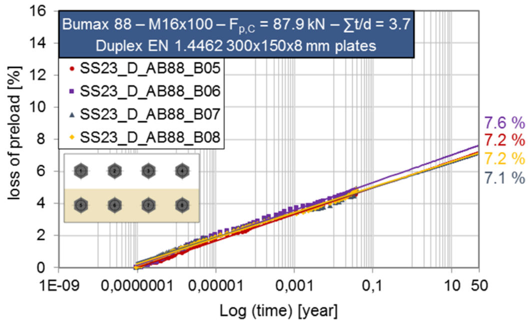


(b) preload losses-log (time) diagrams for eight-bolts specimens - second row

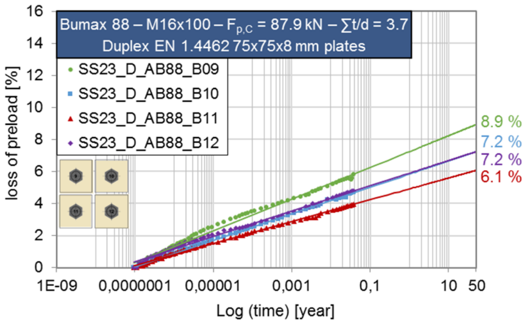


(c) preload losses-log (time) diagrams for one-bolt specimens

| Loss of preload min / mean / max [%] | |
|---|---|
| measured after 14 days | after 50 years (extrapolated) |
| 3.9 / 4.9 / 5.8 | 6.1 / 7.5 / 8.9 |

(d) loss preload measured/extrapolated after 14 days/ 50 years

**Figure 157** Preload losses for SS23

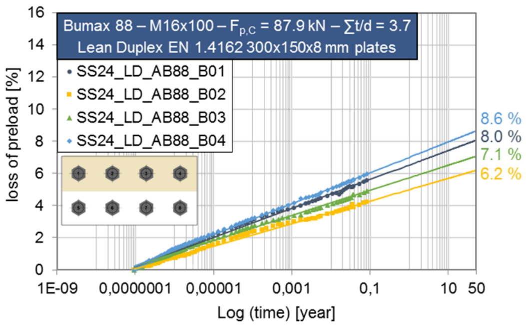


(a) preload losses-log (time) diagrams for eight-bolts specimens - first row

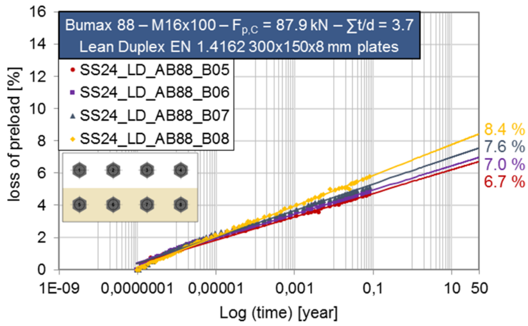


(b) preload losses-log (time) diagrams for eight-bolts specimens - second row

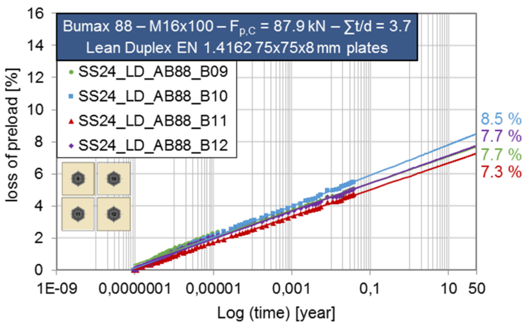


(c) preload losses-log (time) diagrams for one-bolt specimens

| Loss of preload min / mean / max [%] | |
|---|---|
| measured after 14 days | after 50 years (extrapolated) |
| 3.9 / 4.9 / 5.6 | 6.2 / 7.6 / 8.6 |

(d) loss preload measured/extrapolated after 14 days/ 50 years

**Figure 158** Preload losses for SS24

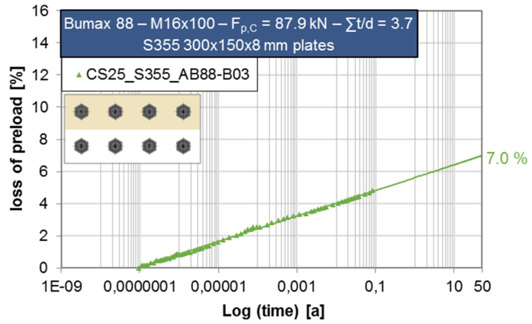


(a) preload losses-log (time) diagrams for eight-bolts specimens - first row

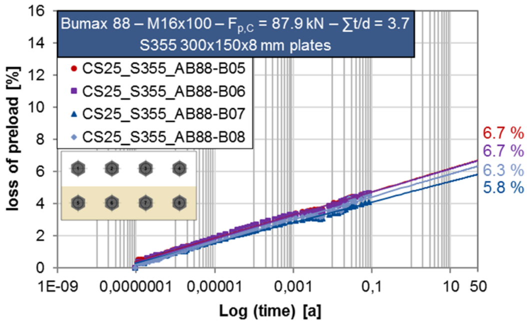


(b) preload losses-log (time) diagrams for eight-bolts specimens - second row

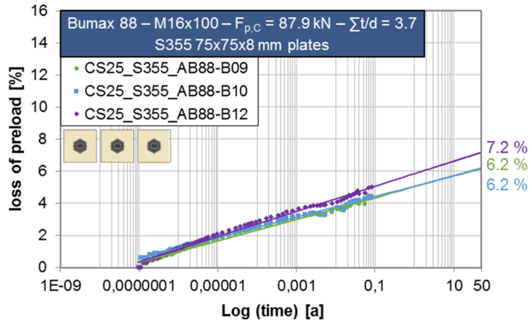


(c) preload losses-log (time) diagrams for one-bolt specimens

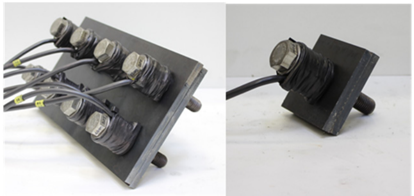

| Loss of preload min / mean / max [%] | |
|---|---|
| measured after 30 days | after 50 years (extrapolated) |
| 4.1 / 4.6 / 5.0 | 5.8 / 6.5 / 7.2 |

(d) loss preload measured/extrapolated after 30 days/ 50 years

**Figure 159** Preload losses for CS25

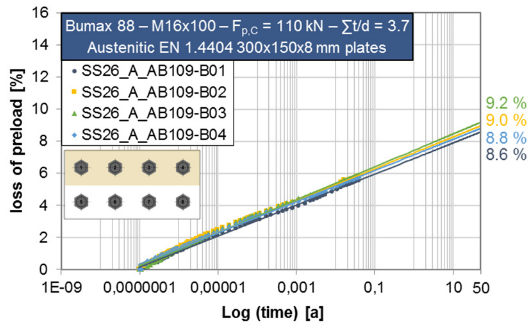


(a) preload losses-log (time) diagrams for eight-bolts specimens - first row

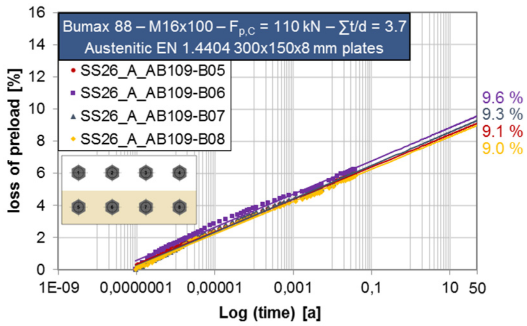


(b) preload losses-log (time) diagrams for eight-bolts specimens - second row

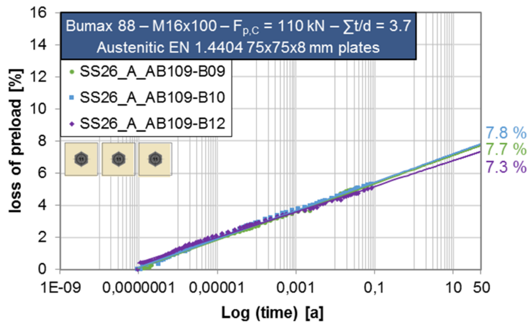


(c) preload losses-log (time) diagrams for one-bolt specimens

| Loss of preload min / mean / max [%] | |
|---|---|
| measured after 14 days | after 50 years (extrapolated) |
| 4.8 / 5.6 / 6.3 | 7.3 / 8.7 / 9.6 |

(d) loss preload measured/extrapolated after 14 days/ 50 years

**Figure 160** Preload losses for SS26

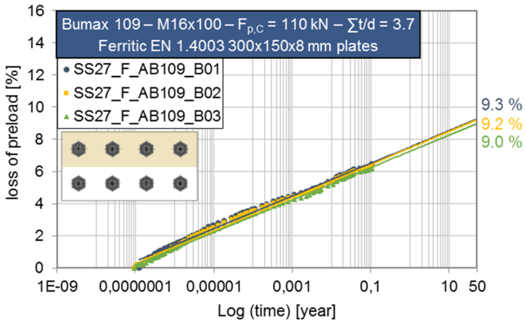


(a) preload losses-log (time) diagrams for eight-bolts specimens - first row

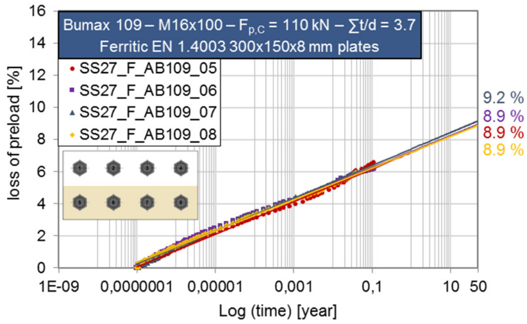


(b) preload losses-log (time) diagrams for eight-bolts specimens - second row

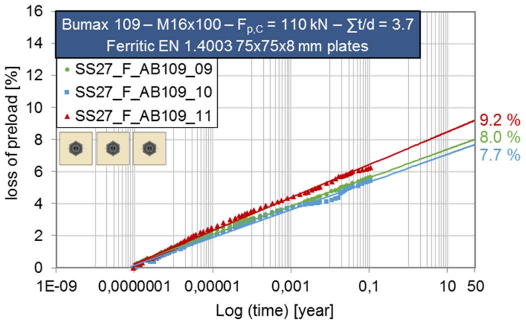


(c) preload losses-log (time) diagrams for one-bolt specimens

| Loss of preload min / mean / max [%] | |
|---|---|
| measured after 40 days | after 50 years (extrapolated) |
| 5.4 / 6.1 / 6.6 | 7.7 / 8.8 / 9.3 |

(d) loss preload measured/extrapolated after 40 days/ 50 years

**Figure 161** Preload losses for SS27

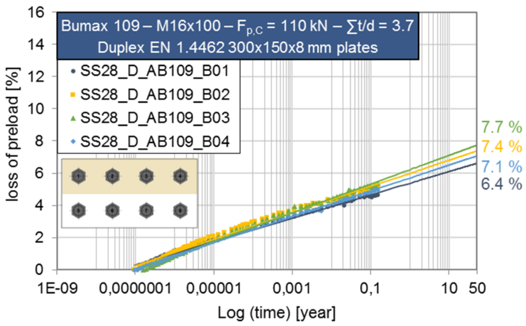


(a) preload losses-log (time) diagrams for eight-bolts specimens - first row

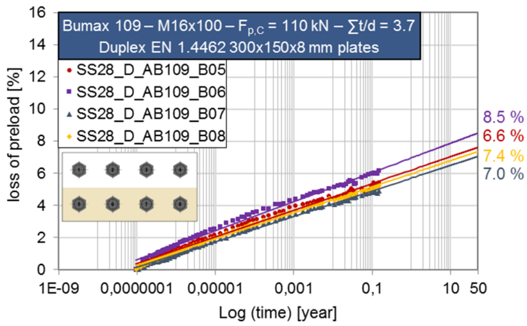


(b) preload losses-log (time) diagrams for eight-bolts specimens - second row

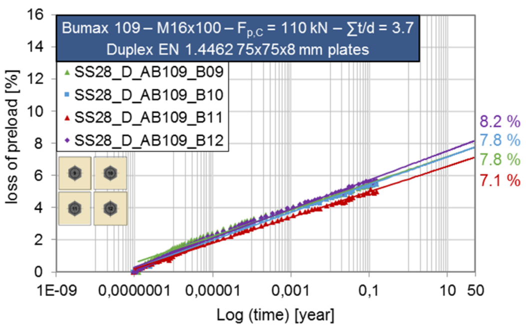


(c) preload losses-log (time) diagrams for one-bolt specimens

| Loss of preload min / mean / max [%] | |
|---|---|
| measured after 55 days | after 50 years (extrapolated) |
| 4.6 / 5.3 / 6.1 | 6.4 / 7.5 / 8.5 |

(d) loss preload measured/extrapolated after 55 days/ 50 years

**Figure 162** Preload losses for SS28

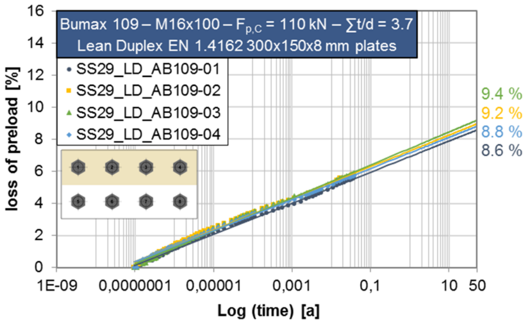


(a) preload losses-log (time) diagrams for eight-bolts specimens - first row

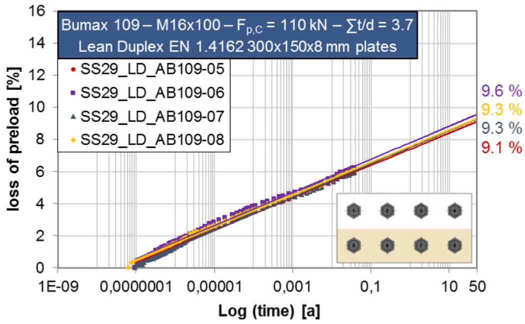


(b) preload losses-log (time) diagrams for eight-bolts specimens - second row

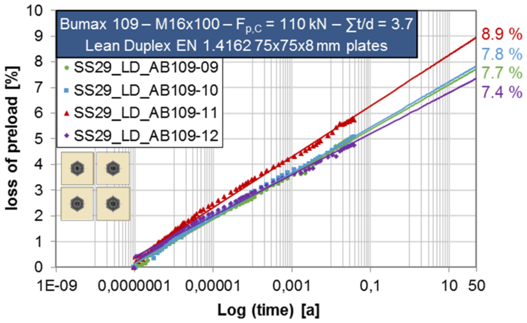


(c) preload losses-log (time) diagrams for one-bolt specimens

| Loss of preload min / mean / max [%] | |
|---|---|
| measured after 14 days | after 50 years (extrapolated) |
| 4.8 / 5.6 / 6.3 | 7.4 / 8.8 / 9.6 |

(d) loss preload measured/extrapolated after 14 days/ 50 years

**Figure 163** Preload losses for SS29

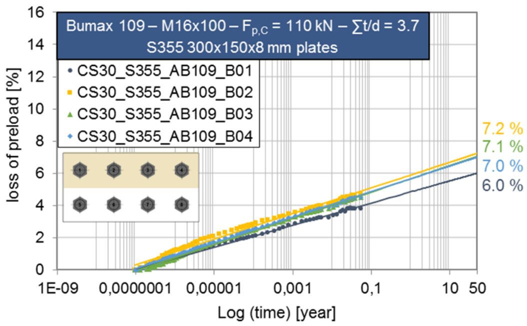


(a) preload losses-log (time) diagrams for eight-bolts specimens - first row

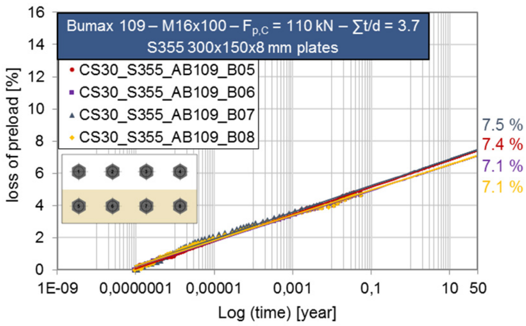


(b) preload losses-log (time) diagrams for eight-bolts specimens - second row

| Loss of preload min / mean / max [%] | |
|---|---|
| measured after 20 days | after 50 years (extrapolated) |
| 3.8 / 4.5 / 4.8 | 6.0 / 7.0 / 7.5 |

(c) loss preload measured/extrapolated after 20 days/ 50 years

**Figure 164** Preload losses for CS30

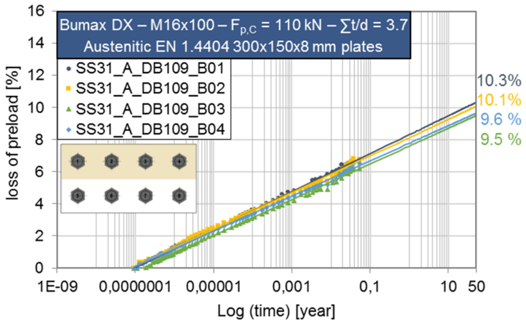


(a) preload losses-log (time) diagrams for eight-bolts specimens - first row

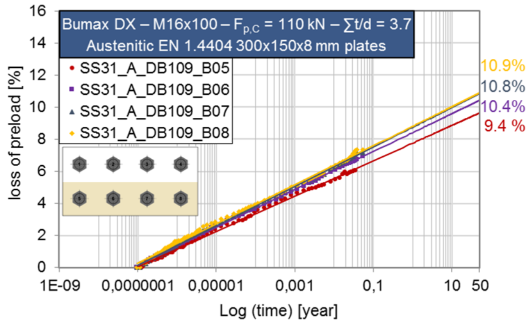


(b) preload losses-log (time) diagrams for eight-bolts specimens - second row

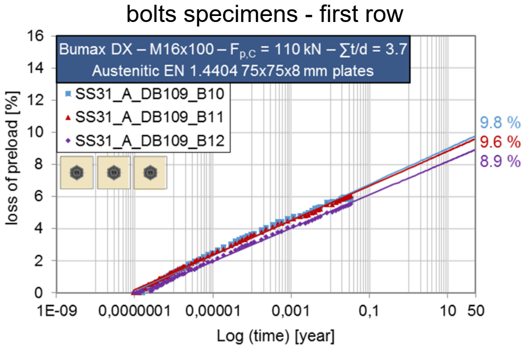


(c) preload losses-log (time) diagrams for one-bolt specimens

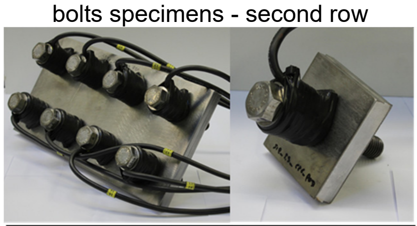

| Loss of preload min / mean / max [%] | |
|---|---|
| measured after 12 days | after 50 years (extrapolated) |
| 5.5 / 6.5 / 7.2 | 8.9 / 9.9 / 10.9 |

(d) loss preload measured/extrapolated after 12 days/ 50 years

**Figure 165** Preload losses for SS31

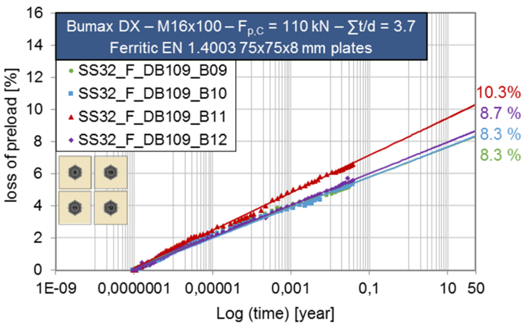


(a) preload losses-log (time) diagrams for one-bolt specimens

| Loss of preload min / mean / max [%] | |
|---|---|
| measured after 14 days | after 50 years (extrapolated) |
| 5.4 / 5.8 / 6.6 | 8.3 / 9.0 / 10.3 |

(b) loss preload measured/extrapolated after 14 days/ 50 years

**Figure 166** Preload losses for SS32

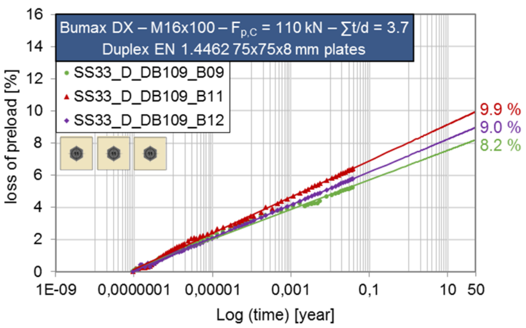


(a) preload losses-log (time) diagrams for one-bolt specimens

| Loss of preload min / mean / max [%] | |
|---|---|
| measured after 14 days | after 50 years (extrapolated) |
| 5.2 / 5.8 / 6.4 | 8.2 / 9.0 / 9.9 |

(b) loss preload measured/extrapolated after 1 days/ 50 years

**Figure 167** Preload losses for SS33

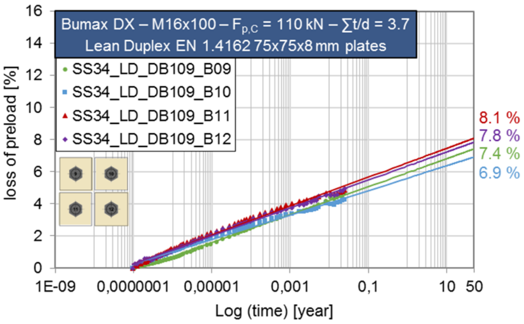


(a) preload losses-log (time) diagrams for one-bolt specimens

| Loss of preload min / max [%] | |
|---|---|
| measured after 9 days | after 50 years (extrapolated) |
| 4.3 / 4.7 / 5.0 | 6.9 / 7.6 / 8.1 |

(b) loss preload measured/extrapolated after 9 days/ 50 years

**Figure 168** Preload losses for SS34

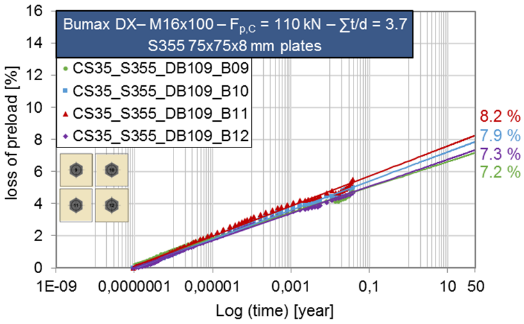


(a) preload losses-log (time) diagrams for one-bolt specimens

| Loss of preload min / max [%] | |
|---|---|
| measured after 14 days | after 50 years (extrapolated) |
| 4.7 / 5.0 / 5.5 | 7.2 / 7.7 / 8.2 |

(b) loss preload measured/extrapolated after 14 days/ 50 years

**Figure 169** Preload losses for CS35

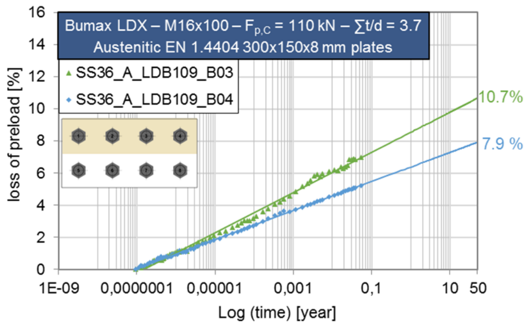


(a) preload losses-log (time) diagrams for eight-bolts specimens - first row

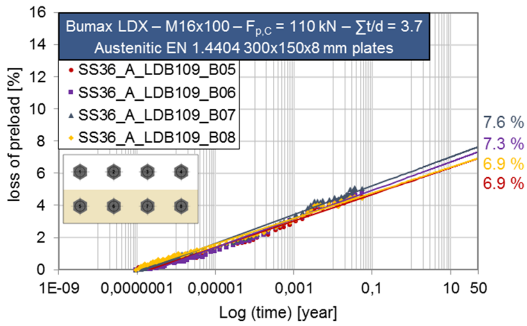


(b) preload losses-log (time) diagrams for eight-bolts specimens - second row

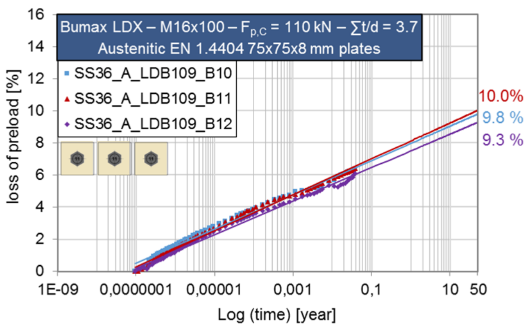


(c) preload losses-log (time) diagrams for one-bolt specimens

| Loss of preload min / mean / max [%] | |
|---|---|
| measured after 14 days | after 50 years (extrapolated) |
| 4.5 / 5.5 / 6.8 | 6.9 / 8.5 / 10.7 |

(d) loss preload measured/extrapolated after 14 days/ 50 years

**Figure 170** Preload losses for SS36

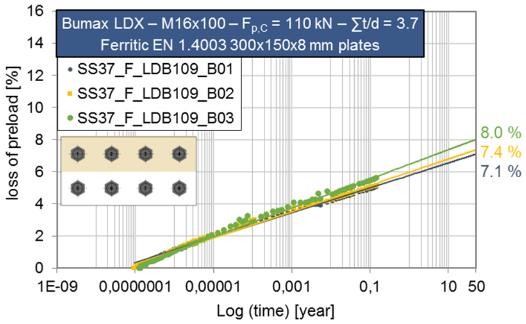


(a) preload losses-log (time) diagrams for eight-bolts specimens - first row

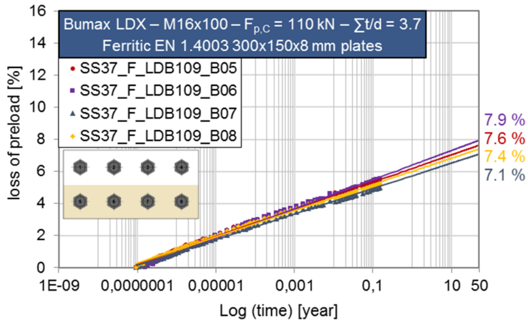


(b) preload losses-log (time) diagrams for eight-bolts specimens - second row

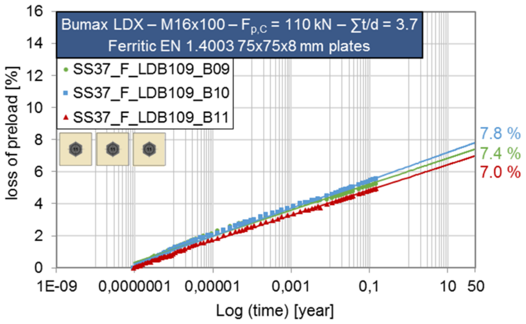


(c) preload losses-log (time) diagrams for one-bolt specimens

| Loss of preload min / mean / max [%] | |
|---|---|
| measured after 55 days | after 50 years (extrapolated) |
| 4.9 / 5.3 / 5.6 | 7.0 / 7.5 / 8.0 |

(d) loss preload measured/extrapolated after 55 days/ 50 years

**Figure 171** Preload losses for SS37

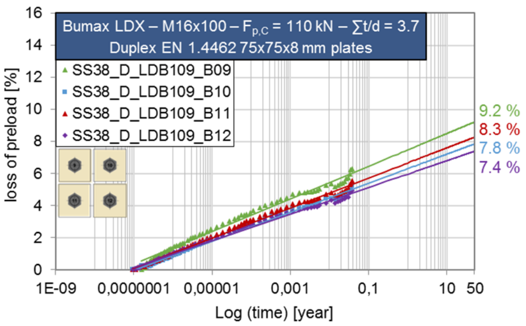


(a) preload losses-log (time) diagrams for one-bolt specimens

| Loss of preload min / mean / max [%] | |
|---|---|
| measured after 14 days | after 50 years (extrapolated) |
| 4.9 / 5.5 / 6.3 | 7.4 / 8.2 / 9.2 |

(b) loss preload measured/extrapolated after 14 days/ 50 years

**Figure 172** Preload losses for SS38

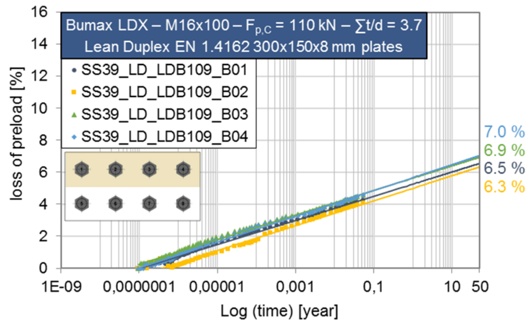


(a) preload losses-log (time) diagrams for eight-bolts specimens - first row

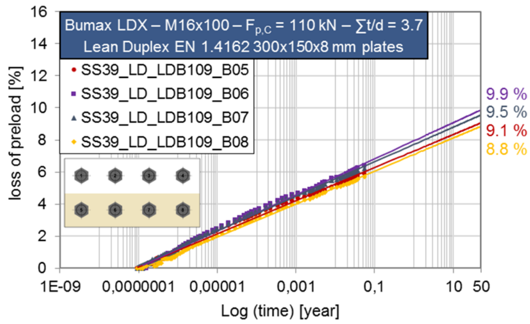


(b) preload losses-log (time) diagrams for eight-bolts specimens - second row

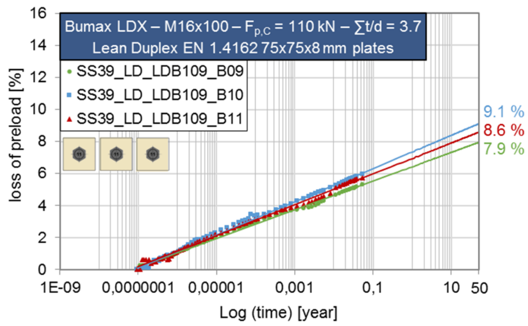


(c) preload losses-log (time) diagrams for one-bolt specimens

| Loss of preload min / mean / max [%] | |
|---|---|
| measured after 20 days | after 50 years (extrapolated) |
| 4.1 / 5.3 / 6.4 | 6.3 / 8.2 / 9.9 |

(d) loss preload measured/extrapolated after 20 days/ 50 years

**Figure 173** Preload losses for SS39

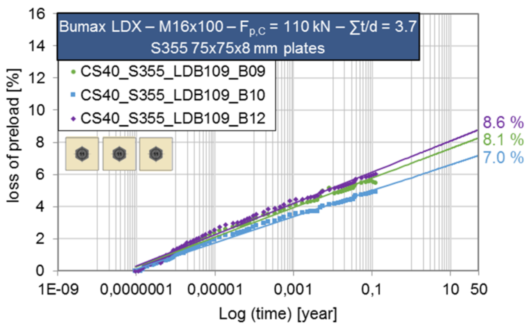


(a) preload losses-log (time) diagrams for one-bolt specimens

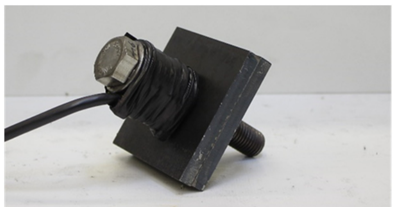

| Loss of preload min / mean / max [%] | |
|---|---|
| measured after 55 days | after 50 years (extrapolated) |
| 5.0 / 5.6 / 6.1 | 7.0 / 7.9 / 8.6 |

(b) loss preload measured/extrapolated after 55 days/ 50 years

**Figure 174** Preload losses for CS40

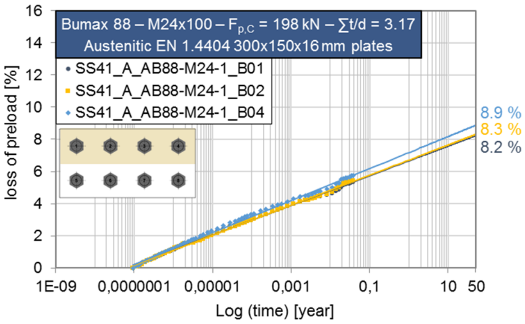


(a) preload losses-log (time) diagrams for eight-bolts specimens - first row

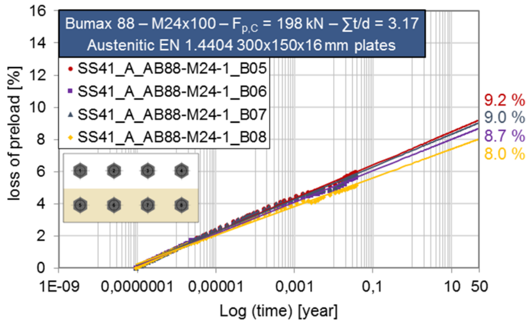


(b) preload losses-log (time) diagrams for eight-bolts specimens - second row

| Loss of preload min / mean / max [%] | |
|---|---|
| measured after 14 days | after 50 years (extrapolated) |
| 5.1 / 5.7 / 6.2 | 8.0 / 8.6 / 9.2 |

(c) loss preload measured/extrapolated after 14 days/ 50 years

**Figure 175** Preload losses for SS41

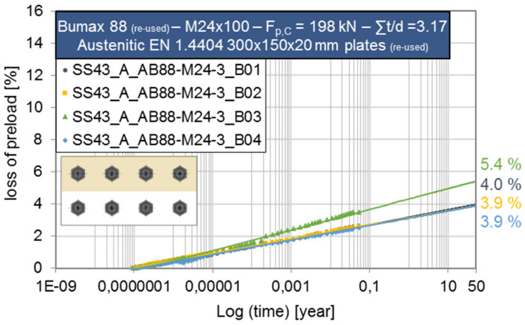


(a) preload losses-log (time) diagrams for eight-bolts specimens - first row

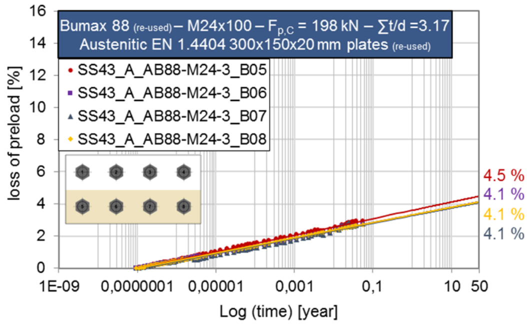


(b) preload losses-log (time) diagrams for eight-bolts specimens - second row

| Loss of preload min / mean / max [%] | |
|---|---|
| measured after 25 days | after 50 years (extrapolated) |
| 2.6 / 2.8 / 3.6 | 3.9 / 4.2 / 5.4 |

(c) loss preload measured/extrapolated after 25 days/ 50 years

**Figure 176** Preload losses for SS42

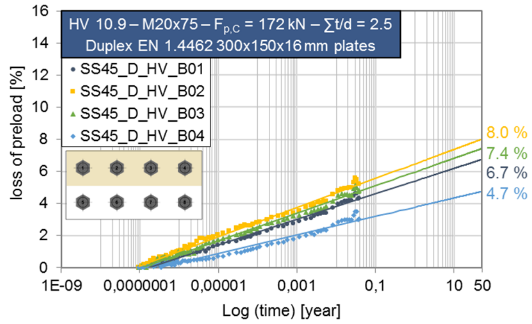


(a) preload losses-log (time) diagrams for eight-bolts specimens - first row

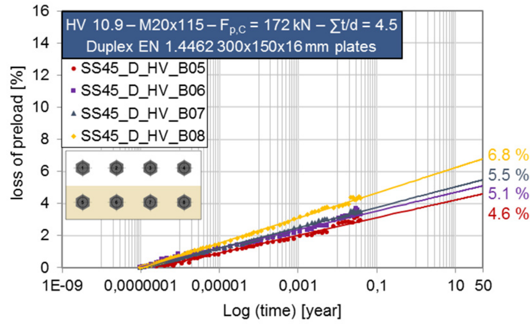


(b) preload losses-log (time) diagrams for eight-bolts specimens - second row

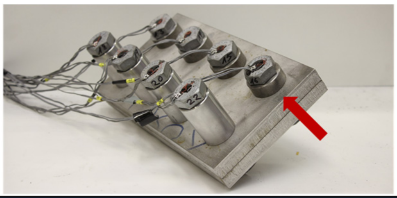

| Loss of preload min / mean / max [%] | |
|---|---|
| measured after 14 days | after 50 years (extrapolated) |
| 3.0 / 4.3 / 5.2 | 4.7 / 6.7 / 8.0 |

(c) preload losses-log (time) diagrams for one-bolt specimens

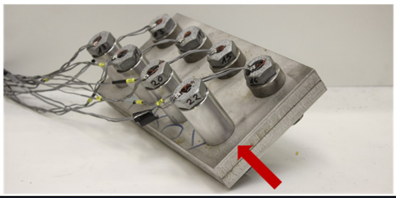

| Loss of preload min / mean / max [%] | |
|---|---|
| measured after 14 days | after 50 years (extrapolated) |
| 2.9 / 3.5 / 4.4 | 4.6 / 5.5 / 6.8 |

(d) loss preload measured/extrapolated after 14 days/ 50 years

**Figure 177** Preload losses for SS45

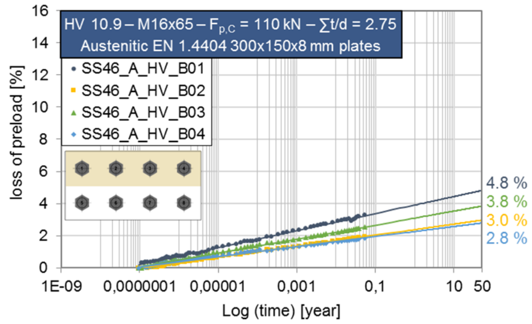


(a) preload losses-log (time) diagrams for eight-bolts specimens - first row

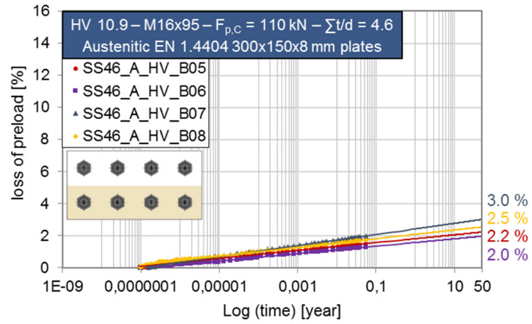


(b) preload losses-log (time) diagrams for eight-bolts specimens - second row

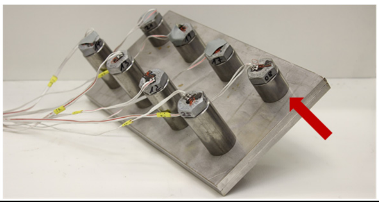

| Loss of preload min / mean / max [%] | |
|---|---|
| measured after 20 days | after 50 years (extrapolated) |
| 1.8 / 2.4 / 3.3 | 2.8 / 3.6 / 4.8 |

(c) preload losses-log (time) diagrams for one-bolt specimens

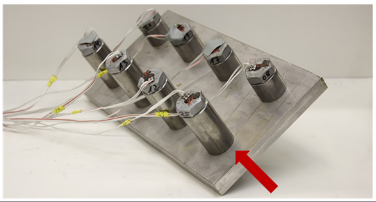

| Loss of preload min / mean / max [%] | |
|---|---|
| measured after 20 days | after 50 years (extrapolated) |
| 1.3 / 1.6 / 2.0 | 2.0 / 2.4 / 3.0 |

(d) loss preload measured/extrapolated after 20 days/ 50 years

**Figure 178** Preload losses for SS46

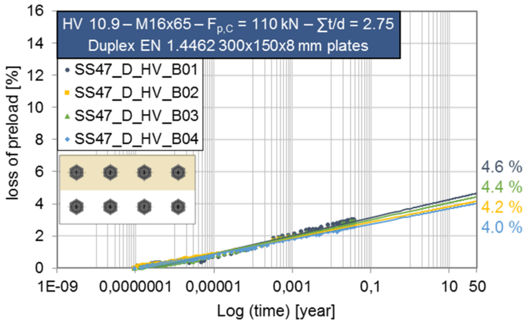


(a) preload losses-log (time) diagrams for eight-bolts specimens - first row

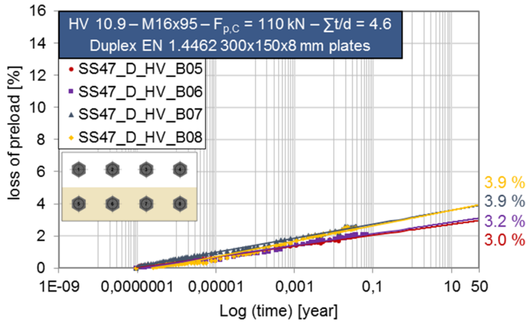


(b) preload losses-log (time) diagrams for eight-bolts specimens - second row

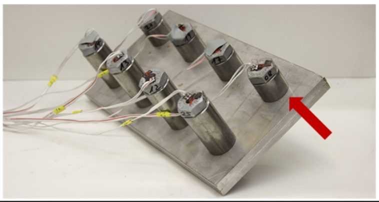

| Loss of preload min / mean / max [%] | |
|---|---|
| measured after 14 days | after 50 years (extrapolated) |
| 2.6 / 2.8 / 3.0 | 4.0 / 4.4 / 4.6 |

(c) preload losses-log (time) diagrams for one-bolt specimens

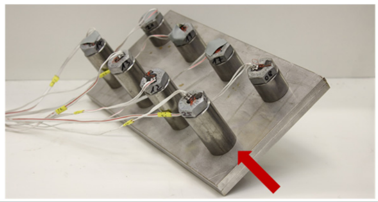

| Loss of preload min / mean / max [%] | |
|---|---|
| measured after 14 days | after 50 years (extrapolated) |
| 2.0 / 2.3 / 2.6 | 3.0 / 3.5 / 3.9 |

(d) loss preload measured/extrapolated after 14 days/ 50 years

**Figure 179** Preload losses for SS47

# 8 Annex B: Rate of loss of preload

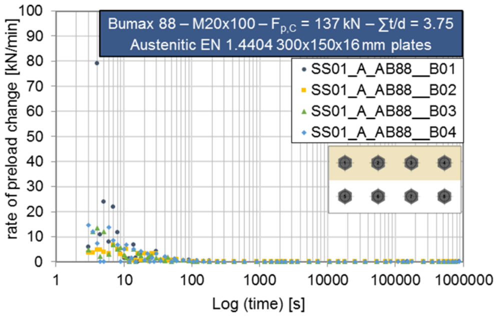


(a) log (rate of loss of preload) – time diagrams for eight-bolts specimens - first row

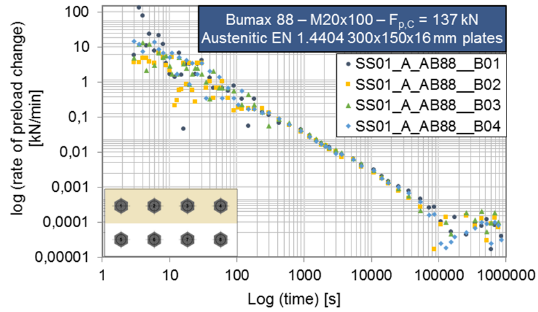


(b) log (rate of loss of preload) – log (time) diagrams for eight-bolts specimens - first row

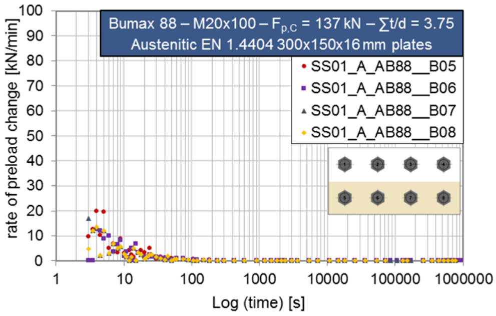


(c) log (rate of loss of preload) – time diagrams for eight-bolts specimens - second row

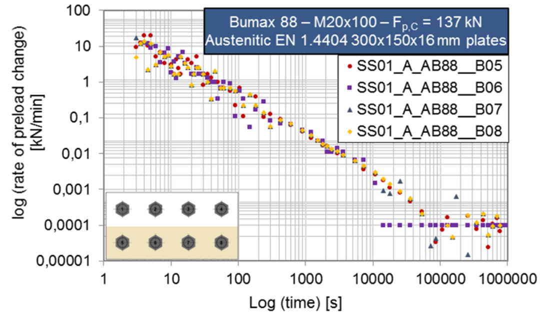


(d) log (rate of loss of preload) – log (time) diagrams for eight-bolts specimens - second row

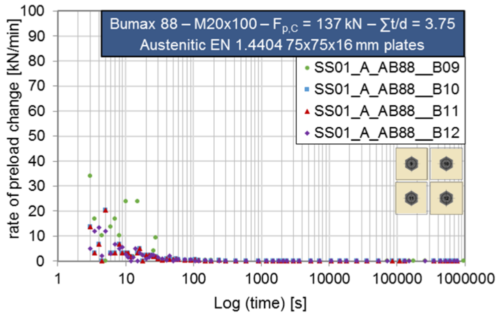


(e) log (rate of loss of preload) – time diagrams for one-bolt specimens

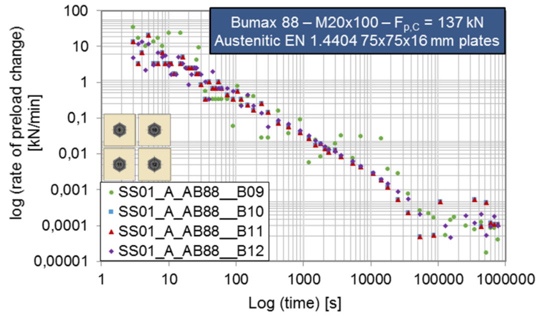


(f) log (rate of loss of preload) – log (time) diagrams for one-bolt specimens

**Figure 180** Rate of loss of preload for SS01 test series (M20 bolting assemblies, preload level: $F_{p,C}$ 172 kN, ∑t/d = 3.75)

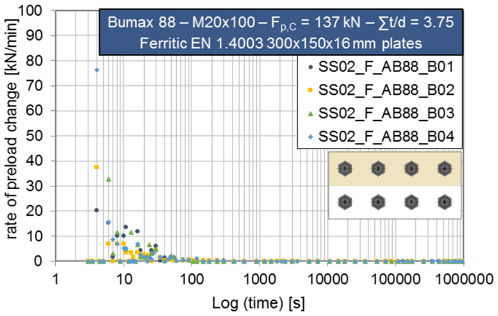


(a) log (rate of loss of preload) – time diagrams for eight-bolts specimens - first row

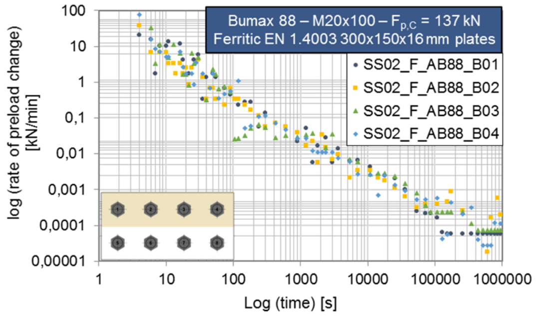


(b) log (rate of loss of preload) – log (time) diagrams for eight-bolts specimens - first row

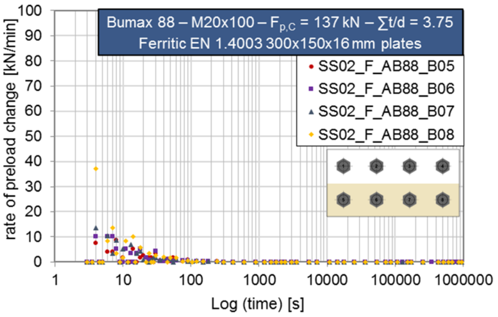


(c) log (rate of loss of preload) – time diagrams for eight-bolts specimens - second row

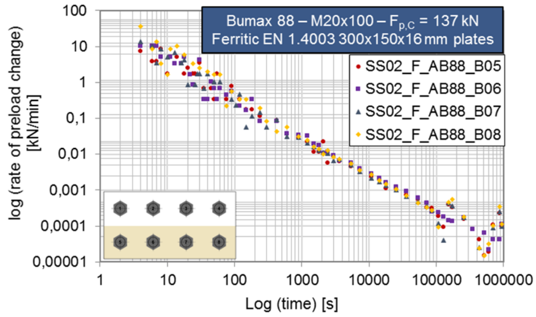


(d) log (rate of loss of preload) – log (time) diagrams for eight-bolts specimens - second row

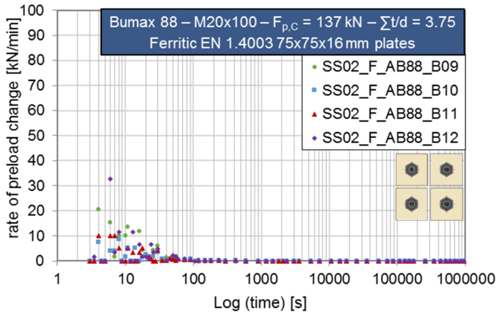


(e) log (rate of loss of preload) – time diagrams for one-bolt specimens

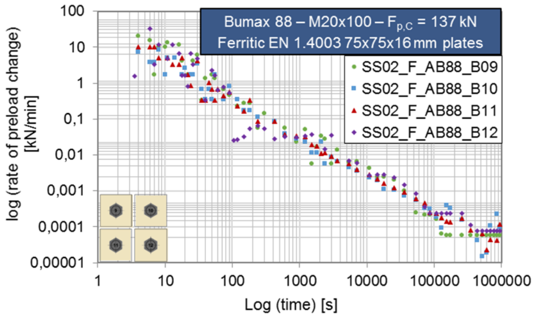


(f) log (rate of loss of preload) – log (time) diagrams for one-bolt specimens

**Figure 181** Rate of loss of preload for SS02 test series (M20 bolting assemblies, preload level: $F_{p,C}$ 172 kN, ∑t/d = 3.75)

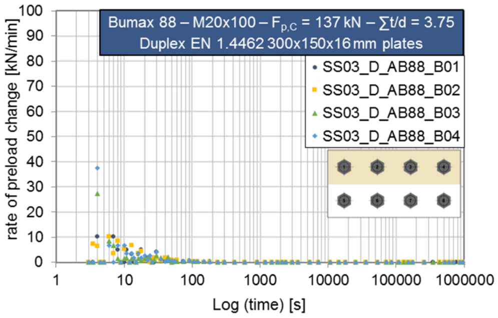


(a) log (rate of loss of preload) – time diagrams for eight-bolts specimens - first row

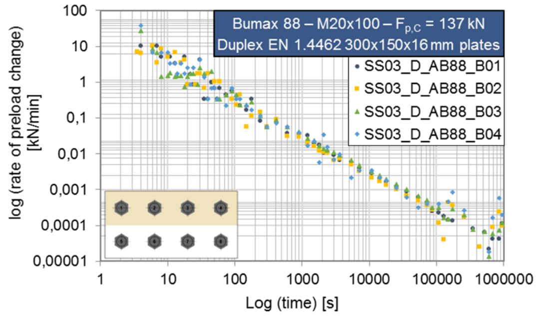


(b) log (rate of loss of preload) – log (time) diagrams for eight-bolts specimens - first row

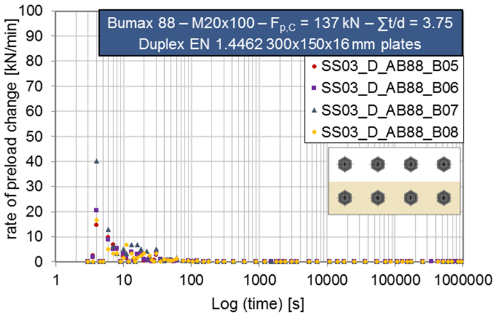


(c) log (rate of loss of preload) – time diagrams for eight-bolts specimens - second row

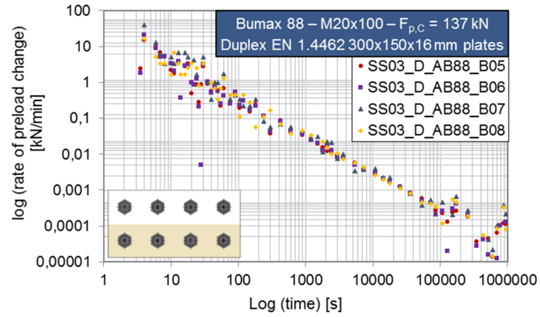


(d) log (rate of loss of preload) – log (time) diagrams for eight-bolts specimens - second row

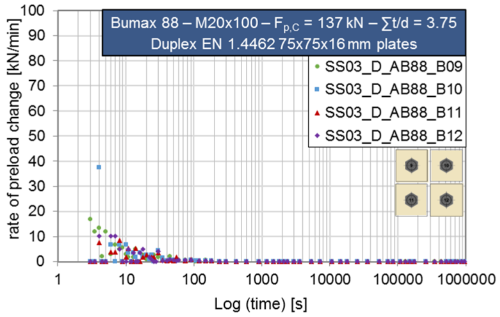


(e) log (rate of loss of preload) – time diagrams for one-bolt specimens

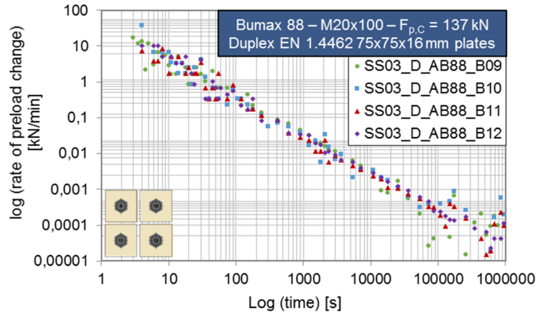


(f) log (rate of loss of preload) – log (time) diagrams for one-bolt specimens

**Figure 182** Rate of loss of preload for SS03 test series (M20 bolting assemblies, preload level: $F_{p,C}$ 172 kN, $\sum t/d = 3.75$)

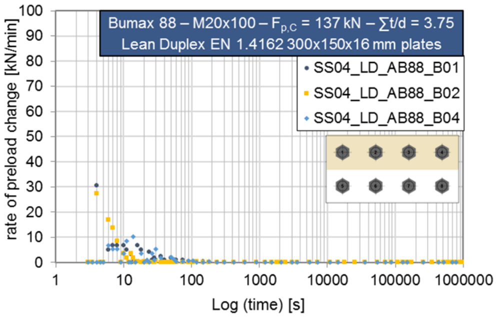


(a) log (rate of loss of preload) – time diagrams for eight-bolts specimens - first row

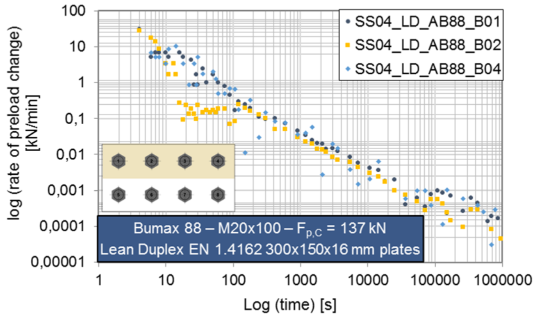


(b) log (rate of loss of preload) – log (time) diagrams for eight-bolts specimens - first row

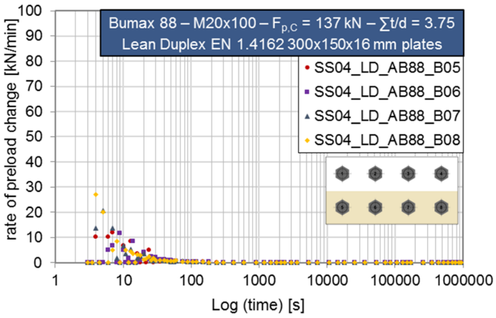


(c) log (rate of loss of preload) – time diagrams for eight-bolts specimens - second row

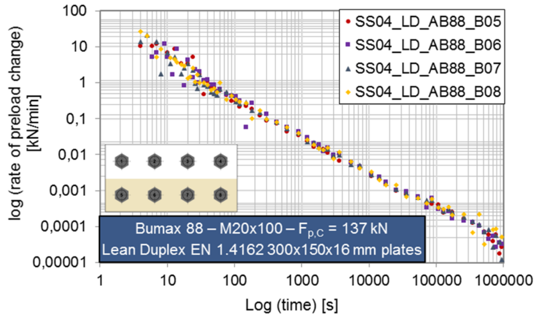


(d) log (rate of loss of preload) – log (time) diagrams for eight-bolts specimens - second row

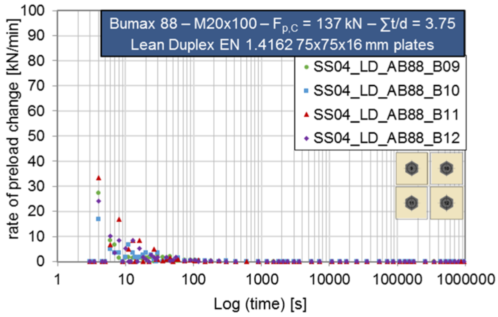


(e) log (rate of loss of preload) – time diagrams for one-bolt specimens

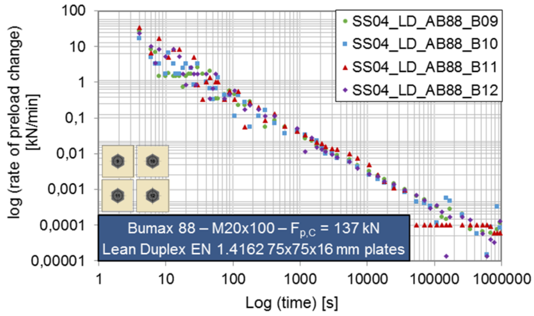


(f) log (rate of loss of preload) – log (time) diagrams for one-bolt specimens

**Figure 183** Rate of loss of preload for SS04 test series (M20 bolting assemblies, preload level: $F_{p,C}$ 172 kN, ∑t/d = 3.75)

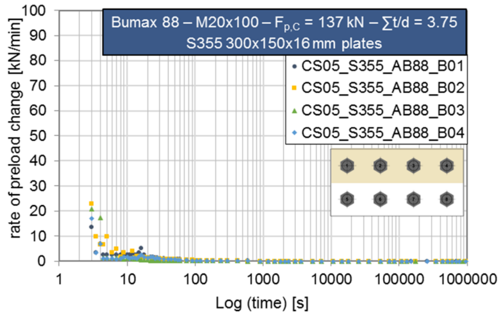


(a) log (rate of loss of preload) – time diagrams for eight-bolts specimens - first row

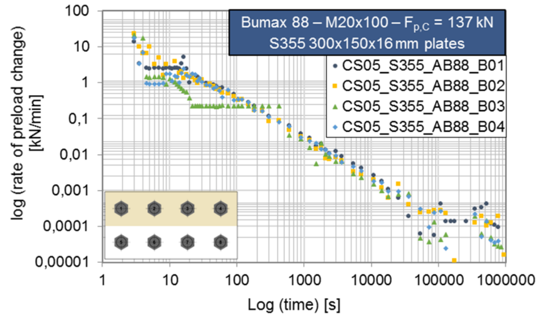


(b) log (rate of loss of preload) – log (time) diagrams for eight-bolts specimens - first row

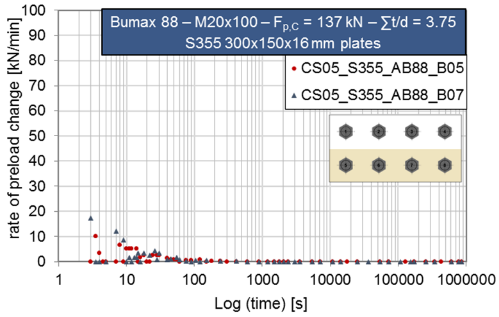


(c) log (rate of loss of preload) – time diagrams for eight-bolts specimens - second row

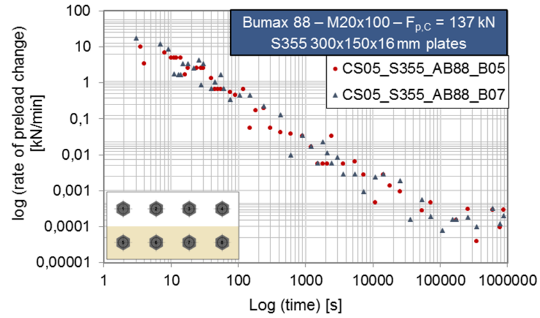


(d) log (rate of loss of preload) – log (time) diagrams for eight-bolts specimens - second row

**Figure 184** Rate of loss of preload for CS05 test series (M20 bolting assemblies, preload level: $F_{p,C}$ 172 kN, ∑t/d = 3.75)

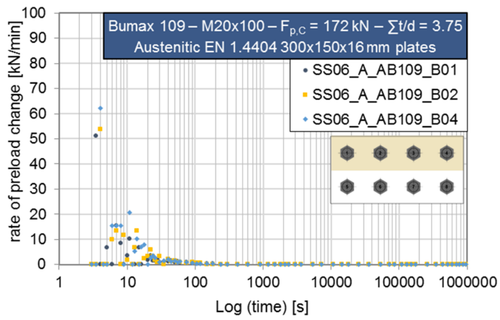


(a) log (rate of loss of preload) – time diagrams for eight-bolts specimens - first row

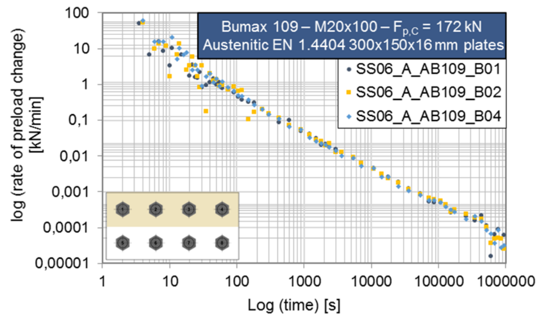


(b) log (rate of loss of preload) – log (time) diagrams for eight-bolts specimens - first row

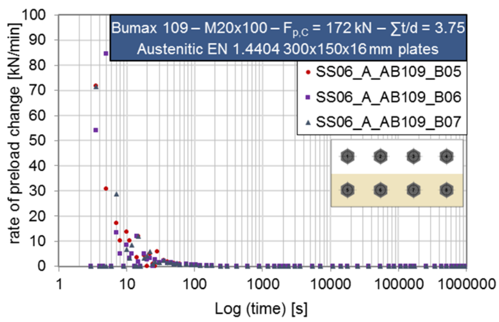


(c) log (rate of loss of preload) – time diagrams for eight-bolts specimens - second row

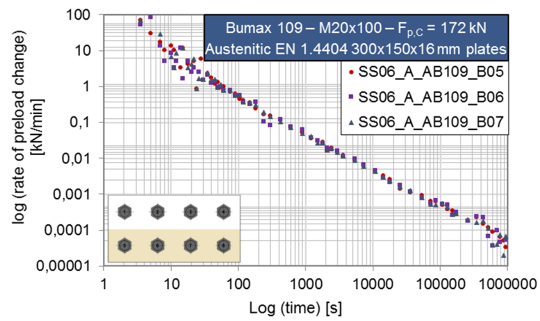


(d) log (rate of loss of preload) – log (time) diagrams for eight-bolts specimens - second row

**Figure 185** Rate of loss of preload for SS06 test series (M20 bolting assemblies, preload level: $F_{p,C}$ 172 kN, ∑t/d = 3.75)

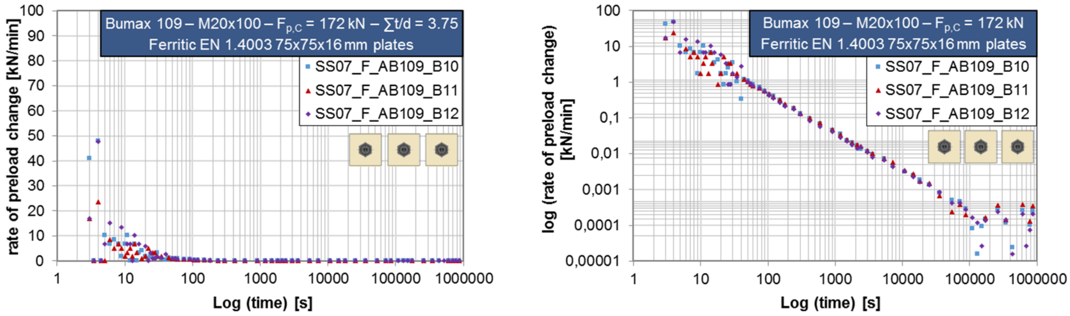


(a) log (rate of loss of preload) – time diagrams for one-bolt specimens

(b) log (rate of loss of preload) – log (time) diagrams for one-bolt specimens

**Figure 186** Rate of loss of preload for SS07 test series (M20 bolting assemblies, preload level: $F_{p,C}$ 172 kN, ∑t/d = 3.75)

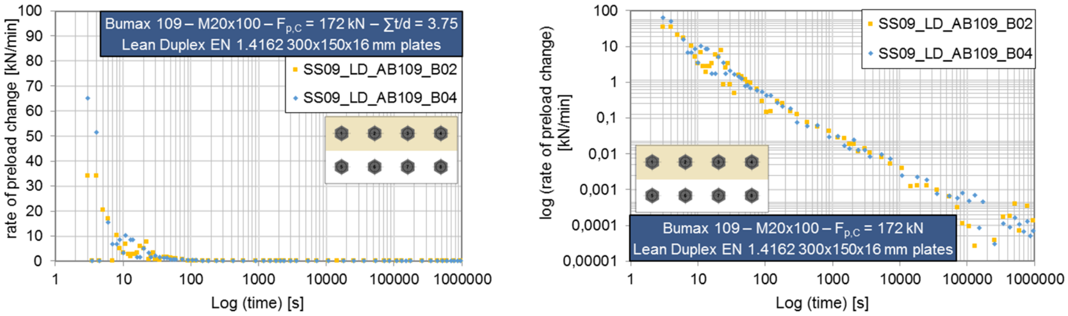


(a) log (rate of loss of preload) – time diagrams for eight-bolts specimens - first row

(b) log (rate of loss of preload) – log (time) diagrams for eight-bolts specimens - first row

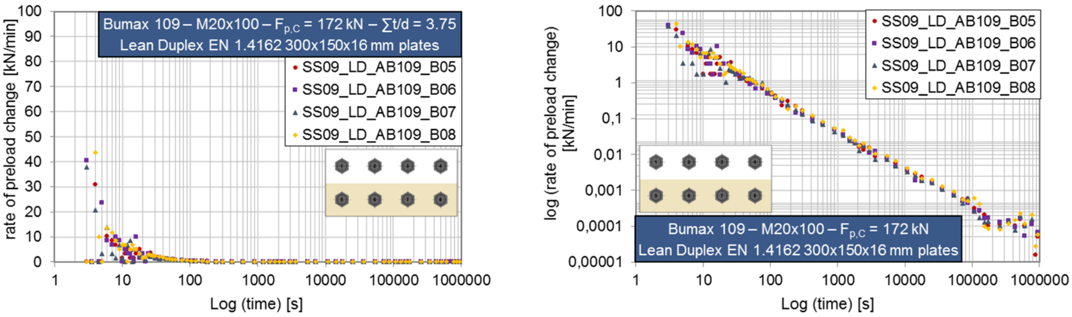


(c) log (rate of loss of preload) – time diagrams for eight-bolts specimens - second row

(d) log (rate of loss of preload) – log (time) diagrams for eight-bolts specimens - second row

**Figure 187** Rate of loss of preload for SS09 test series (M20 bolting assemblies, preload level: $F_{p,C}$ 172 kN, ∑t/d = 3.75)

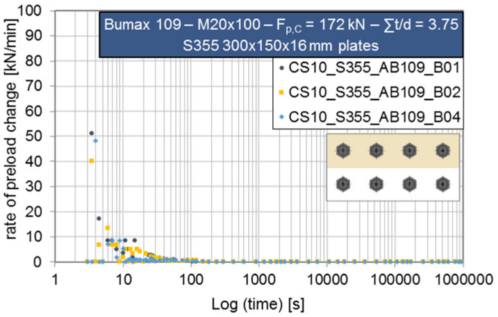


(a) log (rate of loss of preload) – time diagrams for eight-bolts specimens - first row

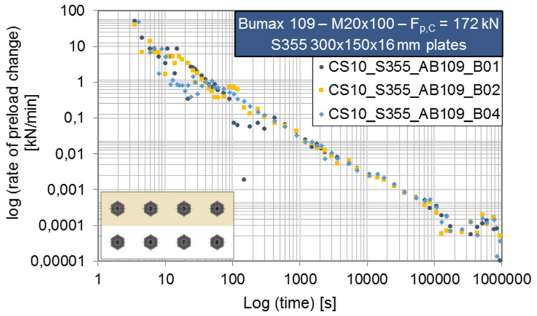


(b) log (rate of loss of preload) – log (time) diagrams for eight-bolts specimens - first row

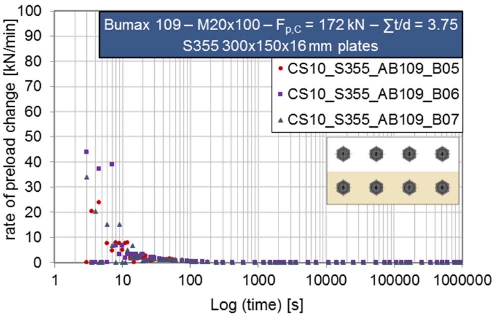


(c) log (rate of loss of preload) – time diagrams for eight-bolts specimens - second row

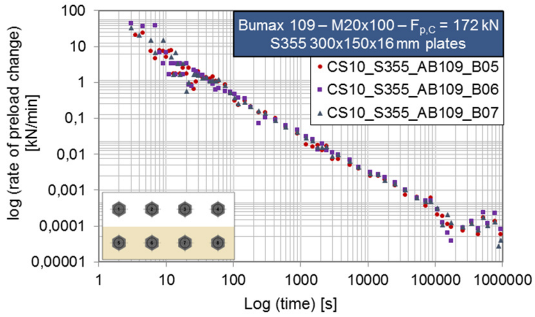


(d) log (rate of loss of preload) – log (time) diagrams for eight-bolts specimens - second row

**Figure 188** Rate of loss of preload for CS10 test series (M20 bolting assemblies, preload level: $F_{p,C}$ 172 kN, $\sum t/d = 3.75$)

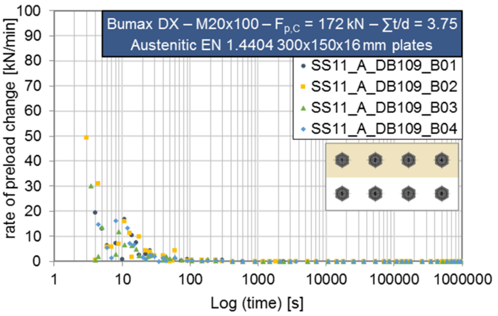


(a) log (rate of loss of preload) – time diagrams for eight-bolts specimens - first row

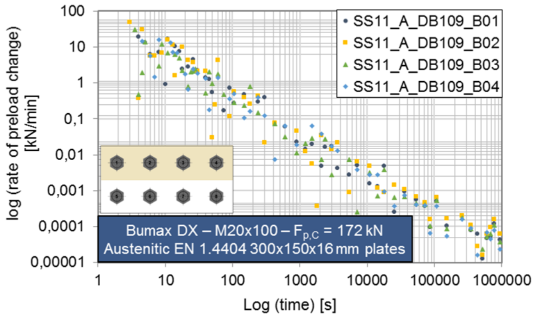


(b) log (rate of loss of preload) – log (time) diagrams for eight-bolts specimens - first row

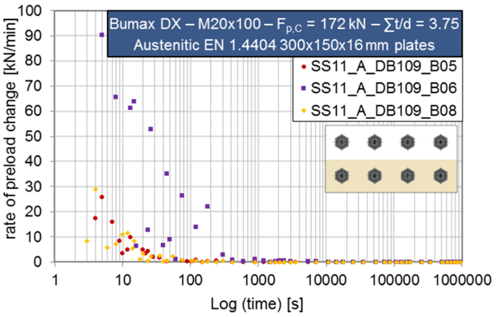


(c) log (rate of loss of preload) – time diagrams for eight-bolts specimens - second row

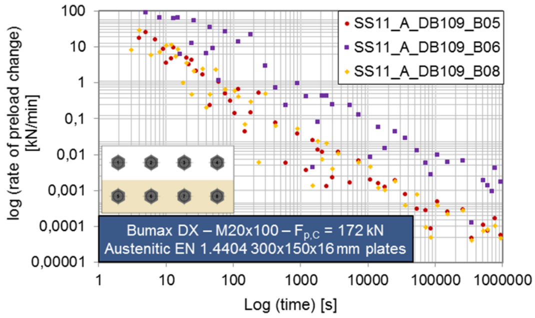


(d) log (rate of loss of preload) – log (time) diagrams for eight-bolts specimens - second row

**Figure 189** Rate of loss of preload for SS11 test series (M20 bolting assemblies, preload level: $F_{p,C}$ 172 kN, $\sum t/d = 3.75$)

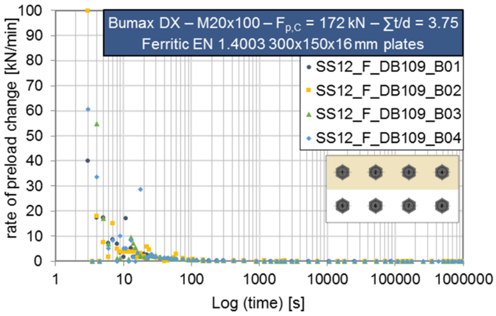


(a) log (rate of loss of preload) – time diagrams for eight-bolts specimens - first row

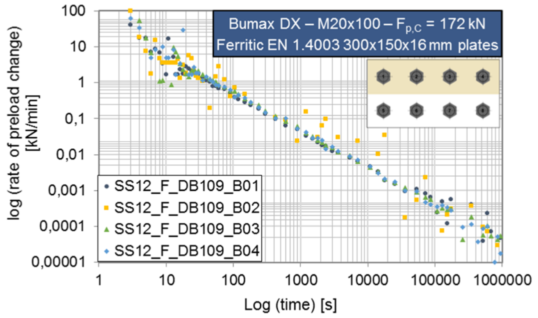


(b) log (rate of loss of preload) – log (time) diagrams for eight-bolts specimens - first row

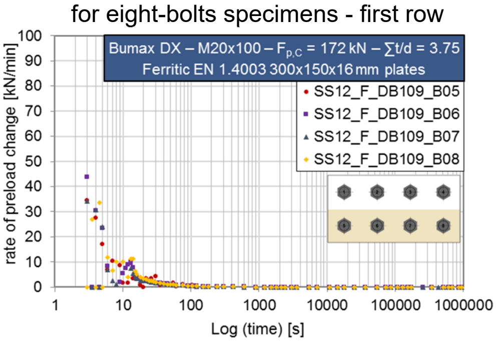


(c) log (rate of loss of preload) – time diagrams for eight-bolts specimens - second row

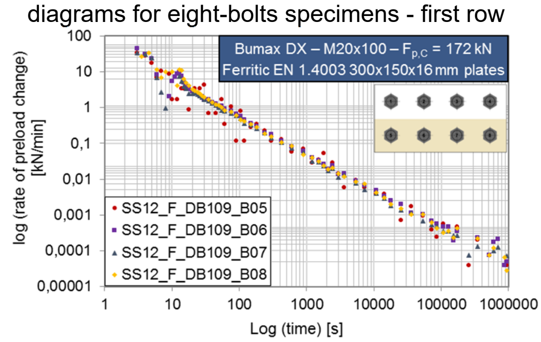


(d) log (rate of loss of preload) – log (time) diagrams for eight-bolts specimens - second row

**Figure 190** Rate of loss of preload for SS12 test series (M20 bolting assemblies, preload level: $F_{p,C}$ 172 kN, ∑t/d = 3.75)

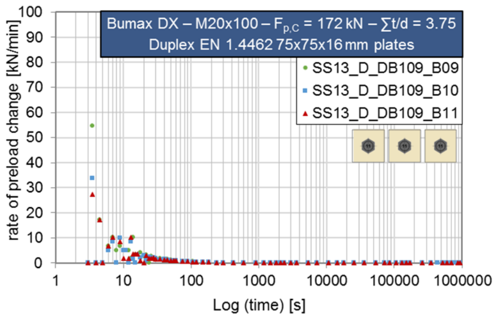


(a) log (rate of loss of preload) – time diagrams for one-bolt specimens

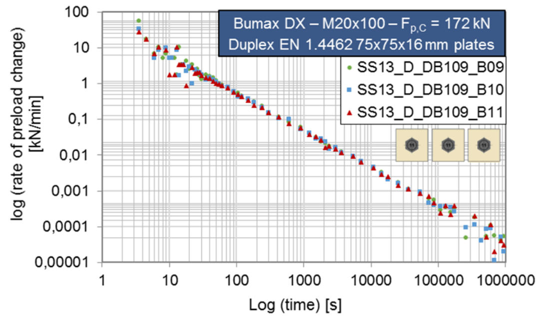


(b) log (rate of loss of preload) – log (time) diagrams for one-bolt specimens

**Figure 191** Rate of loss of preload for SS13 test series (M20 bolting assemblies, preload level: $F_{p,C}$ 172 kN, ∑t/d = 3.75)

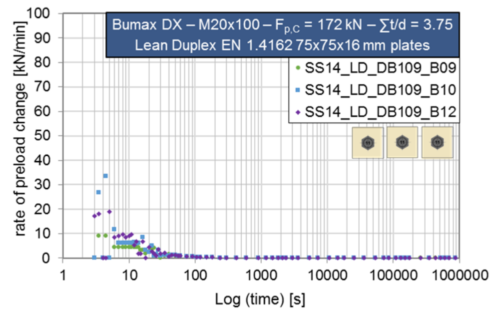


(a) log (rate of loss of preload) – time diagrams for one-bolt specimens

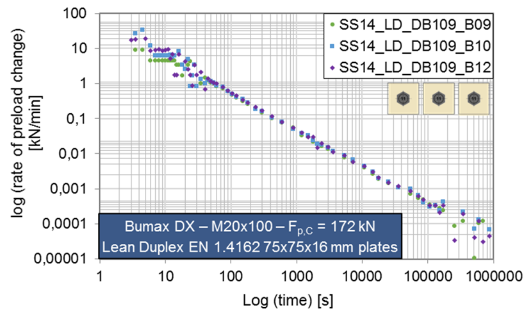


(b) log (rate of loss of preload) – log (time) diagrams for one-bolt specimens

**Figure 192** Rate of loss of preload for SS14 test series (M20 bolting assemblies, preload level: $F_{p,C}$ 172 kN, ∑t/d = 3.75)

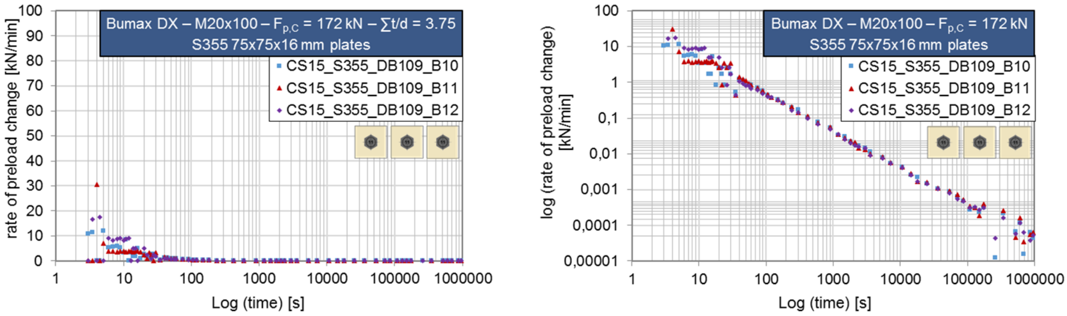


(a) log (rate of loss of preload) – time diagrams for one-bolt specimens

(b) log (rate of loss of preload) – log (time) diagrams for one-bolt specimens

**Figure 193** Rate of loss of preload for CS15 test series (M20 bolting assemblies, preload level: $F_{p,C}$ 172 kN, ∑t/d = 3.75)

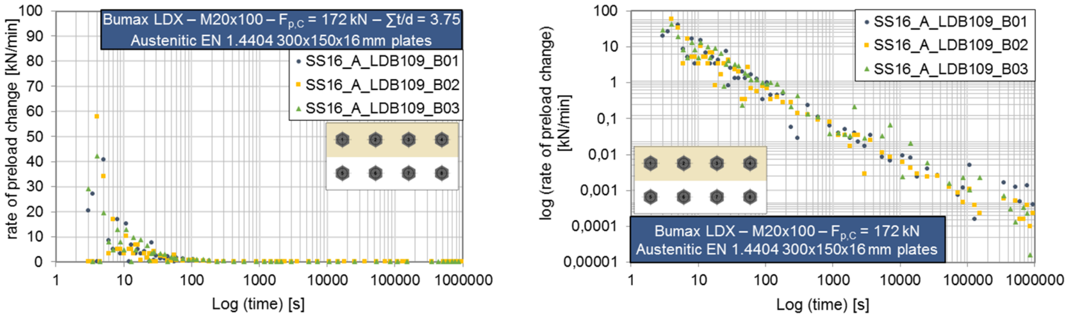


(a) log (rate of loss of preload) – time diagrams for eight-bolts specimens - first row

(b) log (rate of loss of preload) – log (time) diagrams for eight-bolts specimens - first row

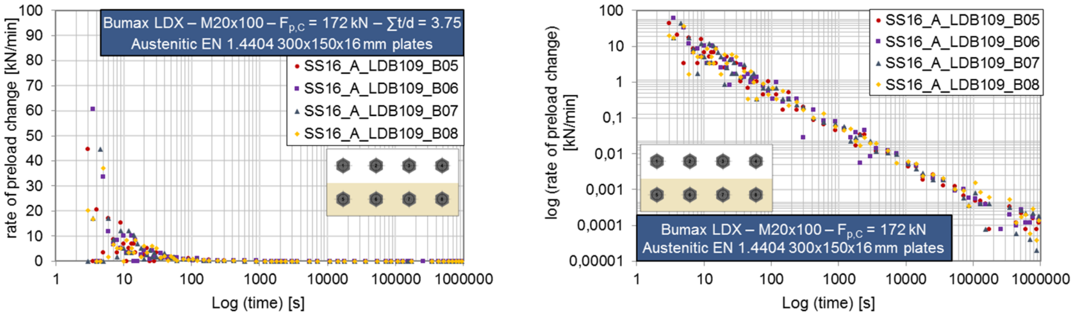


(c) log (rate of loss of preload) – time diagrams for eight-bolts specimens - second row

(d) log (rate of loss of preload) – log (time) diagrams for eight-bolts specimens - second row

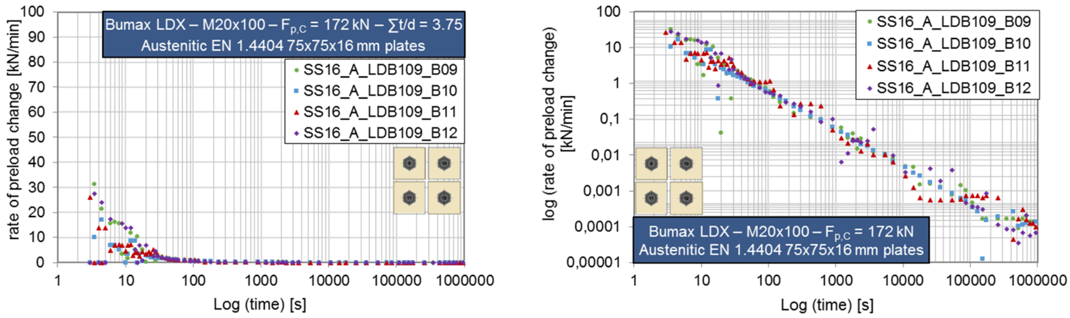


(e) log (rate of loss of preload) – time diagrams for one-bolt specimens

(f) log (rate of loss of preload) – log (time) diagrams for one-bolt specimens

**Figure 194** Rate of loss of preload for SS16 test series (M20 bolting assemblies, preload level: $F_{p,C}$ 172 kN, ∑t/d = 3.75)

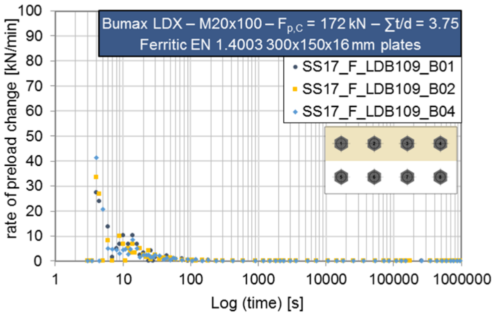


(a) log (rate of loss of preload) – time diagrams for eight-bolts specimens - first row

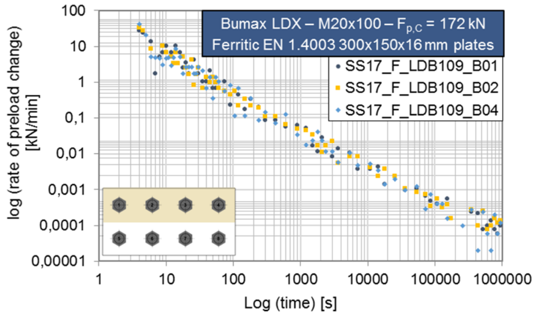


(b) log (rate of loss of preload) – log (time) diagrams for eight-bolts specimens - first row

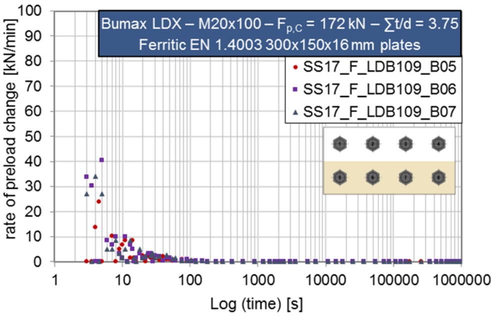


(c) log (rate of loss of preload) – time diagrams for eight-bolts specimens - second row

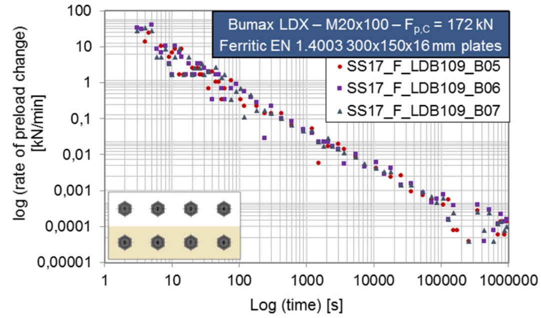


(d) log (rate of loss of preload) – log (time) diagrams for eight-bolts specimens - second row

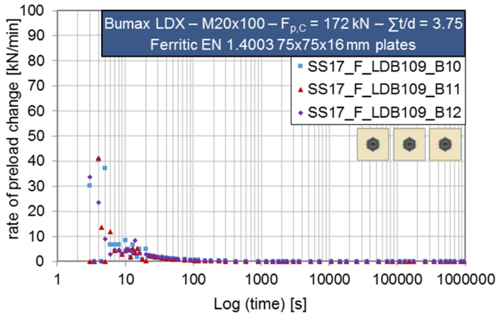


(e) log (rate of loss of preload) – time diagrams for one-bolt specimens

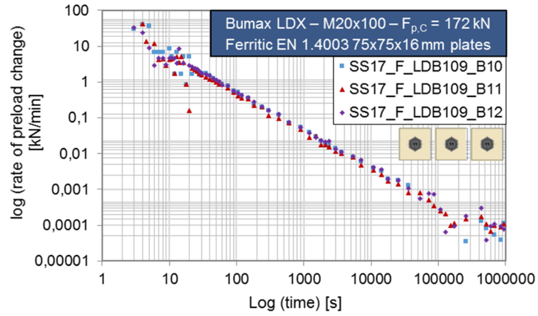


(f) log (rate of loss of preload) – log (time) diagrams for one-bolt specimens

**Figure 195** Rate of loss of preload for SS17 test series (M20 bolting assemblies, preload level: $F_{p,C}$ 172 kN, ∑t/d = 3.75)

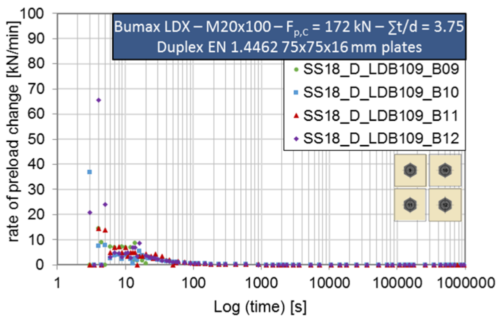


(a) log (rate of loss of preload) – time diagrams for one-bolt specimens

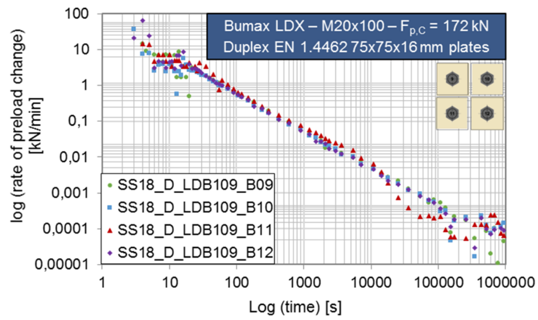


(b) log (rate of loss of preload) – log (time) diagrams for one-bolt specimens

**Figure 196** Rate of loss of preload for SS18 test series (M20 bolting assemblies, preload level: $F_{p,C}$ 172 kN, ∑t/d = 3.75)

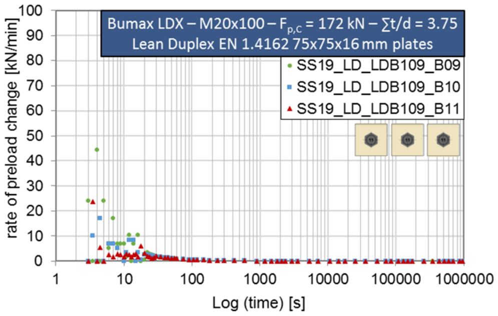


(a) log (rate of loss of preload) – time diagrams for one-bolt specimens

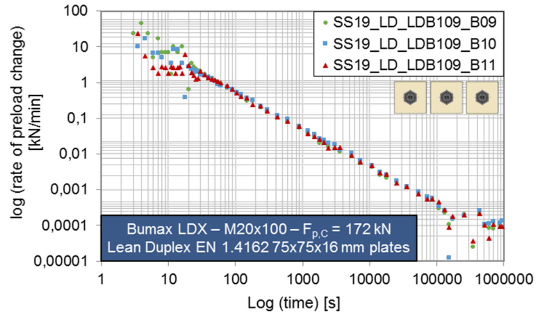


(b) log (rate of loss of preload) – log (time) diagrams for one-bolt specimens

**Figure 197** Rate of loss of preload for SS19 test series (M20 bolting assemblies, preload level: $F_{p,C}$ 172 kN, ∑t/d = 3.75)

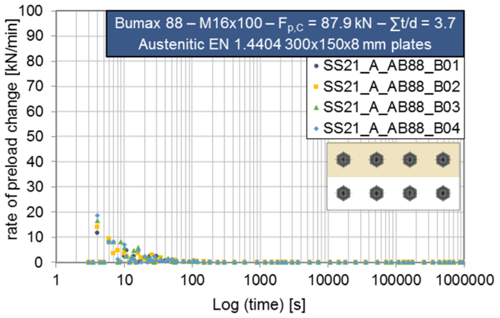


(a) log (rate of loss of preload) – time diagrams for eight-bolts specimens - first row

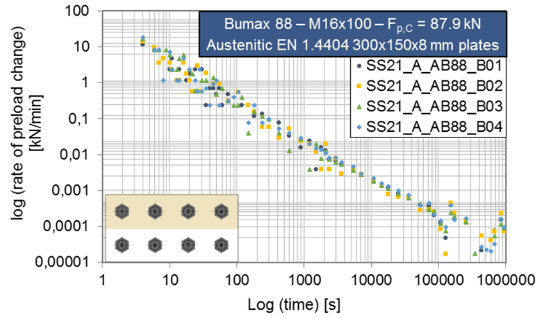


(b) log (rate of loss of preload) – log (time) diagrams for eight-bolts specimens - first row

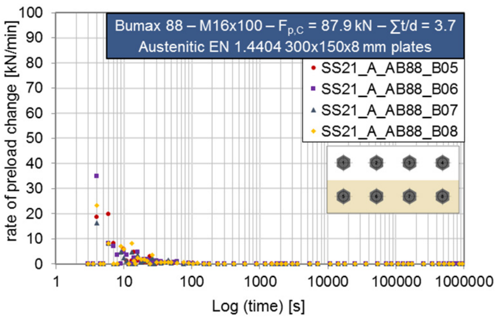


(c) log (rate of loss of preload) – time diagrams for eight-bolts specimens - second row

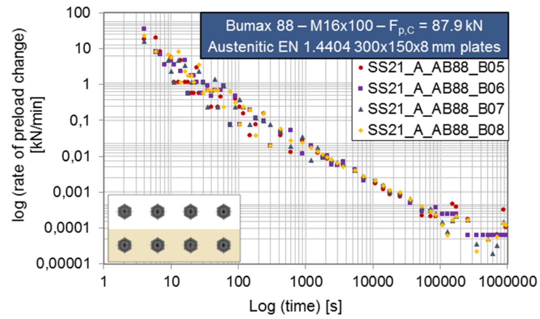


(d) log (rate of loss of preload) – log (time) diagrams for eight-bolts specimens - second row

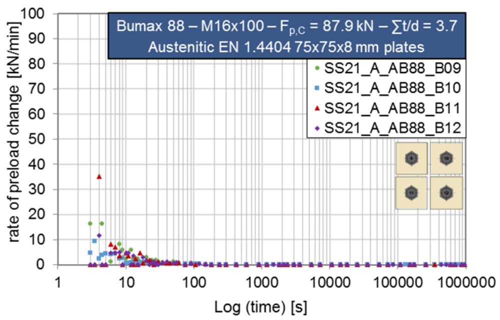


(e) log (rate of loss of preload) – time diagrams for one-bolt specimens

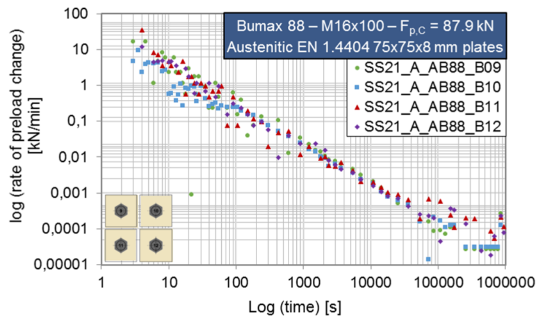


(f) log (rate of loss of preload) – log (time) diagrams for one-bolt specimens

**Figure 198** Rate of loss of preload for SS21 test series (M16 bolting assemblies, preload level: $F_{p,C}$ 87.9 kN, ∑t/d = 3.7)

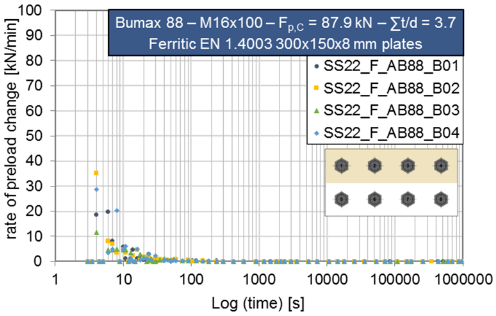


(a) log (rate of loss of preload) – time diagrams for eight-bolts specimens - first row

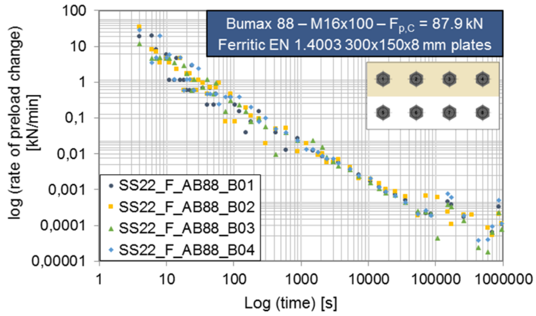


(b) log (rate of loss of preload) – log (time) diagrams for eight-bolts specimens - first row

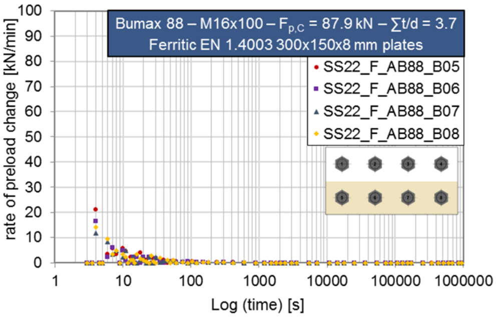


(c) log (rate of loss of preload) – time diagrams for eight-bolts specimens - second row

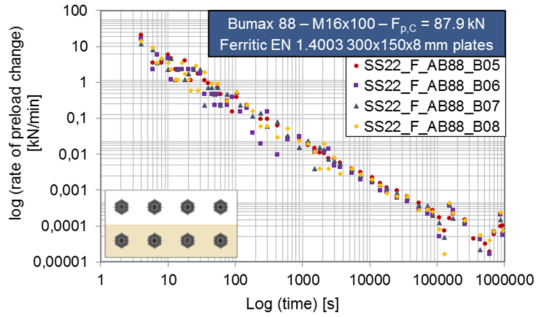


(d) log (rate of loss of preload) – log (time) diagrams for eight-bolts specimens - second row

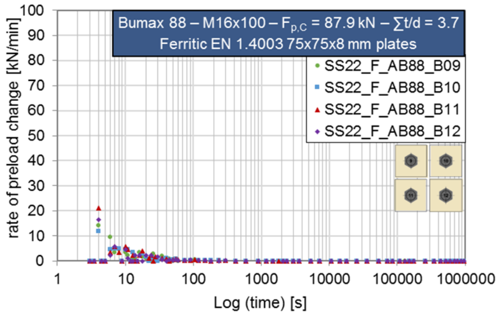


(e) log (rate of loss of preload) – time diagrams for one-bolt specimens

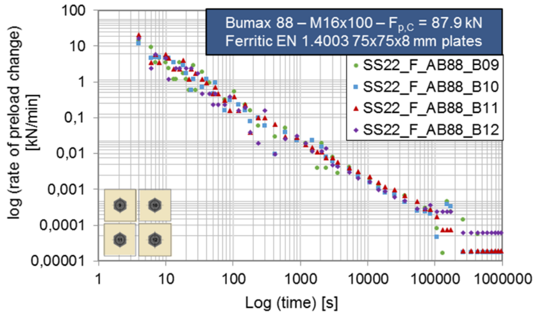


(f) log (rate of loss of preload) – log (time) diagrams for one-bolt specimens

**Figure 199** Rate of loss of preload for SS22 test series (M16 bolting assemblies, preload level: $F_{p,C}$ 87.9 kN, $\sum t/d = 3.7$)

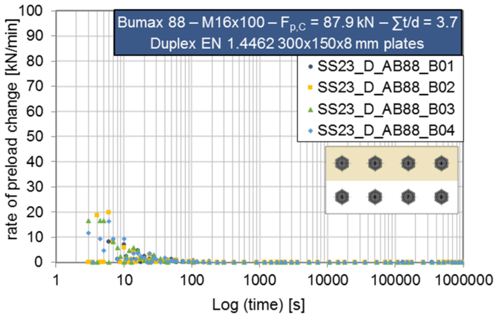


(a) log (rate of loss of preload) – time diagrams for eight-bolts specimens - first row

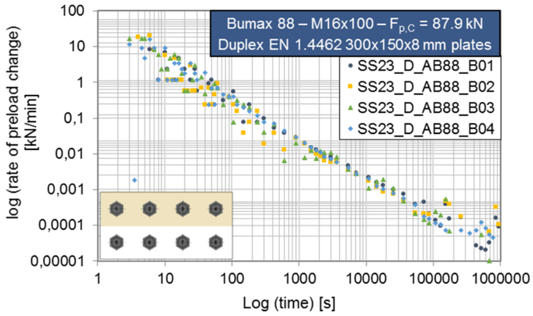


(b) log (rate of loss of preload) – log (time) diagrams for eight-bolts specimens - first row

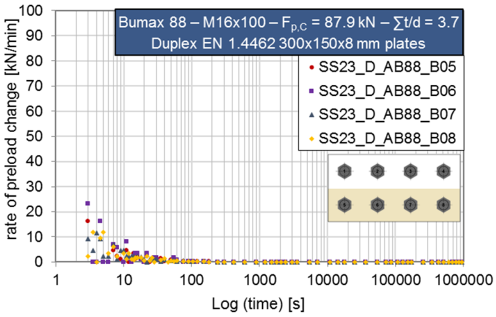


(c) log (rate of loss of preload) – time diagrams for eight-bolts specimens - second row

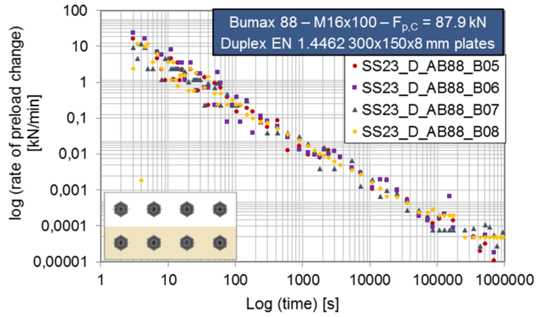


(d) log (rate of loss of preload) – log (time) diagrams for eight-bolts specimens - second row

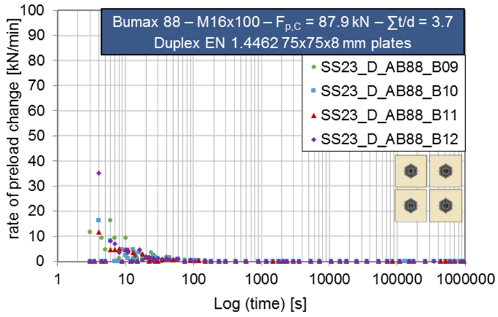


(e) log (rate of loss of preload) – time diagrams for one-bolt specimens

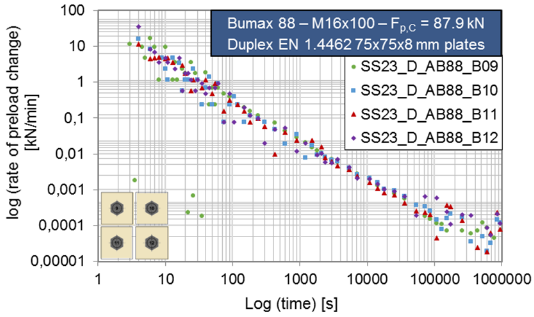


(f) log (rate of loss of preload) – log (time) diagrams for one-bolt specimens

**Figure 200** Rate of loss of preload for SS23 test series (M16 bolting assemblies, preload level: $F_{p,C}$ 87.9 kN, ∑t/d = 3.7)

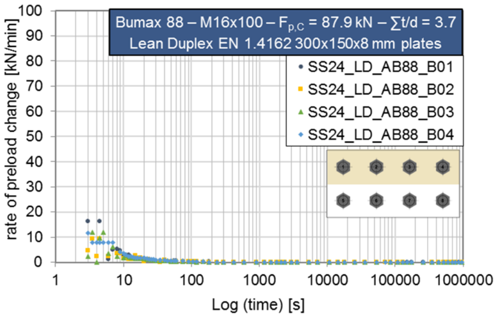


(a) log (rate of loss of preload) – time diagrams for eight-bolts specimens - first row

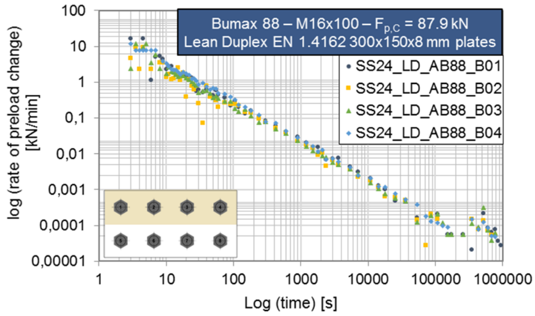


(b) log (rate of loss of preload) – log (time) diagrams for eight-bolts specimens - first row

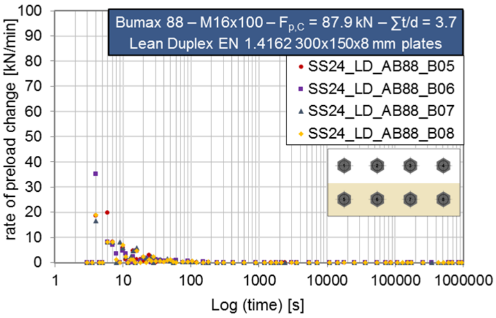


(c) log (rate of loss of preload) – time diagrams for eight-bolts specimens - second row

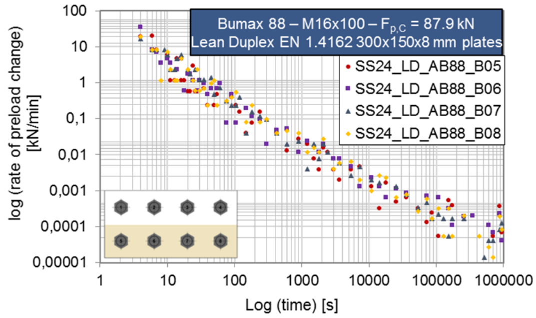


(d) log (rate of loss of preload) – log (time) diagrams for eight-bolts specimens - second row

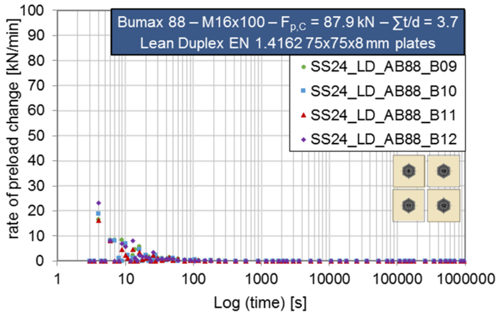


(e) log (rate of loss of preload) – time diagrams for one-bolt specimens

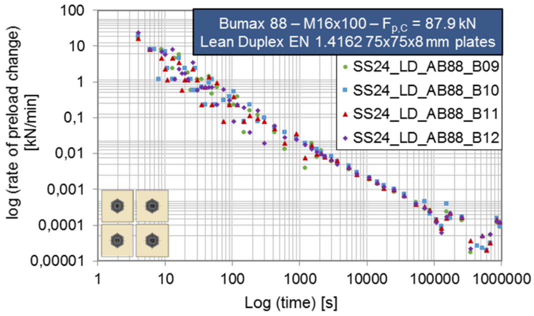


(f) log (rate of loss of preload) – log (time) diagrams for one-bolt specimens

**Figure 201** Rate of loss of preload for SS24 test series (M16 bolting assemblies, preload level: $F_{p,C}$ 87.9 kN, $\sum t/d = 3.7$)

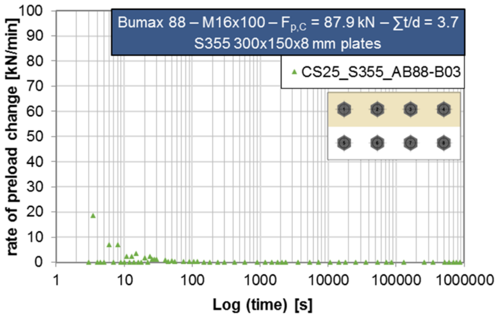


(a) log (rate of loss of preload) – time diagrams for eight-bolts specimens - first row

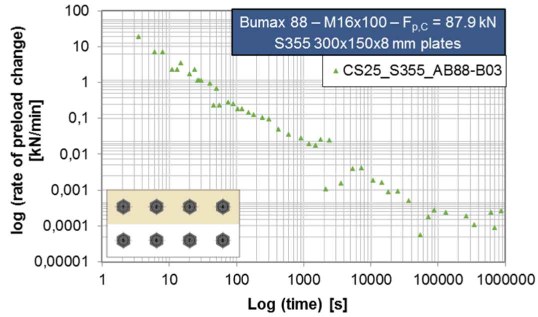


(b) log (rate of loss of preload) – log (time) diagrams for eight-bolts specimens - first row

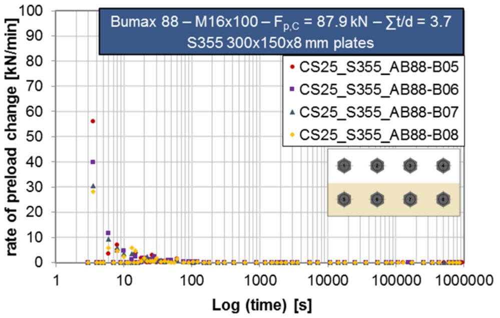


(c) log (rate of loss of preload) – time diagrams for eight-bolts specimens - second row

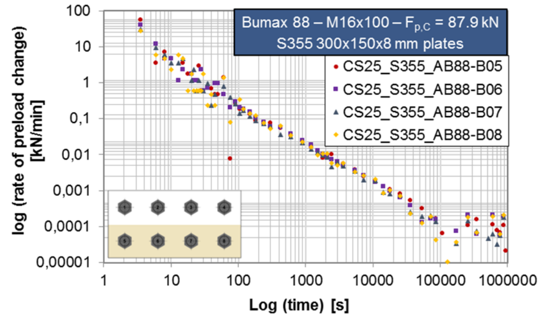


(d) log (rate of loss of preload) – log (time) diagrams for eight-bolts specimens - second row

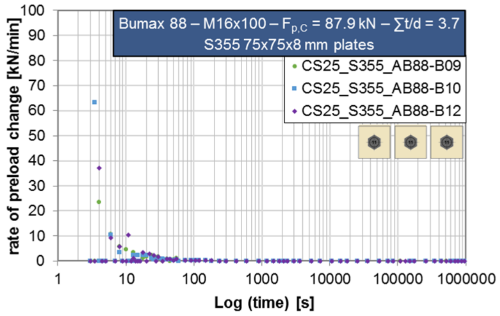


(e) log (rate of loss of preload) – time diagrams for one-bolt specimens

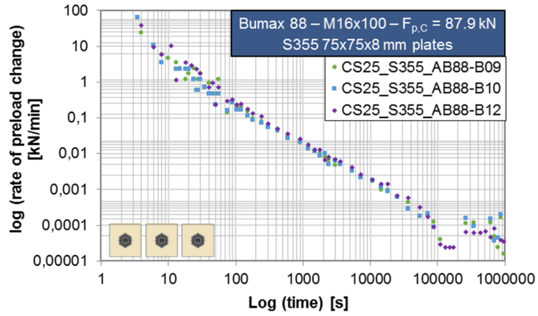


(f) log (rate of loss of preload) – log (time) diagrams for one-bolt specimens

**Figure 202** Rate of loss of preload for CS25 test series (M16 bolting assemblies, preload level: $F_{p,C}$ 87.9 kN, ∑t/d = 3.7)

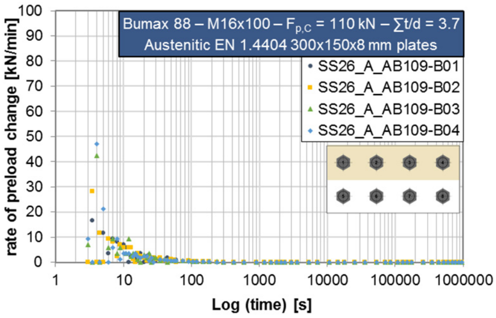


(a) log (rate of loss of preload) – time diagrams for eight-bolts specimens - first row

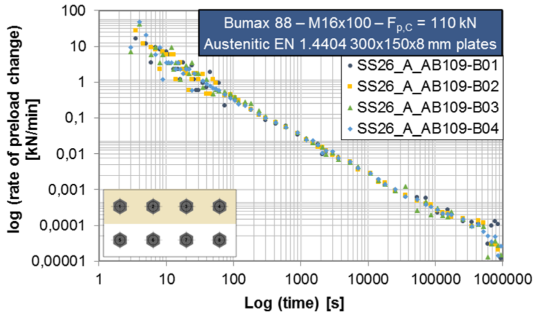


(b) log (rate of loss of preload) – log (time) diagrams for eight-bolts specimens - first row

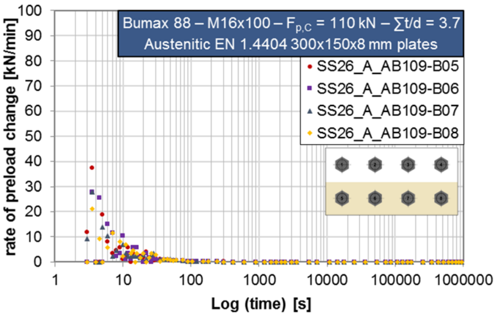


(c) log (rate of loss of preload) – time diagrams for eight-bolts specimens - second row

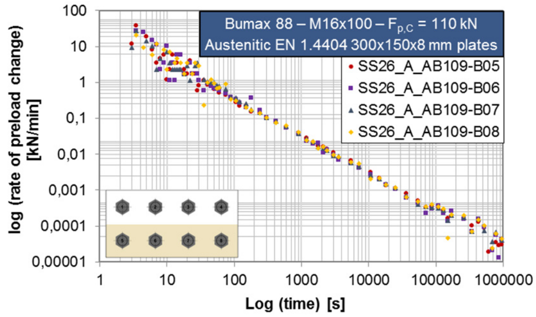


(d) log (rate of loss of preload) – log (time) diagrams for eight-bolts specimens - second row

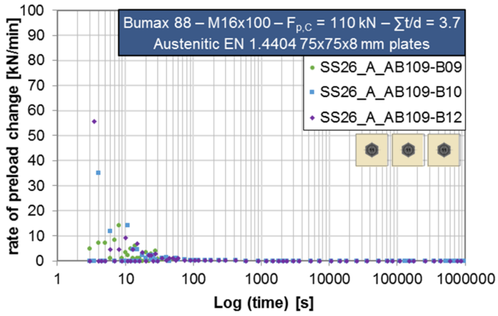


(e) log (rate of loss of preload) – time diagrams for one-bolt specimens

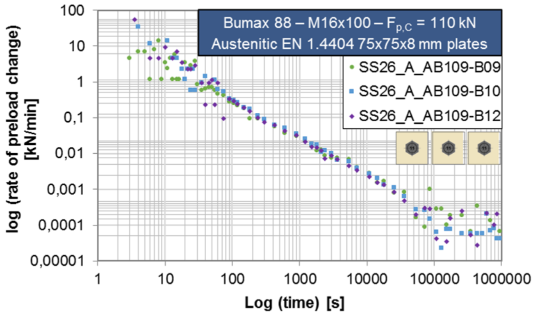


(f) log (rate of loss of preload) – log (time) diagrams for one-bolt specimens

**Figure 203** Rate of loss of preload for SS26 test series (M16 bolting assemblies, preload level: $F_{p,C}$ 110 kN, ∑t/d = 3.7)

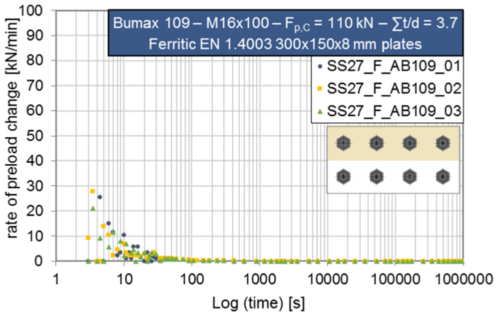


(a) log (rate of loss of preload) – time diagrams for eight-bolts specimens - first row

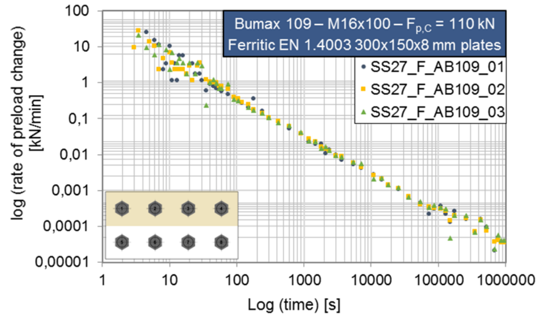


(b) log (rate of loss of preload) – log (time) diagrams for eight-bolts specimens - first row

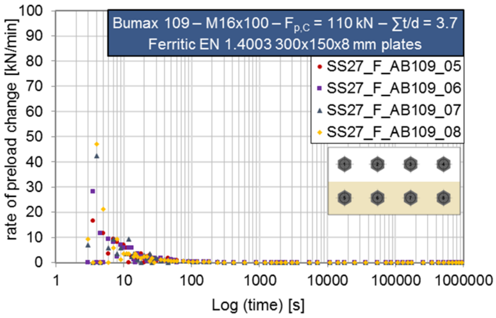


(c) log (rate of loss of preload) – time diagrams for eight-bolts specimens - second row

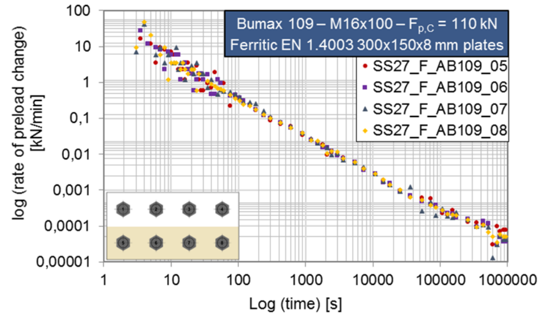


(d) log (rate of loss of preload) – log (time) diagrams for eight-bolts specimens - second row

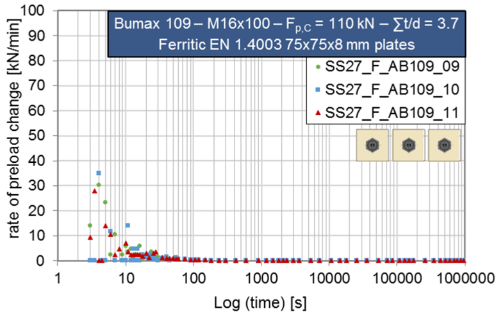


(e) log (rate of loss of preload) – time diagrams for one-bolt specimens

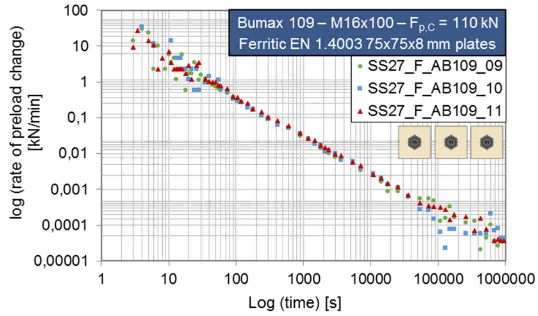


(f) log (rate of loss of preload) – log (time) diagrams for one-bolt specimens

**Figure 204** Rate of loss of preload for SS27 test series (M16 bolting assemblies, preload level: $F_{p,C}$ 110 kN, $\sum t/d = 3.7$)

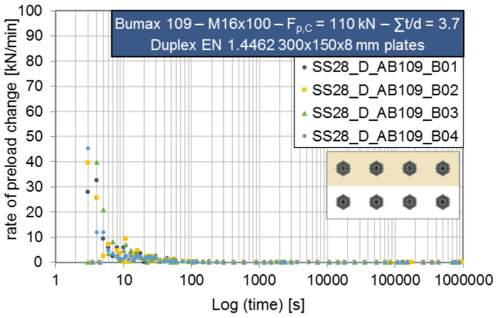


(a) log (rate of loss of preload) – time diagrams for eight-bolts specimens - first row

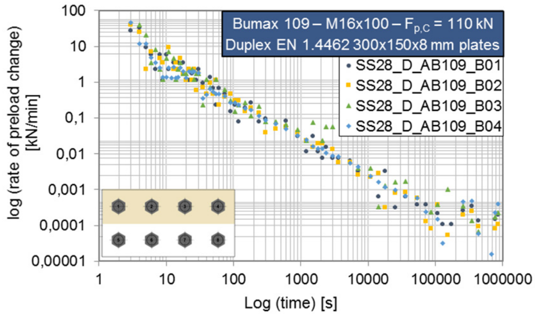


(b) log (rate of loss of preload) – log (time) diagrams for eight-bolts specimens - first row

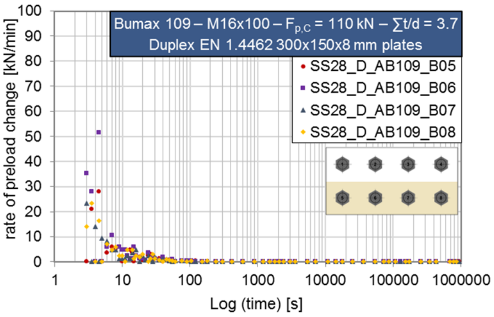


(c) log (rate of loss of preload) – time diagrams for eight-bolts specimens - second row

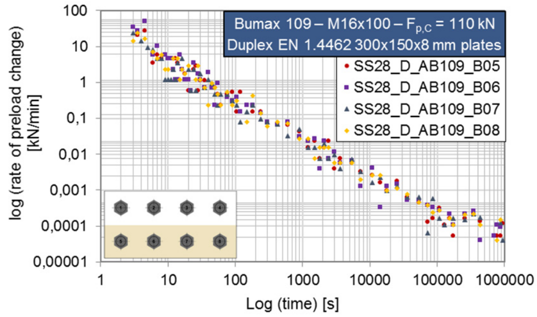


(d) log (rate of loss of preload) – log (time) diagrams for eight-bolts specimens - second row

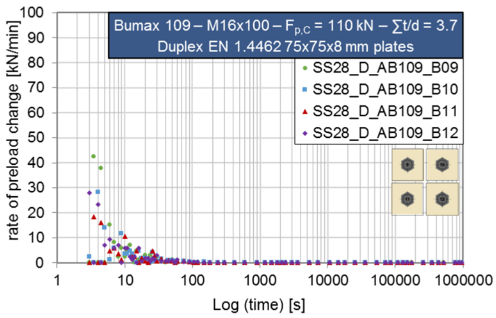


(e) log (rate of loss of preload) – time diagrams for one-bolt specimens

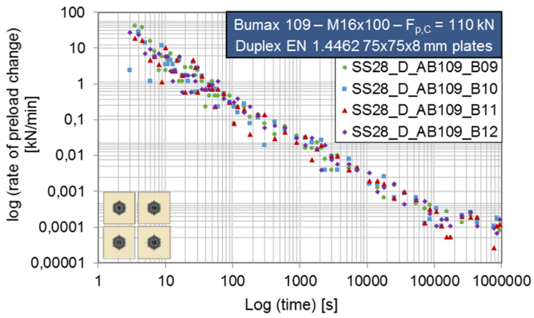


(f) log (rate of loss of preload) – log (time) diagrams for one-bolt specimens

**Figure 205** Rate of loss of preload for SS28 test series (M16 bolting assemblies, preload level: $F_{p,C}$ 110 kN, ∑t/d = 3.7)

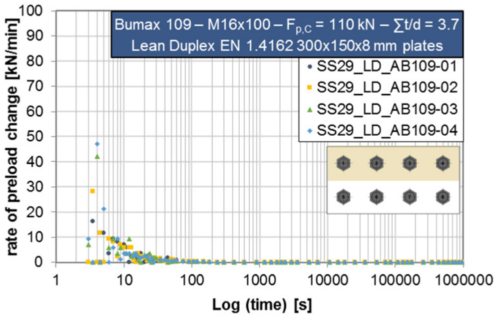


(a) log (rate of loss of preload) – time diagrams for eight-bolts specimens - first row

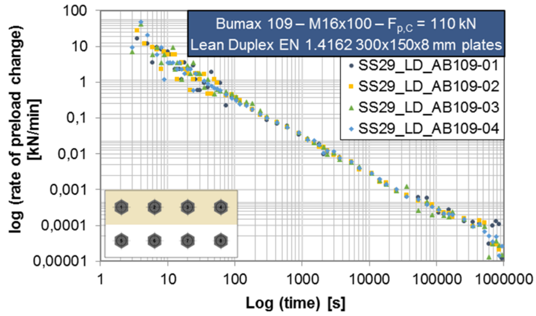


(b) log (rate of loss of preload) – log (time) diagrams for eight-bolts specimens - first row

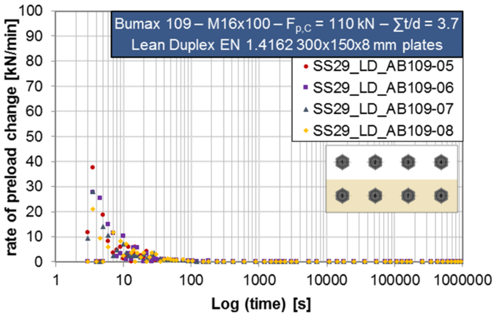


(c) log (rate of loss of preload) – time diagrams for eight-bolts specimens - second row

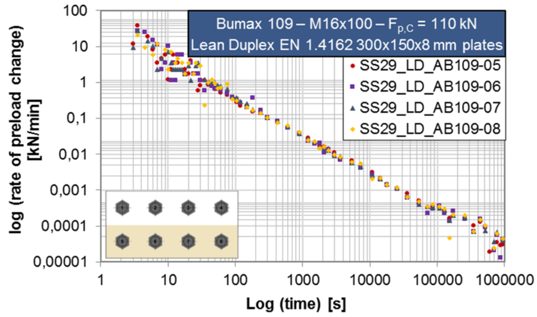


(d) log (rate of loss of preload) – log (time) diagrams for eight-bolts specimens - second row

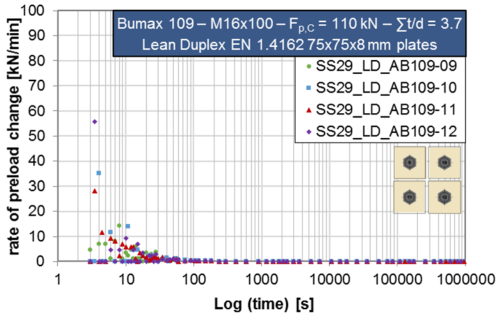


(e) log (rate of loss of preload) – time diagrams for one-bolt specimens

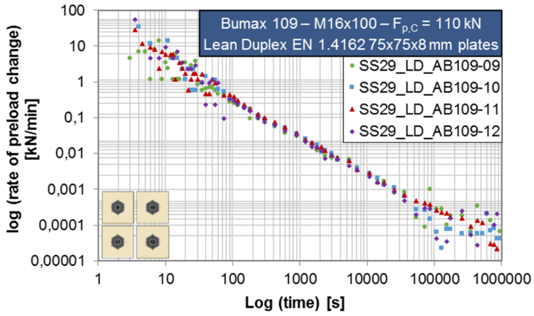


(f) log (rate of loss of preload) – log (time) diagrams for one-bolt specimens

**Figure 206** Rate of loss of preload for SS29 test series (M16 bolting assemblies, preload level: $F_{p,C}$ 110 kN, $\sum t/d = 3.7$)

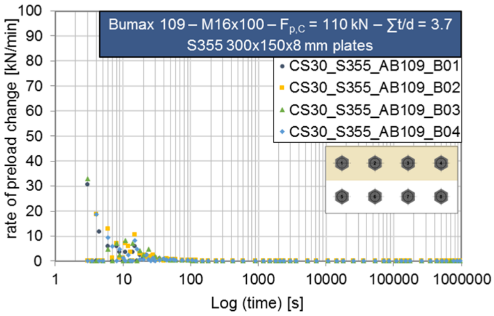


(a) log (rate of loss of preload) – time diagrams for eight-bolts specimens - first row

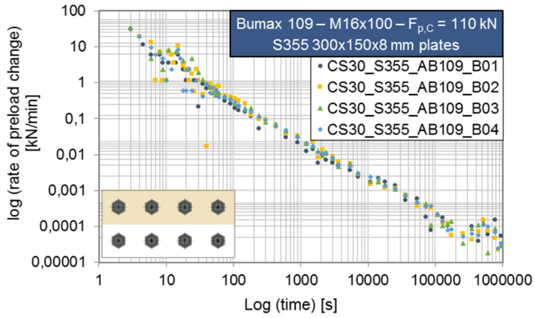


(b) log (rate of loss of preload) – log (time) diagrams for eight-bolts specimens - first row

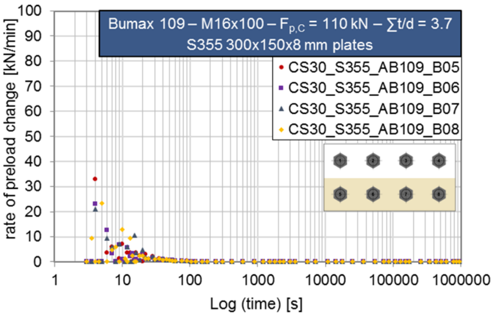


(c) log (rate of loss of preload) – time diagrams for eight-bolts specimens - second row

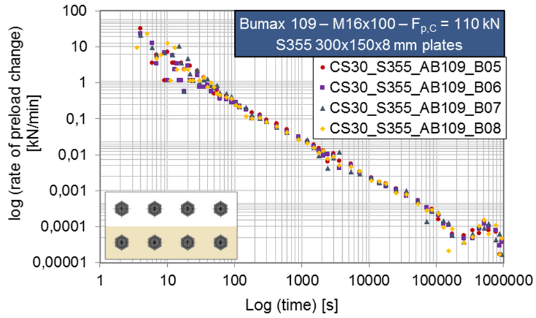


(d) log (rate of loss of preload) – log (time) diagrams for eight-bolts specimens - second row

**Figure 207** Rate of loss of preload for CS30 test series (M16 bolting assemblies, preload level: $F_{p,C}$ 110 kN, $\sum t/d = 3.7$)

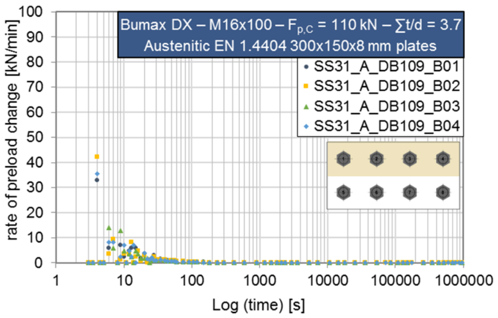


(a) log (rate of loss of preload) – time diagrams for eight-bolts specimens - first row

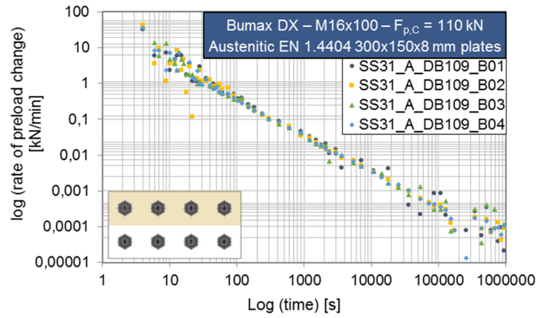


(b) log (rate of loss of preload) – log (time) diagrams for eight-bolts specimens - first row

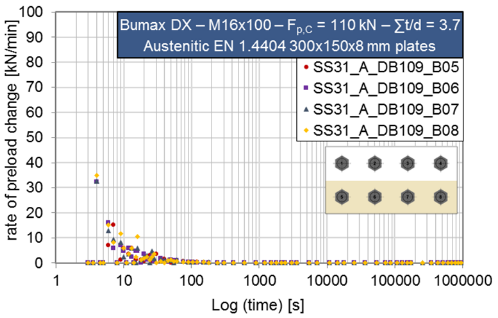


(c) log (rate of loss of preload) – time diagrams for eight-bolts specimens - second row

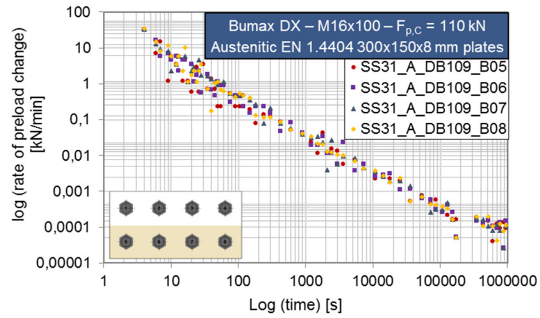


(d) log (rate of loss of preload) – log (time) diagrams for eight-bolts specimens - second row

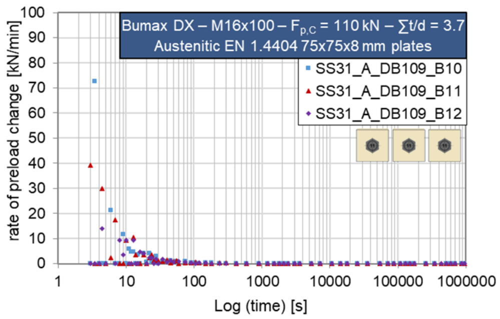


(e) log (rate of loss of preload) – time diagrams for one-bolt specimens

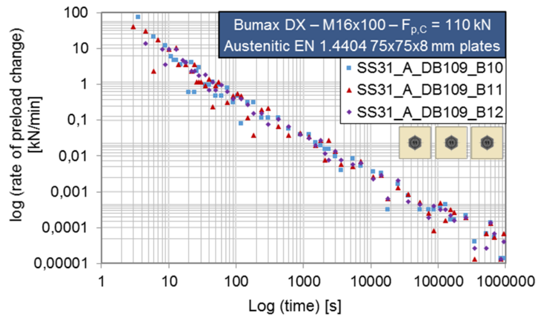


(f) log (rate of loss of preload) – log (time) diagrams for one-bolt specimens

**Figure 208** Rate of loss of preload for SS31 test series (M16 bolting assemblies, preload level: $F_{p,C}$ 110 kN, ∑t/d = 3.7)

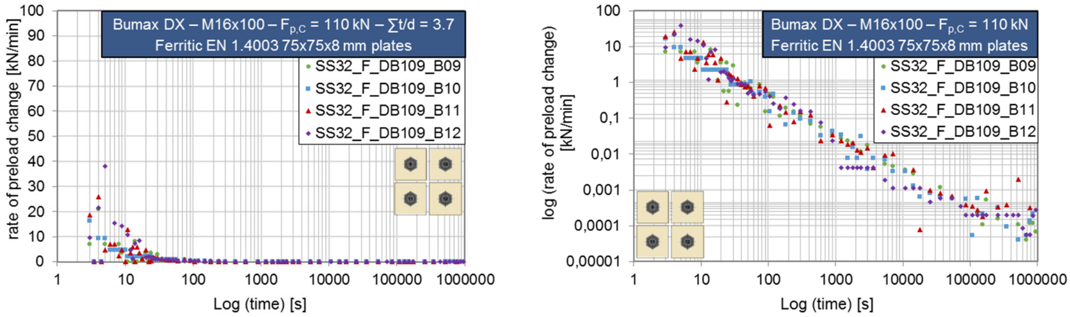


(a) log (rate of loss of preload) – time diagrams for one-bolt specimens

(b) log (rate of loss of preload) – log (time) diagrams for one-bolt specimens

**Figure 209** Rate of loss of preload for SS32 test series (M16 bolting assemblies, preload level: $F_{p,C}$ 110 kN, ∑t/d = 3.7)

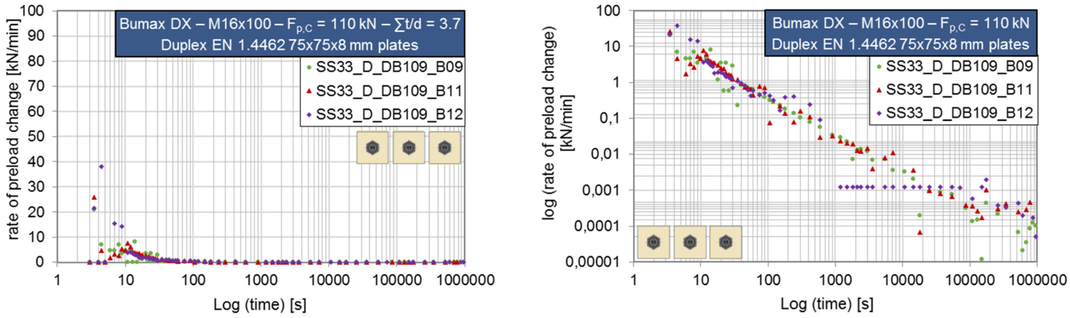


(a) log (rate of loss of preload) – time diagrams for one-bolt specimens

(b) log (rate of loss of preload) – log (time) diagrams for one-bolt specimens

**Figure 210** Rate of loss of preload for SS33 test series (M16 bolting assemblies, preload level: $F_{p,C}$ 110 kN, ∑t/d = 3.7)

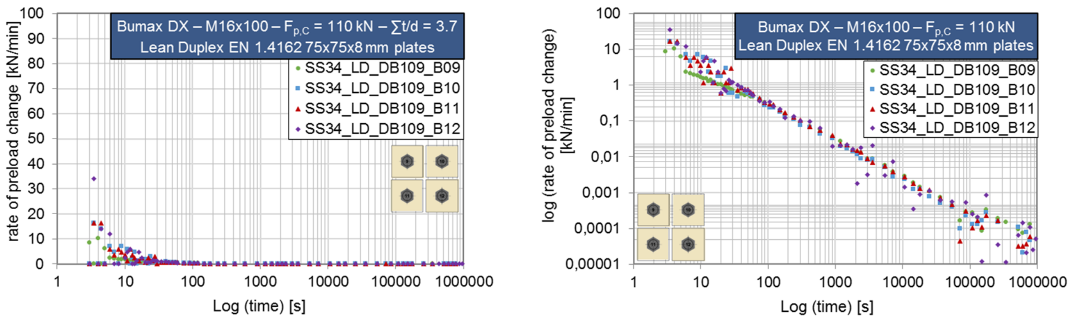


(a) log (rate of loss of preload) – time diagrams for one-bolt specimens

(b) log (rate of loss of preload) – log (time) diagrams for one-bolt specimens

**Figure 211** Rate of loss of preload for SS34 test series (M16 bolting assemblies, preload level: $F_{p,C}$ 110 kN, ∑t/d = 3.7)

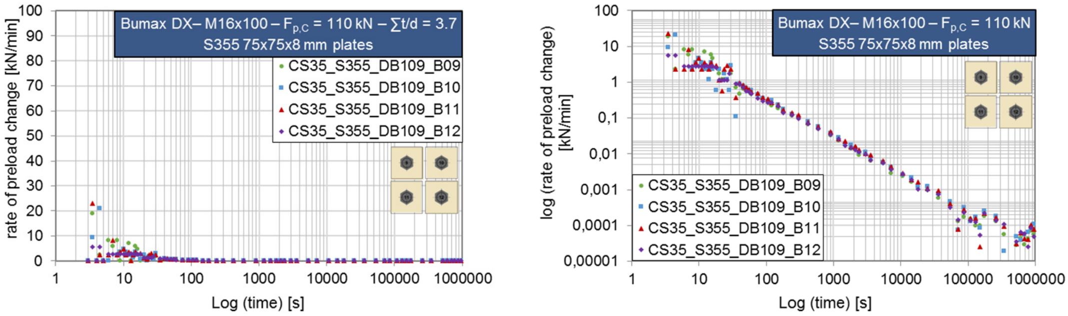


(a) log (rate of loss of preload) – time diagrams for one-bolt specimens

(b) log (rate of loss of preload) – log (time) diagrams for one-bolt specimens

**Figure 212** Rate of loss of preload for CS35 test series (M16 bolting assemblies, preload level: $F_{p,C}$ 110 kN, ∑t/d = 3.7)

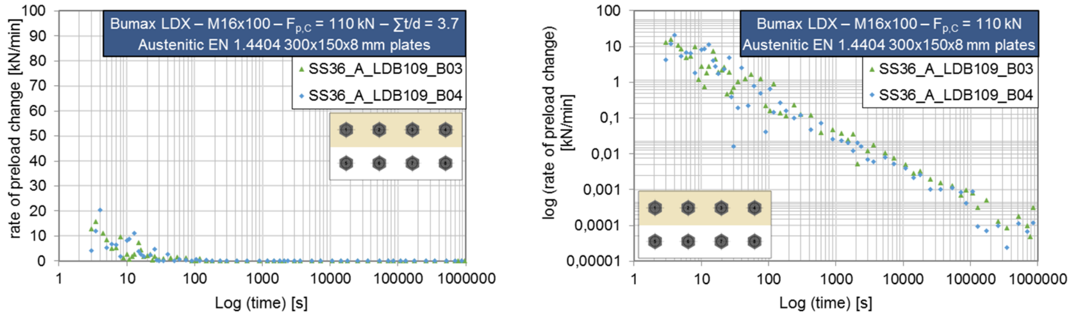


(a) log (rate of loss of preload) – time diagrams for eight-bolts specimens - first row

(b) log (rate of loss of preload) – log (time) diagrams for eight-bolts specimens - first row

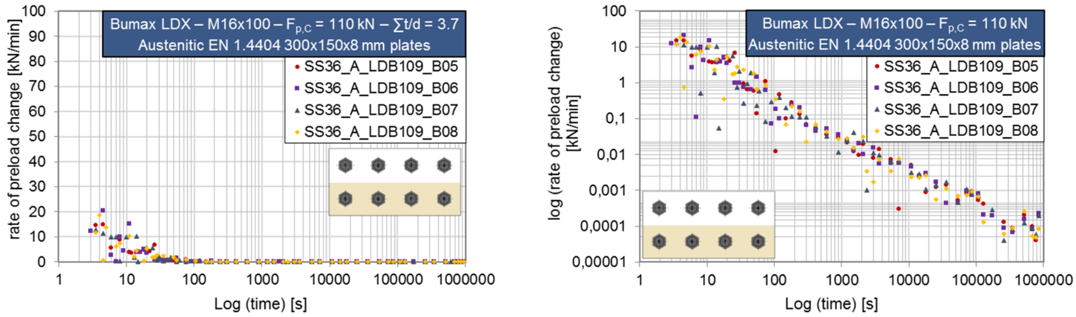


(c) log (rate of loss of preload) – time diagrams for eight-bolts specimens - second row

(d) log (rate of loss of preload) – log (time) diagrams for eight-bolts specimens - second row

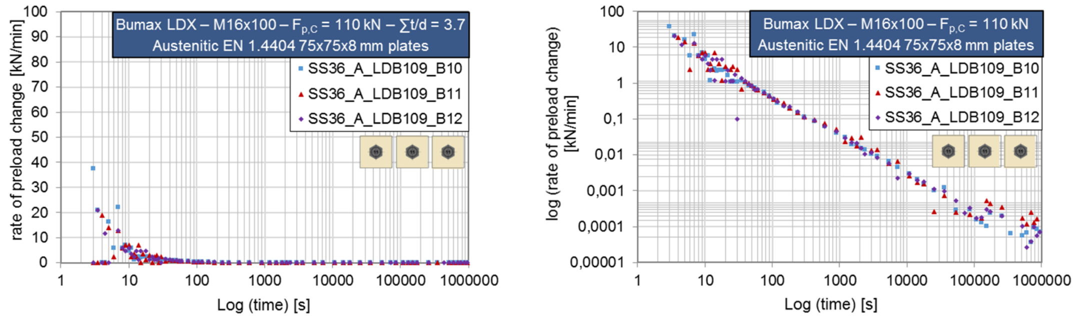


(e) log (rate of loss of preload) – time diagrams for one-bolt specimens

(f) log (rate of loss of preload) – log (time) diagrams for one-bolt specimens

**Figure 213** Rate of loss of preload for SS36 test series (M16 bolting assemblies, preload level: $F_{p,C}$ 110 kN, ∑t/d = 3.7)

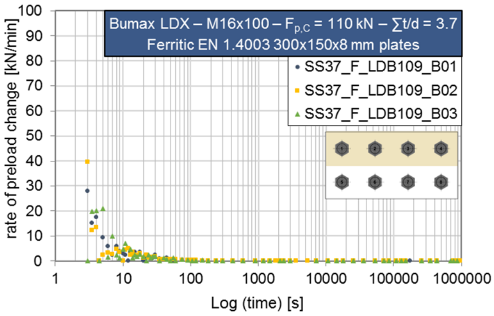


(a) log (rate of loss of preload) – time diagrams for eight-bolts specimens - first row

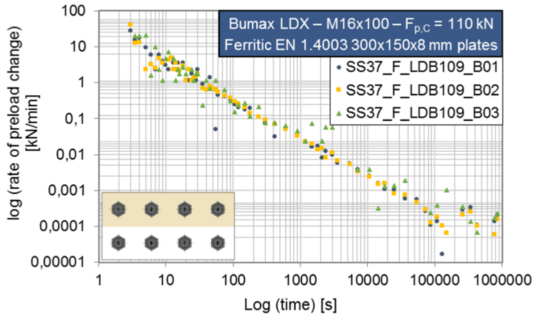


(b) log (rate of loss of preload) – log (time) diagrams for eight-bolts specimens - first row

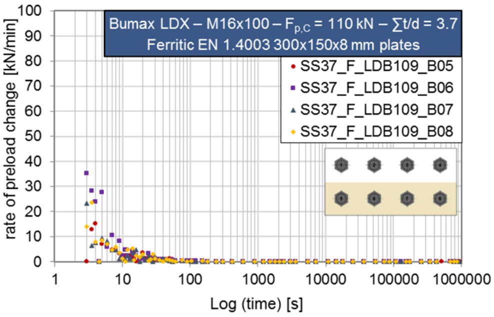


(c) log (rate of loss of preload) – time diagrams for eight-bolts specimens - second row

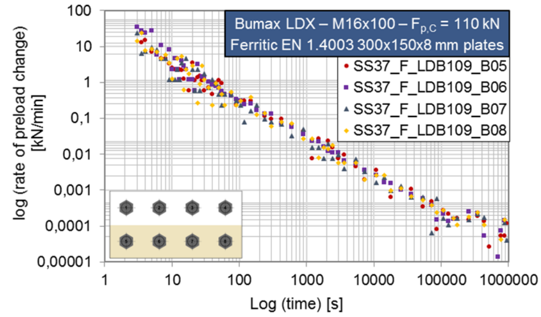


(d) log (rate of loss of preload) – log (time) diagrams for eight-bolts specimens - second row

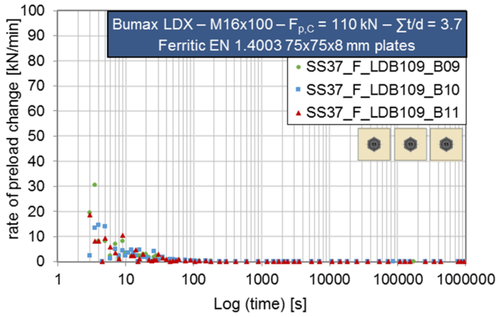


(e) log (rate of loss of preload) – time diagrams for one-bolt specimens

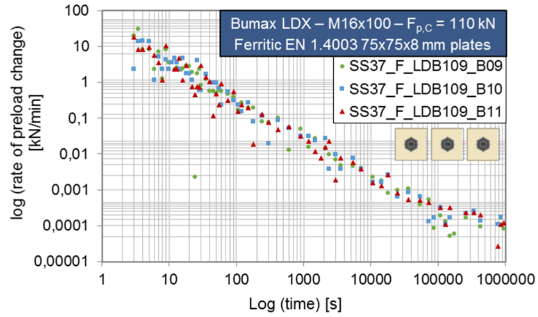


(f) log (rate of loss of preload) – log (time) diagrams for one-bolt specimens

**Figure 214** Rate of loss of preload for SS37 test series (M16 bolting assemblies, preload level: $F_{p,C}$ 110 kN, ∑t/d = 3.7)

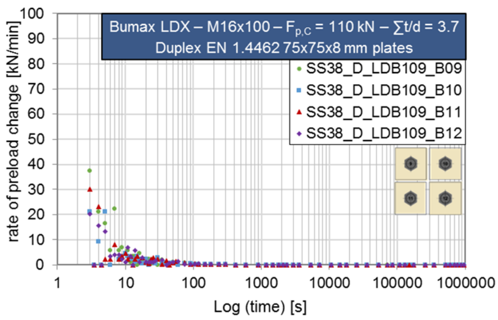


(a) log (rate of loss of preload) – time diagrams for one-bolt specimens

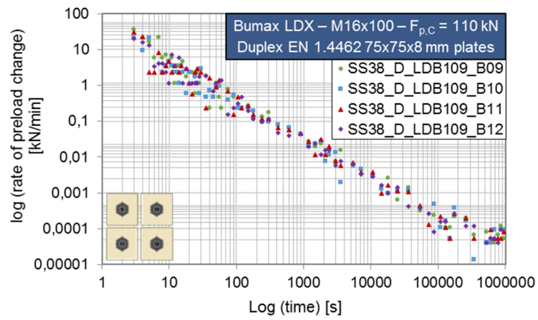


(b) log (rate of loss of preload) – log (time) diagrams for one-bolt specimens

**Figure 215** Rate of loss of preload for SS38 test series (M16 bolting assemblies, preload level: $F_{p,C}$ 110 kN, ∑t/d = 3.7)

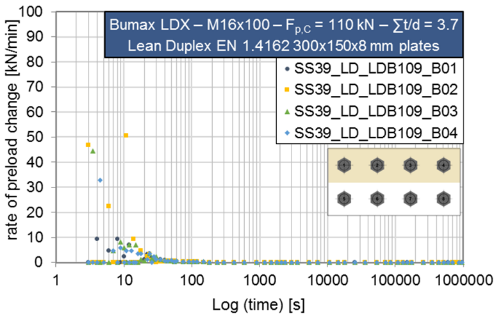


(a) log (rate of loss of preload) – time diagrams for eight-bolts specimens - first row

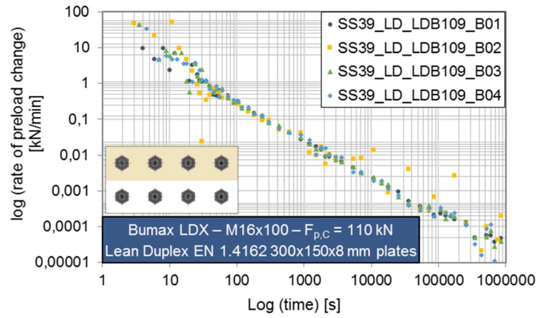


(b) log (rate of loss of preload) – log (time) diagrams for eight-bolts specimens - first row

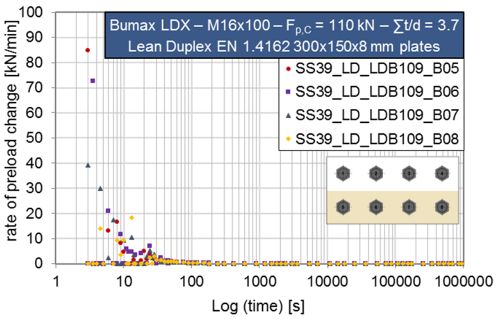


(c) log (rate of loss of preload) – time diagrams for eight-bolts specimens - second row

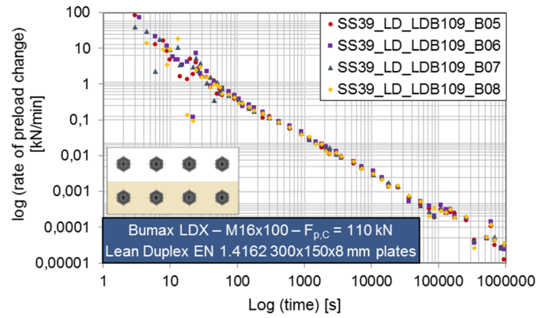


(d) log (rate of loss of preload) – log (time) diagrams for eight-bolts specimens - second row

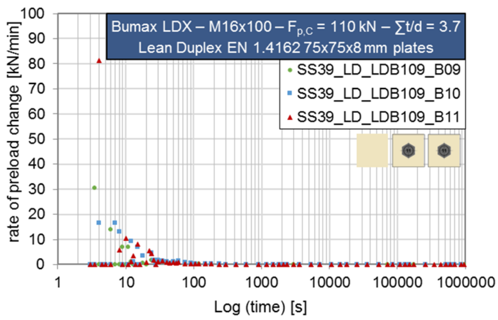


(e) log (rate of loss of preload) – time diagrams for one-bolt specimens

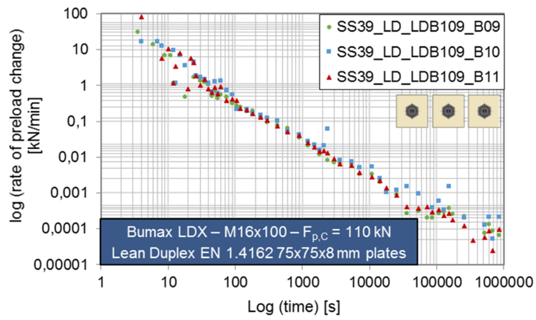


(f) log (rate of loss of preload) – log (time) diagrams for one-bolt specimens

**Figure 216** Rate of loss of preload for SS39 test series (M16 bolting assemblies, preload level: $F_{p,C}$ 110 kN, ∑t/d = 3.7)

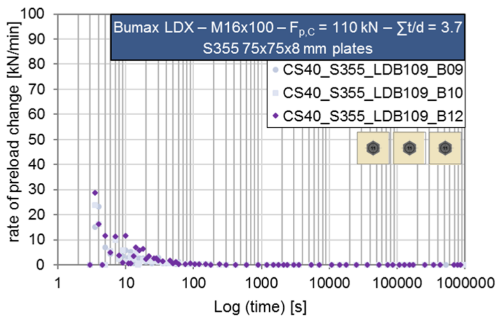


(a) log (rate of loss of preload) – time diagrams for one-bolt specimens

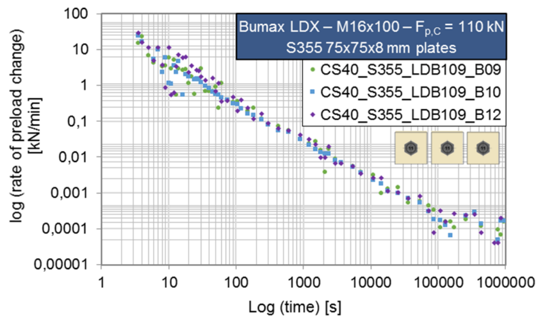


(b) log (rate of loss of preload) – log (time) diagrams for one-bolt specimens

**Figure 217** Rate of loss of preload for CS40 test series (M16 bolting assemblies, preload level: $F_{p,C}$ 110 kN, ∑t/d = 3.7)

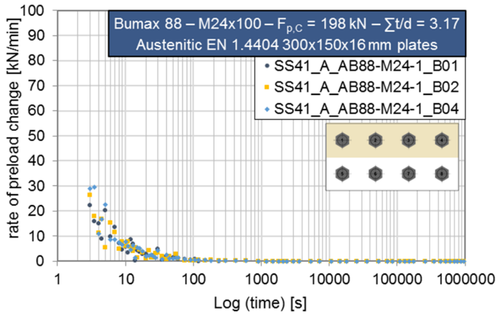


(a) log (rate of loss of preload) – time diagrams for eight-bolts specimens - first row

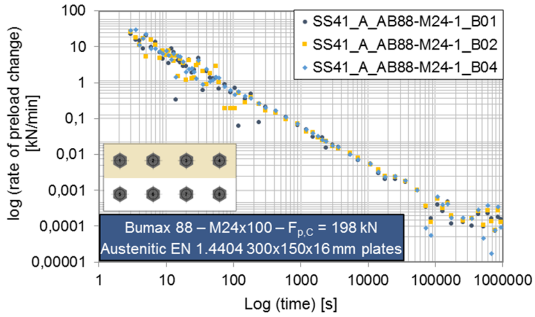


(b) log (rate of loss of preload) – log (time) diagrams for eight-bolts specimens - first row

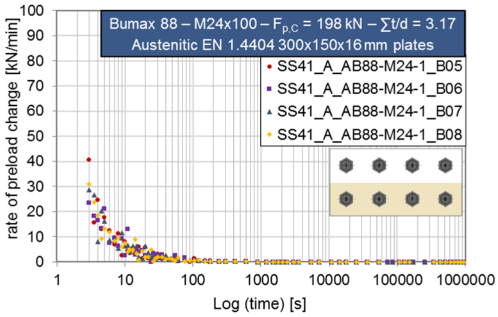


(c) log (rate of loss of preload) – time diagrams for eight-bolts specimens - second row

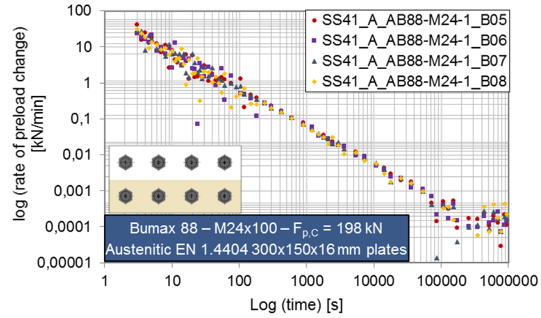


(d) log (rate of loss of preload) – log (time) diagrams for eight-bolts specimens - second row

**Figure 218** Rate of loss of preload for SS41 test series (M24 bolting assemblies, preload level: $F_{p,C}$ 198 kN, ∑t/d = 3.17)

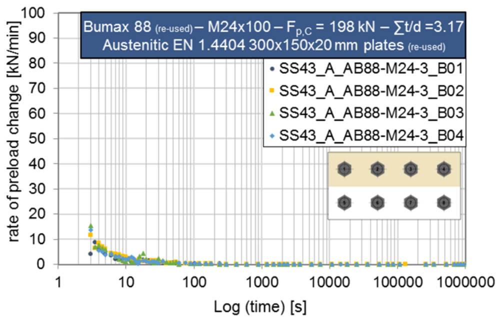


(a) log (rate of loss of preload) – time diagrams for eight-bolts specimens - first row

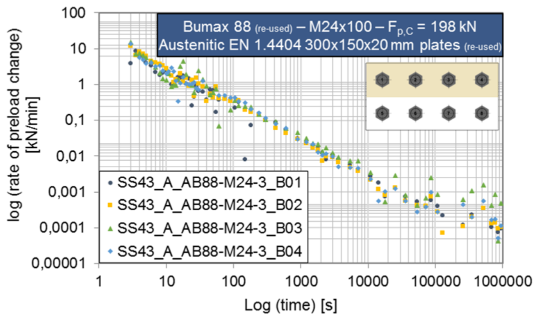


(b) log (rate of loss of preload) – log (time) diagrams for eight-bolts specimens - first row

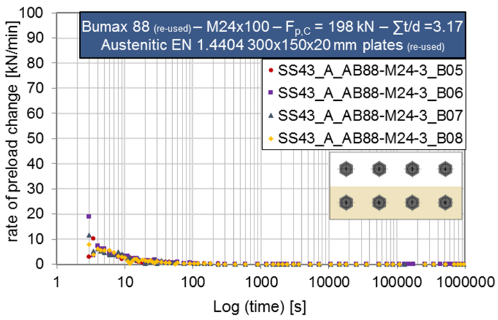


(c) log (rate of loss of preload) – time diagrams for eight-bolts specimens - second row

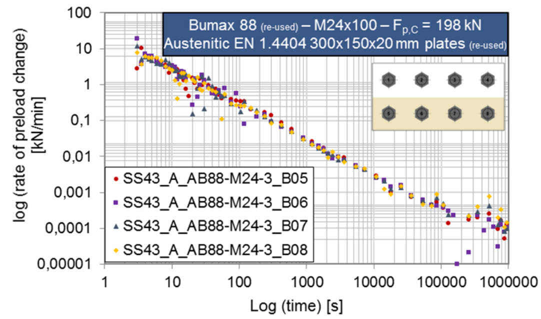


(d) log (rate of loss of preload) – log (time) diagrams for eight-bolts specimens - second row

**Figure 219** Rate of loss of preload for SS43 test series (M24 bolting assemblies, preload level: $F_{p,C}$ 198 kN, ∑t/d = 3.17)

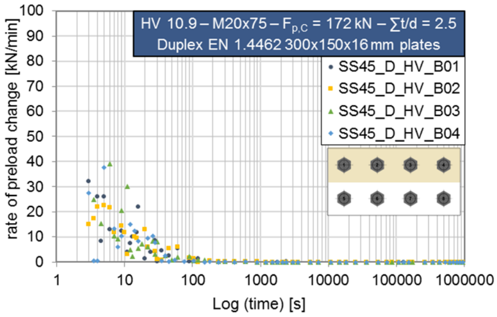


(a) log (rate of loss of preload) – time diagrams for eight-bolts specimens - first row

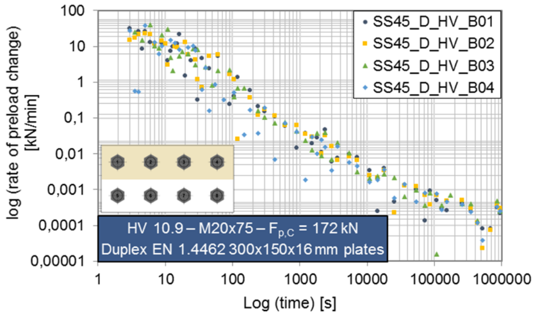


(b) log (rate of loss of preload) – log (time) diagrams for eight-bolts specimens - first row

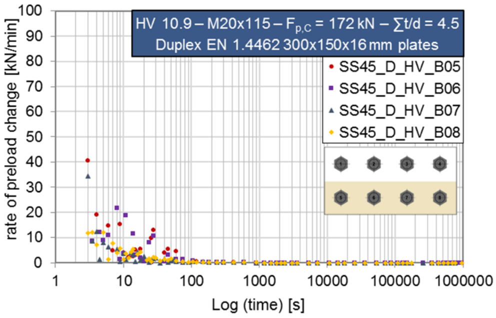


(c) log (rate of loss of preload) – time diagrams for eight-bolts specimens - second row

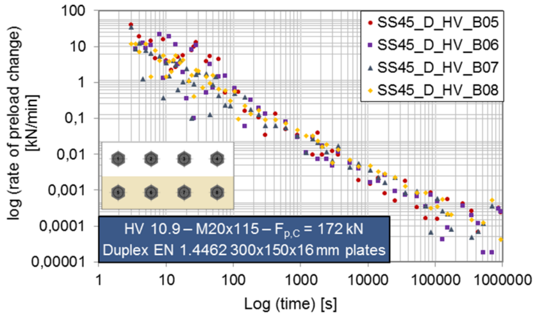


(d) log (rate of loss of preload) – log (time) diagrams for eight-bolts specimens - second row

**Figure 220** Rate of loss of preload for SS45 test series (M20 bolting assemblies, preload level: $F_{p,C}$ 172 kN, ∑t/d = 2.5/4.5)

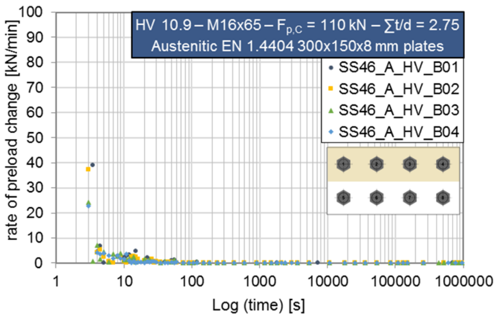


(a) log (rate of loss of preload) – time diagrams for eight-bolts specimens - first row

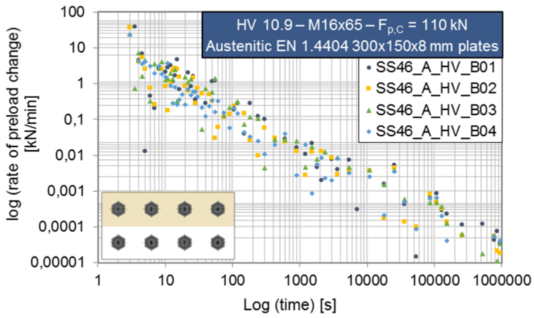


(b) log (rate of loss of preload) – log (time) diagrams for eight-bolts specimens - first row

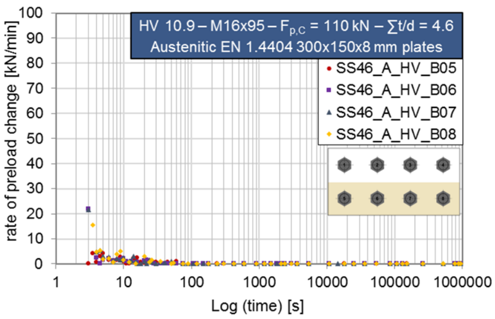


(c) log (rate of loss of preload) – time diagrams for eight-bolts specimens - second row

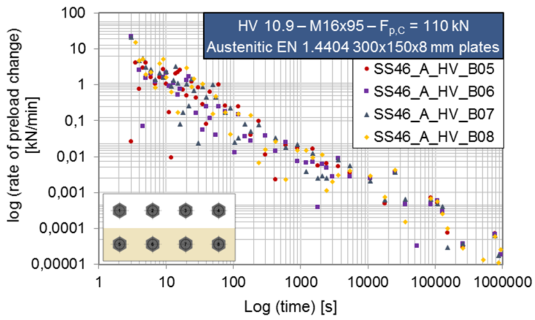


(d) log (rate of loss of preload) – log (time) diagrams for eight-bolts specimens - second row

**Figure 221** Rate of loss of preload for SS46 test series (M16 bolting assemblies, preload level: $F_{p,C}$ 110 kN, ∑t/d = 2.75/4.6)

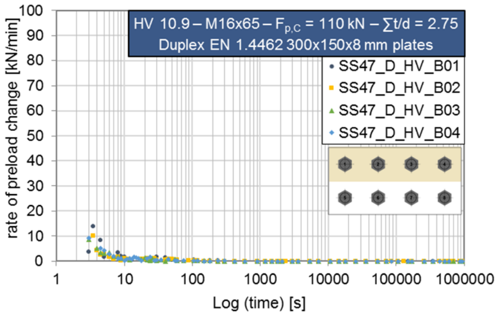


(a) log (rate of loss of preload) – time diagrams for eight-bolts specimens - first row

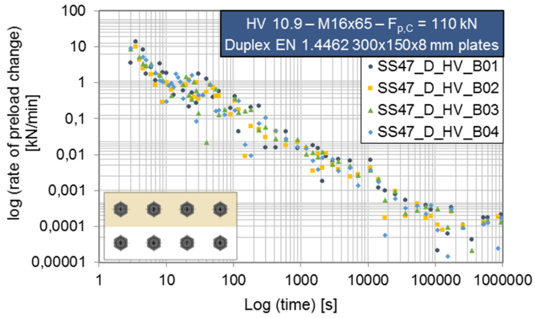


(b) log (rate of loss of preload) – log (time) diagrams for eight-bolts specimens - first row

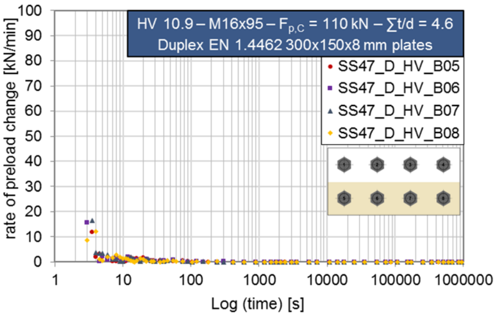


(c) log (rate of loss of preload) – time diagrams for eight-bolts specimens - second row

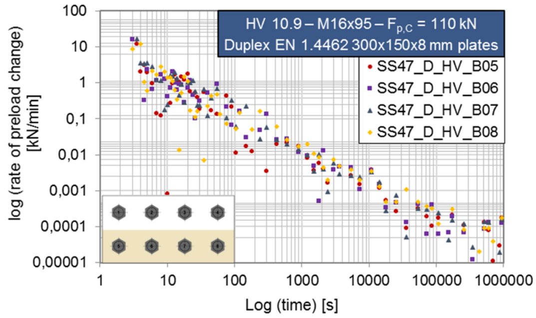


(d) log (rate of loss of preload) – log (time) diagrams for eight-bolts specimens - second row

**Figure 222** Rate of loss of preload for SS47 test series (M16 bolting assemblies, preload level: $F_{p,C}$ 110 kN, ∑t/d = 2.75/4.6)